University of Southampton

Faculty of Engineering and Physical Sciences

Chemistry

The Synthesis of Fluorinated Bile Acid Analogues

by

Rachel Wynn

Thesis for the degree of Doctor of Philosophy

February 2019

University of Southampton

Abstract

Faculty of Faculty of Engineering and Physical Sciences

Chemistry

Thesis for the degree of Doctor of Philosophy

The Synthesis of Fluorinated Bile Acid Analogues

by

Rachel Wynn

Bile acids are a type of acidic steroid found in the bile of mammals and other vertebrates. They are key in the digestion of food but also play a role as signalling molecules, regulating their own synthesis and transport, as well as being involved in the homeostasis of energy and glucose. Because of this role, naturally-occurring and semi-synthetic bile acids have been used to treat a range of liver diseases and disorders for many years. Additionally, bile acids and their derivatives have been investigated for their roles in the treatment of cancer and, more recently, various life-changing neurodegenerative diseases such as Parkinson's disease and Alzheimer's disease.

In drug discovery, fluorine is widely used to modulate the properties of potential drug candidates, including pK_a, hydrogen-bond donating capacity and log$P$/D. Because of this, introduction of fluorine atoms to the polycyclic ring system of a bile acid is of high interest, to investigate the biological effects compared to those of the non-fluorinated analogues. This thesis describes the synthesis of a number of fluorinated bile acid analogues, along with the discussion of the biological activities of selected compounds in liver and neurodegenerative diseases. The crystal packing of a number of the analogues and intermediates in their synthesis is also discussed.

Table of Contents

Table of Tables

Table of Figures

Table of Figures

Table of Figures

Table of Figures

Research Thesis: Declaration of Authorship

Print name:	Rachel Wynn

Title of thesis:	The Synthesis of Fluorinated Bile Acid Analogues

I declare that this thesis and the work presented in it are my own and has been generated by me as the result of my own original research.

I confirm that:

1. This work was done wholly or mainly while in candidature for a research degree at this University;
2. Where any part of this thesis has previously been submitted for a degree or any other qualification at this University or any other institution, this has been clearly stated;
3. Where I have consulted the published work of others, this is always clearly attributed;
4. Where I have quoted from the work of others, the source is always given. With the exception of such quotations, this thesis is entirely my own work;
5. I have acknowledged all main sources of help;
6. Where the thesis is based on work done by myself jointly with others, I have made clear exactly what was done by others and what I have contributed myself;
7. None of this work has been published before submission

Signature:		Date:	

Acknowledgements

Firstly, I would like to thank Professor Bruno Linclau for his endless and invaluable guidance, support and patience throughout my PhD. He has taught me so much and I am thankful for the opportunity to carry out my studies under his supervision. I would also like to thank Dr Alex Weymouth-Wilson for his leadership and insight throughout my time on the bile acid project.

I'd like to thank all of the members in the Linclau group I have worked with throughout my PhD: Ben, Zhong, Gemma, Gert-Jan, Lucas, Julien, Clement, Joe, Hannah, Simon, David, JB, RK, Mariana, Diego, and all of the French students and project students we've had over the past 3 years, you've all made it brilliant. Special thanks must go to Zhong and Joe for teaching me all about the bile acid project when I started my PhD. Special thanks must also go to Ben (aka Bjef, Jeff Benries or King Ben), Gemma and Gert-Jan (GJ) not only for the friendship, great memories and endless laughs, but also for playing Taylor Swift in the lab all the time! I'd like to thank Zhong, Ben, Gemma, Hannah, Simon and David for proof-reading my thesis chapters. Thanks must also go to my friends from the 3rd floor office for all of the chats, meals out and overall support. I'd also like to thank the team at NZP UK in Reading who were so helpful whilst I was on my placement, in meetings and with the many emails throughout my PhD.

Thanks go to Keith and Mark in stores, who, as well as doing an excellent job at providing us with help and consumables, have been wonderful to talk to and have many laughs with over the years. I would also like to thank Neil for running the NMR facilities and helping with many tough samples, John, Julie and Sarah for mass spectrometry services (particularly to Julie for all of her help with highly fragmenting bile acids), and Mark for performing X-Ray crystallography on many not-so-perfect bile acid crystals.

To three important Johns I have met since I started studying Chemistry at college: John Luton, my A-level Chemistry teacher, for showing me how brilliant Chemistry can be and inspiring me to choose it as both a degree and as a career; and Dr John Turner and Professor John Spencer from the University of Sussex who were so inspiring, helpful and supportive throughout my undergraduate degree.

Thanks must go to my friends and my amazing family, Mum, Lucy, James, Auntie Carolyn and Uncle Andy, for the never ending support and care through the highs and lows of the PhD. Finally, to Matt, my wonderful boyfriend, thank you for mopping up all of the Chemistry-induced tears, for helping with all of the PhD stress, for making me laugh and smile even on the hardest days and for always being incredibly supportive throughout my studies.

Definitions and Abbreviations

Aβ	Amyloid β
Ac	Acetyl
AD	Alzheimer's Disease
ADMET	Absorption, distribution, metabolism, excretion and toxicity
AIBN	Azobisisobutyronitrile
APOE	Apolipoprotein E
ATP	Adenosine triphosphate
BA	Bile acid
BBB	Blood-brain-barrier
BPO	Dibenzoyl peroxide
Bz	Benzoyl
CA	Cholic acid
CDCA	Chenodeoxycholic acid
COSY	Correlation spectroscopy
CNS	Central nervous system
CSF	Cerebral spinal fluid
CV	Column Volume(s)
d	Doublet
DAST	Diethylaminosulfur trifluoride
DBU	1,8-Diazabicyclo(5.4.0)undec-7-ene
DCA	Deoxycholic acid
DCM	Dichloromethane
DEAD	Diethyl azodicarboxylate
DIAD	Diisopropyl azodicarboxylate
DIPEA	*N,N*-Diisopropylethylamine
DMAP	4-Dimethylaminopyridine
DMF	Dimethylformamide
DMP	Dess-Martin periodinane
DMSO	Dimethylsulfoxide
DNA	Deoxyribonucleic acid
ER	Endoplasmic reticulum
ESI	Electrospray ionisation
ETC	Electron Transport Chain

EtOAc	Ethyl acetate
FG	Functional Group
FTIR	Fourier-transform infrared
FXR	Farnesoid X receptor
GPCR	G-protein-coupled receptor
GSH	Glutathione
HB	Hydrogen bond
HBA	Hydrogen bond acceptor
HBD	Hydrogen bond donor
HDCA	Hyodeoxycholic acid
HMBC	Heteronuclear multiple-bond correlation spectroscopy
HPLC	High performance liquid chromatography
HSQC	Heteronuclear single-quantum correlation spectroscopy
IMHB	Intramolecular hydrogen bond
IPA	Isopropanol
IR	Infra-red
LCA	Lithocholic acid
LDA	Lithium diisopropylamide
LDH	Lactate dehydrogenase
LRMS	Low resolution mass spectrometry
m	Multiplet
MAPK	Mitogen-activated protein kinase
m-CPBA	*meta*-Chloroperoxybenzoic acid
MDR	Multi-drug resistant
MMP	Mitochondrial membrane potential
MOM	Methoxymethyl
mp	Melting point
MS	Mass spectrometry
NASH	Non-alcoholic steatohepatitis
NCS	*N*-chlorosuccinimide
NfF	Perfluorobutanesulfonyl fluoride
NFT	Neurofibrillary tangle(s)
NMP	N-Methylpyrolidinone
NMR	Nuclear magnetic resonance
NOE(SY)	Nuclear Overhauser effect (spectroscopy)

OCA	Obeticholic acid
O-PCTF	*O*-Phenyl chlorothionoformate
PD	Parkinson's disease
PDC	Pyridinium dichromate
PE	Petroleum ether 40-60
PET	Positron emission tomography
*p*TSA	*para*-Toluenesulfonic acid
PXR	Pregnane X receptor
q	Quartet
R_f	Retention factor
ROS	Reactive oxygen species
RT	Room temperature
s	Singlet
SXR	Steroid and xenobiotic receptor
t	Triplet
TBAB	Tetra-*n*-butylammonium bromide
TBAF	Tetra-*n*-butylammonium fluoride
TBDMS	*tert*-butyldimethylsilyl
TBDPS	*tert*-butyldiphenylsilyl
TEMPO	2,2,6,6-tetramethylpiperidine 1-oxyl
THF	Tetrahydrofuran
TLC	Thin layer chromatography
TMSCl	Chlorotrimethylsilane
TGR5	Takeda G-protein-coupled receptor 5
UDCA	Ursodeoxycholic acid
UV	Ultraviolet
VDR	Vitamin D receptor
VdW	Van der Waals

Chapter 1 Introduction

1.1 Targeted Disease Areas

1.1.1 Neurodegenerative Diseases/Disorders

Neurodegenerative diseases such as Parkinson's, Alzheimer's and Huntingdon's along with other disorders such as Motor Neurone Disease (also known as ALS) and Multiple Sclerosis are prevalent across the world and lack effective treatment.

Alzheimer's disease (AD) is the most common cause of dementia and is a chronic, progressive disease which is prevalent in 10-30% of people over 65 years old.[1] As well as problems with memory, AD can cause confusion, speech and language problems, depression, hallucinations and personality changes in patients. Generally, AD occurs at the same rate throughout the world and is more prevalent in women than in men.[1] Factors increasing the risk of developing AD include diabetes, high blood pressure, obesity, smoking, low educational attainment and physical inactivity.[1]

The disease affects wide areas of the cerebral cortex[i] and hippocampus,[ii] and, in general, is associated with the accumulation of the protein amyloid-β (Aβ) in plaques in extracellular spaces, along with aggregation of tau (a microtubule protein) in neurofibrillary tangles (NFTs) in neurons.[1] This accumulation of amyloid plaques and NFTs leads to neuronal cell death.[2,3] Additionally, a genetic variation in the gene encoding apolipoprotein E (APOE, a lipid transport protein) effects the age of onset of AD and there is substantial evidence to indicate that, along with Aβ and tau, APOE contributes to AD.

The majority of AD patients have the sporadic form of the disease which is caused by the failure to clear Aβ from brain tissue, of which the general age of onset is 80 years or older. A small number of patients (<1%) have the familial form of AD though. Familial AD develops at a much lower age (around 45 years old) and is caused by inherited mutations in genes that effect the processing and production of Aβ.[1] Notably, the disease progression rates of sporadic and familial AD are comparable.

[i] Cerebral cortex: The outer layer of the brain, involved in memory, awareness, perception, language and other key brain processes.
[ii] Hippocampus: A structure located within the temporal lobe of the brain, involved in memory storage and encoding.

Whilst there are several drugs approved to alleviate some of the symptoms of AD, there are no current treatments for the underlying causes of the disease.

Parkinson's disease (PD) is the second-most common neurodegenerative disorder and effects 2-3% of the population over 65 years old in the US. It is a progressive disorder, described as "*the shaking palsy",* and causes severe disability in patients. Common symptoms include bradykinesia (slowness of movement), cognitive impairment, sleep disorders and an impaired sense of smell amongst numerous others. In most populations, PD is twice as common in men than it is in women, potentially due to a proposed protective effect of female sex hormones.[4]

Neuronal loss in the substantia nigra[iii,5,6] (leading to dopamine deficiency) and widespread inclusions of aggregates of α-synuclein (an intracellular protein) are characteristic of Parkinson's disease. Key factors in the pathogenesis of PD include α-synuclein protein homeostasis, mitochondrial dysfunction, oxidative stress and neuroinflammation. Whist the normal function of α-synuclein is not fully understood, it is proposed to have an important role in mitochondrial function. Accumulation of α-synuclein and dysfunction of mitochondria are known to lead to oxidative damage of brain tissue. Additionally, α-synuclein accumulation leads to reduced activity in mitochondrial complex I, a complex that is essential in the electron transport chain of cellular respiration.[4]

The majority of PD cases are sporadic and occur in people with no family history of the disorder, although heritable forms of Parkinson's represent 5-10% of cases. A number of different mutated genes, denoted PARK, are responsible for familial Parkinson's. Some genes including PARK1/4 (SNCA), PARK8 (LRRK2) and PARK17 (VPS35) are autosomal dominant, requiring only one mutated allele to cause the disease, whilst other genes such as PARK2, PARK6 (PINK1), PARK7 (and so on) are autosomal recessive, requiring two mutated alleles to cause the disease.[4,7]

Parkinson's disease is most commonly treated with administration of L-DOPA, a precursor to dopamine, but, like AD, currently no curative treatments exist.[4] There is an obvious need for the development of new therapeutics to target the progression of both PD and AD, rather than just treating the symptoms.

[iii] Substantia Nigra: the long nucleus located in the middle of the brain which, *via* signalling down the spinal cord, controls the muscles of the body. The neurotransmitter Dopamine is made in the Substantia Nigra.

1.1.2 Cancer

The statistic by Cancer Research UK that "*1 in 2 people in the UK born after 1960 will be diagnosed with some form of cancer during their lifetime*"[8] is shocking. In the UK, around 164,000 people die from cancer every year and the disease accounts for over 25% of all deaths.[9] In the US, cancer is the second leading cause of death (after heart disease) and an estimated 610,000 people will die from cancer in 2018.[10] While the incidence rate of all cancers has increased in the UK since 1990s, with a higher rate observed in females than in males,[11] mortality rates for all cancers in general have decreased around 10% in the last decade.[9] Likewise, in the US the cancer death rate between 1991 and 2015 was observed to decrease significantly (by 26%).[10] Part of the decrease in death rates is due to an ever-increasing effort to cure the disease and find new, highly effective treatments for cancer.

More than 360,000 new cancer cases are observed every year in the UK, 53% of which in 2015 were breast, prostate, lung and bowel cancers, the four types that account for almost half of all cancer deaths.[9,11] In UK females, breast cancer is the most common cancer and is the 2nd most common cause of cancer death.[12] Currently, breast cancer is treated with a range of chemotherapy drugs including: Tamoxifen, Doxorubicin, Methotrexate, 5-Fluorouracil, Tarceva and Cisplatin. Whilst these agents are effective at treating breast cancer, in some cases, some patients can become resistant to the drugs during treatment and some do not respond to the treatment at all.[13] Additionally, as well as having life-altering side effects, some chemotherapy agents have been shown to induce genetic damage, potentially causing further carcinogenic effects.[14]

Malignant, cancerous cells form following mutations in normal cells when the genome is damaged. The damage can occur as a result of DNA replication errors, DNA base instability, attack of DNA by free radicals or by interaction of DNA with radiation or carcinogenic chemicals.[14] Some mutations can disrupt apoptosis, the regulated cell death process, leading to initiation of tumour growth as well as tumour progression and the spread of cancerous cells throughout the body.[15] One of the most fundamental traits of cancer cells is their ability to proliferate continuously.[16] Because of this, inducing apoptosis is fundamental in the treatment of cancer and hence, most chemotherapy agents with cytotoxic activity induce apoptosis.[15]

Despite the current availability of a plethora of effective anticancer agents on the worldwide market, there is clear room for improvement in terms of developing agents which are as efficacious (or have a higher efficacy) than current drugs but also have lower toxicity towards normal cells, reducing side effects.

1.2 Bile Acids

1.2.1 Structure and Numbering

Steroid compounds are systematically numbered and named following the IUPAC 1989 recommendations.[17] *Figure 1.1* shows the steroid cholestane (**1.1**) with numbering of positions and lettering of rings, plus the A-ring as drawn conventionally on the bottom left hand side. Substituents on the top face of the ring are denoted β, those below the ring are denoted α. Also shown in *Figure 1.1* is the bile acid chenodeoxycholic acid (CDCA, **1.2**), which along with all of the other naturally occurring bile acids, has a *cis*-A,B ring juncture that is intrinsic in the chemistry and biology of bile acids. Note: when depicting bile acid structures, the stereochemistry of the hydrogen atoms at the 8-, 9- and 14-positions is not always shown, in this case, they are assumed to be: 8β, 9α and 14α.

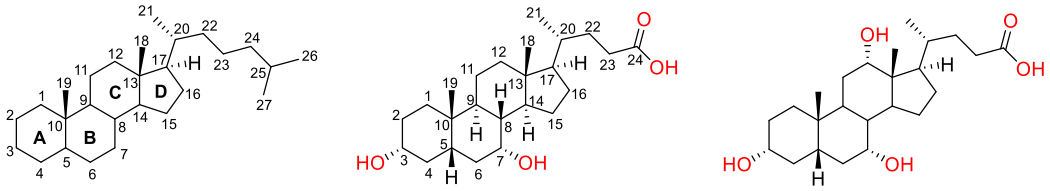

Figure 1.1 - Steroid Numbering and Key Primary Bile Acids in Humans

1.2.2 The Properties, Roles and Biosynthesis of Bile Acids

Found in the bile of vertebrates, bile acids (BAs) are a type of acidic steroid formed as a product of cholesterol catabolism.[18,19] They are classified as primary, secondary or tertiary bile acids: the primary are produced in the liver, whilst the secondary and tertiary are produced in the gut from enzymatic transformations of the primary bile acids by bacteria.[20] In humans, CDCA (**1.2**, *Figure 1.1*) and cholic acid (CA, **1.3**, *Figure 1.1*) are the primary bile acids, which form the secondary and tertiary bile acids shown in *Figure 1.2*: lithocholic acid (LCA, **1.4**), deoxycholic acid (DCA, **1.5**), ursodeoxycholic acid (UDCA, **1.6**) and hyodeoxycholic acid (HDCA, **1.7**).[21,22] LCA is present in trace amounts in the human bile acid pool, whilst UDCA, formed in humans by gut bacteria *via* 7β-epimerisation of CDCA, makes up around 1-3% of the total bile acid pool.[20,23] Notably, LCA is the most toxic of the bile acids and at high concentrations, it can cause liver damage.[24,25] HDCA is a primary bile acid in pigs, formed in humans from LCA by C-6 hydroxylation in the gut.[21]

Normally, 90-95% of bile acids are conjugated to glycine or taurine to form negatively charged bile salts that possess increased aqueous solubility compared to BAs in most physiological pH ranges, but are unable to pass through the epithelium of the small intestine and biliary tract.[19] Bile salts are usually tightly bound to plasma and intracellular proteins, limiting their toxicity.[20,23]

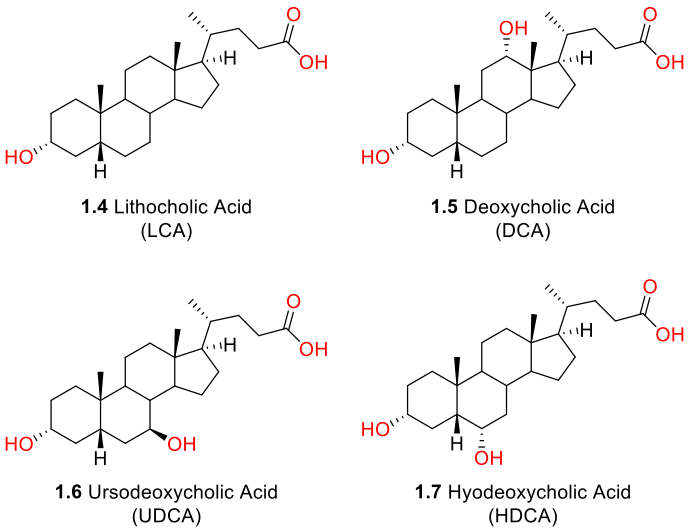

Figure 1.2 - Key Secondary and Tertiary Bile Acids

Bile acids are amphipathic molecules as they possess both a hydrophilic and a hydrophobic face (*Figure 1.3*)[20] which allows them to form mixed micelles with dietary fats and cholesterol, enabling them to act as detergents in the small intestine.[18] They also perform a multitude of tasks, including: facilitating excretion of cholesterol from the liver into the bile (which in turn lowers whole body cholesterol levels);[18] generating bile flow;[20] facilitating the secretion of lipids, endogenous metabolites and xenobiotics from the liver, bile ducts and gall bladder;[20] and aiding digestion and absorption of dietary fats, steroids, drugs and lipophilic vitamins after meal ingestion.[20,26]

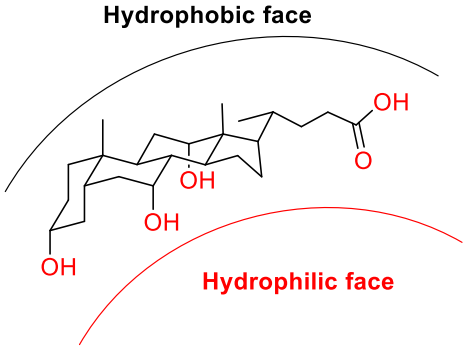

Figure 1.3 - Cholic Acid with Hydrophobic and Hydrophilic Faces Shown

Biosynthesis of primary bile acids from cholesterol occurs in the liver. Every day, in the human (adult) liver, approximately 500 mg of cholesterol is converted into primary bile acids through two major synthetic pathways: the classic (neutral) pathway and the alternative (acidic) pathway (*Figure 1.4*).[21] The classic pathway accounts for around 90% of bile acid production, whilst the alternative pathway produces around 10% of total bile acids under normal physiological conditions.[20] The pathways involve the use of at least 17 different enzymes, many of which are expressed preferentially in the liver.[21] As shown in *Figure 1.4*, the classic and alternative pathways differ mainly on the initiation of bile acid synthesis: the classic pathway is initiated by the use of the

enzyme CYP7A1, converting cholesterol into 7α-hydroxycholesterol, whereas the alternative pathway is initiated by the enzyme CYP27A1, which converts cholesterol into 27-hydroxycholesterol. Both pathways utilise the CYP27A1 enzyme in the later stages of bile acid biosynthesis to form the primary bile acids, CA and CDCA,[20] and the relative amounts of these formed in humans is determined by the level of the enzyme sterol 12α-hydroxylase.[21]

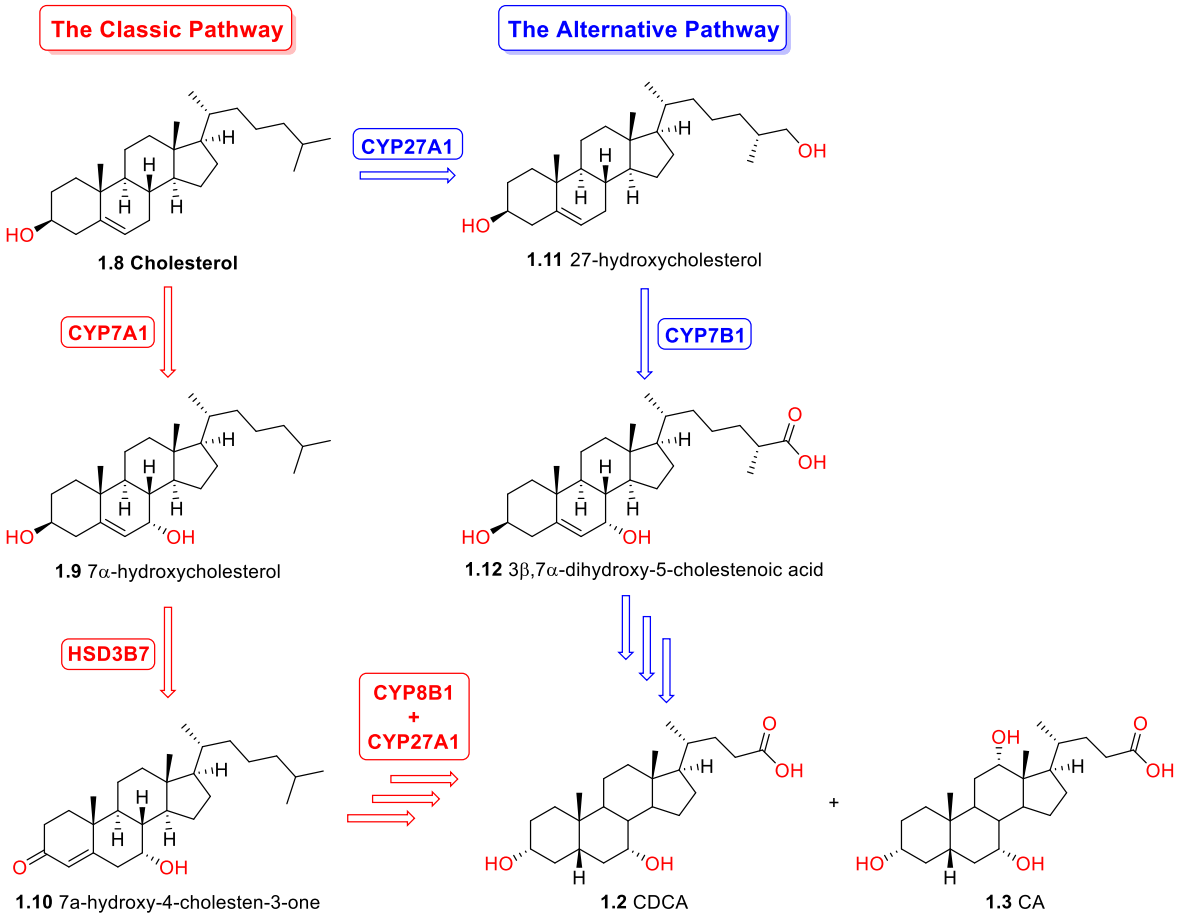

Figure 1.4 - The Classic and Alternative Pathways for the Biosynthesis of Bile Acids[20]

Whilst the primary human bile acids (cholic acid and CDCA) and the secondary bile acids DCA and LCA can be isolated naturally from bovine bile (currently the only economically viable source of bile acids), the bile acid UDCA can only be obtained naturally from the bile of bears. The production of UDCA by extraction from bear bile is highly unsustainable, so extensive research has been conducted to synthesise it from readily more available bile acids, specifically cholic acid. A number of procedures have been utilised in industry to obtain UDCA from cholic acid, some employing full chemically synthetic routes, some exclusively utilising biotransformation reactions and others using a mix of both chemical and biological transformations.[27]

1.2.3 Bile Acids as Signalling Molecules

Along with their primary roles as detergents, bile acids have been shown to act as signalling molecules for a number of intracellular ligand-activated nuclear receptors and cell membrane G-protein-coupled receptors (GPCRs).[20]

Following seminal work published in Science, in 1999 by Makishima *et al.* and Parks *et al.*, bile acids have been discovered to directly activate the nuclear receptors Farnesoid X Receptor (FXR),[28,29] Pregnane X Receptor/Steroid and Xenobiotic Receptor (PXR/SXR)[25] and Vitamin D Receptor (VDR).[24] FXR is an orphan nuclear receptor expressed highly in the liver, intestines and kidneys that plays a role in the secretion of bile acids, cholesterol and phospholipids.[20] When activated by bile acids, FXR represses the expression of CYP7A1 (*Figure 1.4*) and upregulates bile acid transport proteins,[28,30,31] therefore regulating the synthesis and transport of BAs, preventing hepatic bile acid accumulation.[20,28] FXR is activated by both free and conjugated bile acids – CDCA is the most potent natural bile acid activator of FXR, with an EC_{50}[iv,32] of around 7 μM. DCA and LCA are also potent, but to a lesser extent than CDCA,[20,28] whilst cholic acid and UDCA have been shown not to activate FXR, or activate it very weakly.[29]

TGR5 (also known as GPBAR1, M-BAR, BG-37) is a GPCR which is also directly activated by bile acids.[33,34] It is widely expressed throughout the body and has been found in several tissues including the gall bladder, ileum and colon, also in metabolic tissues such as the liver, muscle and brown adipose tissue.[33,35] Both free and conjugated natural bile acids are known to bind to and activate TGR5, with LCA and its taurine conjugate, taurolithocholic acid (TLCA), having the highest activities (EC_{50}) of 530 nM and 290 nM respectively.[22] Cholic acid, DCA, CDCA and HDCA are also known to activate TGR5 at micromolar concentrations,[22,33,34,36] whilst UDCA has very low activity.[34] Activation of TGR5 by bile acids stimulates intracellular cAMP[v,37] production and activation of the mitogen-activated protein kinase (MAPK) pathway,[vi,38] intrinsic in the communication of signals from receptors to DNA in the nucleus of a cell.[20,36,39] TGR5 is also involved in energy and glucose homeostasis, in a fashion independent of FXR.[33,34,36,40,41] Evidence has also shown that activation of TGR5 in the liver by bile acids leads to the protection of the liver endothelium from oxidative stress.[42]

[iv] EC_{50} – the dose at which 50% of the maximum effect is produced or the concentration of drug at which the drug is half-maximally effective.

[v] cAMP – Cyclic adenosine monophosphate, a common "second messenger" that mediates biological responses.

[vi] MAPK pathways are involved in cell proliferation, differentiation, development, transformation and apoptosis.

For both FXR and TGR5, the stereochemistry of the 7-hydroxy of CDCA and UDCA defines their biological activity. As mentioned, UDCA very weakly activates FXR and TGR5, whilst CDCA has micromolar activity, hence a 7α-hydroxy is key for biological activity.

1.2.4 The Uses of Natural and Semi-Synthetic Bile Acids in Liver Disease

Before the discovery of the bile acid activated receptors FXR and TGR5, the medicinal uses of bile acids and bile salts were limited to the dissolution of gallstones,[27,43] the treatment of primary biliary cirrhosis,[44] the treatment of bile acid deficiency and, for several centuries in China, the traditional treatment of digestive diseases.[20] UDCA is still used in modern medicine to improve liver function in choleostatic diseases and decrease cholesterol saturation in bile.[27] More recently, bile acids and bile salts have been used as excipients to aid the solubility, absorption and chemical or enzymatic stability of drugs[45] and in drug formulations as absorption promoters.[46]

Modification of naturally occurring bile acids to form semi-synthetic bile acids is highly common due to their large range of uses. An extensive range of semi-synthetic bile acids have been reported, with the synthesis of: antibacterial agents;[47] antitubercular agents;[48] 22*R*- and 22*S*-hydroxy bile acids;[49] and 23*R*- and 23*S*-fluoro derivatives of bile acids[50] to name a few. Additionally, some fluorinated bile acids have been synthesised and tested against choleostatic liver disease, including derivatives of HDCA (7α-fluoro HDCA, UPF680, shown to prevent LCA synthesis from bile acids)[51] and derivatives of UDCA (6α-fluoro UDCA).[52]

FXR and TGR5 agonists are potential drugs for the treatment of choleostasis (in Primary Biliary Cirrhosis, Primary Sclerosing Cholangitis, Cystic Fibrosis and other diseases[31]) and also metabolic and inflammatory diseases.[20] Due to the differing roles of FXR and TGR5, there is a necessity for agonists that are selective to one of the receptors or at least more potent to one receptor than the other. *Figure 1.5* shows a range of natural and semi-synthetic bile acids and their potency as agonists against TGR5 and FXR. Based on the reasonable efficacy of CDCA towards FXR and TGR5, Pellicciari *et al.* developed the agonist Obeticholic acid (OCA, INT-747, **1.13**, *Figure 1.5*), which had a high potency for both FXR and TGR5, showing the importance of a substituent in the 6α-position for FXR agonism.[31] In 2016, OCA was approved in the USA for the treatment of primary biliary cholangitis (PBC, previously known as primary biliary cirrhosis) when used in combination with UDCA.[53] OCA also is currently (as of 2018) in phase III clinical trials for non-alcoholic steatohepatitis (NASH) with fibrosis, bile acid diarrhoea and a number of other liver diseases.[54,55]

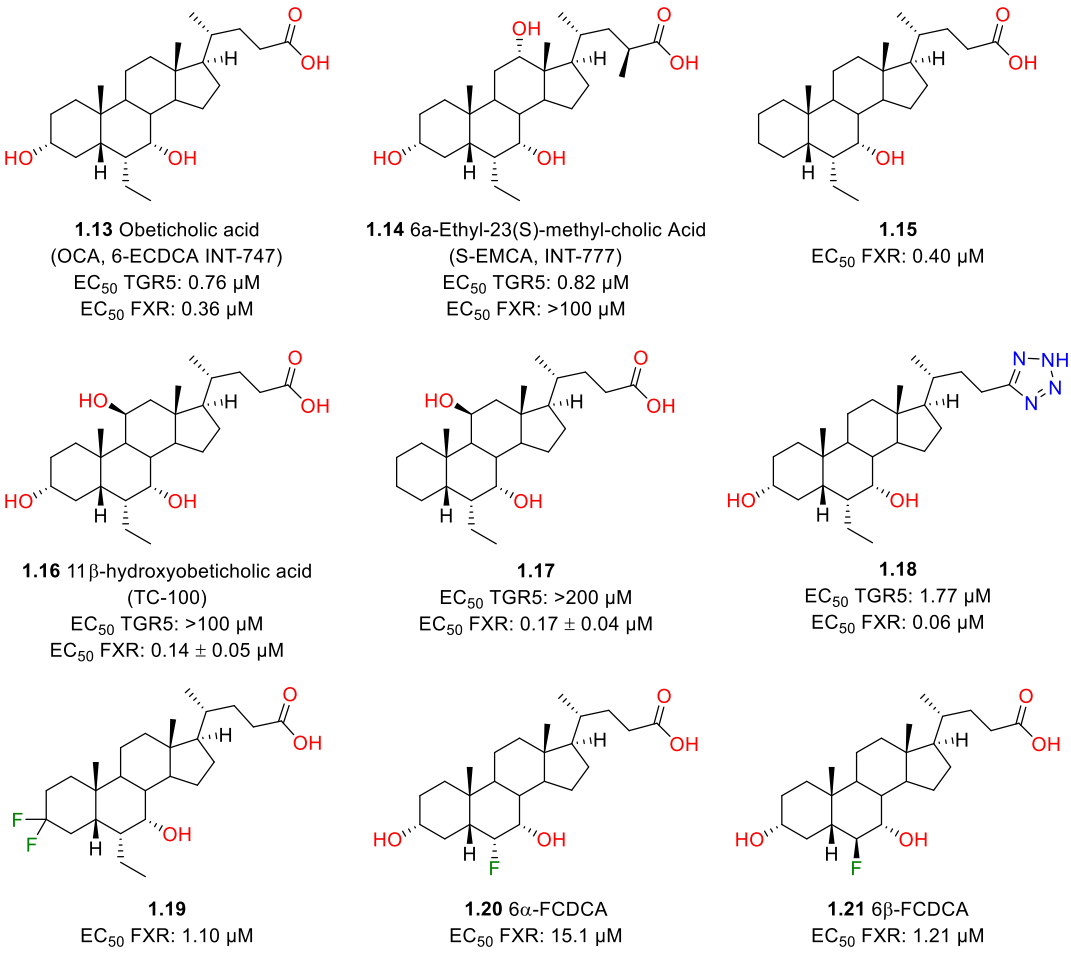

Figure 1.5 - Semi-Synthetic Bile Acids as FXR and TGR5 Agonists[31,35,54-57]

Further research into substituents at the 6α-position of bile acids showed that polar and hydrogen-bonding groups in the 6α-position were not always beneficial, due to the presence of a hydrophobic cavity that the 6α-ethyl group of OCA lies in.[54,57] Moreover, research into CDCA, OCA and their derivatives has found that the 3α-hydroxy of OCA has a low influence on FXR activity – 3-deoxy OCA (**1.15**, *Figure 1.5*) has a comparable FXR EC_{50} to OCA.[54] Conversely, the 7α-hydroxy of OCA is integral for affinity to FXR as it forms hydrogen bonds with the amino acid residues Tyr-366 and Ser-329 of the FXR binding pocket.[54]

Whilst OCA has been shown to be an effective drug, it has two significant side effects: increased levels of LDL-C, known to be the "bad" form of cholesterol; and pruritus (severe skin itching), reported to be caused by activation of TGR5 by OCA.[54] OCA has set a benchmark in terms of activity of bile acid FXR agonists, but there is clear room for improvement in terms of selectivity of FXR over TGR5 to reduce side effects. Selectivity towards TGR5 has been achieved by Pelliciari *et al. via* addition of a 6α-ethyl group and a 23*S*-methyl (α-to the carboxylic acid moiety) to cholic acid, giving INT-777 (S-EMCA, **1.14**, *Figure 1.5*).[35,56] Additionally, Pelliciari *et al.* showed that 11β-hydroxy derivatives of OCA (**1.16** and **1.17**, *Figure 1.5*) were highly selective to FXR, with minimal agonistic activity towards TGR5.[55]

Extensive research has also been carried out to modify the bile acid side chain in the synthesis of FXR and TGR5 agonists. One key agonist with modification of the side chain is the tetrazole OCA derivative **1.18** (*Figure 1.5*), which, on substitution of the carboxylic acid for a tetrazole, saw a significant increase in FXR agonism and a decrease in TGR5 activity compared to OCA.[54] Interestingly, a small number of fluorinated analogues of CDCA and OCA have also been synthesised and tested in assays for FXR agonism. A 3,3-difluoro OCA derivative, **1.19** (*Figure 1.5*), had a lower FXR potency than OCA (EC_{50} = 1.10 μM), but was significantly higher than that of CDCA.[54] The 6α-fluoro and 6β-fluoro CDCA analogues **1.20** and **1.21** (*Figure 1.5*) also had lower efficacies than OCA, but the 6β-fluoro analogue **1.21** had a higher FXR potency than CDCA.[57]

When discussing bile acid agonists of FXR, it is important to note the efficacious, non-bile acid agonists that have been developed. The first key synthetic FXR agonist was GW4064 (**1.22**, *Figure 1.6*), which had nanomolar potency on FXR, higher than any natural or semi-synthetic bile acid.[30] Similarly, Fexaramine (**1.22**, *Figure 1.6*) had high, nanomolar potency on FXR.[58]

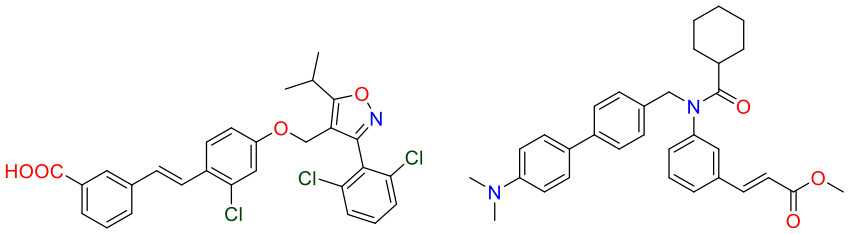

1.22 GW4064
EC_{50} FXR: 15 ± 1 nM

1.23 Fexaramine
EC_{50} FXR: 25 nM

Figure 1.6 - Synthetic FXR/TGR5 Agonists[30,58-61]

1.2.5 The Roles of Bile Acids in Neurodegenerative Diseases and Cancer

1.2.5.1 The Effects of Bile Acids on Apoptosis

Apoptosis plays a key role in neurodegenerative diseases and, as mentioned previously, in the progression and treatment of cancer. It is key in normal cells to maintain cell population, and is a defence mechanism for cells against diseases, chemical agents and anything else that could cause damage to them.[62] Notably, p53, the tumour suppressor protein, is intrinsic in apoptosis as when it is activated, it can cause cell cycle arrest or directly induce apoptosis.[2]

Extensive research has been carried out on the roles naturally occurring bile acids (and their taurine and glycine conjugates) play in apoptosis. Hydrophobic bile acids such as DCA and CDCA are known to induce apoptosis[63] through: an extrinsic pathway *via* activation of death receptors; an intrinsic pathway *via* intracellular stress (causing mitochondrial dysfunction and consequential release of pro-apoptotic factors); and by causing endoplasmic reticulum (ER) stress (inducing apoptotic

signalling).[64] Importantly, cholic acid is not pro-apoptotic – even at high concentrations – and has been shown to not have any obvious effect on cells.[65] UDCA and its taurine conjugate, TUDCA (**1.24**, *Figure 1.7*), are inhibitors of apoptosis though. They modulate apoptosis at several levels and are anti-apoptotic in hepatocytes and non-liver cells,[2,66] interfering with the mitochondrial pathway of cell death.[2,66,67] Through prevention of apoptosis, TUDCA has cytoprotective properties[67] – it can counteract and protect against the hepatotoxicity of other, more hydrophobic bile acids.[68]

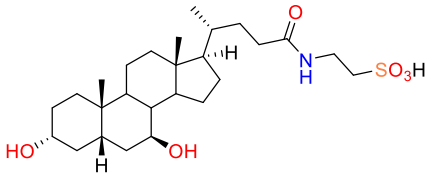

1.24 Tauroursodeoxycholic acid (TUDCA)

Figure 1.7 - TUDCA

1.2.5.2 Bile Acids in Neurodegenerative Diseases

As discussed in **Section 1.1.1**, the function/dysfunction of mitochondria is intrinsic in neurodegenerative diseases. Mitochondria are known to have a prominent role in apoptosis, mediated partly through the release of pro-apoptotic molecules and the permeabilisation of the mitochondrial membrane.[69] The dysfunction of mitochondria has been shown to cause cell death pathways (including apoptosis) to occur in Parkinson's disease and generally, defects in the physiological pathways of apoptosis contribute to neurodegenerative diseases.[3]

In vitro studies have revealed that UDCA and TUDCA inhibit apoptosis in neuronal cells in part by interfering with the mitochondrial pathway of cell death.[2,70] The inhibition of apoptosis allows UDCA and TUDCA to possess a neuroprotective effect in PD, specifically on the human dopaminergic cell line and against inhibitors of mitochondrial complex I. These inhibitors cause changes in mitochondria, inducing apoptosis and degradation of dopaminergic neurons.[3,71] Notably, TUDCA was observed to reduce the loss of dopaminergic neurons in mouse models.[72] Furthermore, oxidative cell stress, an important factor in the pathogenesis of PD, was reduced by UDCA and TUDCA by decreasing the formation of reactive oxygen species (ROS) and maintaining the levels of the antioxidant glutathione (GSH).[3] UDCA is also neuroprotective in both Alzheimer's and Huntingdon's disease,[3,73-76] and also on neuronal cell death caused by cancer chemotherapy, in part by suppressing pro-apoptotic p53.[3,77]

Regarding mitochondria in PD neuronal cells, UDCA and TUDCA can stabilise and preserve mitochondrial membranes,[3,71] maintain energy production[71] and inhibit the loss of mitochondrial membrane potential (MMP), which is important in mitochondrial function.[78] They were also observed experimentally to improve the function of mitochondria in LRRK2 (PARK8) mutant cells.[73]

Mitochondrial stabilisation by TUDCA was also observed in studies for Alzheimer's and Huntingdon's disease, leading to a reduction in neuronal apoptosis.[2,3,70,79] In Huntingdon's rats, UDCA and TUDCA decreased apoptotic cell death in part by decreasing the disruption of the outer membrane of mitochondria.[72] Additionally, in an AD mouse model, TUDCA reduced amyloid-β toxicity by limiting its production and accumulation, leading to a reduction in Aβ deposition.[79] TUDCA can also reduce neuronal apoptosis induced by Aβ by promoting mitochondrial membrane stability and inhibiting mitochondrial membrane permeabilisation.[2,3,70]

Due to the mechanisms of pathogenesis of PD, the rescue of dysfunctional mitochondria is likely to have a strong beneficial effect on Parkinson's brain tissue. A recent study, involving the screening of 2000 compounds for their rescue effect on mitochondria in PD mutant cells, identified the notable rescue effects of UDCA and 5β-cholanic acid (also known as Ursocholanic acid or UCA, **1.25**, *Figure 1.8*) a naturally occurring, deoxygenated bile acid. 5β-cholanic acid and UDCA rescued mitochondrial function in both LRRK2^{G2019S} and PARK2 mutant fibroblasts and completely rescued cellular ATP levels on treatment of LRRK2^{G2019S} mutant fibroblasts. 5β-cholanic acid also rescued and increased the activity of all four respiratory chain complexes of the mitochondrial respiratory chain by 200-500%. The rescue effect by UDCA and cholanic acid was described to potentially be mediated through activation of the glucocorticoid receptor, and suggested a class effect of bile acids and steroids in the rescue of mitochondrial dysfunction.[80] Another study confirmed the rescue effect of UDCA on LRRK2^{G2019S} PD mitochondria, as well as improvement of mitochondrial function by UDCA.[73]

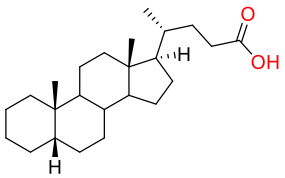

1.25 5β-Cholanic Acid
(Ursocholanic Acid, UCA)

Figure 1.8 - 5β-Cholanic Acid

Finally, it is important to note that in order for bile acids to work as drugs in neurodegenerative diseases, crossing of the blood-brain-barrier (BBB) and penetration of the cerebral spinal fluid (CSF) is imperative. Studies have shown that TUDCA can do both, and can be effectively delivered to the brain.[2,73,81]

1.2.5.3 Bile Acids in Cancer

Naturally occurring bile acids exhibit both positive and negative biological effects with regard to cancer (in general). Whilst the apoptosis-inhibiting bile acid UDCA has been shown to be chemopreventitive of carcinogenesis in the colon,[65,82] DCA and CDCA have been identified as

tumour promoters.[65,83-85] Contrastingly, cholic acid lacks tumour promoting and chemopreventitive activities.[65] In the breast cancer cell lines MCF-7 and MDA-MB-231, LCA exhibits anti-proliferative and pro-apoptotic effects, with an increase in the expression of p53.[86]

As well as having a direct effect on cancerous cells, bile acids have been utilised alongside common chemotherapy agents. Recent research has revealed that CDCA and DCA can reduce tumour resistance to conventional cancer therapies and decrease cancer cell adhesion, impacting the ability for the cells to migrate and invade, therefore mediating cancer progression.[87] Furthermore, the glycine conjugate of CA, glycocholic acid (GCA), has been shown to increase the cytotoxicity of the chemotherapy agent epirubicin in multi-drug resistant (MDR) cancer cells.[88] Other bile acid conjugates such as taurolithocholic acid (TLCA), taurochenodeoxycholic acid (TCDCA) and glycochenodeoxycholic acid (GCDCA) can inhibit drug transport function in MDR cell lines, which also leads to an increase in the cytotoxicity of cancer chemotherapy agents.[89]

A number of steroid derivatives are currently available as drugs on the global market and have been used to treat cancer for many years.[90] With this precedent and the knowledge of the effects of naturally occurring bile acids in cancer, investigation into natural and semi-synthetic bile acids as cancer chemotherapy agents has been extensive. OCA (**1.13**, *Figure 1.5*) has been shown to inhibit the growth of liver cancer cells, with IC_{50}[vii,91] values of 1.07 µM, 1.04 µM and 0.71 µM against the HepG2, Huh7 and SNU-449 cancer cell lines respectively. *Figure 1.9* shows some other semi-synthetic bile acids synthesised in the literature and investigated for their potential use in the treatment of cancer.

When synthesising bile acid analogues, conjugation of the carboxylic acid at C24 to a variety of amines, amino acids, sulfonamides etc. is a relatively straightforward method to produce a library of compounds for biological testing. The cholic acid amide analogue **1.26** (*Figure 1.9*) displayed inhibition of cell growth on the breast cancer cell line MDA-MB-231. With a GI_{50}[viii,92] value of 1.35 µM, the potency was comparable to the chemotherapy agents Doxorubicin and Cis-Platin.[93] As cholic acid has previously been shown not to be cytotoxic towards cell lines, the conjugation to the amino acid aromatic amide is likely to have induced the cytotoxic effect of **1.26**. The thiazole amide LCA derivative **1.27** (*Figure 1.9*) was cytotoxic towards various breast cancer cell lines with IC_{50} values around 7 µM, comparable to those of the established breast cancer drug Tamoxifen.[94]

[vii] IC_{50} – the half-maximum inhibitory concentration of a drug.
[viii] GI_{50} – the concentration of a drug that inhibits cell growth by 50%.

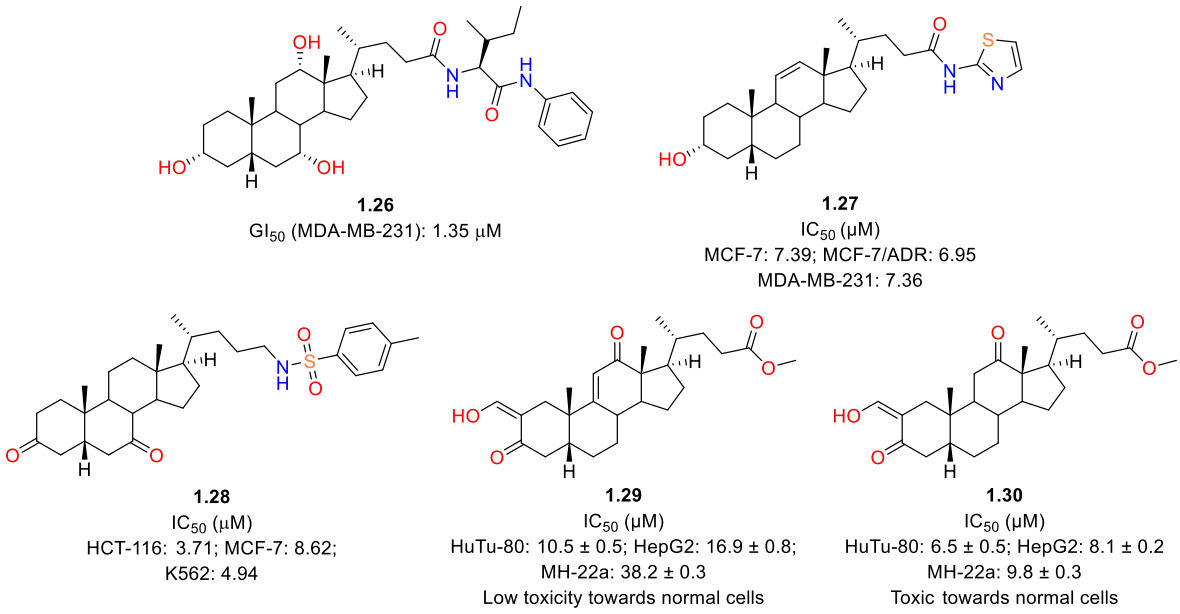

Figure 1.9 - Semi-Synthetic Bile Acid Derivatives as Potential Cancer Drugs[93-96]

Modification of the A-, B- and C-rings of bile acids is also common in the synthesis of potential bile acid-based drugs. Specifically, interest in keto-bile acid derivatives has developed in recent years. The sulfonamide 3,7-diketone bile acid **1.28** (*Figure 1.9*) exhibited anti-tumour activity against HCT-116 (colon), MCF-7 (breast) and K562 (leukaemia) cancer cell lines. With IC_{50} values between 3.71 µM and 8.62 µM, **1.28** showed comparable activity to 5-Fluorouracil.[95] Two diketone DCA derivatives, **1.29** and **1.30** (*Figure 1.9*) displayed cytotoxicity towards HuTu-80 (duodenal), HepG2 (liver) and MH-22a (murine liver) cancer cells, with IC_{50} values in the range of 6.5 to 38.2 µM. Interestingly, the 9,11-alkene analogue **1.29** had low toxicity towards normal cells whilst **1.30**, with full saturation of the C-ring, was cytotoxic towards normal cells.[96]

1.3 Organofluorine Chemistry

Organofluorine compounds are prevalent throughout the chemical industry, appearing in around 25% of pharmaceuticals on the market as well as in important agrochemicals, polymers, organic materials and refrigerants.[97-99] In this section, key aspects of the C-F bond, the effect it has on molecules and the C-F bond's use in drug molecules will be reviewed and discussed.

1.3.1 The C-F Bond and the Effects of the C-F Bond on Conformation and Acidity/Basicity

When bound to carbon, fluorine forms one of the strongest bonds known in organic chemistry with a bond dissociation energy of 105.4 kcal mol^{-1} and a short C-F bond length of 1.35 Å. Generally, the C-F bond strength increases with increasing fluorine substitution, with a strength of 109.6 kcal mol^{-1} for CH_2F_2, 114.6 kcal mol^{-1} for CHF_3 and 116.0 kcal mol^{-1} for CF_4. Due to the high electronegativity of the fluorine atom (4.0 on the Pauling scale), the C-F bond is highly polarised and is more ionic in character than covalent: the fluorine atom bears a partial negative charge (δ^-) and the carbon atom a partial positive charge (δ^+), which are highly attracted to each other.[97,100] The high strength of the C-F bond can give fluorinated organic compounds higher thermal and chemical stability compared to their non-fluorinated counterparts, one example being in fluorinated polymers such as PTFE, which are used in harsh (high temperature and pressure) operating conditions.[98]

Because of its high nuclear charge, fluorine's three lone pairs are held tightly and its Van der Waals radius is one of the smallest in the periodic table (1.47 Å).[97,100] Typically, a fluoride ion is a poor leaving group due to the strength of its bond to carbon, but is known to be a useful leaving group in nucleophilic aromatic substitution reactions (S_NAr), and can be eliminated in highly basic conditions in aliphatic molecules *via* an E1cB mechanism.[97]

The large dipole moment of the C-F bond can affect the conformation of organofluorine compounds. It does so *via*: dipole alignment (the strengths of which define the equilibrium of the conformers);[97,100] dipole-dipole interactions (attractive or repulsive);[97,100,101] interaction with formal charges;[97,102] or hyperconjugation effects – specifically the fluorine *gauche* effect.[100,101] Some of the most prevalent dipole-dipole interactions involving the C-F bond are the interactions of fluorinated drugs with proteins,[97] a topic which will be discussed further in **Section 1.3.4**.

Fluorine's substantial electronegativity can also affect the pK_a of neighbouring functional groups (FGs) when introduced into a molecule. When fluorinating β- or γ- to a carboxylic acid, a decrease in pK_a (and hence an increase in acidity) is observed with an increase in fluorine substitution. The inductive effect of fluorine is responsible for the increase in acidity due to its stabilisation of the

carboxylate anion on deprotonation.[103] A decrease in pK_{aH}[ix] (and hence a decrease in basicity) is observed with β-, γ- and δ- fluorination of amines, decreasing further with a higher fluorine substitution count. Modulation of the pK_{aH} of an amino group with fluorine substitution is of high interest in medicinal chemistry as the changes are associated with the alteration of a molecule's properties, including log*P*/*D*, potency, ability to penetrate the CNS and ADMET (absorption, distribution, metabolism, excretion and toxicity).[103,104]

1.3.2 C-F Hydrogen Bonding and the Effects of Fluorine on Hydrogen Bonding

1.3.2.1 C-F Hydrogen Bonds

The topic of C-F•••H-X hydrogen bonds (HBs) has been extensively discussed, with some reports stating that they are not true hydrogen bonds and that they are instead electrostatic or polar interactions.[105] More recent studies though have shown evidence for the existence of intramolecular and intermolecular C-F•••H-X HBs in a number of different systems, and are unambiguously observed in structures lacking other heteroatoms to act as hydrogen bond acceptors.[102]

With three lone pairs, fluorine is able to participate in hydrogen bonding as a hydrogen bond acceptor (HBA), but as the lone pairs are tightly held, organofluorines only form weak HBs at around 25% of the strength of a typical hydrogen bond, with typical C-F•••H-X contacts between 2.5 and 3.0 Å.[97] Generally, monofluorinated compounds are better HBAs than difluorinated, which are better than trifluorinated compounds.[106,107] One of the defining factors of a C-F•••H-X HB is that the NMR of the structures containing the hydrogen bonds must show deshielding of the proton along with coupling constants with the hydrogen-bonded fluorine.[106]

Despite their weaker strength than normal HBs, the presence of C-F•••H-X intramolecular hydrogen bonds can alter the conformation of a flexible molecule. Research from within the Linclau group has revealed the presence of O-H•••F-C intramolecular hydrogen bonds (IMHBs) which influence the conformational profile of acyclic γ-fluorohydrins, two of which, **1.31** and **1.32**, are shown in *Figure 1.10*. For both **1.31** and **1.32**, the conformers with the highest (computationally calculated) populations contained O-H•••F-C intramolecular hydrogen bonds, indicating that the IMHB increased the stability of the conformer. Significantly, the IMHB of **1.31** had a short distance of 2.0 Å, below the sum of the Van der Waals radii.[108]

[ix] pK_{aH} – The acidity constant of the conjugate acid of a base.

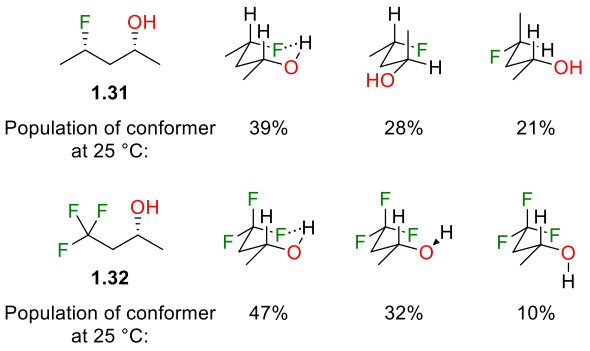

Figure 1.10 - Populations of Conformers of Selected Fluorohydrins[108]

Strong C-F•••H-X intramolecular hydrogen bonds have been observed in molecular systems with a hydrogen bond donor (HBD) close in space to a fluorine atom. Three examples of such systems are shown in *Figure 1.11*, with varying strengths of IMHBs, indicated by $^{h1}J_{H\text{-}F}$ coupling constants from NMR spectral analysis. Both the cyclophane **1.33** and the fluorobenzamide **1.34** (*Figure 1.11*) had moderate strength IMHBs as shown by their relatively low $^{h1}J_{H\text{-}F}$ coupling constants, 6.0 Hz and 11.5 Hz respectively.[106,109] The cage compound **1.35** (*Figure 1.11*) though was shown to have a strong IMHB, with a very large $^{h1}J_{H\text{-}F}$ = 68 Hz coupling constant observed by NMR spectral analysis.[110]

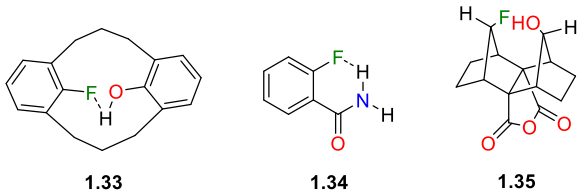

Figure 1.11 - Compounds Containing an IMHB

1.3.2.2 The Effect of Fluorination on Hydrogen Bond Donating Capacity

Past research into the effects of a proximal fluorine on the pK_a and hydrogen bond donating capacity of alcohols has led to the belief that "*fluorination always increases hydrogen bond acidity*".[102,111] More recent studies though have shown that this is not always the case. An investigation of the hydrogen bond donating capacity of eight cyclic, conformationally restricted fluorohydrins was performed recently by the Linclau group, who utilised FTIR spectroscopy to determine alcohol hydrogen bond acidity. In a dilute CCl_4 solution, the decrease in absorbance of the free ν_{OH} stretching band of the alcohols on complexation with *N*-methylpyrolidinone (NMP) was measured and compared to the new OH•••NMP stretching band to determine the pK_{AHY}[x] values.[111]

[x] pK_{AHY} = -log$_{10}K_{AHY}$ = +log$_{10}K$, where K is the thermodynamic equilibrium constant of alcohol complexation with NMP, a measure of hydrogen bond donating capacity.

For the fluorohydrins **1.36** and **1.41** (*Figure 1.12*), an expected increase in pK_{AHY} was observed compared to the parent compounds **1.38** and **1.43** (*Figure 1.12*), as a result of the inductive effect of fluorine. An unexpected decrease in pK_{AHY} was observed though for the other four monofluorinated alcohols, especially so for the 1,3-diaxial fluorohydrin **1.40** (*Figure 1.12*), which displayed almost no ability to act as a hydrogen bond donor. The very low pK_{AHY} value for **1.40** was explained by the presence of an intramolecular O-H•••F-C hydrogen bond (*Figure 1.13*), with a calculated F•••H bond distance of 2.033 Å and a $J_{F\text{-}HO} \approx 12$ Hz coupling constant observed by NMR spectral analysis.[111] For the fluorohydrins **1.39**, **1.44** and **1.45** (*Figure 1.12*), the lower pK_{AHY} values were also attributed to intramolecular C-F•••H-O interactions, but were believed to be weaker hydrogen bonds comparatively.

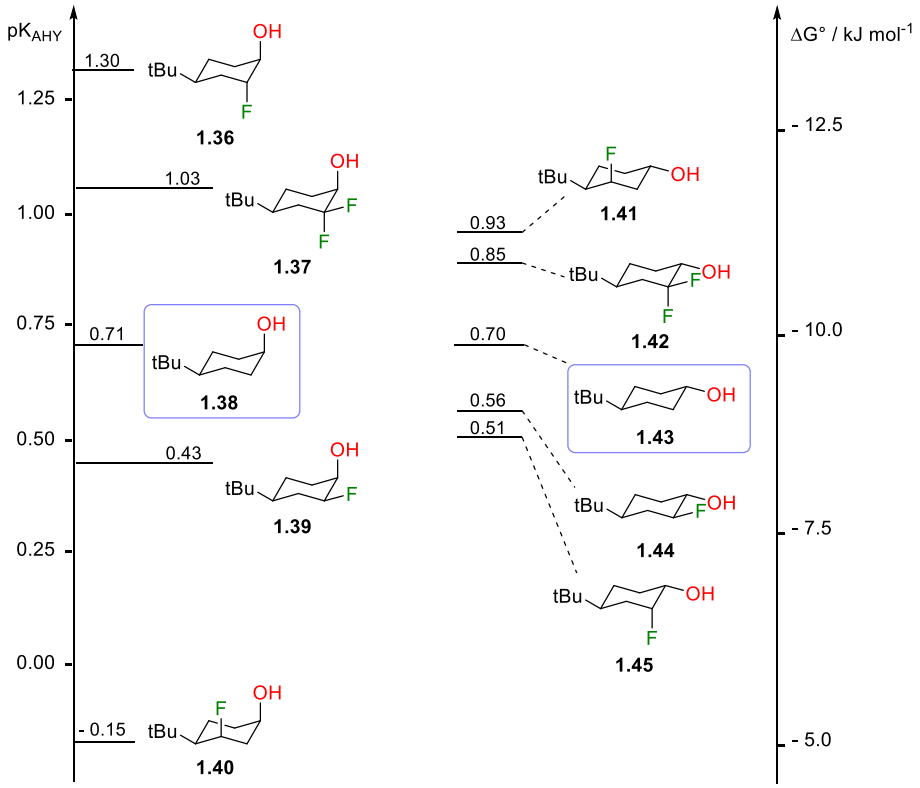

Figure 1.12 - Effect of Fluorination on pK_{AHY} of Cyclic Fluorohydrins, adapted from Ref.[111]

Regarding the difluorinated alcohols **1.37** and **1.42** (*Figure 1.12*), an increase in pK_{AHY} was observed compared to the parent compounds, but unexpectedly, the values were lower than the monofluorinated alcohols **1.36** and **1.41**, despite the larger electron withdrawing effect from two fluorines. This is believed to be due to C-F•••H-O electrostatic interactions (*Figure 1.13*).[111]

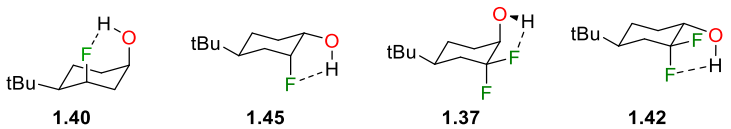

*Figure 1.13 - C-F•••H-O Interactions of **1.40**, **1.45**, **1.37** and **1.42***

1.3.3 The Effect of Fluorination on Lipophilicity

Lipophilicity, expressed as log*P* (the partition coefficient of a compound between octanol or another hydrophobic solvent and water) or log*D* (the distribution coefficient of an ionisable compound at a given pH), is key in the design of effective drug molecules.[112,113] Many drugs are absorbed in the body by passive transport into cells, meaning that the lipophilicity of a drug is key to absorption.[113] Not only does lipophilicity have a vital role in the ADMET properties of a drug, control of log*P*/*D* can also improve the therapeutic success rate and improve the binding affinity of a drug to target proteins.[105,112]

To reduce issues with poor aqueous solubility, high toxicity and low absorption of a drug, a log*P* of less than 5 is required, as stated by Lipinski's rule of five (RO5).[105,113,114] The ability to maintain a low log*P*/*D* while increasing molecular weight is important in the success of a new drug. One method to modulate lipophilicity without introducing heteroatoms like oxygen and nitrogen is by introduction of fluorine.[115] Following a statistical analysis of fluorine substitution of one hydrogen atom on lipophilicity, a generalised statement said, "substitution of a hydrogen atom by fluorine increases lipophilicity…by roughly 0.25 log*P* units", though on analysis of the graph obtained in the study (*Figure 1.14*) there were a significant number of cases in which fluorination decreased the log*D* of a molecule.[105] As the study included a large number of aromatic substrates, in which fluorination is known to increase lipophilicity, it had a heavy bias towards a positive log*D* change overall.[102,116]

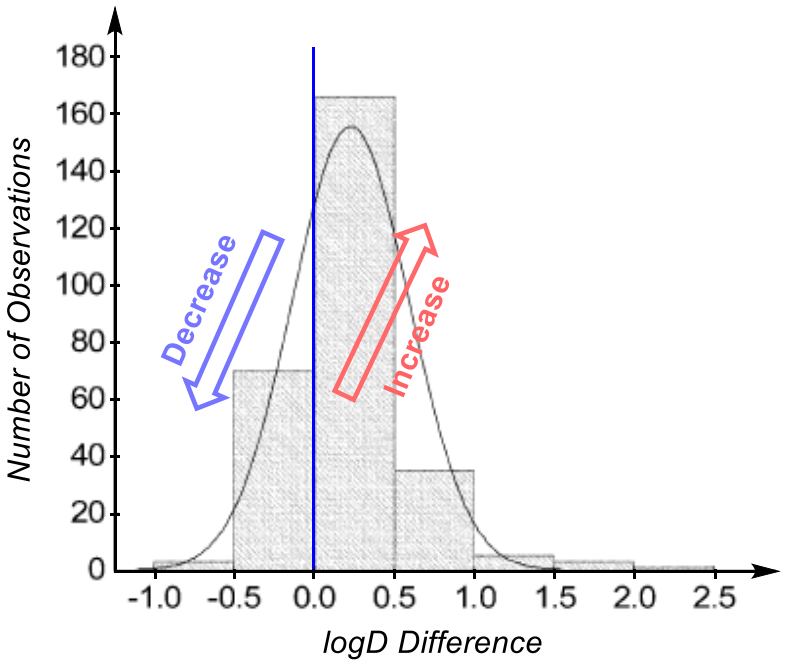

Figure 1.14 - Effect on Lipophilicity of a Molecule on Substitution of a Hydrogen Atom with a Fluorine Atom. Adapted from Ref[105]

The effect of fluorination on the overall lipophilicity of a molecule depends on which of the two opposing effects of fluorination dominates: either an increase in the hydrophobic surface of the molecule, as a result of the larger size of fluorine compared to a hydrogen atom and the non-polarizability of fluorine in polyfluorinated molecules, or an increase in polarity due to fluorine's high electronegativity. For polar compounds, fluorination tends to increase the lipophilicity due to changes in the molecule's hydrophobic surface area and conversely, fluorination of highly apolar compounds tends to decrease the lipophilicity of the molecule due to polar effects.[117]

For alkanes, a significant decrease in lipophilicity upon substitution of hydrogen for fluorine has been observed for both ethane and pentane,[102] explained simply by introduction of polarity arising from the strong inductive effect of fluorine.[113] Studies by Carreira and Müller on fluorinated *n*-propyl chains of benzene have also shown significant decreases in lipophilicity, regardless of the degree of fluorination of the chain.[117] Further investigations into the polarity of fluorinated methyl groups by Carreira and Müller, with analysis of molecular dipole moments, revealed a general polarity trend of: $CH_3 < CF_3 << CH_2F \approx CHF_2$, although the trend was not consistent for some short-chain fluoroalkanes.[117] On investigation of fluorinated *n*-propylindoles, they found that the polarity trend was followed, as exemplified by the corresponding log*P* values of the fluorinated compounds (*Figure 1.15*). In further studies, Carreira and Müller found that *vic*-difluorination of the *n*-propyl chain led to a much larger decrease in lipophilicity (and hence log*P*) than *gem*-difluorination, compared to the non-fluorinated parent compound (Δ = -0.8 vs Δ = -0.5, *Figure 1.15*). This observation was attributed to the much larger dipole moment that a *vic*-difluoro compound possesses compared to the corresponding *gem*-difluoro compound, established by vector analysis of the two moieties.[118]

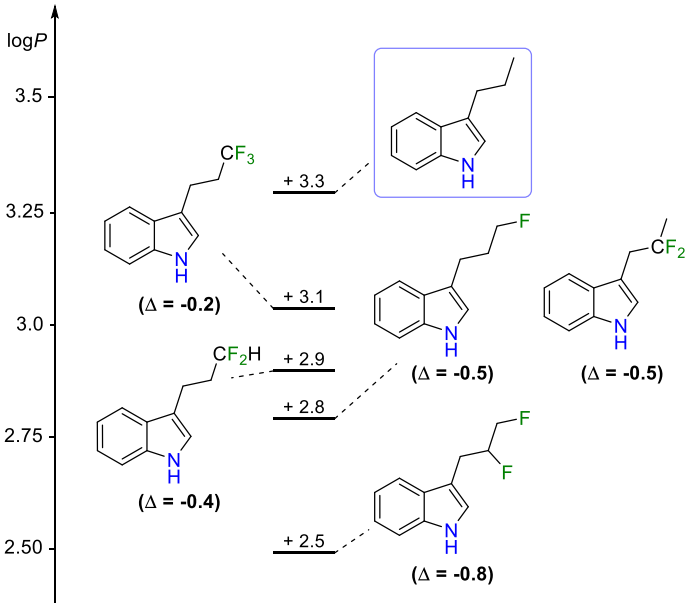

Figure 1.15 - LogP of Indoles with Fluorinated n-Propyl Chains[117,118]

The effect of fluorination on compounds with other functional groups though is not as straight-forward. When introducing a CF_3 group β- to a hydroxy or an amine group, an increase in lipophilicity is observed due to the opposing bond dipoles of C-F and C-O/C-N (*Figure 1.16*). Additionally, the CF_3 group has a strong inductive effect which reduces the nucleophilicity, basicity and polarizability of the neighbouring lone pairs, and hence, increases lipophilicity.[119] Regarding amines, the reduction in basicity leads to a higher ratio of neutral to charged molecules present at pH 7.4, hence leading to a higher value of log*D*.[105,116,120] The strong effect of β-trifluorination is exemplified when comparing the log*P* of trifluoroethanol to its parent compound, ethanol (*Figure 1.16*).[102]

A recent study from within the Linclau group on the lipophilicity of a range of fluorinated alkanols revealed further significant observations on the effect of fluorination on the lipophilicity. Selected alkanols from the ethanol, 1-propanol and 1-pentanol series investigated are shown in *Figure 1.16*.

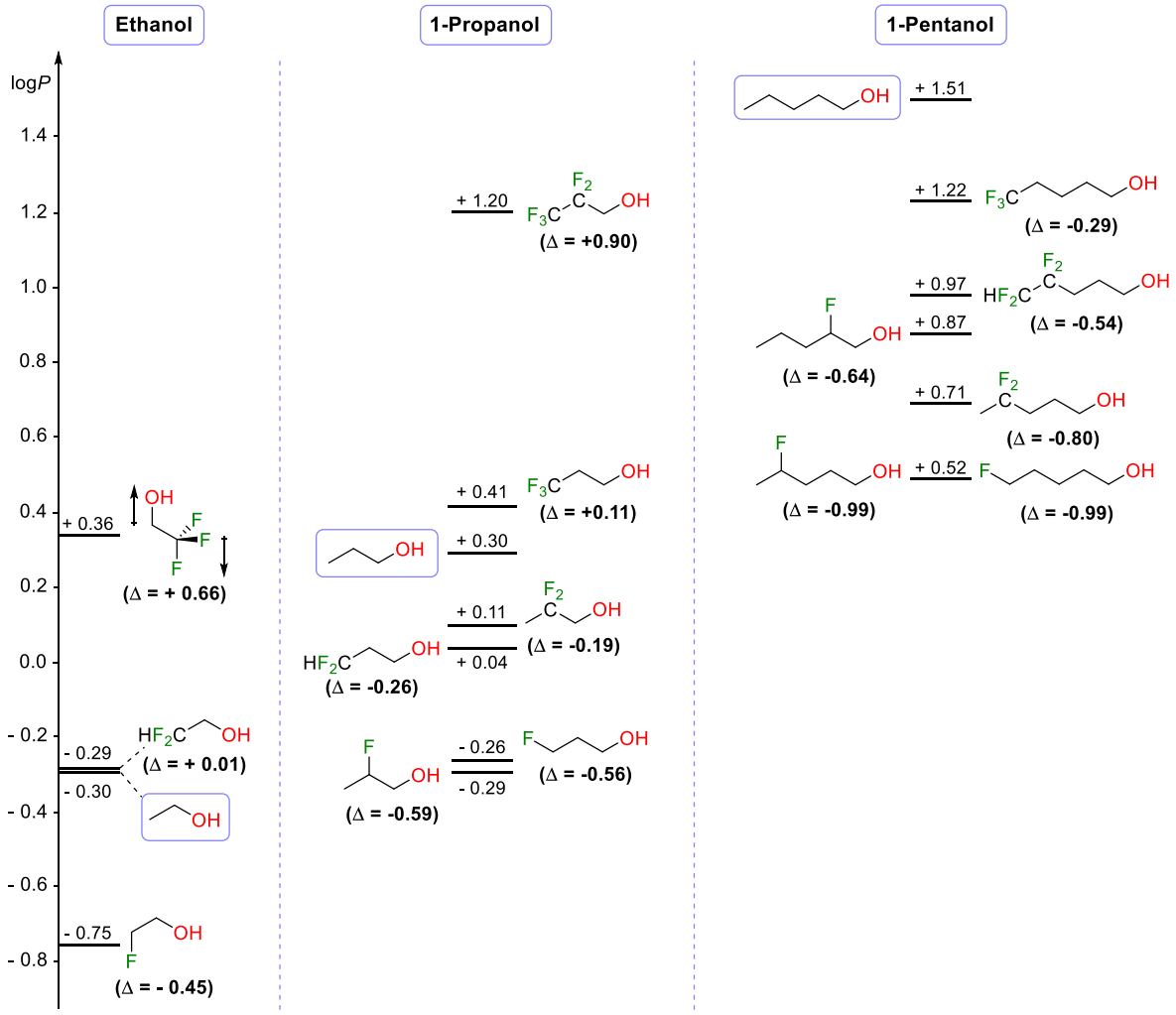

Figure 1.16 - LogP of Selected Fluorinated Alkanols[115]

Firstly, penta-, hexa- and heptafluorination caused an increase in lipophilicity compared to the non-fluorinated parent compound, as is known.[113] Additionally, pentafluorinated alkanols were also

always found to be more lipophilic than the tetrafluorinated alkanols. Whilst trifluorination caused an increase in lipophilicity for ethanol and propanol (*Figure 1.16*), for pentanol, trifluorination caused a significant decrease in log*P* (Δ = - 0.29, *Figure 1.16*), likely due to the domination of polar effects on an apolar molecule. Trifluorinated alkanols always had a higher log*P* than the *gem*-difluorinated compounds (*Figure 1.16*). Except for ethanol, *gem*-difluorination of alkanols, regardless of the position of fluorination, decreased log*P* compared to the parent compound and all *gem*-difluoro compounds were more lipophilic than the monofluorinated alkanols. Finally, monofluorination of the flexible chain alkanols always led to a decrease in lipophilicity, regardless of the proximity of the fluorine to the alcohol (*Figure 1.16*).[115]

The study also included the measurement of log*P* of four of the conformationally restricted alkanols from the hydrogen bonding study previously mentioned in **Section 1.3.2.2** (*Figure 1.12*).

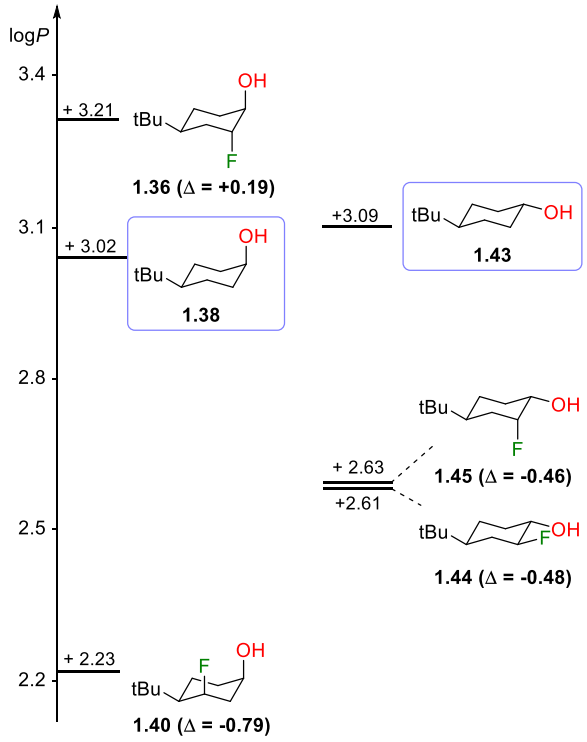

Figure 1.17 - LogP of Conformationally Restricted Fluorohydrins. Adapted from Ref.[115]

An increase in lipophilicity was observed for the 1,2-diaxial fluorohydrin **1.36** (*Figure 1.17*) compared to the non-fluorinated alcohol **1.38** (Δ = + 0.19, *Figure 1.17*), a rare observation of an increase in log*P* upon aliphatic monofluorination. This was attributed to the opposing C-F and C-O dipoles, leading to a decrease in the polarity of the molecule compared to **1.38**. Conversely, the 1,3-diaxial fluorohydrin **1.40** (*Figure 1.17*) displayed a significantly large decrease in log*P* compared to **1.38**, due to the aligned C-F and C-O dipoles. A decrease in lipophilicity was also observed for the equatorial alcohols **1.44** and **1.45** (*Figure 1.17*) compared to the parent compound **1.43**, with very

similar log*P* values obtained regardless of the stereochemistry of the fluorine at the 2-position.[115] This is expected as both **1.44** and **1.45** have the same dihedral angle.

1.3.4 Fluorine in Drug Molecules

Fluorine is prevalent in medicinal chemistry and the use of fluorine in pharmaceuticals is growing. As previously mentioned, around 25% of current pharmaceuticals contain fluorine, which is a substantial increase on the figure from the 1970s of around 2%.[121] The large number of current drugs containing fluorine is somewhat surprising as natural products containing fluorine are very uncommon – only six discrete products have been identified, the majority of which are highly toxic.[122]

Fluorine has a number of attractive properties in drug design, including influence on molecular conformation and modulation of hydrogen bond acidity, pK_a and log*P*/*D*, as previously mentioned. The properties of the fluorine atom and the C-F bond also allow it to act as a bioisostere[xi,123] for a number of moieties. Although fluorine is around 20% larger than hydrogen based on Van der Waals (VdW) radii (1.47 Å and 1.20 Å respectively), it has been shown in a large number of cases to be an effective bioisostere for a hydrogen atom. Its success in this role is owing to a fluorine atom being the most sterically conservative substitution for a hydrogen.[97,124] A C-F or CF_2 can also act as a bioisostere for hydroxyl groups, ketones, amines, nitriles and sulfonyl functionalities.[124] A replacement of C=O for C-F is especially effective as the C-F bond is close in length to that of the carbonyl (1.35 Å and 1.23 Å respectively) and the bonds have comparable dipoles.[124] Replacement of a hydroxyl group for a fluorine atom is also common despite the shorter length of the C-F bond compared to that of the C-OH bond. Both the VdW radius and the electronegativity of fluorine are the most similar to oxygen out of all other bioisosteric atom replacements, and loss of a hydrogen bond donor upon substitution allows exploration of the role of C-OH hydrogen bonds in biological environments.[97,124] One of the rationales of the bioisosteric replacement of atoms or groups with fluorine is that it has the ability to slow down or block oxidative metabolism of drug molecules by cytochrome P450 enzymes, therefore increasing the biological half-life of pharmaceuticals.[105,113]

In addition to reducing metabolism, other roles of fluorine in drug molecules include acting as a leaving group to form covalent bonds between drug molecules and proteins/enzymes ("suicide inhibitors"),[125] and improving interactions between drug molecules and the target proteins/enzymes. Interactions can be improved by modulating conformation, pK_a and log*P*/*D* as

[xi] Bioisosteres are substituents or moieties with similar chemical and physical properties which have similar biological properties. They allow improvement in the properties of drugs whilst retaining biological activity.

discussed previously, or by the introduction of charge-dipole or dipole-dipole interactions of fluorine within the active site of proteins or enzymes. The dipole of the C-F bond can interact with acidic protons and carbonyl groups, adopting a "*Burgi-Dunitz type trajectory*"[97] for amide carbonyls in the backbone of peptides in active sites. These interactions have been experimentally observed to increase ligand binding affinities.[103,124,126]

The earliest fluorinated drug molecules date back to the 1950s, which saw the synthesis of the cancer drug 5-Fluorouracil (5-FU, **1.46**, *Figure 1.18*) and the anti-inflammatory drug Fludrocortisone (**1.47**, *Figure 1.18*).[127,128] Substitution of the 9α-hydrogen of Hydrocortisone for a fluorine gave Fludrocortisone a biological activity 10 times that of Hydrocortisone. Some of the historically highest grossing drugs contain fluorine, including the anti-depressant Prozac (**1.48**, *Figure 1.18*), the statin Lipitor (**1.49**, *Figure 1.18*) and the acid reflux drug Lansoprazole (**1.50**, *Figure 1.18*).[129]

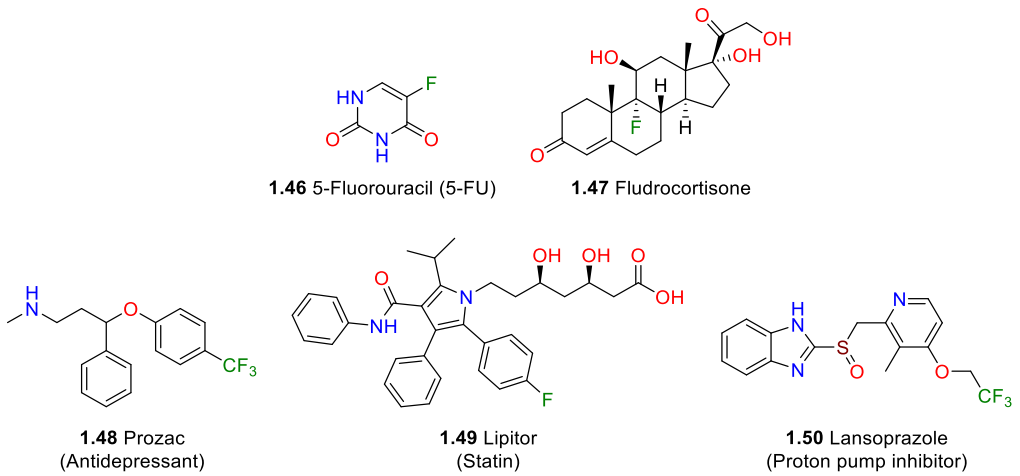

Figure 1.18 - Fluorine Containing Drugs[129]

Fluorinated steroids are also prevalent in medicine. Whilst a great deal of fluorinated steroids are used to treat a range of diseases as anti-inflammatories, they also have roles in other diseases, such as cancer.[90,130] Probably the most notable of fluorinated steroids is Fluticasone Propionate (**1.51**, *Figure 1.19*), sold as Advair Diskus or Seretide when combined with Salmeterol as an oral treatment for Asthma, which has previously been in the top 10 of the world's best-selling drugs.[131] Fluticasone Propionate bears 6α- and 9α-fluorine atoms, both of which are known to heighten the anti-inflammatory properties of steroid-based drug molecules.[130]

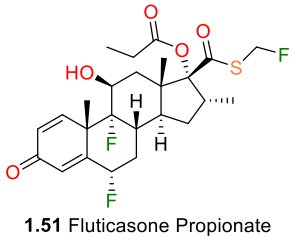

Figure 1.19 - Fluticasone Propionate[130]

A discussion of fluorine's role in medicinal chemistry would not be complete without mentioning its role in PET (Positron Emission Tomography) imaging. PET imaging is a non-invasive medical technique that assesses target engagement and maps functional processes *in vivo*, giving important information about ADMET properties of a drug when administered to a subject.[101,113] [^{18}F] is the most widely used radionuclide for PET imaging as it has a relatively long half-life ($t_{1/2}$) of 110 minutes, which allows multistep synthesis of PET agents with same day imaging. Generated in a cyclotron, the radionuclide can be produced as [^{18}F]-fluoride or [^{18}F]-fluorine gas, either of which can be used directly to synthesise radioligands or to make [^{18}F]-chiral catalysts or [^{18}F]-fluorinating reagents, such as [^{18}F]-Selectfluor or [^{18}F]-TBAF.[101,113] One of the most frequently used PET agents is the commercially available 2-deoxy-2-[^{18}F]fluoro-D-glucose ([^{18}F]-FDG, **1.52**, *Figure 1.20*), which is used in oncology, cardiology and neurology to investigate the metabolic status of tumour cells and a range of organs.[101,113]

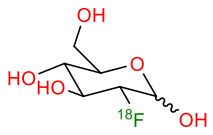

1.52 [^{18}F]-FDG

Figure 1.20 - 2-Deoxy-2-[^{18}F]fluoro-D-glucose

Steroid-based [^{18}F] agents have also been utilised in PET imaging. The [^{18}F] steroids 16β-[^{18}F]fluoro-5α-dihydrotestosterone (FDHT, **1.53**, *Figure 1.21*) and [^{18}F]fluoro furanyl norprogesterone (FFNP, **1.54**, *Figure 1.21*) have been successfully employed in PET imaging for prostate and breast cancers. The synthesis of both ligands is possible in high radiochemical yields (RCY) when using nucleophilic displacement of either a triflate or mesylate with [^{18}F]KF.[132] Additionally, the bile acid-based PET ligand [^{18}F]-LCATD (**1.55**, *Figure 1.21*) is an effective tracer for the investigation of drug interactions and toxicity in hepatic cells.[133]

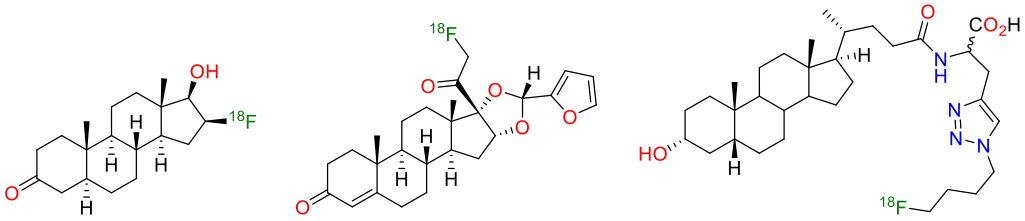

1.53 [^{18}F]-FDHT **1.54** [^{18}F]-FFNP **1.55** [^{18}F]-LCATD

Figure 1.21- [^{18}F] Steroid PET Tracers

1.4 Aims

Our aim is to synthesise fluorinated bile acid analogues to span a number of different therapeutic areas. The positions of fluorination will include those that bear hydroxy groups in the naturally occurring bile acids – 3, 6, 7 and 12 (*Figure 1.22*) – as well as other positions which are synthetically accessible, including the 4-position (*Figure 1.22*). The range of analogues will also include hydroxy groups or ketones at the stated positions.

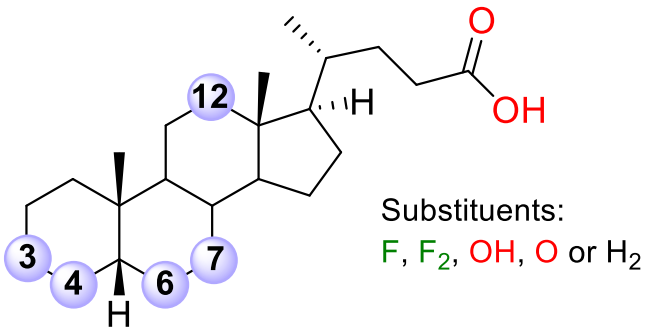

Figure 1.22 - General Bile Acid Structure with Positions Highlighted

Initially, fluorinated 5β-cholanic acid analogues bearing no oxygen-containing functional groups on the A, B, C, D-ring structure (with fluorination at the positions stated) are targeted for neurodegenerative diseases. For 5β-cholanic acid, fluorination is anticipated to decrease the lipophilicity of the bile acid skeleton due to introduction of strong dipoles on a highly lipophilic structure. Additionally for bile acids, substitution of a hydroxy group for a fluorine atom is likely to increase lipophilicity, hence fluorinated 5β-cholanic acid analogues are anticipated to be less polar than UDCA, and therefore will be in between UDCA and 5β-cholanic acid in terms of polarity. All other, oxygenated analogues synthesised will also be tested in assays for neurodegenerative diseases, as the biological activity of semi-synthetic bile acids is not well known.

Fluorinated analogues with hydroxy groups and ketones are specifically of interest for testing in cancer assays. This is because a variety of compounds bearing these moieties have been shown to have activity against numerous different cancer cell lines (*Figure 1.9*). The ketone analogues are also of interest to investigate the effects of removal of a HBD whilst retaining a strong HBA.

Analogues with fluorination next to hydroxy groups are targeted for testing in assays for FXR and TGR5, along with analogues with substitution of hydroxy groups for fluorine atoms. This is because fluorine atoms will introduce dipole effects (compared to non-fluorinated bile acids) and will modulate the hydrogen bond acidity of proximal hydroxy groups, leading to altered biological interactions within the active sites of FXR and TGR5.

Chapter 2 Synthesis of *gem*-Difluorinated Analogues

2.1 Retrosynthetic Analysis of gem-Difluorinated Target Compounds

In this chapter, the synthesis of *gem*-difluorinated bile acid analogues is discussed. Retrosynthetic analysis of the tetra- and difluorinated analogues **2.1** and **2.2** (*Scheme 2.1*) leads to the protected 3,7-diketone **2.3** (*Scheme 2.1*), with forward synthesis possible *via* a deoxofluorination reaction. The diketone **2.3** could be accessed from the naturally occurring bile acid CDCA (*Scheme 2.1*, available from NZP UK) following bis-oxidation.

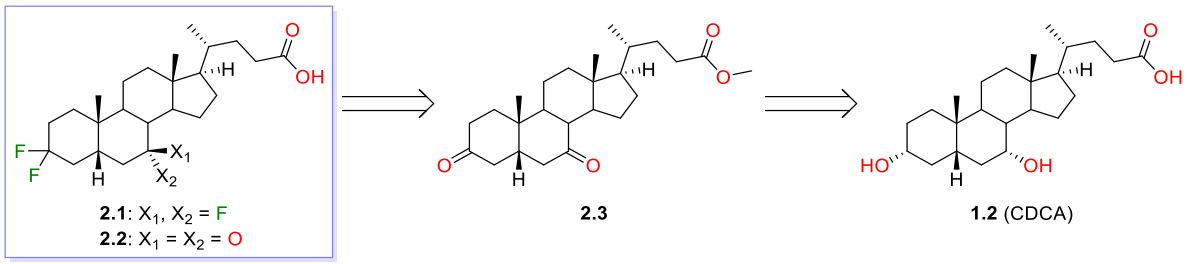

*Scheme 2.1 - Retrosynthetic Analysis of **2.1** and **2.2***

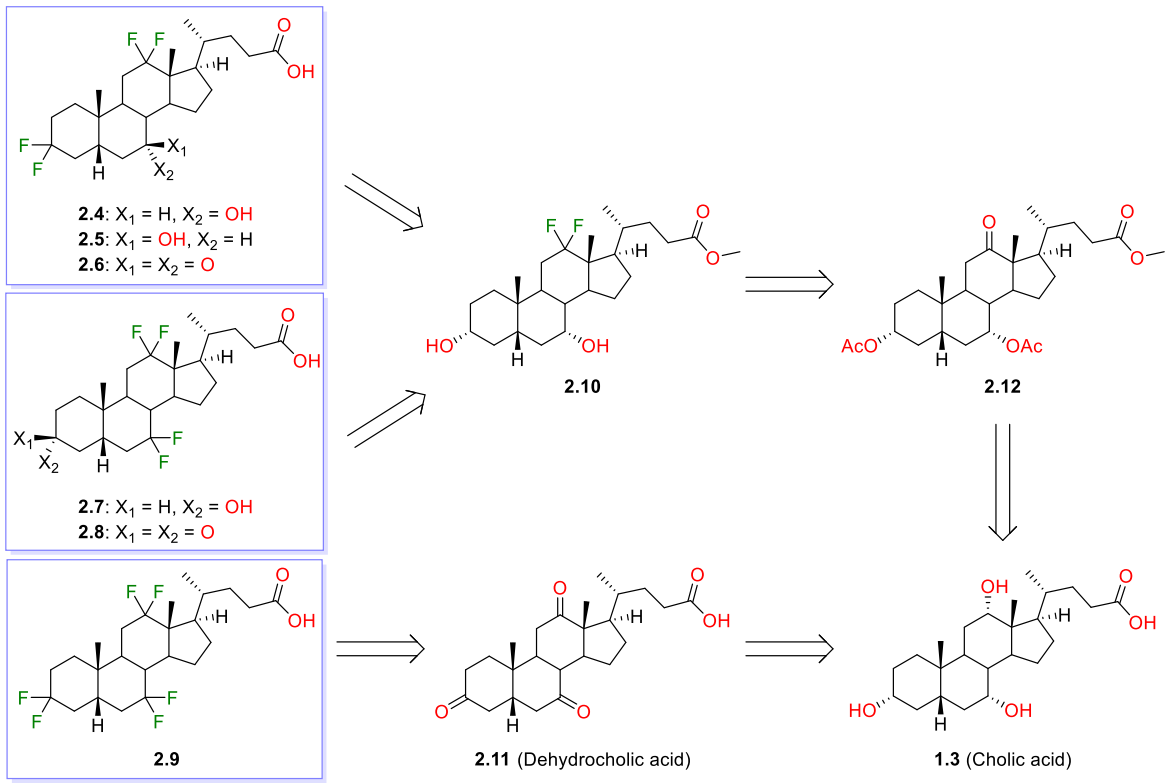

*Scheme 2.2 - Retrosynthetic Analysis of **2.4-2.9***

Regarding analogues with *gem*-difluorination at the 12-position and either the 3- or 7-positions, **2.4** to **2.8** (*Scheme 2.2*), retrosynthetic analysis of all five analogues leads to the 12,12-difluorinated

bile acid ester **2.10** (*Scheme 2.2*). Forward synthesis is possible *via* regioselective oxidation or hydroxy group protection, with further oxidation and deoxofluorination reactions. The ester **2.10** could be synthesised from the 12-ketone ester **2.12**, an intermediate currently available from NZP UK, which is formed from the naturally occurring bile acid cholic acid, **1.3** (*Scheme 2.2*).

The hexafluorinated analogue **2.9** (*Scheme 2.2*) could be accessed from the 3,7,12-triketone dehydrocholic acid (**2.11**, *Scheme 2.2*), *via* deoxofluorination. Dehydrocholic acid is synthesised commercially from cholic acid, **1.3**, and is available from NZP UK and various chemical vendors.

Retrosynthetic analysis of analogues with A-ring deoxygenation, **2.13** and **2.14** (*Scheme 2.3*) lead to their hydroxylated counterparts **2.15** and **2.16** (*Scheme 2.3*), following deoxygenation reactions. The carboxylic acid **2.15** is accessed from 7-keto LCA, **2.17** (*Scheme 2.3*), a derivative of CDCA available from NZP UK, *via* deoxofluorination. The carboxylic acid **2.16** could be accessed from the ester **2.18** (*Scheme 2.3*), also *via* deoxofluorination. Electrophilic fluorination of 7-keto LCA could yield **2.18**.

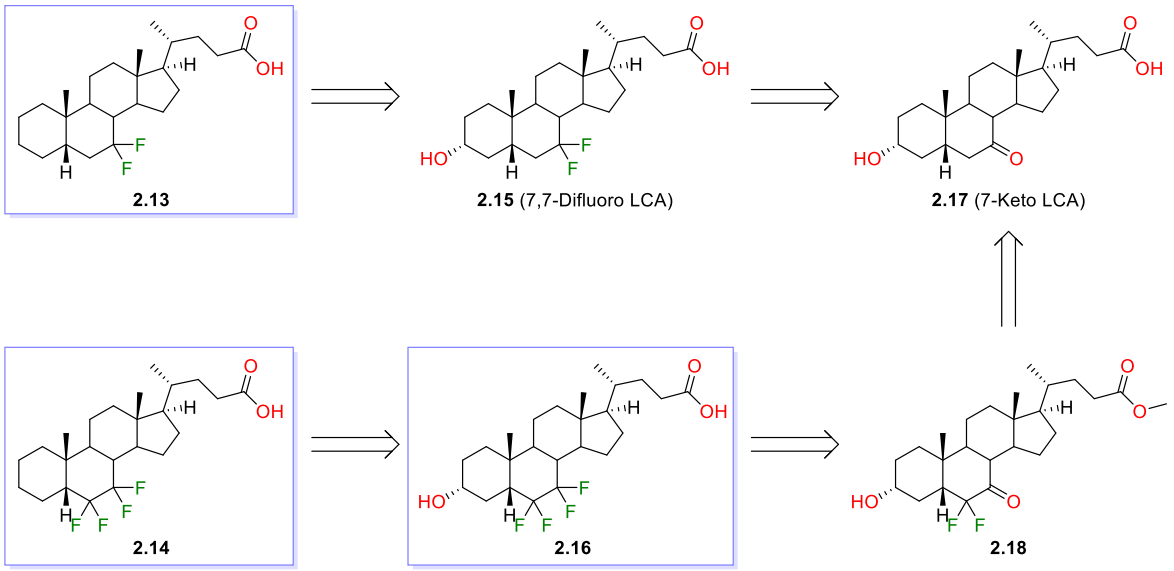

*Scheme 2.3 - Retrosynthetic Analysis of **2.13**, **2.14** and **2.16***

Retrosynthetic analysis of the deoxygenated analogue **2.19** (*Scheme 2.4*) leads to its 3-hydroxy counterpart **2.21**, formed following deoxofluorination of the 12-ketone intermediate **2.23** (*Scheme 2.4*). The ketone ester could be synthesised from the bile acid DCA (**1.5**, *Scheme 2.4*), available from NZP UK. The tetrafluorinated analogue **2.20** (*Scheme 2.4*) could also be synthesised from DCA *via* difluorination of the 3,12-diketone ester **2.22** (*Scheme 2.4*).

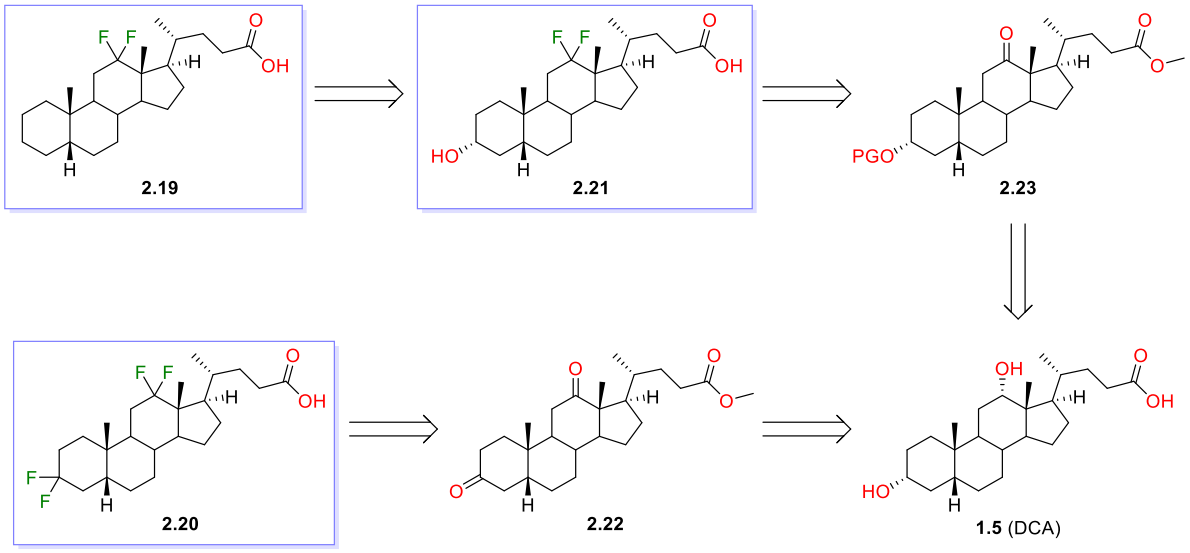

*Scheme 2.4 - Retrosynthetic Analysis of **2.19-2.21***

2.2 Synthesis of Analogues from Chenodeoxycholic Acid

2.2.1 Synthesis of Diketone Intermediate

Protection of the carboxylic acid moiety as a methyl ester is a practice commonly adopted.[134] Following precedent from within the group, Pelliciari and coworkers' high-yielding method for ester formation[135] was used, utilising methanol and *p*-toluenesulfonic acid monohydrate (*p*TSA•H_2O) with sonication to cleanly afford the desired methyl ester **2.24** (*Scheme 2.5*).

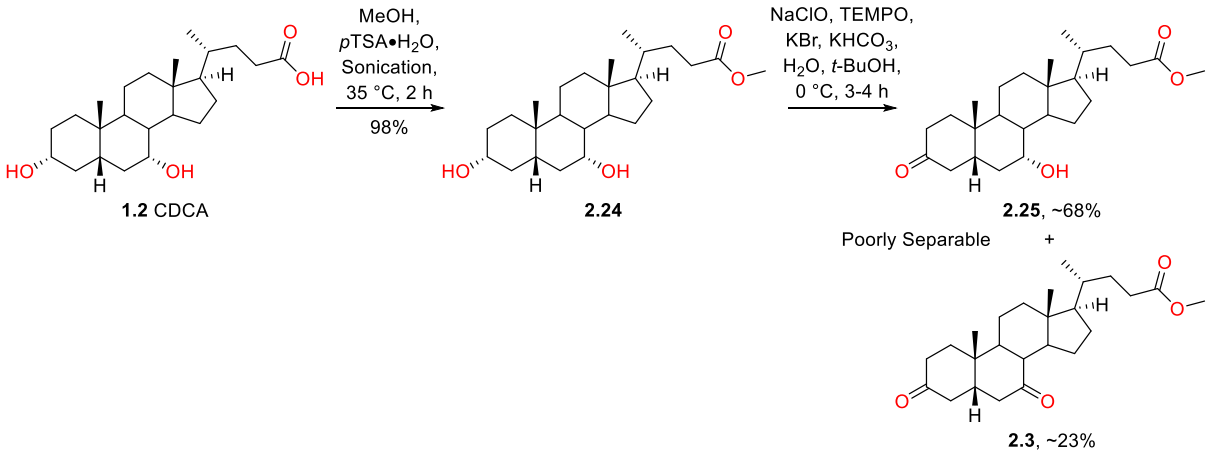

*Scheme 2.5 - Synthesis of **2.3***

Whilst selective oxidation of the 3α-hydroxy of **2.24** was not targeted for the synthesis of the tetra- and difluorinated target analogues, other synthetic routes within the project required the 3-ketone **2.25** (*Scheme 2.5,* see **Chapter 4**). Despite the proposed regioselectivity of the oxidation reaction, the diketone **2.3** (*Scheme 2.5*) was yielded and was hence used in the synthesis of **2.1** and **2.2** (*Scheme 2.5*).

Computational analysis of the 3α- and 7α-hydroxy groups has revealed that the 7α-OH is more reactive towards oxidants than the 3α-OH.[136] Despite this, 3-selective oxidation is possible with the use of a bulky oxidant, as the 3α-hydroxy is significantly less sterically hindered than the 7α-hydroxy. The oxidising agent Ag_2CO_3 on Celite has previously been utilised within the literature to perform 3-selective oxidation of bile acid derivatives with high yields,[137,138] but this method of oxidation was avoided due to the requirement of high temperatures (150 °C), the poor atom economy of the reaction[137,138] and the somewhat high cost of oxidant. Enzymatic 3-selective oxidation is also possible,[139] but the methods are not currently viable due to the equipment and chemicals/biologicals required (along with their high cost).

A procedure by Burns *et al.* for 3-selective oxidation of bile acid derivatives, utilising the readily available reagents sodium hypochlorite (NaClO) and 2,2,6,6-tetramethylpiperidine 1-oxyl (TEMPO,

Scheme 2.6),[140] has been optimised previously within the group to give good yields (60-70%) of 3-oxo bile acid products. Whilst the equivalents of TEMPO used in the reaction are relatively high (1.3 equiv), recovery of the oxidant is possible upon purification by flash chromatography. TEMPO is a bulky, mild oxidising agent of alcohols, used catalytically or stoichiometrically. Under basic conditions, the mechanism of alcohol oxidation is proposed to proceed *via* a catalytic cycle (*Scheme 2.6*).[141]

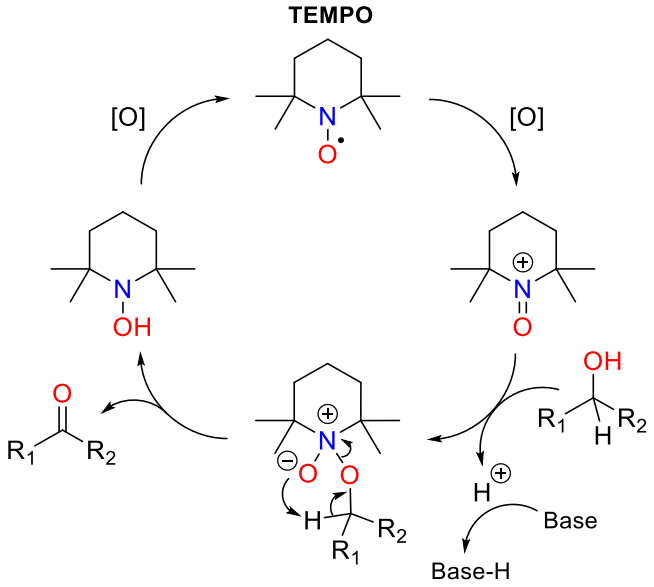

Scheme 2.6 - Proposed Reaction Mechanism for TEMPO-Mediated Oxidation Under Basic Conditions. [O] = Secondary Oxidant. Adapted From Ref.[141]

Using the optimised conditions, with slow addition of 11% NaClO solution over the course of 3-4 h, a mixture of the 3-ketone **2.25** and the diketone **2.3** (*Scheme 2.5*) was observed to have formed on analysis of the ^{1}H NMR spectrum of the crude material. The two compounds were found to be poorly separable by flash column chromatography, hence following two rounds of purification, **2.25** was cleanly isolated in a 14% yield, along with a 7:3 mix of **2.25** and **2.3**.

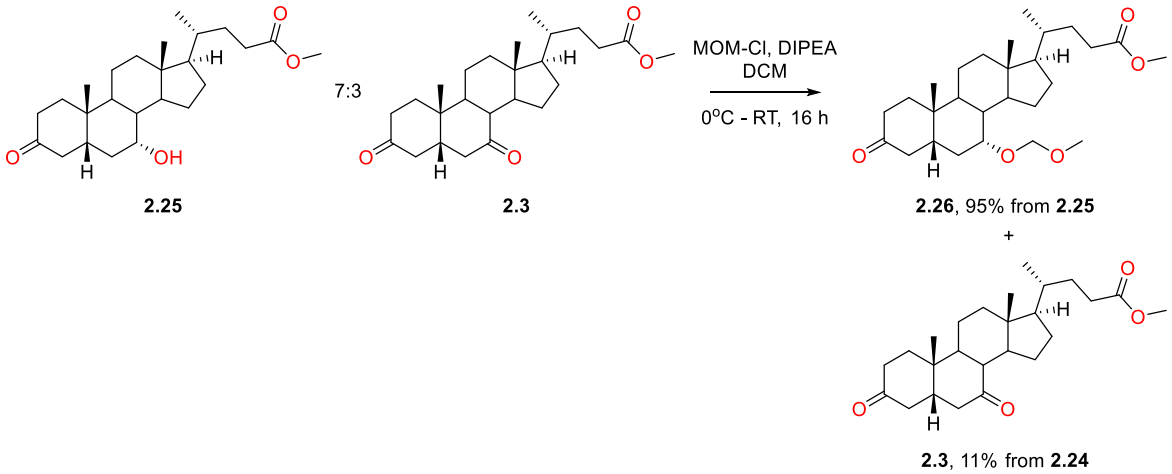

*Scheme 2.7 - MOM-Protection of **2.25/2.3** Mix*

In order to achieve separation of the 7:3 mix of **2.25** and **2.3**, MOM ether-protection of the alcohol of **2.25** was performed using conditions previously optimised from within the group. Protection of the 7α-OH of **2.25** increased its retention factor by thin-layer chromatography, allowing separation from the desired diketone **2.3.** A 95% yield of the MOM-protected ketone **2.26** (*Scheme 2.7*) and an 11% yield of **2.3** were achieved after purification by column chromatography.

2.2.2 Deoxodifluorination of the Diketone Intermediate

To access the desired di- and tetrafluorinated analogues **2.1** and **2.2**, nucleophilic deoxofluorination of the ketones was required. Commonly, deoxofluorination of ketones is carried out with sulfur fluoride reagents such as sulfur tetrafluoride (SF_4),[142] diethylaminosulfur trifluoride (DAST, **2.27**, *Figure 2.1*)[143] or Deoxo-Fluor® (*Figure 2.1*),[144] although SF_4 is seldom used due to its toxicity.

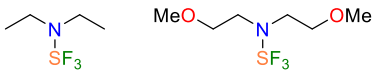

2.27 DAST **2.28** Deoxo-Fluor

Figure 2.1 - DAST and Deoxo-Fluor

The proposed mechanism for DAST-mediated deoxofluorination is shown in *Scheme 2.8*. A reversible elimination of a fluoride ion from DAST **2.27** gives the cation **2.29**, which in turn is attacked by an oxygen lone pair from the carbonyl group, giving the activated oxonium **2.31**. The activated ketone is then attacked by the previously eliminated fluoride ion to give the intermediate **2.32**, which releases a fluoride ion to give **2.33**. At this stage, there are three potential reaction pathways:

1. The red pathway, an S_N2 reaction of a fluoride displacing the -$OSFNEt_2$ leaving group of **2.33** to give the *gem*-difluoro product **2.34**.
2. The blue pathway, a biomolecular elimination (E_2) reaction in which a fluoride ion abstracts a β-hydrogen to eliminate the leaving group, giving the fluoroalkene product **2.36**.
3. The black pathway, in which the -OSF_2NEt_2 group leaves to give the carbocation **2.35**, which can form either the *gem*-difluoro product **2.34** or the fluoroalkene product **2.36** *via* S_N1 or unimolecular elimination (E_1) reactions.

There are arguments for both the unimolecular and bimolecular pathways to the difluoro and fluoroalkene products, as the carbocation **2.35** can be both stabilised and destabilised by fluorine. In principal, fluorine can mesomerically donate a lone pair of electrons, stabilising the carbocation, and inductively withdraw electron density, destabilising the carbocation.

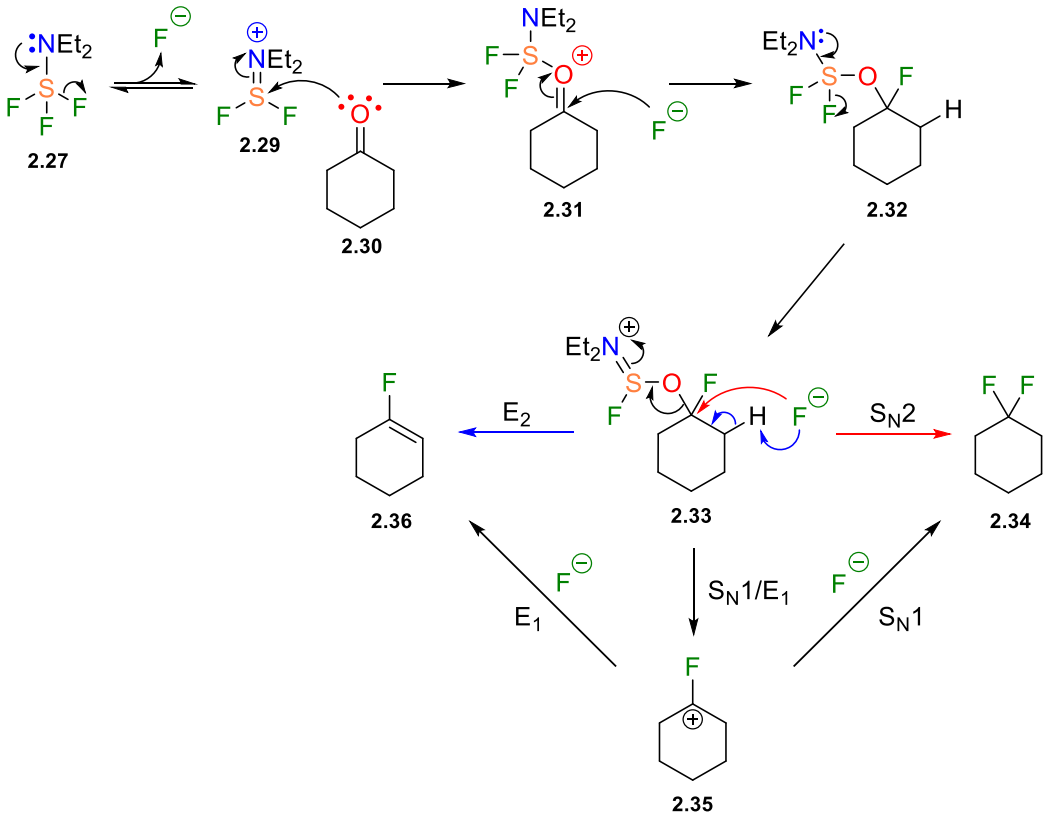

Scheme 2.8 - Proposed Mechanism for Deoxofluorination by DAST

Whilst Deoxo-Fluor is safer to handle than DAST and has a higher thermal stability, previous investigations within the group on difluorination reactions have shown that Deoxo-Fluor is much less effective for bile acid ketones. Hence, fluorination of **2.3** was carried out with DAST (*Scheme 2.9*). Previous work from within the group has also revealed that in order to difluorinate the sterically hindered 7-ketone, neat DAST is required and also, the 3-ketone reacts with DAST at a much higher rate than the 7-ketone, giving selectivity where required. This allowed the synthesis of both of the targeted A- and B-ring tetrafluorinated and difluorinated analogues, from one deoxofluorination reaction.

Initially, the reaction was stirred at room temperature, but after 3 d, ^{1}H and ^{19}F NMR spectral analysis of the reaction mixture showed no reaction of the 7-ketone with DAST. To force the reaction further, the mixture was heated at 50 °C for 3 d. Generally, heating causes a DAST-mediated difluorination reaction to occur faster and increases the yield of *gem*-difluoro products, but it is important to control the internal temperature as the degradation products of DAST (amine and sulfur-based products) are potentially explosive at temperatures above 80 °C.[145] Purification of the crude reaction material after an aqueous workup gave the tetra- and difluorinated esters **2.37** and **2.38**, ~80% and ~90% pure respectively, with inseparable fluoroalkene by-products (*Scheme 2.9*).

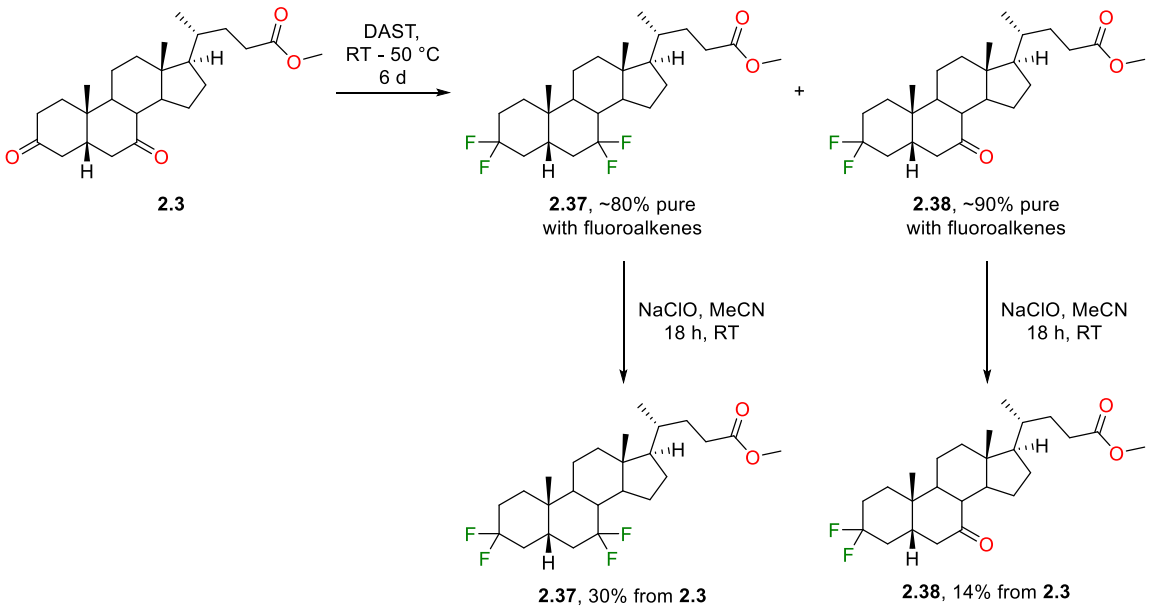

*Scheme 2.9 - Deoxofluorination of **2.3***

To enable separation of **2.37** and **2.38** from the fluoroalkene side products, epoxidation was carried out. Epoxidation allows separation by flash chromatography as fluoroepoxide products are generally more polar than *gem*-difluoro products, and hence have lower retention factors on silica gel. *m*-CPBA is typically used within the group to epoxidize fluoroalkenes, but was not suitable for use on **2.38** as a Baeyer-Villiger (B-V) reaction could occur on the ketone at the 7-position. To avoid the synthesis of further side products, epoxidation was performed using sodium hypochlorite (NaClO) in acetonitrile (*Scheme 2.9*), a method described by Coe *et al.* for the epoxidation of polyfluorocyclohexenes.[146] Following purification, the tetrafluoro and difluoro esters **2.37** and **2.38** were isolated in 30% and 14% yields respectively over two steps and their structures were confirmed by x-ray crystallographic analysis, shown in *Figure 2.2* and *Figure 2.3*.

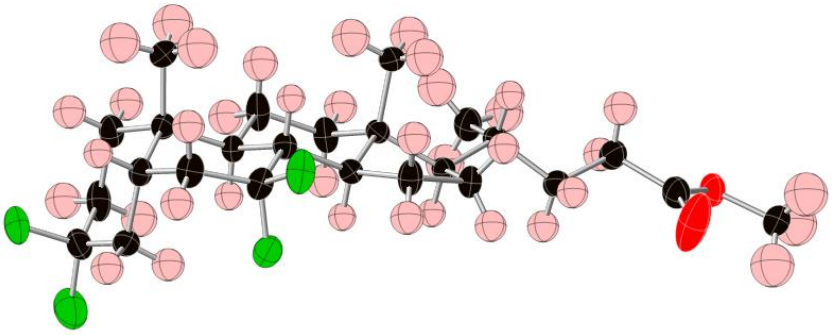

*Figure 2.2 - X-Ray Crystal Structure of **2.37***

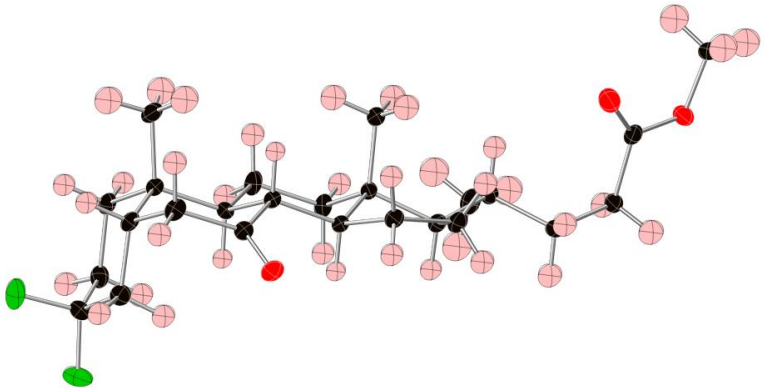

*Figure 2.3 - X-Ray Crystal Structure of **2.38***

2.2.3 Deprotection of *gem*-Difluorinated Esters

The desired fluorinated carboxylic acids were obtained by methyl ester saponification of **2.37** and **2.38** (*Scheme 2.10*). Methods for ester saponification previously used by Pellicciari *et al.* and Carreira *et al.* involved the use of sodium hydroxide in methanol/water with heating up to 120 °C.[57,137] Due to the presence of multiple fluorine atoms in **2.37** and **2.38** that could potentially eliminate under harsh basic conditions, a milder ester hydrolysis method was investigated. The use of aqueous lithium hydroxide, as reported by Dayal and coworkers,[147] gave the corresponding carboxylic acid products **2.1** and **2.2** in high yields without the requirement for further purification (*Scheme 2.10*).

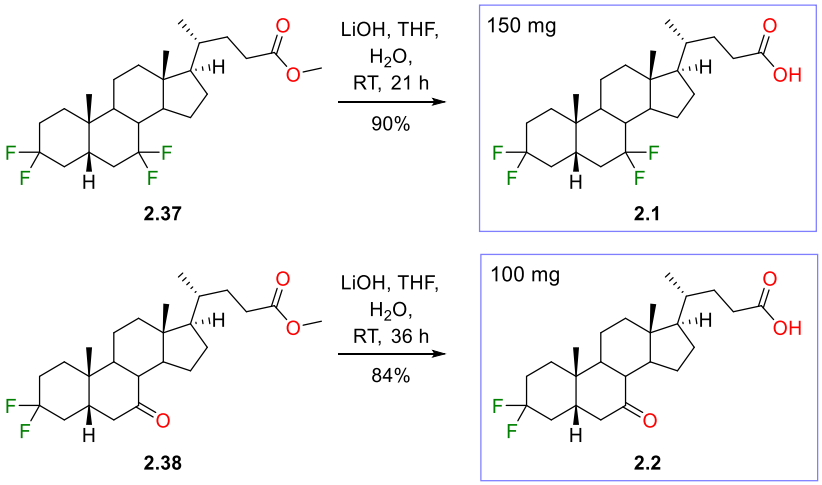

*Scheme 2.10 - Methyl Ester Saponification of **2.37** and **2.38***

2.3 Synthesis of Analogues from Cholic Acid and Its Derivatives

2.3.1 Synthesis of 3,3,12,12-Tetrafluorinated Analogues

2.3.1.1 Synthesis of 3,3,12,12-Tetrafluoro-7α-Hydroxy-5β-Cholanic Acid

Synthesis of the 3,3,12,12-tetrafluorinated analogues **2.4** to **2.6** (*Scheme 2.2*) commenced with deoxofluorination of the advanced intermediate **2.12** (*Scheme 2.11*), supplied by NZP UK. Previous 12,12-difluorination reactions performed within the group have shown the necessity of neat DAST, heated at 50 °C for at least 7 d to synthesise the desired *gem*-difluoro compounds in high yields. Due to the safety concerns of DAST, the scale of the deoxofluorination reaction was limited to 5.0 g of **2.12** in 10 mL (~8 equiv) of neat DAST, with addition of up to a maximum 16 mL (~13 equiv) of DAST throughout the length of the reaction. The reaction was performed four times, with varying isolated yields between 45% and 75% of the desired difluorinated product **2.39** (*Scheme 2.11*), dependent on the quality of DAST used and the frequency of its addition.

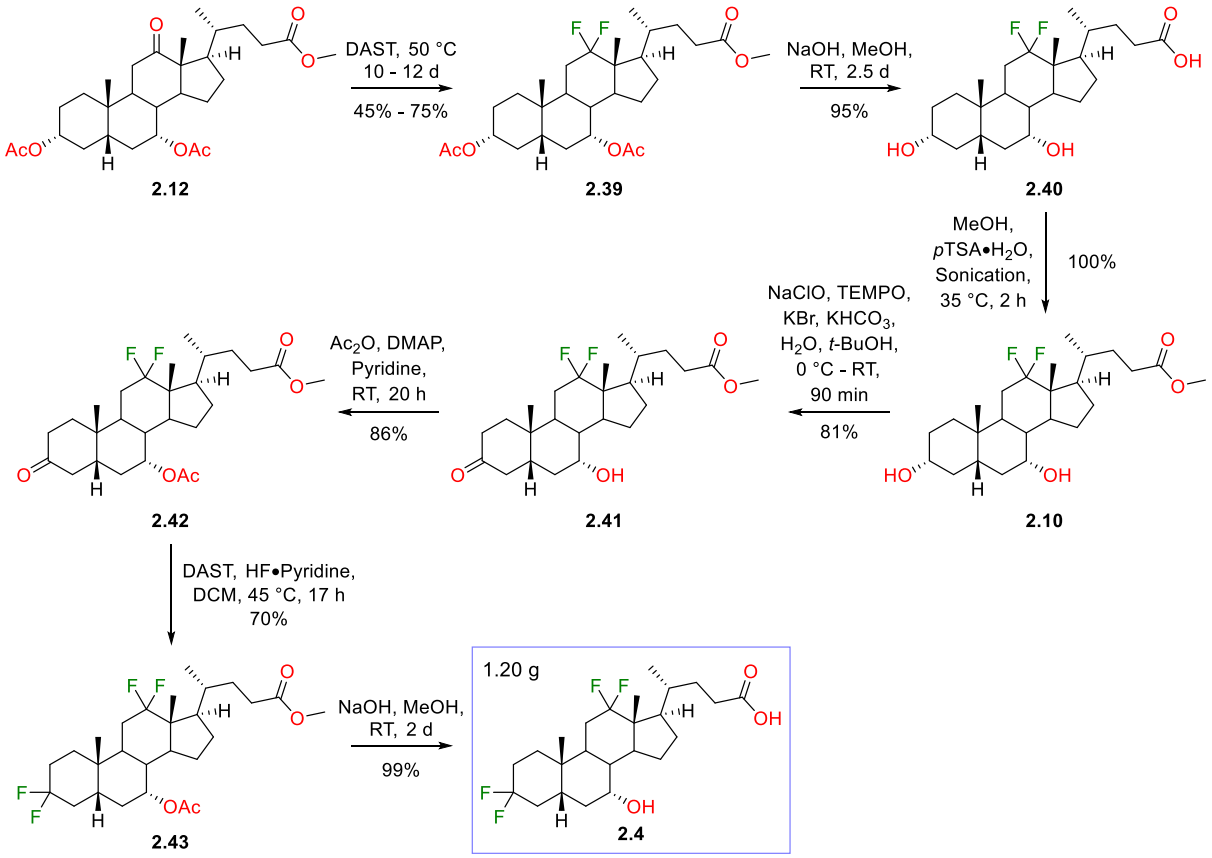

*Scheme 2.11 - Synthesis of **2.4***

While in principal selective acetate methanolysis of **2.39** would be possible, leaving the methyl ester and 7α-acetoxy intact for further reactions, our experience shows that this is difficult to achieve in practice. Hence, to enable further manipulation of the 3- and 7-positions, **2.39** was fully

deprotected to form the carboxylic acid **2.40** (*Scheme 2.11*) using a concentrated NaOH solution in methanol. The forcing conditions were required to completely remove the acetyl group at the hindered 7α-position as milder methods of hydrolysis have been shown to leave the 7α-acetoxy group intact. The carboxylic acid **2.40** was then subjected to facile ester formation using Pellicciari and coworkers' method[135] as previously discussed. Yields of 96% to 100% of **2.10** (*Scheme 2.11*) were achieved across multiple batches without the need for further purification.

Regioselective oxidation of the 3α-hydroxy of **2.10** was then performed using Burns and coworkers' method utilised previously,[140] giving the 3-keto ester **2.41** in an 81% yield (*Scheme 2.11*). Interestingly, only a trace of diketone product formed in the reaction, observed upon analysis of the ^{1}H NMR spectrum of the crude material. This suggests that the 12,12-difluoro group has a deactivating effect on the 7α-OH, likely due to fluorine's electron-withdrawing effect making the hydroxyl group less nucleophilic. Along with NMR spectral analysis of **2.41**, the regioselectivity of the oxidation was confirmed with its x-ray crystal structure, shown in *Figure 2.4*.

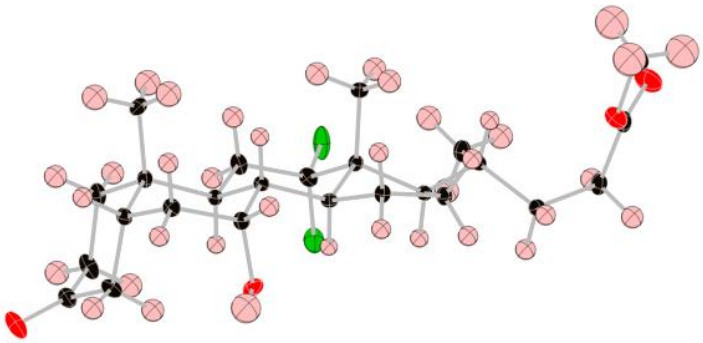

*Figure 2.4 - X-Ray Crystal Structure of **2.41***

Protection of the 7α-hydroxy of **2.41** was carried out using a procedure by Omura and coworkers,[49] utilising acetic anhydride and DMAP. The desired acetate **2.42** (*Scheme 2.11*) was obtained in an 87% yield and crystallised readily, with the x-ray crystal structure shown in *Figure 2.5*.

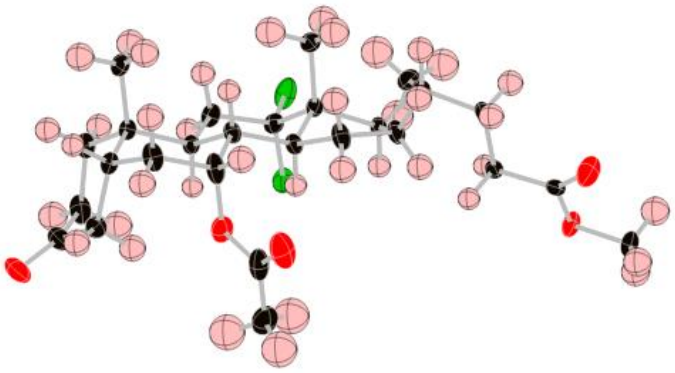

*Figure 2.5 - X-Ray Crystal Structure of **2.42***

Unlike at the 7- or 12-positions, fluorination of a ketone at the 3-position of a bile acid derivative is more straightforward, likely due to the lower steric hindrance in the approach of the fluorinating agent compared to ketones on the B and C-rings. Consequently, neat DAST is not required for fluorination. Conditions for difluorination of a ketone at the 3-position have been previously optimised within the group, using three equivalents of DAST and catalytic HF.Pyridine (Olah's reagent) in DCM under reflux. A high yield of the tetrafluorinated ester **2.43** (*Scheme 2.11*) was achieved using this procedure, with minimal fluoroalkene formation and hence, no issues arising regarding purification. Global deprotection of **2.43** under basic conditions yielded the targeted tetrafluoro carboxylic acid **2.4** (*Scheme 2.11*) in an approximate overall 34% yield from **2.12**.

2.3.1.2 Synthesis of 3,3,12,12-Tetrafluoro-7-Oxo-5β-Cholanic Acid and 3,3,12,12-Tetrafluoro-7β-Hydroxy-5β-Cholanic Acid

With a significant quantity of **2.4** in hand, modification of the 7α-hydroxy was conducted. Oxidation of **2.4** was performed with Dess-Martin Periodinane (DMP), but the desired 7-keto bile acid was inseparable from DMP-related aromatic impurities. To enable separation, methyl ester formation was carried out, followed by flash chromatography purification to cleanly yield **2.44** (*Scheme 2.12*) in a 60% yield over two steps. As is quite common with keto-bile acid derivatives, **2.44** crystallised readily, its x-ray crystal structure is shown in *Figure 2.6*. The methyl ester of **2.44** was then saponified with lithium hydroxide to give the desired tetrafluorinated 7-keto bile acid **2.6** (*Scheme 2.12*).

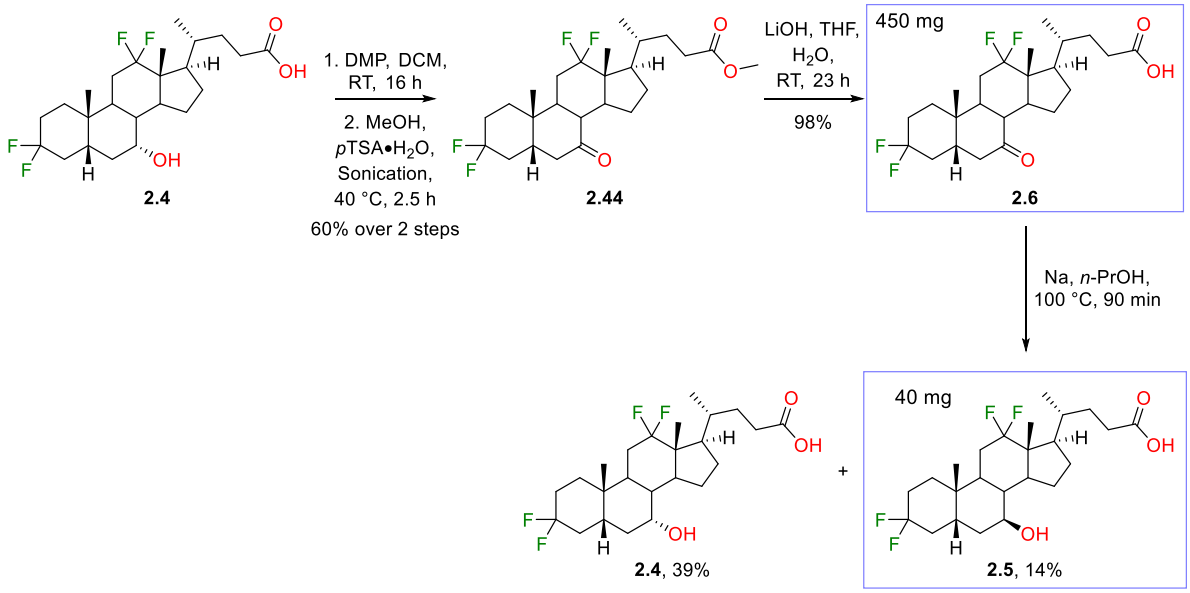

*Scheme 2.12 - Synthesis of **2.5** and **2.6***

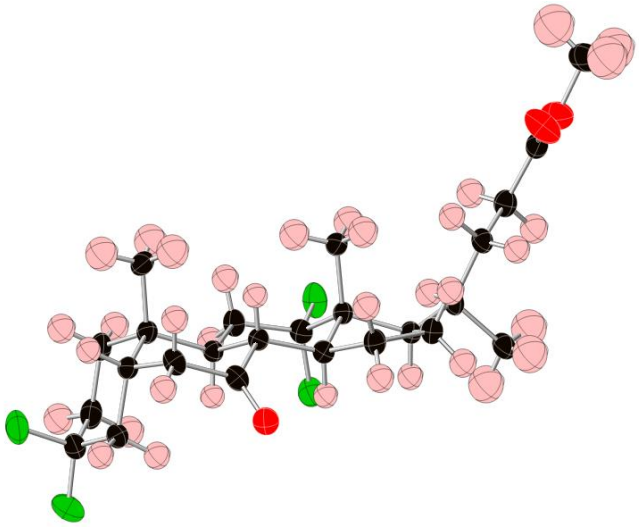

*Figure 2.6 - X-Ray Crystal Structure of **2.44***

To synthesise the final 3,3,12,12-tetrafluorinated-7-oxygenated target compound, β-stereoselective reduction of the 7-ketone of **2.6** was required. When previously performed within the group, reactions of sodium borohydride ($NaBH_4$) with 7-keto bile acids has led to a mix of α- and β-alcohols. When performed on a 12,12-difluorinated bile acid though, low quantities of β-alcohols were isolated, potentially due to steric hindrance (*Figure 2.7*).

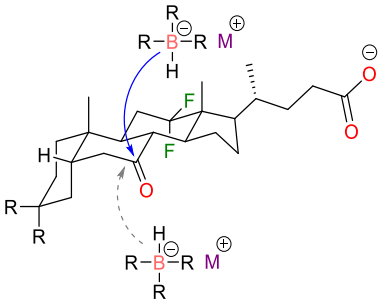

Figure 2.7 - Attack of Boron Reducing Agents on a 12,12-Difluorinated Bile Acid

To form a β-hydroxy group from a ketone at the 7-position, the reducing agent must be small due to the difficulties in the approach of the ketone from the bottom face of the bile acid. Work by Giordano and coworkers investigated the use of alkali metals to reduce the ketone of 7-keto LCA (**2.17**, *Scheme 2.3*), achieving high selectivities of 7β-OH over 7α-OH (between 4:1 and 19:1), and high isolated yields of UDCA.[148] This method was previously used within the group for stereoselective reduction of a 12,12-difluoro-7-oxo bile acid, achieving a β:α diastereomeric ratio of 2:1. Using the same method, stereoselective reduction of **2.6** was conducted using sodium metal in *n*-propanol, heated under reflux for 1.5 h (*Scheme 2.12*).

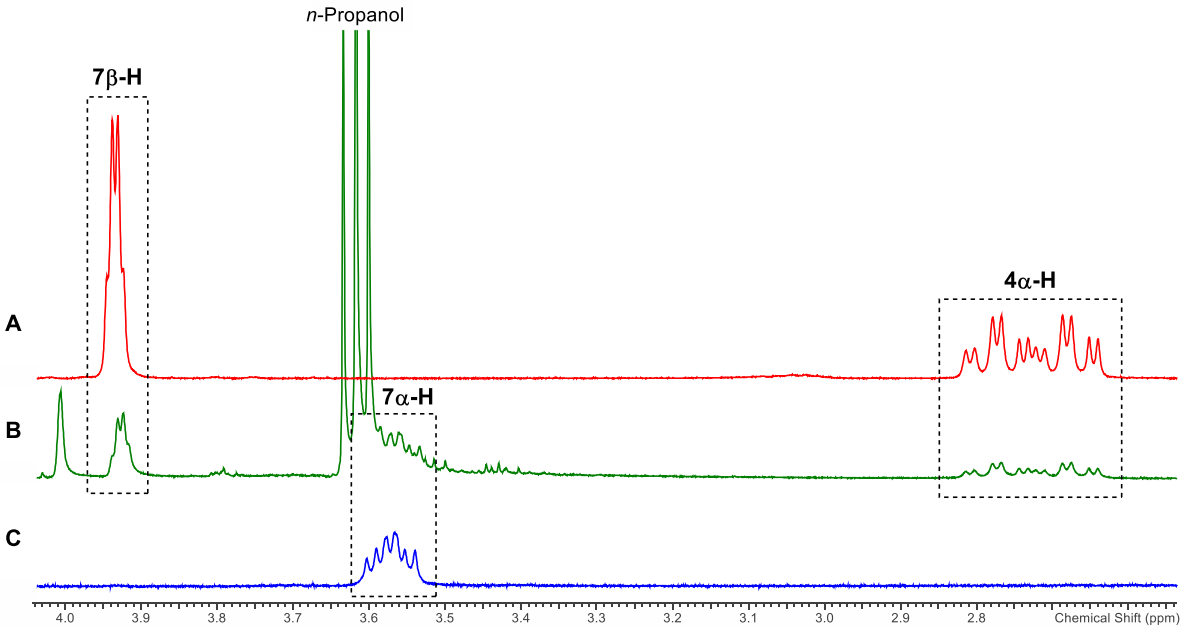

*Figure 2.8 - Section of ^{1}H NMR Spectra of: **A** (red): Clean **2.4**; **B** (green): Crude Material Na/n-Propanol Reduction of **2.6**; **C** (blue): Clean **2.5***

After an aqueous workup, analysis of the ^{1}H NMR spectrum of the crude material (*Figure 2.8*) showed the presence of both a 7α-OH (7β-H q at 3.93 ppm) and a 7β-OH (7α-H td at 3.57 ppm), formed in a ratio of around 1:3 β:α. Following purification by flash chromatography, the 7β-hydroxy compound **2.5** was isolated in a 14% yield (*Scheme 2.12*) and the stereochemistry of the hydroxy group was confirmed with x-ray crystallographic analysis, shown in *Figure 2.9*.

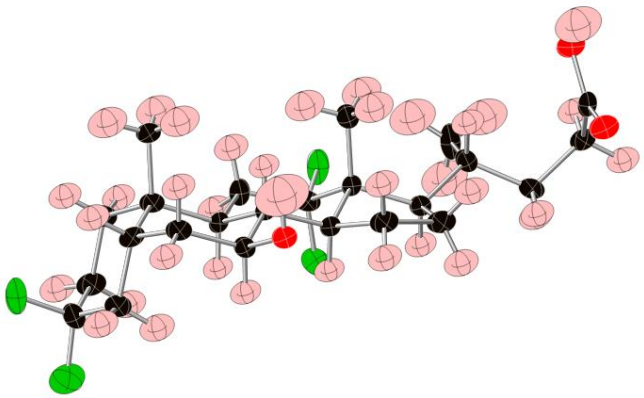

*Figure 2.9 - X-Ray Crystal Structure of **2.5***

The low isolated yield of **2.5** is likely due to the strong electronic effect of two *gem*-difluoro moieties. As mentioned previously, a 2:1 β:α ratio was achieved on reduction of a 12,12-difluoro-7-keto bile acid with sodium. This ratio is significantly lower than that achieved in the literature for 7-keto LCA,[148] suggesting that the *gem*-difluoro group has a negative effect on the formation of a 7β-OH. Accordingly, in the case of **2.5**, with two *gem*-difluoro moieties present, a much lower ratio of around 1:3 β:α was achieved.

2.3.2 Synthesis of 7,7,12,12-Tetrafluorinated Analogues

To synthesise analogues with a 7,7-difluoro moiety, oxidation of the 7α-hydroxy of the key 12,12-difluoro intermediate **2.10** (*Scheme 2.13*) was required. Regioselective oxidation of **2.10** was performed using a NaClO-mediated method developed by Sepe *et al.*,[149] but whilst Sepe's 7-selective oxidation of CDCA was complete within 6 h, 3 d of stirring was required to consume all of **2.10**. After an aqueous workup and purification of the crude material by flash chromatography, a 36% yield of the desired 7-keto ester **2.45** was isolated (*Scheme 2.13*). A mixture of the 3-keto and 3,7-diketone products **2.41** and **2.46** (*Scheme 2.13*) was also isolated. The slow and low yielding oxidation is likely to be as a result of the deactivating effect of 12,12-difluoro group on the 7α-hydroxy, as mentioned previously.

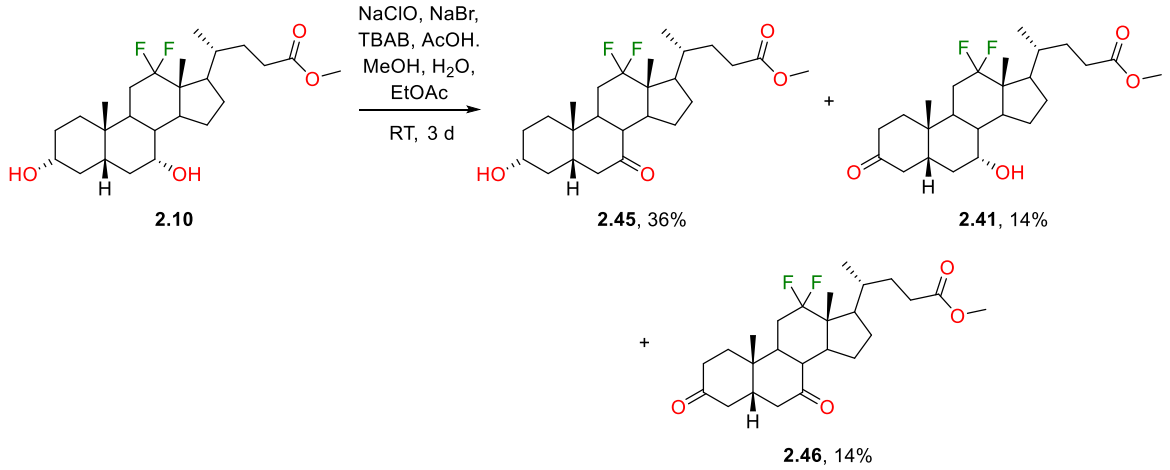

*Scheme 2.13 - 7-Selective Oxidation of **2.10***

Following the unsuccessful regioselective oxidation reaction, 3-selective acetyl protection of **2.10** (*Scheme 2.14*) was carried out. A procedure by Pelliciari *et al.* with acetic anhydride and sodium bicarbonate[135] was used to afford the selectively acetylated product, **2.47** (*Scheme 2.14*), in a 93% yield. Subsequent oxidation of the 7α-hydroxy of **2.47** with DMP was facile, affording the 7-oxo ester **2.48** (*Scheme 2.14*) in a 69% yield.

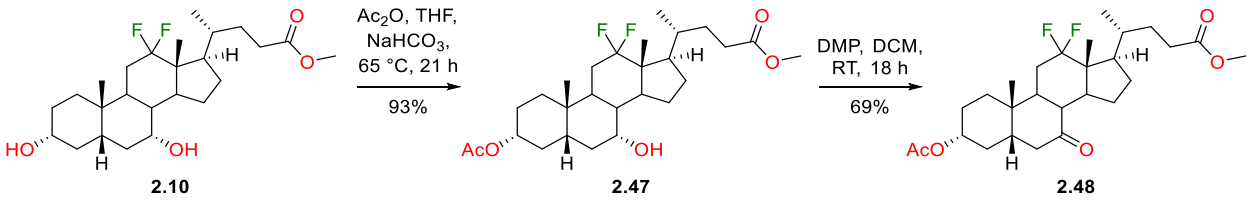

*Scheme 2.14 - Synthesis of **2.48***

As exemplified with the deoxofluorination reaction of **2.3** (*Scheme 2.9*), successful *gem*-difluorination of a bile acid 7-ketone requires the use of neat DAST and heating. Difluorination of **2.48** with DAST gave the desired *gem*-difluoro product **2.49** and the fluoroalkenes **2.50** and **2.51**

(*Scheme 2.15*). Separation of the fluoroalkene products from **2.49** was possible with flash chromatography alone, without the requirement of derivatisation of **2.50** and **2.51**.

Simultaneous acetate cleavage and methyl ester saponification of **2.49** was then performed under basic conditions to give 7,7,12,12-tetrafluoro LCA (**2.7**, *Scheme 2.15*), achieved in 26% yield from the 12,12-difluoro ester **2.10**. The structure of **2.7** was confirmed with its x-ray crystal structure (*Figure 2.10*).

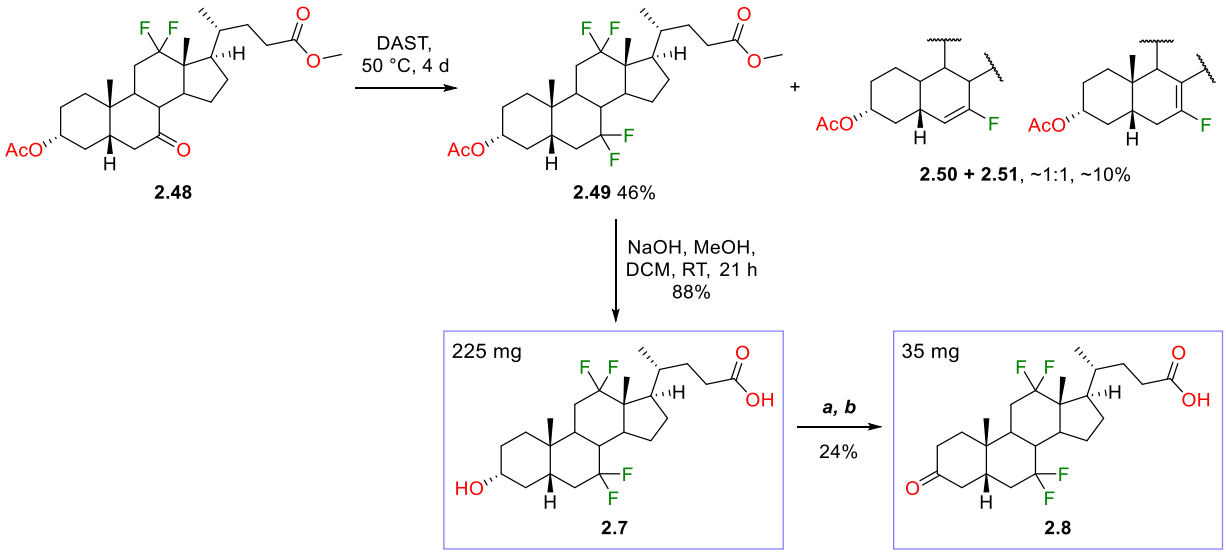

*Scheme 2.15 - Synthesis of **2.7** and **2.8***

a: *NaClO, TBAB, NaBr, MeOH, AcOH, H_2O, AcOEt, RT, 28 h*

b: *NaClO, TEMPO, KBr, $KHCO_3$, t-BuOH, H_2O, MeOH, EtOAc, RT, 3 d*

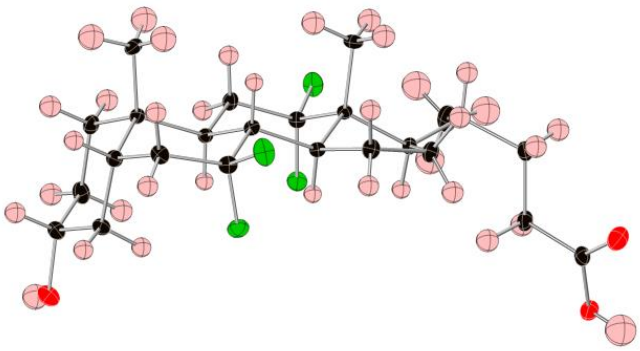

*Figure 2.10 - X-Ray Crystal Structure of **2.7***

To synthesise the 7,7,12,12-tetrafluoro-7-oxo target **2.8** (*Scheme 2.2*), oxidation of the 3α-hydroxy group of **2.7** was initially attempted using an NaClO-mediated oxidation procedure, chosen over DMP in order to avoid the purification issues experienced previously. Following 28 h of stirring and further addition of NaClO, analysis of the reaction mixture by TLC indicated that the reaction was incomplete. After an aqueous workup, the crude material was treated with NaClO and TEMPO using

Burns and coworkers' method[140] in an attempt to force the reaction further. Despite addition of excess NaClO and 3 d of stirring, the reaction mixture contained a 7:3 mix of **2.7** and **2.8** on ^{1}H NMR spectral analysis. Purification of the resulting crude reaction material gave the desired 3-oxo compound **2.8** in a 24% yield (*Scheme 2.15*). As observed previously with tetrafluorinated compounds, the two CF_2 groups had a significant electron withdrawing effect, reducing the nucleophilicity of the 3α-hydroxy group.

2.3.3 Synthesis of 12,12-Difluorinated Ketone Analogues

With the keto ester intermediates **2.41** and **2.45** in hand, saponification of the methyl ester protecting groups was carried out using the mild conditions by Dayal *et al.*,[147] giving the carboxylic acids **2.52** and **2.53** in good yields (*Scheme 2.16*).

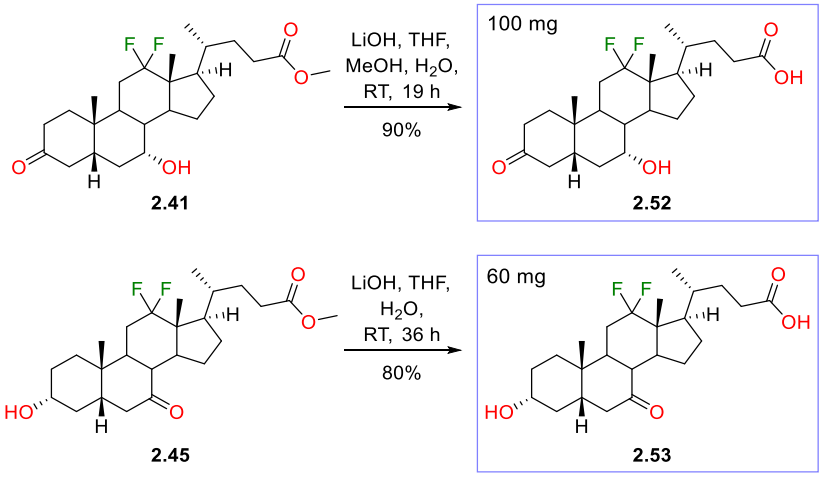

*Scheme 2.16 - Methyl Ester Saponification of **2.41** and **2.45***

The 12,12-difluoro-3,7-diketone **2.46**, previously formed as a by-product of 7-selective oxidation of **2.10** (*Scheme 2.13*) was also of interest, and was hence resynthesized from **2.10** using a high yielding, DMP-mediated oxidation (*Scheme 2.17*). Saponification of the methyl ester then cleanly afforded the carboxylic acid **2.52** (*Scheme 2.17*) in a high yield. Both the diketone ester (**2.46**) and carboxylic acid (**2.54**) readily crystallised, their corresponding x-ray crystal structures are shown in *Figure 2.11* and *Figure 2.12*.

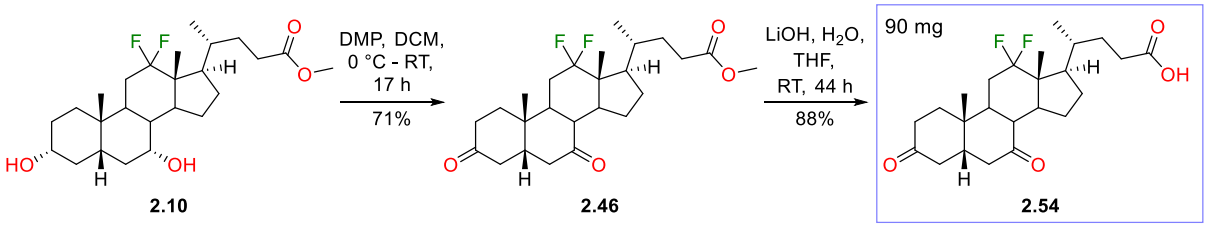

*Scheme 2.17 - Synthesis of **2.52***

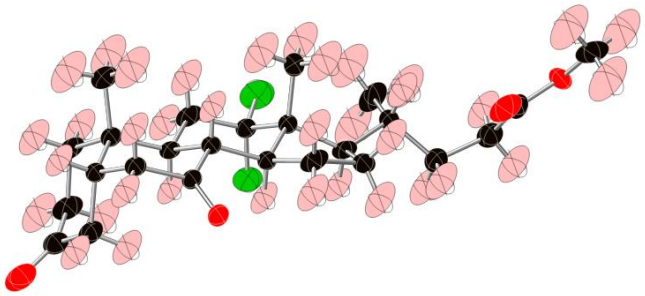

*Figure 2.11 - X-Ray Crystal Structure of **2.46***

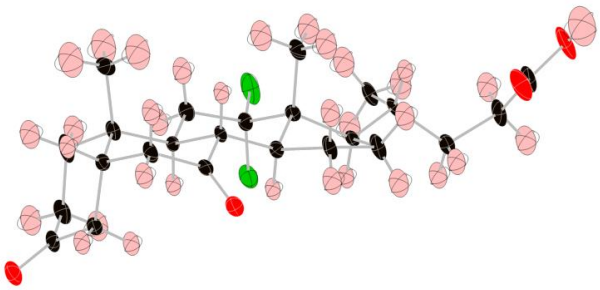

*Figure 2.12 - X-Ray Crystal Structure of **2.54***

2.3.4 Synthesis of 3,3,7,7,12,12-Hexafluoro-5β-Cholanic Acid

Using a base-mediated procedure by Ikonen *et al.*,[150] the methyl ester of dehydrocholic acid (**2.11**, *Scheme 2.18*) was synthesised in a high yield. Pelliciari's acid-catalysed method[135] for methyl esterification was avoided due to potential acetal formation at the 3-ketone.[151] With the carboxylic acid suitably protected, neat DAST deoxofluorination of **2.55** (*Scheme 2.18*) was carried out with heating at 50 °C for 9 d.

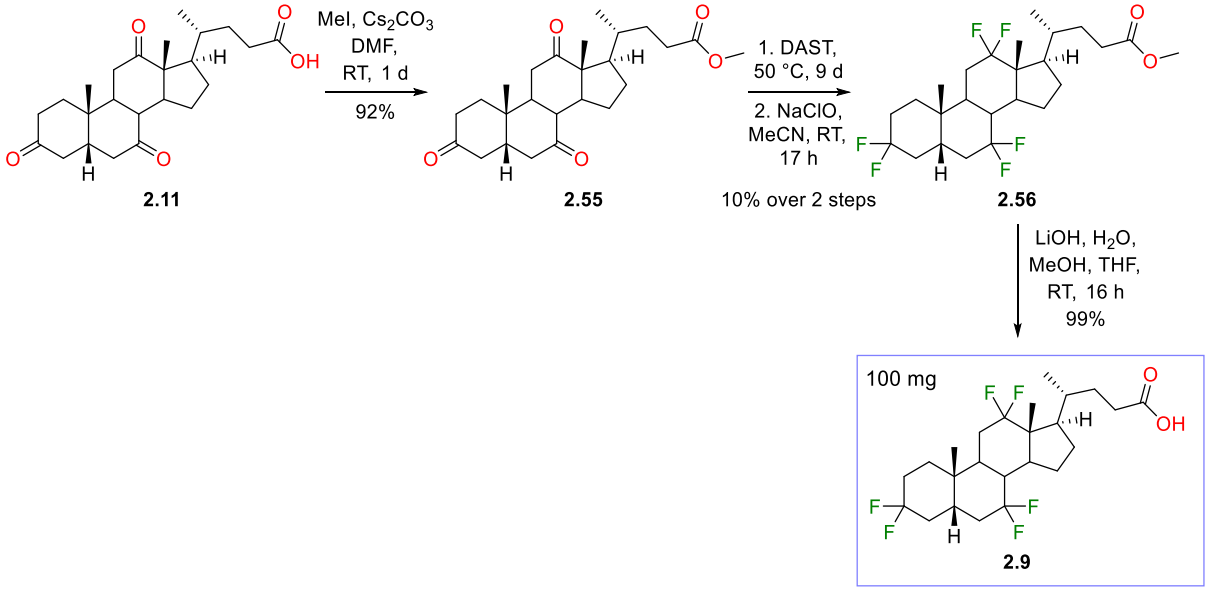

*Scheme 2.18 - Synthesis of **2.9***

Following purification of the crude reaction material, the hexafluorinated ester **2.56** (*Scheme 2.18*) was yielded ~80% pure with fluoroalkene side products. Epoxidation of the fluoroalkene products was performed using the previously utilised method by Coe *et al.*,[146] cleanly giving **2.56** in a 10% yield after flash chromatography. The low yield of hexafluorinated product is likely due to loss of material from the incomplete fluorination reaction of all three ketones. ^{1}H and ^{19}F NMR spectral analysis of the crude material following the DAST reaction showed multiple products bearing ketones and CF_2 moieties. Saponification of **2.56** was then carried out using the mild lithium hydroxide-mediated conditions,[147] giving **2.9** in a 9% yield from dehydrocholic acid (*Scheme 2.18*).

2.4 Synthesis of Analogues from 7-Keto Lithocholic Acid

2.4.1 Optimisation of the Barton-McCombie Deoxygenation

To synthesise the target analogues **2.13**, **2.14** and **2.19** (*Scheme 2.3*, *Scheme 2.4*) from naturally occurring bile acids, deoxygenation of the A-ring is required. Methods for deoxygenation of alcohols and ketones of bile acids have been described in the literature, such as the Barton-McCombie and Wolff-Kishner reactions,[140,152] although the reported methods use toxic reagents such as tributyltin hydride (Bu_3SnH) and hydrazine hydrate. Other non-direct deoxygenation methods have also been reported, involving elimination of leaving groups formed from alcohols and hydrogenation of the resulting alkenes to form the desired CH_2 groups.[153] Whilst this method has been proven to be effective, it is quite long-winded. It is also possible to remove a hydroxy group via deoxychlorination (using a reagent such as SO_2Cl_2), followed by dehalogenation using either hydrogenation over palladium on carbon,[154,155] radical dechlorination with Bu_3SnH and azobisisobutyronitrile (AIBN)[156,157] or indium(III) acetate with phenylsilane ($PhSiH_3$).[158] These methods are disfavoured though as they use toxic heavy metals which are generally avoided in medicinal chemistry.

Previous work within the Linclau group has shown Barton-McCombie deoxygenation methods with trialkylsilanes and dibenzoyl peroxide (BPO) as the radical initiator[159,160] to be successful on fluorinated sugars and aliphatic compounds, achieving high yields with no observation of radical defluorination. Fluorinated bile acids may be unstable to other methods of hydroxy group deoxygenation (such as elimination methods), hence the Barton-McCombie reaction was investigated and optimised.

Prior to testing the Barton-McCombie deoxygenation, the methyl ester of 7-keto LCA (**2.17**, *Scheme 2.19*) was synthesised using Pelliciari's procedure.[135] The ester **2.57** (*Scheme 2.19*) was isolated in a high yield, to be used in testing deoxygenation methodology and synthesising the desired fluorinated B-ring analogues.

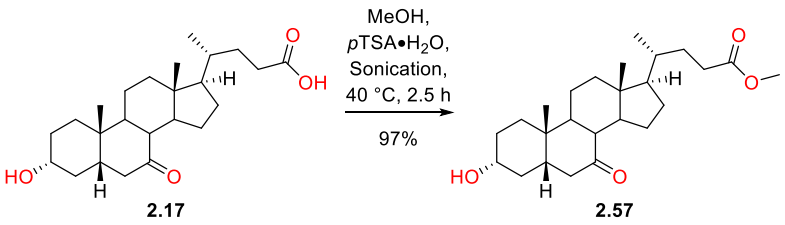

Scheme 2.19 - Methyl Ester Formation on 7-Keto LCA, ***2.17***

To enable deoxygenation, the Barton-McCombie reaction requires the hydroxy group to be converted to a thiocarbamate, thiocarbonate or a xanthate.[161] As the formation of xanthates requires the use of highly toxic carbon disulfide, thiocarbamates and thiocarbonates were

investigated initially. Hence, from the ester **2.57**, the thiocarbamate **2.58** and *O*-phenyl thiocarbonate **2.59** (*Scheme 2.20*) were synthesised in good yields using methods by Burns *et al.*[140] and Kobayashi *et al*.[162]

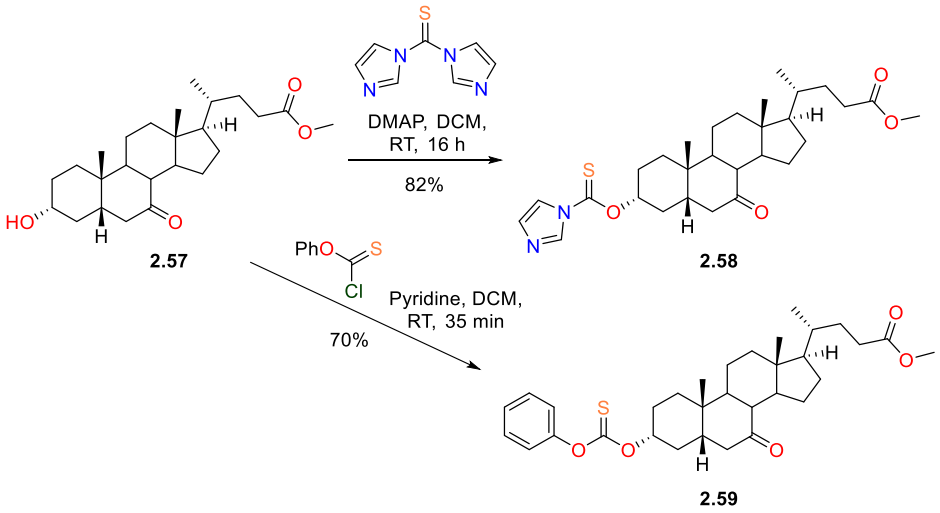

*Scheme 2.20 - Synthesis of Thiocarbamate **2.56** and Thiocarbonate **2.57***

With the thiocarbamate (**2.58**) and thiocarbonate (**2.59**) in hand, deoxygenation conditions were tested (*Table 2.1*). Deoxygenation of thiocarbamate **2.58** was first attempted using a procedure adapted from one by Barton and coworkers, with triethylsilane and BPO.[160] Regardless of reaction times, equivalents of reagent or volumes of solvents used, all reactions led to either a low yield of the impure desired product, **2.60** (*Scheme of Table 2.1*), or degradation of the starting material (Entries 1-3, *Table 2.1*). Deoxygenation of **2.58** was also attempted using Burns and coworkers' conditions with Bu_3SnH (Entry 4, *Table 2.1*), but formed multiple products and only a trace of **2.60**. A triethylborane-mediated deoxygenation reaction was then attempted on **2.58** (Entry 5, *Table 2.1*) using a procedure adapted from one used in the total synthesis of Daphnodorin A by Yuan and coworkers.[163] A low yield of **2.60** was isolated after purification though, likely due to the formation of multiple (unidentified) products in the reaction mixture.

Deoxygenation test reactions then moved onto the thiocarbonate **2.59** (*Table 2.1*). When attempting deoxygenation with triethylsilane in toluene or neat triethylsilane (Entries 6 and 7, *Table 2.1*), good yields of **2.60** were achieved after purification of the crude material. Successful deoxygenation was confirmed with the x-ray crystal structure of **2.60**, shown in *Figure 2.13.* Deoxygenation with triethylborane was also attempted on **2.59** (Entry 8, *Table 2.1*), but proved unsuccessful, with no reaction observed after stirring for 18 h at room temperature. Subsequent deoxygenation reactions on fluorinated substrates hence utilised the thiocarbonate group with triethylsilane and BPO.

Table 2.1 - Barton-McCombie Test/Optimisation Conditions and Results

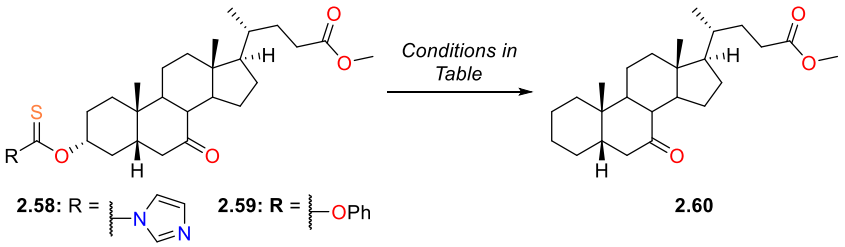

Entry	Starting Material	Conditions	Isolated Yield of 2.60 (Comments)
1	**2.58**	Et_3SiH (10 equiv), BPO (0.5 equiv), Toluene 3.3 mL/100 mg, 110 °C, 18 h	~22% (Impure[1,3])
2	**2.58**	Et_3SiH (15 equiv), BPO (0.8 equiv), Toluene 1 mL/100 mg, 120 °C, 2 h	~30% (Impure[1,3])
3	**2.58**	Et_3SiH (40 equiv), BPO (0.6 equiv), 120 °C, 1.5 h	N/A (Degradation of **2.58** observed[1-3])
4	**2.58**	Bu_3SnH (4 equiv), AIBN (0.2 equiv), Toluene 2.4 mL/100 mg, 120 °C, 4 h	N/A (Multiple unidentified products formed[1-3])
5	**2.58**	BEt_3 (10 equiv), MeOH/H_2O 1:1 (~30 equiv), THF 2.5 mL/100 mg, RT, 75 min	16% (Multiple unidentified products formed[1-3])
6	**2.59**	Et_3SiH (15 equiv), BPO (0.6 equiv), Toluene 1 mL/100 mg, 120 °C, 1.5 h	48%
7	**2.59**	Et_3SiH (40 equiv), BPO (0.4 equiv), 120 °C, 1 h	~60% (Trace aromatic impurities present[1])
8	**2.59**	BEt_3 (10 equiv), MeOH/H_2O 1:1 (~30 equiv), THF 2.5 mL/100 mg, RT, 18 h	N/A (No reaction observed[3])

[1]As shown by analysis of ^1H NMR spectrum of crude material; [2]As shown by analysis of the Mass Spectrum of the crude material; [3]As shown by TLC analysis

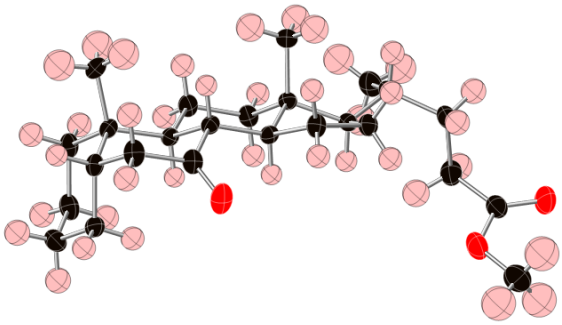

*Figure 2.13 - X-Ray Crystal Structure of **2.60***

The mechanism of deoxygenation of thiocarbonates with triethylsilane and dibenzoyl peroxide is stated to follow the same pathway as radical deoxygenations with tributyltin hydride.[159,160,164] Hence, *Scheme 2.21* shows the proposed deoxygenation mechanism of **2.59**.

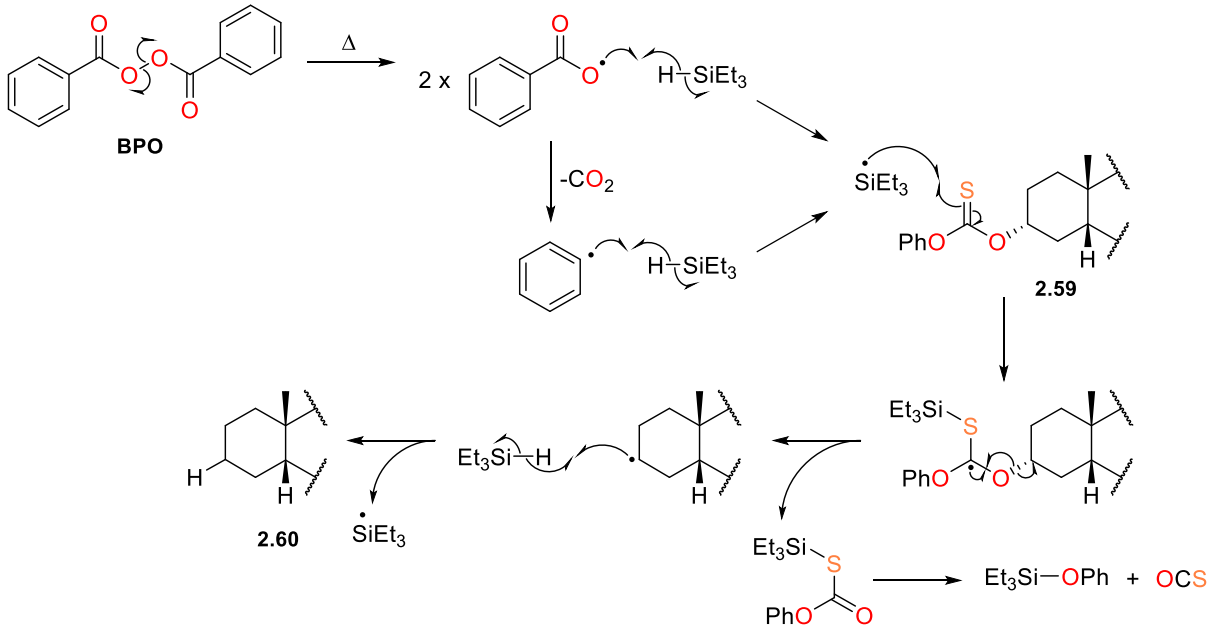

*Scheme 2.21 - Proposed Mechanism of Deoxygenation of **2.59** with Triethylsilane and Benzoyl Peroxide*

A clean sample of the deoxygenated keto ester **2.60** (*Scheme 2.22*) was treated with aqueous lithium hydroxide[147] to form a 7-oxo bile acid analogue, **2.61** (*Scheme 2.22*).

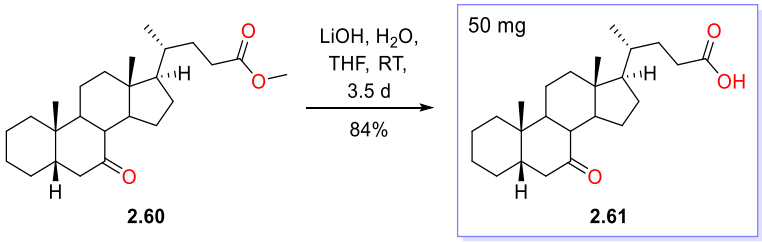

*Scheme 2.22 - Methyl Ester Saponification of **2.60***

2.4.2 Synthesis of 7,7-Difluoro-5β-Cholanic Acid

Following a synthetic route developed within the group for the synthesis of 7,7-difluoro LCA (**2.15**, *Scheme 2.3*), acetylation of the methyl ester **2.57** (*Scheme 2.23*) was performed using Pelliciari's procedure[135] to afford **2.62** (*Scheme 2.23*) in a good yield. The 7-ketone of **2.62** was then difluorinated with neat DAST (with heating) to give a moderate yield of the desired *gem*-difluorinated product **2.63** (*Scheme 2.23*), with ~20% inseparable fluoroalkene products. The ~80% pure product was carried through to basic global deprotection, giving the carboxylic acid **2.15** (*Scheme 2.23*), again ~80% pure. The methyl ester was then re-installed using Pelliciari's method,[135] but fluoroalkene products were still inseparable at this stage of the synthetic route. The impure product was treated with *m*-CPBA, and following purification by flash chromatography, **2.64** (*Scheme 2.23*) was cleanly isolated in a good yield from **2.15**.

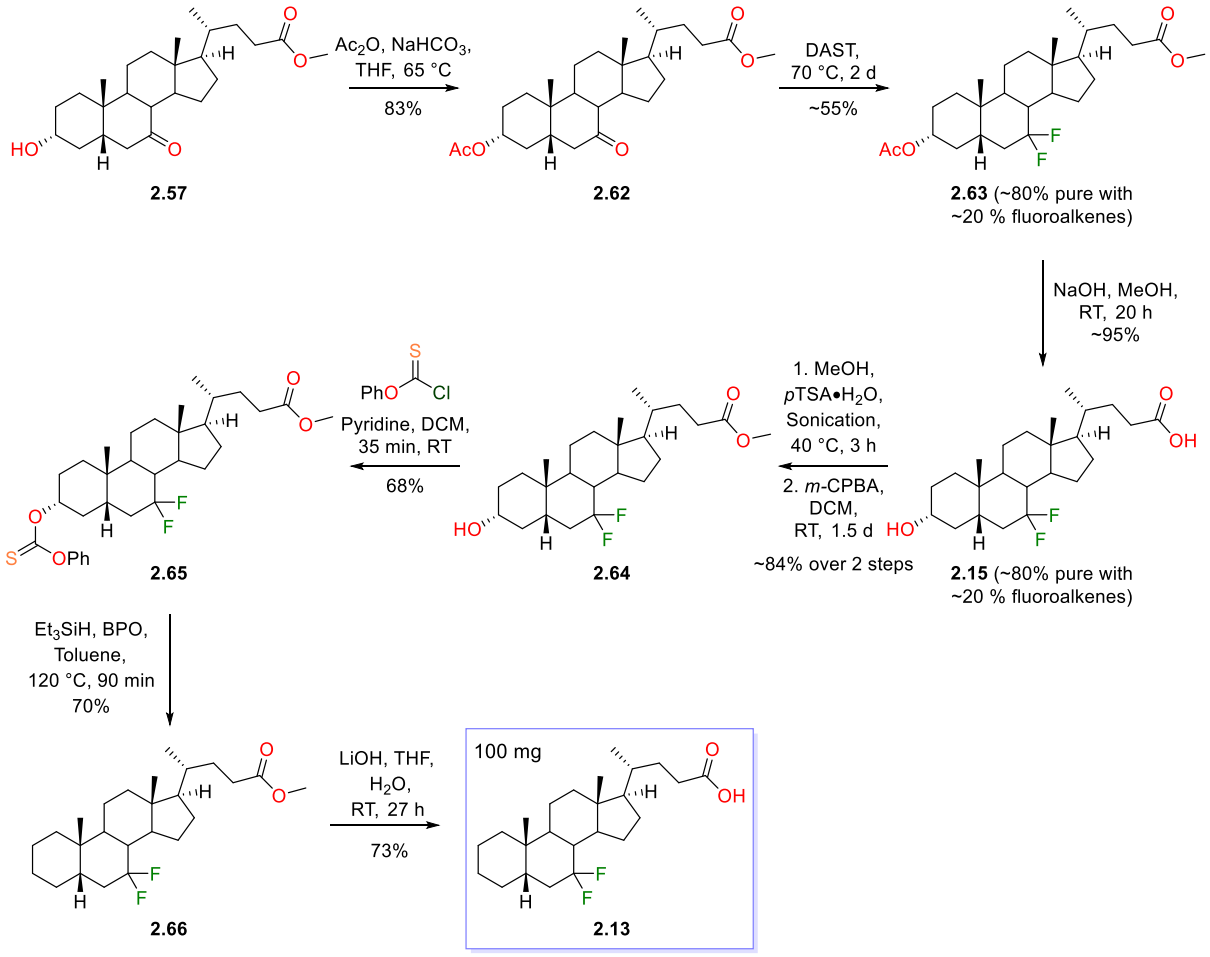

*Scheme 2.23 - Synthesis of **2.13***

Using the previously optimised conditions for alcohol deoxygenation, the 3α-hydroxy of **2.64** was removed by a Barton-McCombie reaction *via* the *O*-phenyl thiocarbonate **2.65** (*Scheme 2.23*). Heating of the thiocarbonate with triethylsilane and BPO gave the 7,7-difluoro methyl ester **2.66** (*Scheme 2.23*) in a 48% yield over two steps. The methyl ester of **2.66** was then saponified under

mild basic conditions[147] to obtain the desired A-ring deoxygenated, 7,7-difluoro bile acid **2.13** (*Scheme 2.23*), in an approximate 12% yield from the methyl ester **2.57**. Both the A-ring deoxygenated 7,7-difluoro methyl ester (**2.66**) and carboxylic acid (**2.13**) crystallised, with their x-ray crystal structures shown in *Figure 2.14* and *Figure 2.15*.

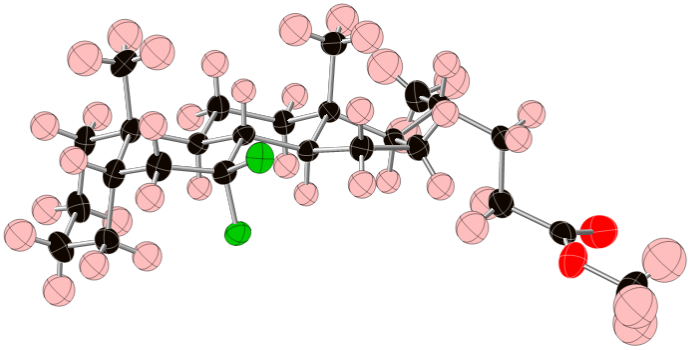

*Figure 2.14 - X-Ray Crystal Structure of **2.66***

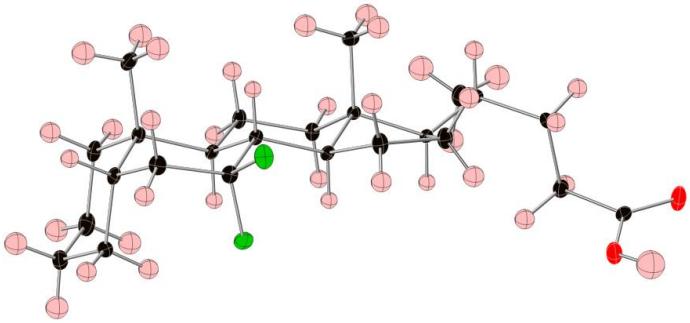

*Figure 2.15 - X-Ray Crystal Structure of **2.13***

2.4.3 Towards the Synthesis of 6,6,7,7-Tetrafluorinated Bile Acids

Using an electrophilic fluorination procedure previously utilised within the group (adapted from a method by Sepe *et al.*[149]), synthesis towards the 6,6,7,7-tetrafluorinated analogues **2.14** and **2.16** (*Scheme 2.3*) commenced with Selectfluor®-mediated fluorination of **2.57** via a silyl enol ether, **2.67** (*Scheme 2.24*). The 6α- and 6β-monofluorinated ketones **2.68** and **2.69** (*Scheme 2.24*) were isolated in good yields from **2.65**. To form the 6,6-*gem*-difluoro intermediate required, the 6β-fluoro ketone **2.69** was treated with LDA and TMSCl to form the fluoro silyl enol ether **2.70** (*Scheme 2.24*). After an aqueous workup, a mixture of the silyl enol ether **2.70** and 6β-fluoro starting material **2.69** was isolated.

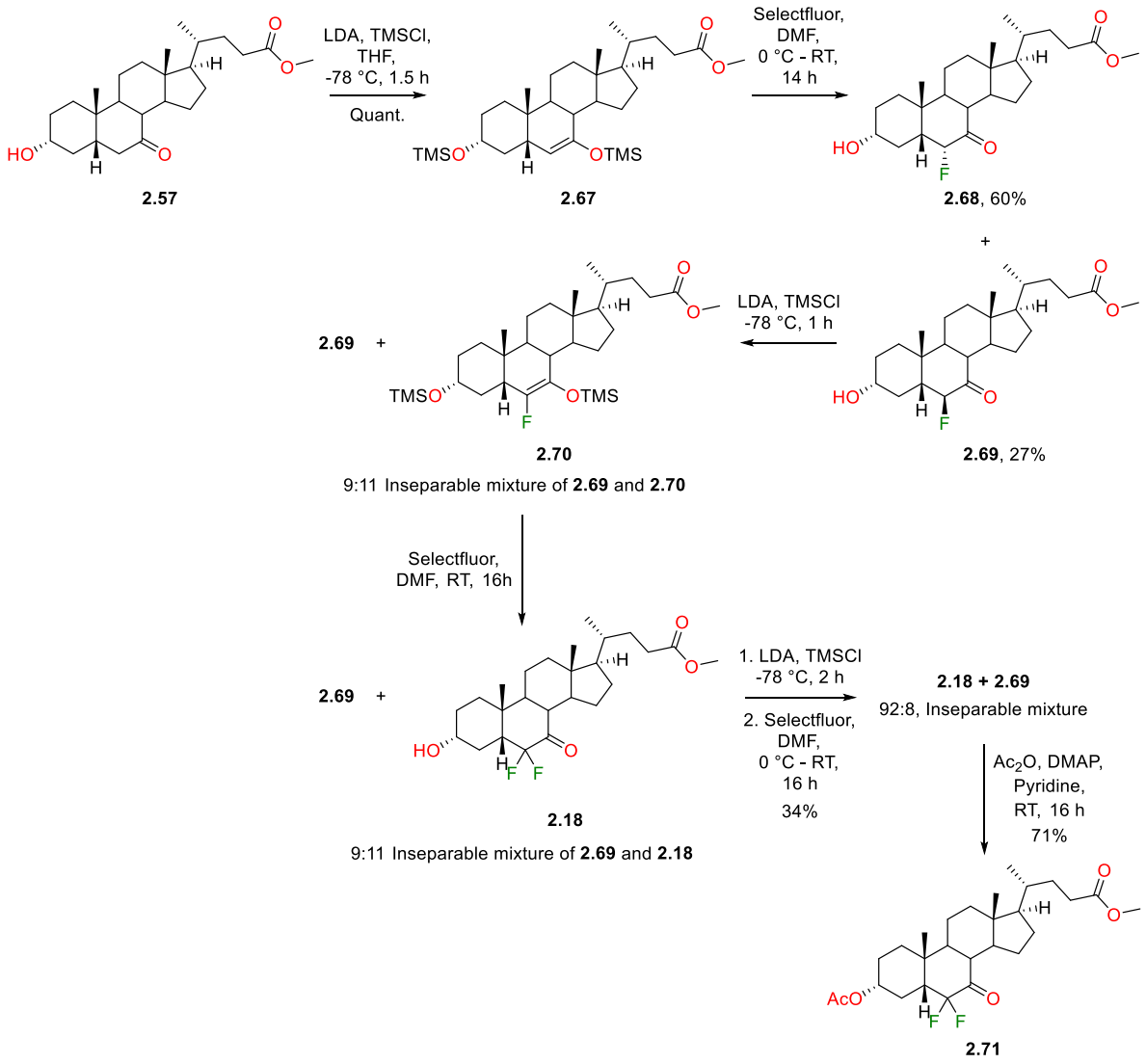

*Scheme 2.24 - Synthesis of the Intermediate **2.71***

Due to the instability of silyl enol ethers, the mixture was fluorinated with Selectfluor® to give an 11:9 mix of the desired difluoro ketone, **2.18** (*Scheme 2.24*), and the 6β-fluoro ketone **2.69**. The two ketones were inseparable by flash chromatography, thus the mixture was reacted with LDA and TMSCl to consume the remaining monofluorinated material, with twice the original reaction time to maximise conversion. The resulting crude material was then treated with Selectfluor® to give a 92:8 mix of **2.18** and **2.69** in a 34% yield from **2.69** (*Scheme 2.24*)**.** The mixture was acetylated with the procedure by Omura *et al.*,[49] allowing separation of the two ketones by flash chromatography. The 3α-acetoxy ester **2.71** was cleanly afforded in a 71% yield (*Scheme 2.24*).

Deoxofluorination of the 7-ketone of **2.71** was then attempted (*Table 2.2*). When first attempting the reactions on **2.71**, it was not known whether the 6,6-difluoro moiety would hinder fluorination of the 7-ketone (due to the steric hindrance around the ketone and potential repulsion from the polar fluorine atoms, *Figure 2.16*) or aid fluorination due to enhancement of the δ+ of the ketone. The first attempt at fluorination of **2.71** used neat DAST, stirred at room temperature (Entry 1, *Table*

2.2). After 6d, no reaction was observed on spectral analysis of the reaction mixture by ^{1}H and ^{19}F NMR. The second attempt at difluorination again utilised neat DAST, but with heating at 50 °C (Entry 2, *Table 2.2*). However, no formation of the tetrafluorinated compound **2.72** (*Scheme of Table 2.2*) was observed after 6 d of heating.

Reactions of **2.71** with neat DAST were then attempted with addition of Lewis Acids, BF_3•Et_2O and catalytic HF•pyridine. No reaction was observed following the addition of BF_3•Et_2O (Entry 3, *Table 2.2*), likely due to the probable *in situ* formation of XtalFluor-E®, a fluorinating reagent which is less reactive than DAST towards steroidal ketones. On addition of catalytic HF•pyridine (Entry 4, *Table 2.2*), no reaction occurred. Despite heating the HF•pyridine reaction, the formation of **2.72** was not observed by NMR spectral analysis. In an attempt to force the reaction as much as we (safely) could with DAST, a fifth reaction was attempted with heating at 80 °C overnight, but yet again, **2.72** was not observed to have formed (Entry 5, *Table 2.2*).

*Table 2.2 - Attempted Difluorination of **2.71***

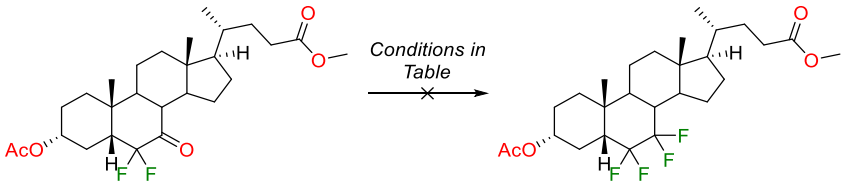

2.71 **2.72**

Entry	Fluorination Conditions	Result
1	DAST, RT, 6 d	No reaction[1]
2	DAST, 50 °C, 6 d	No reaction[1]
3	DAST, BF_3•Et_2O, RT, 3 d	No reaction[1]
4	DAST, HF•Pyridine, RT for 3 d then 50 °C for 1 d	No reaction[1]
5	DAST, 80 °C, 18 h	No reaction[1]
6	Fluolead™, HF•Pyridine, Toluene, 100 °C, 20 h	No reaction[1]

[1]On analysis of the ^{1}H and ^{19}F NMR spectra of the crude material

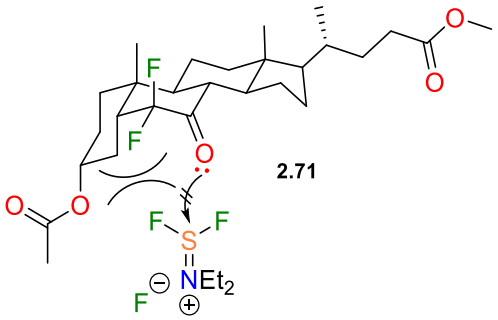

Figure 2.16 - Repulsion of DAST by 6-CF_2

With the lack of success using DAST, another highly reactive deoxofluorination reagent was investigated, 4-*tert*-butyl-2,6-dimethylphenylsulfur trifluoride, Fluolead™ (*Figure 2.17*). Fluolead™ was synthesised by Umemoto and coworkers in 2010 in an attempt to develop a new deoxyfluorination reagent which had a higher thermal stability than DAST and was highly effective at fluorinating alcohols, aldehydes, ketones and carboxylic acids. When used with HF•pyridine, Fluolead has been shown to difluorinate a range of ketones in good yields with minimal fluoroalkene formation.[165]

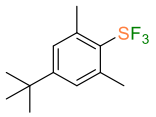

Figure 2.17 - Fluolead™

Previously within the group, deoxyfluorination of a ketone at the 12-position of a bile acid ester was attempted with Fluolead™ and HF•pyridine, but after stirring for 5 d at room temperature, no difluorinated material was isolated. As the decomposition temperature of Fluolead™ is over 200 °C,[165] it was deemed safe to heat a reaction containing it to 100 °C. Hence, difluorination of **2.71** was attempted with Fluolead™ and HF•pyridine in toluene (Entry 6, *Table 2.2*). After 20 h of heating at 100 °C, ^{1}H and ^{19}F NMR spectral analysis showed no reaction had occurred.

With the lack of success testing some the harshest reaction conditions for difluorination, the reaction was abandoned. Whilst 7-keto deoxofluorination of **2.71** with SF_4 may be possible (as it is a significantly stronger fluorinating reagent than DAST), the reaction was not attempted because SF_4 is a highly toxic gas which our group does not have the equipment or resources to handle.

Aside from attempted deoxodifluorination, global deprotection of **2.71** was performed using lithium hydroxide to yield the 6,6-difluoro bile acid analogue, **2.73** (*Scheme 2.25*), in a quantitative yield.

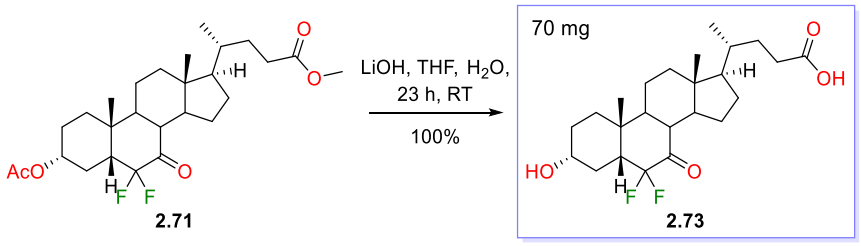

*Scheme 2.25 - Deprotection of **2.71***

Following unsuccessful deoxofluorination of the 7-ketone, an alternative route to install the 7,7-difluoro moiety was investigated. An advanced intermediate bearing a ketone at the 6-position and a 7α-fluoro, **2.74** (*Scheme 2.26*), was available within the group in a low quantity, isolated in previous attempts at the synthesis of 7-fluorinated compounds. Direct electrophilic fluorination of **2.74** was attempted on a small scale with Selectfluor® but after 4 d of stirring at room temperature, the desired difluorinated compound **2.75** (*Scheme 2.26*) was not isolated. Fluorination of **2.74** was also attempted *via* a silyl enol ether, but the reaction with LDA and TMSCl failed to yield the desired 7-fluoro silyl enol ether **2.76** (*Scheme 2.26*), as exemplified by the lack of fluoroalkene peaks (typically around -135 ppm) observed in the ^{19}F NMR of the crude reaction material.

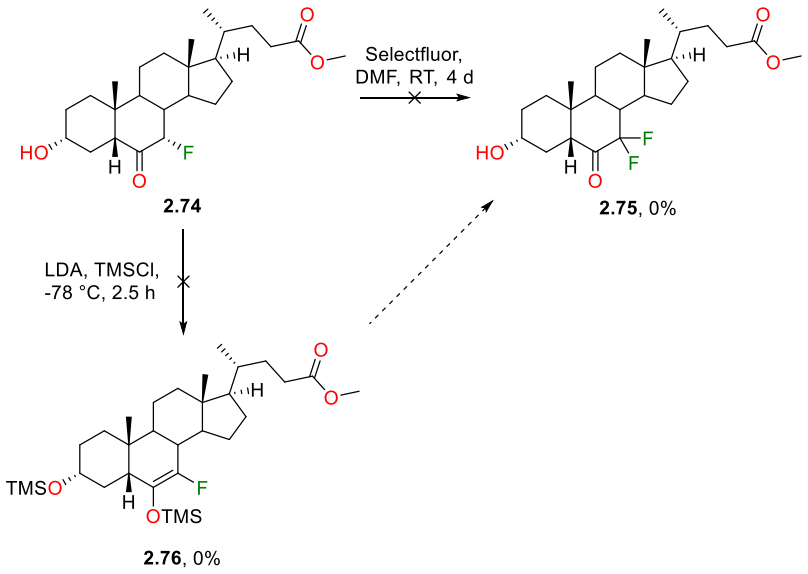

*Scheme 2.26 - Attempted Fluorination and Silyl Enol Ether Formations on Intermediate **2.74***

2.5 Synthesis of Analogues from Deoxycholic Acid

2.5.1 Synthesis of 12,12-Difluoro-5β-Cholanic Acid

Starting from DCA (**1.5**, *Scheme 2.27*), synthesis of the 12,12-difluoro A-ring deoxygenated bile acid **2.19** (*Scheme 2.4*) began with methyl ester formation and 3-selective acetylation, using Pelliciari and coworkers' methods.[135] A 78% yield of the 3α-acetoxy ester **2.79** (*Scheme 2.27*) was achieved, along with a low yield of the diacetoxy ester **2.78** (*Scheme 2.27*). Oxidation of **2.79** using a procedure by Jiang *et al*.,[166] with NaClO and acetic acid, gave the 12-ketone **2.80** (*Scheme 2.27*) in a high yield. Difluorination of **2.80** with neat DAST at 50 °C for 11 d then afforded the 12,12-difluoro ester **2.81** (*Scheme 2.27*), ~90% pure, in a moderate yield. Fluoroalkene products were not observed to have formed in the reaction, based on analysis of the ^{1}H and ^{19}F NMR spectra of the crude material prior to purification. Basic global deprotection of **2.81** cleanly gave 12,12-difluoro LCA (**2.21**, *Scheme 2.27*), the x-ray crystal structure of which is shown in *Figure 2.18*.

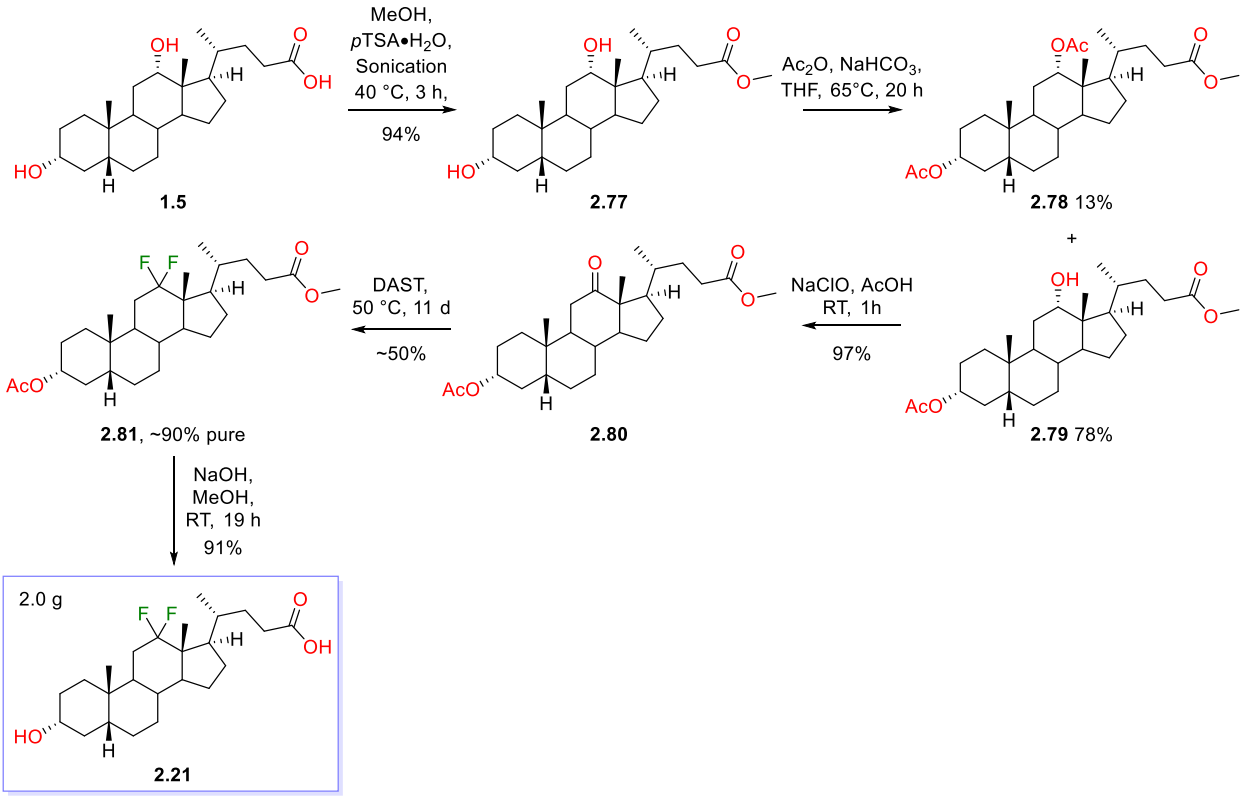

*Scheme 2.27 - Synthesis of **2.21***

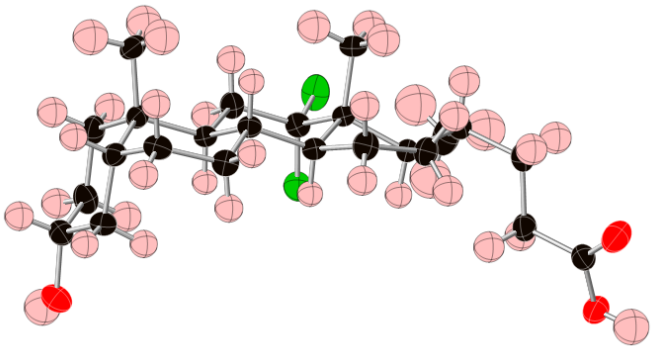

*Figure 2.18 - X-Ray Crystal Structure of **2.21***

The carboxylic acid of **2.21** was re-protected as a methyl ester, giving the intermediate **2.82** (*Scheme 2.28*), which, after treatment with *O*-phenyl chlorothionoformate, gave the thiocarbonate **2.83** (*Scheme 2.28*) ~90% pure with aromatic impurities. A Barton-McCombie deoxygenation with triethylsilane and BPO followed, giving a good yield of the A-ring deoxygenated ester **2.84** (*Scheme 2.28*) again, ~90% pure after flash chromatography purification, with co-eluting aromatic impurities. Saponification of the methyl ester of **2.84** and purification by column chromatography gave the 12,12-difluoro carboxylic acid **2.19** (*Scheme 2.28*), in an overall yield of approximately 10% from DCA. The structure of **2.19** was confirmed by x-ray crystallographic analysis, shown in *Figure 2.19*.

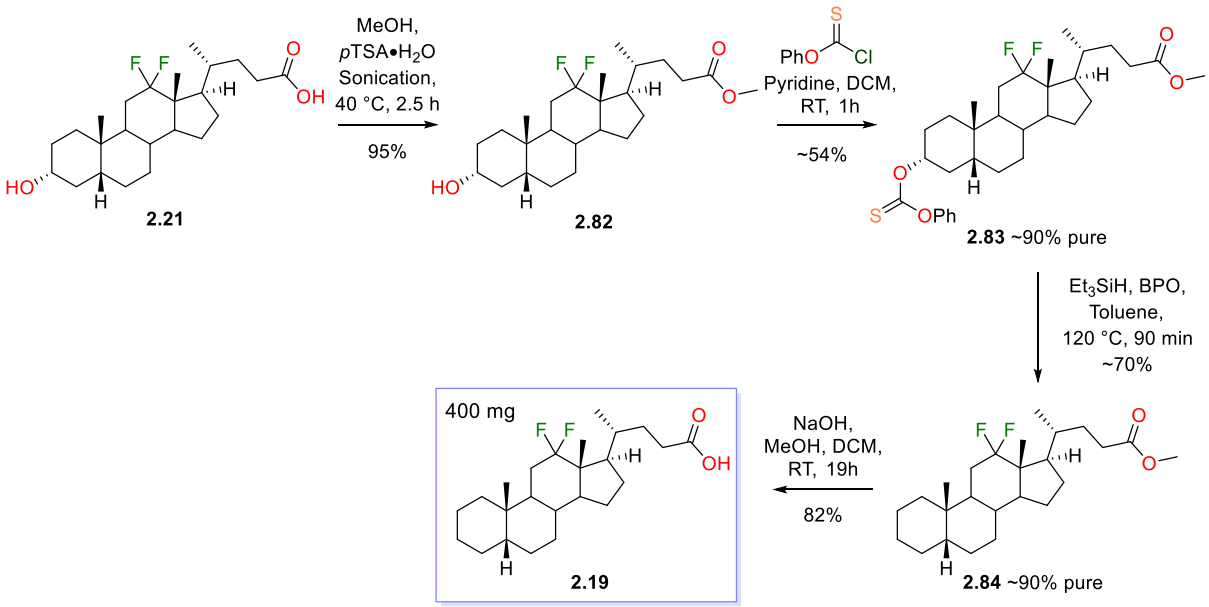

*Scheme 2.28 - Synthesis of **2.19***

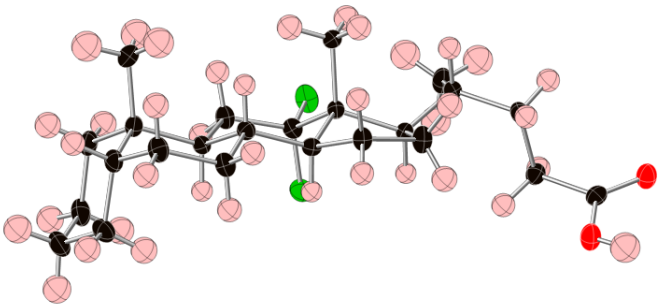

*Figure 2.19 - X-Ray Crystal Structure of **2.19***

The 3-ketone analogue **2.86** (*Scheme 2.29*) was also isolated following bleach oxidation of the intermediate **2.82** (*Scheme 2.29*) and saponification of the methyl ester under mild conditions, in a 66% yield over two steps.

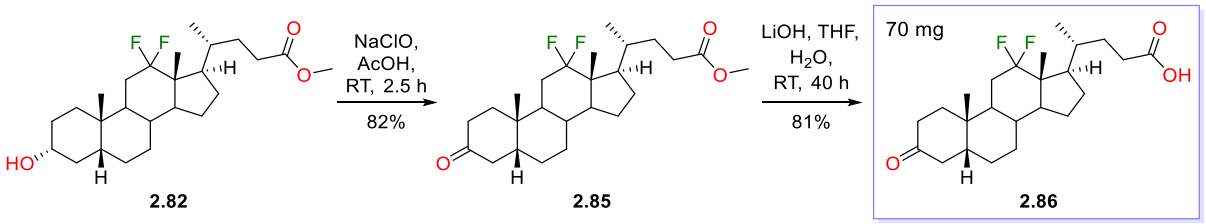

*Scheme 2.29 - Synthesis of **2.86***

2.5.2 Synthesis of 3,3,12,12-Tetrafluoro-5β-Cholanic Acid

Starting from the previously synthesised methyl ester of DCA (**2.77**, *Scheme 2.30*), bis-oxidation of the 3α- and 12α-hydroxy groups using the method by Jiang *et al*.[166] gave the diketone **2.22** in a 91% yield (*Scheme 2.30*). At this stage, tetrafluorination of both ketones could have been carried out with neat DAST and heat, but previous difluorination reactions of a 3-ketone with neat DAST has led to significant formation of fluoroalkene by-products, which require derivatisation to allow separation by column chromatography (*Scheme 2.9*). When using 3 equiv of DAST with catalytic HF•Pyridine in DCM, only traces of fluoroalkenes have been shown to form (*Scheme 2.11*), hence, the mild difluorination conditions were used on **2.22**, giving **2.87** (*Scheme 2.30*) in a 68% yield. Difluorination of the 12-ketone of **2.87** was subsequently carried out using neat DAST at 50 °C, giving the tetrafluoro ester **2.88** (*Scheme 2.30*) in a good yield, followed by methyl ester hydrolysis to afford the 3,3,12,12-tetrafluorinated target compound **2.20** (*Scheme 2.30*). The synthesis of carboxylic acid **2.20** was achieved in a 40% overall yield from deoxycholic acid, and readily crystallised (*Figure 2.20*).

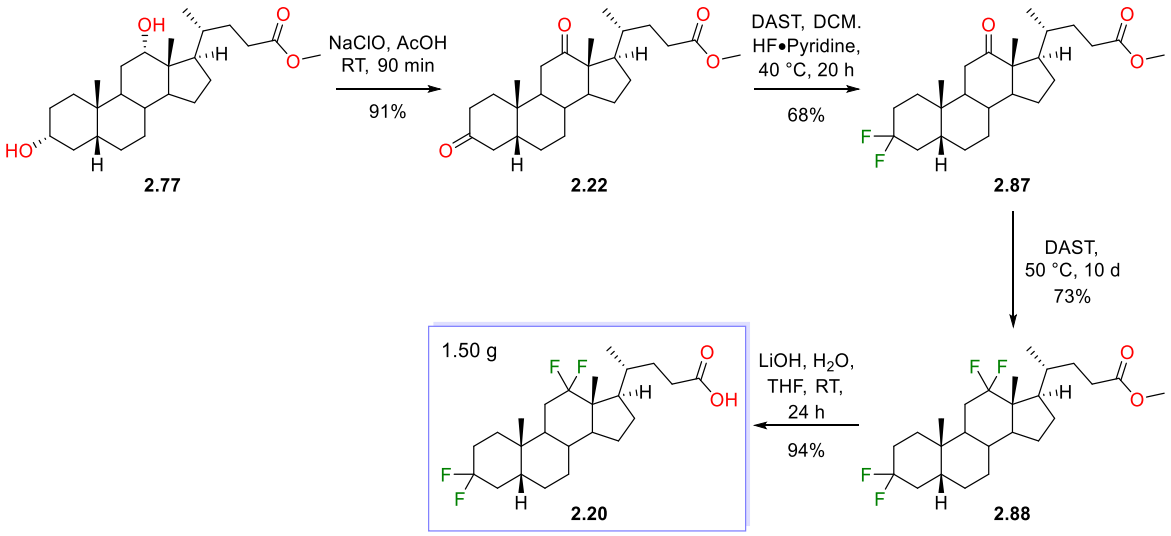

*Scheme 2.30 - Synthesis of **2.20***

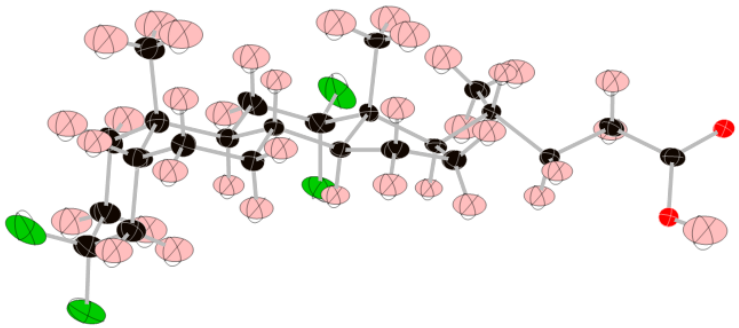

*Figure 2.20 - X-Ray Crystal Structure of **2.20***

A small quantity of **2.87** was taken for methyl ester saponification, giving the carboxylic acid **2.89** (*Scheme 2.31*). Both the 3,3-difluoro-12-keto ester (**2.87**) and carboxylic acid (**2.89**) crystallised, with their respective x-ray crystal structures shown in *Figure 2.21* and *Figure 2.22*.

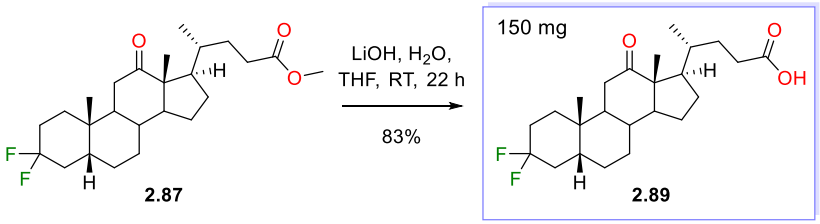

*Scheme 2.31 - Synthesis of **2.87***

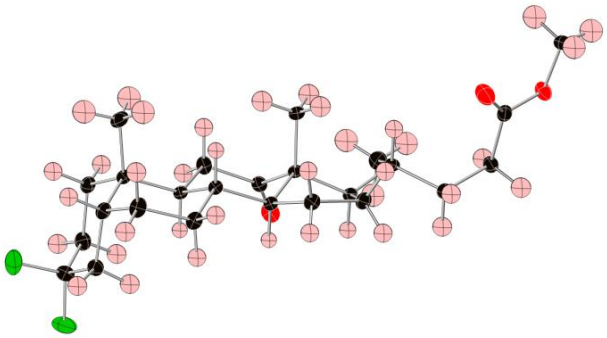

*Figure 2.21 - X-Ray Crystal Structure of **2.87***

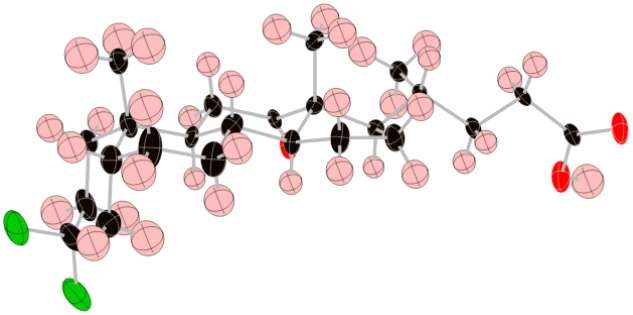

*Figure 2.22 - X-Ray Crystal Structure of **2.89***

2.6 Conclusion

A total of eighteen *gem*-difluorinated bile acid analogues (*Figure 2.23*) were synthesised *via* nucleophilic or electrophilic fluorination reactions.

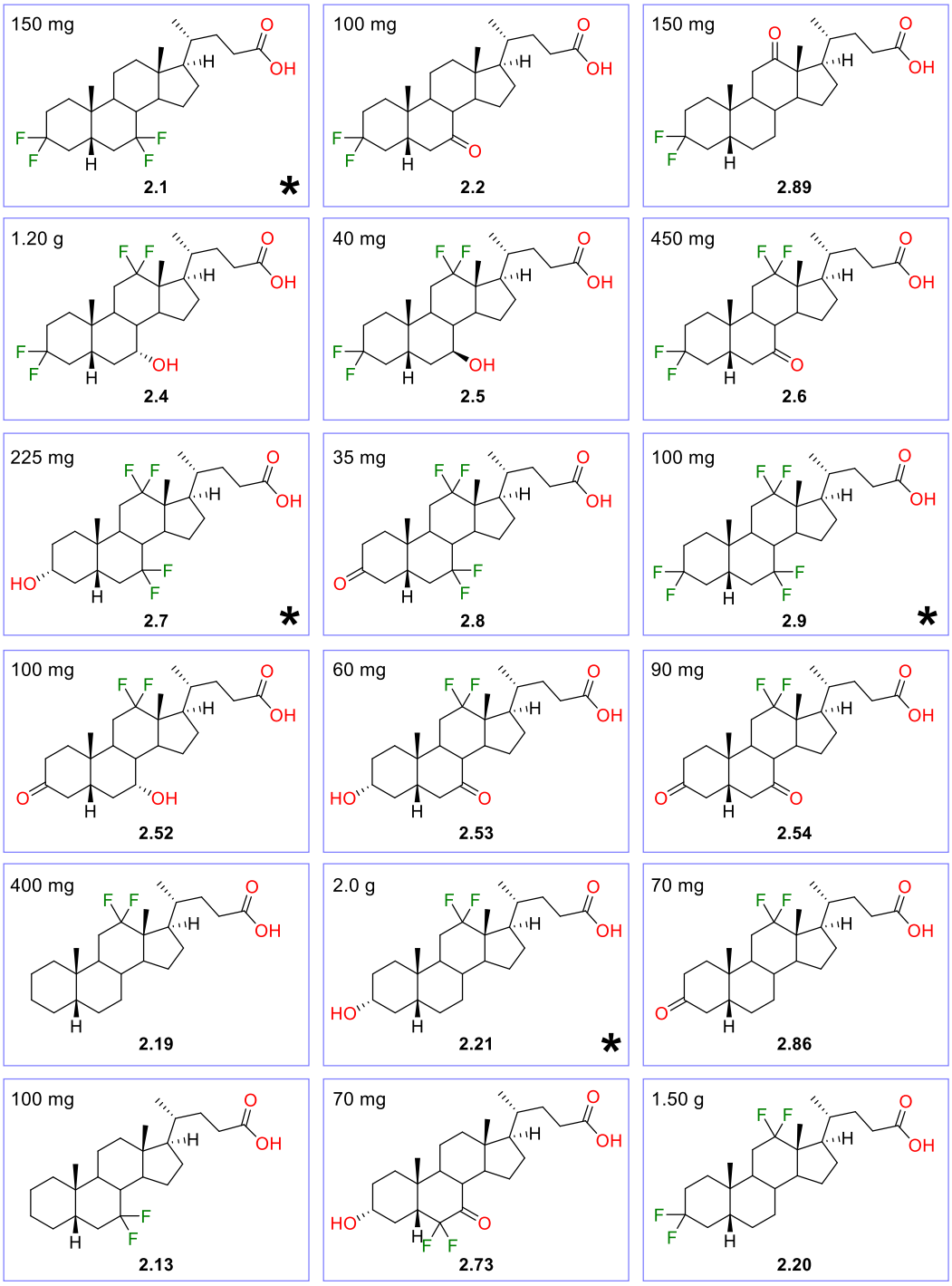

Figure 2.23 - Synthesised gem-Difluorinated Bile Acid Analogues

It is important to note that a number of fluorinated bile acid derivatives were patented by Academia Sinica in March 2017,[167] including those in *Figure 2.23* marked with an asterisk (*). All analogues in this chapter were synthesised prior to publication of the patent.

The target compounds were successfully synthesised from the naturally occurring bile acids chenodeoxycholic acid (CDCA) and deoxycholic acid (DCA) and the advanced intermediates methyl 3α,7α-diacetoxy-12-oxo-5β-cholan-24-oate (**2.12**, *Scheme 2.2*), dehydrocholic acid (**2.11**, *Scheme 2.2*) and 7-keto LCA (**2.17**, *Scheme 2.3*), all provided by NZP UK.

The A- and B-ring *gem*-difluorinated analogues **2.1** and **2.2** (*Figure 2.23*) were synthesised from CDCA following successful esterification, oxidation, deoxofluorination and saponification reactions. Inseparable fluoroalkene by-products of the deoxofluorination reaction were removed by epoxidation and further purification. Both of the target analogues were afforded in excess of 100 mg, sufficient quantities for testing in various biological assays for the receptors FXR and TGR5, cancer and neurodegenerative diseases.

The advanced intermediate methyl 3α,7α-diacetoxy-12-oxo-5β-cholan-24-oate, **2.12** (synthesised in industry from cholic acid) afforded the A- and C-ring *gem*-difluorinated analogues **2.4**, **2.5**, **2.6** and **2.52** (*Figure 2.23*), following deoxofluorination, saponification, esterification, regioselective oxidation and reduction reactions. Despite the low yield of the stereoselective reduction of **2.6** to form **2.5**, the analogues were obtained in quantities of 30 mg to 1.20 g, sufficient for biological testing.

Sufficient quantities of the B- and C-ring *gem*-difluorinated analogues **2.7**, **2.8**, **2.53** and **2.54** (*Figure 2.23*) were also yielded, synthesised from **2.12** as a result of successful deoxofluorination, saponification, esterification, regioselective acetylation and oxidation reactions.

The hexafluorinated analogue **2.9** (*Figure 2.23*) was synthesised from dehydrocholic acid following basic methyl esterification, deoxofluorination and saponification reactions. Despite a low yielding fluorination reaction, 100 mg of the analogue was afforded.

The Barton-McCombie deoxygenation reaction with triethylsilane and dibenzoyl peroxide was optimised for a 7-oxo bile acid ester, and the highest yielding conditions were utilised in the synthesis of the A-ring deoxygenated analogues **2.13** and **2.19** (*Figure 2.23*), synthesised from 7-keto LCA and DCA respectively. Both analogues were isolated in sufficient quantities for biological testing. The 12,12-difluoro analogues **2.21** and **2.86** (*Figure 2.23*) were also obtained during the synthesis of **2.19**, following esterification, oxidation, deoxofluorination and saponification reactions.

DCA was also used to synthesise the 3,3,12,12-tetrafluorinated target analogue **2.20** (*Figure 2.23*) in a high quantity. The 3,3-difluoro-12-oxo analogue **2.89** (*Figure 2.23*) was isolated from saponification of an intermediate in the synthesis of **2.20**.

Synthesis of the 6,6,7,7-tetrafluorinated targets **2.14** and **2.16** (*Scheme 2.3*) was attempted, but deoxofluorination of a ketone next to a 6-CF_2 moiety proved to be challenging, yielding no tetrafluorinated products. A synthetic route *via* electrophilic difluorination was also investigated but was unsuccessful. Currently, a viable route to the 6,6,7,7-tetrafluoro analogues is not known.

During the synthesis of the *gem*-difluorinated analogues, x-ray crystal structures of seventeen bile acid derivatives were obtained, allowing confirmation of product structures and reaction outcomes.

Chapter 3 Synthesis of Mono- and (Non-Geminal) Difluorinated Analogues

3.1 Targeted Mono- and (Non-Geminal) Difluorinated Analogues

With the synthesis of eighteen *gem*-difluorinated target compounds described in the previous chapter, the synthesis of mono- and non-geminal difluorinated bile acid analogues is described here.

3.1.1 4β,6α-Difluorinated Target Analogues

Firstly, 4β-,6α-difluorinated analogues of 5β-cholanic acid and CDCA, **3.1** and **3.2** (*Figure 3.1*), were targeted, along with 4- and 6-fluorinated carboxylic acids of intermediates formed in their synthesis.

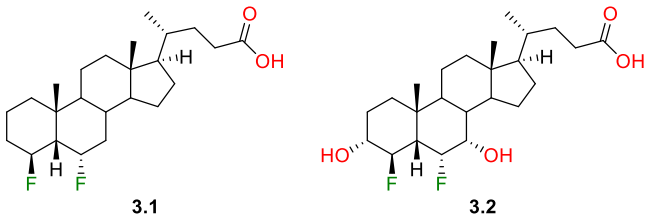

Figure 3.1 - Targeted 4β,6α-Difluorinated Analogues

The deoxygenated analogue **3.1** is of particular interest for neurodegenerative disease studies as a fluorinated analogue of 5β-cholanic acid, which, as noted, has been shown to have mitochondrial rescue effects. The 4β- and 6α-fluoro substituents are co-linear with each other (*Figure 3.2*), meaning that the C-F dipoles are aligned, which, for apolar molecules, is expected to lead to a significant decrease in lipophilicity compared to *gem*-difluorination or monofluorination. The difluorinated carboxylic acid **3.1** should therefore have a lower log*P* value than 5β-cholanic acid, and, in terms of polarity, may serve as an intermediary between 5β-cholanic acid and UDCA, which has also been observed to possess mitochondrial rescue effects.

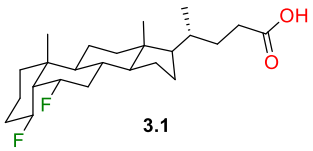

*Figure 3.2 - 3D Representation of **3.1***

4β,6α-Difluoro CDCA, **3.2**, is an intermediate in the synthesis of **3.1** but is also interesting as an analogue for testing in biological assays. The stereochemistry of the fluorine and hydroxy substituents of the A-ring of **3.2** is comparable to the conformationally restricted fluorohydrin **1.44** (*Figure 3.3*), discussed in **Sections 1.3.2.2 and 1.3.3**. Similarly, the B-ring of **3.2** is comparable to the fluorohydrin **1.39** (*Figure 3.3*). Both **1.39** and **1.44** possessed lower pK_{AHY} values than their non-fluorinated parent compounds, therefore it can be assumed that the target analogue **3.2** will have a lower hydrogen-bond donating capacity than CDCA. A lower HB-donating capacity could lead to altered biological effects of **3.2** compared to CDCA, owing to differences in binding to the active site of a biological target. Additionally, the equatorial fluorohydrin **1.44** had a lower log*P* value than its parent compound, it is therefore hypothesised that **3.2** will be less lipophilic than CDCA.

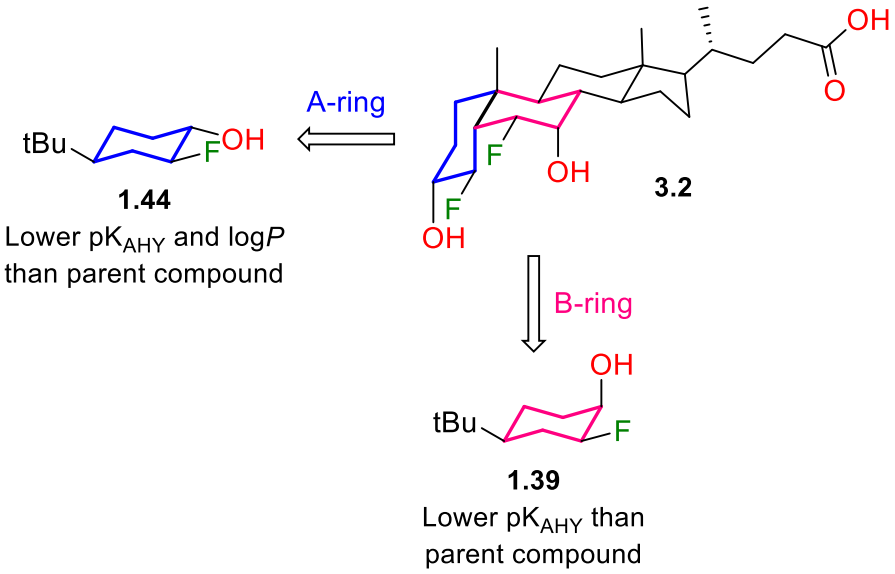

*Figure 3.3 - Comparison of **3.2** to Conformationally Restricted Fluorohydrins **1.39** and **1.44***

3.1.2 7-Fluorinated Target Analogues

A range of 7-fluorinated analogues, **3.3** to **3.10** (*Figure 3.4*) were also targeted. The analogues were of particular interest as preliminary screenings of fluorinated bile acids against FXR and TGR5 revealed that 7,7-difluoro LCA (**2.15**, *Scheme 2.23*) had moderate TGR5 activity. Also, 7β-fluoro LCA, **3.4**, was of special interest in assays for neurodegenerative diseases as it is an analogue of UDCA.

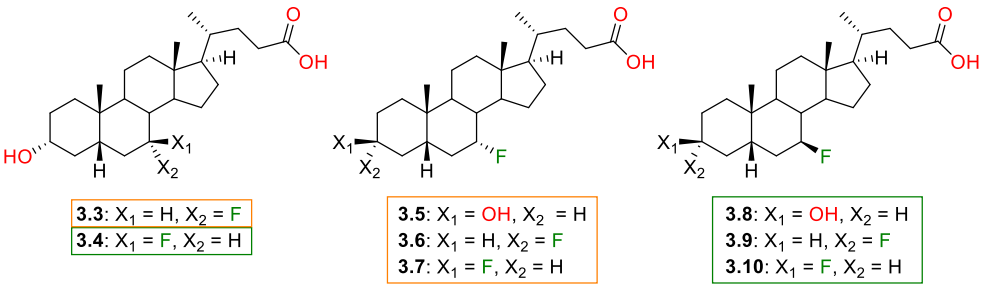

Figure 3.4 - Targeted 7-Fluorinated Analogues

Previous attempts at synthesis of compounds with 7α- and 7β-fluoro substituents within the group have been unsuccessful thus far. Nucleophilic deoxyfluorination of a 7β-hydroxy of a bile acid derivative led to a mixture of 7α- and 7β-fluoro products, which were inseparable by flash chromatography and HPLC at all stages of the synthetic route. Other investigations within the group have shown the ability to synthesise clean 7α- and 7β-fluoro products when introducing them *via* electrophilic fluorination of a 6-keto containing bile acid derivative, but deoxygenation of the ketone using numerous different procedures proved unsuccessful. It was thought that deoxygenation at the 6-position could be achieved *via* a hydroxyl group, potentially utilising a Barton-McCombie reaction.

3.2 Synthesis of 4β,6α-Difluorinated Bile Acid Analogues

3.2.1 Retrosynthetic Analysis

The retrosynthetic analysis of **3.1** and **3.2** (*Scheme 3.1*) leads to the 6α-fluoro-3-keto-7α-hydroxy ester **3.11** (*Scheme 3.1*), which could be obtained from the 6α-fluoro-7-keto ester **2.68** (*Scheme 3.1*). The ester **2.68** is synthesised from 7-keto LCA (**2.17**, *Scheme 3.1*), a derivative of CDCA, following electrophilic fluorination.

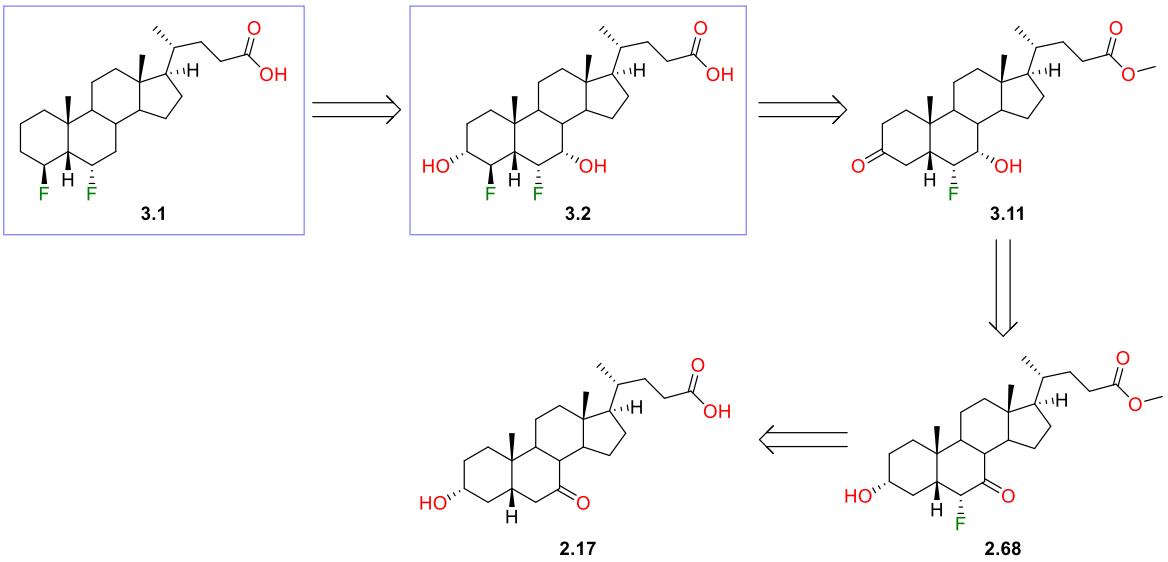

*Scheme 3.1 - Retrosynthetic Analysis of **3.1** and **3.2***

3.2.2 Synthesis of 6α-fluoro Analogues

The 6α-fluoro ester **2.68** (*Scheme 3.2*), previously synthesised in **Section 2.4.3**, was deprotected to give the analogue **3.12** (*Scheme 3.2*) in a good yield.

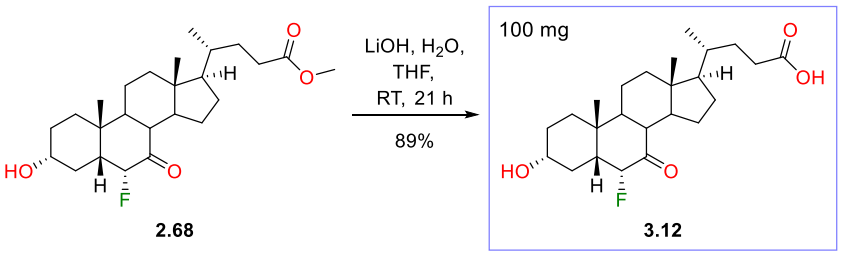

*Scheme 3.2 - Methyl Ester Saponification of **2.68***

Interestingly, treatment of the 6β-fluoro ester **2.69** (*Scheme 3.3*) with lithium hydroxide led to complete epimerisation of the axial 6β-fluoro substituent to the equatorial 6α-fluoro, giving **3.12** in a very high yield (*Scheme 3.3*).

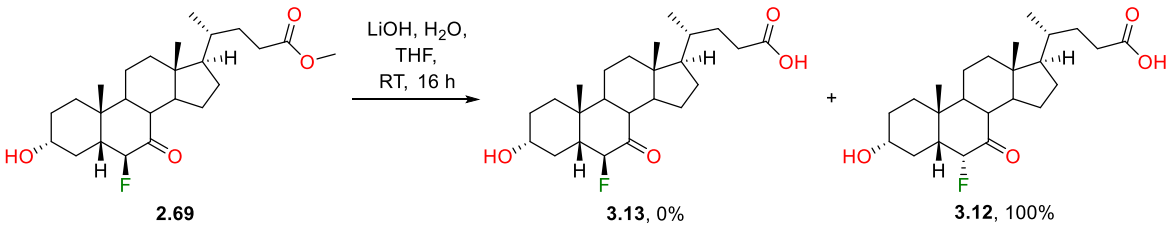

*Scheme 3.3 - Saponification/Epimerisation of **2.69***

As the 6β-fluoro ester was not required for the synthesis of **3.1** and **3.2**, epimerisation/saponification of all stock of **2.69** was carried out. The carboxylic acid of **3.12** was then re-protected as a methyl ester, yielding an ample quantity of **2.68** (*Scheme 3.4*) to be used in the synthesis of **3.1** and **3.2**.

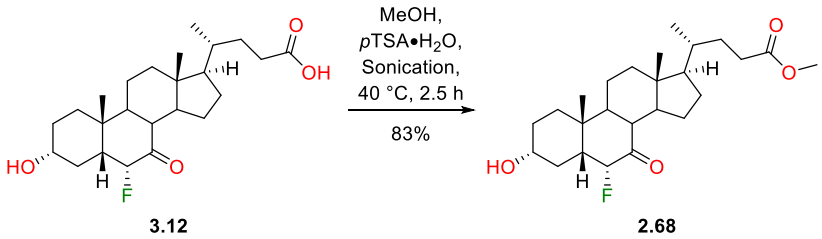

*Scheme 3.4 - Methyl Ester Formation on **3.12***

With **2.68** in hand, reduction of the 7-ketone was carried out with sodium borohydride in THF. When previously performed within the group on the same substrate, the reduction gave yields upwards of 70%. Despite this, the desired 7α-hydroxy ester **3.18** (*Scheme 3.5*) was isolated in a low yield, along with a significant mass of another compound. Upon analysis by ^{1}H NMR, the product was observed to possess a multiplet peak at 4.55 ppm (*Figure 3.5*), reminiscent of a 3β-H of a 3α-acetoxy compound. Based upon mass spectrometry and $^{1}H/^{13}C$ NMR analysis, the product was proposed to be the dimer **3.15** (*Scheme 3.5*).

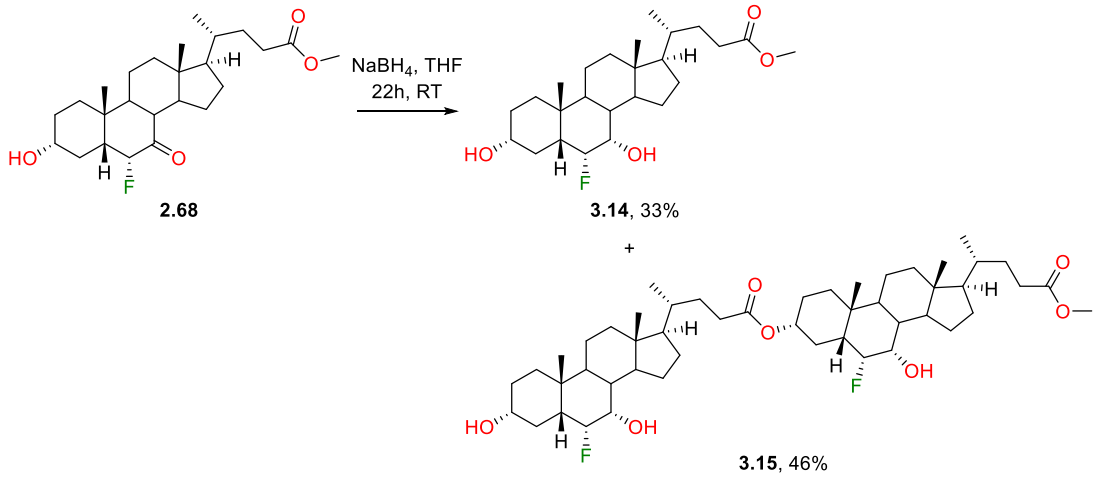

*Scheme 3.5 - Reduction of **2.68***

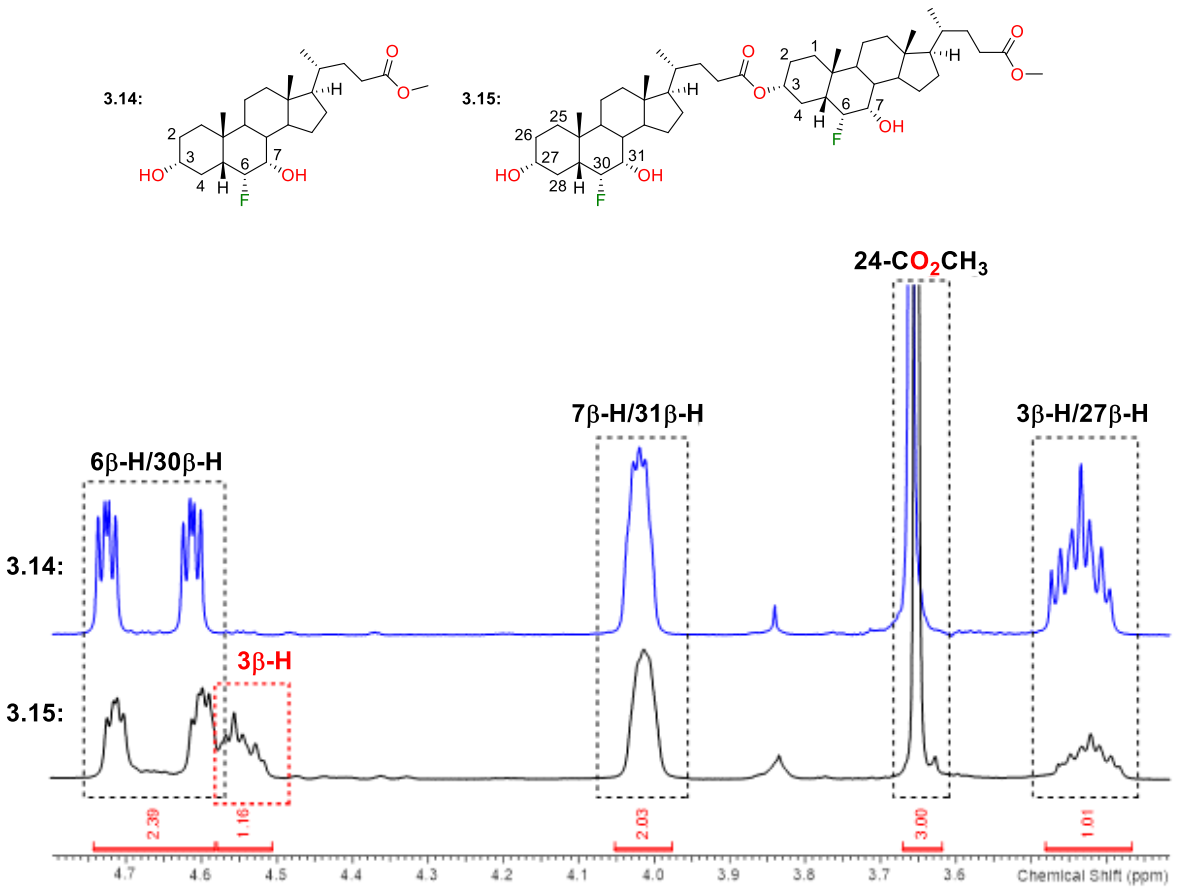

*Figure 3.5 - Section of ^{1}H NMR Spectra of **3.14** (Blue) and **3.15** (Red)*

The dimer **3.15** (*Scheme 3.6*) was readily hydrolysed under basic conditions to give the carboxylic acid **1.20** (*Scheme 3.6*) in a high yield, and after re-forming the methyl ester, **3.14** was isolated in an overall yield of 74% from the 6α-fluoro ketone **2.68**.

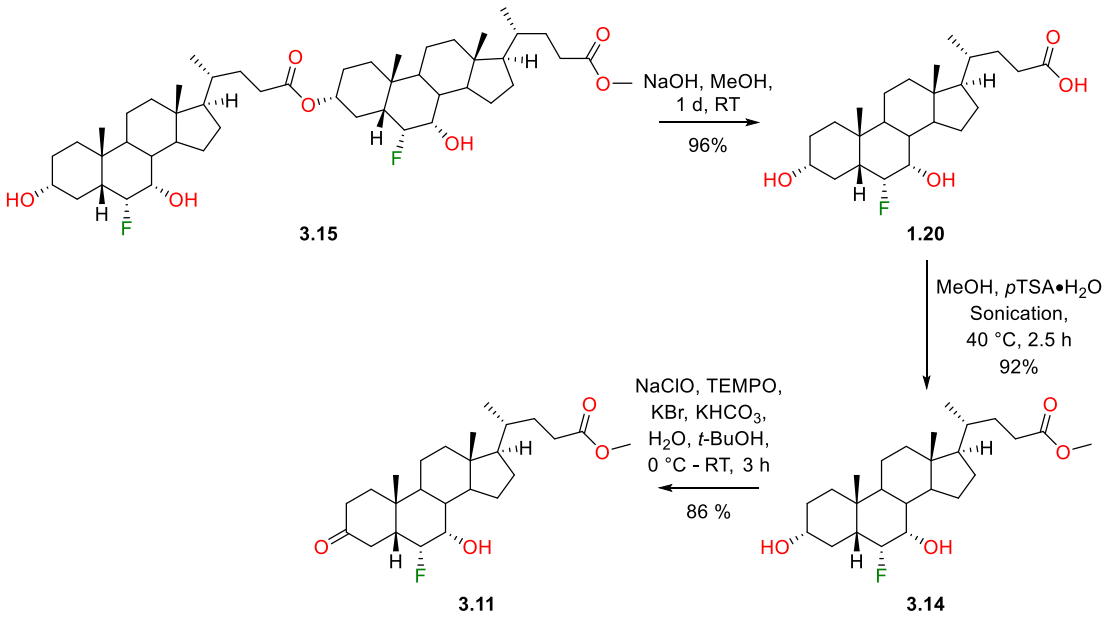

*Scheme 3.6 - Synthesis of Intermediate **3.11***

Regioselective oxidation of **3.14** using Burns and coworkers' method[140] gave **3.11** (*Scheme 3.6*), with the 3-ketone required to install a fluorine atom at the 4-position. As expected, oxidation of the 7α-hydroxy was not observed to have occurred on analysis of the crude material by ^{1}H NMR.

Prior to fluorination, the methyl ester of **3.11** was saponified with lithium hydroxide to give a good yield of the 6α-fluoro-3-keto analogue **3.16** (*Scheme 3.7*), which crystallised readily. Analysis of the x-ray crystal structure of **3.16** (*Figure 3.6*) showed an interesting and significant distortion in the A-ring.

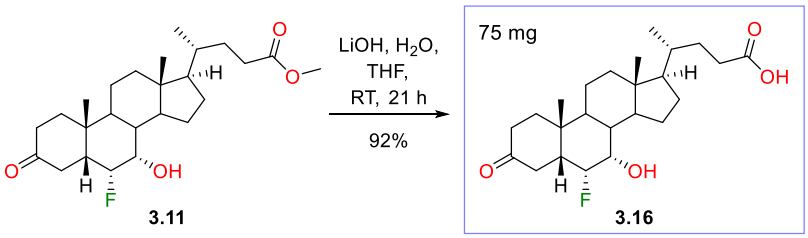

*Scheme 3.7 - Deprotection of **3.11***

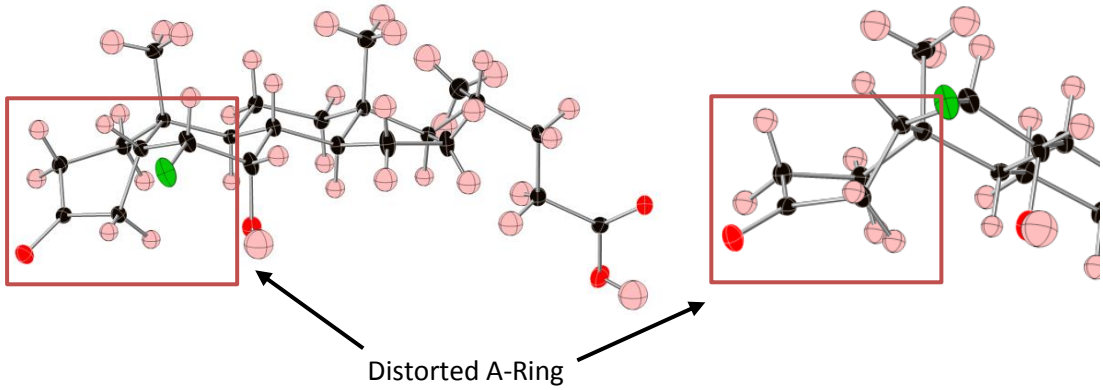

*Figure 3.6 - X-Ray Crystal Structure of **3.16***

3.2.3 Synthesis of 4β,6α-difluoro CDCA

Electrophilic fluorination of **3.11** (*Scheme of Table 3.1*) was achieved with Selectfluor in DMF with heating, a method shown previously within the group on a 3-keto bile acid ester to give high selectivity towards the 4-position over the 2-position. Initial heating of **3.11** with 1.5 equiv of Selectfluor gave a 57% yield of the desired 4β-fluoro product **3.17** (*Scheme of Table 3.1*) as part of an inseparable 9:1 mix with the 2β-fluoro product **3.18** (Entry 1, *Table 3.1*). No 4α- or 2α-fluoro products were observed to have formed on analysis of the crude reaction material by ^{1}H and ^{19}F NMR.

*Table 3.1 - Electrophilic Fluorination of **3.11***

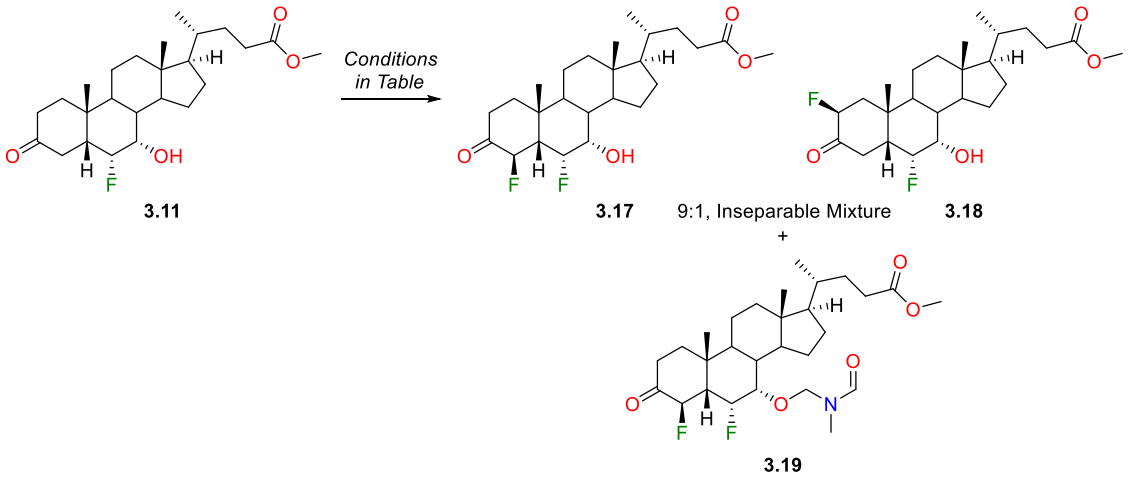

Entry	Conditions (Equiv)	Yield
1	Selectfluor (1.5), DMF, 50 °C, 16 h	**3.17**/**3.18**: 57%; **3.19**: ~15% (70% pure[1])
2	Selectfluor (1.1), DMF, 50 °C, 20 h	**3.17**/**3.18**: 60%; **3.19**: ~3%[1]

[1]As shown by analysis of ^{1}H NMR spectrum of crude material

Interestingly, on analysis of the reaction mixture by TLC, a product with a higher polarity than **3.17** and **3.18** had formed. After flash chromatography purification, the product was isolated around 70% pure and analysed initially by ^{1}H NMR – sections of its ^{1}H NMR spectrum are shown in *Figure 3.7* and *Figure 3.8* (spectrum A, in red), along with the spectrum of the mixture of **3.17** and **3.18** (spectrum B, in green) for comparative purposes. Along with resonances corresponding to residual DMF, a singlet peak typical of a formamide derivative (~8.1 ppm, *Figure 3.7*), two doublet peaks characteristic of a diastereotopic CH_2 between two electronegative atoms (~5.0 ppm and ~4.7 ppm, *Figure 3.7*) and one singlet typical of an N-methyl group (~2.9 ppm, *Figure 3.8*) were present in the ^{1}H NMR spectrum. Following further analysis by ^{13}C NMR, HPLC-LRMS, infra-red spectroscopy and x-ray crystallography, the product was confirmed to be **3.19** (*Scheme of Table 3.1*) an adduct of the 7α-hydroxy group of **3.17** to DMF, with its x-ray crystal structure shown in *Figure 3.9*.

When performing the reaction again with lower equivalents of Selectfluor (Entry 2, *Table 3.1*), the 4β- and 2β-fluoro products **3.17** and **3.18** were isolated in a slightly higher yield of 60%, whilst only a trace of the DMF adduct **3.19** was observed to have formed upon analysis of the ^{1}H NMR spectrum of the crude material.

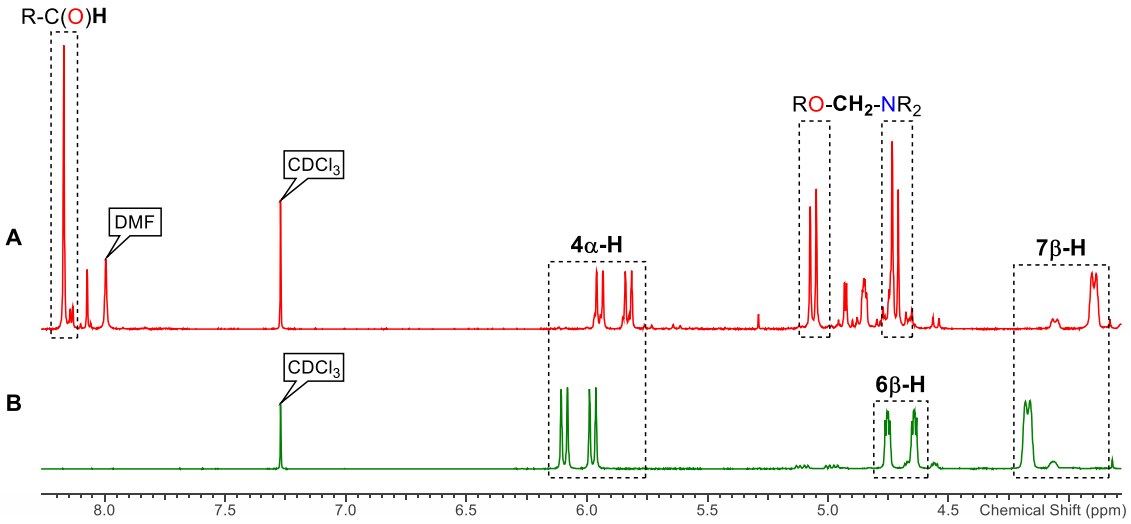

Figure 3.7 - Section of ^{1}H NMR Spectra of: ***A*** *(red):* ***3.19*** *~70% pure;* ***B*** *(green):* ***3.17/3.18*** *Mix*

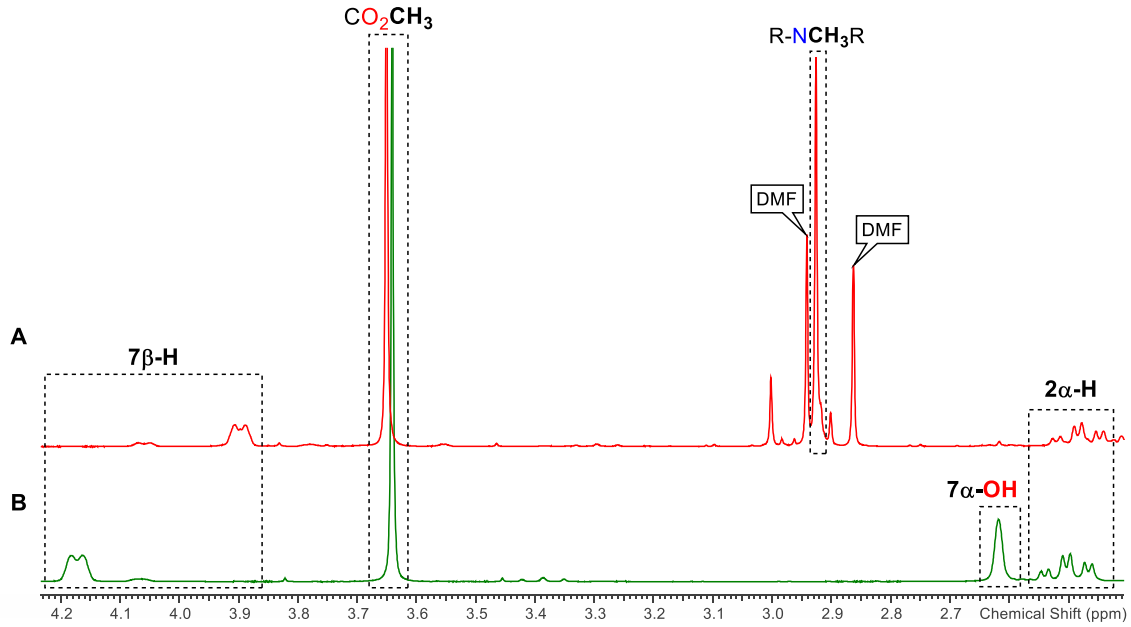

Figure 3.8 - Section of ^{1}H NMR Spectra of: ***A*** *(red):* ***3.19*** *~70% pure;* ***B*** *(green):* ***3.17/3.18*** *Mix*

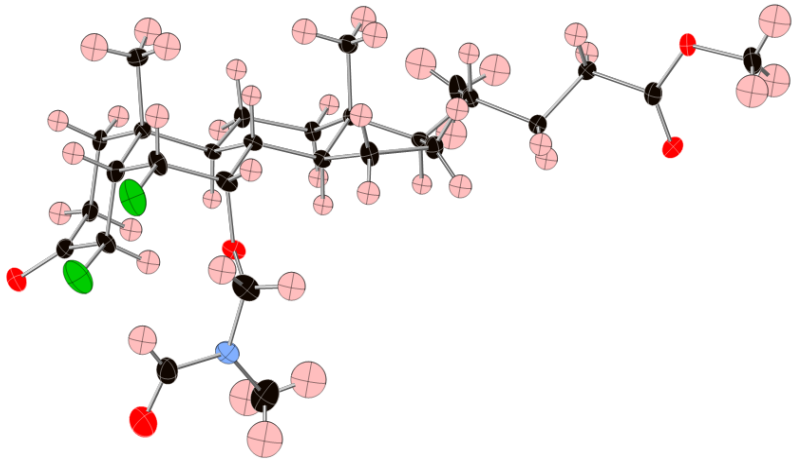

Figure 3.9 - X-Ray Crystal Structure of ***3.19***

Reactions of –OH nucleophiles with DMF to form the same type of adduct have been noted in the literature, generally under oxidative conditions with a catalyst such as a transition metal[168,169] or tetrabutylammonium iodide (TBAI).[170] In a study by Stephenson and coworkers, formation of nucleophile-DMF adducts was reported for a number of different nucleophiles, employing the use of the persulfate anion ($S_2O_8^{2-}$) as an oxidant and either heat (thermolysis) or ruthenium catalysts with visible light (photocatalysis) to catalyse the reactions.[168] In the study, a potential reaction mechanism for adduct formation under oxidative conditions was given, shown in *Scheme 3.8*. Thermal decomposition of $S_2O_8^{2-}$ was proposed to give a sulfate radical anion **3.20**, which abstracted a hydrogen atom from DMF to give the radical **3.21**. With another equivalent of $S_2O_8^{2-}$, the electrophilic species **3.22** was obtained, which could then be attacked by a nucleophile (Nu) to form the desired adduct.

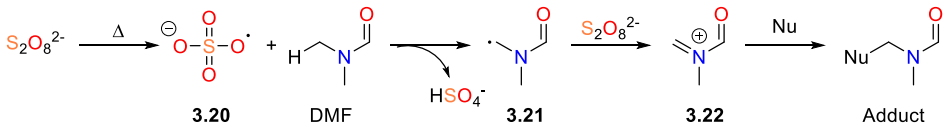

Scheme 3.8 - Nucleophile-Adduct Formation from Stephenson Study[168]

As Selectfluor is known to act as an oxidant as well as a fluorinating reagent,[171] the radical **3.21** and, hence the electrophilic species **3.22** could have formed in the 4β-fluorination reaction mixture under thermal conditions. Following formation of **3.22**, it would be attacked by the 7α-hydroxy of **3.17** (*Scheme 3.9*), giving **3.19** after an aqueous workup.

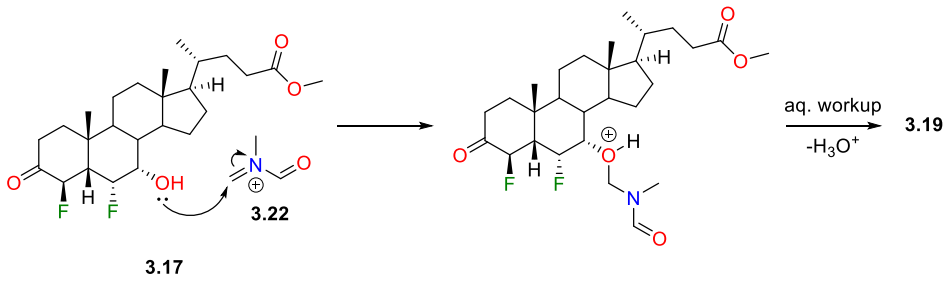

*Scheme 3.9 - Proposed Reaction Mechanism of DMF with **3.17***

Next, with the 9:1 mix of difluorinated ketone products **3.17** and **3.18** in hand, a reduction under Luche conditions,[172] using a procedure by Černý *et al.*,[173] was performed in an attempt to selectively form the desired 3α-hydroxy products. The reaction with $NaBH_4$ and $CeCl_3$ gave an inseparable 92:8 mix of the desired 3α-alcohols **3.23** and **3.24** (*Scheme 3.10*) in a 69% yield and additionally, an inseparable 9:1 mix of the 3β-alcohols **3.25** and **3.26** (*Scheme 3.10*) in a 19% yield. The 3α- and 3β-alcohols were readily separable from each other by flash chromatography. In order to separate the 2β- and 4β-fluorohydrins **3.23** and **3.24** from each other, a number of TLC conditions were tested,

but none were observed to give separation. Also, separation was not observed by normal or reverse-phase HPLC-LRMS.

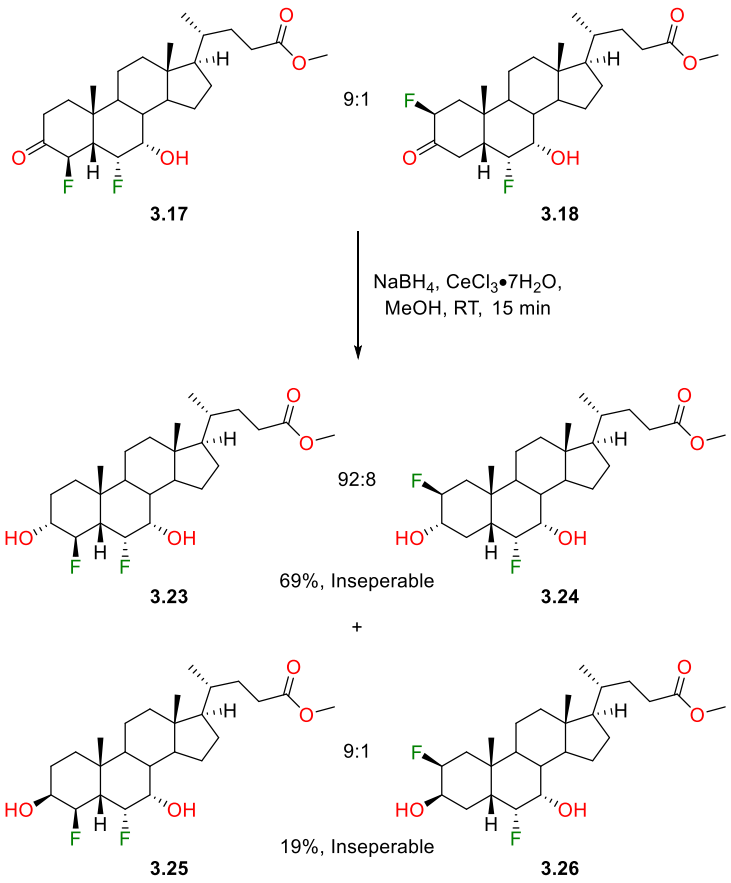

*Scheme 3.10 - Reduction of **3.17** and **3.18***

Occasionally, hydroxy group protection and deprotection reactions of bile acid derivatives allows separation of products that co-elute by flash chromatography and HPLC purification, hence, acetyl protection of the 92:8 mix of **3.23** and **3.24** was carried out (*Scheme 3.11*). Following slow flash chromatography purification, the diacetylated product **3.27** (*Scheme 3.11*) was isolated >97% pure based upon ^{19}F NMR analysis. However, the protected 2β-fluoro product was not cleanly isolated.

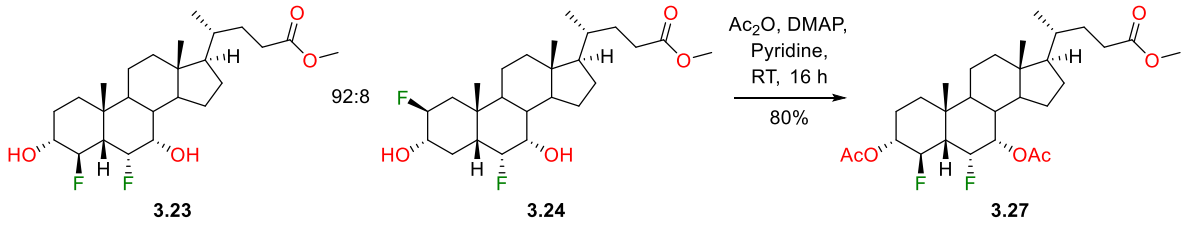

*Scheme 3.11 - Acetylation of **3.23** and **3.24***

The clean 4β,6α-difluoro product **3.27** crystallised (*Figure 3.10*), revealing the predicted close proximity of the two fluorine atoms, observed to possess a *J*=41.6 Hz coupling constant in the ^{19}F [^{1}H] NMR of **3.27** (*Figure 3.11*).

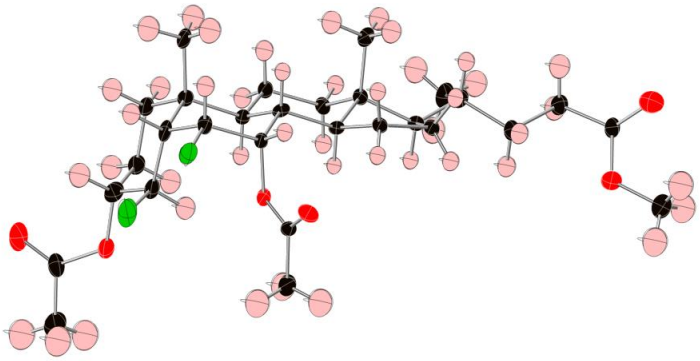

*Figure 3.10 - X-Ray Crystal Structure of **3.27***

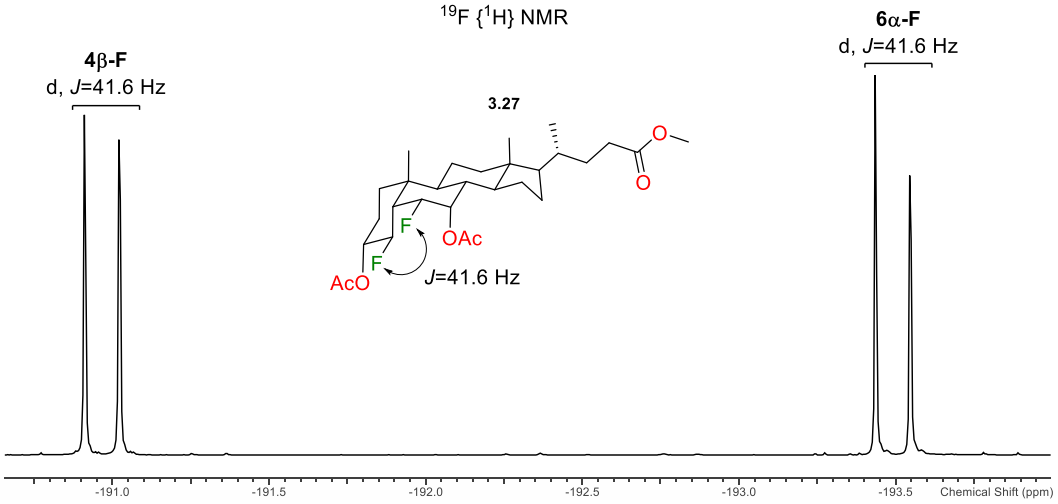

*Figure 3.11 - Section of ^{19}F [^{1}H] NMR of **3.27***

The protecting groups of **3.27** were then removed under strong basic conditions to give the target analogue 4β,6α-difluoro CDCA (**3.2**, *Scheme 3.12*) in a high yield.

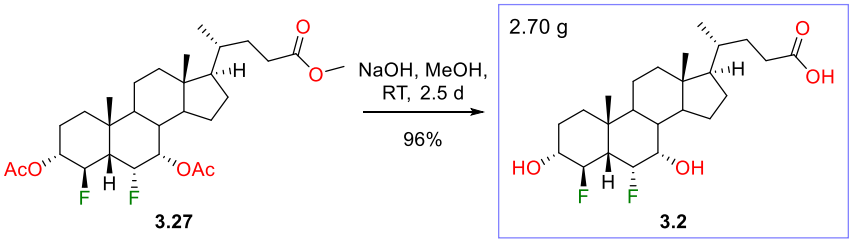

*Scheme 3.12 - Synthesis of **3.2***

3.2.4 Deoxygenation of the A- and B-Rings and Synthesis of 4β,6α-difluoro-5β-cholanic acid

In order to perform deoxygenation reactions on **3.2** (*Scheme 3.13*), its carboxylic acid was protected with a methyl ester to give **3.23** (*Scheme 3.13*) in a high yield.

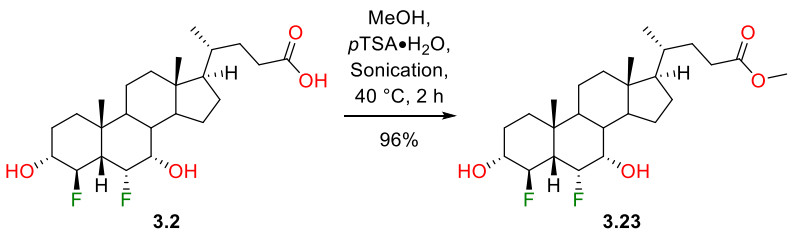

*Scheme 3.13 - Methyl Ester Formation on **3.2***

To successfully synthesise the target analogue **3.1** (*Scheme 3.1*), deoxygenation of both the A- and B-rings was required. Whilst methodology has been optimised for the A-ring of bile acid derivatives, deoxygenation of the B-ring was yet to be explored. The 7-position (of the B-ring) of a bile acid is significantly more sterically hindered than the 3-position as it is on the bottom face of the bile acid and it is proximal to a tertiary centre. Because of this, incorporation of a large group onto the 7α-alcohol can be challenging. Before attempting to deoxygenate the 7α-hydroxy group of any fluorinated material, deoxygenation was performed on the methyl ester of CDCA (**2.24**, *Scheme 3.14*).

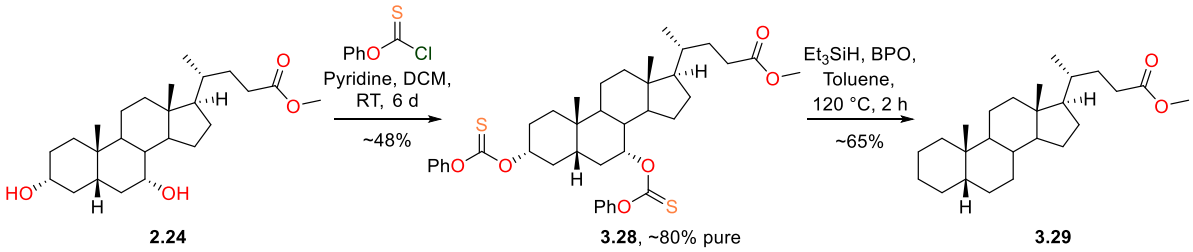

*Scheme 3.14 - Deoxygenation of **2.24***

Previously, when forming the thiocarbonate of an alcohol at the 3-position of a bile acid, complete consumption of the starting material was observed after 30 min – 1 h of stirring on analysis by TLC. In contrast, when synthesising **3.28** (*Scheme 3.14*), after 1 d of stirring at room temperature, analysis of the reaction mixture by HPLC-LRMS showed an incomplete reaction, with a mixture of monothiocarbonate and dithiocarbonate products present in the reaction mixture. Hence, further *O*-phenyl chlorothionoformate (*O*-PCTF) and pyridine were added to the reaction mixture. After 6 d of stirring, analysis of the reaction mixture by HPLC-LRMS showed the presence of only dithiocarbonate. Following two attempts to purify the crude material by flash chromatography, **3.28** was isolated around 80% pure in an approximate 48% yield.

Deoxygenation of **3.28** was then achieved using the normal conditions with triethylsilane and dibenzoyl peroxide with 2 h of heating, giving the desired A,B-ring deoxygenated ester **3.29** (*Scheme 3.14*) in an approximate 65% yield. The methyl ester of **3.29** was then saponified to yield 5β-cholanic acid **1.25** (*Scheme 3.15*).

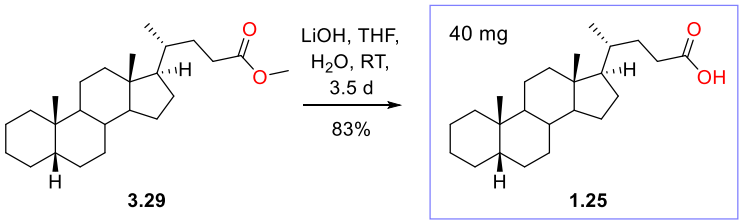

*Scheme 3.15 - Synthesis of **1.25***

With conditions in hand for deoxygenation of the B-ring, deoxygenation of **3.23** was attempted. To try to increase the reaction rate (and hence lower the reaction time) for thiocarbonate formation on **3.23**, DMAP was used along with pyridine to catalyse the first test reaction (Entry 1, *Table 3.2*). Despite the presence of another catalyst, the reaction proceeded very slowly and required addition of further *O*-PCTF to form the dithiocarbonate **3.30** (*Scheme of Table 3.2*). Following 12 d of stirring and purification of the crude material by flash chromatography, an inseparable 1:1 mixture of the di- and monothiocarbonates **3.30** and **3.31** was isolated (*Scheme of Table 3.2*).

The formation of **3.30** was repeated on the same scale, but using a higher number of equivalents of *O*-PCTF (Entry 2, *Table 3.2*). On analysis of the reaction mixture by HPLC-LRMS, in comparison to Entry 1, the reaction proceeded much faster, and after 6 d, a 1:1 mix of **3.30** and **3.31** was yielded. A final test scale reaction was performed, again increasing the quantities of *O*-PCTF and pyridine used whilst also changing the addition time of reagents and removing DMAP (Entry 3, *Table 3.2*). After 6 d, again a 1:1 mix of **3.30** and **3.31** was obtained following purification.

For the full-scale (680 mg) thiocarbonate formation, *O*-phenyl chlorothionoformate and pyridine were added in a large excess only at the start of the reaction (Entry 4, *Table 3.2*). After stirring for 7 d, a 7:3 mix of **3.30** and **3.31** was isolated in a low, 20% yield. Another product was also isolated, but was not fully identified directly after isolation. After attempted deoxygenation of the product (discussion to follow), it was identified to be **3.32** (*Scheme of Table 3.2*), with a phenyl carbonate group on the 7α-hydroxy.

*Table 3.2 - Thiocarbonate Formation on **3.24***

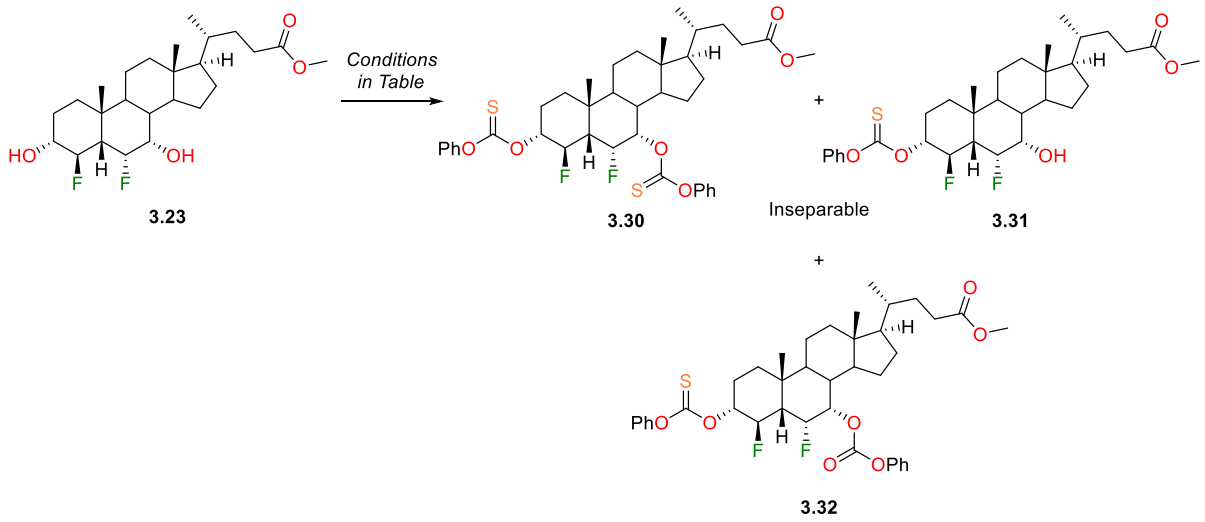

Entry	Conditions	Scale (mg)	Result
1	*O*-PCTF (5 x 2 equiv), DMAP (0.5 equiv), Pyridine (5 x 6 equiv), DCM, 12 d	50	Mix of **3.30** and **3.31** formed (~1:1)[1]
2	*O*-PCTF, (1 x 10 equiv + 1 x 3 equiv), DMAP (1 equiv), Pyridine, THF/DCM, 6 d	50	Mix of **3.30** and **3.31** formed (~1:1)[1]
3	*O*-PCTF (2 x 10 equiv), Pyridine (2 x 20 equiv), DCM, 6 d	50	Mix of **3.30** and **3.31** formed (~1:1)[1]
4	*O*-PCTF (20 equiv), Pyridine (40 equiv), DCM, 7 d	680	Inseparable ~7:3 mixture of **3.30** and **3.31** isolated, ~20%; Impure fraction containing **3.32** also isolated, ~40%[1]

O-PCTF: *O*-Phenyl Chlorothionoformate; [1]As shown by analysis of the ^{1}H NMR spectrum of the material post purification

The obtained 7:3 mixture of **3.30** and **3.31** was deoxygenated with triethylsilane and dibenzoyl peroxide. After 3 h of heating, the reaction gave the desired deoxygenated product **3.33** (*Scheme 3.16*) and the fluorohydrin **3.34** (*Scheme 3.16*), but both were isolated impure and in very low yields of around 16% and 14% respectively, with inseparable aromatic impurities.

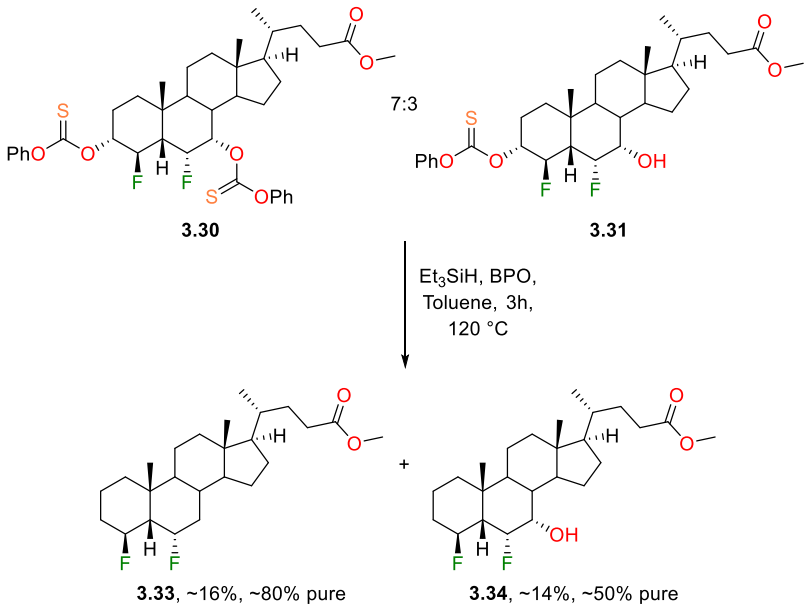

*Scheme 3.16 - Deoxygenation of **3.30/3.31** Mix*

The other product isolated from the thiocarbonate formation (*Scheme of Table 3.2*, revealed to be the phenyl carbonate **3.32** after the reaction), was also deoxygenated using triethysilane and dibenzoyl peroxide.

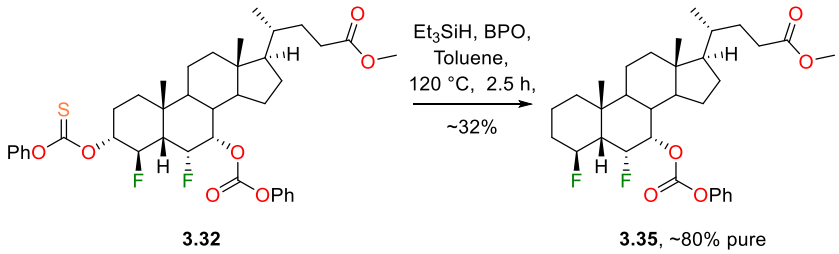

*Scheme 3.17 - Deoxygenation of **3.32***

After purification and analysis by NMR, LRMS and IR, the isolated 80% pure product of deoxygenation was identified to be **3.35** (*Scheme 3.17*), an ester bearing a phenyl carbonate group on the 7α-hydroxy. To ascertain whether the phenyl carbonate group had formed in or was present prior to the deoxygenation reaction, sections of the ^{1}H NMR spectra of **3.30/3.31**, **3.32** and **3.35** were compared, shown in *Figure 3.12*, along with 3D representations of the compounds discussed.

On analysis of the ^{1}H NMR spectrum of **3.30** (shown in blue, *Figure 3.12*), a high chemical shift of the 7β-proton was observed, at 6.05 ppm, whilst analysis of the corresponding spectrum of **3.35** (shown in black, *Figure 3.12*) revealed the chemical shift of the 7β-proton was significantly lower, at around 5.4 ppm. The ^{1}H NMR spectrum of **3.32** (shown in green, *Figure 3.12*) bore two peaks likely to correspond to 7β-protons, one at 6.05 identified to be **3.30** present in the sample after purification, and another at around 5.4 ppm. Due to the similarities in chemical shift and apparent coupling patterns of the 7β-protons of **3.32** and **3.35**, it was determined that the phenyl carbonate

group at the 7α-position of **3.32** was present prior to the attempted deoxygenation reaction. LRMS data provided further evidence to support this theory as the mass spectrum of **3.32** exhibited a typical $[M+NH_4]^+$ peak.

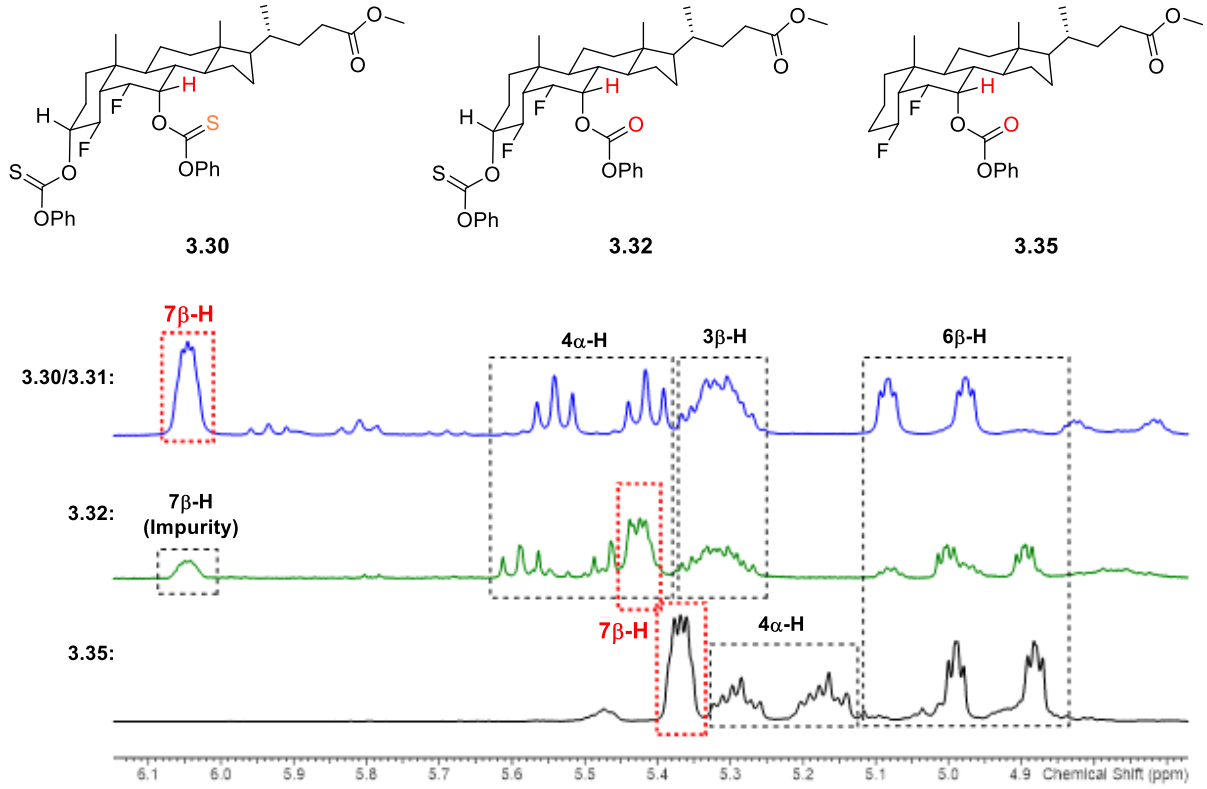

*Figure 3.12 - Structures of **3.30**, **3.32** and **3.35** and Sections of ^{1}H NMR Spectra of **3.30/3.31**, **3.32** and **3.35***

A proposed mechanism for the formation of **3.32** is shown in *Scheme 3.18*. If water ingressed into either the reaction mixture or the stock of *O*-PCTF, a reaction could occur to form **3.36**, which could tautomerise and react through the sulfur atom with another molecule of *O*-PCTF to give the reactive anhydride **3.37** (*Scheme 3.18*). The monothiocarbonate, **3.31**, could then attack **3.37** *via* the red or blue pathways shown in *Scheme 3.18*. If attacked *via* the red pathway, in which the 7α-hydroxy attacks the C=S, the dithiocarbonate **3.30** would be yielded. Conversely, if the anhydride was attacked *via* the blue pathway, in which the 7α-hydroxy attacks the C=O, the phenyl carbonate **3.32** would be obtained.

Alternatively, if the anhydride **3.37** was attacked by pyridine, the reaction again could progress *via* one of two pathways to form the adducts **3.38** or **3.39** (*Scheme 3.18*). When attacking adduct **3.38** with the monothiocarbonate **3.31**, the dithiocarbonate **3.30** would be formed. Conversely, when attacking adduct **3.39** with **3.31**, the phenyl carbonate **3.32** would be formed.

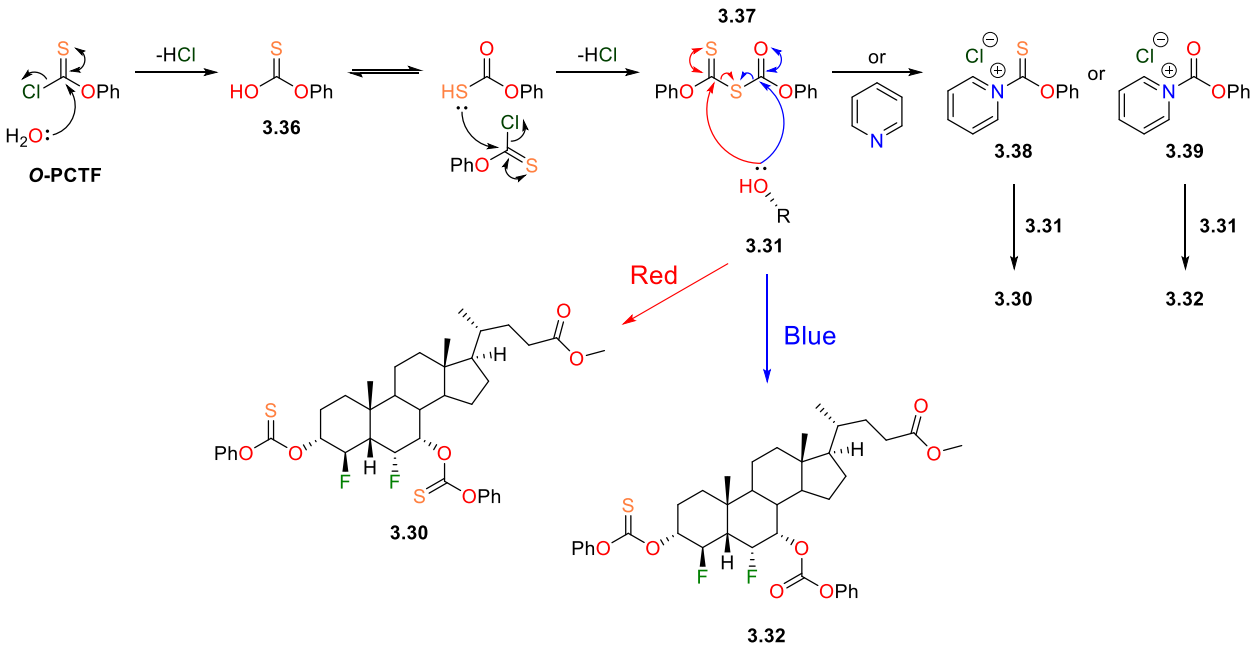

*Scheme 3.18 - Proposed Mechanism of Formation of **3.30** and **3.32***

With the lack of success deoxygenating **3.23** *via* a thiocarbonate, an alternative, smaller group to enable deoxygenation was investigated: a xanthate group. Although the synthesis of xanthates requires the use of highly toxic carbon disulfide (CS_2), it was thought that as CS_2 is small in size, its approach of the hindered 7α-hydroxy may be more facile in comparison to *O*-PCTF.

A procedure by Litvinovskaya *et al.* was first used for testing xanthate ester formation, which utilised CS_2, 1,8-diazabicyclo(5.4.0)undec-7-ene (DBU) and methyl iodide to afford the desired xanthate product.[174] When performed on **3.23** though, the desired compound **3.40** (*Scheme of Table 3.3*) did not form and only a trace of the mono xanthate ester **3.41** (*Scheme of Table 3.3*) was observed on analysis of the ^{1}H NMR spectrum of the crude material (Entry 1, *Table 3.3*). A method using a different base, by Togo *et al.,* with NaH and imidazole[175] was tested on **3.23**, but again yielded 0% of **3.40** and only a trace of **3.41** (Entry 2, *Table 3.3*).

Inoue *et al.* described a procedure for xanthate formation and deoxygenation of a 7α-hydroxy of a 5β-steroid derivative, used in the synthesis of the natural product 19-hydroxysarmentogenin.[176] The procedure used high equivalents of NaH, CS_2 and MeI relative to the reacting steroid (20, 20 and 40 respectively), along with 10 equiv of water, giving high yields of xanthate esters. Inoue's procedure was tested initially on a 50 mg scale of **3.23**, giving a good yield of the desired xanthate **3.40** after purification (*Entry 3*, *Table 3.3*). The reaction was performed again, with half of the equivalents of all reagents initially used (*Entry 4*, *Table 3.3*) but led to only a trace of **3.40** being formed, with evidence of methyl ester hydrolysis on analysis of the ^{1}H NMR of the crude material. Due to the presence of both NaH and water in the reaction mixture, NaOH is likely to have formed, causing saponification of the methyl ester.

The reaction with 10 equiv of CS_2 was attempted once more on **3.23**, omitting water from the reaction mixture to avoid potential ester hydrolysis. A good, 50% yield of **3.40** was achieved after purification (*Entry 5*, *Table 3.3*). A final reaction on a 750 mg scale, which used the same conditions and equivalents of reagents, afforded a significantly higher yield of the desired xanthate **3.40** (*Entry 6*, *Table 3.3*), giving ample material for deoxygenation.

*Table 3.3 - Xanthate Formation on **3.23***

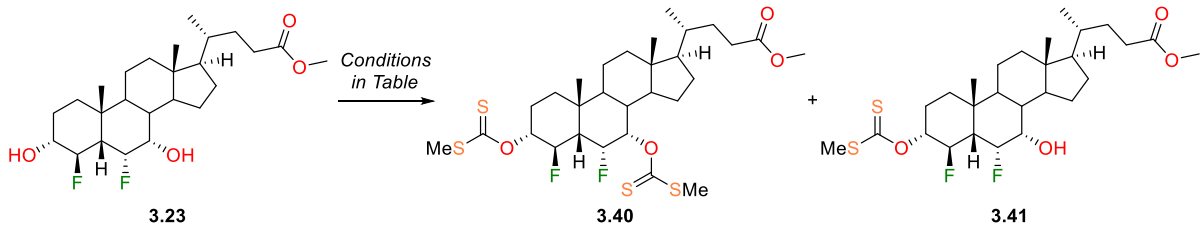

Entry	Conditions (Equiv)	Scale (mg)	Result
1	CS_2 (4), DBU (6), MeI (10), DMF, RT, 2 d[174]	50	**3.40**: 0%; **3.41**: Trace[1]
2	NaH (6), Imidazole (0.03), CS_2 (5), MeI (5), THF, RT, 4 h[175]	50	**3.40**: 0%; **3.41**: Trace[1]
3	NaH (20), CS_2 (20), H_2O (10), MeI (40), THF, RT, 7 h[176]	50	**3.40:** 50%[2]
4	NaH (10), CS_2 (10), H_2O (5), MeI (20), THF, RT, 7 h	100	**3.40**: Trace, potential ester hydrolysis[1]
5	NaH (10), CS_2 (10), MeI (20), THF, RT, 7 h	100	**3.40:** 50%[2]
6	NaH (10), CS_2 (10), MeI (20), THF, RT, 7 h	750	**3.40:** 83%[2]

[1]As shown by analysis of the $^1H/^{19}F$ NMR spectra of the crude material; [2]Isolated Yield

Whilst Inoue *et al.* deoxygenated their 7α-xanthate with AIBN and triphenyltin hydride,[176] this method was not used to avoid the introduction of toxic organotin compounds into the synthesis of **3.1**. The deoxygenation conditions with triethylsilane and benzoyl peroxide were used instead on **3.40** (*Scheme 3.19*), giving a sufficient yield of the deoxygenated ester **3.33** (*Scheme 3.19*). Methyl ester saponification followed, giving the target analogue 4β,6α-difluoro-5β-cholanic acid (**3.1**, *Scheme 3.19*) in a high yield. The fully deoxygenated structure of **3.1** was confirmed with x-ray crystallographic analysis, shown in *Figure 3.13*.

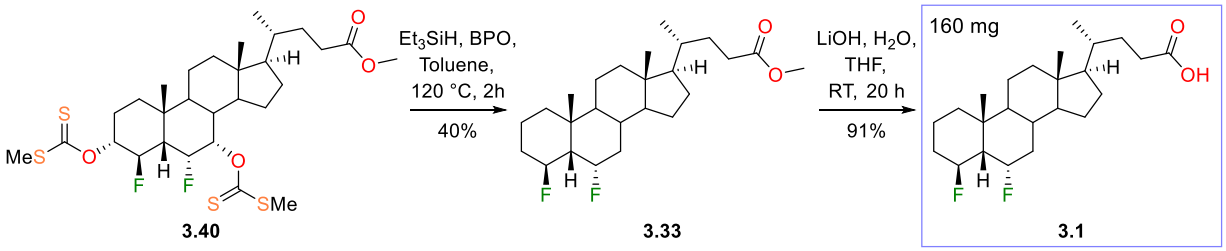

*Scheme 3.19 - Synthesis of **3.1***

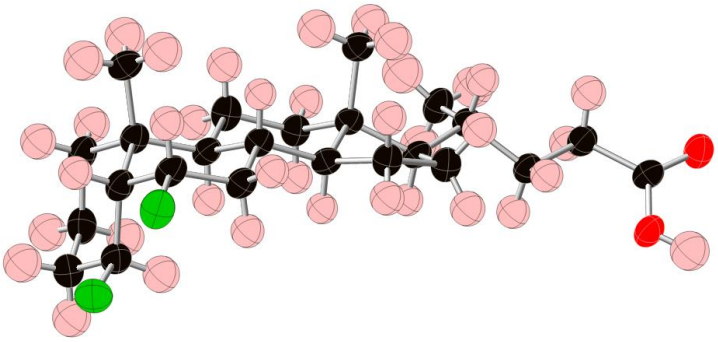

*Figure 3.13 - X-Ray Crystal Structure of **3.1***

3.3 Synthesis of 7-Fluorinated Bile Acid Analogues

3.3.1 Retrosynthetic Analysis

The retrosynthetic analysis of the 7α- and 7β-fluoro target analogues **3.3** to **3.10** is shown in *Scheme 3.20*. The 7α-fluoro analogues **3.5**, **3.6** and **3.7** could be synthesised from 7α-fluoro LCA, **3.3**, which could be accessed from the 7α-fluoro intermediate **2.74** (*Scheme 3.20*, previously mentioned in **Section 2.4.3**) following deoxygenation at the 6-position. Similarly, the 7β-fluoro analogues **3.8**, **3.9** and **3.10** could be formed from 7β-fluoro LCA, **3.4**, which could be synthesised from **3.42** (*Scheme 3.20*). Both **2.74** and **3.42** have been synthesised previously within the group from HDCA (**1.7**, *Scheme 3.20*).

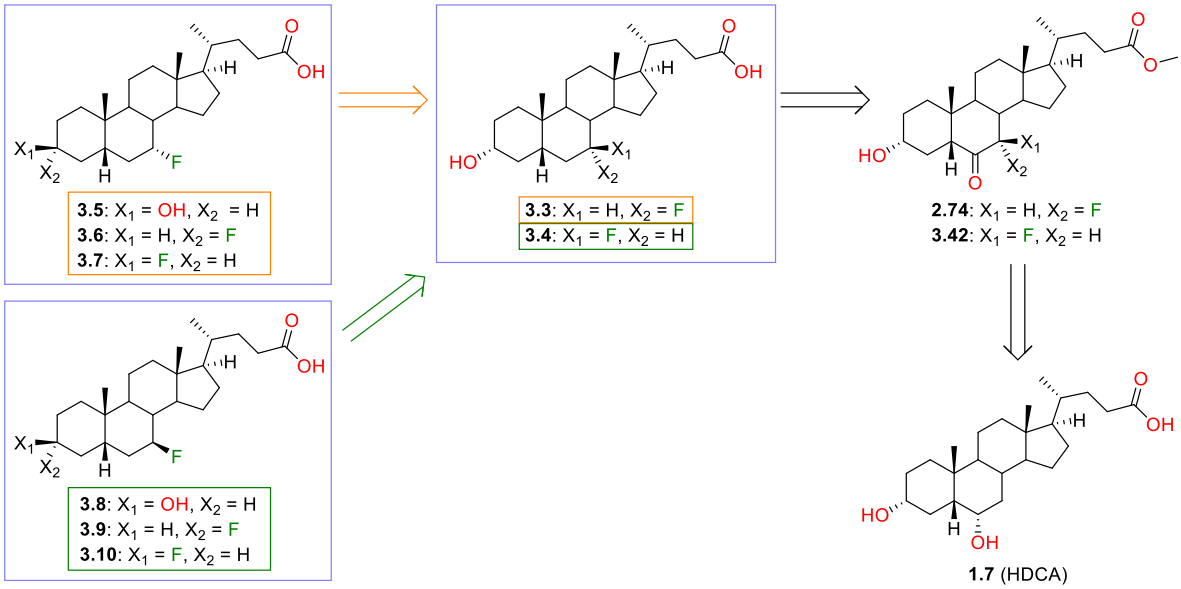

*Scheme 3.20 - Retrosynthetic Analysis of **3.3** - **3.10***

As briefly discussed in **Section 1.2.4**, 7α-fluoro HDCA (**3.43**, UPF680, *Figure 3.14*) has been described in the literature by Clerici *et al*.[51] The synthesis of **3.43** was described with no detailed experimental procedures, though the 7α-fluoro moiety was noted to be installed *via* Selectfluor fluorination of a silyl enol ether, formed from a ketone at the 6-position of a bile acid ester.[51] Notably, the synthetic procedure formerly used within the group to the 7α-fluoro intermediate **2.74** followed the same steps as the literature synthesis of **3.43**, although different methods of methyl ester formation (on HDCA, **1.7**) and 6-selective oxidation were utilised.

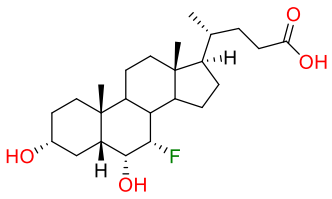

3.43 7α-fluoro HDCA

Figure 3.14 - 7α-fluoro HDCA

3.3.2 Synthesis of 6-keto Intermediate

To synthesise the required intermediate **2.74**, the carboxylic acid of HDCA (**1.7**, *Scheme 3.21*) was protected by a methyl ester under acidic conditions, giving **3.44** (*Scheme 3.21*) in a 99% yield.

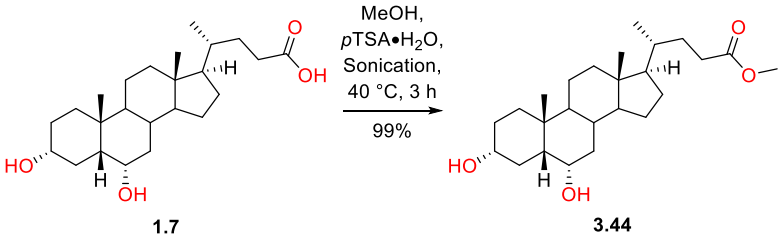

1.7 **3.44**

*Scheme 3.21 - Methyl Ester Formation on **1.7***

Selective protection of the 3-hydroxy group in **3.47** was attempted (*Table 3.4*) to avoid the use of excessive quantities of carcinogenic pyridinium dichromate (PDC), used previously in the synthesis of **2.74** as a regioselective oxidant. All regioselective protection reactions of the 3α-hydroxy were initially attempted with one equivalent of reagent, with further equivalents added if analysis by TLC revealed starting material was present in the reaction mixture after overnight stirring/heating. Reactions were attempted with the benzoyl (Bz), acetyl (Ac), *tert*-butyldiphenylsilyl (TBDPS) and *tert*-butyldimethylsilyl (TBDMS) protecting groups using various procedures on different scales, but none gave a good yield (>50%) of the desired 3-protected products (highlighted in red, Entries 1 to 6, *Table 3.4*).

*Table 3.4 - Attempted 3-Selective Protection of **3.44***

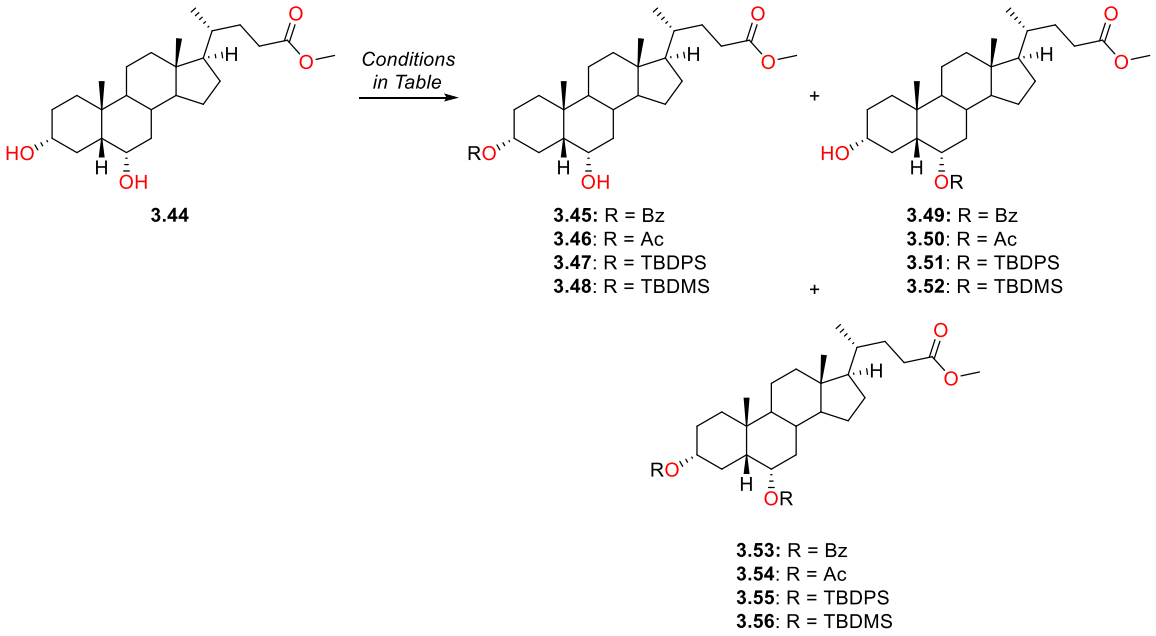

Entry	R	Conditions	Scale	Yield/Result
1	Bz	Bz-Cl, pyridine, toluene, DCM, RT, 18 h	100 mg	**3.45**: ~45%; **3.49**: 0%; **3.53**: ~55%[1]
2	Bz	Bz-Cl, pyridine, toluene, DCM, RT, 1.5 d	1.0 g	**3.45**: ~40%; **3.49**: 40%; **3.53**: ~20%[1]
3	Ac	Ac_2O, $NaHCO_3$, THF, 65°C, 1.5 d	100 mg	**3.46**: ~15%; **3.50**: 0%; **3.54**: ~85%[1]
4	TBDPS	TBDPS-Cl, imidazole, DMF, RT, 6 d[57]	200 mg	**3.47:** ~4%; **3.51**: ~28%; **3.55**: 19%[2]
5	TBDMS	TBDMS-Cl, imidazole, THF, DMF, 0 °C – RT, 4 d[177]	200 mg	No reaction[1]
6	TBDMS	TBDMS-OTf, 2,6-lutidine, DCM, 0 °C – RT, 1,5 d	200 mg	**3.48**: 12%; **3.52**: 0%; **3.56**: 35%[2]

[1]On analysis of the ^{1}H NMR spectrum of the crude material; [2]Approximate yield from mixed fractions after purification

Following the unsuccessful attempts at 3-selective protection of **3.44**, regioselective oxidation with pyridinium dichromate was carried out using a procedure by Yang *et al.*,[178] giving a mixture of the

desired 6-ketone **3.57**, the 3-ketone **3.58** and the diketone **3.59** (*Scheme 3.22*). Note: the reaction was divided into three batches in order to ease workup and purification of the oxidised products. Purification of the desired 6-ketone **3.57** proved challenging as it had a very similar retention factor by TLC to **3.58**. After multiple attempts at flash chromatography purification, full separation of **3.57** from **3.58** was not achieved, hence **3.57** and **3.58** were isolated in 45% and 2% yields (56% and 10% including material in mixed fractions).

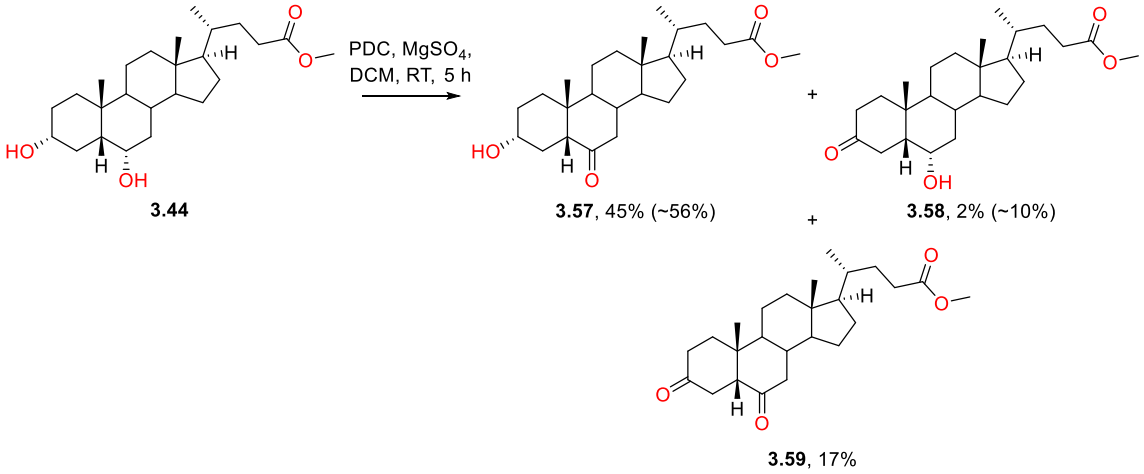

*Scheme 3.22 - PDC Oxidation of **3.44**. Note: Yields in brackets are those including material in mixed fractions.*

3.3.3 Electrophilic Fluorination and 3α-Hydroxy Protection

As the detailed experimental procedure for electrophilic fluorination of **3.57** was not given in the study by Clerici *et al*,[51] the procedure to fluorinate next to a 7-ketone, adapted from a method by Sepe *et al.*[149] (*Scheme 2.24*), was investigated. The same procedure has been applied successfully in the literature to the 6-ketone of a 5α-steroid, giving the desired 7α-fluoro product in a 71% yield.[179] The LDA/TMSCl conditions were employed on **3.57**, giving a quantitative yield of the TMS enolate **3.60** (*Scheme 3.23*). Overnight stirring of **3.60** with Selectfluor then gave the targeted 7α- and 7β-fluoro ketones **2.74** and **3.42** (*Scheme 3.23*) in 62% and 8% yields respectively. The stereochemistry of the fluorine atoms of **2.74** and **3.42** were confirmed by x-ray crystallography (*Figure 3.15*, *Figure 3.16*).

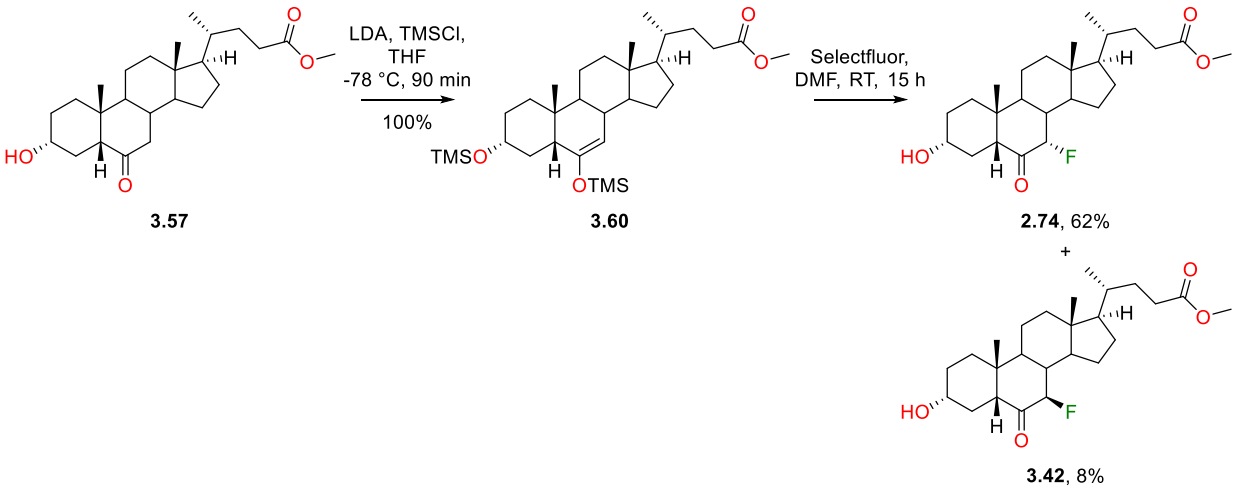

*Scheme 3.23 - Electrophilic Fluorination of **3.57***

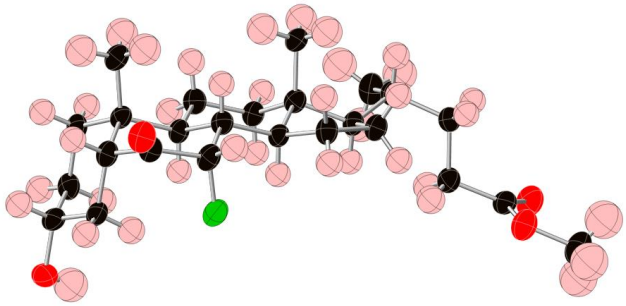

*Figure 3.15 - X-Ray Crystal Structure of **2.74***

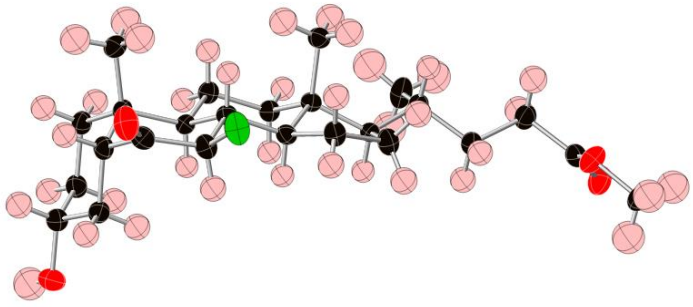

*Figure 3.16 - X-Ray Crystal Structure of **3.42***

As mentioned, deoxygenation at the 6-position was envisioned *via* a Barton-McCombie reaction following reduction of the 6-ketones of **2.74** and **3.42** (*Scheme 3.20*). To ensure that thiocarbonate formation only occurred on an alcohol at the 6-position, the 3α-hydroxy groups of the 7α- and 7β-fluoro products **2.74** and **3.42** were protected as acetate esters (*Table 3.5*). Using Omura and coworkers' procedure for acetylation,[49] the protected products **3.63** and **3.64** were achieved in very high yields.

*Table 3.5 - Acetylation of **2.72** and **3.42***

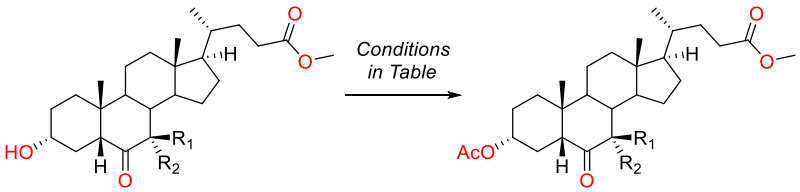

2.74: R_1 = H, R_2 = F
3.42: R_1 = F, R_2 = H

3.61: R_1 = H, R_2 = F
3.62: R_1 = F, R_2 = H

Entry	Starting Material	Conditions	Yield
1	**2.74**	Ac_2O, DMAP, pyridine, RT, 17 h	**3.61**: 99%
2	**3.42**	Ac_2O, DMAP, pyridine, RT, 19 h	**3.62**: 96%

Facile, high-yielding epimerisation of the 5β-H of **3.57** has been described in the literature using acidic (Entry 1, *Table 3.6*) or basic (Entry 2, *Table 3.6*) conditions.[178,180,181] As the acetylation conditions used on **2.74** and **3.42** utilised a base and also formed acetic acid *in situ*, 1D NOE experiments were conducted on the acetylated products **3.61** and **3.62** to ensure the 5β-stereochemistry was retained.

Table 3.6 - Literature Conditions for Epimerisation of 5β-H[178,180,181]

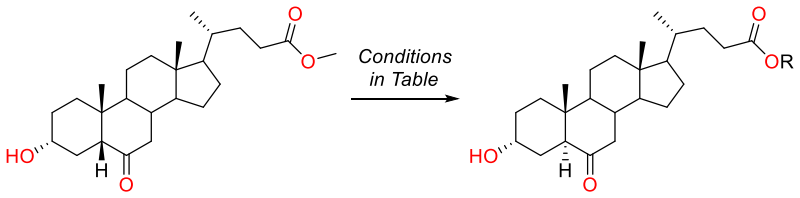

3.57

3.63: R = Me
3.64: R = H

Entry	*Literature Conditions*	*Yield*
1	HCl, MeOH	**3.63**: 94%[178,180]
2	NaOH, 1,4-Dioxane, H_2O	**3.64**: 84%[181]

In the 1D NOE experiment of **3.61**, irradiation of the 19-CH_3 was performed. On irradiation, only protons near in space to the 19-CH_3 group would be observed in the ^{1}H NMR, therefore for **3.61**, the 1β-, 5β-, 8β- and 11β-protons are observed (*Figure 3.17*). *Table 3.7* shows the predicted and experimental multiplicities of the investigated protons.

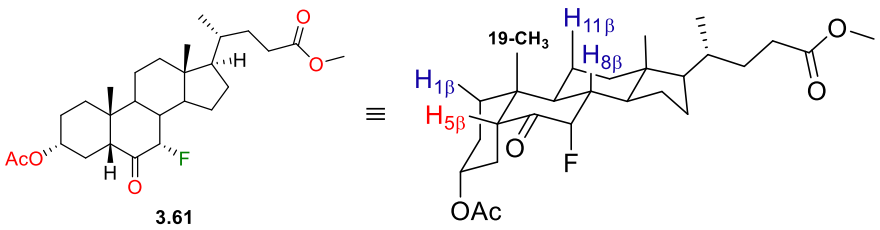

*Figure 3.17 - 3D Representation of **3.61***

*Table 3.7 - Predicted and Observed 1D NOESY Data on **3.61***

Proton	Expected Multiplicity (with *J* values in the region of)	Observed Multiplicity (with *J* values, Hz)	Chemical Shift (ppm)
1β-H	ddd (2 x *J*≈12-14 Hz, 1 x *J*≈3-5 Hz)	Apparent td, *J*=14.3, 3.4	1.14
5β-H	dd (1 x *J*≈12-14 Hz, 1 x *J*≈2-4 Hz)	dd, *J*=13.3, 2.7	2.33
8β-H	dddd (1 x *J*≈38-40 Hz, 2 x *J*≈10-13 Hz, 1 x *J*≈2-4 Hz)	Apparent dtd, *J*=38.5, 11.0, 2.3	1.77
11β-H	dddd (3 x *J*≈11-14 Hz, 1 x *J*≈3-5 Hz)	Apparent qd, *J*=12.8, 3.7	1.38

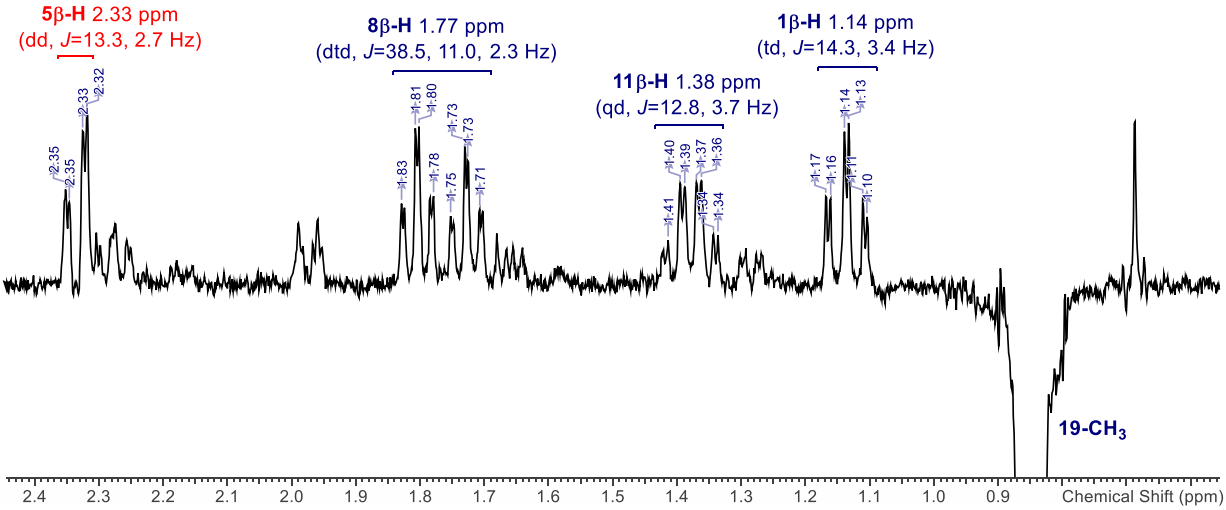

*Figure 3.18 - Section of 1D Selective Gradient NOESY Spectrum at 19-CH_3 (0.85 ppm) of **3.61***

The 1D Selective Gradient NOESY Spectrum of **3.61** (*Figure 3.18*) displayed a dd, *J*=13.3, 2.7 Hz at 2.33 ppm, which was characteristic of and consistent with that of a 5β-H. The experimental data for the other protons investigated also agreed with the predicted data for 5β-stereochemistry, hence **3.61** was confirmed not to have epimerised. If the 5-position had epimerised to a 5α-H (*Figure 3.19*), the axial 4β-H would be visible by 1D NOE experiments instead of the 5-H, and would have an expected multiplicity of td, which was not observed experimentally. Also, the 1β-H would be equatorial in a 5α-steroid rather than axial, and would have an expected multiplicity of ddd (rather

than td for the axial proton), which again was not observed. Further confirmation of the 5β-stereochemistry of **3.61** was provided by x-ray crystallography (*Figure 3.20*).

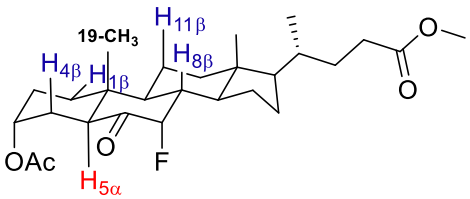

3.65

*Figure 3.19 - Potential 5-H Epimerised Product from **3.61***

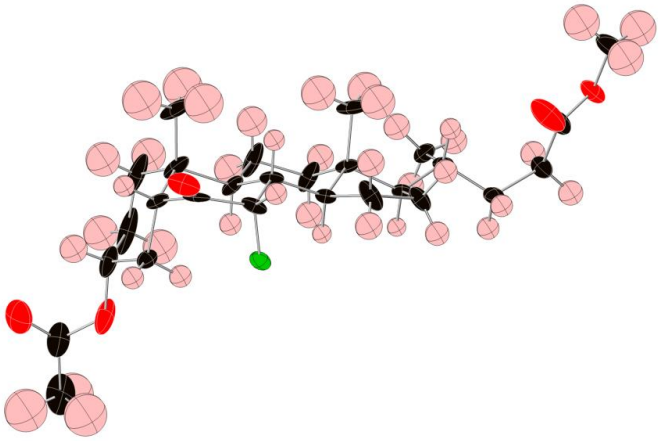

*Figure 3.20 - X-Ray Crystal Structure of **3.61***

The corresponding 1D NOE experiment was then carried out on the 7β-fluoro ketone **3.62**, again with irradiation of the 19-CH_3. Due to the equatorial position of the fluorine atom, the predicted multiplicities of the 5β-H and 8β-H were different to **3.62**: the 5β-H was expected to be a dt, with a small W-coupling to the 7β-F; the 8β-H was predicted to be a quintet, with an axial to equatorial coupling to the 7β-F and strong couplings to three trans-diaxial protons (*Table 3.8*).

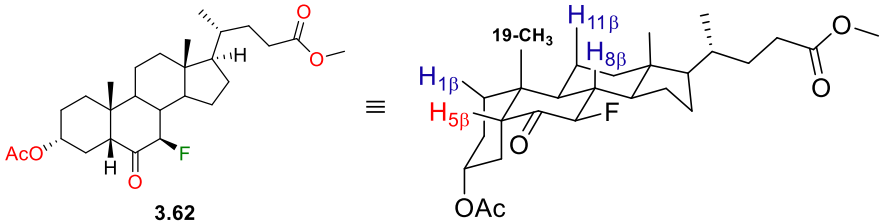

3.62

*Figure 3.21 - 3D Representation of **3.62***

*Table 3.8 - Predicted and Observed 1D NOESY Data on **3.62***

Proton	Expected Multiplicity (with *J* values in the region of)	Observed Multiplicity (with *J* values, Hz)	Chemical Shift (ppm)
1β-H	ddd (2 x *J*≈13-15 Hz, 1 x *J*≈3-5 Hz)	Apparent td, *J*=14.3, 3.4 Hz	1.18
5β-H	ddd (1 x *J*≈12-14 Hz, 2 x *J*≈3-5 Hz)	Apparent dt, *J*=13.7, 4.3 Hz	2.40
8β-H	dddd (4 x *J*≈9-12 Hz)	Apparent quin, *J*=10.1 Hz	1.97
11β-H	dddd (3 x *J*≈11-14 Hz, 1 x *J*≈3-5 Hz)	Apparent qd, *J*=11.9, 3.7 Hz	1.43

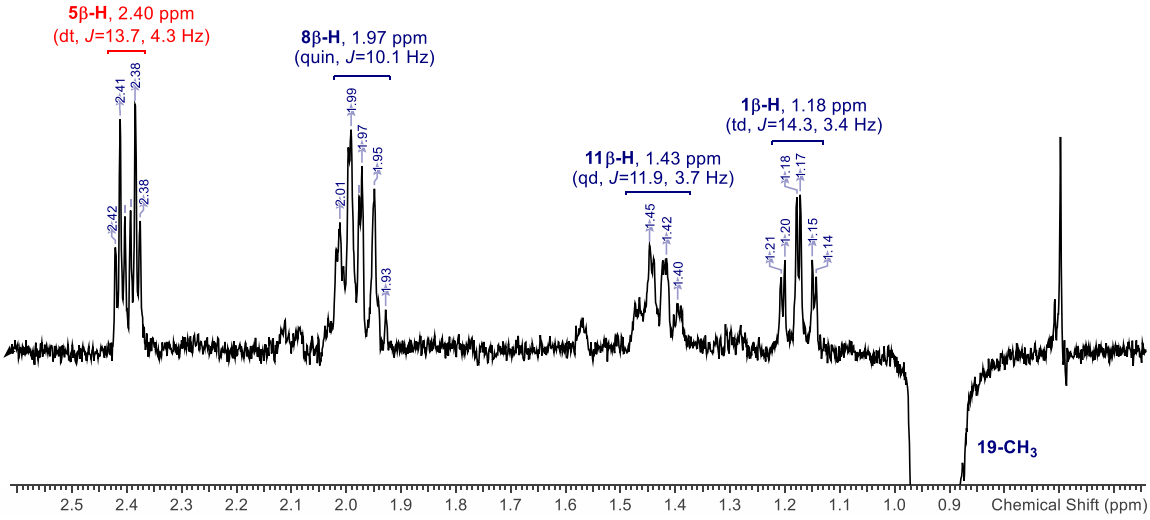

*Figure 3.22 - Section of 1D Selective Gradient NOESY Spectrum at 19-CH_3 (0.91 ppm) of **3.62***

The 1D Selective Gradient NOESY Spectrum of **3.62** (*Figure 3.22*) displayed the expected dt, *J*=13.7, 4.3 Hz at 2.40 ppm, signifying a 5β-H. Additionally, the experimental data for the other protons investigated also agreed with the predicted data for 5β-stereochemistry. Like with **3.62**, if the 5-position had epimerised to a 5α-H (*Figure 3.23*), the axial 4β-H and equatorial 1β-H would be visible by 1D NOE experiments and would have different coupling patterns to the protons observed in *Figure 3.22*. Again, neither were observed experimentally.

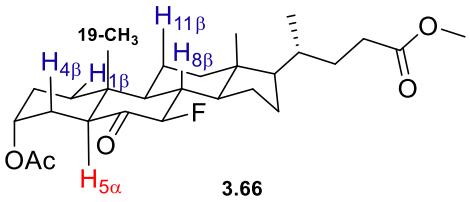

*Figure 3.23 - Potential 5-H Epimerisation Product from **3.62***

Further confirmation of the 5β-stereochemistry of **3.62** was provided by x-ray crystallography (*Figure 3.24*).

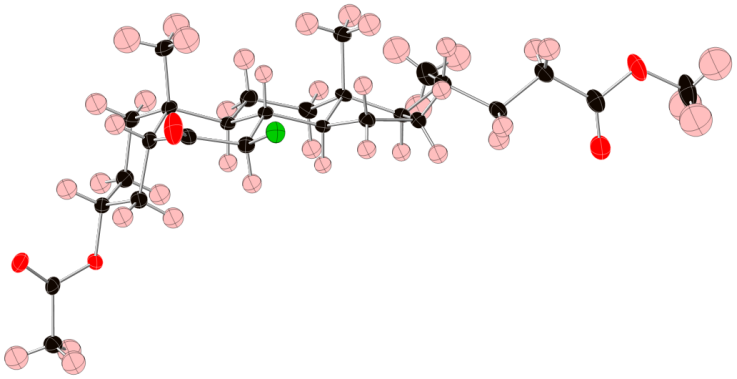

*Figure 3.24 - X-Ray Crystal Structure of **3.62***

3.3.4 Synthesis of 7α-Fluoro Monofluorinated Analogues

Initially focussing on the 7α-fluoro analogues, reduction of the 6-ketone of **3.6** was achieved with sodium borohydride, stirred overnight under anhydrous conditions to give the readily separable 6α- and 6β-alcohols **3.67** and **3.68** (*Scheme 3.24*), in 22% and 57% yields respectively. The 6β-alcohol was then deoxygenated with the previously optimised method *via* the thiocarbonate **3.69** (*Scheme 3.24*), formed following overnight stirring. Heating of **3.69** with triethylsilane and dibenzoyl peroxide gave a high yield of the 7α-fluoro ester **3.70** (*Scheme 3.24*) around 80% pure with inseparable aromatic impurities. As an ample quantity of **3.70** had been obtained, **3.67** was not deoxygenated.

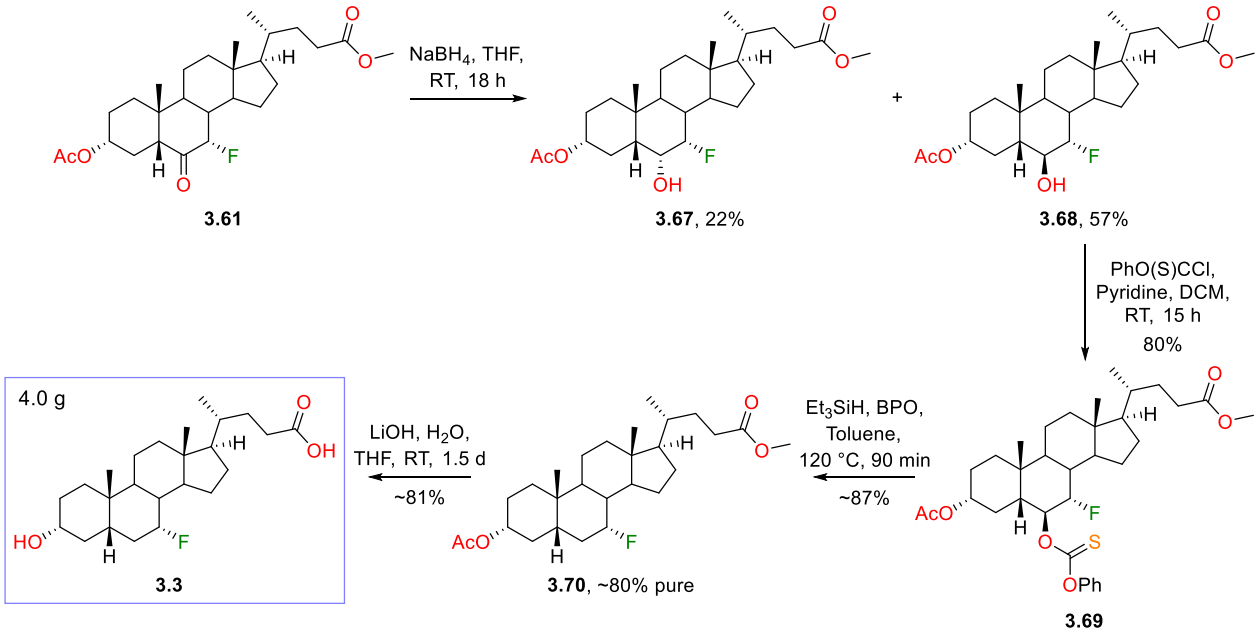

*Scheme 3.24 - Synthesis of **3.3***

Deoxygenation of the 6-position was confirmed by x-ray crystallographic analysis of **3.70** (*Figure 3.25*), which further confirmed the absence of 5H-epimerisation in the reaction conditions prior to the 6-keto reduction.

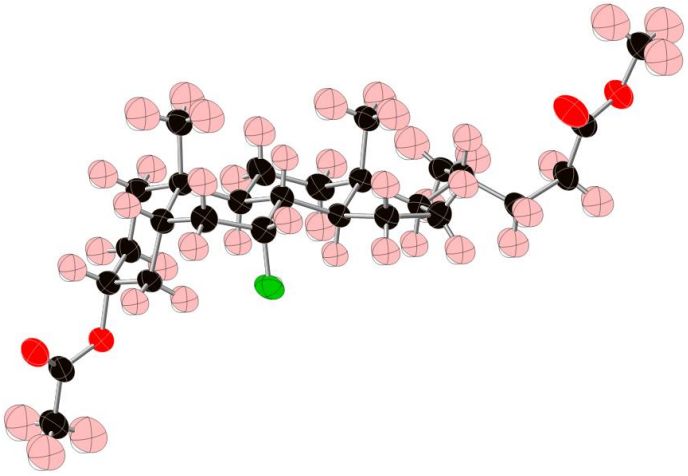

*Figure 3.25 - X-Ray Crystal Structure of **3.70***

Global deprotection of **3.70** followed, giving the target analogue 7α-fluoro LCA (**3.3**, *Scheme 3.24*) in an approximate 9% overall yield from HDCA, with its x-ray crystal structure shown in *Figure 3.26*.

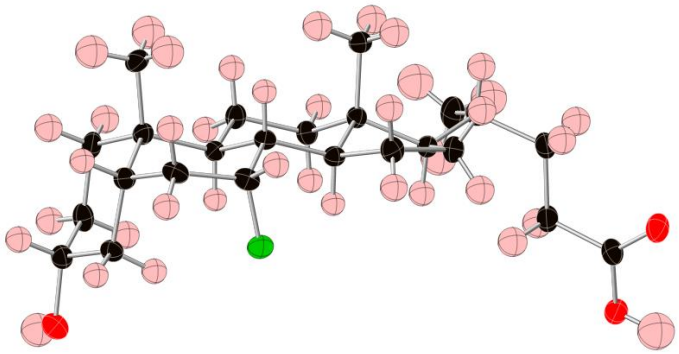

*Figure 3.26 - X-Ray Crystal Structure of **3.3***

7α-fluoro HDCA (**3.43**, *Scheme 3.25*) was then isolated in a high yield following global deprotection of the 6α-hydroxy intermediate **3.67**. The intermediate was also methylated using a procedure by Pellicciari *et al*.[57] to obtain the 6α-methoxy ester **3.71** (*Scheme 3.25*), which was deprotected under basic conditions to give 7α-fluoro-6α-methoxy LCA, **3.72** (*Scheme 3.25*). The 6α-methoxy analogue **3.72** was targeted to test in assays for FXR activity, to investigate the impact on biological activity that substitution of a 7α-hydroxy group for a fluorine atom has, whilst possessing an isostere for a 6α-ethyl.

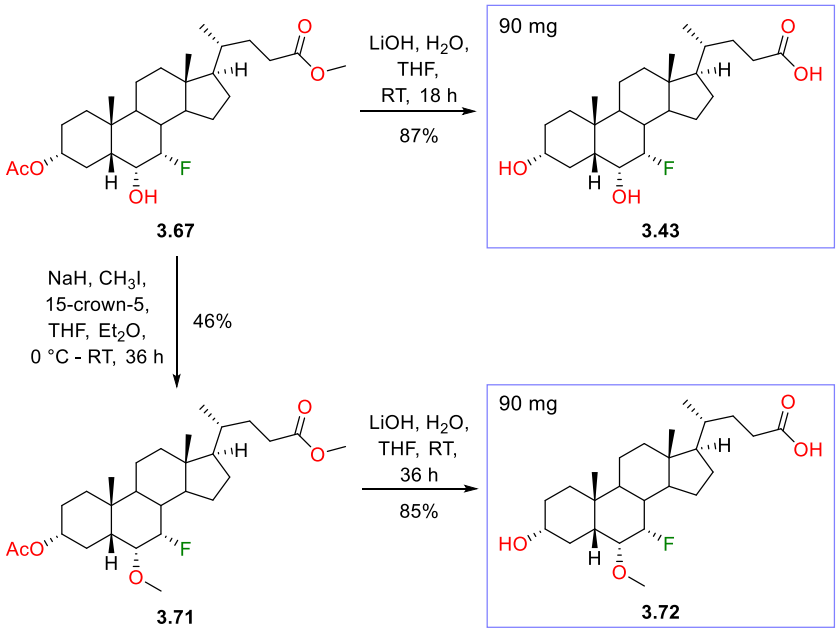

*Scheme 3.25 - Synthesis of **3.43** and **3.72***

3.3.5 Synthesis of 3α/β,7α-Difluoro Analogues

To enable modification of the 3α-hydroxy of **3.3**, the carboxylic acid was protected as a methyl ester, giving **3.73** (*Scheme 3.26*) in a high yield.

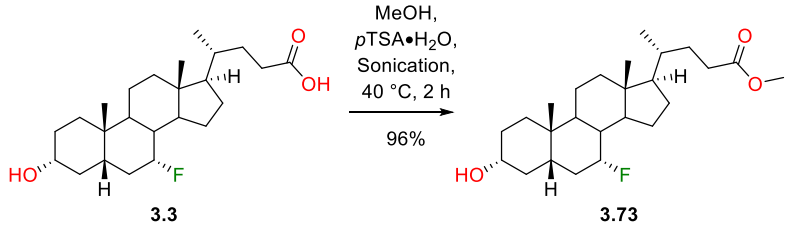

*Scheme 3.26 - Methyl Ester Formation on **3.3***

Fluorination of the 3α-hydroxy of **3.73** was then trialled (*Table 3.9*). Successful deoxyfluorination of alcohols has been performed within the group with a number of different fluorinating reagents. Whilst DAST is usually the first, convenient choice for fluorination, two less commonly used sulfonyl fluoride reagents, PyFluor[182] (*Figure 3.27*) and perfluorobutanesulfonyl fluoride[183] (NfF, *Figure 3.27*), have been shown predominantly to be higher yielding than DAST for various aliphatic substrates.

*Table 3.9 - Fluorination of **3.73***

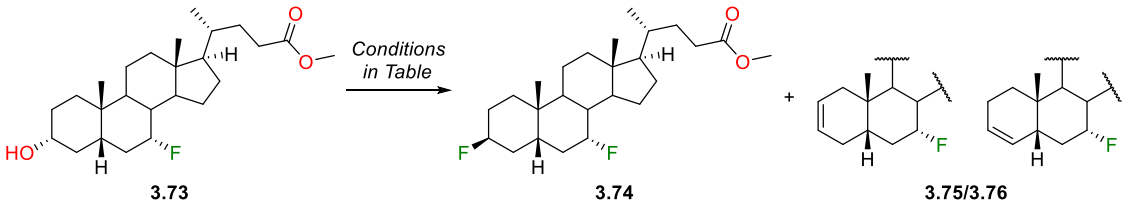

Entry	Conditions	Scale	Yield
1	PyFluor, DBU, Toluene, RT, 19 h	100 mg	**3.74**: 0%
2	NfF, 3HF•NEt_3, NEt_3, Acetonitrile, RT, 17 h	50 mg	**3.74**: ~40%[1] **3.75/3.76**: ~60%[1]
3	DAST, DCM, RT, 21 h	50 mg	**3.74**: ~63%[1] **3.75/3.76**: ~30%[1]
4	1. DAST, DCM, RT, 3 d 2. *m*-CPBA, DCM, RT, 17 h	540 mg	**3.74**: 34%[2]

[1]Approximate yield based on analysis of the ^{1}H NMR spectrum of the crude material; [2]Isolated Yield.

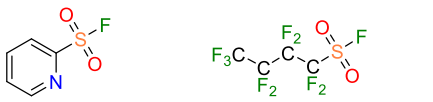

Figure 3.27 - PyFluor and NfF

PyFluor has previously been successfully employed as a fluorinating reagent of bile acid A-ring alcohols within the group with minimal formation of elimination byproducts, but for **3.73**, PyFluor yielded 0% of the 3β-fluoro product (Entry 1, *Table 3.9*). Analysis of the crude material by ^{1}H NMR showed the presence of the sulfonate ester intermediate, formed prior to fluorination. Conversely, fluorination of **3.73** with the other sulfonyl fluoride reagent NfF (Entry 2, *Table 3.9*) was observed by ^{1}H and ^{19}F NMR spectral analysis to form the desired 3β-fluoro product **3.76** (*Scheme of Table 3.9*), although, a comparatively higher percentage of alkene by-products **3.77** and **3.78** (*Scheme of Table 3.9*) were also formed.

Deoxyfluorination with DAST gave the best ratio of 3β-fluoro to alkene products on a test scale (Entry 3, *Table 3.9*), and on the full scale reaction of **3.73** (Entry 4, *Table 3.9*), the difluoro ester **3.74**

was achieved in a 36% yield, following *m*-CPBA-mediated epoxidation of the inseparable alkene by-products. The structure of **3.74** was confirmed by x-ray crystallography (*Figure 3.28*).

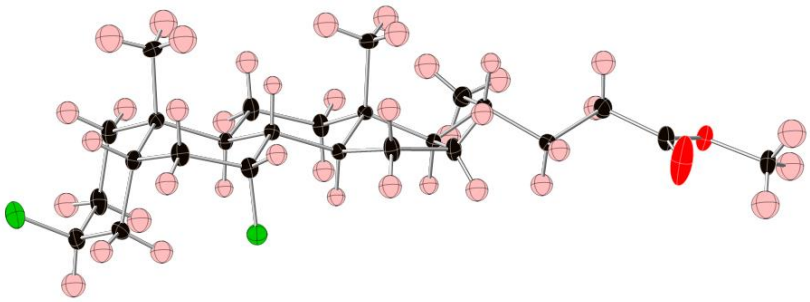

*Figure 3.28 - X-Ray Crystal Structure of **3.74***

Saponification of the methyl ester under mild basic conditions[147] then gave the 3β,7α-difluoro target analogue **3.7** (*Scheme 3.27*), which readily crystallised (*Figure 3.29*).

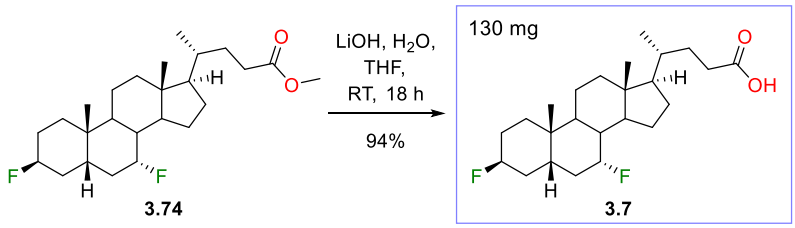

*Scheme 3.27 - Synthesis of **3.7***

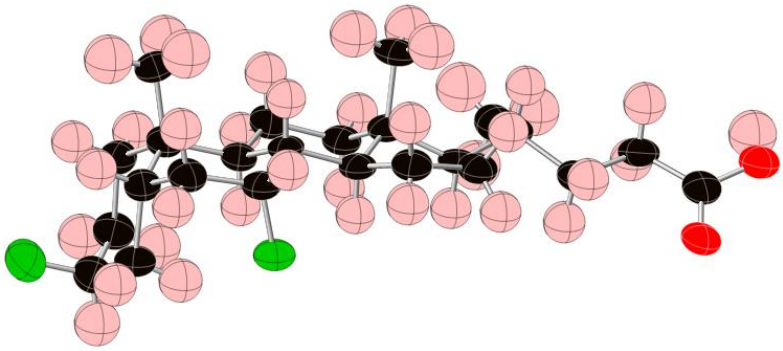

*Figure 3.29 - X-Ray Crystal Structure of **3.7***

Synthesis of the remaining 7α-fluoro target analogues **3.5** and **3.6** (*Scheme 3.20*) commenced with a Mitsunobu inversion of the 3α-hydroxy of **3.73** using a procedure by Geoffroy *et al.*,[184] giving a high yield of the desired 3β-benzoate **3.77** (*Scheme 3.28*).

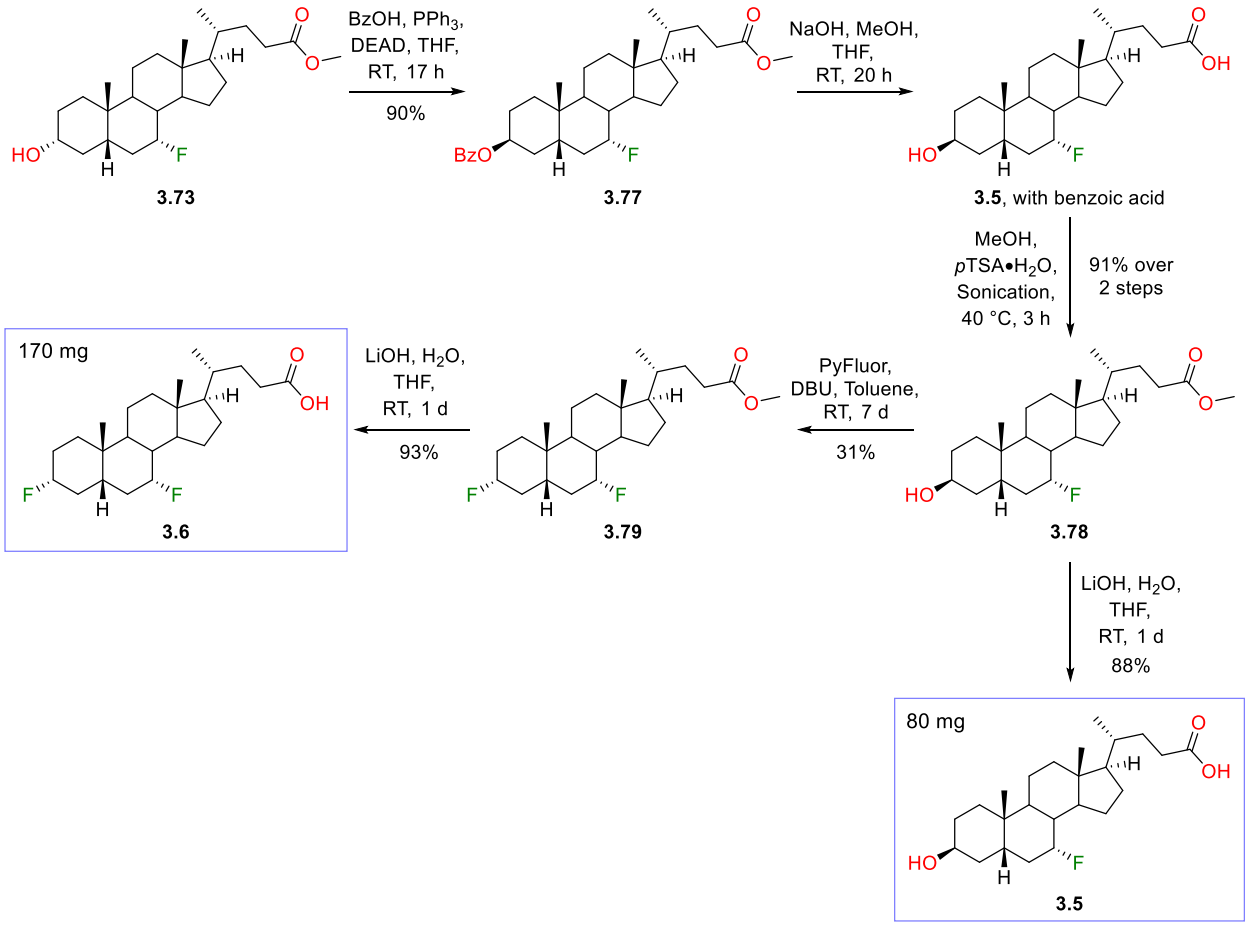

*Scheme 3.28 - Synthesis of **3.5** and **3.6***

Selective deprotection of the benzoyl protecting group of **3.77** was first attempted with potassium carbonate in anhydrous methanol,[185] but no reaction occurred after overnight stirring. The reaction was then attempted with sodium methoxide in methanol, but despite using anhydrous conditions, the methyl ester partially hydrolysed. Instead, global deprotection of **3.77** was carried out with sodium hydroxide, giving the carboxylic acid **3.5** (*Scheme 3.28*) impure with benzoic acid, inseparable by flash chromatography. The methyl ester was reinstalled, yielding **3.78** (*Scheme 3.28*) cleanly after purification by flash chromatography.

Fluorination of **3.78** was then performed using PyFluor. Although PyFluor was unsuccessful at fluorinating the less reactive, equatorial 3α-hydroxy of **3.73**, when used on axial 3β-alcohols, it has been shown within the group to give good yields of 3α-fluoro products. In contrast, DAST has been shown to give significantly lower yields of around 20%. A 31% yield of the 3α,7α-difluoro ester **3.79** (*Scheme 3.28*) was achieved, with loss of yield due to unreacted sulfonate ester. In this case, alkene by-products were separable by flash chromatography without the requirement for derivatisation.

With **3.79** in hand, it was deprotected under basic conditions to give the 3α,7α-difluoro target analogue **3.6** (*Scheme 3.28*), the x-ray crystal structure of which is shown in *Figure 3.30*. The ester

of **3.78** was also saponified to give a clean sample of the 3β-hydroxy-7α-fluoro target analogue **3.5** (*Scheme 3.28*), the structure of which was confirmed by x-ray crystallography (*Figure 3.31*).

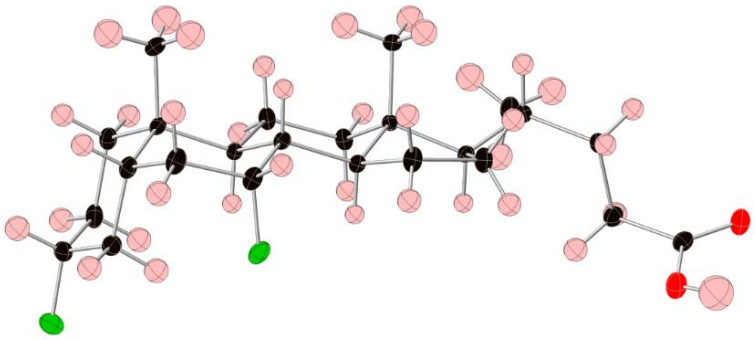

*Figure 3.30 - X-Ray Crystal Structure of **3.6***

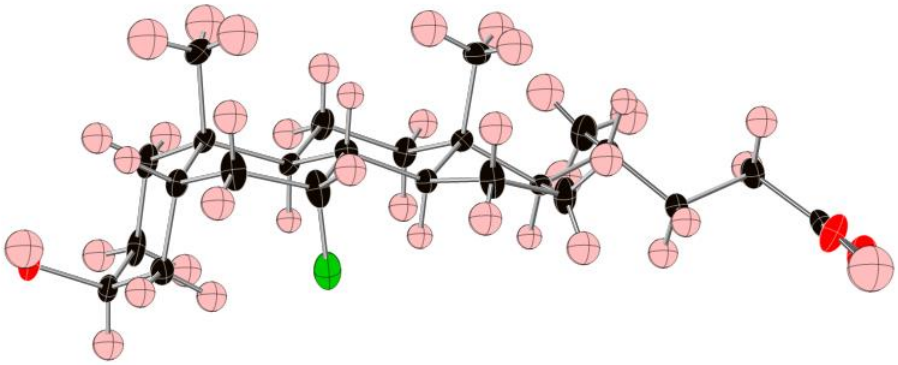

*Figure 3.31 - X-Ray Crystal Structure of **3.5***

3.3.6 Synthesis of 7β-Fluoro Analogues

With the targeted 7α-fluoro analogues in hand, synthesis of the 7β-fluoro analogues commenced. From the 7β-fluoro ketone **3.62**, the 6α- and 6β-hydroxy esters **3.80** and **3.81** (*Scheme 3.29*) were achieved in moderate yields, synthesised *via* reduction with sodium borohydride. Due to the low yielding electrophilic fluorination reaction (*Scheme 3.23*), a significantly lower amount of 7β-fluoro material was available. Hence, thiocarbonate formation and deoxygenation was performed on both **3.80** and **3.81** to ensure the highest possible quantity of deoxygenated material (*Scheme 3.20*) could be obtained.

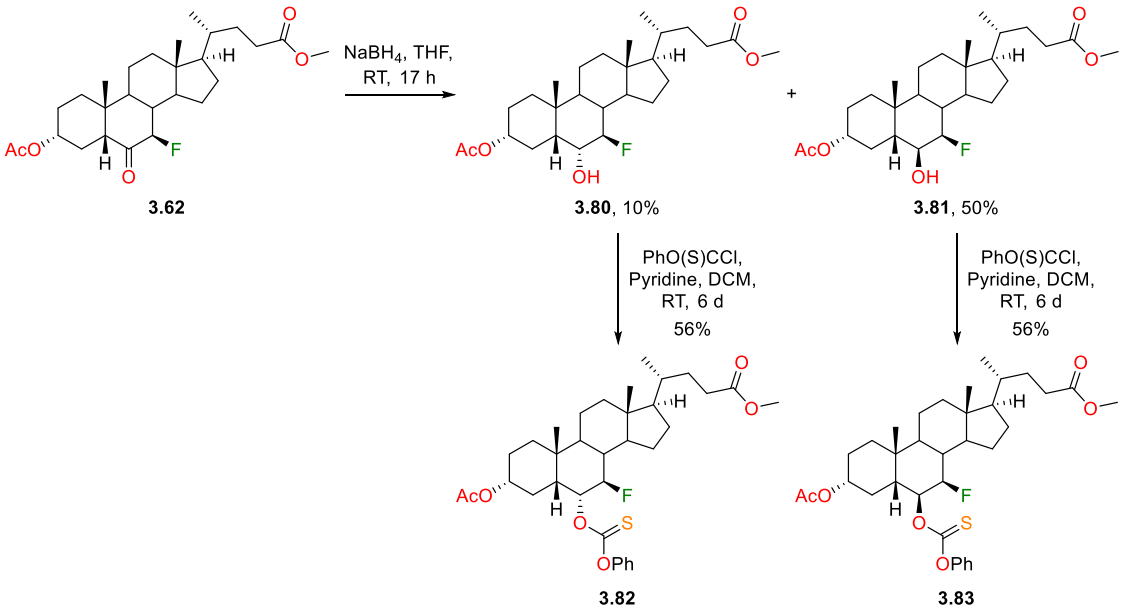

*Scheme 3.29 - Reduction of **3.64** and Thiocarbonate Formation*

Following 6 d of stirring, the 6α- and 6β-thiocarbonates **3.82** and **3.83** (*Scheme 3.29*) were formed, both in 56% yields. Both reactions were observed to be very slow on analysis of the reaction mixture by HPLC-LRMS. The negative inductive effect of the proximal fluorine atom is likely to have reduced the nucleophilicity of the reacting hydroxy group, slowing the reaction. In addition, the reaction could have been slowed by the difficultly in approach of *O*-phenyl chlorothionoformate from either the hindered bottom face of **3.82**, or the top face of **3.83**, where it could clash with both 19-CH_3 and the 7β-fluorine (*Figure 3.32*).

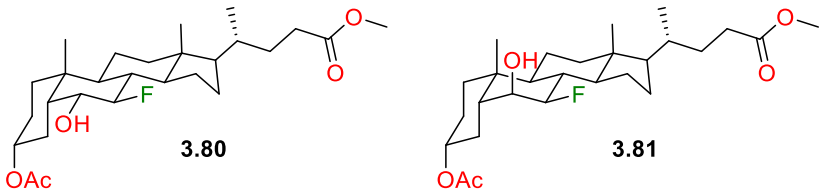

*Figure 3.32 - 3D Representations of **3.80** and **3.81***

Comparatively, deoxygenation of the thiocarbonates, **3.82** and **3.83**, was facile. Following heating with triethylsilane and dibenzoyl peroxide, the 7β-fluoro ester **3.84** (*Scheme 3.30*) was isolated around 85% pure, in approximate yields of 64% and 83% from **3.82** and **3.83** respectively.

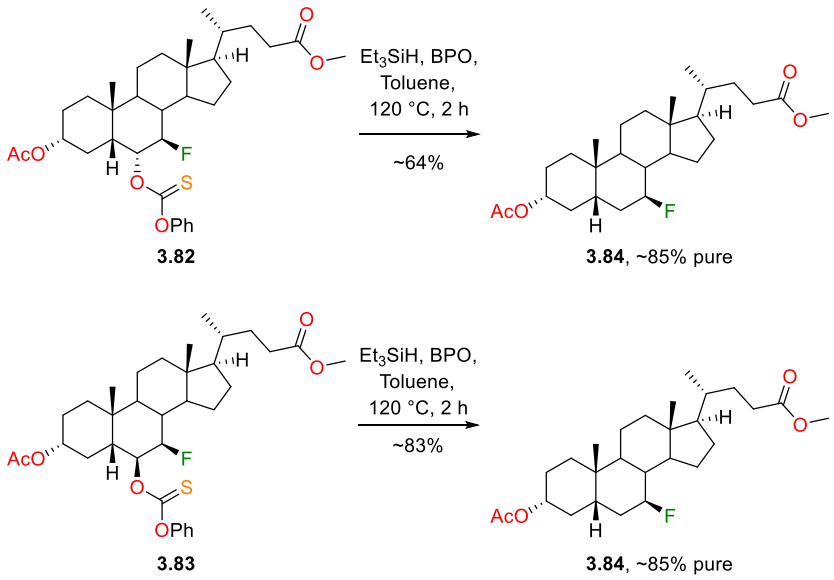

*Scheme 3.30 - Deoxygenation of **3.82** and **3.83***

Finally, global deprotection of **3.84** and flash chromatography purification gave around 250 mg of the target analogue 7β-fluoro LCA, **3.4** (*Scheme 3.31*), in <1% overall yield from HDCA. The structure of **3.4** was confirmed by x-ray crystallography (*Figure 3.33*).

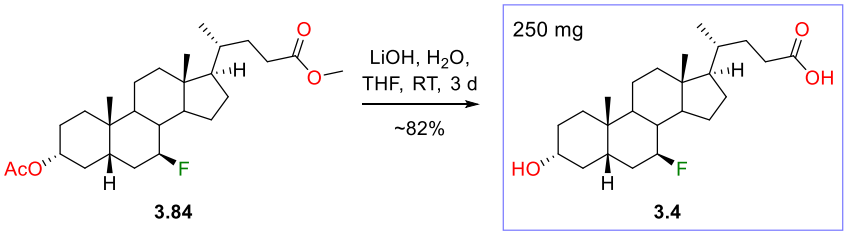

*Scheme 3.31 - Synthesis of **3.4***

As fluorination reactions of the 7α-fluoro A-ring alcohols gave low (~30%) yields of 3-fluoro products (*Scheme 3.28*, *Table 3.9*), functionalisation of the 3α-hydroxy of **3.4** was deemed not to be viable on the low quantity remaining.

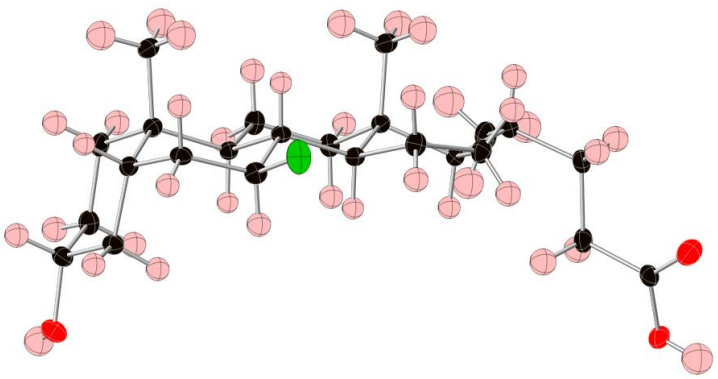

*Figure 3.33 - X-Ray Crystal Structure of **3.4***

3.4 Conclusion

To conclude, eleven mono- and non-geminal difluorinated bile acid analogues (*Figure 3.34*) were successfully synthesised from 7-keto LCA (**2.17**, *Scheme 3.1*) and hyodeoxycholic acid (HDCA, **1.7**, *Scheme 3.20*).

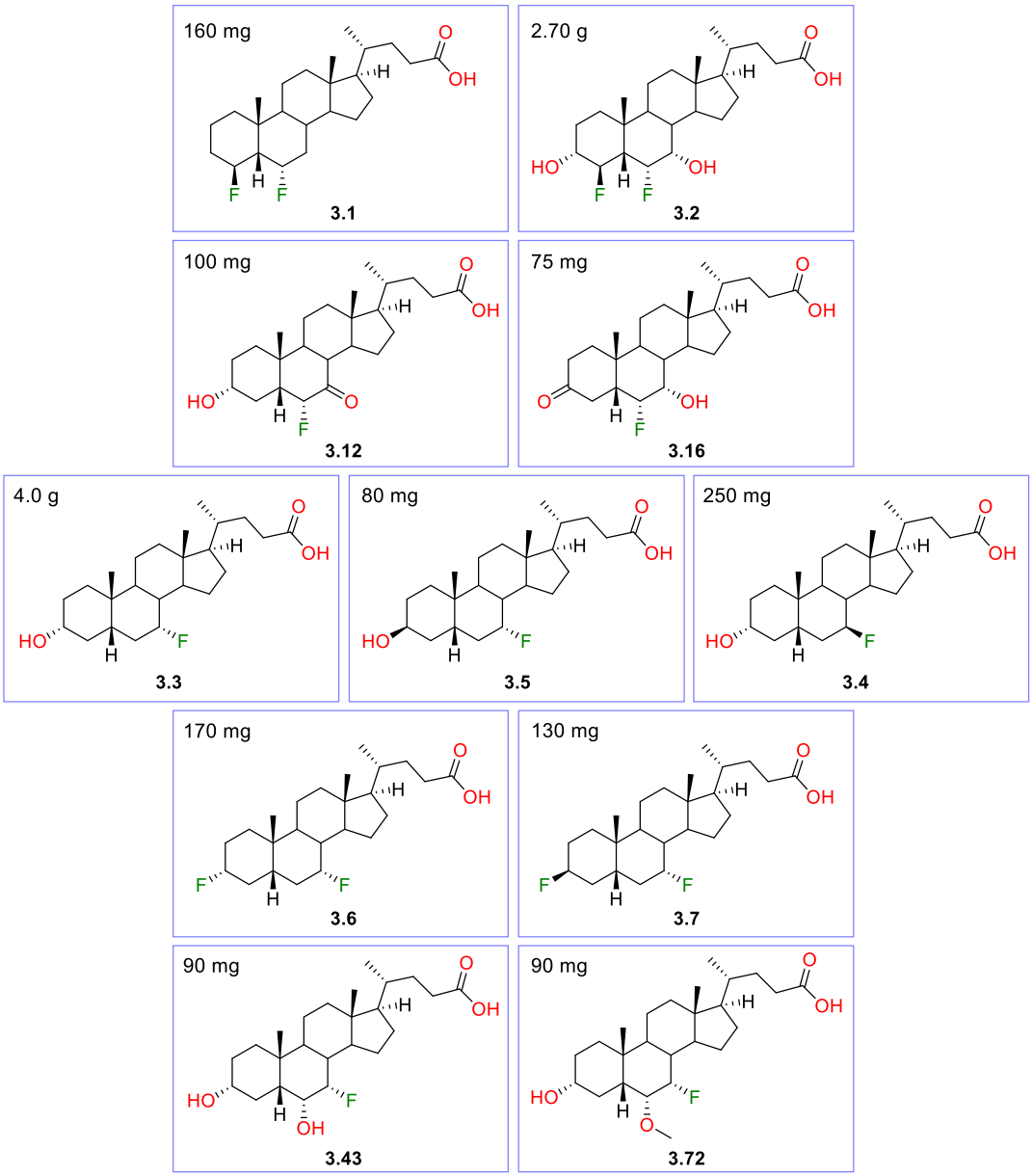

Figure 3.34 - Synthesised Mono- and Difluorinated Bile Acid Analogues

The 4β,6α-difluoro analogues **3.1** and **3.2** (*Figure 3.34*) were synthesised from the 6α-fluoro intermediate **2.68** (*Scheme 3.1*), formed previously from 7-keto LCA, following successful reduction, oxidation, esterification, saponification, electrophilic fluorination and Barton-McCombie deoxygenation reactions. Both analogues were isolated in excess of 150 mg, sufficient quantities for testing in biological assays. The synthesis also saw the formation of an unusual by-product, identified to be an alcohol-DMF adduct by NMR spectroscopic and x-ray crystallographic analysis.

The 6α-fluoro ketone analogues **3.12** and **3.16** (*Figure 3.34*) were also obtained during the synthesis of **3.1** and **3.2**.

The synthesis of diastereomerically pure 7α-fluoro LCA (**3.3**, *Figure 3.34*) and 7β-fluoro LCA (**3.4**, *Figure 3.34*) was achieved from hyodeoxycholic acid. Esterification, regioselective oxidation, electrophilic fluorination, reduction, Barton-McCombie deoxygenation and saponification reactions afforded **3.3** and **3.4** in 4.0 g and 250 mg respectively, ample quantities for various biological assays.

The 7α-fluoro analogues **3.5**, **3.6** and **3.7** (*Figure 3.34*) were synthesised following modification of the 3α-hydroxy of **3.3**. The 3β-hydroxy analogue **3.5** was obtained following a Mitsunobu inversion, whilst the 3-fluoro analogues **3.6** and **3.7** were synthesised *via* deoxyfluorination reactions using DAST and PyFluor. Modification of the 3α-hydroxy of **3.4** was not performed due to earlier isolation of a low mass of 7β-fluoro products.

The 6α-hydroxy and 6α-methoxy analogues **3.43** and **3.72** (*Figure 3.34*) were also isolated, synthesised from a 6α-hydroxy intermediate from the route to **3.3.**

Chapter 4 Synthesis of Chlorinated Analogues

4.1 Retrosynthetic Analysis of Chlorinated Target Compounds

Biological screening of the first fluorinated bile acids synthesised within the group revealed that 3-deoxy-3α-fluoro CDCA (**4.1**, *Figure 4.1*) reduced cell viability and induced apoptosis in breast cancer cell lines, specifically MCF-7 and MDA-MB-231, with IC_{50} values of 6.44 ± 0.37 μM and 7.16 ± 0.03 μM respectively. As a result of these findings, 3α-chlorinated analogues of **4.1** were targeted to test against the same cell lines.

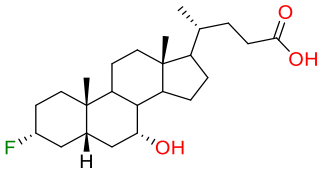

4.1

Figure 4.1 - 3-Deoxy-3α-fluoro CDCA

A retrosynthetic analysis of 3-deoxy-3α-chloro CDCA (**4.2**, *Scheme 4.1*) leads to the 3β-hydroxy ester **4.3** (*Scheme 4.1*), which could be obtained from the previously synthesised 3-keto ester **2.25** (*Scheme 4.1*) following protection and reduction reactions. Whilst a 3β-hydroxy could be installed *via* a Mitsunobu reaction from CDCA, the proposed protection/deprotection strategy required (prior to chlorination) would be long-winded and was therefore avoided.

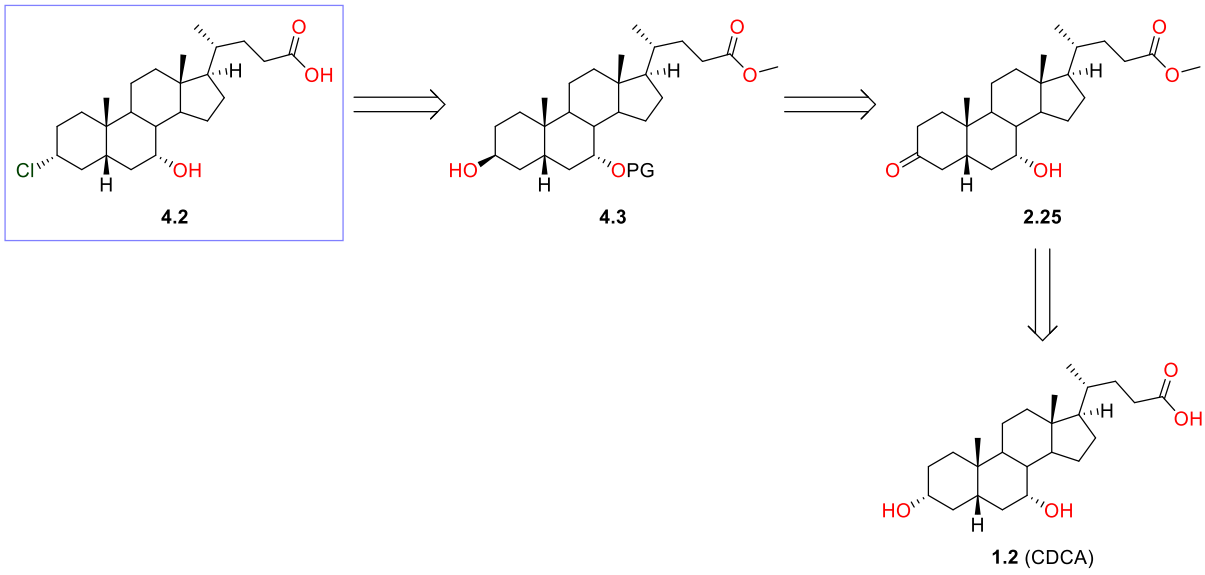

*Scheme 4.1 - Retrosynthetic Analysis of **4.2***

3-deoxy-3α-chloro UDCA (**4.4**, *Scheme 4.2*) could be formed using the same synthetic strategy as **4.2**, starting instead with UDCA (**1.6**, *Scheme 4.2*).

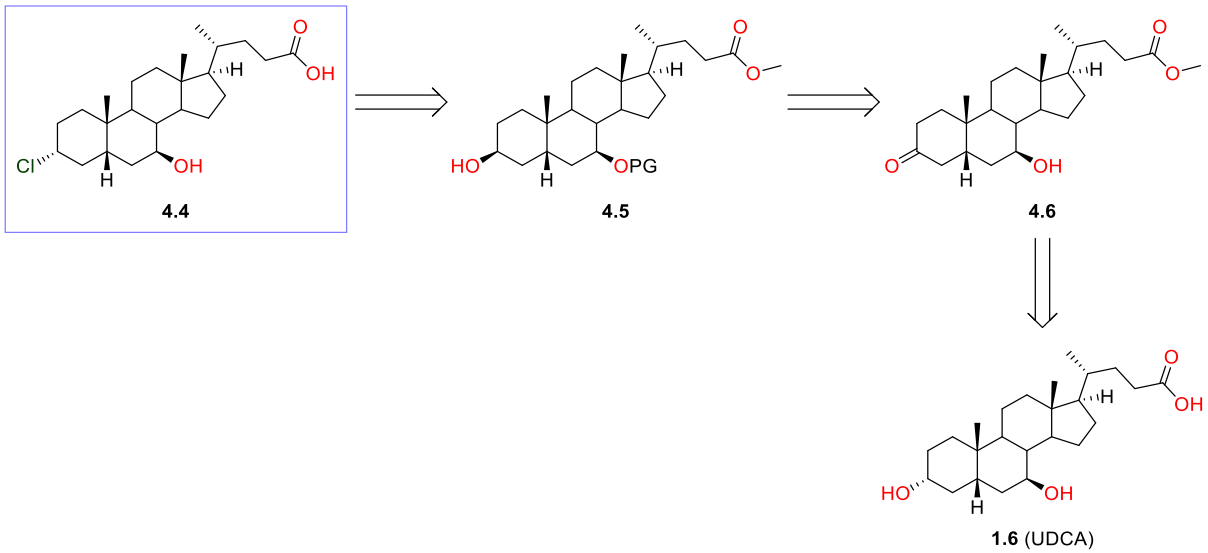

*Scheme 4.2 - Retrosynthetic Analysis of **4.4***

4.2 Synthesis of Analogues from CDCA and its Derivatives

4.2.1 Protection and Stereoselective Reduction

To install a 3α-chloro moiety, a 3β-hydroxy is required. Literature studies have shown that the strong "Selectride" reducing agents (lithium, L-, or potassium, K-) give very high selectivity towards 3β-hydroxy products from 3-keto-5β-steroids,[186,187] due to a preferred equatorial attack of the bulky reducing agent.[188] Notably though, L-Selectride has the ability to reduce esters to alcohols, therefore L-Selectride reduction was first tested on a 3-ketone of a carboxylic acid. The methyl ester of the previously synthesised compound **2.26** (*Scheme 4.3*) was saponified to give the carboxylic acid **4.7** (*Scheme 4.3*), a derivative with no ester groups and a protected 7α-hydroxy group.

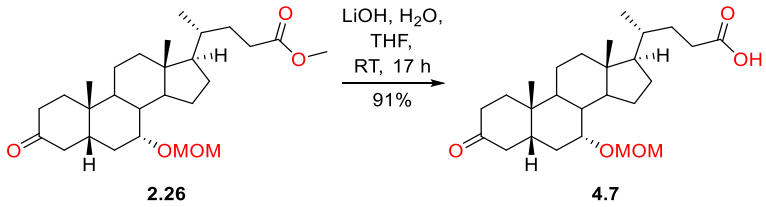

2.26 **4.7**

*Scheme 4.3 - Methyl Ester Saponification of **2.26***

Additionally, to allow the use of a simple protecting group strategy, reduction of the 3-ketone of a methyl ester derivative with L-Selectride was of interest, specifically to investigate the degree of reduction of the ester and determine the viability of the protecting group. To protect the 7α-hydroxy group, an acetyl group was chosen as it is known to be stable in acidic media at room temperature – conditions typical of a chlorination reaction. Also, specifically, a 7α-acetate has been observed to possess low reactivity due to steric hindrance, meaning reduction of the protecting group with L-Selectride is not expected. Hence, the previously synthesised 3-ketone ester **2.25** (*Scheme 4.4*) was acetylated, giving a high yield of **4.8** (*Scheme 4.4*).

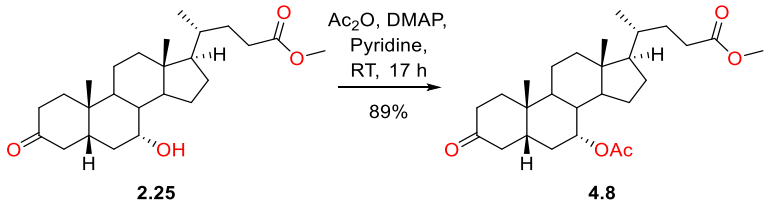

2.25 **4.8**

*Scheme 4.4 - Acetyl Protection of **2.25***

The test scale reduction of **4.7** with L-Selectride was fast, and cleanly gave only the 3β-hydroxy product **4.9** (Entry 1, *Table 4.1*) in a very high yield. With proof of the formation of the desired stereochemistry at the 3-position, the ester **4.8** was reduced with L-Selectride. The reaction was also fast, but led to a lower yield of the desired 3β-hydroxy product **4.10** (Entry 2, *Table 4.1*). The methyl ester (at C24) was also observed on analysis of the ^{1}H NMR spectrum of the crude material

to have reduced partially, although the primary alcohol product **4.11** (*Scheme of Table 4.1*) was not isolated. Notably, reduction of the 7α-acetyl group of **4.8** was not observed. On a 4.0 g scale (Entry 3, *Table 4.1*), reduction of **4.8** gave a significantly higher yield of **4.10**, with the formation of only a trace of **4.11**.

Table 4.1 - Stereoselective Reduction Reactions

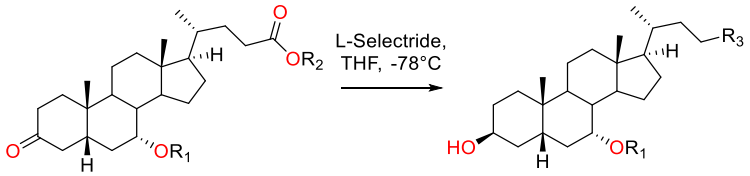

4.7: R_1 = MOM, R_2 = H
4.8: R_1 = Ac, R_2 = Me

4.9: R_1 = MOM, R_3 = COOH
4.10: R_1 = Ac, R_3 = COOMe
4.11: R_1 = Ac, R_3 = CH_2OH

Entry	Starting Material	Scale	Reaction Time	Yield/Result
1	**4.7**	100 mg	10 min	**4.9**: 97%
2	**4.8**	550 mg	15 min	**4.10**: 60%; **4.11**: ~5% (not isolated)
3	**4.8**	4.0 g	15 min	**4.10**: 80%; **4.11**: Trace

The stereochemistry of the 3-hydroxy of **4.9** and **4.10** was confirmed on analysis of the ^{1}H NMR spectra of the clean products. In the ^{1}H NMR spectrum of CDCA methyl ester (**2.24**, *Figure 4.2*), with a 3α-hydroxy group, the 3β-H coupled to two vicinal *trans*-diaxial protons and was observed to be a tt with *J*=11.1, 4.5 Hz. In the ^{1}H NMR spectra of **4.9** and **4.10** (*Figure 4.2*), quartets corresponding to 7β-protons were observed along with broad singlets corresponding to the 3-protons. These did not possess any large ^{1}H-^{1}H coupling constants due to the lack of vicinal *trans*-diaxial protons, hence the 3-alcohol was deemed to be in the β-position for both **4.9** and **4.10**.

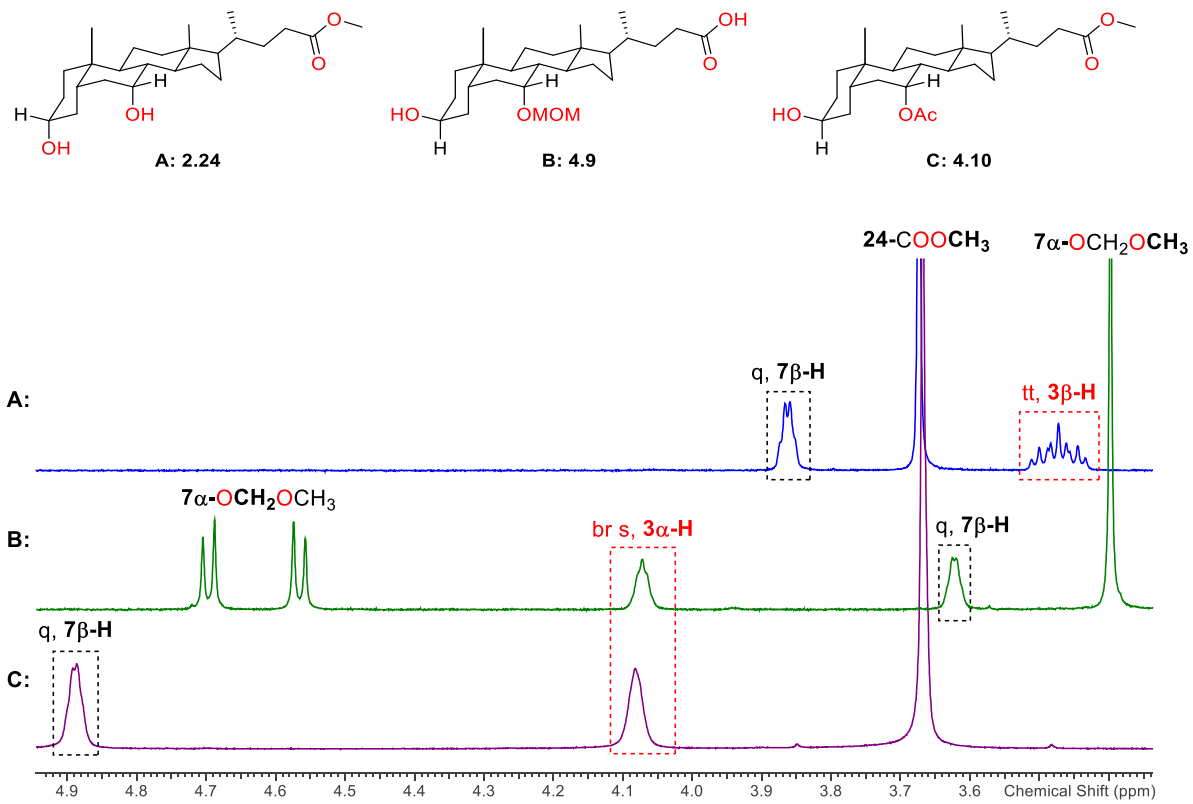

*Figure 4.2 - Structures of **2.24**, **4.9** and **4.10** with Sections of ^{1}H NMR Spectra of: **2.24** (**A**, blue); **4.9** (**B**, green); **4.10** (**C**, purple)*

4.2.2 Chlorination and Deprotection

Chlorination of **4.10** was attempted first with phosphorus oxychloride using a procedure by Kovács *et al.*[189] (Entry 1, *Table 4.2*), but neither the desired 3α-chloro product **4.12** (*Scheme of Table 4.2*) or potential alkene by-products (**4.13**/**4.14**, *Scheme of Table 4.2*) were observed to have formed on analysis of the crude material – only a high level of unidentified degraded material and polymeric material were observed. The reaction was then attempted using a procedure by Babcock *et al.*, with *N*-chlorosuccinimide (NCS) and triphenylphosphine,[190] but after stirring the reaction mixture for 3.5 d at room temperature, analysis of the crude material showed that it contained only ~20% of the desired product (Entry 2, *Table 4.2*). Using a procedure by Schneider *et al.*,[191] a test scale reaction of **4.10** with sulfuryl chloride (SO_2Cl_2) gave an approximate 40% yield of product (based on analysis of the ^{1}H NMR spectrum of the crude material), with no observation of alkene formation (Entry 3, *Table 4.2*).

On 220 mg and 2.5 g scales of **4.10** (Entries 4 and 5, *Table 4.2*), chlorination with SO_2Cl_2 gave yields of 48% and 45% of **4.12** respectively, sufficient for synthesis of the target analogue **4.2**. Along with ^{1}H NMR spectral analysis, the stereochemistry of the chlorine atom of **4.12** was confirmed by x-ray crystallography (*Figure 4.3*).

*Table 4.2 - Chlorination of **4.10***

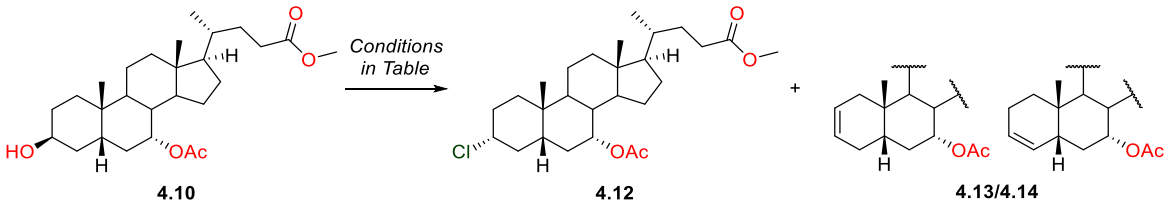

Entry	Conditions	Scale	Yield/Result
1	$POCl_3$, 80 °C, 1 h	80 mg	**4.12, 4.13, 4.14**: 0% Degradation observed[1,2]
2	NCS, PPh_3, THF, 3½ d	20 mg	**4.12**: ~20%; **4.13/4.13**: ~10%; **4.10**: ~70%[1,2]
3	SO_2Cl_2, Pyridine, 30 min	20 mg	**4.12**: ~40%; **4.13/4.14**: 0%[1,2]
4	SO_2Cl_2, Pyridine, 35 min	220 mg	**4.12**: 48%[3]
5	SO_2Cl_2, Pyridine, 20 min	2.5 g	**4.12**: 45%[3]

[1]As shown by analysis of ^{1}H NMR spectrum of crude material; [2]As shown by analysis of the Mass Spectrum of the reaction mixture or crude material; [3]Isolated yield

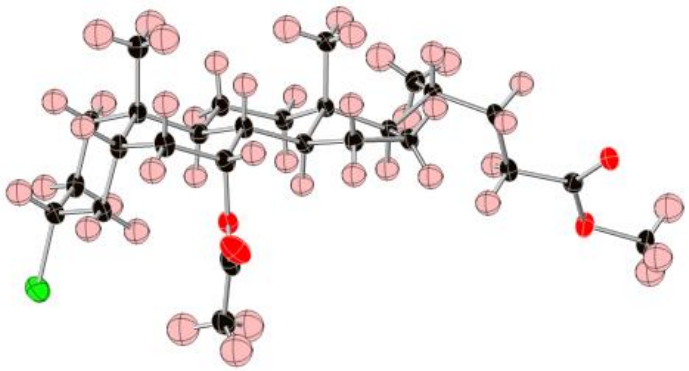

*Figure 4.3 - X-Ray Crystal Structure of **4.12***

As observed previously, deprotection of a 7α-acetoxy group requires strong basic conditions for complete removal, hence global deprotection of **4.12** was performed with a 10% solution of sodium hydroxide in methanol, cleanly yielding the target analogue, 3-deoxy-3α-chloro CDCA (**4.2**, *Scheme 4.5*), in a high yield. The structure of **4.2** was confirmed by x-ray crystallography (*Figure 4.4*).

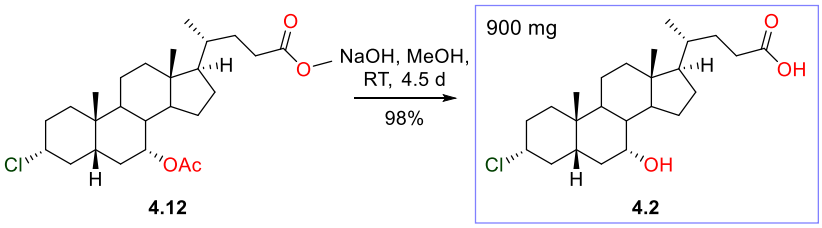

*Scheme 4.5 - Synthesis of **4.2***

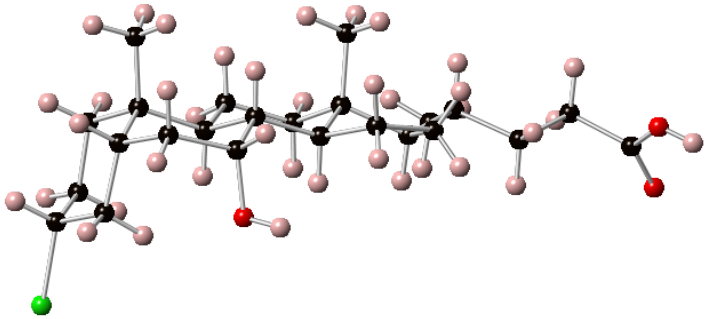

*Figure 4.4 - X-Ray Crystal Structure of **4.2***

4.3 Synthesis of Analogues from UDCA

4.3.1 Attempted Synthesis of 4.4 from UDCA

Following an analogous route to **4.2**, the synthesis towards 3-deoxy-3α-chloro UDCA (**4.4**, *Scheme 4.2*) commenced with the formation of the methyl ester **4.15** (*Scheme 4.6*). Selective oxidation of the 3α-hydroxy of **4.15** followed, using NaClO and TEMPO, yielding only the 3-ketone product **4.5** (*Scheme 4.6*). Note: oxidation of the 7β-hydroxy of **4.15** was not observed upon analysis of the crude material by ^{1}H NMR. Acetyl protection of **4.5** gave **4.16** (*Scheme 4.6*), which was treated with L-Selectride to stereoselectively reduce the 3-ketone to a 3β-hydroxy group. Whilst reduction of the 7α-acetyl protected ester **4.8** gave only 3β-hydroxy products (*Table 4.1*), reduction of **4.16** gave an inseparable, 4:1 mixture of the 3β- and 3α-hydroxy products, **4.17** and **4.18** (*Scheme 4.6*).

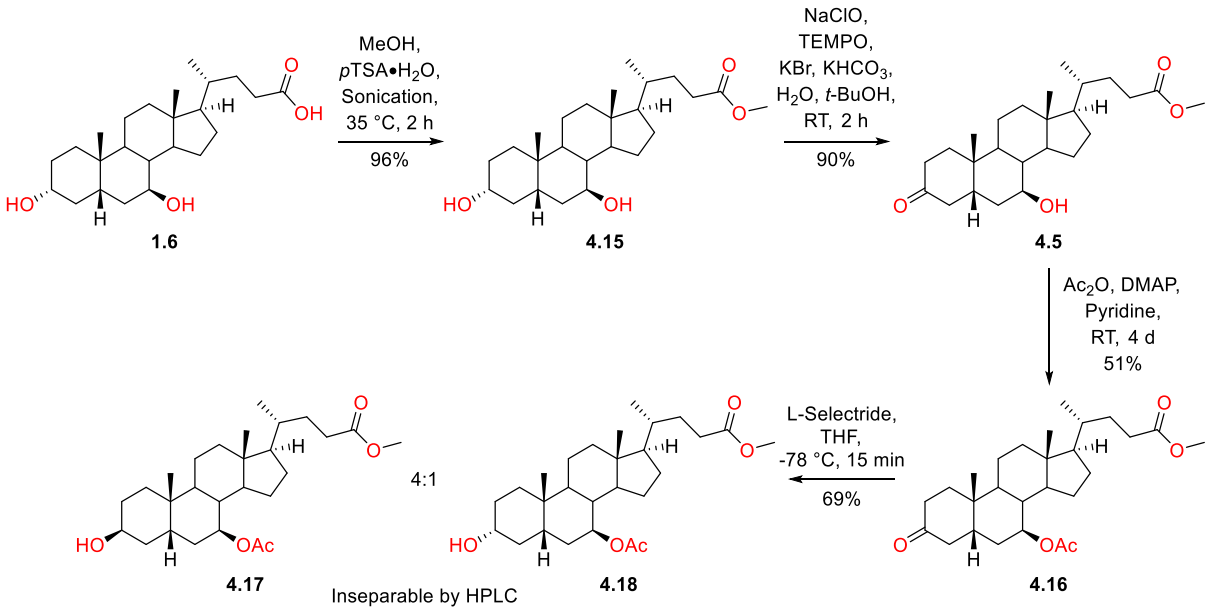

*Scheme 4.6 - Synthesis of **4.17** and **4.18***

As mentioned, L-Selectride is known to give 3β-alcohols from steroidal 3-ketones, although it is possible for the stereoselectivity to be modified by directing effects arising due to the presence of other functional groups. Analysis of the 3D-structure of **4.16** (*Figure 4.5*) reveals that the "up" 7β-acetyl could direct L-Selectride to the top face of the bile acid, therefore explaining the mixture of 3β- and 3α-hydroxy products isolated in the reaction.

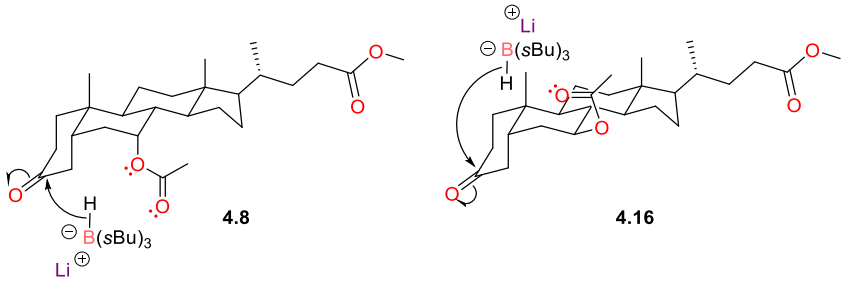

*Figure 4.5 - Proposed Attack of L-Selectride on **4.8** and **4.16***

Attempts at separation of **4.17** and **4.18** by HPLC purification were unsuccessful, hence the 4:1 mixture of alcohols was taken through to the next step of the synthetic route. Chlorination of **4.17** and **4.18** with sulfuryl chloride gave a low yield of the 3α- and 3β-chloro esters **4.19** and **4.20** (*Scheme 4.7*), which, again, were inseparable by HPLC purification.

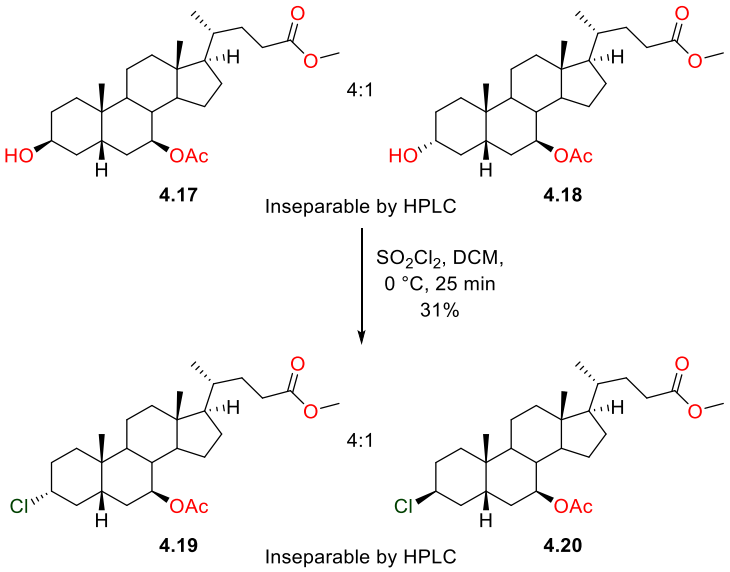

*Scheme 4.7 - Chlorination of **4.17** and **4.18***

It was envisioned that separation may be possible following acetyl deprotection, hence, the mixture of **4.19** and **4.20** was globally deprotected with sodium hydroxide and the crude carboxylic acid was treated with methanol and *p*TSA•H_2O to give the esters **4.21** and **4.22** (*Scheme 4.8*). Unfortunately, the 3α- and 3β-chloro esters were inseparable by HPLC purification.

Following the unsuccessful attempts at achieving a diastereomerically pure sample of **4.21**, saponification of the 4:1 mixture of **4.21** and **4.22** gave 3-deoxy-3α-chloro UDCA (**4.4**, *Scheme 4.8*) around 80% pure, sufficient for initial biological screenings to give an indication of activity.

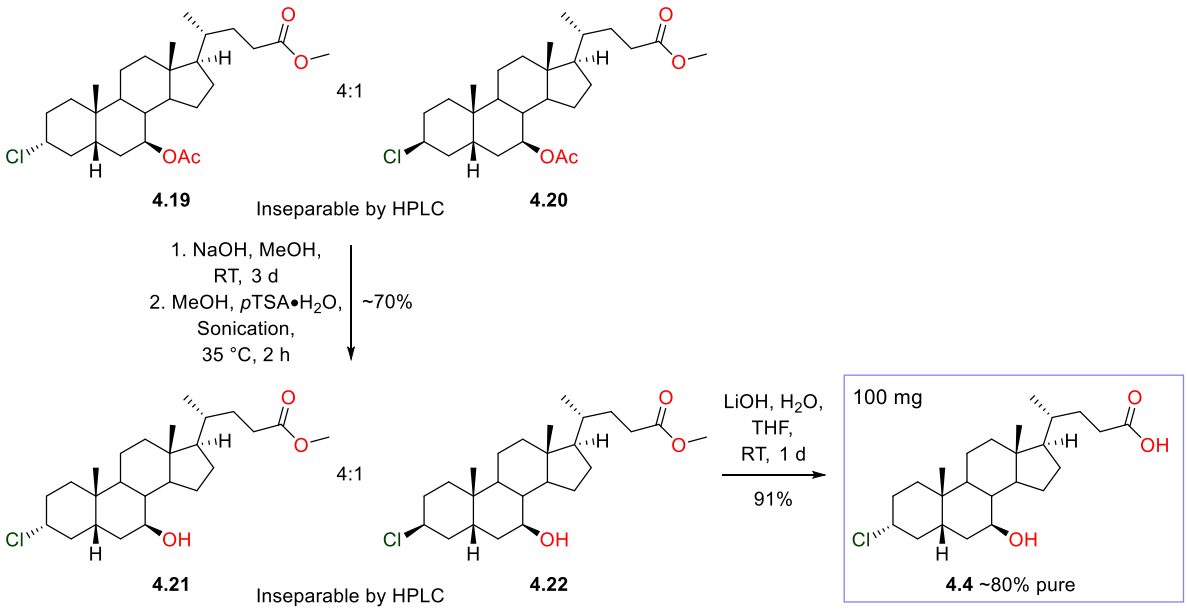

*Scheme 4.8 - Synthesis of **4.4***

4.3.2 Attempted Synthesis of 4.4 from CDCA Derivatives

To obtain **4.4** diastereomerically pure, a synthetic route *via* inversion of the 7α-hydroxy of 3-deoxy-3α-chloro CDCA, **4.2** (*Scheme 4.9*), was attempted. Prior to inversion test reactions, the carboxylic acid of **4.2** was protected with a methyl ester, giving **4.23** (*Scheme 4.9*) in a good yield.

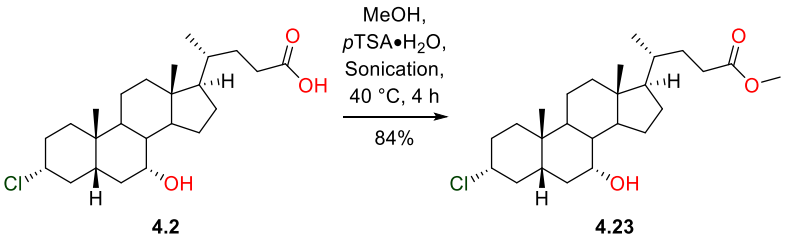

*Scheme 4.9 - Methyl Ester Formation on **4.2***

For bile acids, bile acid esters and 5β-steroids, multiple methods have been reported to obtain a 7β-hydroxy group at the 7-position, five of which are shown in *Scheme 4.10* (**A** to **E**). Inversion of the stereochemistry of the 7α-OH of CDCA (**1.2**, **A**, *Scheme 4.10*) has been reported using microbes such as *Xanthomonas maltophilia*, which utilise the enzymes 7α- and 7β-hydroxysteroid dehydrogenase, giving low to moderate yields of UDCA, **1.6**.[192] The mentioned dehydrogenase enzymes have also been isolated from *Xanthomonas maltophilia*, and used alone in aqueous media to invert the stereochemistry of the 7α-hydroxy of bile acids, achieving high yields of the desired 7β-hydroxy bile acid products.[193]

Using purely chemical methods, 7β-hydroxy formation has been reported by Iida and Chang on a cholic acid derivative *via* a 7α-mesylate (**4.24**, **B**, *Scheme 4.10*) using potassium superoxide and 18-

crown-6 to achieve the inversion of stereochemistry.[194] Techniques utilising stereoselective reduction of a 7-ketone have also been reported, using either sodium metal in hindered alcohol solvents (used previously in **Section 2.3.1.2**, **C**, *Scheme 4.10*) or Al(O*i*Pr)$_3$ in isopropanol (**D**, *Scheme 4.10*). Both methods were shown to achieve high yields of 7β-hydroxy products in the studies.[148,195]

Whilst literature precedent has not yet been set for the inversion of the 7α-OH of a bile acid or derivative using a Mitsunobu reaction, a procedure for the inversion of a 7α-OH of a 5β-steroid derivative was reported by Li *et al.* (**E**, *Scheme 4.10*). Formic acid, diisopropyl azodicarboxylate (DIAD), and triphenylphosphine were used to achieve a 92% yield of the desired 7β-alcohol over two steps.[196]

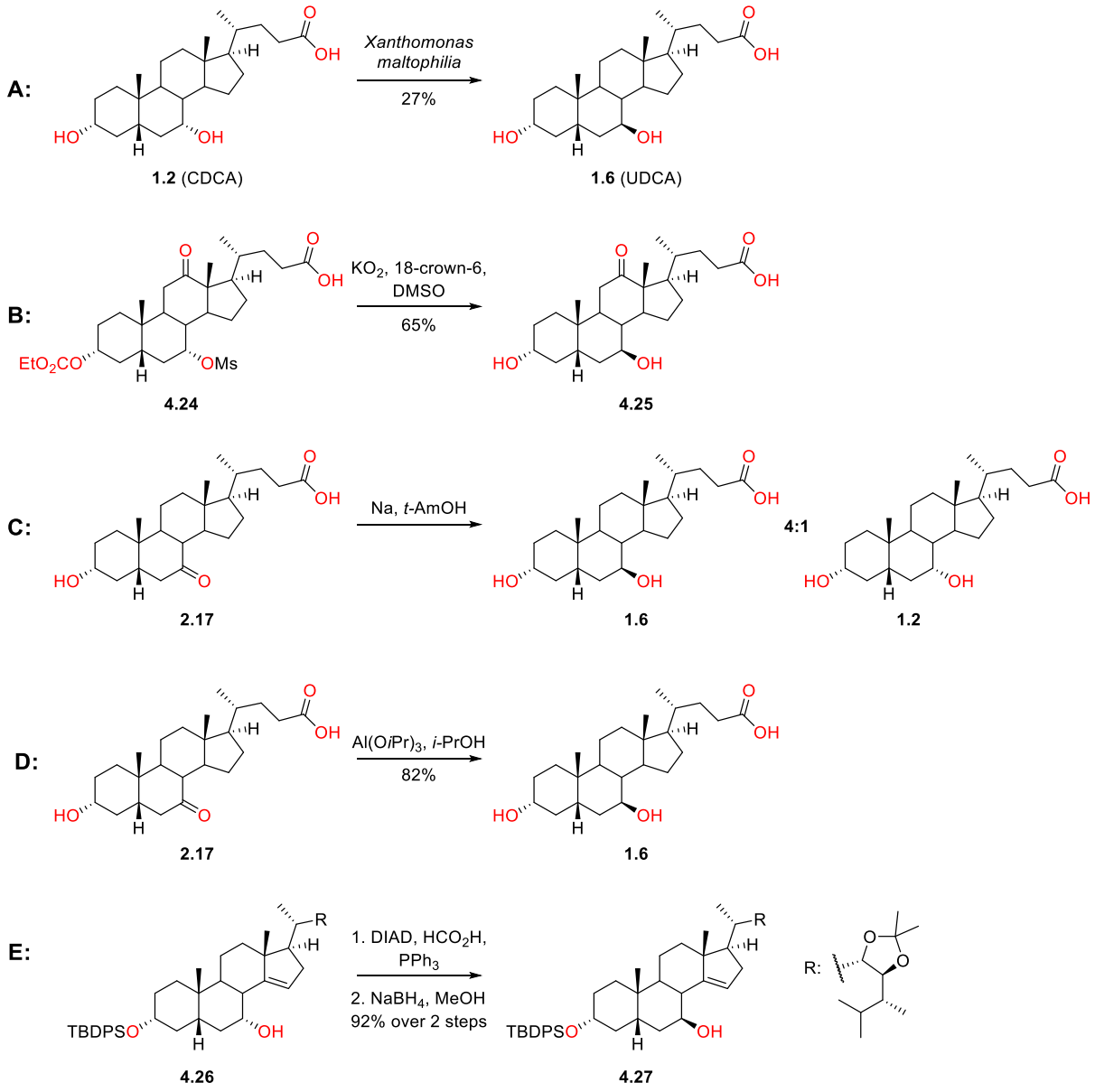

Scheme 4.10 - Literature Conditions for 7β-OH Formation: ***A***[192]*,* ***B***[194]*,* ***C***[148]*,* ***D***[195] *and* ***E***[196]

To invert the stereochemistry of the 7α-hydroxy of **4.23**, microbe or enzymatic methods were not viable due to the equipment and chemicals/biologicals required (along with their high cost) and were hence not attempted. Inversion *via* a mesylate using potassium superoxide was also not attempted due to the explosive nature of potassium superoxide,[xii] and reduction of a 7-ketone using sodium metal was not trialled as sodium has previously been reported to remove a 3β-chloro of a steroid derivative.[197] As a result of this, Mitsunobu reactions on **4.23** were first attempted to introduce a 7β-hydroxy. When using Li and coworkers' procedure for inversion,[196] no reaction was observed by TLC, HPLC-LRMS and ^{1}H NMR analysis after stirring for over 3 d (Entry 1, *Table 4.3*).

*Table 4.3 - Attempted Mitsunobu Reactions on **4.23***

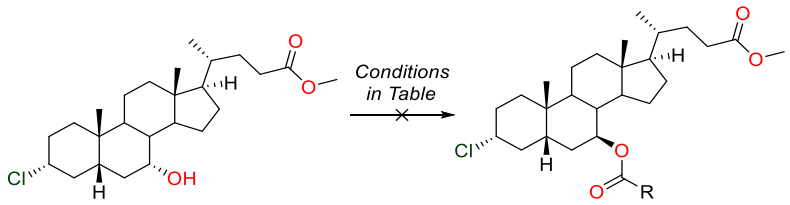

Entry	R	Conditions	Result
1	H	HCOOH, DIAD, PPh_3, THF, RT, 3½ d	**4.28**: 0%[1,2]
2	CH_2Cl	$ClCH_2COOH$, DEAD, PPh_3, Toluene, RT, 20 h	**4.29**: 0%[1,2]

As shown by analysis of the: [1]^{1}H NMR spectrum of the crude material, [2]Mass Spectrum of the crude material

Chloroacetic acid has previously been reported to be a good nucleophile in sterically hindered Mitsunobu reactions.[198] An inversion reaction with chloroacetic acid, triphenylphosphine and DEAD was attempted on **4.23** (Entry 2, *Table 4.3*) but again, HPLC-LRMS and ^{1}H NMR spectral analysis showed that no 7β-ester product (**4.29**, *Scheme of Table 4.3*) had formed.

Following the unsuccessful Mitsunobu reactions on **4.23**, attention turned to stereoselective reduction of a 7-ketone to install a 7β-hydroxy. Bleach-mediated oxidation of **4.23** yielded the 7-keto ester **4.30** (*Scheme 4.11*), the methyl ester of which was saponified with lithium hydroxide to give the 7-oxo analogue **4.31** (*Scheme 4.11*). The 3α-chloro-7-oxo methyl ester **4.30** crystallised readily, hence its structure was confirmed by x-ray crystallography (*Figure 4.6*).

[xii] Noted in its SDS

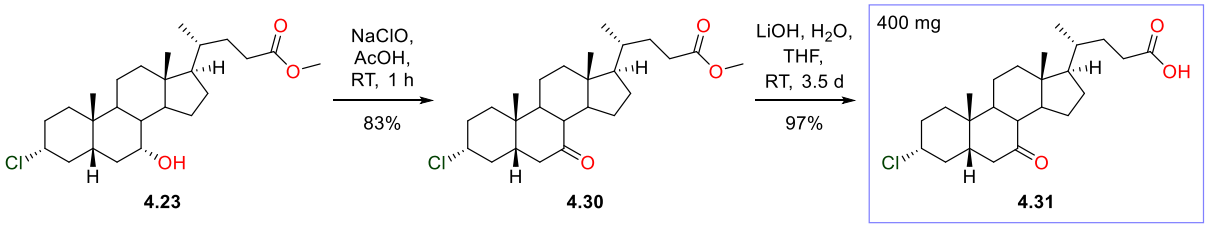

*Scheme 4.11 - Synthesis of **4.31***

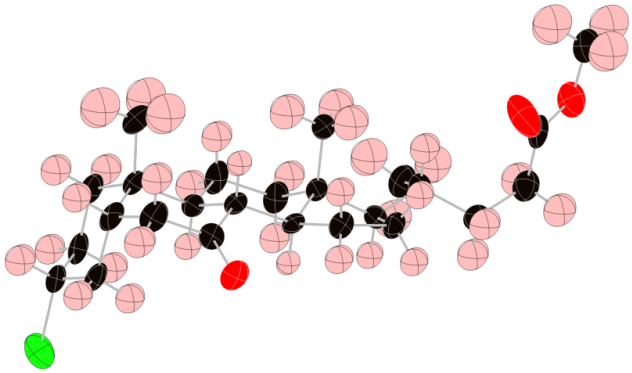

*Figure 4.6 - X-Ray Crystal Structure of **4.30***

Stereoselective reduction of **4.31** was first attempted with aluminium isopropoxide using conditions by Yu *et al*.[195] (Entry 1, *Table 4.4*). After heating for 3 h, ^{1}H NMR spectral analysis of the crude material showed that it contained only the starting material **4.31** and the previously synthesised 7α-hydroxy product **4.2** (*Scheme of Table 4.4*).

*Table 4.4 - Attempted Stereoselective Reduction of **4.31***

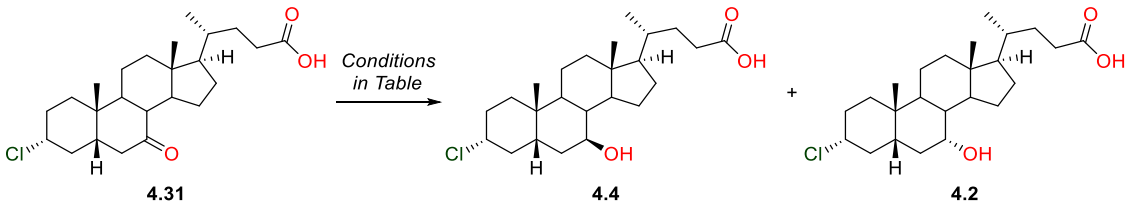

Entry	Conditions	Result
1	$Al(O^{i}Pr)_3$, IPA, 85 °C, 3 h	**4.4**: 0%; **4.31**: 55%; **4.2**: 45%[1]
2	$NaBH_4$, $CeCl_3 \bullet 7H_2O$, MeOH, EtOAc, RT, 30 min	**4.4**: 0%; **4.31**: 40%; **4.2**: 60%[1]

[1]As shown by analysis of the ^{1}H NMR spectrum of the crude material

Reduction of **4.31** was also attempted using Luche reduction conditions. Previously within the group, reduction of a ketone at the 7-position of various fluorinated bile acid derivatives with Luche conditions has yielded both 7α- and 7β-hydroxy products. Treatment of **4.31** with $NaBH_4$ and

$CeCl_3 \bullet 7H_2O$ (Entry 2, *Table 4.4*) though gave, again, a mixture of **4.31** and **4.2**, with no trace of the 7β-hydroxy product **4.4** on analysis of the crude material by ^1H NMR.

Further attempts at the synthesis of diastereomerically pure **4.4** were not performed as the 80% pure material was deemed sufficient enough for testing.

4.4 Conclusion

Three 3α-chloro bile acid analogues (*Figure 4.7*) were successfully synthesised in ample quantities for biological testing.

3-deoxy-3α-chloro CDCA, **4.2** (*Figure 4.7*), was synthesised from the previously synthesised 3-keto ester **2.25** (*Scheme 4.1*) following protection, stereoselective reduction, sulfuryl chloride-mediated deoxychlorination and saponification reactions.

3-deoxy-3α-chloro UDCA, **4.4** (*Figure 4.7*), was synthesised from UDCA following protection, oxidation, reduction, chlorination and deprotection reactions, but was isolated around 80% pure with inseparable 3β-chlorinated material. The synthesis of diastereomerically pure **4.4** was attempted from **4.2** *via* stereoinversion of the 7α-hydroxy, but Mitsunobu and 7β-stereoselective reduction reactions were unsuccessful. Prior to attempts at stereoselective reduction, the 7-keto analogue **4.31** (*Figure 4.7*) was also isolated from **4.2** following oxidation of the 7α-hydroxy.

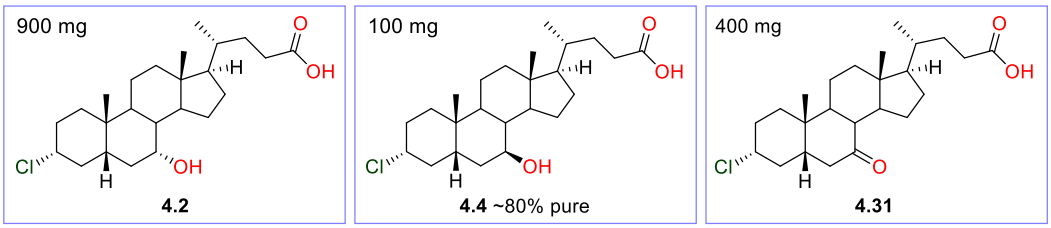

Figure 4.7 - Synthesised Chlorinated Target Analogues

Chapter 5 Biological Testing Results

5.1 Neurodegenerative Disease

5.1.1 Background of Assays

5.1.1.1 Mitochondria and MMP/ATP Assays

As discussed previously in **Section 1.1.1**, dysfunctional mitochondria and reduction in activity of electron transport chain complexes (involved in cellular respiration) are hallmarks of neurodegenerative diseases.

Mitochondria are vital organelles which produce ATP for cells *via* oxidative phosphorylation, a key metabolic pathway. Notably, mitochondria possess outer and inner membranes that encase the intermembrane space[xiii] and the mitochondrial matrix[xiv].[199] Embedded in the inner membrane is the electron transport chain (ETC), consisting of four enzyme complexes that use redox reactions to transfer electrons from complex to complex, along the chain.[200] The ETC is intrinsic in oxidative phosphorylation as it is responsible for the generation of a proton gradient from the matrix to the intermembrane space (through the inner membrane), that drives ATP synthase (also known as complex V), catalysing the synthesis of ATP.[199,201]

The electrochemical gradient generated by the ETC is known as the mitochondrial membrane potential (MMP) and is a key feature of mitochondria.[199,201] As well as catalysing ATP synthesis, the membrane potential is essential in many other mitochondrial functions including mitochondrial homeostasis (allowing elimination of dysfunctional mitochondria),[202] protein import, and the homeostasis of Ca^{2+}, a key signalling ion which, amongst many other roles, is essential in the control of neurotransmitter release and neurogenesis in neurons.[199] In addition, in neurons, mitochondria are vital as they supply intermediates from the citric acid cycle that are used as building blocks to form the neurotransmitters γ-aminobutyric acid (GABA) and glutamate.[199]

Importantly, long-term changes in MMP (compared to the normal levels) may lead to the loss of cell viability,[202] hence, measurement of the mitochondrial membrane potential is indicative of mitochondrial function and cell health.[201,203,204] In practice, the measurement of MMP can be

[xiii] Intermembrane space – the space inbetween the outer and inner mitochondrial membranes.
[xiv] Mitochondrial matrix – the space inside of the inner membrane.

performed in the suspension of mitochondria of cells *in situ*, either by using electrodes to measure the potential or by using spectral methods with fluorescent dyes.[202,203]

As well as MMP assays, the measurement of cellular ATP levels is indicative of mitochondrial health. This is because when mitochondria are dysfunctional, ATP production is lowered due to the impairment of the ETC, leading to loss of the proton gradient which powers ATP synthase.[205] ATP levels can be measured using bioluminescence assays, quantifying the light (luminescence) generated from ATP-dependent reactions of the luciferase enzyme.[206]

5.1.1.2 Cytotoxicity Assay

When investigating potential drug candidates for neurodegenerative diseases, cytotoxicity screenings are of high importance to ensure that the compounds do not cause undesired cell death. The screenings are generally performed early on in the biological testing programmes to ensure that any cytotoxic compounds are eliminated from the project as soon as possible.

Cytotoxicity can be measured by the quantification of lactate dehydrogenase (LDH) levels. LDH is an enzyme that is normally present in the cytoplasm of cells,[xv,207] which gets released into the extracellular space following permeabilisation of the cell membrane. The cell membrane may be permeabilised as a result of necrosis[xvi] (a non-programmed form of cell death)[208] or as a result of external damage to cells.[208] LDH is stable in the extracellular environment and in cell culture media, hence it is easily quantified and its measurement is a commonly used method for determination of cell death, late-stage apoptosis and cell viability.[207] Generally, high LDH levels indicate that the tested drug candidate is cytotoxic towards the cell line being investigated.

In neurodegenerative diseases, the LDH assay and cell viability assays in general are commonly used tools in drug discovery to not only quantify the number of dying cells, but also to determine whether drug candidates have neuroprotective effects.[207]

[xv] Lactate dehydrogenase (LDH) – An enzyme which is intrinsic in glycolysis, a key cell metabolic pathway.
[xvi] Necrosis – A type of cell death characterised by swelling and rupture of organelles within a cell, leading to disruption of the cell membrane.

5.1.2 Activity of Fluorinated Bile Acid Derivatives in Parkinson's Disease

Preliminary screenings (performed by the Sheffield Institute for Translational Neuroscience, SITraN), of bile acid derivatives in MMP and ATP quantification assays in fibroblast cells of sporadic (sPD) and familial (fPD, LRRK2) Parkinson's disease patients indicated that the 12,12-difluoro derivatives **2.52** (JED125, *Figure 5.1*, synthesis discussed in **Section 2.3.3**) and **2.53** (JED129, *Figure 5.1,* synthesis discussed in **Section 2.3.3**) were active, along with the 2,2-difluoro UDCA derivative JED135 (*Figure 5.1*), previously synthesised within the group. In further testing, JED135 was shown to normalise the MMP of, the levels of ROS (reactive oxygen species, which lead to oxidative damage) and ATP levels in patient-derived dopaminergic iNeurons.[xvii,209] Additionally, JED135 was shown to pass through the BBB. Further assays and testing relating to the activity and cytotoxicity of the compounds is currently yet to be finalised.

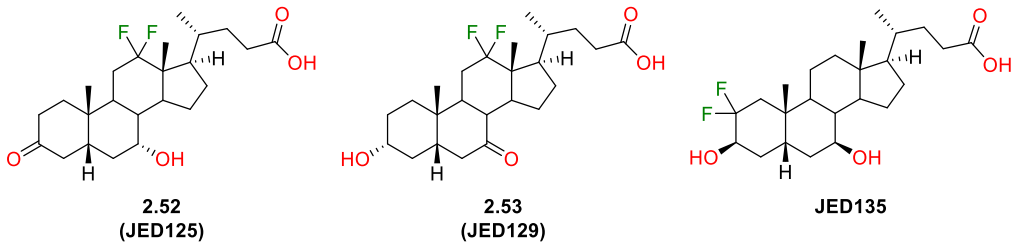

Figure 5.1 - Active Compounds in Assays for PD

5.1.3 Activity of Fluorinated Bile Acid Derivatives in Alzheimer's Disease

A primary drug screen for Alzheimer's Disease was undertaken by SITraN. Screening of 181 bile acid derivatives was performed at 10 µM and 100 nM (including 28 of the bile acid derivatives synthesised in this thesis) against sporadic (random) and familial (genetic or inherited) AD cells from four patients (sAD1, sAD2, fAD1 and fAD2) in ATP quantification and LDH cytotoxicity assays. For both of the assays, DMSO was used a blank and the compounds were compared against UDCA and TUDCA at 10 µM.

5.1.3.1 ATP Assays

Four and three ATP assays were performed for the sAD1/fAD1 and sAD2/fAD2 cells respectively. The hits were described as either "strong" or "moderate", with a strong hit being defined as a compound with activity in 3/4 or 4/4 assays for sAD1/fAD1 and 2/3 for sAD2/fAD2, and a moderate hit was defined as a compound with activity in 2/4 assays for sAD1/fAD1 and 1/3 for sAD2/fAD2 at

[xvii] iNeurons (induced neurons) or iDA neurons (induced dopaminergic neurons) are a type of cell directly formed from human fibroblasts. They "*exhibit functional dopaminergic neurotransmission and relieve locomotor symptoms in animal models of Parkinson's disease*"

both concentrations tested. Note: A hit compound increased cellular ATP levels compared to DMSO.

Table 5.1 - ATP Quantification Assay for Sporadic AD Cells (sAD1 and sAD2)

ATP Quantification Assay (Sporadic AD)			
sAD1		**sAD2**	
Compound[1]	**Hit Level**	**Compound**[1]	**Hit Level**
JED105	Strong	JED106	Strong
JED108 (**2.9**)	Strong	JED108 (**2.9**)	Moderate
JED133	Moderate	JED133	Strong
JED136	Strong	JED135	Moderate
JED137	Moderate	JED136	Strong
JED140	Moderate	JED383	Strong
JED383	Strong		
JED384	Moderate		
JED385	Strong		

[1]For structures, see *Figure 5.2*.

Of the 181 compounds tested, fifteen fluorinated bile acid derivatives were hits in the ATP assays against sporadic AD cells: nine were hits against sAD1 cells and six were hits against sAD2 cells, as shown in *Table 5.1*. In the sAD1 cell ATP assay, notably, the hexafluorinated bile acid **2.9** (JED108, *Figure 5.2*, synthesis discussed in **Section 2.3.4**) was a strong hit at 100 nM. Additionally, **2.9** was a moderate hit at both concentrations tested in the ATP assay of sAD2 cells. Strong hits in the sporadic AD cell assays were also observed for the trifluoromethyl compound JED105, 2,2-difluoro CDCA (JED136), 4α-fluoro CDCA (JED106), the fluoroalkene derivative JED133 and the 3α-fluoro sulfonamide derivatives JED383 and JED384 (*Figure 5.2*).

Interestingly, the majority of compounds which exhibited strong or moderate hits in the assays against both sporadic AD cell lines (active compounds) had quite different structures. The only observed similarity was that polar groups were present at the 3- and 7-positions of the A- and B-

rings, with fluorination predominantly on the A ring (except for JED105). It is worth noting that a number of compounds with similar structures to the hits were not active.

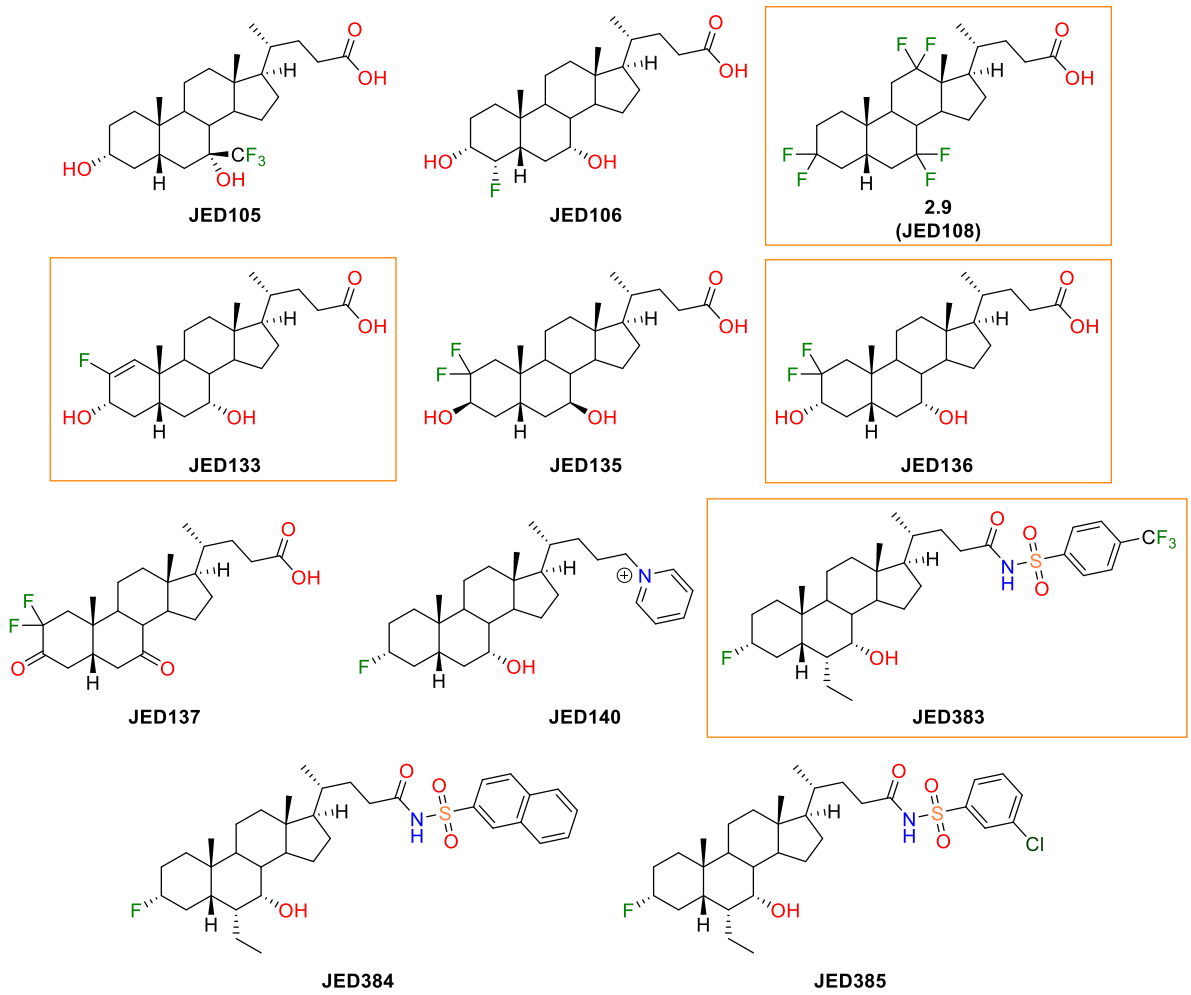

Figure 5.2 - Tested Fluorinated Bile Acid Derivatives with ATP Activity in Sporadic AD Cells

Of the four compounds with hits in both sporadic AD cell lines (**2.9**, JED133, JED136 and JED383, highlighted in orange in *Figure 5.2*), only two bore similar structures, JED133 and JED136, differing only at the 1- and 2-positions, although the shape of the A-ring of JED133 was significantly different to JED136 as it contained an endocyclic alkene. When comparing JED133, JED136 and JED383 to **2.9**, the structures were very different. Not only did it not bear any hydroxy groups, **2.9** bore a CF_2 moiety at the 12-position (on the C-ring), whilst the other compounds bore a CH_2 moiety at the same position.

Despite the great differences in structure, the mean values of the experimental average ATP increases of the four hit sporadic AD compounds were remarkably similar (*Table 5.2*). The hexafluoro bile acid, **2.9**, displayed the highest mean increase in cellular ATP levels in sAD1 and sAD2 cells at over 30%, indicating that mitochondrial function was partially restored by **2.9**. Whilst

JED133 and JED383 exhibited higher percentages of ATP increases in sAD1 cells, their mean increase percentages were lower than **2.9** overall.

Table 5.2 - Average ATP Increase of Compounds with Strong Hits Against Sporadic AD Cells (sAD1 and sAD2)

	Average ATP Increase for Sporadic AD Cells (%)[2]		
Compound	**sAD1**	**sAD2**	**Mean**
JED108 (2.9)	31.5	31.0	31.3
JED133	32.4	25.9	29.2
JED136	29.0	23.1	26.1
JED383	32.2	23.3	27.8

[2]The average ATP increase was measured based on the comparison to the sAD1 or sAD2 cells dosed with DMSO.

Regarding familial AD cells, sixteen different bile acid derivatives synthesised in Southampton were observed to be active in the ATP assays against the fAD1 and fAD2 cells: ten were hits in fAD1 cells and seven in fAD2 cells, with JED143 (2,2-difluoro UDCA, *Figure 5.3*) being a hit against both cell lines (*Table 5.3*). Interestingly, four compounds synthesised in this thesis were strong hits against the familial AD cells: the 3,3,12,12-tetrafluoro derivative **2.4** (JED126, *Figure 5.3*, synthesis discussed in **Section 2.3.1**) and 6α-fluoro-7-keto LCA (**3.12**, JED452, *Figure 5.3*, synthesis discussed in **Section 3.2.2**) were strong hits against the fAD1 cells; 7-keto-5β-cholanic acid (**2.61**, JED160, *Figure 5.3*, synthesis discussed in **Section 2.4.1**) and 12,12-difluoro-5β-cholanic acid (**2.19**, JED427, *Figure 5.3*, synthesis discussed in **Section 2.5.1**) were active against fAD2 cells. Notably though, none of the four compounds were observed to be active in ATP assays for either of the sporadic cell lines. Strong hits were also observed for the 3,7-diketo fluoroalkene derivative JED134 (*Figure 5.3*), the 3α-fluoro sulfonamide derivative JED382 (*Figure 5.3*), 2,2-difluoro UDCA (JED143), and the taurine conjugate of 7,7,-difluoro LCA, JED418 (*Figure 5.3*), along with the previously mentioned derivatives JED135 and JED140 (*Figure 5.2*). Additionally, the strongly active compounds against sporadic AD cells, the hexafluoro derivative **2.9** (JED108) and the CDCA fluoroalkene derivative JED133, were observed to be active in fAD1 and fAD2 cells respectively, albeit at a moderate level.

Table 5.3 - ATP Quantification Assay for Familial AD Cells (fAD1 and fAD2)

ATP Quantification Assay (Familial AD)			
fAD1		**fAD2**	
Compound[3]	**Hit Level**	**Compound**[3]	**Hit Level**
JED108 (**2.9**)	Moderate	JED127 (**2.2**)	Moderate
JED126 (**2.4**)	Strong	JED129 (**2.53**)	Moderate
JED134	Strong	JED133	Moderate
JED135	Strong	JED143	Strong
JED140	Strong	JED160 (**2.61**)	Strong
JED142	Moderate	JED418	Strong
JED143	Moderate	JED427 (**2.19**)	Strong
JED154	Moderate		
JED382	Strong		
JED452 (**3.12**)	Strong		

[3]For structures, see *Figure 5.3*.

Similarly to the ATP assays of the sporadic AD cells, the active compounds exhibited quite different structures to one another. For the fAD1 cells, the strong hits (**2.4**, JED134, JED135, JED140, JED382 and **3.12**) all bore a strong HBA at the 7-position, either a hydroxy group or a ketone, with varying degrees of hydroxylation and fluorination across the A,B and C-rings. The strong hits against the fAD2 cells (JED143, **2.61**, JED418 and **2.19**) differed though. All bore significantly different collections of moieties on the A,B and C-rings, again with varying degrees of fluorination, and neither JED418 nor **2.19** bore a HBA at the 7-position like the hits against the fAD1 cells. Based upon the presence of polar moieties and hydrogen-bonding groups, the fAD2 hit compounds had very different polarities to each other: intriguingly, both the lipophilic, deoxygenated 12,12-difluoro bile acid derivative **2.19** and highly polar 2,2-difluoro UDCA (JED143) were both strong hits, despite having very different structures.

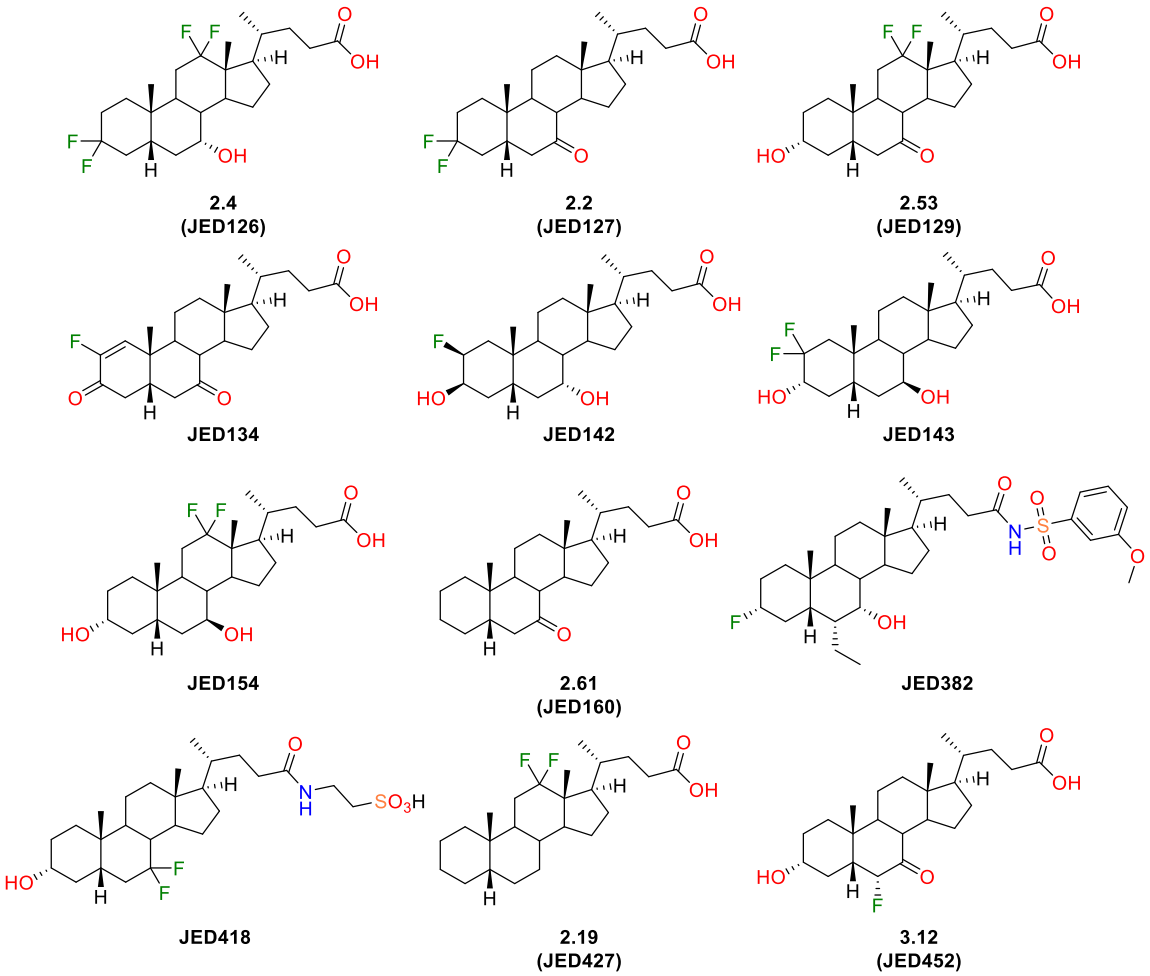

Figure 5.3 - Tested Fluorinated Bile Acid Derivatives with ATP Activity in Familial AD Cells

Of all of the compounds tested, only the hexafluoro derivative **2.9** and the CDCA fluoroalkene derivative JED133 were hits in both sporadic cell lines and a familial AD cell line, hence, **2.9** and JED133 were established as important candidates to be investigated further. The 2,2-difluoro derivative JED135 (*Figure 5.2*) and the pyridinium salt derivative JED140 (*Figure 5.2*) were also observed to have activity against either the sAD1 or sAD2 cell line and the fAD1 cell line, but the hits were not as strong as **2.9** and JED133.

Currently, the mode of action of the bile acid derivatives increasing ATP levels in the AD cell lines tested is not known, but biological studies are being carried out to investigate this further.

5.1.3.2 Cytotoxicity Assays

With the results of the primary activity screening in hand, LDH cytotoxicity studies were performed on the 181 bile acid derivatives previously tested. As noted prior, the measurement of a high level of LDH indicates a compound has high cytotoxicity and would cause cell death. For all of the sporadic and familial cell lines (sAD1, sAD2, fAD1 and fAD2), three LDH assays were performed per compound. A strong hit was defined as a hit in 3/3 assays (or 3 assays from both concentrations)

and a moderate hit was a hit in 2/3 assays. Notably, a hit compound indicated that the compound was cytotoxic towards the tested cell line.

Table 5.4 - Cytotoxicity Assay Results in Sporadic AD Cells for Fluorinated Bile Acid Derivatives

LDH Cytotoxicity Assay (Sporadic AD)			
sAD1		**sAD2**	
Compound[4]	**Hit Level**	**Compound**[4]	**Hit Level**
JED132	Strong	JED105	Strong
JED154	Strong	JED106	Strong
JED676 (**3.43**)	Moderate	JED148	Strong
		JED149	Moderate
		JED154	Strong
		JED378	Moderate

[4]For structures, see *Figure 5.4*.

Regarding the sporadic AD cell lines, the results of the LDH assay revealed that three fluorinated bile acid derivatives displayed cytotoxicity towards the sAD1 cell line and six towards the sAD2 cells. For sAD1, the 2-fluoroalkene UDCA derivative JED132 (*Figure 5.4*) and 12,12-difluoro UDCA (JED154, *Figure 5.3*) were strong hits in the LDH assays, whilst for the sAD2 cells, the trifluormethyl CDCA analogue JED105 (*Figure 5.2*), 4α-fluoro CDCA (JED106, *Figure 5.2*), the 3α-fluoro amide derivative JED148 (*Figure 5.4*) were strong hits as well as 12,12-difluoro UDCA (JED154). Additionally, 7α-fluoro HDCA (**3.43**, JED676, *Figure 5.4*, synthesis discussed in **Section 3.3.4**) had moderate cytotoxicity towards the sAD1 cell line. Notably, none of the hit compounds in the sAD1/sAD2 LDH assays were active in the sAD1/sAD2 ATP assays.

When comparing the structures of the cytotoxic fluorinated bile acid derivatives, the positions of fluorination were not consistent, although the compounds all bore numerous polar groups both on the polycyclic ring structure and the chain at C-17. Interestingly, all hit compounds bore a hydroxy group on the B-ring.

As only 12,12-difluoro UDCA (JED154) was a strong hit against both sporadic AD cell lines, its LDH percentage increase was measured, revealing increases of 56.6% and 79.5% in sAD1 and sAD2 cell

lines respectively. The observed high cytotoxicity of JED154 may be due to the fact that it is an analogue of the (normally) cytoprotective bile acid UDCA, but bears a deactivating CF_2 group, meaning its reactivity is altered compared to UDCA. Whilst cytotoxicity is undesired for a potential neurodegenerative disease drug, for other disease targets such as cancer, cytotoxicity is desired towards specific cell lines. Because of this, 12,12-difluoro UDCA could be considered in assays against cancer cell lines in the future.

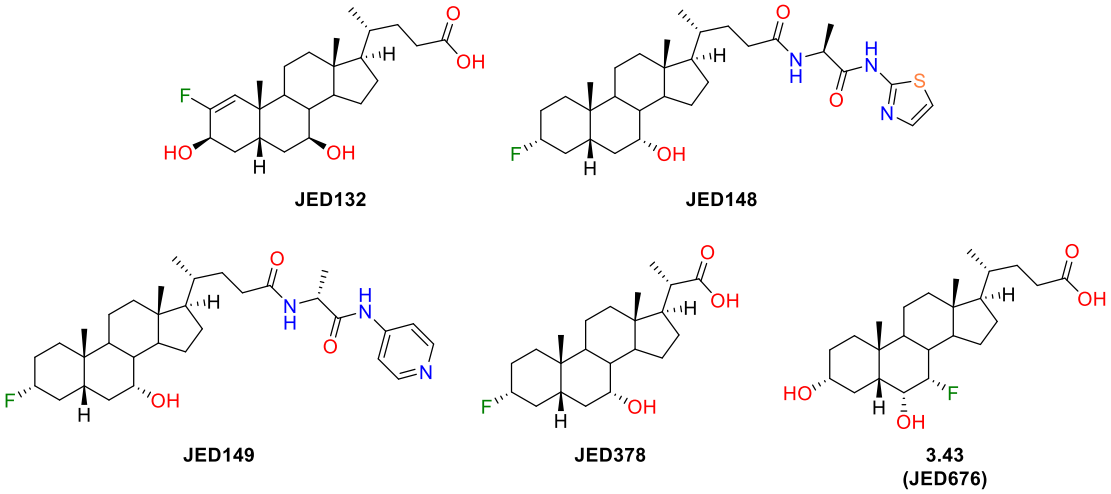

Figure 5.4 - Cytotoxic Fluorinated Bile Acid Derivatives (Towards sAD1 and sAD2 Cells)

For the familial AD cell lines, eight different derivatives were revealed to have moderate or strong cytotoxicity. The 3,3-difluoro OCA derivative JED151 (*Figure 5.5*) and the amide conjugates JED147 (*Figure 5.5*) and JED149 (*Figure 5.4*) were all strong hits against both fAD1 and fAD2 cells, whilst the conjugate JED148 (*Figure 5.4*) was only a strong hit against fAD1 cells. Strong hits were also observed for 12,12-difluoro LCA (**2.21**, JED428, *Figure 5.5*, synthesis discussed in **Section 2.5.1**), 6,6-difluoro-7-keto LCA (**2.73**, JED675, *Figure 5.5*, synthesis discussed in **Section 2.4.3**) and the 7α-fluoro-3β-hydroxy derivative **3.5** (JED695, *Figure 5.5*, synthesis discussed in **Section 3.3.5**), along with 7-keto-5β-cholanic acid (**2.61**, JED160) which, notably, was previously observed to be a strong hit in the ATP assay for fAD2 cells.

On comparison of the structures of the fAD1/fAD2 LDH assay hits, the compounds did not display much similarity, though, like with the hit compounds in the sAD1/sAD2 LDH assays, most bore numerous polar groups. Reasoning behind why the compounds were cytotoxic is not currently known, although it is interesting to observe though that some of the hit compounds of the ATP assays mentioned previously have similar structures to a number of the cytotoxic compounds, with only minor differences observed, e.g. JED132 (*Figure 5.4*) vs JED133 (*Figure 5.2*).

Table 5.5 - Cytotoxicity Assay Results in Familial AD Cells for Fluorinated Bile Acid Derivatives

LDH Cytotoxicity Assay (Familial AD)			
fAD1		**fAD2**	
Compound[5]	**Hit Level**	**Compound**[5]	**Hit Level**
JED147	Strong	JED147	Strong
JED148	Strong	JED149	Strong
JED151	Strong	JED151	Strong
JED695 (**3.5**)	Strong	JED160 (**2.61**)	Strong
		JED428 (**2.21**)	Strong
		JED675 (**2.73**)	Strong

[5]For structures, see *Figure 5.5*.

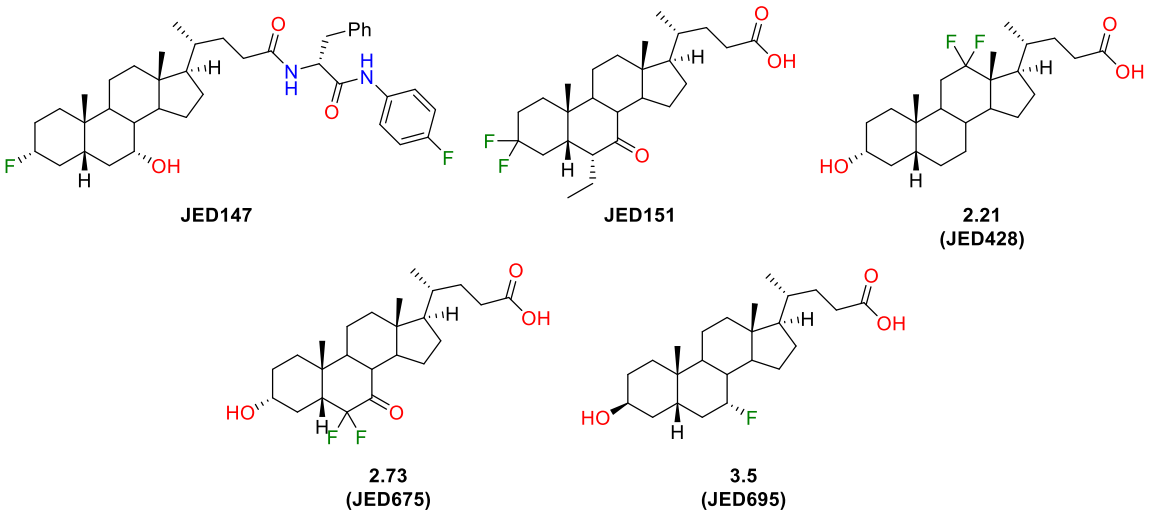

Figure 5.5 - Cytotoxic Fluorinated Bile Acid Derivatives (Towards fAD1 and fAD2 Cells)

Importantly, the hit compounds from the ATP assays of both the sporadic and familial AD cells, **2.9** and JED133, were not observed to be cytotoxic towards the sAD or fAD cell lines tested and can hence be carried through to further testing in assays for Alzheimer's disease in both sporadic and familial patient cells.

5.2 FXR/TGR5

In 2016, DiscoverX (now Eurofins) screened 104 bile acid derivatives against primary assays for FXR and TGR5 activity. FXR agonism was determined in a PathHunter® NHR biosensor cell line using PathHunter® NHR Protein Interaction and Nuclear Translocation assays. Additionally, TGR5 agonism was determined using a Hit Hunter® cAMP agonist assay. Following a period of incubation of the cells with the compounds, the assays utilised the production of chemiluminescent signals to determine the activity of the bile acid derivatives. Of the 104 derivatives tested in both the FXR and TGR5 assays, two synthesised in this thesis were included: 7,7,12,12-tetrafluoro LCA (**2.7**, *Figure 5.6,* synthesis discussed in **Section 2.3.2**) and 3,3,7,7,12,12-hexafluoro-5β-cholanic acid (**2.9**, *Figure 5.6*). Sadly, when compared to OCA (103% efficacy at 2.38 µM), neither **2.7** nor **2.9** exhibited an appreciable level of efficacy (>10%) in either the FXR or TGR5 assays at their tested concentrations (2.23 µM and 2.13 µM respectively).

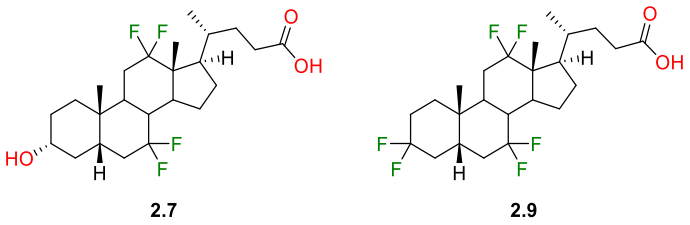

Figure 5.6 - Compounds Synthesised in This Thesis Tested in FXR and TGR5 Assays

Following this screening, only compounds with 6α-ethyl moieties or 6α-ethyl isosteres were pursued further in FXR agonist screenings. As the 7α-fluoro-6α-methoxy bile acid derivative **3.72** (*Figure 5.7*) bore a 6α-ethyl isostere, it was screened in a recent (2018) FXR assay, but was not observed to be active compared to OCA.

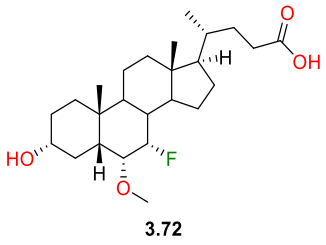

Figure 5.7 - 7α-fluoro-6α-methoxy LCA, ***3.72***

5.3 Conclusion

Preliminary screenings of fluorinated bile acid derivatives in activity assays for Parkinson's Disease indicated that the 12,12-difluorinated keto-bile acid derivatives **2.52** and **2.53** (*Figure 5.8*) had activity, though further testing is currently ongoing.

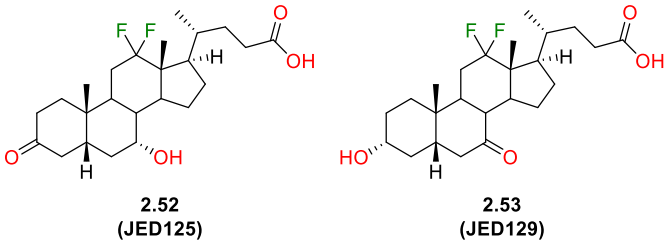

2.52
(JED125)

2.53
(JED129)

*Figure 5.8 - 12,12-Difluoro Derivatives **2.52** and **2.53***

Regarding testing of compounds in assays for Alzheimer's Disease, a diverse range of fluorinated bile acid derivatives were found to be strong hits in ATP assays against both sporadic and familial AD cell lines, indicating that a number of fluorinated bile acid derivatives can increase, and hence rescue, cellular ATP levels. The hexafluorinated bile acid derivative **2.9** (*Figure 5.9*) was found to increase cellular ATP levels in sporadic AD cells by around 31% and importantly, was found not to be cytotoxic against any of the AD cell lines tested.

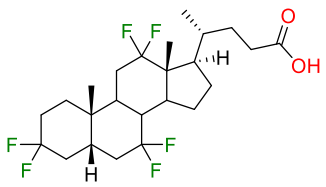

2.9
(JED108)

*Figure 5.9 - 3,3,7,7,12,12-Hexafluoro-5β-Cholanic Acid (**2.9**)*

In assays for FXR and TGR5 agonism, no compounds synthesised in this thesis displayed an appreciable level of activity compared to the benchmark bile acid compound, OCA. Further FXR and TGR5 testing will focus mainly on compounds with a 6α-ethyl chain or a 6α-ethyl isostere.

Due to the heavy focus on neurodegenerative diseases and FXR/TGR5, testing of bile acid derivatives in assays for cancer have not yet been conducted since the initial screening in 2015.

Chapter 6 X-Ray Crystallographic Studies of Bile Acids and Their Derivatives

6.1 Introduction

X-ray crystallography is described to be the "*most comprehensive technique*" for determination of molecular structure and is vital in a number of scientific disciplines including chemistry, drug discovery, molecular biology and materials science. Specifically, x-ray diffraction studies of organic compounds allow the investigation of bonds and the absolute configuration of molecules.[210] X-ray crystallography of proteins provides key information on biological molecules at an atomic level, including the structures of active sites or ligand-binding domains of proteins, which allows the elucidation of the chemical space for potential drug molecules to target the proteins under analysis. The analysis of proteins co-crystallised with drug molecules can also reveal how drugs interact with active sites of proteins.[210-212]

For rigid, conformationally restricted compounds, molecular arrangement within a crystal is determined by the relative energies of the different orientations of the molecules and their accompanying intermolecular interactions. Generally, the crystal structure that is observed experimentally has the lowest energy of all of the possible arrangements. For flexible molecules, crystal packing is less straight-forward though due to the ability of the molecules to adopt multiple conformations. Experimental observations reveal that the lowest energy conformation of a flexible molecule is not always adopted within a crystal structure and that other, higher energy conformers sometimes have a better balance of intra- and intermolecular interactions in terms of energy.[213] Additionally, the same molecule can give rise to different crystal packing arrangements, especially if its conformations are of similar energy.

For uncharged organic molecules, hydrogen bonds are the strongest intermolecular interactions.[214] As they are directionally specific, they are heavily used in crystal design to manipulate packing patterns and arrangement.[215] Next to hydrogen bonds, weaker interactions such as Van der Waals forces, π-stacking, dipole-dipole interactions and halogen bonds (where the halogen atom is electrophilic in the contact) all play a role in the arrangement of molecules in a crystal.[214] Notably in halogen bonding, iodine has the highest interaction energy and fluorine has the lowest.[216]

Despite its low interaction energy in halogen bonding, fluorine atoms can have a significant impact on crystal packing – replacement of a hydrogen atom for a fluorine atom can contribute to changes in the arrangement of molecules, potentially leading to altered crystal structures.[217,218] Interactions

of F-atoms with C-H or C-F groups in crystal structures are generally weak in nature, but become significant when hydrogen bonding is not present.[218] C-H•••F-C interactions can lead to the formation of dimers, chains, tetramers and so on.[217] When multiple fluorine atoms are present in a molecule, the sum of the weak F•••H interactions can have a noticeable influence on the packing and arrangement of molecules, and hence, on the overall crystal structure.[218]

Throughout this thesis, the crystal structures of 35 bile acid derivatives have been obtained following x-ray crystallography, performed by the Southampton X-Ray Crystallography service. Hence, this chapter will contain comparisons of the observed crystal packing modes of a selection of derivatives containing CF_2 and C-F groups with those containing alcohols and C-H moieties at the same positions. Note: the term "isostructural" will be used for compounds exhibiting matching crystal packing modes. Additionally, hydrogen atoms are removed for simplification when analysing crystal packing. When discussing the crystal packing of bile acids and their derivatives, the terms "head" and "tail" will be used: the term "head" describes the A-ring of the bile acid and the term "tail" describes the terminal carboxylic acid or ester moiety, as illustrated by the x-ray crystal structure of **2.38** (*Figure 6.1*). Also, for clarity, the "top/upper" and "bottom/under" faces of the bile acid are defined.

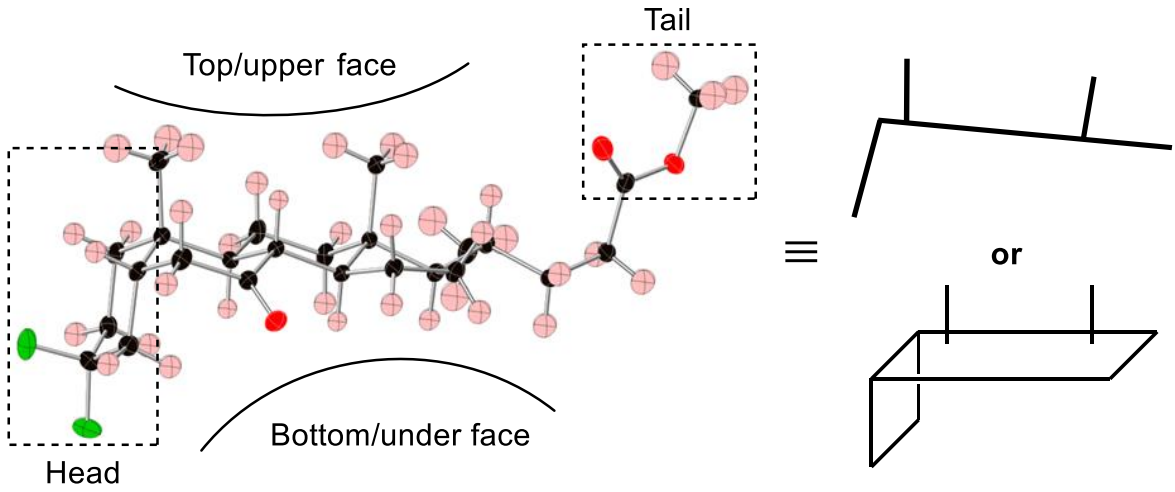

*Figure 6.1 - X-Ray Crystal Structure of **2.38** and 3D-Representation*

For fluorinated bile acids and their derivatives, the strongest intermolecular interactions are observed between terminal carboxylic acid moieties, if present, as they possess strong hydrogen-bonding interactions, typically giving rise to "tail to tail" crystal packing. In structures lacking free carboxylic acids, e.g. methyl esters, hydrogen bonding between alcohols, ketones and esters dominate the crystal packing, along with dipolar interactions of esters. The next strongest interactions in bile acids/derivatives are dipolar interactions of carbonyls, along with interactions of a ketone with acidic protons α-to a ketone moiety, followed by interactions of C-F/CF_2 dipoles. The weakest of all possible interactions are Van der Waals forces between apolar moieties.

Notably about bile acids/derivatives, the polycyclic system they possess is a rigid, conformationally restricted structure, whilst the chain is flexible and can adopt multiple different conformations. Along with intermolecular interactions, this overall shape can also dictate the molecular arrangement within crystals. As observed in the crystal structure of **2.38** (*Figure 6.1*), the 5β-stereochemistry of bile acids and their derivatives gives the polycyclic structure a non-linear shape, with an approximate right angle corresponding to the join between the A- and B-rings.

6.2 Alcohol to C-F Comparison

6.2.1 3-Hydroxy *vs* 3-Fluoro

On exchange of the 3α-hydroxy of **3.3** for a 3α-fluoro at the head of the bile acid, giving **3.6**, significant changes in crystal packing were observed (*Figure 6.2*). The 3α-hydroxy bile acid **3.3** exhibited a head-to-tail packing motif, whilst **3.6** was observed to have a molecular arrangement dominated by tail-to-tail interactions, with interactions of the heads and the bottom faces of the bile acids.

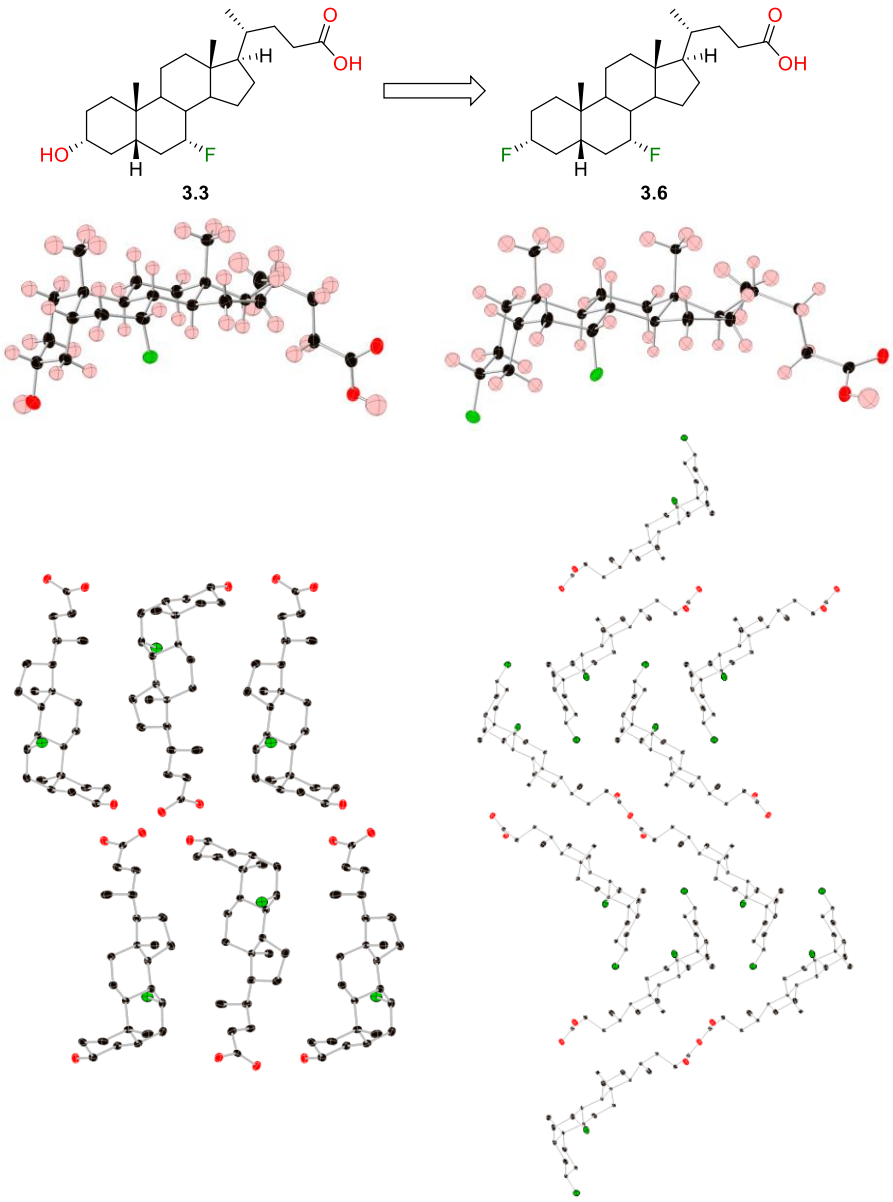

*Figure 6.2 - Crystal Packing of **3.3** (left, 2018sot0004) and **3.6** (right, 2018sot0019)*

On a closer analysis of the crystal packing of **3.3**, a network of hydrogen bonds was observed between layers of the 3α-hydroxy groups and the carboxylic acids, as shown in *Figure 6.3*. Short,

1.66 Å, hydrogen bonds were observed between the carboxylic acid protons and the lone pairs of the 3α-hydroxy groups, whilst the hydrogen bonds between the 3α-hydroxy group proton and the carboxylic acid carbonyl were slightly larger, at 1.90 Å. These differences are likely due to the differences in hydrogen bond donating ability – the carboxylic acid proton is a better HBD than the 3α-hydroxy group proton as it is more acidic. Conversely, the 3α-fluoro bile acid **3.6** did not exhibit a network of hydrogen bonds as no HBD was present at the head of the bile acid. Fluorine is a weaker HBA compared to a hydroxy group and was not observed to partake in hydrogen bonding with the terminal carboxylic acid moieties. Intermolecular hydrogen bonds were observed only between the carboxylic acid moieties, with a bond distance of 1.87 Å (*Figure 6.4*).

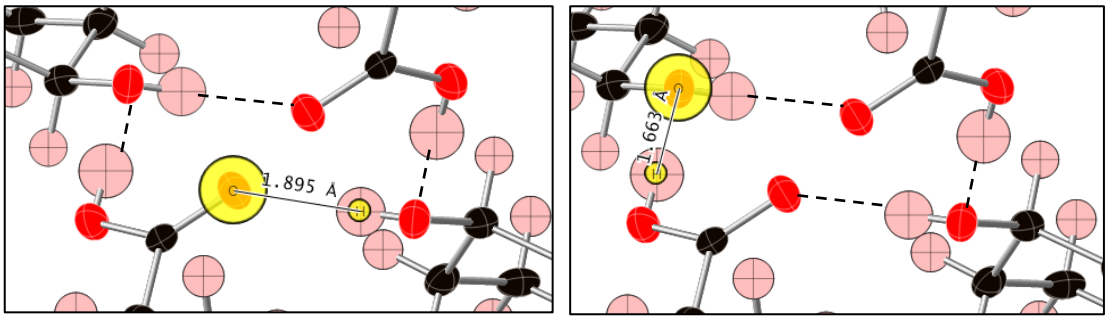

*Figure 6.3 - Hydrogen Bonding Network of **3.3** (2018sot0004)*

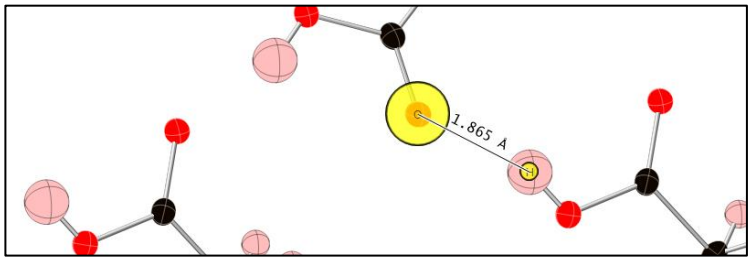

*Figure 6.4 - Hydrogen Bonding Interactions of **3.6** (2018sot0019)*

On analysis of the fluorine atoms of **3.3**, interestingly, the C-F bonds (and hence C-F dipoles) were observed to be aligned (left, *Figure 6.5*), as a result of the head-to-tail packing motif. For **3.6**, alignment of C-F dipoles was also observed, but due to the observed tail-to-tail packing with head/under face interactions, the two sets of C-F dipoles were observed to be at an approximate right angle to each other (right, *Figure 6.5*).

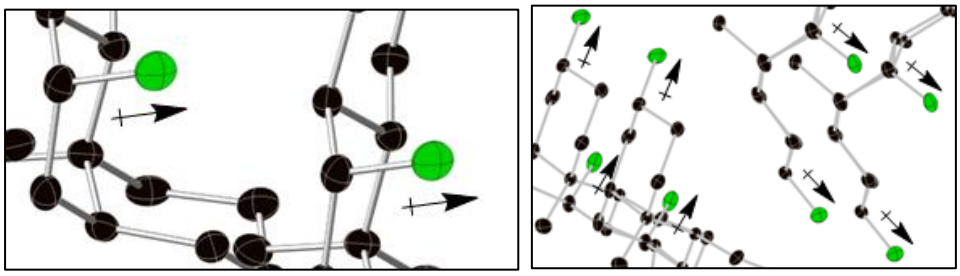

*Figure 6.5 - C-F Dipoles in **3.3** (left, 2018sot0004) and **3.6** (right, 2018sot0019)*

Similarly to **3.3** and **3.6**, differences in the crystal packing of the 3β-hydroxy and 3β-fluoro bile acids **3.5** and **3.7** were also observed, likely because of the removal of a HBD and a strong HBA at the head of the bile acid (*Figure 6.6*). Due to the β-stereochemistry of the 3-hydroxy group, complex arrangements of the heads and tails of **3.5** were observed, leading to a complicated crystal structure. The structure of **3.7** was much simpler though, with head-to-head and tail-to-tail interactions and defined layers.

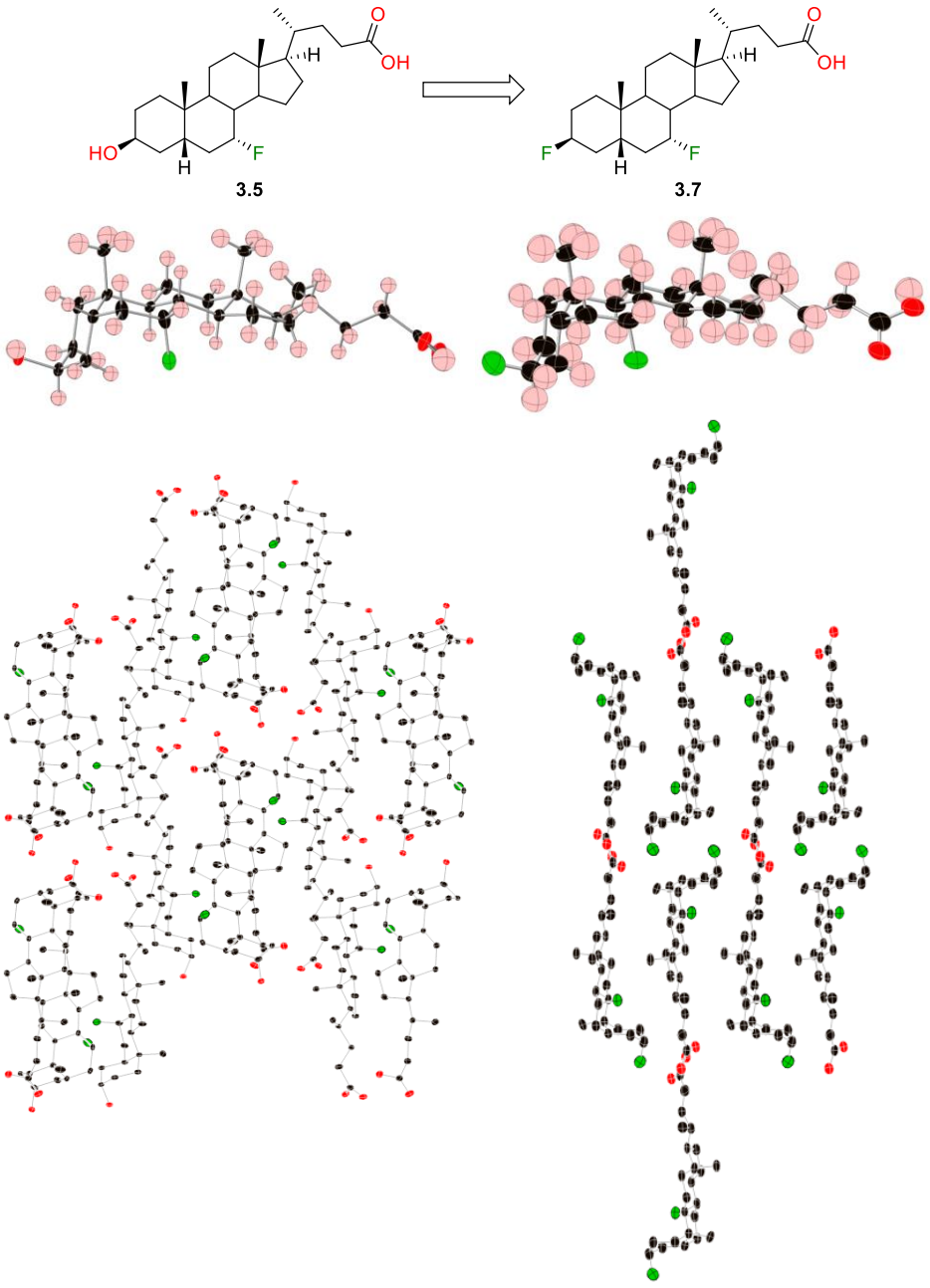

*Figure 6.6 - Crystal Packing of **3.5** (left, 2018sot0017) and **3.7** (right, 2018sot0015)*

On closer analysis of the complex molecular arrangement of **3.5**, intermolecular hydrogen bonds were observed between the 3β-hydroxy groups and between the carboxylic acid moieties and hydroxy groups. The bonds were observed to have similar distances, both around 2.0 Å (*Figure 6.7*).

For **3.7**, the hydrogen bonds were much simpler to analyse and only occurred between carboxylic acid moieties, with a short bond distance of 1.81 Å observed between all of the carboxylic acid protons and carbonyl groups analysed (*Figure 6.8*).

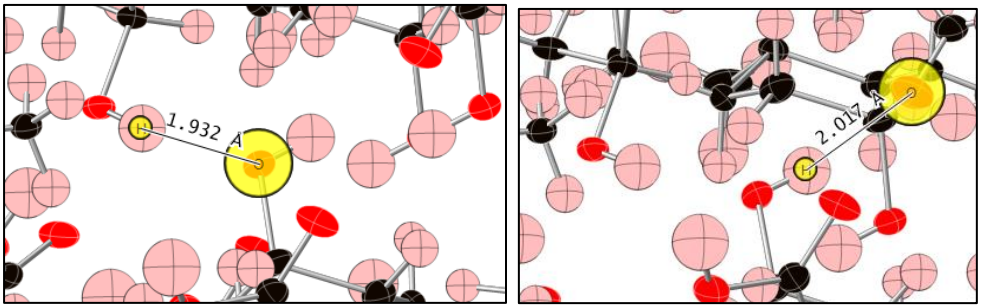

*Figure 6.7 - Hydrogen Bonding Interactions of **3.5** (2018sot0017): Left – Alcohol/Alcohol; Right – Alcohol/Carboxylic Acid*

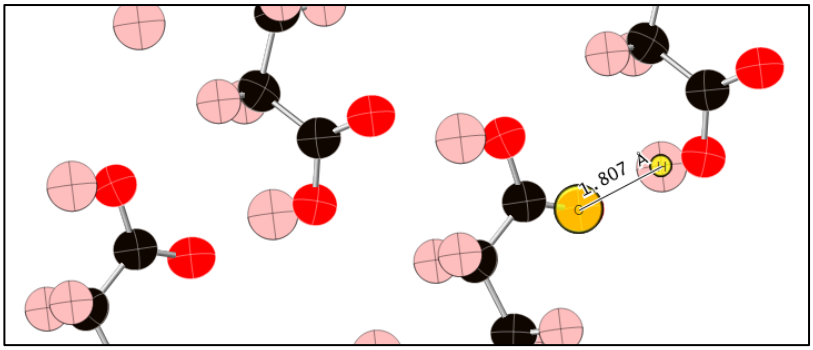

*Figure 6.8 - Carboxylic Acid Hydrogen Bonding Interactions of **3.7** (2018sot0015)*

Interestingly for **3.5**, analysis of the C-F bonds revealed that the C-F dipoles were at approximate right angles to each other (right, *Figure 6.9*), likely due to the molecular arrangement being dominated by the complex hydrogen bonding network. For **3.7**, the orientation of the C-F dipoles was quite different. The 3β-fluorine atoms were arranged (almost) parallel to each other, opposing each other at the head-to-head interface, likely contributing strongly to the observed packing motif.

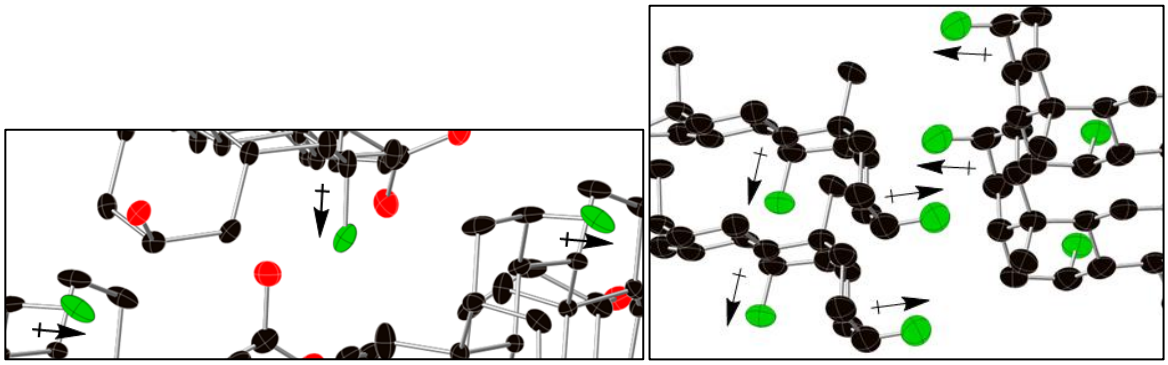

*Figure 6.9 - C-F Dipoles of **3.5** (left, 2018sot0017) and **3.7** (right, 2018sot0015)*

6.2.2 7-Hydroxy *vs* 7-Fluoro

Removal of a strong HBA and a strong HBD from the 7-position, replacing a 7α-hydroxy with a 7α-fluoro (**1.2** to **3.3**), also proved to yield significant changes in molecular arrangement within the crystals (*Figure 6.10*). Note: The x-ray crystal structure of CDCA, **1.2**, was retrieved from the Cambridge Structural Database (CSD)[xviii] and did not show hydrogen atoms.

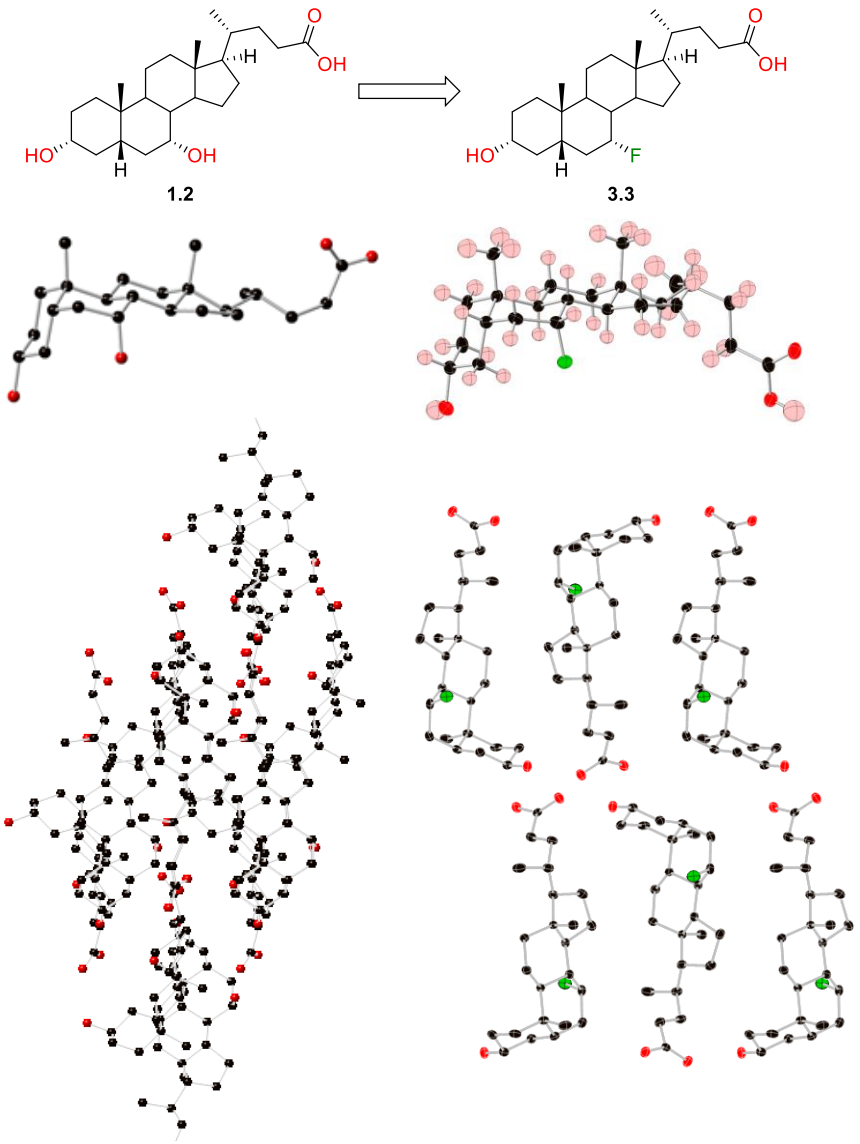

*Figure 6.10 - Crystal Packing of **1.2** (left) and **3.3** (right, 2018sot0004)*

The same effect was observed when exchanging the 7β-hydroxy of UDCA for a 7β-fluoro (**1.6** to **3.4**, *Figure 6.11*), going from a complex crystal structure with intricate hydrogen bonding networks between the hydroxy groups and carboxylic acids of **1.6**, to a more straight-forward, layered structure with hydrogen bonds between the 3α-hydroxy groups and carboxylic acids of **3.4** (*Figure*

[xviii] Crystal structure of **1.2** (chenodeoxycholic acid) retrieved from https://www.ccdc.cam.ac.uk/structures/, Deposition Number: 1124444

6.12). Note: The x-ray crystal structure of UDCA was also retrieved from the CSD[xix] and did not show hydrogen atoms.

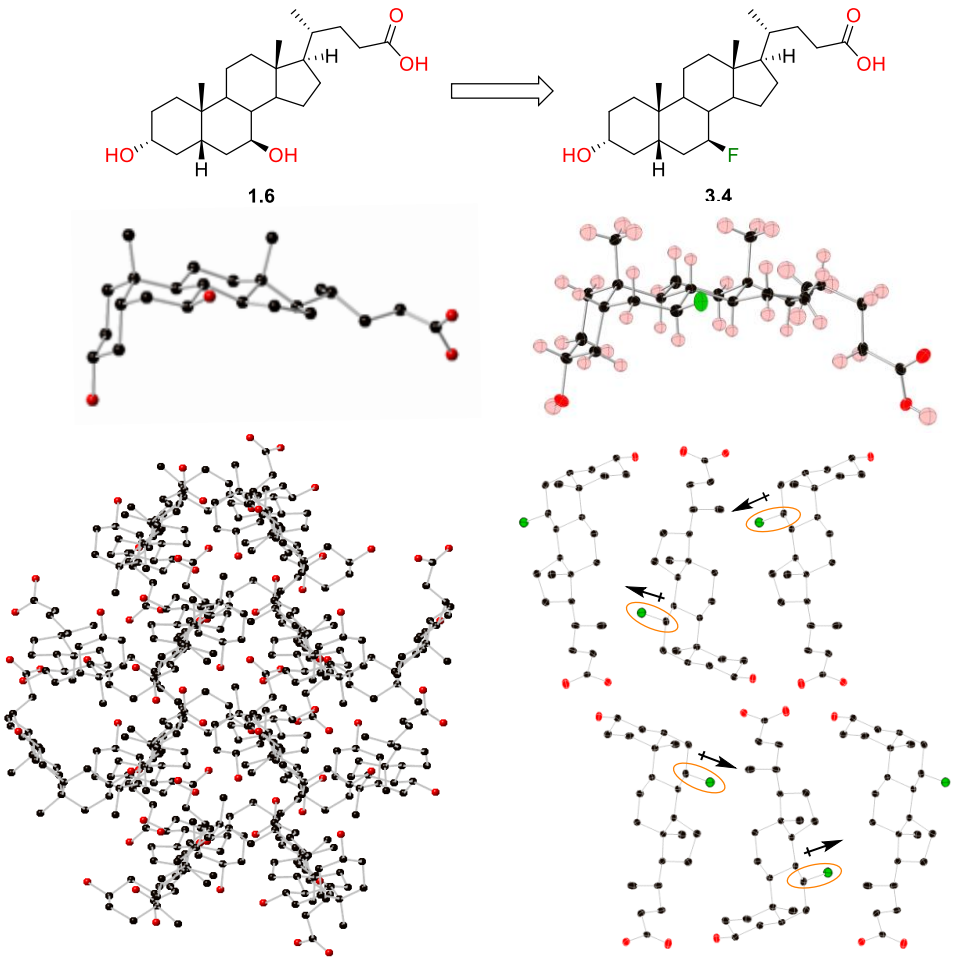

*Figure 6.11 - Crystal Packing of **1.6** (left) and **3.4** (right, 2018sot0020)*

Interestingly, the C-F bonds of **3.4** (right, *Figure 6.12*) were observed to be aligned in stacks, with opposing dipoles in alternating stacks as highlighted in *Figure 6.11* (right).

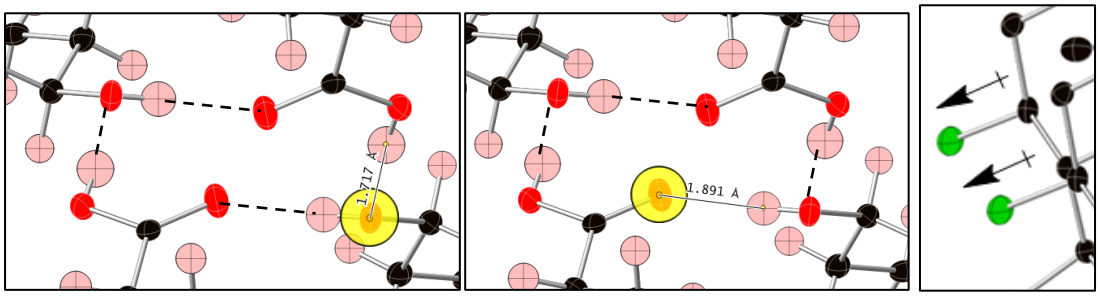

*Figure 6.12 - Hydrogen Bonding Network (left, middle) and C-F Dipoles (right) of a Section of **3.4** (2018sot0020)*

[xix] Crystal structure of **1.6** (ursodeoxycholic acid) retrieved from https://www.ccdc.cam.ac.uk/structures/, Deposition Number: 1153516

6.2.3 3,7-Dihydroxy *vs* 3,7-Difluoro

Accordingly, exchange of both the 3α- and 7α-hydroxy groups for fluorine atoms lead to large, predicted changes in crystal packing (**1.2** to **3.6**, *Figure 6.13*). Removal of all strong HBAs and HBDs from the A,B,C,D-ring system removed complex hydrogen bonding networks, giving **3.6** a crystal structure dominated by tail-to-tail hydrogen bonding interactions.

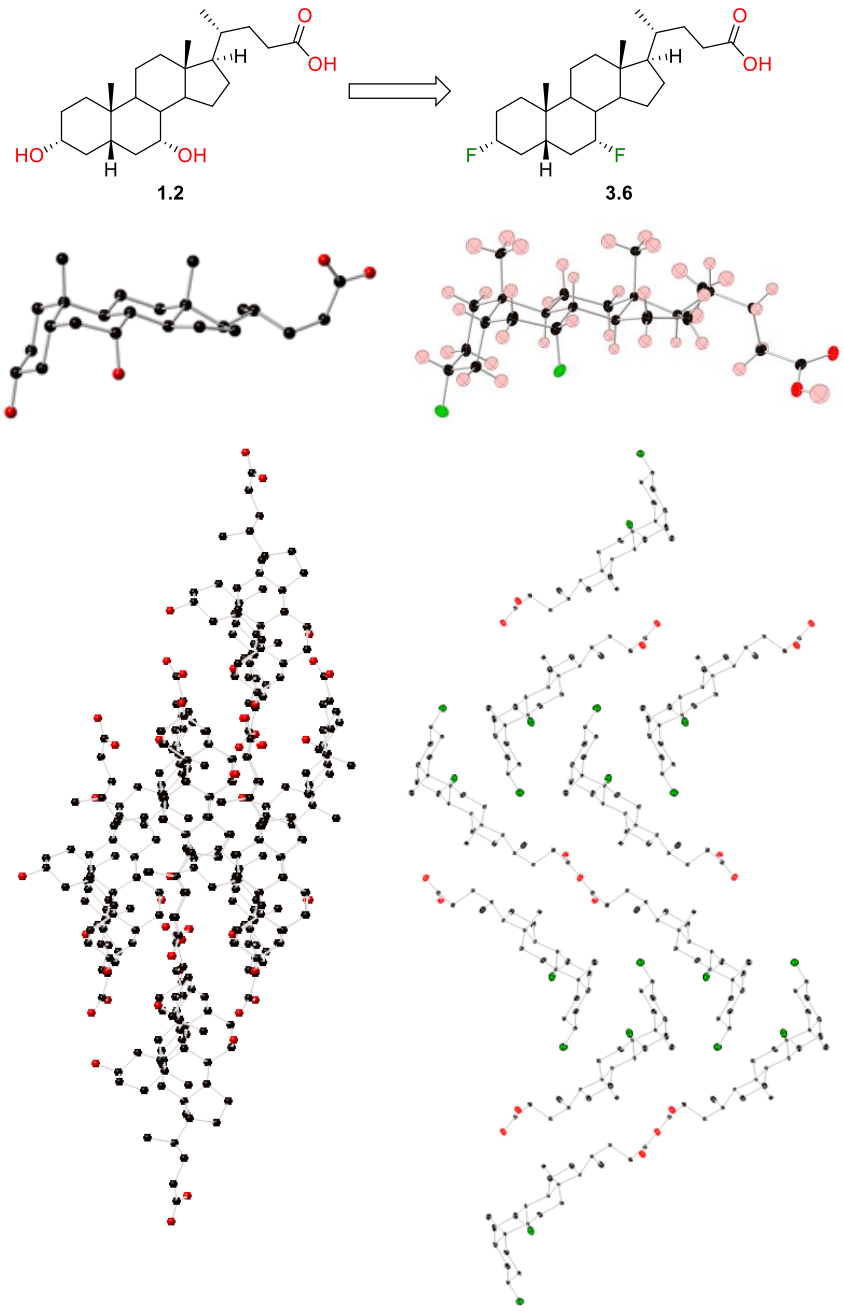

*Figure 6.13 - Crystal Packing of **1.2** (left) and **3.6** (right, 2018sot0019)*

6.3 C-H to C-F/CF_2 Comparison

6.3.1 7-H *vs* 7-fluoro and 7-CF_2

Conversely, comparison of the crystal packing of LCA (**1.4**) and 7α-fluoro LCA (**3.3**) revealed that **1.4** and **3.3** were isostructural with each other (*Figure 6.14*) – exchange of a 7α-hydrogen for a 7α-fluoro yielded no impact on the crystal packing mode. Notably, both **1.4** and **3.4** had four molecules in their unit cell and the crystal structure was dominated by hydrogen bonding interactions of the 3α-hydroxy groups with the terminal carboxylic acid moieties, giving layers of a head-to-tail packing motif. Note: The x-ray crystal structure of LCA, **1.4**, was retrieved from the CSD.[xx]

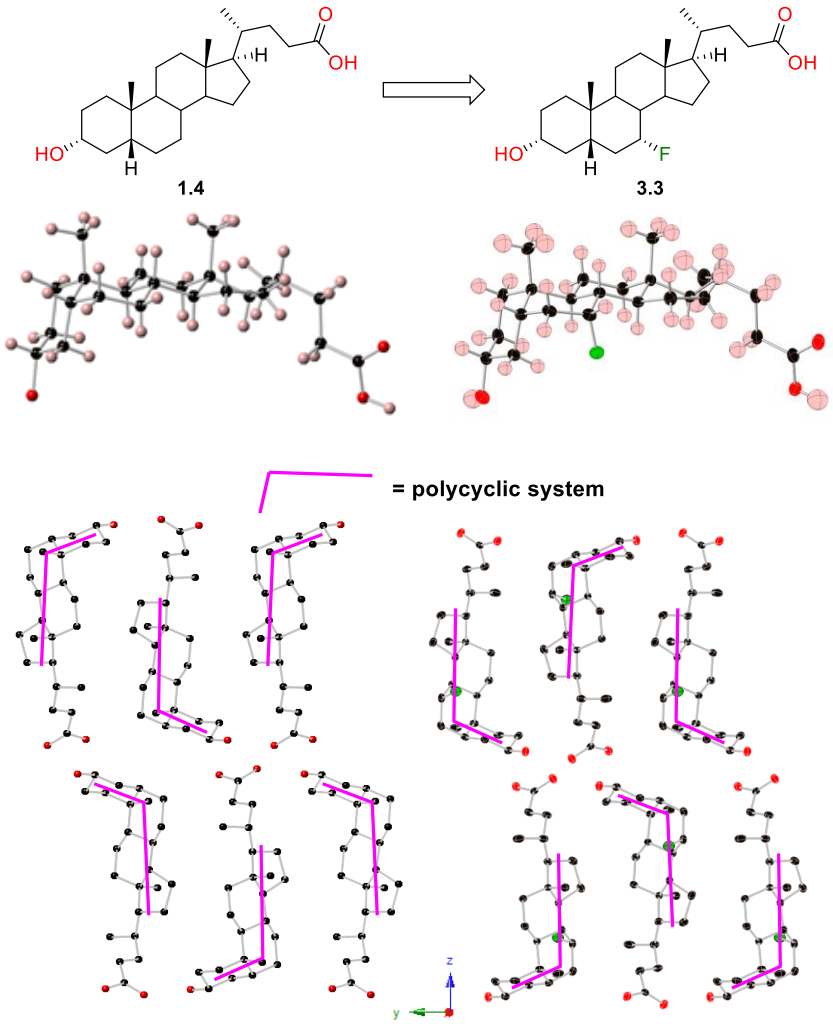

*Figure 6.14 - Crystal Packing of **1.4** (left) and **3.3** (right, 2018sot0004)*

[xx] Crystal structure of **1.4** (lithocholic acid) retrieved from https://www.ccdc.cam.ac.uk/structures/, Deposition Number: 1204431

LCA exhibited a hydrogen bonding network between the 3α-hydroxy groups and the carboxylic acid moieties, with bond distances of around 1.6 Å, values comparable to those of **3.3** (*Figure 6.15*).

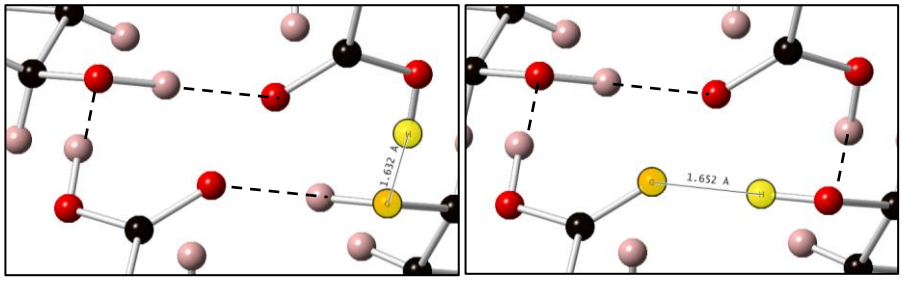

*Figure 6.15 - Hydrogen Bonding Network of **1.4***

Analysis of the crystal packing of 7β-fluoro LCA (**3.4**, *Figure 6.16*) revealed that, remarkably, inverting the stereochemistry of the 7-fluoro group had no effect on the overall crystal packing. LCA was isostructural with **3.4**, which confirmed that when a moiety that could partake in hydrogen bonding as a donor and an acceptor was present on the A-ring of a bile acid derivative, exchange of a C-H at the 7-position for a C-F had no effect on the molecular arrangement of bile acid derivatives, regardless of stereochemistry.

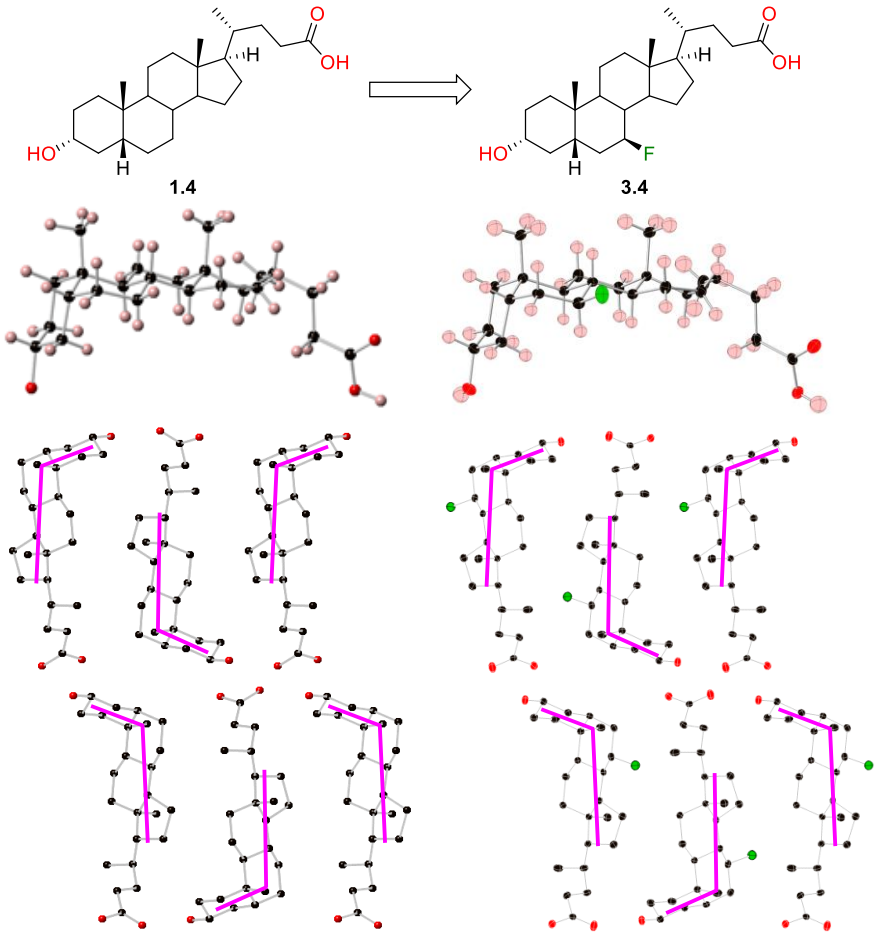

*Figure 6.16 - Crystal Packing of **1.4** (left) and **3.4** (right, 2018sot0020)*

Additionally, replacement of the 7-CH_2 of 12,12-difluoro LCA (**2.21**) with a 7-CF_2 (**2.7**) yielded no change in crystal packing (*Figure 6.17*), despite having different numbers of molecules in their unit cells (eight and four respectively). Again, the molecular arrangement within the crystal was controlled by hydrogen bonding between the 3α-hydroxy and the carboxylic acid groups, with a head-to-tail crystal packing mode.

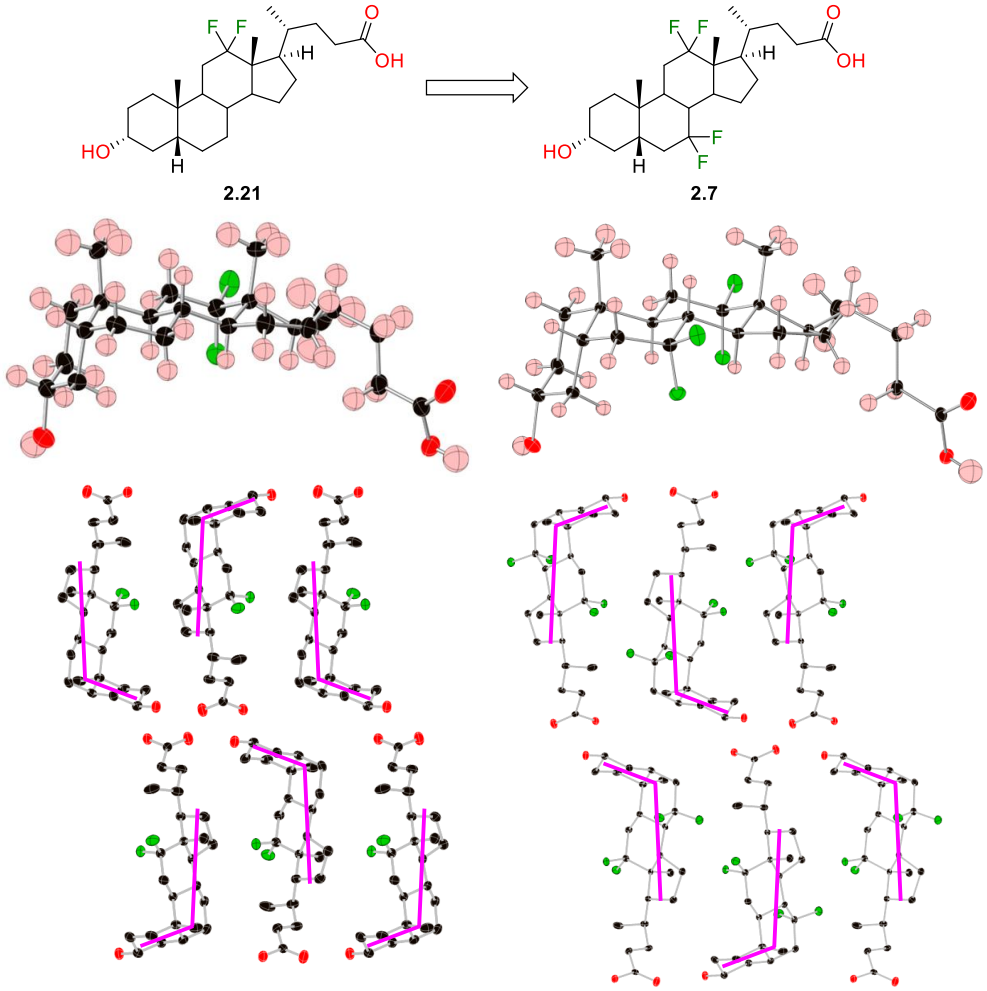

*Figure 6.17 - Crystal Packing of **2.21** (left, 2017sot0040) and **2.7** (right, 2016sot0068)*

Like with the other fluorinated LCA analogues, a network of hydrogen bonds was observed between the 3α-hydroxy groups and the carboxylic acid moieties of **2.21**, with similar bond distances (*Figure 6.18*). A similar hydrogen bonding network was also observed for **2.7**, with minor differences observed in hydrogen bond distances (*Figure 6.19*).

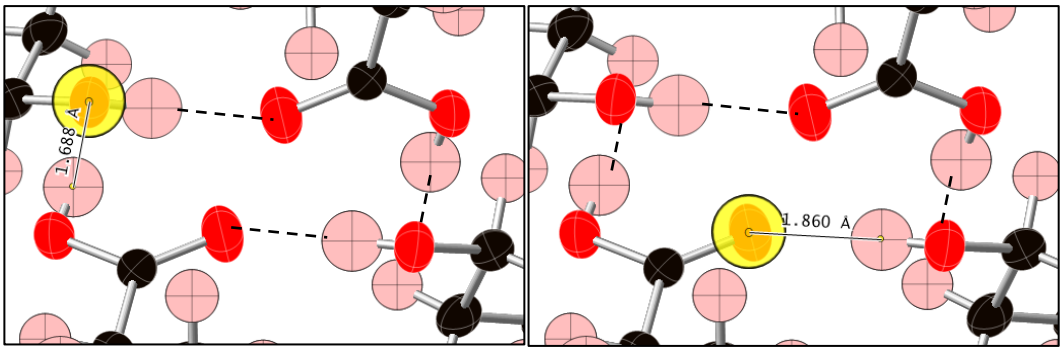

*Figure 6.18 - Hydrogen Bonding Network of **2.21** (2017sot0040)*

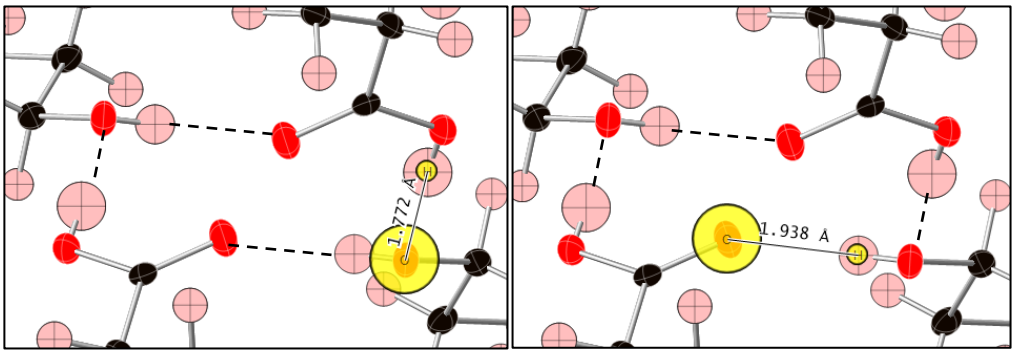

*Figure 6.19 - Hydrogen Bonding Network of **2.7** (2016sot0068)*

For both **2.21** (left, *Figure 6.20*) and **2.7** (right, *Figure 6.20*), the 7-CF_2 and 12-CF_2 groups (and hence their dipoles) were observed to be aligned. Notably, the 7-CF_2 and 12-CF_2 moieties of **2.7** were not parallel.

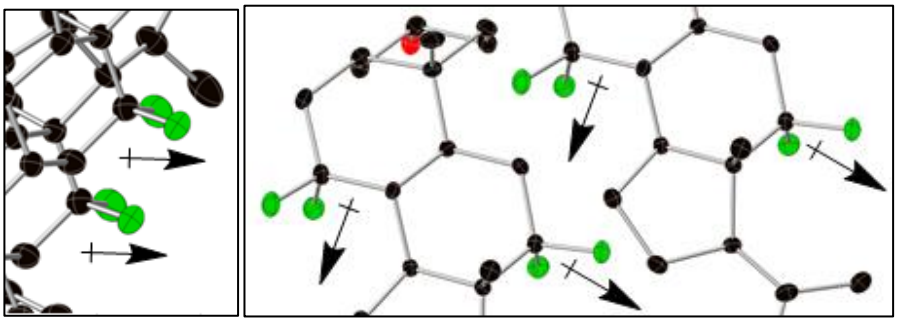

*Figure 6.20 - CF_2 Dipoles of **2.21** (left, 2017sot0040) and **2.7** (right, 2016sot0068)*

Interestingly, comparison of the crystal packing of **2.21** (*Figure 6.17*) with that of its non-fluorinated counterpart, LCA (*Figure 6.14*), revealed that introduction of a CF_2 group at the 12-position had no overall effect on crystal packing. Additionally, 7,7,12,12-tetrafluoro LCA (**2.7**) was also isostructural with LCA. It is intriguing to observe that all of the fluorinated LCA derivatives mentioned (**3.3**, **3.4**, **2.21** and **2.7**) are isostructural with LCA, regardless of the fluorination position on the B- or C-ring, indicating that fluorination of the B- and C-rings had no effect on crystal packing. Also, the observation added further confirmation that moieties at the head of the bile acid are vital in determining the crystal packing mode.

6.4 Stereochemical Comparison of C-F Moieties

As previously discussed in **Section 6.3.1**, inversion of the stereochemistry of the 7α-F of **3.3** (*Figure 6.14*) to a 7β-F (**3.4**, *Figure 6.16*) resulted in isostructurality, i.e. no change in the mode of crystal packing. Hence, investigation of the inversion in stereochemistry of a fluorine at other positions became of interest. Contrastingly to 7-fluoro stereochemical inversion, when comparing the crystal structures of the 3α-fluoro and 3β-fluoro bile acid derivatives, **3.6** (left, *Figure 6.21*) and **3.7** (right, *Figure 6.21*), significant differences were observed. As mentioned, hydrogen bonding of the carboxylic acid moieties of **3.6** and **3.7** dominated their crystal packing modes, although **3.6** displayed head-to-bottom face interactions, whilst head-to-head interactions were observed for **3.7**. Significantly, the C-F dipoles of **3.6** appeared to be aligned (*Figure 6.5*), whilst the C-F dipoles of **3.7** appeared to be parallel and opposing each other (*Figure 6.9*), likely contributing to the packing motif.

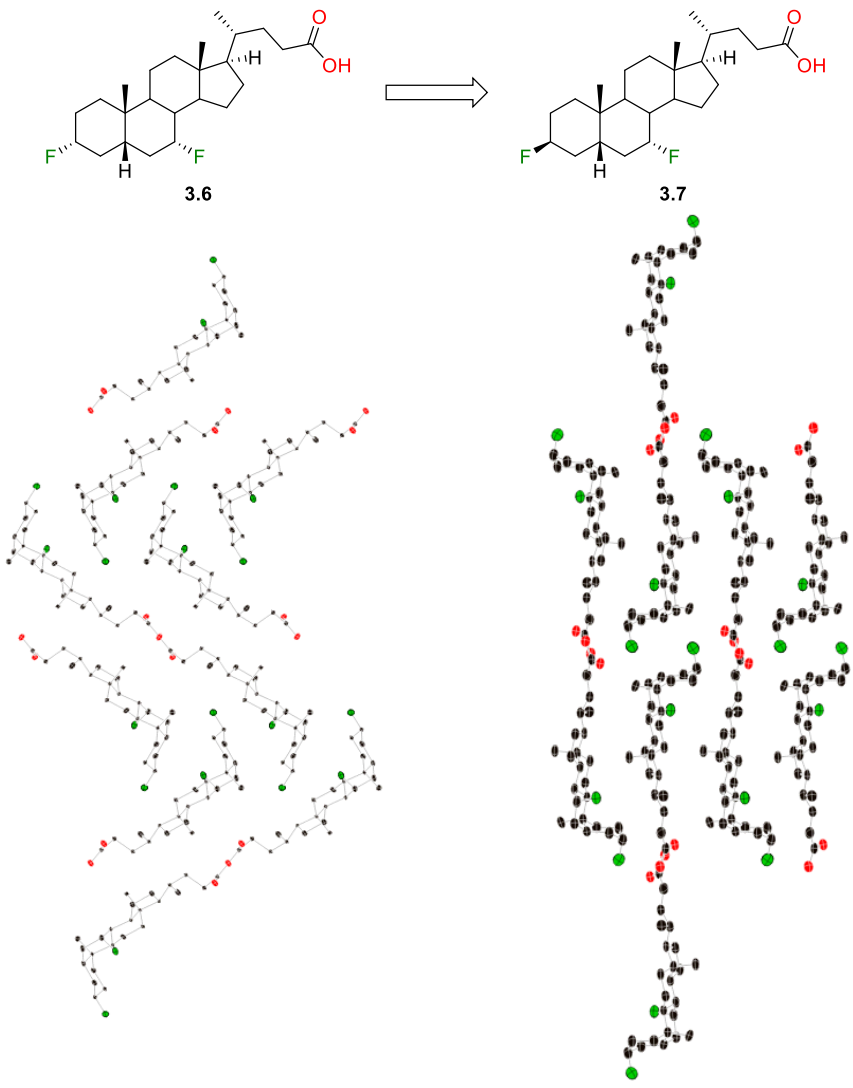

*Figure 6.21 - Crystal Packing of **3.6** (left, 2018sot0019) and **3.7** (right, 2018sot0015)*

6.5 A-Ring Deoxygenated Analogues

As observed previously, when the A-ring of a bile acid derivative bears no oxygen-containing functional groups (with a strong HBA or HBD), the crystal packing is dominated by tail-to-tail interactions. Following on from the observation made above, the bile acid analogues **2.19**, **3.1** and **3.6**, bearing fluorination at different positions of the A-, B- and C-rings, were found to be isostructural with each other (*Figure 6.22*), all exhibiting interactions between the head of the derivatives with the bottom faces. It was also observed that the C-F group on the A-ring of **3.6** did not provide a strong enough HBA to participate in hydrogen bonding with the carboxylic acid moiety, hence was involved only in weaker intermolecular interactions. Based on this observation, it can be assumed that, other than the hydrogen-bonding interactions between carboxylic acid moieties, alignment of C-F/CF_2 dipoles and Van der Waals forces between the C-H and C-F groups contribute to the crystal packing of these compounds. Notably, the fluorine atoms of different molecules were not closely orientated, hence it was believed that no C-F•••F-C interactions were present.

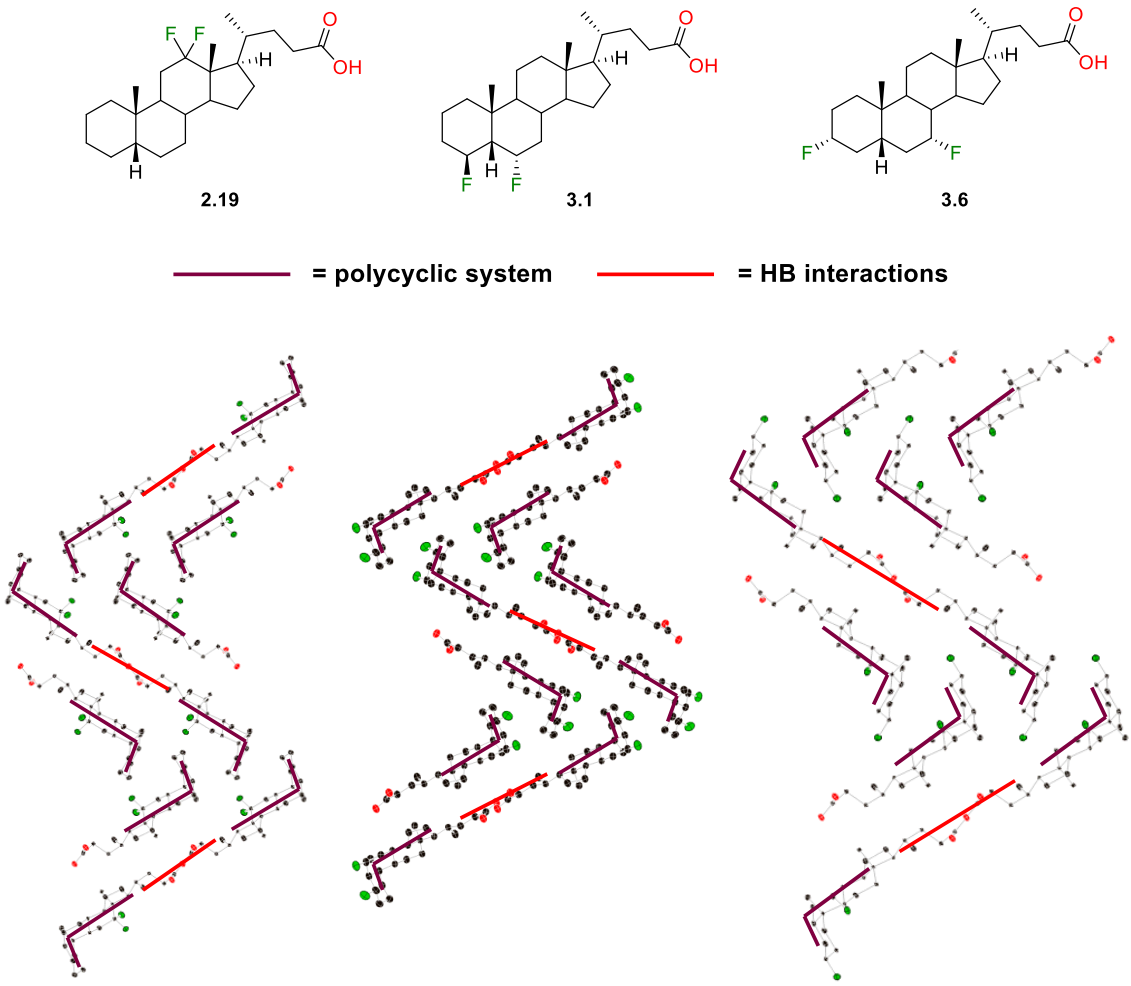

*Figure 6.22 - Crystal Packing of **2.19** (2017sot0044), **3.1** (2018sot0016) and **3.6** (2018sot0019)*

Despite the lack of oxygen-containing functional groups, the 7,7-difluoro and 3β,7α-difluoro bile acid analogues, **2.13** and **3.7**, possessed different modes of crystal packing to **2.19**, **3.1** and **3.6**, but were isostructural with each other (*Figure 6.23*). Whilst the molecular arrangements of **2.13** and **3.7** were still (mainly) controlled by hydrogen bonding between carboxylic acid groups, head-to-head interactions were also observed, giving a more linear mode of crystal packing compared to **2.19**, **3.1** and **3.6**. As mentioned, the parallel, opposite C-F dipoles of **3.7** gave rise to its head-to-head packing, but the reasoning behind the orientation of the molecules of **2.13** is not currently known.

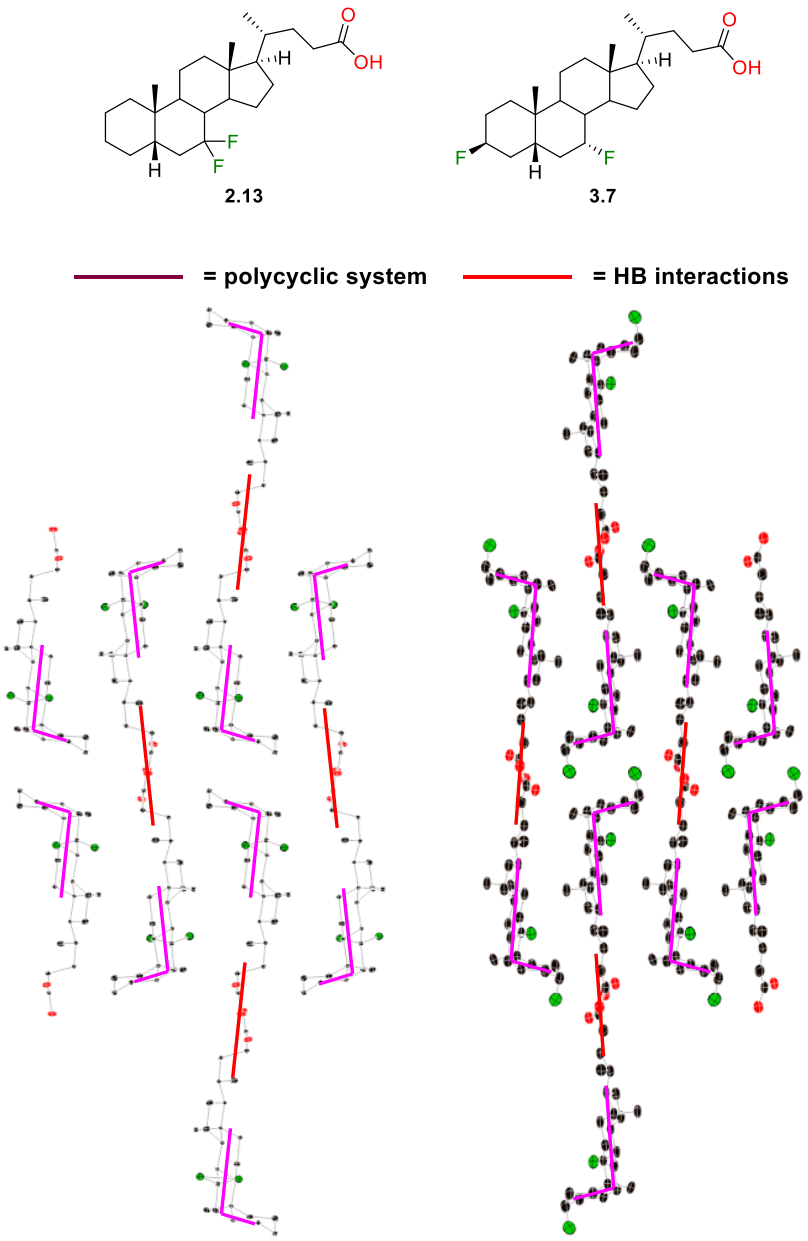

*Figure 6.23 - Crystal Packing of **2.13** (2017sot0028) and **3.7** (2018sot0015)*

6.6 Conclusion

To conclude, it has been observed that moieties at the 3-position, at the head of a bile acid derivative, are key in how molecules arrange within a crystal. When no hydrogen-bond donating groups were present on the A-ring, tail-to-tail interactions were observed to control crystal packing. Additionally, deoxygenation of the A-ring gave rise to similar packing modes in compounds bearing fluorine atoms in different positions of the A-, B- and C-rings.

Replacement of hydroxy groups on the 3- and 7-positions with fluorine atoms always lead to changes in crystal packing mode. This was likely due to the lack of strong hydrogen bond acceptors and donors, removing some of the strong hydrogen bonding interactions. When replacing a C-H or CH_2 with a C-F or CF_2 at the 7- and 12-positions, isostructurality after fluorination was observed. This was true for the investigated 3α-hydroxy derivatives, although the crystal structures of corresponding derivatives with deoxygenation at the 3-position were not available. Additionally and importantly, the stereochemistry of a C-F at the 7-position had no impact on crystal packing when a 3α-hydroxy group was present at the head of the bile acid to participate in hydrogen bonding. Contrastingly, inversion of the stereochemistry of a 3-fluoro changed the crystal packing mode significantly. These observations form the basis for further study within the group of the crystal packing of fluorinated bile acid derivatives.

Chapter 7 Experimental

7.1 General Methods

Unless otherwise stated, all reagents were obtained from commercial suppliers and used without further purification as received from the supplier (Sigma-Aldrich, Alfa Aesar, VWR, Fisher Scientific, Fluorochem and NZP UK). Anhydrous solvents were distilled immediately prior to use or used from dry, sealed bottles under nitrogen/argon, purchased from commercial sources. Water and air sensitive reactions were performed under inert atmosphere (argon) using dry solvents and all glassware was flame-dried under vacuum.

Reactions were monitored by thin layer chromatography using aluminium foil supported silica plates (Merck Keiselgel 60 F_{254}), run in the solvents stated and developed using either a cerium ammonium molybdate solution, potassium permanganate solution, *p*-anisaldehyde solution, vanillin solution or UV light.

Chromatography columns were prepared using Merck Geduran Si 60 40-63 µm silica gel. Column chromatography was also performed using a Biotage® Isolera One instrument with the solvents and column stated (10 g, 25 g, 30 g, 50 g, 100 g or 120 g prepacked Biotage® SNAP KP-Sil, SNAP Ultra HP-Sphere 25 µm or ZIP KP-Sil columns). Preparative HPLC was carried out using a Biorad Bio-Sil D 90-10 column (250×22 mm at 15mL min^{-1}).

Nuclear magnetic resonance spectra were recorded using either a Bruker Ultrashield 400 MHz or 500 MHz spectrometer with spectra being assigned using COSY, HSQC, HMBC, Dept Q and Dept 135. All chemical shifts are quoted on the δ scale in ppm relative to residual solvent peaks as appropriate. ^{19}F NMR were externally referenced to $CFCl_3$. The coupling constants (*J*) are given in Hertz (Hz). The proton NMR signals were designated as follows: s (singlet), d (doublet), t (triplet), q (quartet), quin (quintet), sxt (sextet), spt (septet), m (multiplet), or a combination of the above.

Low resolution mass spectra were recorded using a Waters (Manchester, UK) Acquity UPC^2 TQD tandem quadrupole mass spectrometer. Ultrahigh performance supercritical fluid chromatography was undertaken using a UPC^2 BEH C18 (or equivalent) column (Waters, 100 mm x 3.0 mm 1.7µm). Gradient elution from 90% CO_2:10% methanol modifier (25mM ammonium acetate) to 60% CO_2:40% methanol modifier (25 mM ammonium acetate) was performed over three min at a flow rate of 1.5 mL/min with an Active Back Pressure Regulator (ABPR) pressure of 150 bar. A make-up flow solvent (methanol 1% formic acid) was pumped at a flow rate of 0.45 mL/min into the mass spectrometer. Low resolution mass spectra were also recorded using a Waters Acquity TQD mass

tandem quadrupole mass spectrometer. Ultrahigh performance liquid chromatography was undertaken using Waters BEH C18 (or equivalent) column (50 mm x 2.1mm 1.7µm). Gradient elution from 20% acetonitrile (0.2% formic acid) to 100% acetonitrile (0.2% formic acid) was performed over five/ten min at a flow rate of 0.6 mL/min.

High resolution mass spectra were recorded using a MaXis (Bruker Daltonics, Bremen, Germany) time of flight (TOF) mass spectrometer. Ultrahigh performance liquid chromatography was performed using a Waters UPLC BEH C18 (50 mm x 2.1 mm 1.7µm) column. Gradient elution from 20% acetonitrile (0.2% formic acid) to 100% acetonitrile (0.2% formic acid) was performed in five min at a flow rate of 0.6 mL/min.

IR spectra were recorded neat or as a thin-film on either a Thermofisher Scientific™ Nicolet iS5 or Nicolet 380 FTIR Spectrometer with an iD7 ATR accessory. Absorption peaks are given in cm^{-1} and the intensities were designated as follows: w (weak), m (medium), s (strong), br (broad).

Optical rotations were recorded on an OPTICAL ACTIVITY POLAAR 2001 polarimeter at 589 nm.

Melting points were recorded on a Gallenkamp melting point apparatus fitted with a microscope and are uncorrected.

^{1}H, ^{13}C and ^{19}F NMR spectra are assigned using the steroid numbering system, presented again in *Figure 7.1* for convenience.

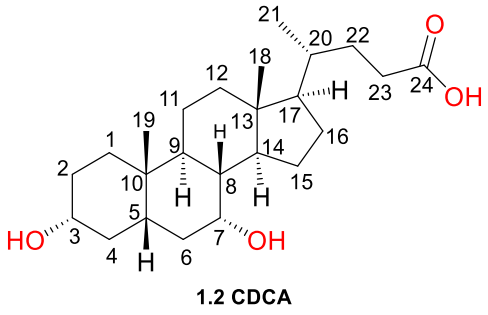

1.2 CDCA

*Figure 7.1 - CDCA (**1.2**) with Numbering*

7.2 General Procedures

Note: For each procedure, the crude material was purified by flash chromatography as required. Purification details are included in the experimental procedure for each product.

7.2.1 Procedure A for carboxylic acid protection as a methyl ester

The carboxylic acid (1.0 equiv) was dissolved in methanol (20 mL/g) and *p*TSA•H_2O (0.10 equiv) was added. The solution was sonicated at 40 °C for 2 h, after which the reaction mixture was reduced *in vacuo*. The resulting residue was dissolved in EtOAc (15 mL/g) and washed with saturated $NaHCO_3$, water and brine (all 15 mL/g) before drying over Na_2SO_4 and reducing *in vacuo* to yield the crude ester.

7.2.2 Procedure B for selective oxidation of a 3α-hydroxy group

The alcohol (1.0 equiv) was dissolved in a mixture of water (2.5 mL/g) and *t*-butanol (10 mL/g). To this solution KBr (2.0 equiv), $KHCO_3$ (10 equiv) and TEMPO (1.3 equiv) were added. The solution was cooled to 0 °C before adding an 11% NaClO solution (2.0 equiv) portionwise over the course of 2-4 h. The reaction mixture then was quenched with saturated sodium thiosulfate solution (20 mL/g) and the aqueous phase was extracted with EtOAc (2 x 20 mL/g). The combined organic phases were washed with water and brine (both 20 mL/g), before drying over Na_2SO_4 and reducing *in vacuo* to give the crude ketone.

7.2.3 Procedure C for lithium hydroxide-mediated ester saponification

The ester (1 equiv) was dissolved in THF (20 – 40 mL/g, as required for full solubility) and LiOH (2M in H_2O, 10 equiv) was added. After stirring at RT for 17 h-4 d, the reaction mixture was acidified with 2M HCl (50 mL/g, until pH ~3/4) and the aqueous phase was extracted with EtOAc (2/3 x 50 mL/g). The combined organic phases were washed with water and brine (both 50 mL/g) before drying over Na_2SO_4 and reducing *in vacuo* to yield the crude carboxylic acid.

7.2.4 Procedure D for sodium hydroxide-mediated ester saponification

The ester (1.0 equiv) was dissolved in MeOH (25 – 50 mL/g, as required for full solubility, 1 – 4 mL/g of DCM occasionally added to aid solubility) and NaOH (~40 equiv, w/w 10% solution in MeOH) was added. After 17 h-4 d, the reaction mixture was reduced *in vacuo* and the resulting residue acidified with 2M HCl (50 mL/g, until pH ~3/4). The aqueous phase was extracted with EtOAc (3 x 25 mL/g)

and the combined organic phases were washed with water and brine (both 50 mL/g) before drying over Na_2SO_4 and reducing *in vacuo* to yield the crude carboxylic acid.

7.2.5 Procedure E for protection with an acetyl group using acetic anhydride, DMAP and pyridine

The alcohol (1.0 equiv) was dissolved in dry pyridine (5-10 mL/g) and acetic anhydride (10 equiv per hydroxy group) and DMAP (0.1 equiv) were added. After 16 h-3 d of stirring at RT, MeOH (10 mL/g) was added to the reaction mixture portionwise and the solvents were removed *in vacuo*. The resulting residue was dissolved in EtOAc (50 mL/g) and the organic phase was washed with 2M HCl, saturated $NaHCO_3$ solution, water and brine (all 50 mL/g) before drying over Na_2SO_4 and reducing *in vacuo* to yield the crude ester.

7.2.6 Procedure F for selective protection of a 3α-hydroxy moiety with an acetyl group using acetic anhydride and $NaHCO_3$

The alcohol (1.0 equiv) was dissolved in dry THF (20 mL/g) and acetic anhydride (10 equiv) and $NaHCO_3$ (10 equiv) were added. After heating under reflux (65 °C) for 17-21 h, the reaction mixture was diluted with water (50 mL/g) and the aqueous phase was extracted with EtOAc (3 x 50 mL/g). The combined organic phases were washed with water and brine (both 50 mL/g) before drying over $NaSO_4$ and reducing *in vacuo* to yield the crude ester.

7.2.7 Procedure G for thiocarbonate formation

The alcohol (1.0 equiv) was dissolved in dry DCM (15 mL/g) and dry pyridine (3.0 equiv) and *O*-phenyl chlorothionoformate (1.1 equiv) were added. After stirring at RT for 30 min-1h, the reaction mixture was diluted with EtOAc (50 mL/g) and washed with water and brine (both 50 mL/g) before drying over Na_2SO_4 and reducing *in vacuo* to yield the crude thiocarbonate product.

7.2.8 Procedure H for thiocarbonate or xanthate deoxygenation with Et_3SiH and BPO

The thiocarbonate or xanthate (1.0 equiv), Et_3SiH (40 equiv) and dry toluene (5-10 mL/g, as required for solubility) were added to a flame-dried flask under argon. The mixture was degassed with argon for 5 min and heated to 120 °C. Dibenzoyl peroxide (BPO, 0.2 equiv) was then added in 30 min intervals (at 120 °C) until the reaction mixture was deemed complete by TLC (generally 0.6-1.0 equiv BPO added over 1.5-2.5 h). The reaction mixture was then allowed to cool to RT and was reduced *in vacuo* to yield the crude deoxygenated material.

7.3 Synthesis of *gem*-Difluorinated Analogues

7.3.1 Synthesis of Analogues from CDCA

Methyl 3α,5β,7α-cholan-24-oate (2.24)

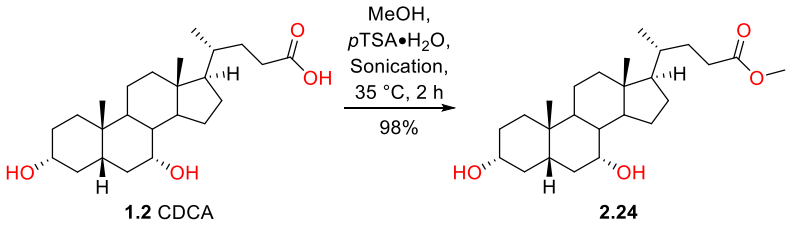

Following general procedure A, CDCA (**1.2**, 25.0 g, 64.0 mmol, 1.0 equiv) was protected to yield **2.24** as a white solid (25.4 g, 62.5 mmol, 98%) with no further purification.

mp 72 – 74 °C (lit. 66 – 68 °C[219]). **R_f** 0.47 (EtOAc/PE 50/50). **^{1}H NMR** (400 MHz, $CDCl_3$) δ 3.86 (apparent br d, *J*=2.8 Hz, 1H, 7β-**H**), 3.67 (s, 3H, 24-COO**CH_3**), 3.47 (tt, *J*=11.1, 4.5 Hz, 1H, 3β-**H**), 2.36 (ddd, *J*=15.4, 10.1, 5.3 Hz, 1H, 23-**H'**), 0.97-2.29 (m), 0.94 (d, *J*=6.5 Hz, 3H, 21-**CH_3**), 0.92 (s, 3H, 19-**CH_3**), 0.67 (s, 3H, 18-**CH_3**) ppm. **^{13}C NMR** (100 MHz, $CDCl_3$) δ 174.7 (**24-COO**CH_3), 72.0 (**3-CH**), 68.5 (**7-CH**), 55.8 (CH), 51.5 (**24**-COO**CH_3**), 50.4 (CH), 42.7 (C), 41.5 (CH), 39.9 (CH_2), 39.6 (CH_2), 39.4 (CH), 35.4 (CH), 35.3 (CH_2), 35.0 (C), 34.6 (CH_2), 32.8 (CH), 31.0 (CH_2), 31.0 (CH_2), 30.7 (CH_2), 28.1 (CH_2), 23.7 (CH_2), 22.8 (**19-CH_3**), 20.6 (CH_2), 18.2 (**21-CH_3**), 11.7 (**18-CH_3**) ppm. ^{1}H and ^{13}C NMR data agree with literature.[219-221]

Methyl 3-oxo-7α-hydroxy-5β-cholan-24-oate (2.25), Methyl 3,7-dioxo-5β-cholan-24-oate (2.3)

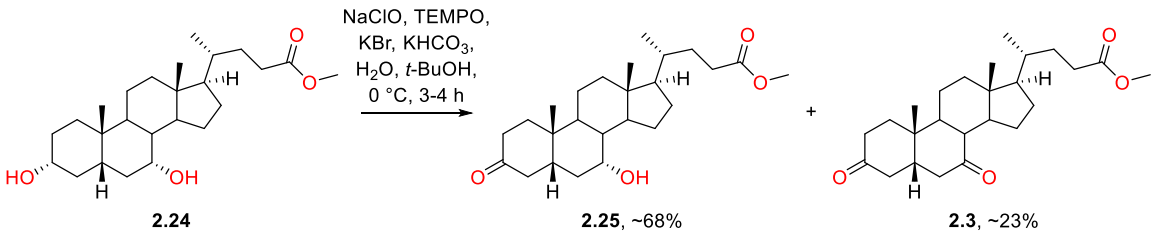

Following general procedure B, **2.24** (19.8 g, 48.6 mmol, 1.0 equiv) was oxidised. The crude material was combined with the crude from another batch of the reaction for purification (60.9 mmol of **2.24**). The crude material was purified by flash chromatography (EtOAc/PE: 20%/80% → 35%/65%), giving 19.7 g of a mix of **2.25** and **2.3** (7:3) and pure **2.25** (3.00 g, 12%). 5 g of the mix of **2.25** and **2.3** was further purified by flash chromatography (Biotage SNAP HP-Sphere 50 g cartridge, EtOAc/PE: 25%/75% → 35%/65%), giving 4.00 g of a mix of **2.25** and **2.3** (7:3) and **2.25** (0.56 g, 2%). The 7:3 mix of **2.25** and **2.3** (~19 g) was used in further reactions without further purification.

2.25: **mp** 118 – 120 °C (lit. 128 – 129 °C[219]). **R_f** 0.29 (EtOAc/PE 35/65). **^{1}H NMR** (400 MHz, $CDCl_3$) δ 3.92 (apparent br d, *J*=2.3 Hz, 1H, 7β-**H**), 3.66 (s, 3H, 24-COO**CH_3**), 3.39 (dd, *J*=14.8, 13.8 Hz, 1H, 4α-**H**), 2.47-1.06 (m), 1.00 (s, 3H, 19-**CH_3**), 0.94 (d, *J*=6.4 Hz, 3H, 21-**CH_3**), 0.70 (s, 3H, 18-**CH_3**) ppm. **^{13}C NMR** (100 MHz, $CDCl_3$) δ 213.2 (**3-C**), 174.7 (**24-COO**CH_3), 68.4 (**7-CH**), 55.8 (CH), 51.5 (**24**-COO**CH_3**), 50.3 (CH), 45.6 (CH_2), 43.2 (CH), 42.7 (C), 39.5 (CH_2), 39.3 (CH), 36.9 (CH_2), 36.8 (CH_2), 35.3 (CH), 35.3 (C), 33.9 (CH_2), 33.3 (CH), 31.0 (CH_2), 30.9 (CH_2), 28.1 (CH_2), 23.6 (CH_2), 21.9 (**19-CH_3**), 20.9 (CH_2), 18.2 (**21-CH_3**), 11.8 (**18-CH_3**) ppm. ^{1}H and ^{13}C NMR data agree with literature.[138,219,220]

Methyl 3-oxo-7α-methoxymexthoxyl-5β-cholan-24-oate (2.26), Methyl 3,7-dioxo-5β-cholan-24-oate (2.3)

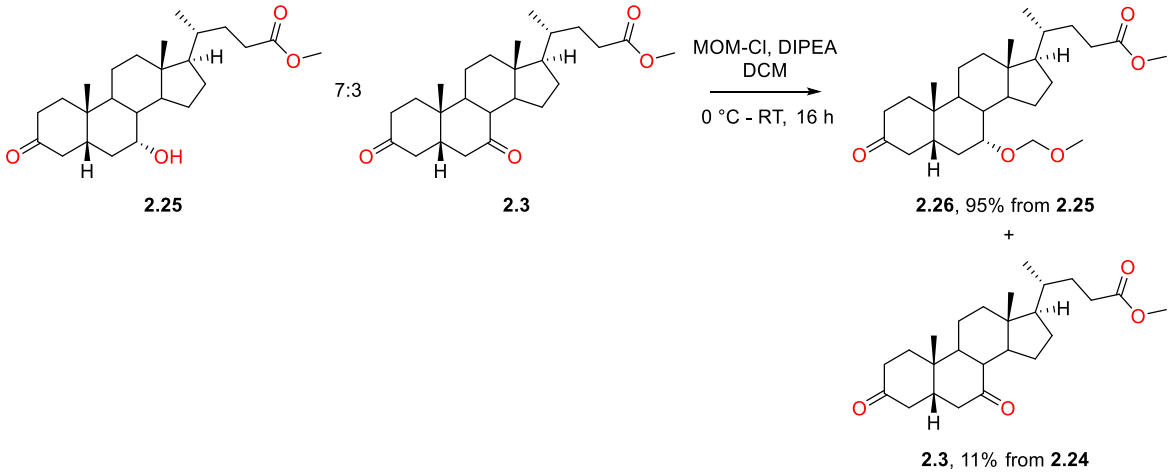

The 7:3 mix of **2.25** and **2.3** (14 g, ~9.8 g of **2.25**, ~24 mmol, ~1 equiv) was dissolved in dry DCM (250 mL) and cooled to 0 °C before adding MOM-Cl (9.20 mL, 121 mmol, 5.0 equiv) and DIPEA (11.9 mL, 72.7 mmol, 3.0 equiv). The reaction mixture was stirred at RT for 16 h, after which it was quenched with water (150 mL) and MeOH (100 mL) before separating the phases and extracting the aqueous phase with EtOAc (4 x 200 mL). The combined organic phases were washed with water (250 mL) and brine (300 mL) before drying over Na_2SO_4 and reducing *in vacuo*, giving around 16 g of an oily yellow solid. The crude material was purified by flash chromatography (EtOAc/PE: 15%/85% → 25%/75%), firstly giving **2.26** (10.3 g, 23.0 mmol, 95%), then **2.3** (2.77 g, 6.88 mmol, 11% from **2.24**), both as white powders.

2.26: **mp** 100 – 102 °C (lit. 103 °C[220]). **R_f** 0.26 (EtOAc/PE 20/80). **^{1}H NMR** (400 MHz, $CDCl_3$) δ 4.67 (d, *J*=6.8 Hz, 1H, 7α-O**CH_2**OCH_3), 4.53 (d, *J*=6.8 Hz, 1H, 7α-O**CH_2**OCH_3), 3.66 (br s, 4H, 7β-**H** and 24-COO**CH_3**), 3.36 (s, 3H, 7α-OCH_2O**CH_3**), 3.32 (br t, *J*=14.2 Hz, 1H, 4α-**H**), 2.43-1.03 (m), 1.01 (s, 3H, 19-**CH_3**), 0.93 (d, *J*=6.5 Hz, 3H, 21-**CH_3**), 0.68 (s, 3H, 18-**CH_3**). **^{13}C NMR** (100 MHz, $CDCl_3$) δ 213.1 (**3-C**), 174.6 (**24-COO**CH_3), 95.9 (**7α-OCO**CH_3), 75.0 (**7-C**), 56.3 (**7α**-OCO**CH_3**), 55.6 (CH), 51.4 (**24**-COO**CH_3**), 49.7 (CH), 45.1 (CH_2), 43.1 (CH), 42.5 (C), 39.4 (CH), 39.3 (CH_2), 36.8 (CH_2), 36.7 (CH_2), 35.3 (CH), 35.2 (C), 33.7 (CH), 31.0 (CH_2), 31.0 (CH_2), 30.4 (CH_2), 28.1 (CH_2), 23.7 (CH_2), 21.9 (**19-CH_3**), 20.9 (CH_2),

18.3 (**21-CH_3**), 11.7 (**18-CH_3**) ppm. ^{1}H NMR and melting point data agree with literature.[220] ^{13}C NMR data not available. ^{1}H and ^{13}C NMR data consistent with data from within the group.

2.3: **mp** 158 – 160 °C (lit. 152 – 155 °C[222]). **R_f** 0.26 (EtOAc/PE 25/75). **^{1}H NMR** (400 MHz, $CDCl_3$) δ 3.66 (s, 3H, 24-COO**CH_3**), 2.88 (dd, *J*=12.7, 5.2 Hz, 1H, 6β-**H**), 2.49 (t, *J*=11.3 Hz, 1H, 8β-**H**), 0.95-2.40 (m), 1.30 (s, 3H, 19-**CH_3**), 0.93 (d, *J*=6.4 Hz, 3H, 21-**CH_3**), 0.69 (s, 3H, 18-**CH_3**) ppm. **^{13}C NMR** (100 MHz, $CDCl_3$) δ 211.1 (**3-C**), 210.2 (**7-C**), 174.6 (**24-COO**CH_3), 54.8 (CH), 51.5 (**24**-COO**CH_3**), 49.5 (CH), 48.8 (CH), 47.7 (CH), 45.0 (CH_2), 42.9 (CH_2), 42.8 (CH), 42.6 (C), 38.8 (CH_2), 36.7 (CH_2), 35.4 (CH_2), 35.4 (C), 35.2 (CH), 31.0 (CH_2), 30.9 (CH_2), 28.2 (CH_2), 24.7 (CH_2), 22.4 (**19-CH_3**), 22.1 (CH_2), 18.3 (**21-CH_3**), 12.0 (**18-CH_3**) ppm. ^{1}H NMR and melting point data agree with literature.[47,222] ^{13}C NMR data not available. ^{1}H and ^{13}C NMR data consistent with data from within the group.

Methyl 3α,3β,7α,7β-tetrafluoro-5β-cholan-24-oate (2.37), Methyl 3α,3β-difluoro-7-oxo-5β-cholan-24-oate (2.38)

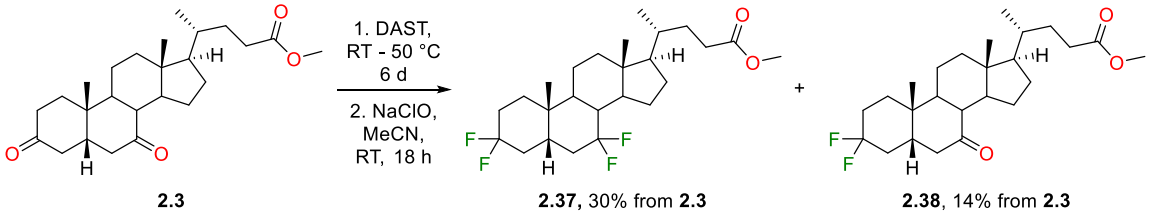

To a flame-dried flask with condenser attached, **2.3** (1.50 g, 3.70 mmol, 1.0 equiv) and DAST (5.0 mL, 38 mmol, 10 equiv) were added. The mixture was stirred at RT for 3 d, then heated to 50 °C. After 3 d of heating, the reaction mixture was allowed to cool, added DCM (50 mL) and decanted dropwise (~5 mL per min) into icy saturated $NaHCO_3$ solution (~200 mL). After achieving a neutral pH, the phases were separated and the aqueous phase was extracted with DCM (2 x 50 mL). The combined organic phases were washed with saturated $NaHCO_3$ solution (75 mL), water (75 mL) and brine (75 mL) before drying over Na_2SO_4 and reducing *in vacuo* to yield the crude (1.8 g) as a brown oil. The crude material was purified by flash chromatography (EtOAc/PE 0%/100% → 10%/90%), yielding two main fractions: a fraction (860 mg) containing around 80% **2.37** and around 20% of fluoroalkene products and a fraction (370 mg) containing around 90% **2.38** and around 10% of fluoroalkene products.

The impure fraction containing **2.37** was dissolved in acetonitrile (20 mL) and treated with NaClO (11%, 0.7 mL, 1.2 mmol, ~3 equiv based on fluoroalkene content). After stirring at RT for 18 h, water (50 mL) was added to the reaction mixture and the aqueous phase was extracted with EtOAc (2 x 50 mL). The combined organic phases were washed with saturated sodium thiosulfate solution (100 mL), water (50 mL) and brine (50 mL) before drying over Na_2SO_4 and reducing *in vacuo* to yield the crude (780 mg) as a pale gum. The crude material was purified by flash chromatography (EtOAc/PE:

8%/92%), yielding **2.37** as a white solid (500 mg, 1.12 mmol, 30% from **2.3**). Fluoroepoxide or fluoroalkene products were not isolated after flash chromatography.

2.37: **mp** 140 – 141 °C. **R_f** 0.35 (EtOAc/PE 10/90). **$[\alpha]_D$** + 22.2 (c = 1.35, $CHCl_3$, 20 °C). **^{1}H NMR** (400 MHz, $CDCl_3$) δ 3.67 (s, 3H, 24-COO**CH_3**), 2.36 (ddd, *J*=15.4, 10.1, 5.3 Hz, 1H, 23-**H'**), 2.29-1.04 (m), 1.01 (s, 3H, 19-**CH_3**), 0.93 (d, *J*=6.5 Hz, 3H, 21-**CH_3**), 0.68 (s, 3H, 18-**CH_3**) ppm. **^{13}C NMR** (100 MHz, $CDCl_3$) δ 174.6 (**24-COO**CH_3), 124.4 (t, *J*=245.0 Hz, **7-C**), 121.1 (br t, *J*=239.2 Hz, **3-C**), 54.9 (**17-CH**), 51.5 (**24**-COO**CH_3**), 48.5 (d, *J*=3.7 Hz, **14-CH**), 43.1 (**13-C**), 41.7 (dd, *J*=23.5, 19.8 Hz, **8-CH**), 39.3 (CH_2), 39.2 (t, *J*=9.5 Hz, **9-CH**), 36.5 (d, *J*=8.8 Hz, **5-CH**), 35.3 (**20-CH**), 35.3 (br t, *J*=23.5 Hz, ***4-CH_2 or 6-CH_2***), 35.2 (dd, *J*=24.9, 22.0 Hz, ***4-CH_2 or 6-CH_2***), 34.3 (**10-C**), 32.3 (d, *J*=8.8 Hz, **1-CH_2**), 31.0 (CH_2), 30.9 (CH_2), 29.1 (dd, *J*=25.3, 22.4 Hz, **2-CH_2**), 28.2 (d, *J*=1.5 Hz, CH_2), 25.3 (d, *J*=4.4 Hz, CH_2), 22.1 (d, *J*=2.9 Hz, **19-CH_3**), 21.2 (CH_2), 18.3 (**21-CH_3**), 11.8 (**18-CH_3**) ppm. **^{19}F NMR** (376MHz, $CDCl_3$) δ -84.93 (br d, *J*=242.8 Hz, 1F, 7β-**F**), -89.91 (br d, *J*=234.1 Hz, 1F, 3α-**F**), -101.65 (dddd, *J*=242.8, 39.9, 26.0, 13.9 Hz, 1F, 7α-**F**), -102.35 (dtt, *J*=234.1, 32.9, 8.7 Hz, 1F, 3β-**F**) ppm. **^{19}F [^{1}H] NMR** (376MHz, $CDCl_3$) δ -84.93 (d, *J*=242.8 Hz, 1F, 7β-**F**), -89.91 (d, *J*=234.1 Hz, 1F, 3α-**F**), -101.63 (dd, *J*=242.8, 3.5 Hz, 1F, 7α-**F**), -102.36 (dd, *J*=234.1, 3.5 Hz, 1F, 3β-**F**) ppm. **LRMS (ESI+)** m/z: 464.6 $[M+NH_4]^+$, 444.5 $[M+NH_4-HF]^+$. **HRMS (ESI+)** $C_{25}H_{38}F_4NaO_2$ $[M+Na]^+$. Calculated: 469.2700; Found: 469.2706 (1.3 ppm error). **IR** (neat, cm^{-1}) 2947 – 2884 (m), 1737 (s), 1193 (m), 1095 (s).

The impure fraction containing **2.38** was dissolved in acetonitrile (10 mL) and treated with NaClO (11%, 0.2 mL, 0.30 mmol, ~3 equiv based on fluoroalkene content). After stirring at RT for 18 h, water (25 mL) was added to the reaction mixture and the aqueous phase was extracted with EtOAc (2 x 25 mL). The combined organic phases were washed with saturated sodium thiosulfate solution (50 mL), water (50 mL) and brine (50 mL) before drying over Na_2SO_4 and reducing *in vacuo* to yield the crude (330 mg) as a white solid. The crude material was purified by flash chromatography (EtOAc/PE: 13%/87%) yielding **2.38** as a white solid (220 mg, 0.52 mmol, 14% from **2.3**). Fluoroepoxide or fluoroalkene products were not isolated after flash chromatography.

2.38: **mp** 152 – 153 °C. **R_f** 0.27 (EtOAc/PE 15/85). **$[\alpha]_D$** - 37.1 (c = 0.55, $CHCl_3$, 20 °C). **^{1}H NMR** (400 MHz, $CDCl_3$) δ 3.66 (s, 3H, 24-COO**CH_3**), 2.88 (ddd, *J*=12.7, 6.0, 1.9 Hz, 1H, 6β-**H**), 2.42 (t, *J*=11.3 Hz, 1H, 8β-**H**), 2.35 (ddd, *J*=15.3, 10.0, 5.0 Hz, 1H, 23-**H'**), 0.94-2.26 (m), 1.25 (s, 3H, 19-**CH_3**), 0.92 (d, *J*=6.4 Hz, 3H, 21-**CH_3**), 0.66 (s, 3H, 18-**CH_3**) ppm. **^{13}C NMR** (100 MHz, $CDCl_3$) δ 211.3 (**7-C**), 174.6 (**24-COO**CH_3), 123.2 (dd, *J*=242.8, 238.4 Hz, **3-C**), 54.7 (**17-CH**), 51.5 (**24**-COO**CH_3**), 49.4 (**8-CH**), 48.8 (**14-CH**), 44.5 (**6-CH_2**), 44.2 (d, *J*=9.5 Hz, **5-CH**), 42.6 (**13-C**), 42.3 (CH), 38.8 (CH_2), 35.5 (dd, *J*=26.4, 22.0 Hz, **4-CH_2**), 35.2 (CH), 35.1 (d, *J*=1.5 Hz, **10-C**), 31.9 (d, *J*=9.5 Hz, **1-CH_2**), 31.0 (CH_2), 30.9 (CH_2), 29.0 (dd, *J*=25.7, 22.7 Hz, **2-CH_2**), 28.2 (CH_2), 24.7 (CH_2), 22.5 (d, *J*=2.2 Hz, **19-CH_3**), 22.0 (CH_2), 18.3 (**21-CH_3**), 12.0 (**18-CH_3**) ppm. **^{19}F NMR** (376MHz, $CDCl_3$) δ -90.13 (br d, *J*=237.6 Hz, 1F, 3α-**F**), -100.03

(dtt, *J*=236.9, 34.1, 11.3 Hz, 1F, 3β-**F**) ppm. **^{19}F [^{1}H] NMR** (376MHz, $CDCl_3$) δ -90.25 (d, *J*=235.8 Hz, 1F, 3α-**F**), -100.10 (d, *J*=235.8 Hz, 1F, 3β-**F**) ppm. **LRMS (ESI+)** m/z: 442.5 $[M+NH_4]^+$. **HRMS (ESI+)** $C_{25}H_{42}F_2NO_3$ $[M+NH_4]^+$. Calculated: 442.3127; Found: 442.3127. **IR** (neat, cm^{-1}) 2947 – 2884 (m), 1737 (s), 1373 (m), 1193 (m), 1095 (s).

3α,3β,7α,7β-Tetrafluoro-5β-cholanic acid (2.1)

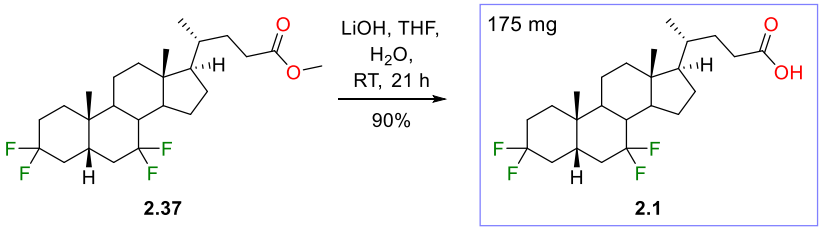

Following general procedure C, **2.37** (200 mg, 0.45 mmol, 1 equiv) was deprotected to yield **2.1** as a white powder (175 mg, 0.40 mmol, 90%) with no further purification.

mp 184 – 185 °C. **R_f** 0.59 (EtOAc/PE 80/20). **$[\alpha]_D$** + 23.5 (c = 0.82, $CHCl_3$, 20 °C). **^{1}H NMR** (400 MHz, $CDCl_3$) δ 2.41 (ddd, *J*=15.4, 10.1, 5.3 Hz, 1H, 23-**H'**), 1.09-2.34 (m), 1.02 (s, 3H, 19-**CH_3**), 0.95 (d, *J*=6.5 Hz, 3H, 21-**CH_3**), 0.69 (s, 3H, 18-**CH_3**) ppm. **^{13}C NMR** (100 MHz, $CDCl_3$) δ 179.9 (**24-COOH**), 124.5 (t, *J*=245.0 Hz, **7-C**), 123.5 (br t, *J*=240.6 Hz, **3-C**), 54.9 (**17-CH**), 48.5 (d, *J*=3.7 Hz, **14-CH**), 43.1 (**13-C**), 41.7 (dd, *J*=22.7, 19.8 Hz, **8-CH**), 39.3 (CH_2), 39.2 (t, *J*=11.0 Hz, CH), 36.5 (d, *J*=9.5 Hz, **5-CH**), 35.3 (br t, *J*=23.5 Hz, ***4-CH₂ or 6-CH₂***), 35.2 (**20-CH**), 35.2 (br t, *J*=23.5 Hz, ***4-CH₂ or 6-CH₂***), 34.3 (**10-C**), 32.3 (br d, *J*=10.3 Hz, **1-CH_2**), 30.9 (CH_2), 30.7 (CH_2), 29.1 (dd, *J*=25.7, 22.7 Hz, **2-CH_2**), 28.2 (CH_2), 25.3 (d, *J*=3.7 Hz, CH_2), 22.1 (d, *J*=2.9 Hz, **19-CH_3**), 21.2 (CH_2), 18.3 (**21-CH_3**), 11.8 (**18-CH_3**) ppm. **^{19}F NMR** (376MHz, $CDCl_3$) δ -84.92 (br d, *J*=242.8 Hz, 1F, 7β-**F**), -89.91 (br d, *J*=234.1 Hz, 1F, 3α-**F**), -101.65 (dddd, *J*=244.5, 38.1, 26.0, 13.9 Hz, 1F, 3β-**F**), -102.35 (dtt, *J*=234.1, 32.9, 8.7 Hz, 1F, 7α-**F**) ppm. **^{19}F [^{1}H] NMR** (376MHz, $CDCl_3$) δ -84.93 (d, *J*=244.5 Hz, 1F, 7β-**F**), -89.90 (d, *J*=234.1 Hz, 1F, 3α-**F**), -101.67 (dd, *J*=242.8, 3.5 Hz, 1F, 3β-**F**), -102.35 (dd, *J*=234.1, 3.5 Hz, 1F, 7α-**F**) ppm. **LRMS (ESI+)** m/z: 450.4 $[M+NH_4]^+$, 430.3 $[M+NH_4\text{-}HF]^+$. **HRMS (ESI+)** $C_{24}H_{36}F_4NaO_2$ $[M+Na]^+$. Calculated: 455.2544; Found: 455.2539 (1.0 ppm error). **IR** (neat, cm^{-1}) 2946 – 2879 (m), 1706 (s), 1098 (s), 909 (s).

3α,3β-Difluoro-7-oxo-5β-cholanic acid (2.2)

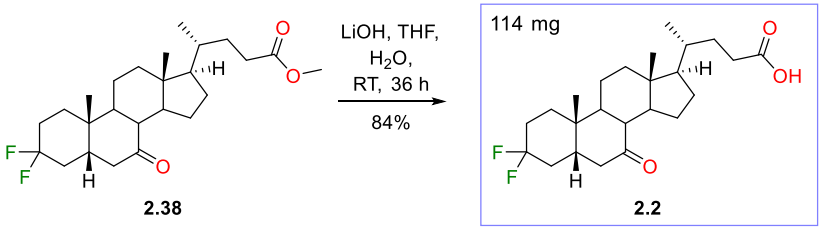

Following general procedure C, **2.38** (138 mg, 0.33 mmol, 1.0 equiv) was deprotected to yield **2.2** as a white solid (114 mg, 0.28 mmol, 84%) with no further purification.

mp 169 – 170 °C. **R_f** 0.27 (EtOAc/PE 40/60). **$[\alpha]_D$** -37.9 (c = 1.04, $CHCl_3$, 20 °C). **^{1}H NMR** (400 MHz, $CDCl_3$) δ 2.88 (ddd, *J*=12.7, 6.1, 1.8 Hz, 1H, 6β-**H**), 0.95 – 2.48 (m), 1.26 (s, 3H, 19-**CH_3**), 0.94 (d, *J*=6.5 Hz, 3H, 21-**CH_3**), 0.67 (s, 3H, 18-**CH_3**) ppm. **^{13}C NMR** (100 MHz, $CDCl_3$) δ 211.4 (**7-C**), 180.1 (**24-COOH**), 123.6 (dd, *J*=242.8, 238.4 Hz, **3-C**), 54.7 (**17-CH**), 49.5 (**8-CH**), 48.8 (**14-CH**), 44.5 (**6-CH_2**), 44.2 (d, *J*=9.5 Hz, **5-CH**), 42.6 (**13-C**), 42.3 (**9-CH**), 38.8 (**12-CH_2**), 35.4 (br dd, *J*=26.4, 22.0 Hz, **4-CH_2**), 35.1 (**20-CH**), 35.1 (**10-C**), 31.9 (d, *J*=9.5 Hz, **1-CH_2**), 31.0 (CH_2), 30.7 (CH_2), 29.0 (dd, *J*=25.7, 22.0 Hz, **2-CH_2**), 28.2 (CH_2), 24.7 (CH_2), 22.5 (d, *J*=2.9 Hz, **19-CH_3**), 22.0 (CH_2), 18.3 (**21-CH_3**), 12.0 (**18-CH_3**) ppm. **^{19}F NMR** (376MHz, $CDCl_3$) δ -90.14 (br d, *J*=237.6 Hz, 1F, 3α-**F**), -100.04 (dtt, *J*=236.9, 34.1, 11.3 Hz, 1F, 3β-**F**) ppm. **^{19}F [^{1}H] NMR** (376MHz, $CDCl_3$) δ -90.22 (d, *J*=237.6 Hz, 1F, 3α-**F**), -100.04 (d, *J*=235.8 Hz, 1F, 3β-**F**) ppm. **LRMS (ESI+)** m/z: 428.4 $[M+NH_4]^+$. **HRMS (ESI+)** $C_{24}H_{36}F_2NaO_3$ $[M+Na]^+$. Calculated: 433.2525; Found: 433.2518 (1.6 ppm error). **IR** (neat, cm^{-1}) 2950 – 2871 (m), 1704 (s), 1091 (s), 1050 (s), 953 (s).

7.3.2 Synthesis of Analogues from Cholic Acid and Its Derivatives

Methyl 12α,12β-difluoro-3α,7α-acetoxy-5β-cholan-24-oate (2.39)

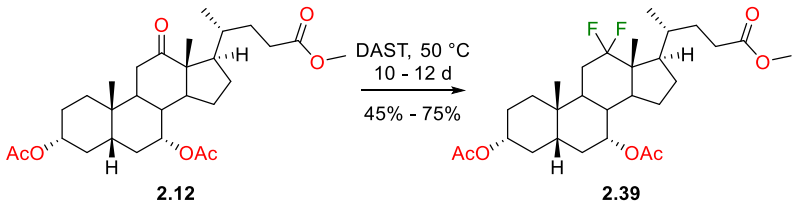

2.12 **2.39**

To a flame-dried flask with condenser attached, under argon, the ketone **2.12** (5.00 g, 9.91 mmol, 1.0 equiv) and DAST (10 mL, ~76 mmol, ~8 equiv) were added. The reaction mixture was heated to 50 °C. Over the course of 4 d, 16 mL of DAST was added to the reaction mixture at RT in a 4 mL portion, a 2 mL portion and a 10 mL portion. After 10 d of heating, the reaction mixture was allowed to cool to RT, added DCM (50 mL) and decanted dropwise (~5 mL per min) into icy, saturated $NaHCO_3$ solution (~ 750 mL). After achieving a neutral pH, the phases were separated and the aqueous phase was extracted with DCM (3 x 100 mL). The DCM phases were combined, washed with water (250 mL) brine (250 mL) before drying over Na_2SO_4 and reducing *in vacuo*, giving around 8 g of brown crude. The crude was purified by flash chromatography (Biotage ZIP KP-Sil 120 g cartridge, EtOAc/PE: 15%/85% → 25%/75%), yielding **2.39** as a yellow solid (3.93 g, 7.46 mmol, 75%).

mp 132 – 134 °C (decomp.). **R_f** 0.23 (EtOAc/PE 25/75). **^{1}H NMR** (400 MHz, $CDCl_3$) δ 4.92 (apparent br d, *J*=2.7 Hz, 1H, 7β-**H**), 4.59 (tt, *J*=11.3, 4.3 Hz, 1H, 3β-**H**), 3.67 (s, 3H, 24-COO**CH_3**), 2.38 (ddd, *J*=15.5, 10.0, 5.3 Hz, 1H, 23-**H'**), 2.26 (ddd, *J*=16.3, 9.7, 6.7 Hz, 1H, 23-**H''**), 2.16 (td, *J*=12.4, 4.8 Hz, 1H, 9α-**H**), 2.07 (s, 3H, 7α-OCO**CH_3**), 2.04 (s, 3H, 3α-OCO**CH_3**), 1.06-2.02 (m), 0.99 (dd, *J*=6.5, 1.8 Hz, 3H, 21-**CH_3**), 0.94 (s, 3H, 19-**CH_3**), 0.83 (s, 3H, 18-**CH_3**) ppm. **^{13}C NMR** (100 MHz, $CDCl_3$) δ 174.6 (**24-COO**CH_3), 170.6 (**3α-OCO**CH_3), 170.2 (**7α-OCO**CH_3), 126.2 (t, *J*=246.5 Hz, **12-C**), 73.7 (**3-C**), 70.1 (**7-C**), 51.5 (**24-**COO**CH_3**), 49.0 (t, *J*=19.8 Hz, **13-C**), 47.6 (d, *J*=2.9 Hz, **17-CH**), 46.7 (d, *J*=6.6 Hz, **14-CH**), 40.5 (**5-CH**), 36.7 (**8-CH**), 34.7 (CH_2), 34.5 (CH_2), 34.4 (**10-C**), 33.0 (**20-CH**), 31.6 (d, *J*=9.5 Hz, **9-CH**), 31.5 (**23-CH_2**), 31.1 (CH_2), 31.0 (br t, *J*=26.0 Hz, **11-CH_2**), 30.3 (**22-CH_2**), 26.6 (**2-CH_2**), 26.0 (CH_2), 22.4 (CH_2), 22.3 (**19-CH_3**), 21.5 and 21.4 (**3α-**OCO**CH_3** or **7α-**OCO**CH_3**), 19.0 (d, *J*=10.3 Hz, **21-CH_3**), 10.4 (d, *J*=5.1 Hz, **18-CH_3**) ppm. **^{19}F NMR** (376 MHz, $CDCl_3$) δ -91.87 (br d, *J*=230.6 Hz, 1F, 12β-**F**), -112.25 (ddd, *J*=12.1, 35.5, 231.5 Hz, 1F, 12α-**F**). **^{19}F [^{1}H] NMR** (376 MHz, $CDCl_3$) δ -91.87 (d, *J*=230.6 Hz, 1F, 12β-**F**), -112.25 (d, *J*=232.3 Hz, 1F, 12α-**F**). **LRMS (ESI+)** m/z: 544.5 $[M+NH_4]^+$, 549.4 $[M+Na]^+$. ^{1}H, ^{13}C and ^{19}F NMR data consistent with data from within the group.

12α,12β-Difluorochenodeoxycholic acid (2.40)

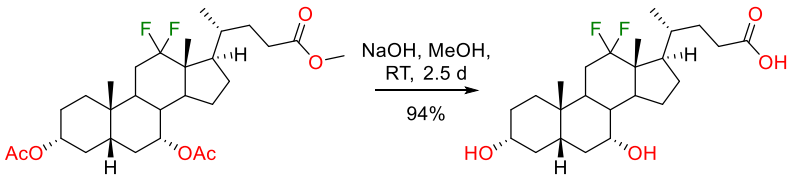

2.39 **2.40**

Following general procedure D, **2.39** (3.80 g, 7.21 mmol, 1.0 equiv) was deprotected to yield **2.40** as an off-white solid (2.91 g, 6.80 mmol, 94%) with no further purification.

mp 202 – 203 °C. **R_f** 0.07 (EtOAc/PE 70/30). **[α]$_D$** + 33.0 (c=0.535, MeOH, 23 °C). **^{1}H NMR** (400 MHz, MeOH-d_4) δ 3.83 (apparent br d, *J*=2.8 Hz, 1H, 7β-**H**), 3.38 (tt, *J*=11.2, 4.4 Hz, 1H, 3β-**H**), 2.15-2.40 (m, 4H), 1.26-2.01 (m), 1.06 (td, *J*=14.1, 3.4 Hz, 1H, 1β-**H**), 1.01 (dd, *J*=6.7, 1.7 Hz, 3H, 21-**CH_3**), 0.94 (s, 3H, 19-**CH_3**), 0.86 (s, 3H, 18-**CH_3**) ppm. **^{13}C NMR** (100 MHz, MeOH-d_4) δ 178.2 (**24-COOH**), 127.8 (dd, *J*=249.4, 246.5 Hz, **12-C**), 72.7 (**3-CH**), 68.3 (**7-CH**), 50.3 (t, *J*=20.5 Hz, **13-C**), 49.3 (br d, *J*=2.2 Hz, **17-CH**), 48.4 (d, *J*=7.3 Hz, **14-CH**), 42.9 (**5-CH**), 40.4 (CH_2), 39.7 (**8-CH**), 36.5 (**1-CH_2**), 35.9 (CH_2), 35.9 (**10-C**), 34.7 (**20-CH**), 32.6 (**23-CH_2**), 32.2 (br t, *J*=26.4 Hz, **11-CH_2**), 31.9 (**22-CH_2**), 31.9 (d, *J*=9.5 Hz, **9-CH**), 31.3 (CH_2), 27.5 (CH_2), 23.6 (CH_2), 23.1 (**18-CH_3**), 19.7 (d, *J*=11.0 Hz, **21-CH_3**), 11.0 (d, *J*=4.4 Hz, **18-CH_3**) ppm. **^{19}F NMR** (376MHz, MeOH-d_4) δ -91.43 (br d, *J*=230.6 Hz, 1F, 12β-**F**), -112.68 (ddd, *J*=231.0, 35.1, 13.0 Hz, 1F, 12α-**F**) ppm. **^{19}F [^{1}H] NMR** (376MHz, MeOH-d_4) δ -91.43 (d, *J*=230.6 Hz, 1F, 12β-**F**), -112.68 (d, *J*=230.6 Hz, 1F, 12α-**F**) ppm. **LRMS (ESI+)** m/z: 446.4 $[M+NH_4]^+$. **HRMS (ESI+)** $C_{24}H_{38}F_2NaO_4$ $[M+Na]^+$. Calculated: 451.2630; Found: 451.2626 (1.0 ppm error). **IR** (neat, cm^{-1}) 3444-

3300 (b), 2968-2864 (m), 1703 (s), 1074 (s), 1030 (s). ^{1}H, ^{13}C and ^{19}F NMR data consistent with data from within the group.

Methyl 12α,12β-difluoro-3α,7α-dihydroxy-5β-cholan-24-oate (2.10)

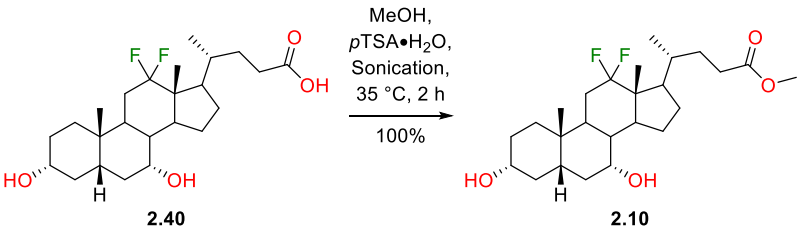

Following general procedure A, **2.40** (2.80 g, 6.53 mmol, 1.0 equiv) was protected to yield **2.10** as an off-white solid (2.77 g, 6.26 mmol, 96%) with no further purification.

mp 55 – 56 °C. **R_f** 0.15 (EtOAc/PE 50/50). **^{1}H NMR** (400 MHz, $CDCl_3$) δ 3.89 (apparent br d, *J*=2.4 Hz, 1H, 7β-**H**), 3.67 (s, 3H, 24-COO**CH_3**), 3.47 (br tt, *J*=10.9, 4.0 Hz, 1H, 3β-**H**), 1.12-2.32 (m), 1.06 (td, *J*=13.6, 2.7 Hz, 1H, 1β-**H**), 1.00 (dd, *J*=6.5, 1.5 Hz, 3H, 21-**CH_3**), 0.91 (s, 3H, 19-**CH_3**), 0.83 (s, 3H, 18-**CH_3**) ppm. **^{13}C NMR** (100 MHz, $CDCl_3$) δ 174.7 (**24-COO**CH_3), 126.4 (t, *J*=249.4 Hz, **12-C**), 71.7 (**3-CH**), 67.6 (**7-CH**), 51.5 (**24-**COO**CH_3**), 48.9 (t, *J*=20.5 Hz, **13-C**), 47.6 (d, *J*=2.2 Hz, **17-CH**), 46.8 (d, *J*=7.3 Hz, **14-CH**), 41.1 (**5-CH**), 39.6 (CH_2), 38.2 (**8-CH**), 35.1 (**1-CH_2**), 34.7 (CH_2), 34.6 (**10-C**), 33.2 (**20-CH**), 31.5 (**23-CH_2**), 31.0 (t, *J*=26.0 Hz, **11-CH_2**), 30.5 (**22-CH_2**), 30.4 (CH_2), 30.4 (d, *J*=8.1 Hz, **9-CH**) 26.2 (CH_2), 22.6 (CH_2), 22.4 (**19-CH_3**), 19.0 (d, *J*=11.0 Hz, **21-CH_3**), 10.4 (d, *J*=4.4 Hz, **18-CH_3**) ppm. **^{19}F NMR** (376MHz, $CDCl_3$) δ -91.53 (br d, *J*=230.6 Hz, 1F, 12β-**F**), -112.05 (ddd, *J*=230.6, 34.7, 12.1 Hz, 1F, 12α-**F**) ppm. **^{19}F [^{1}H] NMR** (376MHz, $CDCl_3$) δ -91.53 (br d, J=229.8 Hz, 1F, 12β-**F**), -112.07 (d, J=230.6 Hz, 1F, 12α-**F**) ppm. **LRMS (ESI+)** m/z: 367 $[M+H-2HF-2H_2O]^+$, 385 $[M+H-2HF-H_2O]^+$, 403 $[M+H-2HF]^+$, 465 $[M+Na]^+$, 885 $[2M+H]^+$, 907 $[2M+Na]^+$. ^{1}H, ^{13}C and ^{19}F NMR data consistent with data from within the group.

Methyl 12α,12β-difluoro-3-oxo-7α-hydroxy-5β-cholan-24-oate (2.41)

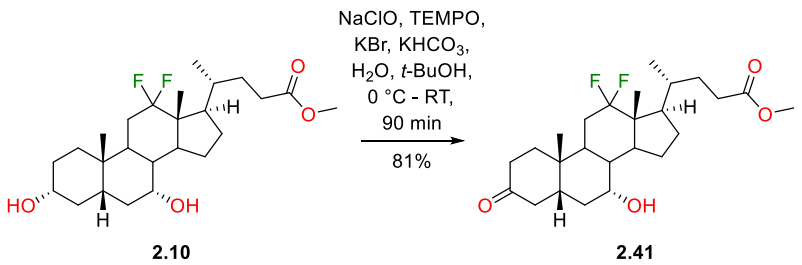

Following general procedure B, **2.10** (2.40 g, 5.42 mmol, 1.0 equiv) was oxidised. The crude material was purified by flash chromatography (Biotage ZIP KP-Sil 80 g Cartridge, EtOAc/PE 25%/75% → 40%/60%), yielding **2.41** as a white solid (1.94 g, 4.40 mmol, 81%).

mp 115 – 117 °C. **R_f** 0.30 (EtOAc/PE 40/60). **$[\alpha]_D$** + 33.6 (c = 0.89, $CHCl_3$, 21 °C). **^{1}H NMR** (400 MHz, $CDCl_3$) δ 3.97 (br s, 1H, 7β-**H**), 3.67 (s, 3H, 24-COO**CH_3**), 3.37 (br t, J=14.6 Hz, 1H, 4α-**H**), 2.49-1.16 (m), 1.02 (s, 3H, 19-**CH_3**), 1.00 (dd, *J*=6.2, 1.6 Hz, 1H, 21-**CH_3**), 0.87 (s, 3H, 18-**CH_3**) ppm. **^{13}C NMR** (100 MHz, $CDCl_3$) δ 212.3 (**3-C**), 174.6 (**24-COO**CH_3), 126.2 (dd, *J*=250.2, 247.2 Hz, **12-C**), 67.6 (**7-CH**), 51.5 (**24**-COO**CH_3**), 49.0 (t, *J*=20.5 Hz, **13-C**), 47.6 (d, *J*=2.2 Hz, **17-CH**), 46.7 (d, *J*=6.6 Hz, **14-CH**), 45.4 (**4-CH_2**), 42.6 (**5-CH**), 38.2 (**8-CH**), 36.7 (***1-CH_2* or *2-CH_2***), 36.5 (***1-CH_2* or *2-CH_2***), 34.9 (**10-C**), 33.9 (**6-CH_2**), 33.2 (**20-CH**), 31.5 (**23-CH_2**), 31.3 (t, *J*=26.4 Hz, **11-CH_2**), 31.0 (d, *J*=10.3 Hz, **9-CH**), 30.4 (**22-CH_2**), 26.2 (***15-CH_2* or *16-CH_2***), 22.6 (***15-CH_2* or *16-CH_2***), 21.6 (**19-CH_3**), 19.0 (d, *J*=11.0 Hz, **21-CH_3**), 10.4 (d, *J*=4.4 Hz, **18-CH_3**) ppm. **^{19}F NMR** (376MHz, $CDCl_3$) δ -91.75 (br d, *J*=232.4 Hz, 1F, 12β-**F**), -112.17 (ddd, *J*=231.5, 34.7, 13.0 Hz, 1F, 12α-**F**) ppm. **^{19}F [^{1}H] NMR** (376MHz, $CDCl_3$) δ -91.75 (d, *J*=230.6 Hz, 1F, 12β-**F**), -112.17 (d, *J*=230.6 Hz, 1F, 12α-**F**) ppm. **LRMS (ESI+)** m/z: 383.5 $[M+H-2HF-H_2O]^+$, 401.4 $[M+H-2HF]^+$, 421.4 $[M+H-HF]^+$, 458.5 $[M+NH_4]^+$, 463.5 $[M+Na]^+$, 881.7 $[2M+H]^+$. **HRMS (ESI+)** $C_{25}H_{42}F_2NO_4$ $[M+NH_4]^+$. Calculated: 458.3076; Found: 458.3067. **IR** (neat, cm^{-1}) 3451 (br, w), 2946-2888 (m), 1739 (s), 1705 (s), 1257 (s), 1021 (s).

Methyl 12α,12β-difluoro-3-oxo-7α-acetoxy-5β-cholan-24-oate (2.42)

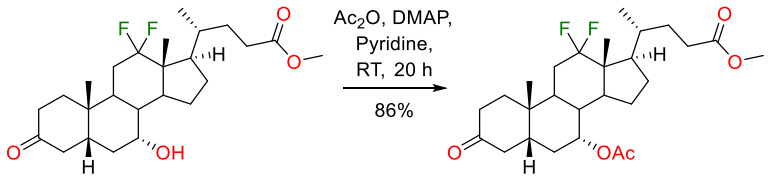

2.41 **2.42**

Following general procedure E, **2.41** (1.85 g, 4.20 mmol, 1.0 equiv) was protected. The crude material was purified by flash chromatography (Biotage ZIP KP-Sil 30 g Cartridge, EtOAc/PE: 20%/80% → 35%/65%), yielding **2.42** as a white, gummy solid which solidified overnight (1.77 g, 3.67 mmol, 87%).

mp 84 – 85 °C. **R_f** 0.21 (EtOAc/PE 30/70). **$[\alpha]_D$** + 22.7 (c = 0.82, $CHCl_3$, 21 °C). **^{1}H NMR** (400 MHz, $CDCl_3$) δ 5.01 (apparent br d, *J*=2.8 Hz, 1H, 7β-**H**), 3.67 (s, 3H, 24-COO**CH_3**), 2.94 (t, *J*=14.4 Hz, 1H, 4α-**H**), 2.48-2.06 (m), 2.05 (s, 3H, 7α-OCO**CH_3**), 2.03-1.13 (m), 1.04 (s, 3H, 19-**CH_3**), 1.00 (dd, *J*=1.8, 6.6 Hz, 3H, 21-**CH_3**), 0.87 (s, 3H, 18-**CH_3**) ppm. **^{13}C NMR** (100 MHz, $CDCl_3$) δ 211.4 (**3-C**), 174.5 (**24-COO**CH_3), 170.0 (**7α-OCO**CH_3), 125.8 (dd, *J*=250.9, 246.5 Hz, **12-C**), 70.0 (**7-CH**), 51.5 (**24**-COO**CH_3**), 49.1 (t, *J*=20.5 Hz, **13-C**), 47.6 (d, *J*=2.2 Hz, **17-CH**), 46.6 (d, *J*=7.3 Hz, **14-CH**), 44.4 (**4-CH_2**), 41.9 (CH), 36.8 (CH), 36.6 (CH_2), 36.2 (CH_2), 34.5 (**10-C**), 33.0 (CH), 32.5 (d, *J*=10.3 Hz, **9-CH**), 31.4 (**23-CH_2**), 31.4 (t, *J*=26.4 Hz, **11-CH_2**), 30.8 (CH_2), 30.3 (CH_2), 25.9 (CH_2), 22.4 (CH_2), 21.5 (**19-CH_3**), 21.4 (**7α**-OCO**CH_3**), 19.0 (d, *J*=10.3 Hz **21-CH_3**), 10.4 (d, *J*=4.4 Hz, **18-CH_3**) ppm. **^{19}F NMR** (376MHz, $CDCl_3$) δ -92.14 (br d, *J*=232.3 Hz, 1F, 12β-**F**), -112.36 (ddd, *J*=232.3, 347, 12.1 Hz, 1F, 12α-**F**) ppm. **^{19}F [^{1}H] NMR** (376MHz, $CDCl_3$) δ -92.20 (d, *J*=232.3 Hz, 1F, 12β-**F**), -112.36 (d, *J*=232.4 Hz, 1F, 12α-**F**) ppm. **LRMS (ESI+)** m/z:

383.5 $[M+H-2HF-AcOH]^+$, 403.4 $[M+H-HF-AcOH]^+$, 443.5 $[M+H-2HF]^+$, 505.5 $[M+Na]^+$. **HRMS (ESI+)** $C_{27}H_{40}F_2NaO_5$ $[M+Na]^+$. Calculated: 505.2736; Found: 505.2736. **IR** (neat, cm^{-1}) 2959 – 2878 (m), 1732 (s), 1715 (s), 1293 (m), 1210 (m), 1023 (m).

Methyl 3α,3β,12α,12β-tetrafluoro-7α-acetoxy-5β-cholan-24-oate (2.43)

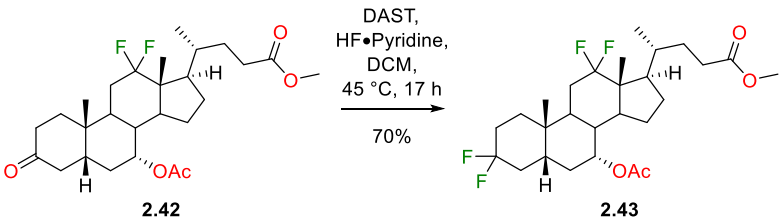

The ketone **2.42** (1.70 g, 3.52 mmol, 1.0 equiv) was dissolved in dry DCM (30 mL) and DAST (1.40 mL, 10.6 mmol, 3.0 equiv) and HF•Pyridine (70% HF, ~0.02 mL, ~0.18 mmol, ~0.05 equiv) were added. After heating under reflux for 18 h, the reaction mixture was cooled, diluted with DCM (30 mL) and saturated $NaHCO_3$ solution (50 mL) was added to the reaction mixture dropwise. The phases were separated and the aqueous phase was extracted with DCM (50 mL). The combined organic phases were washed with saturated $NaHCO_3$ solution (100 mL), water (100 mL) and brine (100 mL) before drying over Na_2SO_4 and reducing *in vacuo* to yield around 150 mg of crude material. The crude was purified by flash chromatography (Biotage ZIP KP-Sil 30 g Cartridge, EtOAc/PE: 12%/88% → 25%/75%), yielding **2.43** as a white gummy solid (1.24 g, 2.46 mmol, 70%).

R_f 0.26 (EtOAc/PE 20%/80%). **$[\alpha]_D$** + 15.8 (c = 1.32, $CHCl_3$, 22 °C). **^{1}H NMR** (400 MHz, $CDCl_3$) 4.97 (q, *J*=2.9 Hz, 1H, 7β-**H**), 3.67 (s, 3H, 24-COO**CH_3**), 2.45-2.22 (m, 3H), 2.07 (s, 3H, 7α-OCO**CH_3**), 2.06-1.10 (m), 1.03-0.96 (m, 6H, dd of 21-**CH_3** and s of 19-**CH_3**), 0.84 (s, 3H, 18-**CH_3**) ppm. **^{13}C NMR** (100 MHz, $CDCl_3$) 174.5 (**24-COO**CH_3), 170.1 (**7α-OCO**CH_3), 126.5 (dd, *J*=250.9, 246.5 Hz, **12-C**), 122.7 (dd, *J*=241.4, 239.9 Hz, **3-C**), 69.9 (**7-CH**), 51.5 (**24**-COO**CH_3**), 49.1 (t, *J*=19.8 Hz, **13-C**), 47.6 (d, *J*=2.2 Hz, **17-CH**), 46.7 (d, *J*=7.3 Hz, **14-CH**), 38.6 (d, *J*=9.5 Hz, **5-CH**), 36.7 (**8-CH**), 36.3 (dd, *J*=24.2, 21.3 Hz, **4-CH_2**), 34.3 (**10-C**), 33.0 (**20-CH**), 32.6 (d, *J*=9.5 Hz, **1-CH_2**), 31.4 (**23-CH_2**), 31.0 (t, *J*=26.4 Hz, **11-CH_2**), 31.0 (br d, *J*=9.5 Hz, **9-CH**), 30.4 (**6-CH_2**), 30.3 (**22-CH_2**), 29.1 (dd, *J*=25.3, 22.4 Hz, **2-CH_2**), 26.0 (***15-CH_2* or *16-CH_2***), 22.4 (***15-CH_2* or *16-CH_2***), 21.8 (d, *J*=2.2 Hz, **19-CH_3**), 21.4 (**7α**-OCO**CH_3**), 19.0 (d, *J*=10.3 Hz, **21-CH_3**), 10.4 (d, *J*=4.4 Hz, **18-CH_3**) ppm. **^{19}F NMR** (376MHz, $CDCl_3$) δ -89.64 (br d, *J*=234.1 Hz, 1F, 3α-**F**), -92.04 (br d, *J*=232.4 Hz, 1F, 12β-**F**), -103.31 (ttd, *J*=233.9, 34.1, 11.1 Hz, 1F, 3β-**F**), -112.24 (ddd, *J*=231.9, 34.2, 13.0 Hz, 1F, 12α-**F**) ppm. **^{19}F [^{1}H] NMR** (376MHz, $CDCl_3$) δ -89.65 (d, *J*=234.1 Hz, 1F, 3α-**F**), -92.04 (d, *J*=232.4 Hz, 1F, 12β-**F**), -103.31 (d, *J*=234.1 Hz, 1F, 3β-**F**), -112.24 (d, *J*=232.3 Hz, 1F, 12α-**F**) ppm. **LRMS (ESI+)** m/z: 522.4 $[M+NH_4]^+$. **HRMS (ESI+)** $C_{27}H_{40}F_4NaO_4$ $[M+Na]^+$. Calculated: 527.2755; Found: 527.2755. **IR** (neat, cm^{-1}) 2953 (m), 1733 (s), 1370 (s), 1225 (s), 1097 (s), 1016 (s).

3α,3β,12α,12β-Tetrafluoro-7α-hydroxy-5β-cholanic acid (2.4)

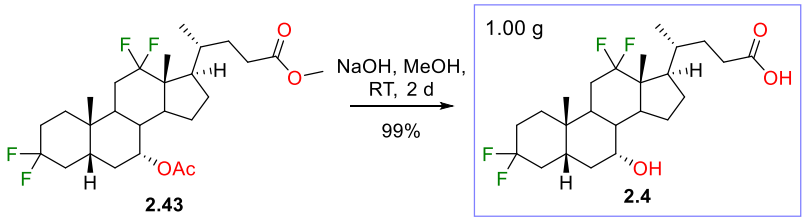

Following general procedure D, **2.43** (1.15 g, 2.28 mmol, 1.0 equiv) was deprotected to yield **2.4** as a white gummy solid (1.01 g, 2.25 mmol, 99%) with no further purification.

R_f 0.24 (EtOAc/PE 40/60). **$[\alpha]_D$** + 0.19 (c = 0.63, $CHCl_3$, 20 °C). **^{1}H NMR** (400 MHz, $CDCl_3$) δ 3.93 (apparent br d, *J*=2.7 Hz, 1H, 7β-**H**), 2.72 (dtd, *J*=36.9, 14.1, 4.5 Hz, 1H, 4α-**H**), (ddd, *J*=15.8, 10.0, 5.3 Hz, 1H, 23-**H'**), 2.31 (ddd, *J*=16.3, 9.7, 6.6 Hz, 1H, 23-**H''**), 2.10 (td, *J*=12.3, 4.8 Hz, 1H, 9α-**H**), 1.09-2.06 (m), 1.02 (dd, *J*=1.8, 6.6 Hz, 3H, 21-**CH_3**), 0.97 (s, 3H, 19-**CH_3**), 0.85 (s, 3H, 18-**CH_3**) ppm. **^{13}C NMR** (100 MHz, $CDCl_3$) δ 180.0 (d, *J*=2.2 Hz, **24-COOH**), 125.7 (dd, *J*=250.2, 247.2 Hz, **12-C**), 121.4 (dd, *J*=241.4, 238.4 Hz, **3-C**), 67.5 (**7-C**), 49.0 (t, *J*=19.8 Hz, **13-C**), 47.6 (d, *J*=2.2 Hz, **17-CH**), 46.8 (d, *J*=7.3 Hz, **14-CH**), 38.9 (d, *J*=9.5 Hz, **5-CH**), 38.1 (**8-CH**), 37.1 (dd, *J*=24.2, 21.3 Hz, **4-CH_2**), 34.6 (**10-C**), 33.6 (**6-CH_2**), 33.2 (**20-CH**), 32.7 (d, *J*=8.8 Hz, **1-CH_2**), 31.4 (**23-CH_2**), 31.3 (br t, *J*=26.4 Hz, **11-CH_2**), 30.2 (**22-CH_2**), 29.8 (d, *J*=10.3 Hz, **9-CH**), 29.1 (dd, *J*=24.9, 22.0 Hz, **2-CH_2**), 26.3 (***15-CH_2* or *16-CH_2***), 22.6 (***15-CH_2* or *16-CH_2***), 21.9 (d, *J*=2.9 Hz, **19-CH_3**), 18.9 (d, *J*=11.0 Hz, **21-CH_3**), 10.4 (d, *J*=4.4 Hz, **18-CH_3**) ppm. **^{19}F NMR** (376MHz, $CDCl_3$) δ -89.73 (br d, *J*=232.3 Hz, 1F, 3α-**F**), -91.50 (br d, *J*=230.6 Hz, 1F, 12β-**F**), -103.74 - -102.57 (m, 1F, 3β-**F**), -112.07 (ddd, *J*=230.6, 34.7, 12.1 Hz, 1F, 12α-**F**) ppm. **^{19}F [^{1}H] NMR** (376MHz, $CDCl_3$) δ -89.73 (d, *J*=232.3 Hz, 1F, 3α-**F**), -91.50 (d, *J*=230.6 Hz, 1F, 12β-**F**), -103.11 (d, *J*=232.3 Hz, 1F, 3β-**F**), -112.07 (d, *J*=232.3 Hz, 1F, 12α-**F**) ppm. **LRMS (ESI+)** m/z: 466.4 $[M+NH_4]^+$. **HRMS (ESI+)** $C_{24}H_{36}F_4NaO_3$ $[M+Na]^+$. Calculated: 471.2493; Found: 471.2495 (-0.6 ppm error). **IR** (neat, cm^{-1}) 2943 (m), 1705 (s), 1369 (s), 1098 (s), 754 (s).

Methyl 3α,3β,12α,12β-tetrafluoro-7-oxo-5β-cholan-24-oate (2.44)

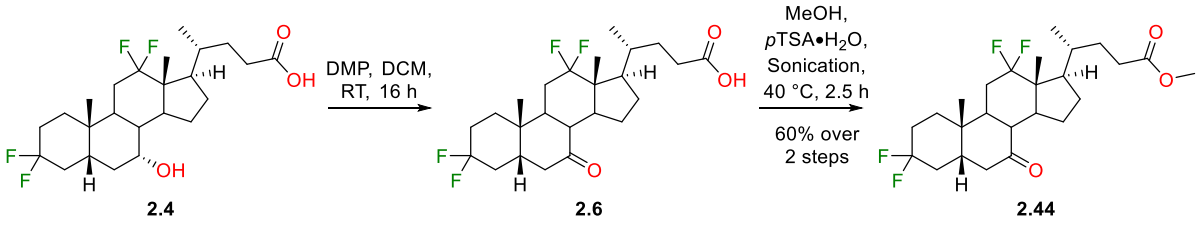

The alcohol **2.4** (900 mg, 2.01 mmol, 1.0 equiv) was dissolved in DCM (15 mL) and DMP (1.02 g, 2.41 mmol, 1.2 equiv) was slowly added at 0 °C. After 16 h of stirring, the reaction mixture was diluted with DCM (50 mL) and quenched with saturated $NaHCO_3$ solution (50 mL) and saturated sodium thiosulfate solution (50 mL). The mixture was extracted with DCM (3 x 50 mL) and the combined

organic phases were washed with saturated $NaHCO_3$ (100 mL), water (100 mL) and brine (100 mL) before drying over Na_2SO_4 and reducing *in vacuo*, giving around 920 mg of crude material. The crude material was purified by flash chromatography (Biotage SNAP KP-Sil 25g Cartridge, DCM/MeOH: 100%/0% → 90%/10%), yielding 835 mg of a fraction containing **2.6** and aromatic, DMP-related impurities. Following general procedure A, the fraction (835 mg, ~1.9 mmol of **2.6**, ~1 equiv) was protected. The crude material was purified by flash chromatography (Biotage ZIP KP-Sil 30 g Cartridge, EtOAc/PE: 15%/85% → 25%/75%), yielding **2.44** as a white solid (560 mg, 1.22 mmol, 60% from **2.4**).

mp 164 – 165 °C. **R_f** 0.39 (EtOAc/PE 20/80). **$[\alpha]_D$** - 14.0 (c = 1.0, $CHCl_3$, 25 °C). **^{1}H NMR** (400 MHz, $CDCl_3$) δ 3.66 (s, 3H, 24-COO**CH_3**), 2.88 (ddd, *J*=13.0, 6.0, 1.8 Hz, 1H, 6β-**H**), 2.33-2.48 (m, 2H overlapping t *J*=11.3 Hz 8β-**H**, ddd *J*=15.3, 9.9, 5.4 Hz 23-**H'**), 2.14-2.32 (m, 3H), 1.29-2.04 (m), 1.26 (s, 3H, 19-**CH_3**), 1.00-1.13 (m, 1H 15α-**H**), 0.98 (dd, *J*=6.7, 2.0 Hz, 3H, 21-**CH_3**), 0.84 (s, 3H, 18-**CH_3**) ppm. **^{13}C NMR** (100 MHz, $CDCl_3$) δ 209.4 (d, *J*=2.2 Hz, **7-C**), 174.5 (**24-COO**CH_3), 124.5 (dd, *J*=250.2. 247.2 Hz, **12-C**), 120.7 (dd, *J*=243.6, 238.4 Hz, **3-C**), 51.5 (**24-**COO**CH_3**), 48.9 (dd, *J*=22.0, 19.8 Hz, **13-C**), 47.9 (**8-CH**), 47.0 (**17-CH**), 45.5 (d, *J*=7.3 Hz, **14-CH**), 44.3 (**6-CH_2**), 43.8 (d, *J*=9.5 Hz, **5-CH**), 39.3 (d, *J*=9.5 Hz, **9-CH**), 35.3 (dd, *J*=26.4, 22.7 Hz, **4-CH_2**), 34.7 (**10-C**), 32.7 (**20-CH**), 31.9 (t, *J*=27.1 Hz, **11-CH_2**), 31.7 (d, *J*=8.8 Hz, **1-CH_2**), 31.6 (**23-CH_2**), 30.2 (**22-CH_2**), 28.8 (dd, *J*=25.7, 22.7 Hz, **2-CH_2**), 25.9 (**16-CH_2**), 23.6 (**15-CH_2**), 22.2 (d, *J*=2.2 Hz, **19-CH_3**), 19.2 (d, *J*=10.3 Hz, **21-CH_3**), 10.7 (d, *J*=4.4 Hz, **18-CH_3**) ppm. **^{19}F NMR** (376MHz, $CDCl_3$) δ -90.59 (br d, *J*=237.6 Hz, 1F, 3α-**F**), -93.46 (br d, *J*=232.3 Hz, 1F, 12β-**F**), -100.29 (dtt, *J*=238.1, 33.8, 11.9 Hz, 1F, 3β-**F**), -112.90 (ddd, *J*=232.3, 31.2, 10.4 Hz, 1F, 12α-**F**) ppm. **^{19}F [^{1}H] NMR** (376MHz, $CDCl_3$) δ -90.66 (d, *J*=237.6 Hz, 1F, 3α-**F**), -93.46 (d, *J*=232.3 Hz, 1F, 12β-**F**), -100.29 (d, *J*=237.6 Hz, 1F, 3β-**F**), -112.99 (d, *J*=234.1 Hz, 1F, 12α-**F**) ppm. **LRMS (ESI+)** m/z: 921.8 $[2M+H]^+$, 441.5 $[M+H-HF]^+$. **HRMS (ESI+)** $C_{25}H_{36}F_4NaO_3$ $[M+Na]^+$. Calculated: 483.2493; Found: 483.2489 (0.9 ppm error). **IR** (neat, cm^{-1}) 2971 (m), 1729 (s), 1711 (s), 1093 (s).

3α,3β,12α,12β-Tetrafluoro-7-oxo-5β-cholanic acid (2.6)

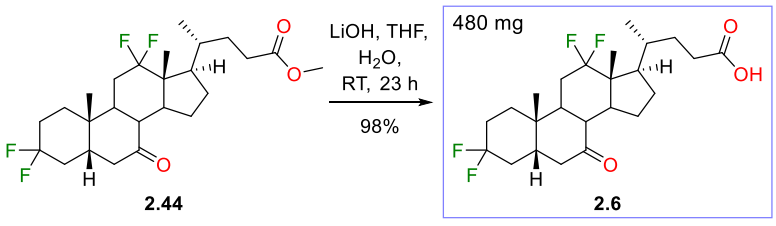

Following general procedure C, **2.44** (500 mg, 1.09 mmol, 1.0 equiv) was deprotected to yield **2.6** as a white solid (480 mg, 1.07 mmol, 98%) with no further purification.

mp 144 – 145 °C. **R_f** 0.41 (EtOAc/PE 50/50). **$[\alpha]_D$** - 15.3 (c = 0.99, $CHCl_3$, 22 °C). **^{1}H NMR** (400 MHz, $CDCl_3$) δ 2.88 (ddd, *J*=12.9, 5.8, 1.8 Hz, 1H, 6β-**H**), 2.38-2.49 (m, 2H, 8β-**H** and 23-**H'**), 2.24-2.36 (m,

2H, 23-**H''** and 15β-**H**), 2.14-2.24 (m, 1H, 5β-**H**), 1.30-2.11 (m), 1.27 (s, 3H, 19-**CH_3**), 1.02-1.14 (m, 1H, 15α-**H**), 1.00 (dd, *J*=6.5, 1.5 Hz, 3H, 21-**CH_3**), 0.84 (s, 3H, 18-**CH_3**) ppm. **^{13}C NMR** (100 MHz, $CDCl_3$) δ 209.5 (**7-C**), 180.2 (**24-COOH**), 124.5 (dd, *J*=250.9, 247.2 Hz, **12-C**), 120.4 (dd, *J*=243.6, 238.4 Hz, **3-C**), 48.9 (dd, *J*=20.5, 20.5 Hz, **13-C**), 47.9 (**8-CH**), 47.0 (**17-CH**), 45.5 (d, *J*=7.3 Hz, **14-CH**), 44.3 (**6-CH_2**), 43.8 (d, *J*=9.5 Hz, **5-CH**), 39.3 (d, *J*=10.3 Hz**,** **9-CH**), 35.3 (dd, *J*=26.4, 22.7 Hz, **4-CH_2**), 34.7 (**10-C**), 32.7 (**20-CH**), 31.9 (t, *J*=26.4 Hz, **11-CH_2**), 31.7 (d, *J*=9.5 Hz, **1-CH_2**), 31.6 (**23-CH_2**), 30.0 (**22-CH_2**), 28.8 (dd, *J*=25.7, 22.7 Hz, **2-CH_2**), 26.0 (**16-CH_2**), 23.6 (**15-CH_2**), 22.2 (d, *J*=2.9 Hz, **19-CH_3**), 19.1 (d, *J*=10.3 Hz, **21-CH_3**), 10.7 (d, *J*=5.1 Hz, **18-CH_3**) ppm. **^{19}F NMR** (376MHz, $CDCl_3$) δ -90.57 (br d, *J*=237.6 Hz, 1F, 3α-**F**), -93.29 (br d, *J*=232.4 Hz, 1F, 12β-**F**), -100.28 (dtt, *J*=237.6, 34.0, 11.9 Hz, 1F, 3β-**F**), -113.69--112.26 (m, 1F, 12α-**F**) ppm. **^{19}F [^{1}H] NMR** (376MHz, $CDCl_3$) δ -90.57 (d, *J*=237.6 Hz, 1F, 3α-**F**), -93.29 (d, *J*=234.1 Hz, 1F, 12β-**F**), -100.28 (d, *J*=237.6 Hz, 1F, 3β-**F**), -112.88 (d, *J*=234.1 Hz, 1F, 12α-**F**) ppm. **LRMS (ESI+)** m/z: 893.8 $[2M+H]^+$, 427.6 $[M+H-HF]^+$, 407.5 $[M+H-2HF]^+$. **HRMS (ESI+)** $C_{24}H_{34}F_4NaO_3$ $[M+Na]^+$. Calculated: 469.2336; Found: 469.2343 (1.3 ppm error). **IR** (neat, cm^{-1}) 2954 (m), 1708 (s), 1093 (s), 959 (m), 753 (m).

3α,3β,12α,12β-Tetrafluoro-7β-hydroxy-5β-cholanic acid (2.5)

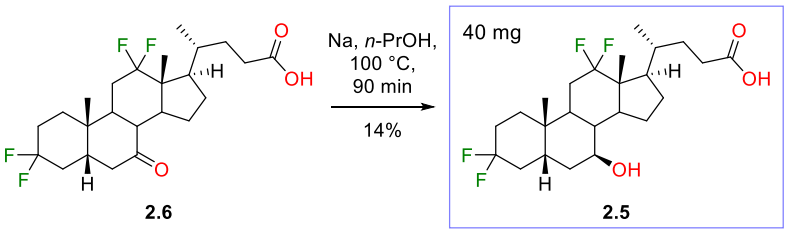

The ketone **2.6** (300 mg, 0.67 mmol, 1.0 equiv) was dissolved in dry *n*-propanol (15 mL) and Na *metal* (600 mg, 26.1 mmol, ~39 equiv) was slowly added in small portions. After heating under reflux for 1.5 h, the reaction mixture was cooled and diluted with water (20 mL) before acidifying with 2M HCl (30 mL). The aqueous phase was extracted with EtOAc (2 x 25 mL) and the combined organic phases were washed with water (50 mL) and brine (50 mL) before drying over Na_2SO_4 and reducing *in vacuo*, giving around 320 mg of crude material. The crude was purified by flash chromatography (Biotage ZIP KP-Sil 10 g Cartridge, EtOAc/PE: 24%/65% → 45%/65%), yielding **2.5** as a white solid (43 mg, 0.096 mmol, 14%).

mp 153 – 154 °C. **R_f** 0.15 (EA/PE 40/60). **$[\alpha]_D$** + 60.5 (c = 0.36, $CHCl_3$, 24 °C). **^{1}H NMR** (400 MHz, $CDCl_3$) δ 3.50-3.63 (m, 1H, 7α-**H**), 2.43 (ddd, *J*=15.8, 10.1, 5.4 Hz, 1H, 23-**H'**), 2.32 (ddd, *J*=16.1, 9.7, 6.6 Hz, 1H, 23-**H''**), 1.33-2.02 (m), 0.98-1.05 (m, 6H, 19-**CH_3** and 21-**CH_3**), 0.88 (s, 3H, 18-**CH_3**) ppm. **^{13}C NMR** (100 MHz, $CDCl_3$) δ 179.8 (**24-COOH**), 125.1 (dd, *J*=250.9, 245.8 Hz, **12-C**), 121.0 (dd, *J*=242.8, 239.2 Hz, **3-C**), 70.2 (**7-CH**), 51.9 (d, *J*=7.3 Hz, **14-CH**), 49.9 (dd, *J*=21.3, 19.8 Hz, **13-C**), 46.5 (d, *J*=2.9 Hz, **17-CH**), 42.0 (**8-CH**), 40.1 (d, *J*=8.8 Hz, ***5-CH or 9-CH***), 35.8 (**6-CH_2**), 35.3 (d, *J*=8.8 Hz, ***5-***

CH or 9-CH), 35.2 (dd, *J*=24.9, 22.0 Hz, **4-CH₂**), 33.6 (**10-C**), 32.9 (**20-CH**), 32.3 (d, *J*=9.5 Hz, **1-CH₂**), 31.6 (**23-CH₂**), 31.6 (t, *J*=26.4 Hz, **11-CH₂**), 30.0 (**22-CH₂**), 29.0 (dd, *J*=24.9, 22.0 Hz, **2-CH₂**), 26.2 (***15-CH₂ or 16-CH₂***), 25.5 (***15-CH₂ or 16-CH₂***), 22.4 (d, *J*=2.2 Hz, **19-CH₃**), 19.1 (d, *J*=9.5 Hz, **21-CH₃**), 10.6 (br d, *J*=3.7 Hz, **18-CH₃**) ppm. **^{19}F NMR** (376MHz, $CDCl_3$) δ -89.64 (br d, *J*=235.8 Hz, 1F, 3α-**F**), -93.01 (br d, *J*=230.6 Hz, 1F, 12β-**F**), -101.86--100.46 (m, 1F, 3β-**F**), -111.98 (ddd, *J*=232.4, 32.9, 13.9 Hz, 1F, 12α-**F**) ppm. **^{19}F [^{1}H] NMR** (376MHz, $CDCl_3$) δ -89.70 (d, *J*=235.8 Hz, 1F, 3α-**F**), -93.01 (br d, *J*=230.6 Hz, 1F, 12β-**F**), -101.10 (d, *J*=235.8 Hz, 1F, 3β-**F**), -112.00 (br d, *J*=232.3 Hz, 1F, 12α-**F**) ppm. **LRMS (ESI+)** m/z: 471.4 $[M+Na]^+$, 409.6 $[M+H-2HF]^+$. **HRMS (ESI+)** $C_{24}H_{36}F_4NaO_3$ $[M+Na]^+$. Calculated: 471.2493; Found: 471.2486 (1.4 ppm error). **IR** (neat, cm^{-1}) 3276 (b), 2973 – 2869 (m), 1680 (s), 1258 (m), 1015 (m).

Methyl 12α,12β-difluoro-3α-hydroxy-7-oxo-5β-cholan-24-oate (2.45)

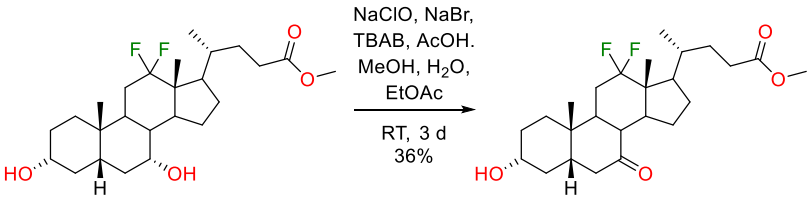

The alcohol **2.10** (240 mg, 0.54 mmol, 1.0 equiv) was dissolved in a mix of MeOH/AcOH/H_2O/EtOAc (3:1:0.25:6.5, 10.75 mL total), NaBr (~5 mg, ~0.03 mmol, ~0.06 equiv) and TBAB (575 mg, 1.80 mmol, 3.3 equiv) were added and the mixture was stirred until a homogeneous solution was obtained. The solution was cooled to 0 °C and NaClO (11%, 0.34 mL, 0.60 mmol, 1.1 equiv) was added dropwise. After 1 d of stirring at RT, the reaction was not deemed complete by TLC. NaClO (11%, 0.34 mL, 0.60 mmol, 1.1 equiv) was added to the reaction mixture at RT. After a total of 3 d of stirring at RT, the reaction mixture was quenched with saturated sodium thiosulfate solution (~ 5 mL), water (~20 mL) was added and the mixture was stirred for 15 min. The mixture was extracted with EtOAc (2 x 25 mL) and the combined organic phases were washed with sat. sodium thiosulfate solution (50 mL), water (50 mL) and brine (50 mL) before drying over Na_2SO_4 and reducing *in vacuo* to yield around 200 mg of crude material. The crude was purified by flash chromatography (EtOAc/PE: 28%/72% → 52%/48%), yielding **2.45** as a colourless gum (86.0 mg, 0.20 mmol, 36%).

R_f 0.21 (EtOAc/PE 50/50). **$[\alpha]_D$** - 6.90 (c = 0.47, $CHCl_3$, 20 °C). **^{1}H NMR** (400 MHz, $CDCl_3$) δ 3.54-3.72 (m, 4H, 24-COO**CH₃** and 3β-**H**), 2.86 (dd, *J*=12.8, 6.1 Hz, 1H, 6β-**H**), 1.23-2.44 (m), 1.22 (s, 3H, 19-**CH₃**), 1.02-1.17 (m, 2H), 0.99 (dd, *J*=6.7, 1.9 Hz, 3H, 21-**CH₃**), 0.84 (s, 3H, 18-**CH₃**) ppm. **^{13}C NMR** (100 MHz, $CDCl_3$) δ 210.2 (**7-C**), 174.5 (**24-COO**CH_3), 125.4 (dd, *J*=249.4, 246.5 Hz, **12-C**), 70.4 (**3-CH**), 51.4 (**24-**COO**CH₃**), 48.9 (br t, *J*=19.8 Hz, **13-C**), 47.9 (CH), 46.9 (**17-CH**), 45.6 (CH), 45.5 (d, *J*=7.3 Hz, **14-CH**), 45.1 (**6-CH₂**), 39.6 (d, *J*=9.5 Hz, **9-CH**), 37.1 (**4-CH₂**), 34.6 (**10-C**), 33.9 (CH_2), 32.7 (**20-CH**), 31.6

(t, *J*=26.4 Hz, **11-CH_2**), 31.5 (CH_2), 30.2 (CH_2), 29.6 (CH_2), 25.8 (CH_2), 23.6 (CH_2), 22.6 (**19-CH_3**), 19.1 (d, *J*=10.3 Hz, **21-CH_3**), 10.6 (d, *J*=5.1 Hz, **18-CH_3**) ppm. **^{19}F NMR** (376MHz, $CDCl_3$) δ -93.27 (br d, *J*=232.4 Hz, 1F, 12β-**F**), -112.91 (ddd, *J*=232.3, 29.5, 15.6 Hz, 1F, 12α-**F**) ppm. **^{19}F [^{1}H] NMR** (376MHz, $CDCl_3$) δ -93.27 (br d, *J*=232.4 Hz, 1F, 12β-**F**), -112.92 (br d, *J*=232.4 Hz, 1F, 12α-**F**) ppm. **LRMS (ESI+)** m/z: 458.5 $[M+NH_4]^+$. **HRMS (ESI+)** $C_{25}H_{42}F_2NO_4$ $[M+NH_4]^+$. Calculated: 458.3076; Found: 458.3067 (2.1 ppm error). **IR** (neat, cm^{-1}) 3399.5 (b), 2930-2876 (m), 1734 (s), 1710 (s), 1018 (s), 732 (m). ^{1}H, ^{13}C and ^{19}F NMR data consistent with data from within the group.

Methyl 12α,12β-difluoro-3α-acetoxy-7α-hydroxy-5β-cholan-24-oate (2.47)

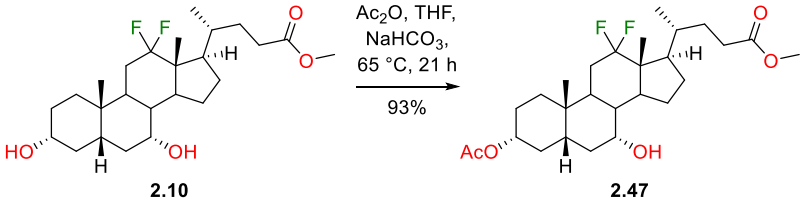

2.10 **2.47**

Following general procedure F, **2.10** (1.30 g, 2.94 mmol, 1.0 equiv) was selectively protected to yield **2.47** (95% pure) as a pale brown gum (1.33 g, 2.74 mmol, 93%) with no further purification.

R_f 0.59 (EtOAc/PE 30/70). **^{1}H NMR** (400 MHz, $CDCl_3$) δ 4.58 (tt, *J*=11.4, 4.5 Hz, 1H, 3β-**H**), 3.90 (br s, 1H, 7β-**H**), 3.67 (s, 3H, 24-COO**CH_3**), 2.13-2.45 (m, 4H), 2.02 (s, 3H, 3α-OCO**CH_3**), 1.05-2.00 (m), 1.00 (dd, *J*=6.7, 1.8 Hz, 3H, 21-**CH_3**), 0.92 (s, 3H, 19-**CH_3**), 0.84 (s, 3H, 18-**CH_3**) ppm. **^{13}C NMR** (100 MHz, $CDCl_3$) δ 174.6 (**24-COO**CH_3), 170.7 (**3α-OCO**CH_3), 126.1 (dd, *J*=250.2, 247.2 Hz, **12-C**), 74.0 (**3-CH**), 67.4 (**7-CH**), 51.4 (**24-**COO**CH_3**), 48.9 (t, *J*=20.5 Hz, **13-C**), 47.6 (d, *J*=2.2 Hz, **17-CH**), 46.8 (d, *J*=7.3 Hz, **14-CH**), 40.8 (**5-CH**), 38.2 (CH), 35.1 (CH_2), 34.8 (CH_2), 34.6 (**10-C**), 34.5 (CH_2), 33.1 (**20-CH**), 31.4 (CH_2), 31.0 (t, *J*=26.0 Hz, **11-CH_2**), 30.4 (br d, *J*=9.5 Hz, **9-CH**), 30.3 (CH_2), 26.4 (**1-CH_2**), 26.1 (CH_2), 22.5 (CH_2), 22.3 (**19-CH_3**), 21.4 (**3α-**OCO**CH_3**), 18.9 (d, *J*=10.3 Hz, **21-CH_3**), 10.4 (d, *J*=4.4 Hz, **18-CH_3**) ppm. **^{19}F NMR** (376MHz, $CDCl_3$) δ -91.51 (br d, *J*=230.6 Hz, 1F, 12β-**F**), -112.07 (ddd, *J*=230.6, 34.7, 12.1 Hz, 1F, 12α-**F**) ppm. **^{19}F [^{1}H] NMR** (376MHz, $CDCl_3$) δ -91.51 (br d, *J*=230.6 Hz, 1F, 12β-**F**), -112.08 (d, *J*=230.6 Hz, 1F, 12α-**F**) ppm. **LRMS (ESI+)** m/z: 502.5 $[M+NH_4]^+$. **HRMS (ESI+)** $C_{27}H_{42}F_2NaO_5$ $[M+Na]^+$. Calculated: 507.2893; Found: 507.2894 (0.4 ppm error). **IR** (neat, cm^{-1}) 3525 (b), 2942 – 2873 (m), 1731 (s), 1244 (s), 1023 (s). ^{1}H, ^{13}C and ^{19}F NMR data consistent with data from within the group.

Methyl 12α,12β-difluoro-3α-acetoxy-7-oxo-5β-cholan-24-oate (2.48)

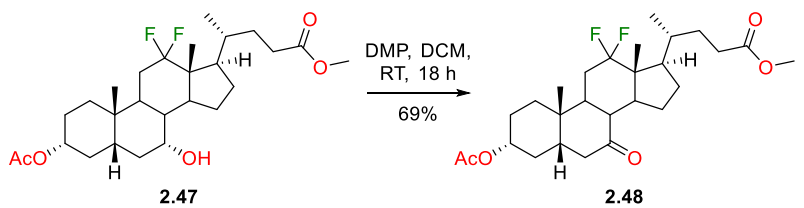

2.47 **2.48**

The alcohol **2.47** (1.23 g, 2.54 mmol, 1.0 equiv) was dissolved in DCM (25 mL) and DMP (1.29 g, 3.05 mmol, 1.2 equiv) was slowly added in portions at 0°C. After 18 h, the reaction mixture was diluted with DCM (25 mL) and quenched with addition of saturated sodium thiosulfate solution (50 mL) and saturated $NaHCO_3$ solution (50 mL). The quenched reaction mixture was extracted with DCM (3 x 50 mL) and the combined organic phases were washed with saturated $NaHCO_3$ (100 mL), water (100 mL) and brine (100 mL) before drying over Na_2SO_4 and reducing *in vacuo* giving 1.22 g of crude. The crude was purified by flash chromatography (Biotage 25 g KP-Sil cartridge, EtOAc/PE: 0%/100% → 30%/70%) yielding **2.48** as a white solid (840 mg, 1.74 mmol, 69%).

mp 107 – 108 °C. **R_f** 0.39 (EtOAc/PE 30/70). **$[\alpha]_D$** + 20.0 (c = 1.07, $CHCl_3$, 23 °C). **^{1}H NMR** (400 MHz, $CDCl_3$) δ 4.61-4.72 (m, 1H, 3β-**H**), 3.60-3.68 (m, 3H, 24-COO**CH_3**), 2.84 (dd, *J*=13.0, 6.3 Hz, 1H, 6β-**H**), 2.07-2.44 (m, 5H), 1.99 (s, 3H, 3α-OCO**CH_3**), 1.70-1.98 (m), 1.23-1.58 (m), 1.21 (s, 3H, 19-**CH_3**), 1.00-1.11 (m, 1H), 0.97 (dd, *J*=6.7, 1.8 Hz, 3H, 21-**CH_3**), 0.82 (s, 3H, 18-**CH_3**) ppm. **^{13}C NMR** (100 MHz, $CDCl_3$) δ 209.7 (d, *J*=1.5 Hz, **7-C**), 174.5 (**24-COO**CH_3), 170.4 (**3α-OCO**CH_3), 125.3 (dd, *J*=250.2, 246.5 Hz, **12-C**), 72.4 (**3-CH**), 51.4 (**24-**COO**CH_3**), 48.9 (br t, *J*=19.8 Hz, **13-C**), 47.9 (**8-CH**), 46.9 (br s, **17-CH**), 45.5 (d, *J*=7.3 Hz, **14-CH**), 45.3 (**5-CH**), 45.0 (**6-CH_2**), 39.6 (d, *J*=10.3 Hz, **9-CH**), 34.7 (**10-C**), 33.6 (CH_2), 33.0 (**4-CH_2**), 32.7 (**20-CH**), 31.7 (br t, *J*=26.4 Hz, **11-CH_2**), 31.5 (**23-CH_2**), 30.2 (**22-CH_2**), 25.8 (CH_2), 25.8 (CH_2), 23.6 (CH_2), 22.6 (**19-CH_3**), 21.2 (**3α-**OCO**CH_3**), 19.1 (d, *J*=10.3 Hz, **21-CH_3**), 10.6 (d, *J*=4.4 Hz, **18-CH_3**) ppm. **^{19}F NMR** (376MHz, $CDCl_3$) δ -93.33 (br d, *J*=234.1 Hz, 1F, 12β-**F**), -112.97 (ddd, *J*=232.8, 31.6, 14.7 Hz, 1F, 12α-**F**) ppm. **^{19}F [^{1}H] NMR** (376MHz, $CDCl_3$) δ -93.33 (d, *J*=232.4 Hz, 1F, 12β-**F**), -112.97 (d, *J*=232.3 Hz, 1F, 12α-**F**) ppm. **LRMS (ESI+)** m/z: 500.5 $[M+NH_4]^+$. **HRMS (ESI+)** $C_{27}H_{40}F_2NaO_5$ $[M+Na]^+$. Calculated: 505.2736; Found: 505.2725 (2.1 ppm error). **IR** ($CDCl_3$, cm^{-1}) 2950 – 2877 (m), 1732 (s), 1713 (s), 1241 (s), 1048 (s), 1023 (s), 731 (m).

Methyl 7α,7β,12α,12β-tetrafluoro-3α-acetoxy-5β-cholan-24-oate (2.49)

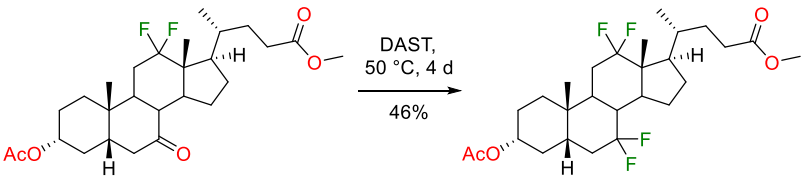

2.48 **2.49**

To a flame-dried flask with condenser attached, under argon, **2.48** (740 mg, 1.53 mmol, 1.0 equiv) and DAST (5.0 mL, 38 mmol, ~25 equiv) were added. The reaction mixture was heated to 50 °C. After 4 d, the reaction mixture was allowed to cool to RT, was diluted with DCM (50 mL) and the mixture was decanted into icy, saturated $NaHCO_3$ solution (~400 mL) portionwise (~5 mL per min). After the mixture was neutralised fully, the layers were separated and the aqueous phase was extracted with DCM (3 x 50 mL). The combined organic phases were washed with water (150 mL) and brine (150 mL) before drying over Na_2SO_4 and reducing *in vacuo*, giving 1.15 g of crude. The

crude was purified twice by flash chromatography (Biotage 25 g KP-Sil cartridge, EtOAc/PE: 15%/85% → 35%/65%; Biotage 25 g KP-Sil cartridge, EtOAc/PE: 15%/85% → 28%/72%) to yield **2.49** as a yellow solid (353 mg, 0.70 mmol, 46%).

mp 116 – 117 °C. **R_f** 0.32 (EtOAc/PE 20/80). **$[\alpha]_D$** + 57.0 (c = 0.765, $CHCl_3$, 22 °C). **^{1}H NMR** (400 MHz, $CDCl_3$) δ 4.57-4.69 (m, 1H, 3β-**H**), 3.66 (s, 3H, 24-COO**CH_3**), 2.33-2.43 (m, 1H, 23-**H'**), 2.05-2.31 (m, 2H), 2.02 (s, 3H, 3α-OCO**CH_3**), 1.13-2.01 (m), 0.95-1.02 (m, 6H, 19-**CH_3** and 21-**CH_3**), 0.85 (s, 3H, 18-**CH_3**) ppm. **^{13}C NMR** (100 MHz, $CDCl_3$) δ 174.5 (**24-COO**CH_3), 170.5 (**3α-OCO**CH_3), 125.4 (dd, *J*=249.4, 246.5 Hz, **12-C**), 121.4 (t, *J*=245.0 Hz, **7-C**), 73.0 (**3-CH**), 51.4 (**24-**COO**CH_3**), 49.4 (br t, *J*=19.8 Hz, **13-C**), 46.7 (d, *J*=2.2 Hz, **17-CH**), 45.1 (br dd, *J*=6.6, 4.4 Hz, **14-CH**), 40.1-41.1 (m, 2C, overlapping dd, *J*=22.0, 19.8 Hz, **8-CH** and d, *J*=11.0 Hz, **5-CH**), 35.9 (t, *J*=23.1 Hz, **6-CH_2**), 34.0-34.3 (m, 2 C, overlapping d, *J*=19.0 Hz, **9-CH** and s, CH_2), 33.9 (**10-C**), 32.9 (**20-CH**), 32.8 (d, *J*=4.4 Hz, **4-CH_2**), 31.5 (**23-CH_2**), 31.1 (t, *J*=26.4 Hz, **11-CH_2**), 30.2 (**22-CH_2**), 26.1 (CH_2), 25.9 (br s, CH_2), 24.1 (d, *J*=4.4 Hz, **15-CH_2**), 22.2 (**19-CH_3**), 21.3 (**3α-**OCO**CH_3**), 19.1 (d, *J*=10.3 Hz, **21-CH_3**), 10.4 (d, *J*=5.1 Hz, **18-CH_3**) ppm. **^{19}F NMR** (376MHz, $CDCl_3$) δ -85.48 (br d, *J*=244.5 Hz, 1F, 7β-**F**), -93.31 (br d, *J*=232.3 Hz, 1F, 12β-**F**), -101.59 (dddd, *J*=242.8, 38.1, 24.3, 13.9 Hz, 1F, 7α-**F**), -112.05 (ddd, *J*=232.3, 34.7, 12.1 Hz, 1F, 12α-**F**) ppm. **^{19}F [^{1}H] NMR** (376MHz, $CDCl_3$) δ -85.49 (d, *J*=242.8 Hz, 1F, 7β-**F**), -93.31 (d, *J*=232.3 Hz, 1F, 12β-**F**), -101.59 (d, *J*=242.8 Hz, 1F, 7α-**F**), -112.05 (d, *J*=234.1 Hz, 1F, 12α-**F**) ppm. **LRMS (ESI+)** m/z: 522.5 $[M+NH_4]^+$. **HRMS (ESI+)** $C_{27}H_{40}F_4NaO_4$ $[M+Na]^+$. Calculated: 527.2755; Found: 527.2763 (1.6 ppm error). **IR** (neat, cm^{-1}) 2976-2875 (m), 1733 (s), 1248 (s), 1054 (m), 1020 (s). ^{1}H, ^{13}C and ^{19}F NMR data consistent with data from within the group.

7α,7β,12α,12β-Tetrafluorolithocholic acid (2.7)

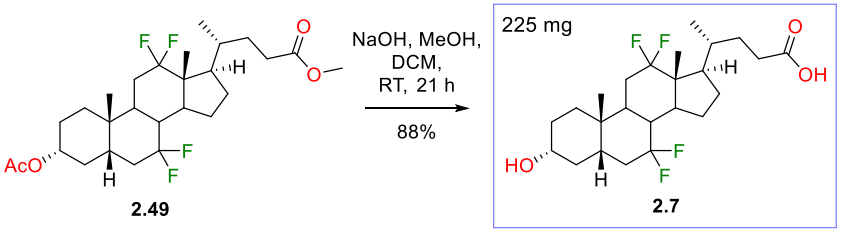

Following general procedure D, **2.49** (290 mg, 0.57 mmol, 1.0 equiv) was deprotected to yield **2.7** as an off-white solid (225 mg, 0.50 mmol, 88%) with no further purification.

mp 193 – 194 °C. **R**: 0.28 (EtOAc/PE 50/50). **$[\alpha]_D$** + 51.0 (c = 0.71, MeOH, 22 °C). **^{1}H NMR** (400 MHz, MeOH-d_4) δ 3.42-3.54 (m, 1H, 3β-**H**), 2.31-2.41 (m, 1H, 23-**H**), 2.14-2.31 (m, 2H), 1.11-2.08 (m), 0.96-1.05 (m, 6H, 19-**CH_3** and 21-**CH_3**), 0.90 (s, 3H, 18-**CH_3**) ppm. **^{13}C NMR** (100 MHz, MeOH-d_4) δ 178.1 (**24-COOH**), 127.0 (dd, *J*=249.4, 245.8 Hz, **12-C**), 123.2 (t, *J*=245.0 Hz, **7-C**), 71.7 (**3-CH**), 50.9 (t, *J*=20.5 Hz, **13-C**), 48.4 (d, *J*=2.2 Hz, **17-CH**), 46.9 (br dd, *J*=6.6, 5.1 Hz, **14-CH**), 42.4 (br d, *J*=10.3 Hz**, 5-CH**), 42.0 (br t, *J*=19.8 Hz, **8-CH**), 38.1 (d, *J*=4.4 Hz, **4-CH_2**), 37.3 (t, *J*=23.1 Hz, **6-CH_2**), 35.8 (t, *J*=9.5 Hz, **9-**

CH), 35.6 (CH_2), 35.2 (**10-C**), 34.4 (**20-CH**), 32.7 (**23-CH_2**), 32.3 (t, *J*=26.8 Hz, **11-CH_2**), 31.8 (**22-CH_2**), 30.9 (CH_2), 27.2 (CH_2), 25.4 (d, *J*=3.7 Hz, **15-CH_2**), 22.8 (**19-CH_3**), 19.8 (d, *J*=10.3 Hz, **21-CH_3**), 11.0 (d, *J*=3.7 Hz, 18-**CH_3**) ppm. **^{19}F NMR** (376MHz, MeOH-d_4) δ -85.43 (br d, *J*=242.8 Hz, 1F, 7β-**F**), -93.59 (br d, *J*=234.1 Hz, 1F, 12β-**F**), -102.01 (dddd, *J*=242.8, 39.9, 26.0, 15.6 Hz, 1F, 7α-**F**), -112.83 (ddd, *J*=232.8, 33.4, 13.0 Hz, 1F, 12α-**F**) ppm. **^{19}F [^{1}H] NMR** (376MHz, MeOH-d_4) δ -85.43 (d, *J*=242.8 Hz, 1F, 7β-**F**), -93.59 (d, *J*=232.4 Hz, 1F, 12β-**F**), -102.01 (d, *J*=242.8 Hz, 1F, 7α-**F**), -112.83 (d, *J*=234.1 Hz, 1F, 12α-**F**) ppm. **LRMS (ESI+)** m/z: 466.5 $[M+NH_4]^+$. **HRMS (ESI+)** $C_{24}H_{36}F_4NaO_3$ $[M+Na]^+$. Calculated: 471.2493; Found: 471.2496 (0.7 ppm error). **IR** (MeOH-d_4, cm^{-1}) 3320 (b), 2957-2876 (m), 1708 (s), 1126 (s), 982 (m). ^{1}H, ^{13}C and ^{19}F NMR data consistent with data from within the group.

7α,7β,12α,12β-Tetrafluoro-3-oxo-5β-cholanic acid (2.8)

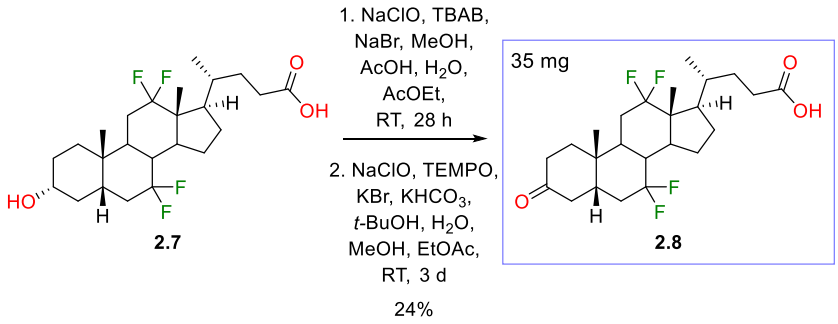

The alcohol **2.7** (155 mg, 0.35 mmol, 1.0 equiv) was dissolved in a mix of MeOH/AcOH/H_2O/EtOAc (3:1:0.25:6.5, 10.75 mL total) and NaBr (~2 mg, ~0.02 mmol, ~0.06 equiv) and TBAB (372 mg, 1.16 mmol, 3.3 equiv) were added before stirring until a homogeneous solution was obtained. The solution was cooled to 0 °C and was added NaClO (11%, 0.40 mL, 0.70 mmol, 2.0 equiv) dropwise. After 23 h of stirring at RT, NaClO (11%, 0.40 mL, 0.70 mmol, 2.0 equiv) and AcOH (1 mL) were added to the reaction mixture. After 5 h, the reaction mixture was quenched with saturated sodium thiosulfate solution (5 mL) and was added water (20 mL). The aqueous phase was extracted with EtOAc (2 x 25 mL) and the combined organic phases were washed with saturated sodium thiosulfate solution (50 mL), water (50 mL) and brine (50 mL) before drying over Na_2SO_4 and reducing *in vacuo* to yield 147 mg of crude. Following general procedure B, the crude (147 mg, ~0.33 mmol, 1.0 equiv) was oxidised. Note: additional NaClO (11%, 0.56 mL, 0.99 mmol, 3.0 equiv) was added to the reaction mixture after 1 d of stirring. After 3 d of stirring in total, the reaction mixture was quenched and worked up. The crude was purified by flash chromatography (Biotage SNAP KP-Sil 10 g cartridge, EtOAc/PE: 35%/65% → 60%/40%), yielding **2.8** as a white gummy solid (37.0 mg, 0.083 mmol, 24%).

mp 159 – 160 °C. **R_f** 0.35 (EtOAc/PE 50/50). **$[\alpha]_D$** + 44.0 (c = 0.53, $CHCl_3$, 21 °C). **^{1}H NMR** (400 MHz, $CDCl_3$) δ 2.70 (t, *J*=14.9 Hz, 1H, 4α-**H**), 1.12-2.52 (m), 1.08 (s, 3H, 19-**CH_3**), 1.01 (br dd, *J*=6.5, 1.6 Hz, 3H, 21-**CH_3**), 0.89 (s, 3H, 18-**CH_3**) ppm. **^{13}C NMR** (100 MHz, $CDCl_3$) δ 210.3 (**3-C**), 179.7 (**24-COOH**),

124.9 (dd, *J*=250.2, 246.5 Hz, **12-C**), 121.2 (t, *J*=244.3 Hz, **7-C**), 49.3 (t, *J*=20.5 Hz, **13-C**), 46.6 (d, *J*=2.2 Hz, **17-CH**), 44.9 (br dd, *J*=7.3, 4.4 Hz, **14-CH**), 42.6 (d, *J*=4.4 Hz, **4-CH₂**), 42.3 (br d, *J*=10.3 Hz, **5-CH**), 40.6 (dd, *J*=22.0, 20.5 Hz, **8-CH**), 36.2 (CH_2), 35.5 (CH_2), 35.4 (t, *J*=23.5 Hz, **6-CH₂**), 34.5 (t, *J*=9.5 Hz, **9-CH**), 34.0 (**10-C**), 32.8 (**20-CH**), 31.4 (**23-CH₂**), 31.4 (t, *J*=27.1 Hz, **11-CH₂**), 29.9 (**22-CH₂**), 25.9 (CH_2), 23.9 (d, *J*=3.7 Hz, **15-CH₂**), 21.4 (**19-CH₃**), 18.9 (d, *J*=10.3 Hz, **21-CH₃**), 10.3 (d, *J*=4.4 Hz, **18-CH₃**) ppm. **^{19}F NMR** (376MHz, $CDCl_3$) δ -85.35 (br d, *J*=246.2 Hz, 1F, 7β-**F**), -93.36 (br d, *J*=234.1 Hz, 1F, 12β-**F**), -101.60 (dddd, *J*=246.2, 36.8, 23.8, 13.9 Hz, 1F, 7α-**F**), -112.04 (ddd, *J*=233.2, 32.9, 13.0 Hz, 1F, 12α-**F**) ppm. **^{19}F [^{1}H] NMR** (376MHz, $CDCl_3$) δ -85.35 (d, *J*=246.2 Hz, 1F, 7β-**F**), -93.36 (d, *J*=234.1 Hz, 1F, 12β-**F**), -101.60 (d, *J*=246.2 Hz, 1F, 7α-**F**), -112.04 (d, *J*=234.1 Hz, 1F, 12α-**F**) ppm. **LRMS (ESI+)** m/z: 464.5 $[M+NH_4]^+$. **HRMS (ESI+)** $C_{24}H_{34}F_4NaO_3$ $[M+Na]^+$. Calculated: 469.2336; Found: 469.2332 (1.0 ppm error). **IR** ($CDCl_3$, cm^{-1}) 2961 – 2884 (m), 1709 (s), 1126 (s), 1048 (m), 733 (m).

12α,12β-Difluoro-3-oxo-7α-hydroxy-5β-cholanic acid (2.52)

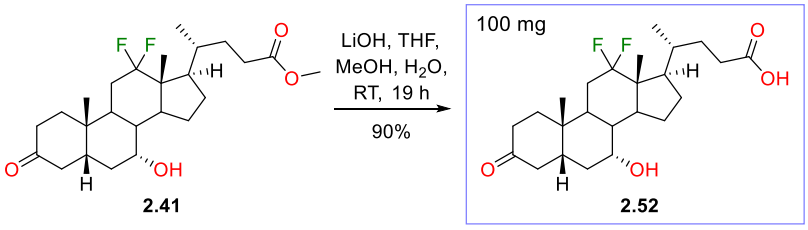

Following general procedure C, **2.41** (122 mg, 0.28 mmol, 1.0 equiv) was deprotected to yield **2.52** as a white solid (106 mg, 0.25 mmol, 90%) with no further purification.

mp 195 – 196 °C (decomp.). **R_f** 0.37 (EtOAc/PE 80/20). **$[\alpha]_D$** + 30.4 (c = 0.75, $CHCl_3$, 20 °C). **^{1}H NMR** (400 MHz, $CDCl_3$) δ 3.97 (apparent br d, *J*=2.7 Hz, 1H, 7β-**H**), 3.37 (br t, *J*=14.7 Hz, 1H, 4α-**H**), 1.21-2.48 (m), 0.98-1.05 (m, 6H, overlapping 19-**CH₃** and 21-**CH₃**), 0.87 (s, 3H, 18-**CH₃**) ppm. **^{13}C NMR** (100 MHz, $CDCl_3$) δ 212.7 (**3-C**), 179.3 (**24-COOH**), 125.9 (dd, *J*=250.2, 247.2 Hz, **12-C**), 67.5 (**7-CH**), 49.0 (t, *J*=20.5 Hz, **13-C**), 47.6 (d, *J*=2.2 Hz, **17-CH**), 46.7 (d, *J*=7.3 Hz, **14-CH**), 45.3 (**4-CH₂**), 42.6 (**5-CH**), 38.2 (**8-CH**), 36.6 (***1-CH₂ or 2-CH₂***), 36.4 (***1-CH₂ or 2-CH₂***), 34.8 (**10-C**), 33.9 (**6-CH₂**), 33.2 (**20-CH**), 31.6 (t, *J*=26.4 Hz, **11-CH₂**), 31.3 (**23-CH₂**), 31.0 (d, *J*=9.5 Hz, **9-CH**), 30.2 (**22-CH₂**), 26.3 (***15-CH₂ or 16-CH₂***), 22.6 (***15-CH₂ or 16-CH₂***), 21.6 (**19-CH₃**), 18.9 (d, *J*=11.0 Hz, **21-CH₃**), 10.4 (d, *J*=4.4 Hz, **18-CH₃**) ppm. **^{19}F NMR** (376MHz, $CDCl_3$) δ -91.50 (br d, *J*=230.6 Hz, 1F, 12β-**F**), -112.14 (ddd, *J*=230.6, 12.1, 4.7 Hz, 1F, 12α-**F**) ppm. **^{19}F [^{1}H] NMR** (376MHz, $CDCl_3$) δ -91.51 (d, *J*=232.3 Hz, 1F, 12β-**F**), -112.14 (d, *J*=230.6 Hz, 1F, 12α-**F**) ppm. **LRMS (ESI+)** m/z: 444.5 $[M+NH_4]^+$. **HRMS (ESI+)** $C_{24}H_{36}F_2NaO_4$ $[M+Na]^+$. Calculated: 449.2474; Found: 449.2478 (0.9 ppm error). **IR** (neat, cm^{-1}) 3523 (m), 2908 (m), 1712 (s), 1247 (m), 1006 (m).

12α,12β-Difluoro-7-oxolithocholic acid (2.53)

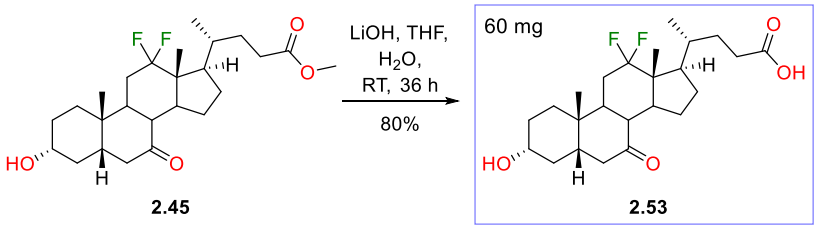

Following general procedure C, **2.45** (77.0 mg, 0.18 mmol, 1.0 equiv) was deprotected to yield **2.53** as a white solid (60 mg, 0.14 mmol, 80%) with no further purification.

mp 169 – 170 °C. **R_f** 0.17 (EtOAc/PE 80/20). **$[\alpha]_D$** - 7.70 (c = 0.63, $CHCl_3$, 21 °C). **^{1}H NMR** (400 MHz, $CDCl_3$) δ 3.57-3.67 (m, 1H, 3β-**H**), 2.86 (dd, *J*=12.8, 5.9 Hz, 1H, 6β-**H**), 2.24-2.50 (m), 2.10-2.21 (m, 1H, 9-**CH**), 1.23-2.04 (m), 1.22 (s, 3H, 19-**CH_3**), 1.04-1.16 (m, 1H), 1.01 (dd, *J*=6.6, 1.8 Hz, 3H, 21-**CH_3**), 0.84 (s, 3H, 18-**CH_3**) ppm. **^{13}C NMR** (100 MHz, $CDCl_3$) δ 210.2 (**7-C**), 179.5 (**24-COOH**), 125.4 (dd, *J*=250.2, 246.5 Hz, **12-C**), 70.6 (**3-CH**), 49.0 (br t, *J*=20.5 Hz, **13-C**), 47.9 (CH), 47.0 (**17-CH**), 45.6 (CH), 45.5 (d, *J*=7.3 Hz, **14-CH**), 45.2 (**6-CH_2**), 39.6 (d, *J*=9.5 Hz, **9-CH**), 37.1 (CH_2), 34.7 (**10-C**), 33.9 (CH_2), 32.8 (**20-CH**), 31.6 (t, *J*=26.4 Hz, **11-CH_2**), 31.5 (CH_2), 30.0 (CH_2), 29.6 (CH_2), 26.0 (CH_2), 23.7 (CH_2), 22.7 (**19-CH_3**), 19.1 (d, *J*=10.3 Hz, **21-CH_3**), 10.7 (d, *J*=5.1 Hz, **18-CH_3**) ppm. **^{19}F NMR** (376MHz, $CDCl_3$) δ -93.16 (br d, *J*=232.4 Hz, 1F, 12β-**F**), -112.89 (ddd, *J*=232.3, 29.5, 15.6 Hz, 1F, 12α-**F**) ppm. **^{19}F [^{1}H] NMR** (376MHz, $CDCl_3$) δ -93.16 (br d, *J*=232.4 Hz, 1F, 12β-**F**), -112.90 (br d, *J*=232.4 Hz, 1F, 12α-**F**) ppm. **LRMS (ESI+)** m/z: 444.6 $[M+NH_4]^+$. **HRMS (ESI+)** $C_{24}H_{36}F_2NaO_4$ $[M+Na]^+$. Calculated: 449.2474; Found: 449.2465 (2.0 ppm error). **IR** (neat, cm^{-1}) 3400 (b,m), 1705 (s), 1059 (m), 1019 (m).

Methyl 12α,12β-difluoro-3,7-dioxo-5β-cholan-24-oate (2.46)

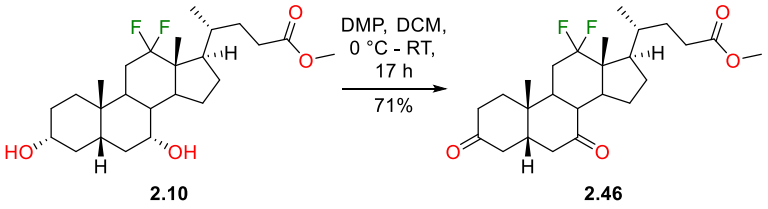

The alcohol **2.10** (400 mg, 0.90 mmol, 1.0 equiv) was dissolved in dry DCM (10 mL) and DMP (840 mg, 1.98 mmol, 2.2 equiv) was slowly added in portions at 0 °C. After stirring for 17 h, the reaction mixture was diluted with DCM (20 mL) and quenched with saturated $NaHCO_3$ solution (20 mL) and saturated sodium thiosulfate solution (20 mL). The mixture was extracted with DCM (3 x 25 mL) and the combined organic phases were washed with saturated $NaHCO_3$ (100 mL), water (100 mL) and brine (100 mL) before drying over Na_2SO_4 and reducing *in vacuo*, giving around 520 mg of crude material. The crude was purified by flash chromatography (Biotage SNAP KP-Sil 10g cartridge, EtOAc/PE: 30%/70% → 40%/60%), yielding **2.46** as a white solid (281 mg, 0.64 mmol, 71%).

mp 166 – 167 °C. **R_f** 0.30 (EtOAc/PE 35/65). **$[\alpha]_D$** - 9.38 (c = 0.48, $CHCl_3$, 24 °C). **^{1}H NMR** (400 MHz, $CDCl_3$) δ 3.66 (s, 3H, 24-COO**CH_3**), 2.88 (dd, *J*=13.0, 5.7 Hz, 1H, 6β-**H**), 2.49 (t, *J*=11.4 Hz, 1H, 8β-**H**), 2.38 (ddd, *J*=15.4, 9.8, 5.4 Hz, 1H, 23-**H'**), 1.77-2.34 (m), 1.33-1.67 (m), 1.31 (s, 3H, 19-**CH_3**), 1.03-1.16 (m, 1H, 15α-**H**), 0.98 (dd, *J*=6.6, 1.7 Hz, 3H, 21-**CH_3**), 0.87 (s, 3H, 18-**CH_3**) ppm. **^{13}C NMR** (100 MHz, $CDCl_3$) δ 209.2 (s, 2 C, **3-C** and **7-C**), 174.5 (**24-COO**CH_3), 125.2 (dd, *J*=250.2, 246.5 Hz, **12-C**), 51.5 (**24**-COO**CH_3**), 49.0 (dd, *J*=21.3, 19.8 Hz, **13-C**), 48.0 (**8-CH**), 47.2 (**5-CH**), 47.0 (br d, *J*=1.5 Hz, **17-CH**), 45.5 (d, *J*=7.3 Hz, **14-CH**), 44.8 (**6-CH_2**), 42.7 (**4-CH_2**), 39.7 (d, *J*=10.3 Hz, **9-CH**), 36.4 (***1-CH_2 or 2-CH_2***), 35.1 (***1-CH_2 or 2-CH_2***), 34.9 (**10-C**), 32.7 (**20-CH**), 32.1 (t, *J*=26.8 Hz, **11-CH_2**), 31.6 (**23-CH_2**), 30.2 (**22-CH_2**), 25.8 (**16-CH_2**), 23.6 (**15-CH_2**), 22.1 (**19-CH_3**), 19.2 (d, *J*=10.3 Hz, **21-CH_3**), 10.7 (d, *J*=4.4 Hz, **18-CH_3**) ppm. **^{19}F NMR** (376MHz, $CDCl_3$) δ -93.54 (br d, *J*=232.4 Hz, 1F, 12β-**F**), -112.90 (ddd, *J*=232.3, 32.9, 12.1 Hz, 1F. 12α-**F**) ppm. **^{19}F [^{1}H] NMR** (376MHz, $CDCl_3$) δ -93.54 (d, *J*=234.1 Hz, 1F, 12β-**F**), -112.83 (d, *J*=234.1 Hz, 1F, 12α-**F**) ppm. **LRMS (ESI+)** m/z: 877.6 $[2M+H]^+$ 461.7 $[M+Na]^+$, 456.7 $[M+NH_4]^+$. **HRMS (ESI+)** $C_{25}H_{36}F_2NaO_4$ $[M+Na]^+$. Calculated: 461.2474; Found: 461.2483 (2.1 ppm error). **IR** (neat, cm^{-1}) 2957 – 2880 (m), 1731 (s), 1706 (s), 1046 (m).

12α,12β-Difluoro-3,7-dioxo-5β-cholanic acid (2.54)

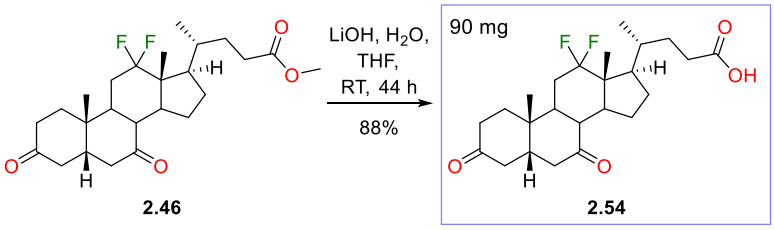

Following general procedure C, **2.46** (110 mg, 0.25 mmol, 1.0 equiv) was deprotected to yield **2.54** as a white solid (93.0 mg, 0.22 mmol, 88%) with no further purification.

mp 186 – 187 °C. **R_f** 0.21 (EtOAc/PE 50/50). **$[\alpha]_D$** - 8.08 (c = 0.50, $CHCl_3$, 22 °C). **^{1}H NMR** (400 MHz, $CDCl_3$) δ 2.88 (dd, *J*=13.0, 5.7 Hz, 1H, 6β-**H**), 2.38-2.54 (m, 2H, t of 8β-**H** and ddd of 23-**H'**), 1.80-2.36 (m), 1.34-1.67 (m), 1.31 (s, 3H, 19-**CH_3**), 1.09 (qd, *J*=12.2, 5.6 Hz, 1H, 15α-**H**), 1.00 (dd, *J*=6.5, 1.5 Hz, 3H, 21-**CH_3**), 0.87 (s, 3H, 18-**CH_3**) ppm. **^{13}C NMR** (100 MHz, $CDCl_3$) δ 209.4 (d, *J*=1.5 Hz, **7-C**), 209.3 (**3-C**), 179.9 (**24-COOH**), 125.2 (dd, *J*=250.9, 246.5 Hz, **12-C**), 49.0 (dd, *J*=20.5, 20.5 Hz, **13-C**), 48.0 (**8-CH**), 47.2 (**5-CH**), 47.0 (**17-CH**), 45.5 (d, *J*=7.3 Hz, **14-CH**), 44.8 (**6-CH_2**), 42.7 (**4-CH_2**), 39.8 (d, *J*=9.5 Hz, **9-CH**), 36.4 (***1-CH_2 or 2-CH_2***), 35.1 (***1-CH_2 or 2-CH_2***), 34.9 (**10-C**), 32.7 (**20-CH**), 32.1 (t, *J*=26.8 Hz, **11-CH_2**), 31.5 (**23-CH_2**), 30.0 **(22-CH_2**), 25.9 (**16-CH_2**), 23.6 (**15-CH_2**), 22.1 (**19-CH_3**), 19.1 (d, *J*=10.3 Hz, **21-CH_3**), 10.7 (d, *J*=4.4 Hz, **18-CH_3**) ppm. **^{19}F NMR** (376MHz, $CDCl_3$) δ -93.36 (br d, *J*=234.1 Hz, 1F, 12β-**F**), -112.86 (ddd, *J*=234.1, 32.9, 12.1 Hz, 1F, 12α-**F**) ppm. **^{19}F [^{1}H] NMR** (376MHz, $CDCl_3$) δ -93.36 (d, *J*=232.4 Hz, 1F, 12β-**F**), -112.86 (d, *J*=234.1 Hz, 1F, 12α-**F**) ppm. **LRMS (ESI+)** m/z: 840.0 $[2M+H]^+$, 447.5 $[M+Na]^+$. **HRMS (ESI+)** $C_{24}H_{34}F_2NaO_4$ $[M+Na]^+$. Calculated: 447.2317; Found: 447.2319 (0.4 ppm error). **IR** (neat, cm^{-1}) 2967 – 2873 (m), 1704 (s), 1047 (m), 1022 (m), 846 (m).

Methyl 3,7,12-trioxo-5β-cholan-24-oate (2.55)

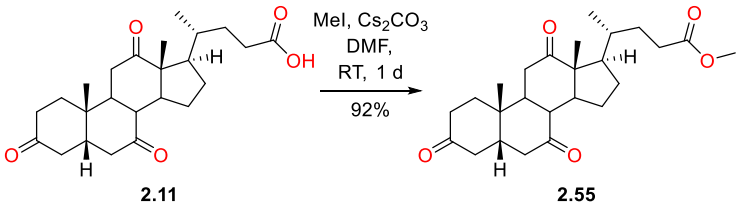

2.11 **2.55**

The carboxylic acid **2.11** (2.00 g, 5.00 mmol, 1.0 equiv) was dissolved in DMF (20 mL) and Cs_2CO_3 (2.10 g, 6.50 mmol, 1.3 equiv) and methyl iodide (1.9 mL, 30 mmol, ~6 equiv) were added. The mixture was stirred at RT for 24 h, after which water (100 mL) was added and the resulting precipitate was filtered. The precipitate was dissolved in EtOAc (100 mL) and DCM (15 mL) and the organic phase was washed with brine (150 mL) before drying over Na_2SO_4 and reducing *in vacuo* to yield **2.55** as a white solid (1.91 g, 4.58 mmol, 92%).

mp 239 – 241 °C (lit 238 – 240 °C[223]). **R_f** 0.27 (EtOAc/PE 50/50). **^{1}H NMR** (400 MHz, $CDCl_3$) δ 3.67 (s, 3H, 24-COO**CH_3**), 2.97-2.81 (m, 3H), 2.46-1.53 (m, 19H), 1.41 (s, 3H, 19-**CH_3**), 1.40-1.21 (m, 4H), 1.08 (s, 3H, 18-**CH_3**), 0.86 (d, *J*=6.6 Hz, 3H, 21-**CH_3**) ppm. **^{13}C NMR** (100 MHz, $CDCl_3$) δ 211.9 (**3-C**), 209.0 (**7-C**), 208.7 (**12-C**), 174.5 (**24-COO**CH_3), 56.9 (C), 51.7 (CH), 51.5 (**24-**COO**CH_3**), 49.0 (CH), 46.8 (CH), 45.6 (CH), 45.5 (CH), 45.0 (CH_2), 42.8 (CH_2), 38.6 (CH_2), 36.5 (CH_2), 36.0 (C), 35.5 (CH), 35.3 (CH_2), 31.3 (CH_2), 30.4 (CH_2), 27.6 (CH_2), 25.1 (CH_2), 21.9 (**19-CH_3**), 18.6 (**21-CH_3**), 11.8 (**18-CH_3**) ppm. **LRMS (ESI+)** m/z: 417.3 $[M+H]^+$, 434.3 $[M+NH_4]^+$, 439.3 $[M+Na]^+$. ^{1}H, ^{13}C and melting point data agree with literature.[223,224]

Methyl 3α,3β,7α,7β,12α,12β-hexafluoro-5β-cholan-24-oate (2.56)

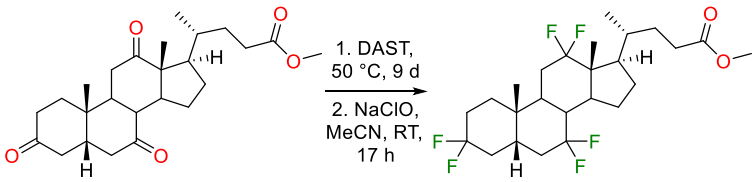

2.55 10% over 2 steps **2.56**

To a flame-dried flask with condenser attached, **2.55** (1.80 g, 4.30 mmol, 1.0 equiv) and DAST (10 mL, 76 mmol, ~18 equiv) were added. The reaction mixture was heated to 50 °C. Over the course of 8 d, 9 mL of DAST was added to the reaction mixture at RT in 1, 2 or 4 mL portions, followed by heating back up to 50 °C. After 9 d, the reaction mixture was allowed to cool to RT, added DCM (100 mL) and decanted dropwise (~5 mL per min) into icy, saturated $NaHCO_3$ solution (~ 500 mL). After achieving a neutral pH, the phases were separated and the aqueous phase was extracted with DCM (2 x 100 mL). The organic phases were combined and washed with saturated $NaHCO_3$ solution (150 mL), water (150 mL) and brine (150 mL) before drying over Na_2SO_4 and reducing *in vacuo* to yield

around 2.8 g of oily, brown crude. The crude was purified by flash chromatography (EtOAc/PE: 0%/100% → 10%/90%), giving a fraction (440 mg) containing around 80% **2.56** and around 20% of fluoroalkene products. The impure fraction obtained was dissolved in acetonitrile (10 mL) and NaClO (11%, 0.32 mL, 0.57 mmol, ~3 equiv based on fluoroalkene content) was added to the stirring solution. After 18 h of stirring at RT, water (25 mL) was added to the reaction mixture and the aqueous phase was extracted with EtOAc (2 x 25 mL). The combined organic phases were washed with saturated sodium thiosulfate solution (50 mL), water (50 mL) and brine (50 mL) before drying over Na_2SO_4 and reducing *in vacuo* to yield around 400 mg of pale yellow crude. The crude was purified by flash chromatography (EtOAc/PE 10%/90% → 30%/70%), yielding **2.56** as a white solid (220 mg, 0.46 mmol, 10% from **2.55**). Fluoroepoxide or fluoroalkene products were not isolated after flash chromatography.

mp 106 – 107°C. $\mathbf{R_f}$ 0.51 (EtOAc/PE 20/80). $\mathbf{[\alpha]_D}$ + 38.0 (c = 0.88, $CHCl_3$, 21 °C). **^{1}H NMR** (400 MHz, $CDCl_3$) δ 3.68 (s, 3H, 24-COO**CH_3**), 2.40 (ddd, *J*=15.4, 9.9, 5.3 Hz, 1H, 23-**H'**), 2.27 (ddd, *J*=15.8, 9.3, 6.8 Hz, 1H, 23-**H''**), 1.31-2.23 (m), 1.03 (s, 3H, 19-**CH_3**), 1.00 (dd, J=2.0, 6.7 Hz, 3H, 21-**CH_3**), 0.87 (s, 3H, 18-**CH_3**) ppm. **^{13}C NMR** (125 MHz, $CDCl_3$) δ 174.5 (**24-COO**CH_3), 125.1 (dd, *J*=250.6, 246.5 Hz, **12-C**), 123.7 (t, *J*=244.6 Hz, **7-C**), 123.0 (dd, *J*=242.7, 238.9 Hz, **3-C**), 51.5 (**24-**COO**CH_3**), 49.4 (t, *J*=20.6 Hz, **13-C**), 46.7 (d, *J*=2.4 Hz, **17-CH**), 45.1 (dd, *J*=6.8, 4.6 Hz, **14-CH**), 40.7 (br t, *J*=21.0 Hz, **8-CH**), 39.0 (br t, *J*=10.4 Hz, ***5-CH or 9-CH***), 35.1 (t, *J*=23.6 Hz, **6-CH_2**), 35.1 (br ddd, *J*=25.3, 22.4, 5.5 Hz, **4-CH_2**), 33.9 (**10-C**), 33.7 (t, *J*=9.3 Hz, ***5-CH or 9-CH***), 32.9 (**20-CH**), 32.1 (d, *J*=9.3 Hz, **1-CH_2**), 31.6 (**23-CH_2**), 31.4 (t, *J*=26.7 Hz, **11-CH_2**), 30.2 (**22-CH_2**), 28.8 (dd, *J*=25.4, 22.5 Hz, **2-CH_2**), 25.9 (d, *J*=1.2 Hz, ***15-CH_2 or 16-CH_2***), 24.1 (d, *J*=4.1 Hz, ***15-CH_2 or 16-CH_2***), 21.8 (d, *J*=2.4 Hz, **19-CH_3**), 19.1 (d, *J*=10.0 Hz, **21-CH_3**), 10.5 (dd, *J*=5.0, 1.2 Hz, **18-CH_3**) ppm. **^{19}F NMR** (376MHz, $CDCl_3$) δ -85.66 (br d, *J*=246.2 Hz, 1F, 7β-**F**), -90.42 (br d, *J*=235.8 Hz, 1F, 3α-**F**), -93.46 (br d, *J*=234.1 Hz, 1F, 12β-**F**), -100.97 - -102.99 (m, 2F, overlapping dddd, *J*=246.2, 38.2, 24.3, 13.9 Hz, 7α-**F** and dtt, *J*=239.2, 38.2, 20.8, 8.7 Hz, 3β-**F**), -112.01 (ddd, *J*=232.3, 32.9, 12.1 Hz, 1F, 12α-**F**) ppm. **^{19}F [^{1}H] NMR** (376MHz, $CDCl_3$) δ -85.75 (d, *J*=244.5 Hz, 1F, 7β-**F**), -90.42 (d, *J*=235.8 Hz, 1F, 3α-**F**), -93.46 (d, *J*=232.4 Hz, 1F, 12β-**F**), -101.68 (dd, *J*=244.5, 3.5 Hz, 1F, 7α-**F**), -102.36 (dd, *J*=235.8, 3.5 Hz, 1F, 3β-**F**), -111.93 (d, *J*=234.1 Hz, 1F, 12α-**F**) ppm. **LRMS (ESI+)** m/z: 403.5 $[M+H-4HF]^+$, 423.5 $[M+H-3HF]^+$, 443.5 $[M+H-2HF]^+$, 463.6 $[M+H-HF]^+$. **HRMS (ESI+)** $C_{25}H_{36}F_6NaO_2$ $[M+Na]^+$. Calculated: 505.2512; Found: 505.2504 (1.6 ppm error). **IR** (neat, cm^{-1}) 2957 – 2889 (m), 1737 (s), 1098 (s), 1023 (m).

3α,3β,7α,7β,12α,12β-Hexafluoro-5β-cholanic acid (2.9)

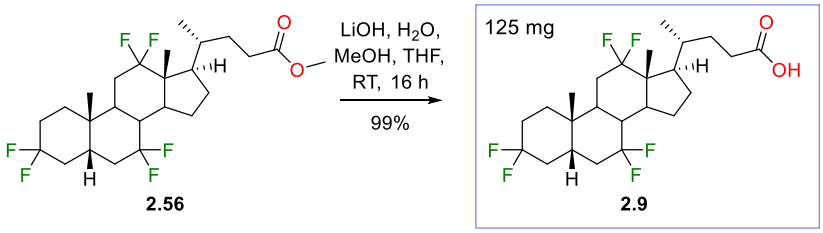

Following general procedure C, **2.56** (130 mg, 0.27 mmol, 1.0 equiv) was deprotected to yield **2.9** as a white powder (125 mg, 0.27 mmol, 99%) with no further purification.

mp 165 – 166 °C. **R_f** 0.36 (EtOAc/PE 30/70). **^{1}H NMR** (500 MHz, $CDCl_3$) 2.44 (ddd, *J*=15.5, 9.8, 5.1 Hz, 1H, 23-**H'**), 2.32 (ddd, *J*=16.2, 9.3, 6.7 Hz, 1H, 23-**H''**), 2.26-1.21 (m), 1.04 (s, 3H, 19-**CH_3**), 1.01 (dd, *J*=1.6, 6.6 Hz, 3H, 21-**CH_3**), 0.87 (s, 3H, 18-**CH_3**) ppm. **^{13}C NMR** (126 MHz, $CDCl_3$) δ 179.0 (**24-COOH**), 125.3 (dd, *J*=250.6, 246.5 Hz, **12-C**), 123.7 (t, *J*=244.9 Hz, **7-C**), 123.0 (dd, *J*=242.9, 238.9 Hz, **3-C**), 49.4 (t, *J*=20.7 Hz, **13-C**), 46.7 (d, *J*=2.4 Hz, **17-CH**), 45.2 (dd, *J*=6.7, 4.5 Hz **14-CH**), 40.7 (dd, *J*=23.1, 20.5 Hz, **8-CH**), 39.0 (br t, *J*=10.3 Hz, ***5-CH or 9-CH***), 35.2 (t, *J*=23.6 Hz, **6-CH_2**), 35.1 (ddd, *J*=25.0, 22.2, 5.5 Hz**,** **4-CH_2**), 33.9 (**10-C**), 33.7 (br t, *J*=9.5 Hz, CH, ***5-CH or 9-CH***), 33.0 (**20-CH**), 32.2 (br d, *J*=9.3 Hz, **1-CH_2**), 31.4 (**23-CH_2**), 31.4 (t, *J*=27.4 Hz, **11-CH_2**), 30.1 (**22-CH_2**), 28.9 (dd, *J*=25.5, 22.6 Hz, **2-CH_2**), 26.0 (***15-CH_2* or *16-CH_2***), 24.1 (d, *J*=3.8 Hz, ***15-CH_2* or *16-CH_2***), 21.8 (d, *J*=2.4 Hz, **19-CH_3**), 19.1 (d, *J*=10.5 Hz, **21-CH_3**), 10.5 (d, *J*=3.8 Hz, **18-CH_3**) ppm. **^{19}F NMR** (471 MHz, $CDCl_3$) δ -85.42 (br d, *J*=245.6 Hz, 1F, 7β-**F**), -90.18 (br d, *J*=236.3 Hz, 1F, 3α-**F**), -93.05 (br d, *J*=232.9 Hz, 1F, 12β-**F**), -101.00 - -102.58 (m, 2F overlapping dddd, 7α-**F** and dtt, 3β-**F**), -111.75 (ddd, *J*=233.2, 33.6, 12.6 Hz, 1F, 12α-**F**) ppm. **^{19}F [^{1}H] NMR** (471 MHz, $CDCl_3$) δ -85.42 (br d, *J*=245.7 Hz, 1F, 7β-**F**), -90.18 (d, *J*=235.7 Hz, 1F, 3α-**F**), -93.05 (br d, *J*=233.2 Hz, 1F, 12β-**F**), -101.43 (br dd, *J*=245.3, 2.9 Hz, 1F, 7α-**F**), -102.12 (br dd, *J*=235.7, 2.9 Hz, 1F, 3β-**F**), -111.75 (br d, *J*=233.5 Hz, 1F, 12α-**F**) ppm. **LRMS (ESI+)** m/z: 369.5 $[M+H-5HF]^+$, 389.4 $[M+H-4HF]^+$, 409.3 $[M+H-3HF]^+$, 429.4 $[M+H-2HF]^+$, 449.4 $[M+H-HF]^+$. **HRMS (ESI+)** $C_{24}H_{34}F_6NaO_2$ $[M+Na]^+$. Calculated: 491.2355; Found: 491.2359 (0.4 ppm error). **IR** (neat, cm^{-1}) 2962 (m), 1706 (s), 1252 (m), 1099 (s), 922 (m).

7.3.3 Synthesis of Analogues from 7-Keto LCA

Methyl 7-oxo-lithocholate (2.57)

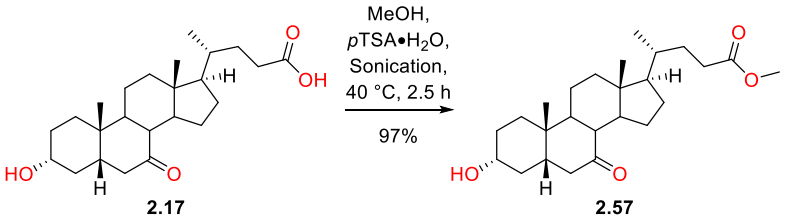

Following general procedure A, **2.17** (20.0 g, 51.2 mmol, 1 equiv) was protected to yield **2.57** as an off white solid (20.0 g, 49.4 mmol, 97%) with no further purification.

mp 90 – 91 °C (lit. 107 – 108 °C[225]). **R_f** 0.30 (EtOAc/PE 50/50). **^{1}H NMR** (400 MHz, $CDCl_3$) 3.65 (s, 3H, 24-COO**CH_3**), 3.52-3.63 (m, 1H, 3β-**H**), 2.84 (dd, *J*=12.5, 5.9 Hz, 1H, 6β-**H**), 2.28-2.42 (m, 2H, 8β-**H** and 23-**H'**), 2.12-2.26 (m, 2H, 23-**H''** and 15β-**H**), 1.62-2.06 (m), 1.19-1.56 (m), 1.18 (s, 3H, 19-**CH_3**), 0.93-1.17 (m, 3H), 0.91 (d, *J*=6.2 Hz, 3H, 21-**CH_3**), 0.64 (s, 3H, 18-**CH_3**) ppm. **^{13}C NMR** (100 MHz, $CDCl_3$) δ 212.0 (**7-C**), 174.6 (**24-COO**CH_3), 70.8 (**3-CH**), 54.7 (**17-CH**), 51.4 (**24-**COO**CH_3**), 49.5 (**8-CH**), 48.9 (**14-CH**), 46.0 (**5-CH**), 45.3 (**6-CH_2**), 42.7 (**9-CH**), 42.6 (**13-C**), 38.9 (**12-CH_2**), 37.3 (**4-CH_2**), 35.2 (**20-CH**), 35.1 (**10-C**), 34.1 (**1-CH_2**), 31.0 (**23-CH_2**), 30.9 (**22-CH_2**), 29.8 (**16-CH_2**), 28.2 (**2-CH_2**), 24.8 (**15-CH_2**), 23.0 (**19-CH_3**), 21.6 (**11-CH_2**), 18.3 (**21-CH_3**), 12.0 (**18-CH_3**) ppm. **LRMS (ESI+)** m/z: 422.2 $[M+NH_4]^+$. ^{1}H and ^{13}C NMR data agree with literature.[225,226]

Methyl 3α-*O*-thiocarbonylimidazole-7-oxo-5β-cholan-24-oate (2.58)

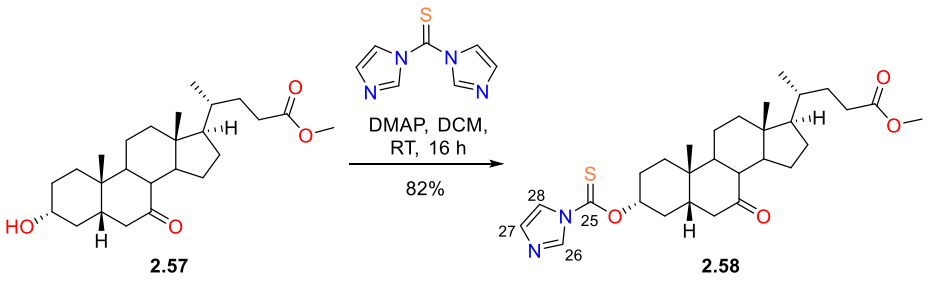

The alcohol **2.58** (2.00 g, 4.94 mmol, 1.0 equiv) was dissolved in dry DCM (20 mL) and 1,1'-thiocarbonyl diimidazole (TCDI, 1.76 g, 9.88 mmol, 2.0 equiv) and DMAP (60 mg, 0.49 mmol, 0.1 equiv) were added. After stirring at RT for 16 h, saturated NH_4Cl solution (40 mL) was added to the reaction mixture, which was then extracted with EtOAc (3 x 50 mL). The combined organic phases were then washed with saturated $NaHCO_3$ (100 mL), water (100 mL) and brine (100 mL) before drying over Na_2SO_4 and reducing *in vacuo* to yield 2.5 g of crude material. The crude was purified by flash chromatography (Biotage ZIP KP-Sil 80 g cartridge, EtOAc/PE: 35%/65% → 45%/55%), yielding **2.58** as a white powder (2.08 g, 4.04 mmol, 82%).

mp 163 – 164 °C. **R_f** 0.39 (EtOAc/PE 40/60). **$[\alpha]_D$** - 1.60 (c = 1.08, $CHCl_3$, 22 °C). **^{1}H NMR** (400 MHz, $CDCl_3$) δ 8.29 (t, *J*=0.9 Hz, 1H, 26-**H**), 7.57 (t, *J*=1.5 Hz, 1H, 27-**H**), 7.00 (dd, *J*=1.7, 0.9 Hz, 1H, 28-**H**), 5.41 (tt, *J*=11.4, 4.6 Hz, 1H, 3β-**H**), 3.54 (s, 3H, 24-COO**CH_3**), 2.91 (dd, *J*=12.6, 5.9 Hz, 1H, 6β-**H**), 2.43 (t, *J*=11.3 Hz, 1H, 8β-**H**), 2.33 (ddd, *J*=15.8, 10.1, 5.3 Hz, 1H, 23-**H'** or 23-**H''**), 2.14-2.27 (m, 2H), 1.73-2.09 (m), 1.26-1.62 (m), 1.25 (s, 3H, 19-**CH_3**), 1.06-1.23 (m, 2H), 0.93-1.02 (m, 1H, 15α-**H** or 15β-**H**), 0.91 (d, *J*=6.5 Hz, 3H, 21-**CH_3**), 0.66 (s, 3H, 18-**CH_3**) ppm. **^{13}C NMR** (100 MHz, $CDCl_3$) δ 211.5 (**7-C**), 183.3 (**25-C=S**), 174.5 (**24-COO**CH_3), 136.8 (**26-CH**), 130.7 (**28-CH**), 117.7 (**27-CH**), 82.5 (**3-CH**), 54.7 (**17-CH**), 51.4 (**24-**COO**CH_3**), 49.4 (**8-CH**), 48.8 (**14-CH**), 45.8 (**5-CH**), 45.1 (**6-CH_2**), 42.9 (**9-CH**), 42.5

(**13-C**), 38.8 (**12-CH$_2$**), 35.1 (**10-C**), 35.1 (**20-CH**), 33.4 (**1-CH$_2$**), 32.2 (**4-CH$_2$**), 30.9 (**23-CH$_2$**), 30.9 (**22-CH$_2$**), 28.2 (**16-CH$_2$**), 25.3 (**2-CH$_2$**), 24.6 (**15-CH$_2$**), 22.9 (**19-CH$_3$**), 21.7 (**11-CH$_2$**), 18.3 (**21-CH$_3$**), 12.0 (**18-CH$_3$**) ppm. **LRMS (ESI+)** m/z: 537.6 $[M+Na]^+$, 515.6 $[M+H]^+$, 387.5 $[M+H\text{-}C_4H_4N_2OS]^+$. **HRMS (ESI+)** $C_{29}H_{43}N_2O_4S$ $[M+H]^+$. Calculated: 515.2938; Found: 515.2948 (1.9 ppm error). **IR** (neat, cm^{-1}) 2949 – 2870 (m), 1731 (s), 1708 (s), 1226 (m), 981 (m).

Methyl 3α-(phenoxycarbonothioyl)oxy-7-oxo-5β-cholan-24-oate (2.59)

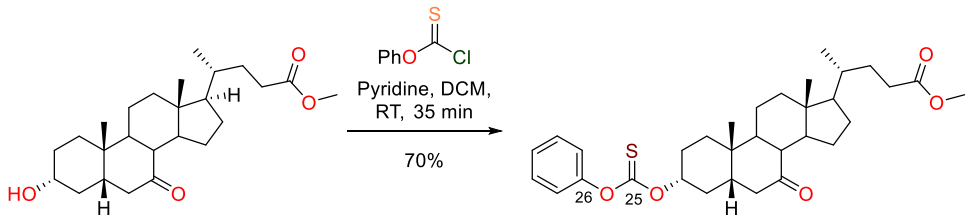

2.57 **2.59**

Following general procedure G, the thiocarbonate of **2.57** (1.00 g, 2.47 mmol, 1.0 equiv) was formed. The crude material was purified by flash chromatography (Biotage SNAP KP-Sil 25 g cartridge, acetone/PE: 5%/95% → 15%/85%), yielding **2.59** as an off-white, gummy solid (930 mg, 1.72 mmol, 70%).

R$_f$ 0.20 (Acetone/PE 10/90). **[α]$_D$** + 34.6 (c = 0.99, $CHCl_3$, 22 °C). **^{1}H NMR** (400 MHz, $CDCl_3$) δ 7.38-7.45 (m, 2H, *meta*-**CH**), 7.26-7.31 (m, 1H, *para*-**CH**), 7.05-7.12 (m, 2H, *ortho*-**CH**), 5.18 (tt, *J*=11.2, 4.4 Hz, 1H, 3β-**H**), 3.67 (s, 3H, 24-COO**CH$_3$**), 2.89 (dd, *J*=12.8, 5.8 Hz, 1H, 6β-**H**), 2.31-2.47 (m, 2H, 8β-**H** and 23-**H'**), 2.18-2.28 (m, 2H, 23-**H''** and 15β-**H**), 1.74-2.11 (m), 1.26-1.63 (m), 1.24 (s, 3H, 19-**CH$_3$**), 1.05-1.21 (m, 2H, 17α-**H** and 12α-**H**), 0.95-1.03 (m, 1H, 15α-**H**), 0.93 (d, *J*=6.2 Hz, 3H, 21-**CH$_3$**), 0.67 (s, 3H, 18-**CH$_3$**) ppm. **^{13}C NMR** (100 MHz, $CDCl_3$) δ 211.4 (**7-C**), 194.1 (**25-C=S**), 174.6 (**24-COO**CH_3), 153.2 (**26-C**), 129.4 (2C, ***meta*-C**), 126.4 (***para*-C**), 121.9 (2C, ***ortho*-C**), 83.2 (**3-CH**), 54.7 (**17-CH**), 51.4 (**24**-COO**CH$_3$**), 49.4 (**8-CH**), 48.8 (**14-CH**), 45.7 (**5-CH**), 45.1 (**6-CH$_2$**), 42.7 (**9-CH**), 42.6 (**13-C**), 38.9 (**12-CH$_2$**), 35.1 (**10-C**), 35.1 (**20-CH**), 33.6 (**1-CH$_2$**), 32.1 (**4-CH$_2$**), 31.0 (**23-CH$_2$**), 30.9 (**22-CH$_2$**), 28.2 (**16-CH$_2$**), 25.3 (**2-CH$_2$**), 24.7 (**15-CH$_2$**), 22.9 (**19-CH$_3$**), 21.7 (**11-CH$_2$**), 18.3 (**21-CH$_3$**), 12.0 (**18-CH$_3$**) ppm. **LRMS (ESI+)** m/z: 558.5 $[M+NH_4]^+$. **HRMS (ESI+)** $C_{32}H_{44}NaO_5S$ $[M+Na]^+$. Calculated: 563.2802; Found: 563.2795 (1.2 ppm error). **IR** (neat, cm^{-1}) 2933 – 2868 (m), 1735 (s), 1697 (s), 1285 (s), 1196 – 1160 (b, s), 1003 (m).

Methyl 7-oxo-5β-cholan-24-oate (2.60)

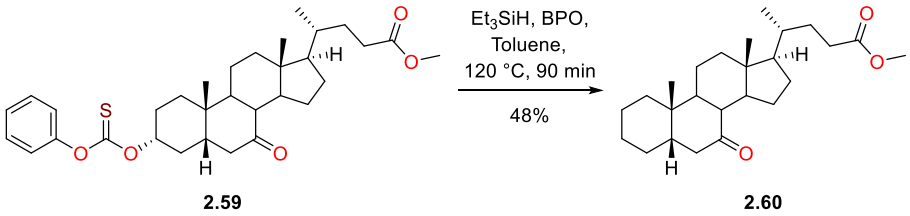

2.59 **2.60**

Following general procedure H, **2.59** (200 mg, 0.37 mmol, 1.0 equiv) was deoxygenated. The crude material was purified by flash chromatography (Biotage SNAP KP-Sil 10 g cartridge, acetone/PE: 0%/100% → 5%/95%), yielding **2.60** as a white gummy solid (70 mg, 0.18 mmol, 49%).

R_f 0.30 (Acetone/PE 5/95). **$[\alpha]_D$** - 54.8 (c = 0.49, $CHCl_3$, 22 °C). **^{1}H NMR** (400 MHz, $CDCl_3$) δ 3.67 (s, 3H, 24-COO**CH_3**), 2.88 (dd, *J*=11.9, 5.9 Hz, 1H, 6β-**H**), 2.31-2.43 (m, 2H, 8β-**H** and 23-**H'**), 2.16-2.28 (m, 2H, 23-**H''** and 15β-**H**), 1.88-2.02 (m, 3H), 1.74-1.86 (m, 4H), 1.67-1.74 (m, 1H), 1.21-1.51 (m), 1.19 (s, 3H, 19-**CH_3**), 1.03-1.18 (m, 3H), 0.94-1.01 (m, 1H, 15α-**H**), 0.93 (d, *J*=6.4 Hz, 3H, 21-**CH_3**), 0.66 (s, 3H, 18-**CH_3**) ppm. **^{13}C NMR** (100 MHz, $CDCl_3$) δ 212.5 (**7-C**), 174.5 (**24-COO**CH_3), 54.7 (**17-CH**), 51.4 (**24-**COO**CH_3**), 49.5 (**8-CH**), 48.9 (**14-CH**), 47.5 (**5-CH**), 45.8 (**6-CH_2**), 42.7 (**9-CH**), 42.6 (**13-C**), 39.0 (**12-CH_2**), 36.4 (CH_2), 35.8 (**10-C**), 35.1 (**20-CH**), 31.0 (**23-CH_2**), 30.9 (**22-CH_2**), 28.2 (**4-CH_2**), 28.0 (**16-CH_2**), 26.5 (CH_2), 24.8 (**15-CH_2**), 23.8 (**19-CH_3**), 21.5 (**11-CH_2**), 20.6 (CH_2), 18.3 (**21-CH_3**), 12.0 (**18-CH_3**) ppm. **LRMS (ESI+)** m/z: 359.5 $[M+H]^+$. **HRMS (ESI+)** $C_{25}H_{41}O_3$ $[M+H]^+$. Calculated: 389.3050; Found: 389.3042 (2.2 ppm error). **IR** (neat, cm^{-1}) 2970 – 2860 (m), 1740 (s), 1702 (s), 1159 (m), 1094 (m).

7-Oxo-5β-cholanic acid (2.61)

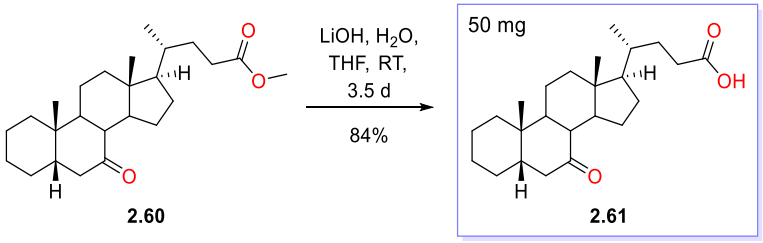

2.60 **2.61**

Following general procedure C, **2.60** (60 mg, 0.15 mmol, 1.0 equiv) was deprotected to yield **2.61** as a white solid (47 mg, 0.13 mmol, 84%) with no further purification.

mp 125 – 126 °C. **R_f** 0.23 (EtOAc/PE 30/70). **$[\alpha]_D$** - 53.6 (c = 0.5, $CHCl_3$, 22 °C). **^{1}H NMR** (400 MHz, $CDCl_3$) δ 2.87 (dd, *J*=12.3, 6.0 Hz, 1H, 6β-**H**), 2.34-2.44 (m, 2H, 8β-**H** and 23-**H'**), 2.15-2.30 (m, 2H, 23-**H''** and 15β-**H**), 1.66-2.02 (m), 1.20-1.52 (m), 1.18 (s, 3H, 19-**CH_3**), 1.03-1.17 (m, 3H), 0.94-1.02 (m, 1H, 15α-**H**), 0.93 (d, *J*=6.5 Hz, 3H, 21-**CH_3**), 0.65 (s, 3H, 18-**CH_3**) ppm. **^{13}C NMR** (100 MHz, $CDCl_3$) δ 212.9 (**7-C**), 180.3 (**24-COOH**), 54.7 (**17-CH**), 49.5 (**8-CH**), 48.9 (**14-CH**), 47.6 (**5-CH**), 45.8 (**6-CH_2**), 42.7 (**9-CH**), 42.6 (**13-C**), 39.0 (**12-CH_2**), 36.4 (CH_2), 35.8 (**10-C**), 35.1 (**20-CH**), 31.0 (**23-CH_2**), 30.7 (**22-**

CH_2), 28.2 (**4-CH_2**), 28.1 (CH_2), 26.5 (CH_2), 24.8 (**15-CH_2**), 23.9 (**19-CH_3**), 21.6 (CH_2), 20.6 (CH_2), 18.3 (**21-CH_3**), 12.0 (**18-CH_3**) ppm. **LRMS (ESI+)** m/z: 375.5 $[M+H]^+$. **HRMS (ESI+)** $C_{24}H_{39}O_3$ $[M+H]^+$. Calculated: 375.2894; Found: 375.2888 (1.6 ppm error). **IR** (neat, cm^{-1}) 2924 – 2860 (b, m), 1701 (s), 1253 (m), 944 (m).

Methyl 3α-acetoxy-7-oxo-5β-cholan-24-oate (2.62)

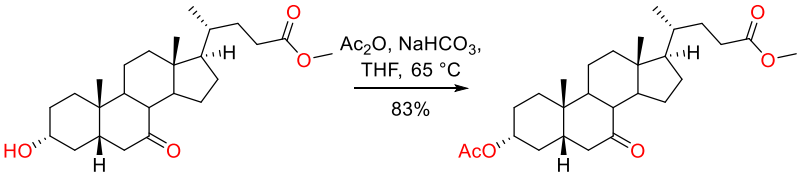

2.57 **2.62**

Following general procedure F, **2.57** (2.50 g, 6.18 mmol, 1.0 equiv) was protected to yield **2.62** as a white solid (2.29 g, 5.13 mmol, 83%) with no further purification.

mp 124 – 125 °C. **R_f** 0.75 (EtOAc/PE 40/60). **$[\alpha]_D$** - 7.39 (c = 1.0, $CHCl_3$, 22 °C). **^{1}H NMR** (400 MHz, $CDCl_3$) δ 4.70 (tt, *J*=11.1, 4.8 Hz, 1H, 3β-**H**), 3.67 (s, 3H, 24-COO**CH_3**), 2.86 (dd, *J*=12.8, 5.9 Hz, 1H, 6β-**H**), 2.31-2.44 (m, 2H, 8β-**H** and 23-**H'**), 2.16-2.28 (m, 2H, 23-**H''** and 15β-**H**), 2.01 (s, 3H, 3α-OCO**CH_3**), 1.66-2.00 (m), 1.24-1.53 (m), 1.21 (s, 3H, 19-**CH_3**), 1.07-1.20 (m, 2H, 12α-**H** and 17α-**H**), 0.94-1.02 (m, 1H, 15α-**H**), 0.93 (d, *J*=6.4 Hz, 3H, 21-**CH_3**), 0.66 (s, 3H, 18-**CH_3**) ppm. **^{13}C NMR** (100 MHz, $CDCl_3$) δ 211.6 (**7-C**), 174.6 (**24-COO**CH_3), 170.4 (3α-**OCO**CH_3), 72.9 (**3-CH**), 54.7 (**17-CH**), 51.4 (**24-**COO**CH_3**), 49.4 (**8-CH**), 48.8 (**14-CH**), 45.8 (**5-CH**), 45.2 (**6-CH_2**), 42.7 (**9-CH**), 42.6 (**13-C**), 38.9 (**12-CH_2**), 35.1 (**20-CH**), 35.1 (**10-C**), 33.8 (**1-CH_2**), 33.0 (**4-CH_2**), 31.0 (**23-CH_2**), 30.9 (**22-CH_2**), 28.2 (**16-CH_2**), 26.0 (**2-CH_2**), 24.7 (**15-CH_2**), 23.0 (**19-CH_3**), 21.7 (**11-CH_2**), 21.2 (**3α-**OCO**CH_3**), 18.3 (**21-CH_3**), 12.0 (**18-CH_3**) ppm. **LRMS (ESI+)** m/z: 893.9 $[2M+H]^+$, 447.5 $[M+H]^+$. **HRMS (ESI+)** $C_{27}H_{42}NaO_5$ $[M+Na]^+$. Calculated: 469.2924; Found: 469.2937 (2.6 ppm error). **IR** (neat, cm^{-1}) 2978 – 2567 (m), 1730 (s), 1703 (s), 1256 (s), 1169 (m). ^{1}H and ^{13}C NMR data agree with data from within the group.

Methyl 7α,7β-difluoro-3α-acetoxy-5β-cholan-24-oate (2.63)

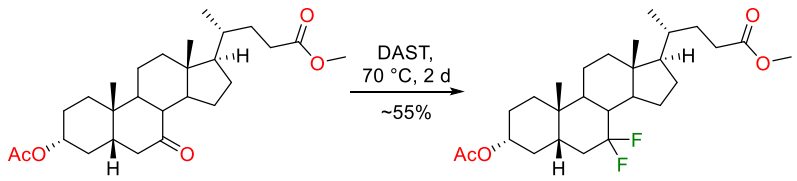

2.62 **2.63** (~80% pure with ~20 % fluoroalkenes)

To a flame-dried flask with condenser attached, under argon **2.62** (2.36 g, 5.28 mmol, 1.0 equiv) and DAST (~12 mL, ~91 mmol, ~17 equiv) were added. The reaction mixture was heated to 70 °C and after two days of heating, was allowed to cool to RT, diluted with DCM (50 mL) and the mixture

was slowly decanted (~5 mL per min) into icy, saturated $NaHCO_3$ solution (~650 mL). After the mixture was fully neutralised it was extracted with DCM (3 x 100 mL). The combined organic phases were then washed with saturated $NaHCO_3$ (200 mL), water (200 mL) and brine (200 mL) before drying over Na_2SO_4 and reducing *in vacuo* to yield 3.9 g of crude material. The crude was purified twice by flash chromatography (1st: Biotage ZIP KP-Sil 80 g cartridge, acetone/PE: 10%/90% → 20%/70%; 2nd: Biotage SNAP KP-Sil 100 g cartridge, acetone/PE: 4%/96% → 9%/91%), yielding **2.63** around 80% pure as a yellow solid (1.75 g total, ~1.4 g **2.63**, ~3.0 mmol, ~56%). HPLC purification was to be attempted on the 80% pure extract of **2.63** but it failed to dissolve in the HPLC eluent.

R_f 0.21 (Acetone/Hexane 5/95). **^{1}H NMR** (400 MHz, $CDCl_3$) δ 5.06 (ddd, *J*=18.2, 6.0, 2.0 Hz, 0.1H, 6-**H** of FA), 4.58-4.76 (m, 1H, 3β-**H**), 3.67 (s, 3H, 24-COO**CH$_3$**), 2.35 (ddd, *J*=15.4, 10.1, 5.3 Hz, 1H, 23-**H'**), 2.04-2.28 (m, 2H, 23-**H''** and 6β-**H**), 2.01-2.04 (m, 3H, 3α-OCO**CH$_3$**), 1.04-2.01 (m), 0.86-0.99 (m, 6H, 19-**CH$_3$** and 21-**CH$_3$**), 0.62-0.72 (m, 3H, 18-**CH$_3$**) ppm. **^{13}C NMR** (100 MHz, $CDCl_3$) δ 174.6 (**24-COO**CH_3), 170.6 (**3α-OCO**CH_3), 124.6 (br t, *J*=243.6 Hz, **7-C**), 73.4 (**3-C**), 55.0 (**17-CH**), 51.5 (**24-**COO**CH$_3$**), 48.6 (d, *J*=4.4 Hz, **14-CH**), 43.1 (**13-C**), 41.8 (dd, *J*=23.1, 19.4 Hz, **8-CH**), 41.0 (d, *J*=10.3 Hz, ***5-CH or 9-CH***), 39.4 (**12-CH$_2$**), 37.0 (d, *J*=8.8 Hz, ***5-CH or 9-CH***), 36.0 (t, *J*=23.5 Hz, **6-CH$_2$**), 35.3 (**20-CH**), 34.4 (**1-CH$_2$**), 34.3 (d, *J*=1.5 Hz, **10-C**), 33.0 (d, *J*=5.1 Hz, **4-CH$_2$**), 31.0 (**23-CH$_2$**), 31.0 (**22-CH$_2$**), 28.3 (br s, **16-CH$_2$**), 26.3 (**2-CH$_2$**), 25.3 (d, *J*=4.4 Hz, **15-CH$_2$**), 22.6 (**19-CH$_3$**), 21.4 (**3α**-OCO**CH$_3$**), 20.9 (**11-CH$_2$**), 18.3 (**21-CH$_3$**), 11.8 (**18-CH$_3$**) ppm. **^{19}F NMR** (376MHz, $CDCl_3$) δ -84.74 (br d, *J*=241.0 Hz, 1F, 7β-**H**), -101.51 (dddd, *J*=240.8, 37.9, 24.7, 13.9 Hz, 1F, 7α-**H**) ppm. **^{19}F [^{1}H] NMR** (376MHz, $CDCl_3$) δ -84.74 (d, *J*=241.0 Hz, 1F, 7β-**H**), -101.52 (br d, *J*=241.0 Hz, 1F, 7α-**H**) ppm. **LRMS (ESI+)** m/z: 409.6 $[M+H-AcOH]^+$, 389.5 $[M+H-AcOH-HF]^+$, 369.5 $[M+H-AcOH-2HF]^+$.

7α,7β-Difluorolithocholic acid (2.15)

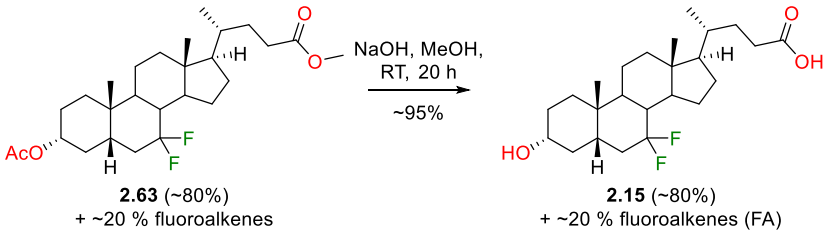

2.63 (~80%)
+ ~20 % fluoroalkenes

2.15 (~80%)
+ ~20 % fluoroalkenes (FA)

Following general procedure D, **2.63** (~80% pure, 1.68 g, ~2.9 mmol, 1.0 equiv) was deprotected to yield **2.15** as an off-white solid, around 80% pure (1.42 g (~1.14 g), ~2.76 mmol, ~95%) with no further purification.

R_f 0.06 (EtOAc/PE 30/70). **^{1}H NMR** (400 MHz, MeOH-d_4) δ 5.08 (ddd, *J*=18.2, 6.0, 1.8 Hz, 0.1H, 6-**H** of FA), 3.41-3.60 (m, 1H, 3β-**H**), 2.29-2.39 (m, 1H, 23-**H'**), 2.16-2.29 (m, 2H, 23-**H''** and 6β-**H**), 1.03-2.15 (m), 0.85-1.02 (m, 6H, 19-**CH$_3$** and 21-**CH$_3$**), 0.65-0.77 (m, 3H, 18-**CH$_3$**) ppm. **^{13}C NMR** (100 MHz, MeOH-d_4) δ 178.2 (**24-COOH**), 126.0 (dd, *J*=245.0, 242.8 Hz, **7-C**), 112.2-112.4 (**FA**), 107.5-107.8

(**FA**), 72.1 (**3-CH**), 56.6 (**17-CH**), 50.3 (d, *J*=4.4 Hz, **14-CH**), 44.4 (**13-C**), 43.3 (dd, *J*=23.1, 19.4 Hz, **8-CH**), 42.7 (br d, *J*=10.3 Hz, ***5-CH or 9-CH***), 41.0 (**12-CH_2**), 38.6 (d, *J*=8.8 Hz, ***5-CH or 9-CH***), 38.3 (d, *J*=4.4 Hz, CH_2), 37.5 (br t, *J*=21.6 Hz, **6-CH_2**), 36.8 (**20-CH**), 35.9 (**10-C**), 35.5 (CH_2), 32.5 (**22-CH_2**), 32.1 (**23-CH_2**), 31.1 (CH_2), 29.5 (d, *J*=1.5 Hz, CH_2), 26.7 (d, *J*=4.4 Hz, CH_2), 23.2 (**19-CH_3**), 22.2 (CH_2), 19.0 (**21-CH_3**), 12.4 (**18-CH_3**) ppm. **^{19}F NMR** (376MHz, MeOH-d_4) δ -84.70 (br d, *J*=241.0 Hz, 1F, 7β-**F**), -101.97 (dddd, *J*=240.8, 38.4, 24.3, 13.9 Hz, 1F, 7α-**F**), -108.16 (br d, *J*=19.1 Hz, 0.1F, 6-**F** of FA), -111.73--111.40 (m, 0.1F, 6-**F** of FA) ppm. **^{19}F [^{1}H] NMR** (376MHz, MeOH-d_4) δ -84.70 (d, *J*=241.0 Hz, 1F, 7β-**F**), -101.97 (d, *J*=241.0 Hz, 1F, 7α-**F**), -108.16 (s, 1F, 6-**F** of FA), -111.53 (s, 1F, 6-**F** of FA) ppm. **LRMS (ESI+)** m/z: 430.3 $[M+NH_4]^+$. ^{1}H, ^{13}C and ^{19}F NMR data consistent with data from within the group.

Methyl 7α,7β-difluoro-3α-hydroxy-5β-cholan-24-oate (2.64)

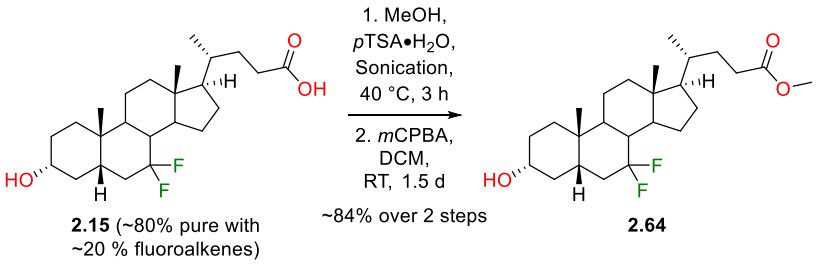

2.15 (~80% pure with ~20 % fluoroalkenes)

2.64

Following general procedure A, **2.15** (~80% pure, 1.35 g, ~2.6 mmol, 1.0 equiv) was protected to give 1.28 g of crude material. An attempt was made at purification of the crude material (Biotage ZIP KP-Sil 30 g cartridge, acetone/PE 15%/85% → 25%/75%), but the fluoroalkene products co-eluted with **2.64**, giving 1.12 g of ~80% pure material. The 80% pure material (1.12 g, ~2.1 mmol, 1.0 equiv) was dissolved in DCM (55 mL) and *m*-CPBA (~70%, ~260 mg, ~1.0 mmol, ~0.5 equiv) was added. After stirring at RT for 1.5 d, the reaction mixture was quenched with sat. $NaHCO_3$ (100 mL). The organic and aqueous phases were separated and the aqueous phase was extracted with DCM (2 x 100 mL). The combined organic phases were washed with sat. $NaHCO_3$ (100 mL), water (100 mL) and brine (100 mL) before drying over Na_2SO_4 and reducing *in vacuo* to give 1.0 g of crude material. The crude was purified by flash chromatography (Biotage ZIP KP-Sil 30 g cartridge, EtOAc/PE: 25%/75% → 40%/60%), cleanly yielding **2.64** as a white solid (745 mg, 1.75 mmol, ~84% from **2.15**). No fluoroalkene or fluoroepoxide products were cleanly isolated following purification.

mp 133 – 134 °C. **R_f** 0.25 (EtOAc/PE 30/70). **[α]$_D$** + 27.2 (c = 1.06, $CHCl_3$, 22 °C). **^{1}H NMR** (400 MHz, $CDCl_3$) δ 3.66 (s, 3H, 24-COO**CH_3**), 3.54 (tt, *J*=10.6, 5.1 Hz, 1H, 3β-**H**), 2.35 (ddd, *J*=15.4, 10.1, 5.3 Hz, 1H, 23-**H'**), 0.99-2.28 (m), 0.95 (s, 3H, 19-**CH_3**), 0.92 (d, *J*=6.4 Hz, 3H, 21-**CH_3**), 0.66 (s, 3H, 18-**CH_3**) ppm. **^{13}C NMR** (100 MHz, $CDCl_3$) δ 174.7 (**24-COO**CH_3), 124.6 (dd, *J*=245.8, 243.6 Hz, **7-C**), 71.3 (**3-CH**), 54.9 (**17-CH**), 51.5 (**24-**COO**CH_3**), 48.5 (d, *J*=4.4 Hz, **14-CH**), 43.1 (**13-C**), 41.8 (dd, *J*=23.1, 19.4 Hz, **8-CH**), 41.2 (d, *J*=11.0 Hz, ***5-CH or 9-CH***), 39.4 (**12-CH_2**), 37.2 (d, *J*=4.4 Hz, CH_2), 37.0 (d, *J*=8.8 Hz,

5-CH or 9-CH), 36.2 (t, *J*=23.1 Hz, **6-CH₂**), 35.2 (**20-CH**), 34.6 (CH_2), 34.2 (**10-C**), 31.0 (**23-CH₂**), 30.9 (**22-CH₂**), 30.1 (CH_2), 28.3 (d, *J*=1.5 Hz, CH_2), 25.3 (d, *J*=4.4 Hz, CH_2), 22.6 (**19-CH₃**), 20.8 (CH_2), 18.3 (**21-CH₃**), 11.8 (**18-CH₃**) ppm. **^{19}F NMR** (376MHz, $CDCl_3$) δ -84.58 (br d, *J*=239.3 Hz, 1F, 7β-**F**), -101.41 (dddd, *J*=241.0, 38.1, 26.0, 13.9 Hz, 1F, 7α-**F**) ppm. **^{19}F [^{1}H] NMR** (376MHz, $CDCl_3$) δ -84.58 (br d, *J*=239.3 Hz, 1F, 7β-**F**), -101.41 (dddd, *J*=241.0, 38.1, 26.0, 13.9 Hz, 7α-**F**) ppm. **LRMS (ESI+)** m/z: 444.5 $[M+NH_4]^+$. **HRMS (ESI+)** $C_{25}H_{40}F_2NaO_3$ $[M+Na]^+$. Calculated: 449.2838; Found: 449.2848 (2.3 ppm error). **IR** (neat, cm^{-1}) 3513 (m, s), 2953 – 2868 (m), 1710 (s), 1101 (s), 980 (m).

Methyl 7α,7β-difluoro-3α-(phenoxycarbonothioyl)oxy-5β-cholan-24-oate (2.65)

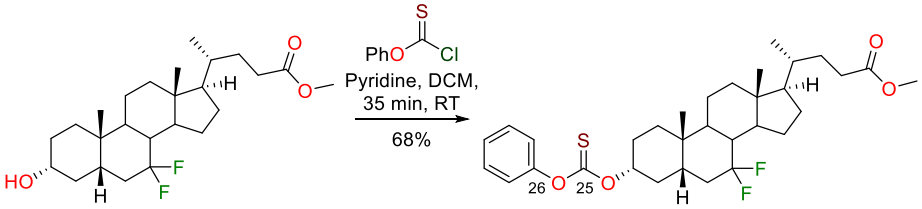

2.64 **2.65**

Following general procedure G, the thiocarbonate of **2.64** (640 mg, 1.50 mmol, 1.0 equiv) was formed. The crude material was purified by flash chromatography (Biotage SNAP KP-Sil 25 g cartridge, acetone/PE: 0%/100% → 5%/95%), yielding **2.65** as a white solid (575 mg, 1.02 mmol, 68%).

mp 131 – 132 °C. **R_f** 0.28 (Acetone/PE 5/95). **$[\alpha]_D$** + 51.3 (c = 1.08, $CHCl_3$, 22 °C). **^{1}H NMR** (400 MHz, $CDCl_3$) δ 7.42 (br t, *J*=7.7 Hz, 2H, *meta* **CH**), 7.30 (br t, *J*=7.5 Hz, 1H, *para*-**CH**), 7.11 (d, *J*=7.7 Hz, 2H, *ortho*-**CH**), 5.06-5.21 (m, 1H, 3β-**H**), 3.68 (s, 3H, 24-COO**CH₃**), 2.37 (ddd, *J*=15.4, 10.3, 5.3 Hz, 1H, 23-**H'**), 2.10-2.30 (m, 2H, 23-**H''** and 6β-**H**), 1.06-2.07 (m), 1.00 (s, 3H, 19-**CH₃**), 0.95 (d, *J*=6.2 Hz, 3H, 21-**CH₃**), 0.69 (s, 3H, 18-**CH₃**) ppm. **^{13}C NMR** (100 MHz, $CDCl_3$) δ 194.3 (**25-C=S**), 174.6 (**24-COO**CH_3), 153.3 (**26-C**), 129.4 (2 C, ***meta*-C**), 126.4 (***para*-C**), 122.0 (2 C, ***ortho*-C**), 124.7 (br t, *J*=245.0 Hz, **7-C**), 83.8 (**3-CH**), 54.9 (**17-CH**), 51.4 (**24**-COO**CH₃**), 48.5 (d, *J*=3.7 Hz, **14-CH**), 43.1 (**13-C**), 41.7 (dd, *J*=22.7, 19.8 Hz, **8-CH**), 40.9 (br d, *J*=11.0 Hz, ***5-CH or 9-CH***), 39.4 (**12-CH₂**), 37.0 (d, *J*=8.8 Hz, ***5-CH or 9-CH***), 36.0 (br t, *J*=23.8 Hz, **6-CH₂**), 35.2 (**20-CH**), 34.3 (**10-C**), 34.1 (**1-CH₂**), 32.0 (d, *J*=4.4 Hz, **4-CH₂**), 31.0 (**23-CH₂**), 30.9 (**22-CH₂**), 28.3 (**16-CH₂**), 25.6 (**2-CH₂**), 25.3 (d, *J*=3.7 Hz, **15-CH₂**), 22.5 (**19-CH₃**), 20.9 (**11-CH₂**), 18.3 (**21-CH₃**), 11.8 (**18-CH₃**) ppm. **^{19}F NMR** (376MHz, $CDCl_3$) δ -84.89 (br d, *J*=242.8 Hz, 1F, 7β-**F**), -101.50 (dddd, *J*=242.8, 38.1, 26.0, 13.9 Hz, 1F, 7α-**F**) ppm. **^{19}F [^{1}H] NMR** (376MHz, $CDCl_3$) δ -84.89 (br d, *J*=241.0 Hz, 1F, 7β-**F**), -101.50 (br d, *J*=242.8 Hz, 1F, 7α-**F**) ppm. **LRMS (ESI+)** m/z: 580.3 $[M+NH_4]^+$, 563.3 $[M+H]^+$. **HRMS (ESI+)** $C_{32}H_{44}F_2NaO_4S$ $[M+Na]^+$. Calculated: 585.2821; Found: 585.2804 (2.8 ppm error). **IR** (DCM, cm^{-1}) 2946 – 2873 (m), 1735 (s), 1193 (s), 1062 (m).

Methyl 7α,7β-difluoro-5β-cholan-24-oate (2.66)

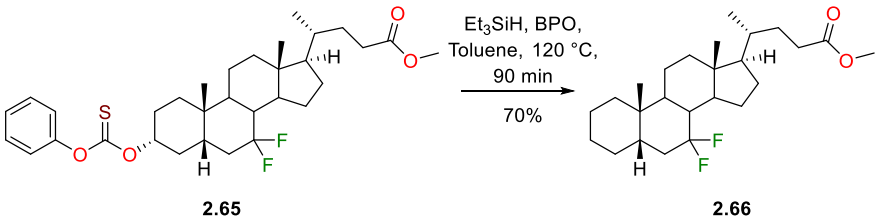

Following procedure H, **2.65** (415 mg, 0.74 mmol, 1.0 equiv) was deoxygenated. The crude material was purified by flash chromatography (Biotage SNAP KP-Sil 25 g cartridge, acetone/PE: 0%/100% → 3%/97%), yielding **2.66** as a white solid (215 mg, 0.52 mmol, 70%).

mp 68 – 69 °C. **R_f** 0.33 (Acetone/PE 5/95). **$[\alpha]_D$** + 30.1 (c = 0.49, $CHCl_3$, 22 °C). **^{1}H NMR** (400 MHz, $CDCl_3$) δ 3.67 (s, 3H, 24-COO**CH_3**), 2.36 (ddd, *J*=15.5, 10.4, 5.3 Hz, 1H, 23-**H'**), 2.07-2.28 (m, 2H, 23-**H''** and 6β-**H**), 1.99 (dt, *J*=12.3, 3.2 Hz, 1H, 12β-**H**), 1.04-1.95 (m), 0.96-1.04 (m, 1H, 1β-**H**), 0.95 (s, 3H, 19-**CH_3**), 0.93 (d, *J*=6.5 Hz, 3H, 21-**CH_3**), 0.67 (s, 3H, 18-**CH_3**) ppm. **^{13}C NMR** (100 MHz, $CDCl_3$) δ 174.7 (**24-COO**CH_3), 125.0 (dd, *J*=245.8, 242.8 Hz, **7-C**), 55.0 (**17-CH**), 51.5 (**24**-COO**CH_3**), 48.6 (d, *J*=3.7 Hz, **14-CH**), 43.1 (**13-C**), 42.8 (d, *J*=10.3 Hz, **5-CH**), 41.8 (dd, *J*=23.1, 19.4 Hz, **8-CH**), 39.5 (**12-CH_2**), 37.0 (**1-CH_2**), 37.0 (br d, *J*=8.8 Hz, **9-CH**), 36.6 (t, *J*=22.7 Hz, **6-CH_2**), 35.3 (**20-CH**), 35.0 (d, *J*=1.5 Hz, **10-C**), 31.0 (**23-CH_2**), 31.0 (**22-CH_2**), 28.3 (d, *J*=1.5 Hz, **16-CH_2**), 27.9 (d, *J*=3.7 Hz, **4-CH_2**), 27.1 (**3-CH_2**), 25.4 (d, *J*=3.7 Hz, **15-CH_2**), 23.5 (**19-CH_3**), 21.0 (**2-CH_2**), 20.8 (**11-CH_2**), 18.3 (**21-CH_3**), 11.8 (**18-CH_3**) ppm. **^{19}F NMR** (376MHz, $CDCl_3$) δ -84.02 (br d, *J*=237.6 Hz, 1F, 7β-**F**), -101.02 (dddd, *J*=238.6, 38.4, 23.8, 14.7 Hz, 1F, 7α-**F**) ppm. **^{19}F [^{1}H] NMR** (376MHz, $CDCl_3$) δ -84.02 (d, *J*=239.3 Hz, 1F, 7β-**F**), -101.02 (d, *J*=237.6 Hz, 1F, 7α-**F**) ppm. **LRMS (ESI+)** m/z: 428.4 $[M+NH_4]^+$. **HRMS (ESI+)** $C_{25}H_{40}F_2NaO_2$ $[M+Na]^+$. Calculated: 433.2889; Found: 433.2884 (1.1 ppm error). **IR** ($CDCl_3$, cm^{-1}) 2926 – 2852 (m), 1736 (s), 1437 (m), 1008 (m).

7α,7β-Difluoro-5β-cholanic acid (2.13)

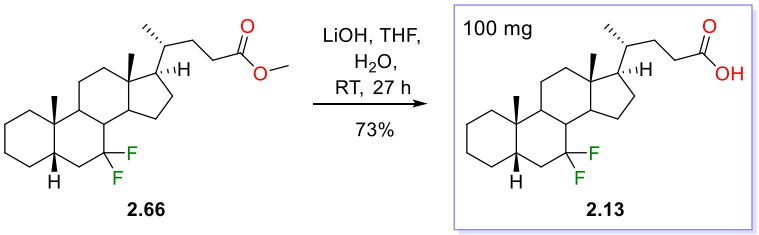

Following general procedure C, **2.66** (170 mg, 0.41 mmol, 1.0 equiv) was deprotected to yield **2.13** as a white solid (118 mg, 0.30 mmol, 73%) with no further purification.

mp 176 – 177 °C. **R_f** 0.29 (EtOAc/PE 25/75). **$[\alpha]_D$** + 30.7 (c = 0.51, $CHCl_3$, 22 °C). **^{1}H NMR** (500 MHz, $CDCl_3$) δ 11.27 (br s, 1H, 24-CO**OH**), 2.41 (ddd, *J*=15.6, 10.3, 5.2 Hz, 1H, 23-**H'**), 2.27 (ddd, *J*=15.9,

9.7, 6.5 Hz, 1H, 23-**H''**), 2.16 (dddd, *J*=38.6, 13.9, 7.4, 6.1 Hz, 1H, 6β-**H**), 2.00 (dt, *J*=12.5, 3.3 Hz, 1H, 12β-**H**), 1.65-1.94 (m), 1.07-1.54 (m), 0.97-1.04 (m, 1H, 1β-**H**), 0.93-0.97 (m, 6H, 19-**CH_3** and 21-**CH_3**), 0.68 (s, 3H, 18-**CH_3**) ppm. **^{13}C NMR** (126 MHz, $CDCl_3$) δ 180.4 (**24-COOH**), 125.0 (dd, *J*=246.2, 242.8 Hz, **7-C**), 55.0 (**17-CH**), 48.6 (d, *J*=4.1 Hz, **14-CH**), 43.2 (**13-C**), 42.8 (d, *J*=10.3 Hz, **5-CH**), 41.9 (dd, *J*=23.1, 19.1 Hz, **8-CH**), 39.5 (**12-CH_2**), 37.0 (**1-CH_2**), 37.0 (br d, *J*=8.8 Hz, **9-CH**), 36.6 (t, *J*=22.9 Hz, **6-CH_2**), 35.2 (**20-CH**), 35.1 (d, *J*=1.2 Hz, **10-C**), 31.0 (**23-CH_2**), 30.7 (**22-CH_2**), 28.3 (d, *J*=1.7 Hz, **16-CH_2**), 27.9 (d, *J*=4.3 Hz, **4-CH_2**), 27.1 (**3-CH_2**), 25.4 (d, *J*=4.1 Hz, **15-CH_2**), 23.5 (**19-CH_3**), 21.0 (**2-CH_2**), 20.9 (**11-CH_2**), 18.3 (**21-CH_3**), 11.8 (**18-CH_3**) ppm. **^{19}F NMR** (471MHz, $CDCl_3$) δ -83.80 (br d, *J*=238.9 Hz, 1F, 7β-**F**), -100.80 (dddd, *J*=238.9, 40.1, 25.8, 15.0 Hz, 1F, 7α-**F**) ppm. **^{19}F [^{1}H] NMR** (471MHz, $CDCl_3$) δ -83.80 (d, *J*=238.9 Hz, 1F, 7β-**F**), -100.80 (d, *J*=238.9 Hz, 1F, 7α-**F**) ppm. **LRMS (ESI+)** m/z: 414.2 $[M+NH_4]^+$. **HRMS (ESI+)** $C_{24}H_{38}F_2NaO_2$ $[M+Na]^+$. Calculated: 419.2732; Found: 419.2722 (2.5 ppm error). **IR** (neat, cm^{-1}) 2924 – 2860 (m), 1718 (s), 1005 (m), 876 (m).

Methyl 3α,7-bis(trimethylsilyloxy)-5β-cholan-6-en-24-oate (2.67)

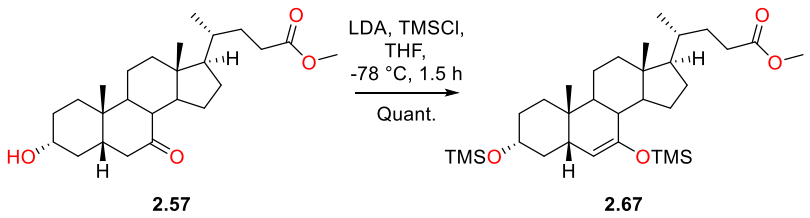

2.57 **2.67**

To a flame-dried flask under argon diisopropylamine (18.2 mL, 130 mmol, 5.0 equiv) and dry THF (150 mL) were added. The solution was cooled to -78 °C and *n*-BuLi (2.5 M in hexanes, 52 mL, 130 mmol, 5.0 equiv) was added dropwise over 20 min. After stirring for 30 min, chlorotrimethylsilane (16.5 mL, 130 mmol, 5.0 equiv) was added to the reaction mixture. After stirring for a further 30 min, a solution of **2.57** (10.5 g, 26.0 mmol, 1.0 equiv) in dry THF (120 mL) was added to the reaction mixture at -78 °C. After stirring for 90 min, NEt_3 (36 mL, 260 mmol, 10 equiv) was added to the reaction mixture. After stirring for a further 1 h, the reaction mixture was warmed to -10 °C and added sat. $NaHCO_3$ (60 mL). Following a further 20 min of stirring, the mixture was extracted with EtOAc (2 x 250 mL). The combined organic phases were then washed with sat. $NaHCO_3$ (300 mL), water (300 mL) and brine (300 mL) before drying over Na_2SO_4 and reducing *in vacuo* to yield **2.67** (15.5 g, ~99% yield). The crude material was used in the next reaction without purification.

R_f 0.94 (EtOAc/PE 50/50). **^{1}H NMR** (400 MHz, $CDCl_3$) δ 4.71-4.77 (m, 1H, 6-**H**), 3.67 (s, 3H, 24-COO**CH_3**), 3.45-3.59 (m, 1H, 3β-**H**), 2.35 (ddd, *J*=15.3, 10.1, 5.3 Hz, 1H, 23-**H'**), 2.23 (ddd, *J*=15.9, 9.5, 6.7 Hz, 1H, 23-**H''**), 0.95-2.04 (m), 0.91-0.95 (m, 3H, 21-**CH_3**), 0.83 (s, 3H, 19-**CH_3**), 0.68 (s, 3H, 18-**CH_3**), 0.16 (s, 9H, 7-OSi(**CH_3**)$_3$), 0.11 (s, 9H, 3α-OSi(**CH_3**)$_3$) ppm. **^{13}C NMR** (100 MHz, $CDCl_3$) δ 174.7 (**24-COO**CH_3), 151.7 (**7-C**), 108.8 (**6-CH**), 71.5 (**3-CH**), 54.8 (**17-CH**), 54.1 (**14-CH**), 51.4 (**24-**COO**CH_3**),

44.4 (**13-C**), 42.7 (**5-CH**), 41.0 (**8-CH**), 40.9 (CH_2), 40.3 (**9-CH**), 40.1 (**12-CH_2**), 35.3 (**20-CH**), 34.6 (CH_2), 33.0 (**10-C**), 31.1 (**23-CH_2**), 31.0 (**22-CH_2**), 30.6 (CH_2), 28.7 (CH_2), 27.1 (CH_2), 22.5 (**19-CH_3**), 20.9 (CH_2), 18.4 (**21-CH_3**), 12.2 (**18-CH_3**), 0.3 (**7-OSi(CH_3)$_3$**), 0.2 (**3α-OSi(CH_3)$_3$**) ppm. **LRMS (ESI+)** m/z: 549.3 $[M+H]^+$. ^{1}H NMR data agrees with data from within the group and literature,[227] ^{13}C NMR data agrees with data from within the group.

Methyl 6α-fluoro-3α-hydroxy-7-oxo-5β-cholan-24-oate (2.68), Methyl 6β-fluoro-3α-hydroxy-7-oxo-5β-cholan-24-oate (2.69)

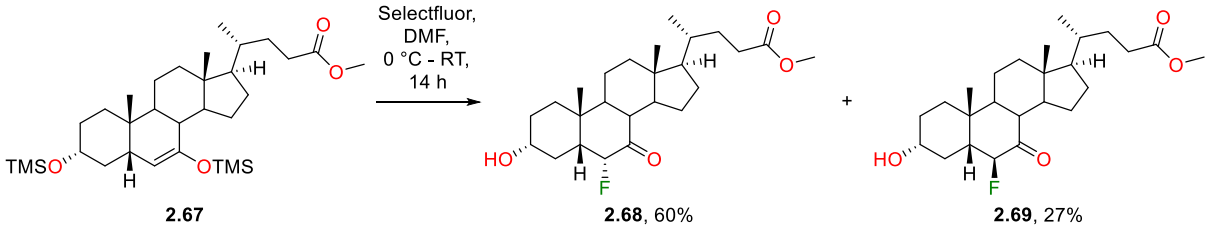

2.67 **2.68**, 60% **2.69**, 27%

The silyl enol ether **2.67** (15.4 g, 26 mmol, 1.0 equiv) was dissolved in dry DMF (60 mL), cooled to 0 °C and a suspension of Selectfluor® (13.8 g, 39.0 mmol, 1.5 equiv) in dry DMF (60 mL) was added. After stirring for 14 h, the reaction mixture was quenched with water (400 mL) and the resulting mixture was extracted with EtOAc (3 x 150 mL). The combined organic phases were washed with brine (400 mL) and dried over Na_2SO_4, before reducing *in vacuo* to give 12.3 g of crude material. The crude was purified by flash chromatography (acetone/PE: 15%/85% → 20%/80%), firstly giving **2.68** (3.00 g, 7.10 mmol, 27%), followed by **2.69** (6.60 g, 15.6 mmol, 60%), both as white gummy solids.

2.68: **R_f** 0.18 (Acetone/PE 20/80). **^{1}H NMR** (400 MHz, $CDCl_3$) δ 5.20 (dd, *J*=49.6, 6.6 Hz, 1H, 6β-**H**), 3.64 (s, 3H, 24-COO**CH_3**), 3.51-3.61 (m, 1H, 3β-**H**), 2.16-2.41 (m, 5H, overlapping 5β-**H**, 23-**H'**, 23-**H''**, 8β-**H**, 15-**H**), 1.62-2.11 (m), 1.22-1.58 (m), 1.20 (s, 3H, 19-**CH_3**), 0.92-1.18 (m, 4H), 0.90 (d, *J*=6.4 Hz, 3H, 21-**CH_3**), 0.63 (s, 3H, 18-**CH_3**) ppm. **^{13}C NMR** (100 MHz, $CDCl_3$) δ 205.8 (d, *J*=13.2 Hz, **7-C**), 174.6 (**24-COO**CH_3), 91.8 (d, *J*=193.7 Hz, **6-CH**), 70.0 (**3-CH**), 54.6 (**17-CH**), 51.4 (**24-**COO**CH_3**), 50.8 (d, *J*=15.4 Hz, **5-CH**), 48.4 (**14-CH**), 47.6 (**8-CH**), 42.6 (**13-C**), 42.5 (**9-CH**), 38.6 (**12-CH_2**), 35.9 (d, *J*=6.6 Hz, **10-C**), 35.1 (**20-CH**), 34.2 (**1-CH_2**), 31.0 (**23-CH_2**), 30.9 (**22-CH_2**), 30.0 (d, *J*=5.1 Hz, **4-CH_2**), 29.4 (**2-CH_2**), 28.1 (**16-CH_2**), 24.3 (**15-CH_2**), 23.2 (**19-CH_3**), 21.5 (**11-CH_2**), 18.2 (**21-CH_3**), 11.9 (**18-CH_3**) ppm. **^{19}F NMR** (376MHz, $CDCl_3$) δ -201.88 (br d, *J*=50.3 Hz, 1F, 6α-**F**) ppm. **^{19}F [^{1}H] NMR** (376MHz, $CDCl_3$) δ -201.88 (s, 1F, 6α-**F**) ppm. **LRMS (ESI+)** m/z: 440.2 $[M+NH_4]^+$. ^{1}H and ^{13}C NMR data agree with data from within the group and partial literature data.[228] ^{19}F NMR data agrees with data from within the group.

2.69: **R_f** 0.27 (Acetone/PE 20/80). **^{1}H NMR** (400 MHz, $CDCl_3$) δ 4.28 (dd, *J*=51.7, 3.1 Hz, 1H, 6α-**H**), 3.65 (s, 3H, 24-COO**CH_3**), 3.56-3.63 (m, 1H, 3β-**H**), 2.97 (td, *J*=11.3, 5.1 Hz, 1H, 8β-**H**), 2.34 (ddd,

J=15.4, 10.1, 5.3 Hz, 1H, 23-**H'**), 2.13-2.26 (m, 2H, 23-**H''** and 5β-**H**), 1.26-2.12 (m), 1.24 (d, *J*=3.3 Hz, 3H, 19-**CH_3**), 0.93-1.22 (m), 0.91 (d, *J*=6.4 Hz, 3H, 21-**CH_3**), 0.69 (s, 3H, 18-**CH_3**) ppm. **^{13}C NMR** (100 MHz, $CDCl_3$) δ 208.3 (d, *J*=22.0 Hz, **7-C**), 174.6 (**24-COO**CH_3), 97.9 (d, *J*=184.1 Hz, **6-CH**), 70.1 (d, *J*=2.9 Hz, **3-CH**), 54.8 (**17-CH**), 51.5 (**24-**COO**CH_3**), 49.7 (d, *J*=18.3 Hz, **5-CH**), 48.1 (**14-CH**), 45.7 (d, *J*=2.9 Hz, **8-CH**), 44.2 (**9-CH**), 42.3 (**13-C**), 38.8 (**12-CH_2**), 35.2 (**20-CH**), 34.8 (d, *J*=1.5 Hz, **10-C**), 34.5 (**1-CH_2**), 32.2 (d, *J*=10.3 Hz, **4-CH_2**), 31.0 (**23-CH_2**), 30.9 (**22-CH_2**), 29.6 (**2-CH_2**), 28.1 (**16-CH_2**), 24.8 (d, *J*=6.6 Hz, **19-CH_3**), 24.2 (**15-CH_2**), 21.6 (**11-CH_2**), 18.3 (**21-CH_3**), 11.9 (**18-CH_3**) ppm. **^{19}F NMR** (376MHz, $CDCl_3$) δ -178.11 (br dd, *J*=51.2, 13.0 Hz, 1F, 6β-**F**) ppm. **^{19}F [^{1}H] NMR** (376MHz, $CDCl_3$) δ -178.11 (s, 1F, 6β-**F**) ppm. ^{1}H, ^{13}C and ^{19}F NMR data agree with data from within the group.

Methyl 6-fluoro-3α,7-bis(trimethylsilyloxy)-5β-cholan-6-en-24-oate (2.70)

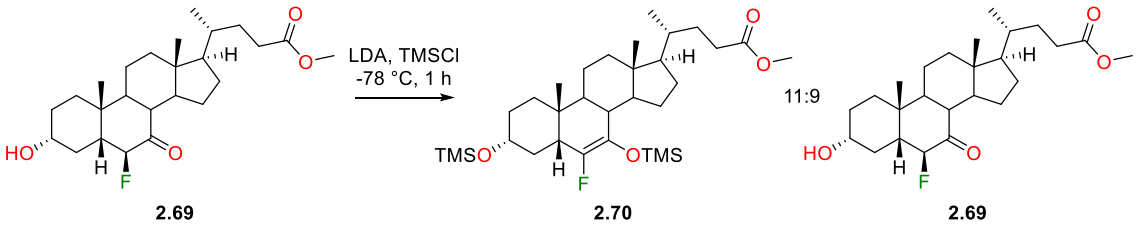

2.69 **2.70** **2.69**

To a flame-dried flask under argon diisopropylamine (8.5 mL, 60 mmol, 5.0 equiv) and dry THF (75 mL) were added. The solution was cooled to -78 °C and *n*-BuLi (2.5 M in hexanes, 24 mL, 60 mmol, 5.0 equiv) was added dropwise over 15 min. After stirring for 30 min, chlorotrimethylsilane (7.5 mL, 60 mmol, 5.0 equiv) was added to the reaction mixture. After stirring for a further 30 min, a solution of **2.69** (5.03 g, 11.9 mmol, 1.0 equiv) in dry THF (550 mL) was added to the reaction mixture at -78 °C. After stirring for 60 min, NEt_3 (17 mL, 120 mmol, 10 equiv) was added to the reaction mixture. After stirring for a further 30 min, the reaction mixture was warmed to -10 °C and added sat. $NaHCO_3$ (30 mL). Following a further 20 min of stirring, the mixture was extracted with EtOAc (3 x 80 mL). The combined organic phases were then washed with sat. $NaHCO_3$ (200 mL), water (200 mL) and brine (200 mL) before drying over Na_2SO_4 and reducing *in vacuo* to yield an 11:9 mixture of **2.70** and **2.69** (6.8 g, ~50% yield). The crude material was used in the next reaction without purification.

R_f 0.93 (Acetone/PE 20/80). **Selected ^{1}H NMR** (400 MHz, $CDCl_3$) 3.66 (s, 3H, 24-COO**CH_3**), 3.50-3.62 (m, 1H, 3β-**H**), 2.35 (ddd, *J*=15.4, 9.7, 5.4 Hz, 1H, 23-**H'**), 0.92 (br d, *J*=6.4 Hz, 3H, 21-**CH_3**), 0.85 (s, 2H, 18-**CH_3**), 0.68 (s, 2H, 18-**CH_3**), 0.16 (d, *J*=1.6 Hz, 6H, 7-OSi**Me_3**), 0.11 (s, 5H, 3α-OSi**Me_3**) ppm. **Selected ^{13}C NMR** (100 MHz, $CDCl_3$) δ 174.7 (**24-COO**CH_3), 146.9 (d, *J*=246.5 Hz, **6-C**), 131.9 (d, *J*=9.5 Hz, **7-C**), 70.7 (**3-C**), 51.4 (**24-**COO**CH_3**), 22.4 (**19-CH_3**), 18.4 (**21-CH_3**), 12.2 (**18-CH_3**), 0.5 (d, *J*=2.9 Hz, **7-OSiMe_3**), 0.2 (**3-OSiMe_3**) ppm. **Selected ^{19}F NMR** (376MHz, $CDCl_3$) δ -135.21 (br s, 1F, 6-**F**) ppm.

Selected ^{19}F [^{1}H] NMR (376MHz, $CDCl_3$) δ -135.20 (s, 1F, 6-**F**) ppm. **LRMS (ESI+)** m/z: 584.3 $[M+NH_4]^+$, 567.3 $[M+H]^+$.

Methyl 6,6-difluoro-3α-hydroxy-7-oxo-5β-cholan-24-oate (2.18)

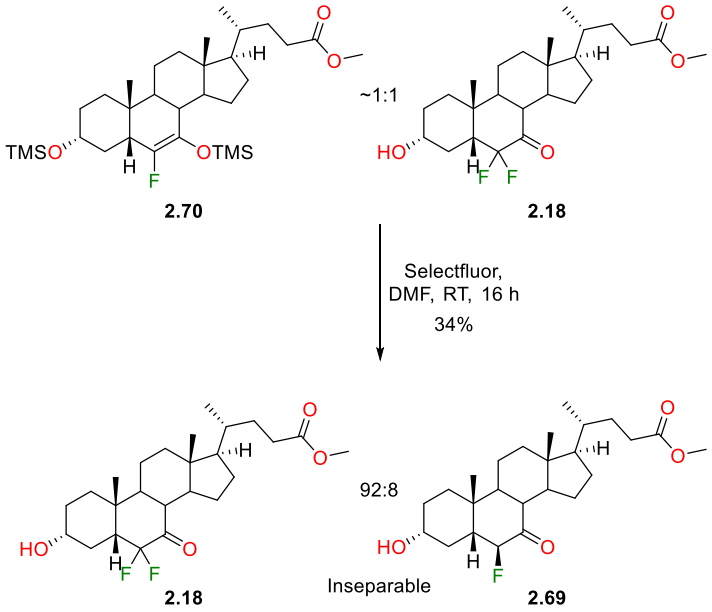

The ~1:1 mixture of silyl enol ether **2.70** and ketone **2.18** (5.85 g, 10.6 mmol, 1.0 equiv) was dissolved in dry DMF (25 mL), cooled to 0 °C and a suspension of Selectfluor® (5.63 g, 15.9 mmol, 1.5 equiv) in dry DMF (2 mL) was added. After stirring for 14 h, the reaction mixture was quenched with water (250 mL) and the resulting mixture was extracted with EtOAc (3 x 100 mL). The combined organic phases were washed with brine (2 x 200 mL) and dried over Na_2SO_4, before reducing *in vacuo* to give 4.2 g of crude material. The crude was purified by flash chromatography (Biotage ZIP KP-Sil 120 g cartridge, acetone/PE: 15%/85% → 30%/70%) to yield a 92:8 mixture of **2.18** and **2.69** as a white solid (1.90 g, ~4.0 mmol, ~34%).

R_f 0.26 (Acetone/PE 20/80). **^{1}H NMR** (400 MHz, $CDCl_3$) δ 3.65 (s, 3H, 24-COO**CH_3**), 3.55-3.63 (m, 1H, 3β-**H**), 2.81 (td, *J*=11.3, 5.4 Hz, 1H, 8β-**H**), 2.35 (ddd, *J*=15.3, 9.9, 5.4 Hz, 1H, 23-**H'**), 1.25-2.28 (m), 1.23 (d, *J*=4.2 Hz, 3H, 19-**CH_3**), 0.94-1.21 (m), 0.92 (d, *J*=6.4 Hz, 3H, 21-**CH_3**), 0.68 (s, 3H, 18-**CH_3**) ppm. **^{13}C NMR** (100 MHz, $CDCl_3$) δ 200.1 (dd, *J*=28.6, 22.0 Hz, **7-C**), 174.6 (**24-COO**CH_3), 117.4 (dd, *J*=259.7, 249.4 Hz, **6-C**), 69.5 (**3-CH**), 54.6 (**17-CH**), 52.2 (dd, *J*=19.8, 16.9 Hz, **5-CH**), 51.5 (**24-COOCH_3**), 48.3 (**14-CH**), 46.5 (**8-CH**), 42.9 (**9-CH**), 42.5 (**13-C**), 38.5 (**12-CH_2**), 35.5 (d, *J*=5.9 Hz, **10-C**), 35.1 (**20-CH**), 34.5 (**1-CH_2**), 31.0 (**23-CH_2**), 30.9 (**22-CH_2**), 30.5 (t, *J*=5.9 Hz, **4-CH_2**), 29.4 (CH_2), 28.1 (CH_2), 24.2 (CH_2), 24.1 (d, *J*=6.6 Hz, **19-CH_3**), 21.4 (**11-CH_2**), 18.3 (**21-CH_3**), 11.9 (**19-CH_3**) ppm. **^{19}F NMR** (376MHz, $CDCl_3$) δ -100.72 (br dd, *J*=249.7, 13.9 Hz, 1F, 6β-**F**), -117.56 (br d, *J*=248.0 Hz, 1F, 6α-**F**) ppm. **^{19}F [^{1}H] NMR** (376MHz, $CDCl_3$) δ -100.65 (d, *J*=248.0 Hz, 1F, 6β-**F**), -117.56 (d, *J*=248.0

Hz, 1F, 6α-**F**) ppm. **LRMS (ESI+)** m/z: 458.3 $[M+NH_4]^+$. **HRMS (ESI+)** $C_{25}H_{38}F_2NaO_4$ $[M+Na]^+$. Calculated: 463.2630; Found: 463.2635 (0.9 ppm error).

Methyl 6α,6β-difluoro-3α-acetoxy-7-oxo-5β-cholan-24-oate (2.71)

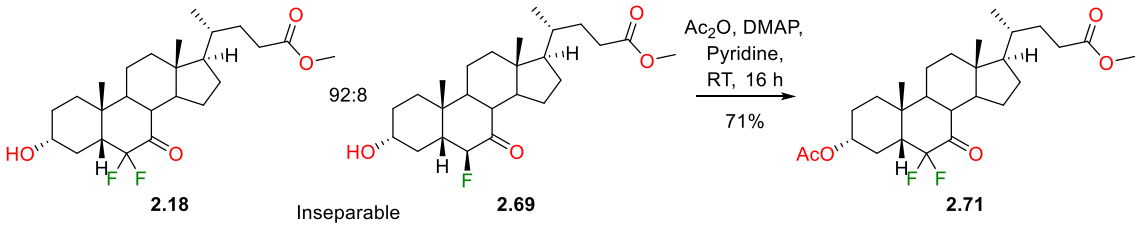

Following general procedure E, the 92:8 mixture of **2.18** and **2.69** (1.82 g, ~4.1 mmol, 1.0 equiv) was protected. The crude material was purified twice by flash chromatography (1st: Biotage SNAP KP-Sil 100 g cartridge, acetone/PE: 0%/100% → 60%/40% over 18 CV; 2nd: Biotage SNAP KP-Sil 50 g cartridge, acetone/PE 0%/100% → 35%/65% over 17 CV) to yield **2.71** as a white solid (1.40 g, 2.90 mmol, ~70%).

mp 149 – 150 °C. $\mathbf{R_f}$ 0.21 (Acetone/PE 10/90). $\mathbf{[\alpha]_D}$ - 43.4 (c = 1.0, $CHCl_3$, 21 °C). **^{1}H NMR** (400 MHz, $CDCl_3$) δ 4.68 (tt, *J*=11.1, 4.5 Hz, 1H, 3β-**H**), 3.66 (s, 3H, 24-COO**CH_3**), 2.83 (td, *J*=11.3, 5.3 Hz, 1H, 8β-**H**), 2.10-2.40 (m, 4H, overlapping 5β-**H**, 23-**H'**, 23-**H''** and 15α-**H**), 2.00-2.05 (m, 1H, 12β-**H**), 1.99 (s, 3H, 3α-OCO**CH_3**), 1.69-1.98 (m), 1.26-1.61 (m), 1.24 (d, *J*=4.3 Hz, 3H, 19-**CH_3**), 1.06-1.21 (m), 0.93-1.05 (m, 1H, 15β-**H**), 0.92 (d, *J*=6.5 Hz, 3H, 21-**CH_3**), 0.68 (s, 3H, 18-**CH_3**) ppm. **^{13}C NMR** (100 MHz, $CDCl_3$) δ 199.9 (dd, *J*=28.2, 22.4 Hz, **7-C**), 174.5 (**24-COO**CH_3), 170.2 (**3α-OCO**CH_3), 117.1 (dd, *J*=261.2, 249.4 Hz, **6-C**), 71.4 (d, *J*=2.2 Hz, **3-CH**), 54.7 (**17-CH**), 52.0 (dd, *J*=20.5, 16.9 Hz, **5-CH**), 51.4 (**24-**COO**CH_3**), 48.2 (**14-CH**), 46.4 (**8-CH**), 43.0 (**9-CH**), 42.5 (**13-C**), 38.5 (**12-CH_2**), 35.5 (d, *J*=5.1 Hz, **10-C**), 35.1 (**20-CH**), 34.2 (**1-CH_2**), 31.0 (**23-CH_2**), 30.9 (**22-CH_2**), 28.1 (**16-CH_2**), 26.7 (t, *J*=6.6 Hz, **4-CH_2**), 25.8 (**2-CH_2**), 24.2 (**15-CH_2**), 24.1 (d, *J*=6.6 Hz, **19-CH_3**), 21.5 (**11-CH_2**), 21.1 (**3α-**OCO**CH_3**), 18.3 (**21-CH_3**), 11.9 (**18-CH_3**) ppm. **^{19}F NMR** (376MHz, $CDCl_3$) δ -101.44--100.32 (m, contains d *J*=249.7 Hz, 1F, 6β-**F**), -117.71 (br d, *J*=249.7 Hz, 1F, 6α-**F**) ppm. **^{19}F [^{1}H] NMR** (376MHz, $CDCl_3$) δ -100.85 (d, *J*=249.7 Hz, 1F, 6β-**F**), -117.71 (d, *J*=249.7 Hz, 1F, 6α-**F**) ppm. **LRMS (ESI+)** m/z: 500.2 $[M+NH_4]^+$. **HRMS (ESI+)** $C_{27}H_{40}F_2NaO_5$ $[M+Na]^+$. Calculated: 505.2736; Found: 505.2745 (1.8 ppm error). **IR** (neat, cm^{-1}) 2950 – 2873 (m), 1738 (s), 1254 (m), 1040 (m).

6α,6β-Difluoro-7-oxo-lithocholic acid (2.73)

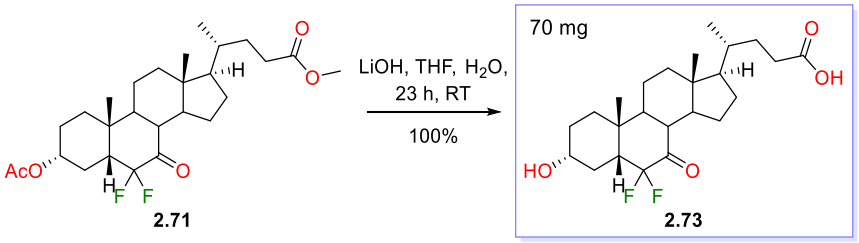

Following general procedure C, **2.71** (80 mg, 0.16 mmol, 1.0 equiv) was deprotected to yield **2.73** as a white solid (69 mg, 0.16 mmol, 100%) with no further purification.

mp 185 – 186 °C. **R_f** 0.18 (EtOAc/PE 70/30). **$[\alpha]_D$** - 48.1 (c = 0.45, MeOH, 21 °C). **^{1}H NMR** (400 MHz, MeOH-d_4) δ 3.49-3.61 (m, 1H, 3β-**H**), 2.86 (td, *J*=11.2, 5.3 Hz, 1H, 8β-**H**), 2.11-2.40 (m, 4H, overlapping 23-**H'**, 23-**H''**, 5β-**H** and 15α-**H**), 2.07 (br d, *J*=13.0 Hz, 1H, 12β-**H**), 1.27-2.03 (m), 1.25 (br d, *J*=4.2 Hz, 3H, 19-**CH_3**), 1.15-1.24 (m, 2H), 0.99-1.09 (m, 2H), 0.98 (d, *J*=6.5 Hz, 3H, 21-**CH_3**), 0.74 (s, 3H, 18-**CH_3**) ppm. **^{13}C NMR** (100 MHz, MeOH-d_4) δ 201.6 (dd, *J*=28.6, 22.0 Hz, **7-C**), 178.1 (**24-COOH**), 119.0 (dd, *J*=259.7, 248.7 Hz, **6-C**), 70.3 (**3-CH**), 56.2 (**17-CH**), 53.4 (dd, *J*=19.4, 17.2 Hz, **5-CH**), 49.8 (**14-CH**), 47.9 (**8-CH**), 44.4 (**9-CH**), 43.8 (**13-C**), 40.0 (**12-CH_2**), 36.8 (d, *J*=5.9 Hz, **10-C**), 36.6 (**20-CH**), 35.6 (**1-CH_2**), 32.4 (**22-CH_2**), 32.1 (**23-CH_2**), 31.5 (br t, *J*=5.9 Hz, **4-CH_2**), 30.4 (**2-CH_2**), 29.3 (**16-CH_2**), 25.5 (**15-CH_2**), 24.7 (br d, *J*=6.6 Hz, **19-CH_3**), 22.7 (**11-CH_2**), 19.0 (**21-CH_3**), 12.5 (**18-CH_3**) ppm. **^{19}F NMR** (376MHz, MeOH-d_4) δ -101.49--100.62 (m, contains d *J*=249.7 Hz, 1F, 6β-**F**), -118.26 (br d, *J*=249.7 Hz, 1F, 6α-**F**) ppm. **^{19}F [^{1}H] NMR** (376MHz, MeOH-d_4) δ -101.05 (d, *J*=249.7 Hz, 1F, 6β-**F**), -118.26 (d, *J*=249.7 Hz, 1F, 6α-**F**) ppm. **LRMS (ESI+)** m/z: 444.2 $[M+NH_4]^+$. **HRMS (ESI+)** $C_{24}H_{36}F_2NaO_4$ $[M+Na]^+$. Calculated: 449.2474; Found: 449.2477 (0.6 ppm error). **IR** (neat, cm^{-1}) 3386 (b), 2942 – 2873 (m), 1744 (s), 1708 (s), 1048 (s).

7.3.4 Synthesis of Analogues from DCA

Methyl 3α,12α-dihydroxy-5β-cholan-24-oate (2.77)

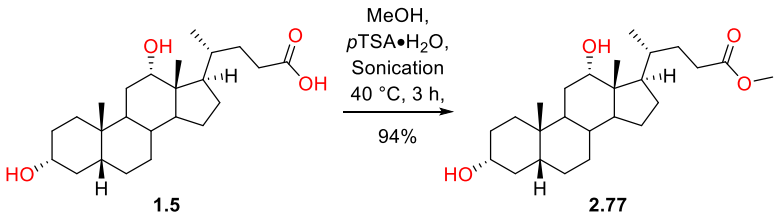

Following general procedure A, DCA (**1.5**, 7.00 g, 17.8 mmol, 1.0 equiv) was protected to yield **2.77** as a white solid (7.00 g, 17.2 mmol, 97%) with no further purification.

mp 63 – 64 °C (lit. 58 °C/149 °C[96,220]). **R_f** 0.44 (EtOAc/PE 50/50). **^{1}H NMR** (400 MHz, $CDCl_3$) δ 3.98 (br s, 1H, 12β-**H**), 3.66 (s, 3H, 24-COO**CH_3**), 3.61 (tt, *J*=11.0, 4.9 Hz, 1H, 3β-**H**), 2.37 (ddd, *J*=15.4, 10.3,

5.3 Hz, 1H, 23-**H'**), 2.24 (ddd, *J*=15.8, 9.5, 6.7 Hz, 1H, 23-**H''**), 1.00-1.93 (m), 0.97 (d, *J*=6.2 Hz, 3H, 21-**CH_3**), 0.91 (s, 3H, 19-**CH_3**), 0.68 (s, 3H, 18-**CH_3**) ppm. **^{13}C NMR** (100 MHz, $CDCl_3$) δ 174.7 (**24-COO**CH_3), 73.1 (**12-CH**), 71.8 (**3-CH**), 51.5 (**24**-COO**CH_3**), 48.2 (CH), 47.3 (CH), 46.5 (**13-C**), 42.0 (CH), 36.4 (CH_2), 36.0 (CH), 35.2 (CH_2), 35.1 (**20-CH**), 34.1 (**10-C**), 33.6 (CH), 31.1 (**23-CH_2**), 30.9 (**22-CH_2**), 30.4 (CH_2), 28.6 (CH_2), 27.4 (CH_2), 27.1 (CH_2), 26.1 (CH_2), 23.6 (CH_2), 23.1 (**19-CH_3**), 17.3 (**21-CH_3**), 12.7 (**18-CH_3**) ppm. **LRMS (ESI+)** m/z: 814.0 $[2M+H]^+$, 429.6 $[M+Na]^+$, 389.5 $[M+H-H_2O]^+$, 371.6 $[M+H-2H_2O]^+$. ^{1}H and ^{13}C NMR data agree with literature.[229]

Methyl 3α,12α-diacetoxy-5β-cholan-24-oate (2.78), Methyl 3α-acetoxy-12α-hydroxy-5β-cholan-24-oate (2.79)

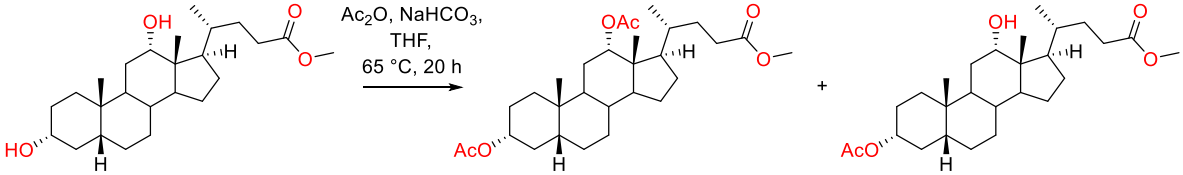

2.77 **2.78**, 13% **2.79**, 78%

Following general procedure F, **2.77** (6.94 g, 17.1 mmol, 1.0 equiv) was protected. The crude material was purified by flash chromatography (acetone/PE 5%/95% → 10%/90%), firstly yielding **2.78** (1.10 g, 2.24 mmol, 13%), then **2.79** (6.02 g, 13.4 mmol, 78%), both as white gummy solids.

2.78: **R_f** 0.33 (Acetone/PE 10/90). **^{1}H NMR** (400 MHz, $CDCl_3$) δ 5.08 (br t, *J*=2.8 Hz, 1H, 12β-**H**), 4.70 (tt, *J*=11.4, 4.5 Hz, 1H, 3β-**H**), 3.66 (s, 3H, 24-COO**CH_3**), 2.33 (ddd, *J*=15.4, 10.1, 5.3 Hz, 1H, 23-**H'**), 2.19 (ddd, *J*=15.9, 9.5, 6.8 Hz, 1H, 23-**H''**), 2.10 (s, 3H, 12α-OCO**CH_3**), 2.03 (s, 3H, 3α-OCO**CH_3**), 0.94-1.94 (m), 0.90 (s, 3H, 19-**CH_3**), 0.80 (d, *J*=6.4 Hz, 3H, 21-**CH_3**), 0.72 (s, 3H, 18-**CH_3**) ppm. **^{13}C NMR** (100 MHz, $CDCl_3$) δ 174.5 (**24-COO**CH_3), 170.5 (**3α-OCO**CH_3), 170.4 (**12α-OCO**CH_3), 75.9 (**12-CH**), 74.2 (**3-CH**), 51.5 (**24**-COO**CH_3**), 49.4 (**14-CH**), 47.6 (**17-CH**), 45.0 (**13-C**), 41.8 (**5-CH**), 35.6 (**8-CH**), 34.7 (**1-CH_2**), 34.7 (**20-CH**), 34.4 (**9-CH**), 34.0 (**10-C**), 32.2 (CH_2), 30.9 (**23-CH_2**), 30.8 (**22-CH_2**), 27.3 (CH_2), 26.9 (CH_2), 26.6 (**2-CH_2**), 25.8 (CH_2), 25.6 (CH_2), 23.4 (CH_2), 23.0 (**19-CH_3**), 21.4 (**3α**-OCO**CH_3**), 21.3 (**12α**-OCO**CH_3**), 17.5 (**21-CH_3**), 12.4 (**19-CH_3**) ppm. **LRMS (ESI+)** m/z: 508.2 $[M+NH_4]^+$. ^{1}H NMR data agrees with partial literature data,[230] ^{13}C NMR data agrees with literature data.[231]

2.79: **R_f** 0.26 (Acetone/PE 10/90). **^{1}H NMR** (400 MHz, $CDCl_3$) δ 4.70 (tt, *J*=11.4, 4.8 Hz, 1H, 3β-**H**), 3.98 (br q, *J*=3.4 Hz, 1H, 12β-**H**), 3.66 (s, 3H, 24-COO**CH_3**), 2.36 (ddd, *J*=15.4, 10.1, 5.1 Hz, 1H, 23-**H'**), 2.23 (ddd, *J*=15.8, 9.4, 6.7 Hz, 1H, 23-**H''**), 2.01 (s, 3H, 3α-OCO**CH_3**), 0.98-1.93 (m), 0.97 (d, *J*=6.4 Hz, 3H, 21-**CH_3**), 0.91 (s, 3H, 19-**CH_3**), 0.67 (s, 3H, 18-**CH_3**) ppm. **^{13}C NMR** (100 MHz, $CDCl_3$) δ 174.6 (**24-COO**CH_3), 170.6 (**3α-OCO**CH_3), 74.2 (**3-CH**), 73.1 (**12-CH**), 51.5 (**24**-COO**CH_3**), 48.2 (**14-CH**), 47.3 (**17-CH**), 46.5 (**13-C**), 41.8 (**5-CH**), 35.9 (**8-CH**), 35.0 (**20-CH**), 34.8 (CH_2), 34.1 (**10-C**), 33.6 (**9-CH**), 32.1 (CH_2), 31.0 (**23-CH_2**), 30.9 (**22-CH_2**), 28.7 (CH_2), 27.4 (CH_2), 26.9 (CH_2), 26.5 (**1-CH_2**), 26.0 (CH_2), 23.6

(CH_2), 23.1 (**19-CH_3**), 21.4 (**3α**-OCO**CH_3**), 17.3 (**21-CH_3**), 12.7 (**18-CH_3**) ppm. **LRMS (ESI+)** m/z: 466.2 $[M+NH_4]^+$. ^1H and ^{13}C NMR data agree with literature.[232]

Methyl 3α-acetoxy-12-oxo-5β-cholan-24-oate (2.80)

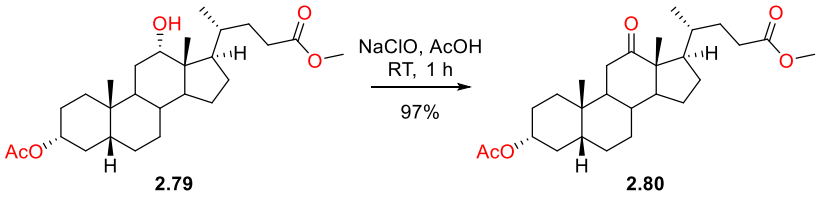

2.79 **2.80**

The alcohol **2.79** (6.02 g, 13.4 mmol, 1.0 equiv) was dissolved in acetic acid (75 mL) and NaClO (~11% in H_2O, ~25 mL, ~40 mmol, ~3 equiv) was added dropwise over the course of 1 h. After the full addition of NaClO, the reaction mixture was diluted with water and filtered. The resulting solid residue was dissolved in EtOAc (250 mL) and the organic phase was washed with sat. $NaHCO_3$ (200 mL), water (200 mL) and brine (200 mL) before drying over Na_2SO_4 and reducing *in vacuo* to yield **2.80** as a white solid (5.78 g, 12.9 mmol, 97%).

mp 134 – 135 °C. **R_f** 0.56 (EtOAc/PE 25/75). **^{1}H NMR** (400 MHz, $CDCl_3$) δ 4.69 (tt, *J*=11.2, 4.0 Hz, 1H, 3β-**H**), 3.65 (s, 3H, 24-COO**CH_3**), 2.47 (t, *J*=12.1 Hz, 1H, 11β-**H**), 2.38 (ddd, *J*=15.4, 9.8, 5.1 Hz, 1H, 23-**H'**), 2.25 (ddd, *J*=15.7, 9.1, 6.8 Hz, 1H, 23-**H''**), 2.01-2.06 (m, 2H), 2.00 (s, 3H, 3α-OCO**CH_3**), 1.04-1.98 (m), 0.95-1.04 (m, 6H, 19-**CH_3** and 18-**CH_3**), 0.84 (d, *J*=6.5 Hz, 3H, 21-**CH_3**) ppm. **^{13}C NMR** (100 MHz, $CDCl_3$) δ 214.6 (**12-C**), 174.6 (**24-COO**CH_3), 170.6 (**3α-OCO**CH_3), 73.7 (**3-CH**), 58.6 (**14-CH**), 57.5 (**13-C**), 51.4 (**24**-COO**CH_3**), 46.4 (**17-CH**), 44.0 (**9-CH**), 41.3 (**5-CH**), 38.1 (**11-CH_2**), 35.6 (**8-CH**), 35.6 (**20-CH**), 35.3 (**10-C**), 34.9 (**1-CH_2**), 32.1 (CH_2), 31.3 (**23-CH_2**), 30.5 (**22-CH_2**), 27.5 (CH_2), 26.9 (CH_2), 26.3 (**2-CH_2**), 26.0 (CH_2), 24.3 (CH_2), 22.7 (**19-CH_3**), 21.4 (**3α**-OCO**CH_3**), 18.5 (**21-CH_3**), 11.6 (**18-CH_3**) ppm. **LRMS (ESI+)** m/z: 464.2 $[M+NH_4]^+$. ^1H and ^{13}C NMR data agree with literature[232]

Methyl 12α,12β-difluoro-3α-acetoxy-5β-cholan-24-oate (2.81)

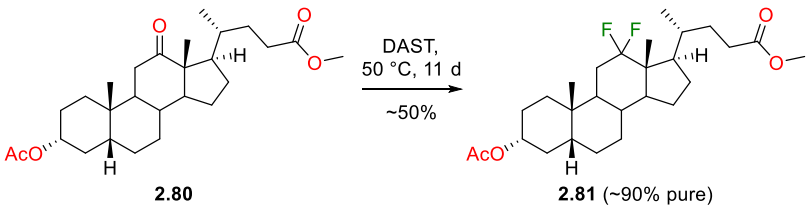

2.80 **2.81** (~90% pure)

The ketone **2.80** (5.03 g, 11.3 mmol, 1.0 equiv) and DAST (12 mL, 90.8 mmol, ~8 equiv) were added to a flame-dried flask under argon and heated to 50 °C. After 3 d, further DAST (4 mL, ~30 mmol, ~2.5 equiv) was added to the reaction mixture at RT and was heated again at 50 °C. 5 d following the start of the reaction, further DAST (10 mL, ~76 mmol, ~6.5 equiv) was added. 11 d after starting the reaction, the reaction mixture was cooled to RT, diluted with DCM (100 mL) and quenched by

the slow addition of the reaction mixture (~5 mL per min) to icy sat. $NaHCO_3$ solution (~600 mL). The mixture was extracted with DCM (3 x 100 mL) and the combined organic phases were washed with sat. $NaHCO_3$ (500 mL) and brine (1 L). Full separation of the organic phase from the aqueous phase was not achieved, so the wet organics were reduced *in vacuo* and the resulting wet crude material was dissolved in EtOAc (400 mL). The organic phase was then washed with brine (300 mL) and dried over Na_2SO_4 before reducing *in vacuo* to give 11 g of crude material. The crude was purified by flash chromatography twice (1st: acetone/PE 4%/96% → 5%/95%; 2nd: acetone/PE 4%/96% → 6%/94%), yielding **2.81** around 90% pure as a light-brown solid (2.7 g, ~5.7 mmol, ~50%).

R_f 0.39 (Acetone/PE 10/90). **^{1}H NMR** (400 MHz, $CDCl_3$) δ 4.71 (tt, *J*=11.4, 4.5 Hz, 1H, 3β-**H**), 3.66 (s, 3H, 24-COO**CH_3**), 2.37 (ddd, *J*=15.4, 10.0, 5.3 Hz, 1H, 23-**H'**), 2.26 (ddd, *J*=16.1, 9.7, 6.7 Hz, 1H, 23-**H''**), 2.02 (s, 3H, 3α-OCO**CH_3**), 1.01-1.98 (m), 0.98 (dd, *J*=6.6, 1.7 Hz, 3H, 21-**CH_3**), 0.93 (s, 3H, 19-**CH_3**), 0.81 (s, 3H, 18-**CH_3**) ppm. (DAST impurity at 3.92 ppm). **^{13}C NMR** (100 MHz, $CDCl_3$) δ 174.6 (**24-COO**CH_3), 170.6 (**3α-OCO**CH_3), 126.4 (dd, *J*=250.5, 246.9 Hz, **12-C**), 73.9 (**3-CH**), 52.5 (d, *J*=7.3 Hz, **14-CH**), 51.4 (**24**-COO**CH_3**), 49.2 (dd, *J*=21.3, 19.8 Hz, **13-C**), 47.8 (d, *J*=2.2 Hz, **17-CH**), 41.4 (**5-CH**), 37.1 (d, *J*=9.5 Hz, **9-CH**), 34.8 (**1-CH_2**), 34.6 (**8-CH**), 34.1 (**10-C**), 33.2 (**20-CH**), 32.0 (**4-CH_2**), 31.5 (**23-CH_2**), 31.3 (br t, *J*=24.9 Hz, **11-CH_2**), 30.4 (**22-CH_2**), 26.7 (***15-CH_2* or *16-CH_2***), 26.4 (**2-CH_2**), 26.2 (***6-CH_2* or *7-CH_2***), 25.4 (d, *J*=1.5 Hz, ***15-CH_2* or *16-CH_2***), 23.0 (***6-CH_2* or *7-CH_2***), 22.9 (**19-CH_3**), 21.4 (**3α**-OCO**CH_3**), 18.9 (d, *J*=11.0 Hz, **21-CH_3**), 10.5 (dd, *J*=5.1, 1.5 Hz, **18-CH_3**) ppm. **^{19}F NMR** (376MHz, $CDCl_3$) δ -91.20 (br d, *J*=228.9 Hz, 1F, 12β-**F**), -112.21 (ddd, *J*=230.6, 34.7, 12.1 Hz, 1F, 12α-**F**) ppm. **^{19}F [^{1}H] NMR** (376MHz, $CDCl_3$) δ -91.20 (br d, *J*=228.9 Hz, 1F, 12β-**F**), -112.15 (d, *J*=230.6 Hz, 1F, 12α-**F**) ppm. **LRMS (ESI+)** m/z: 486.2 $[M+NH_4]^+$. **HRMS (ESI+)** $C_{27}H_{42}F_2NaO_4$ $[M+Na]^+$. Calculated: 491.2943; Found: 491.2950 (-1.5 ppm error).

12α,12β-Difluorolithocholic acid (2.21)

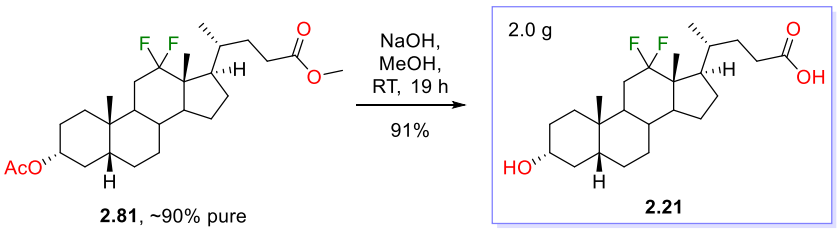

2.81, ~90% pure

2.21

Following general procedure D, **2.81** (~90% pure, 2.55 g, ~5.44 mmol, 1.0 equiv) was deprotected to yield **2.21** as an off-white solid (2.05 g, 4.97 mmol, ~91%) with no further purification.

mp 184 – 185 °C. **R_f** 0.09 (Acetone/PE 20/80). **[α]$_D$** + 56.2 (c = 0.25, $CHCl_3$/MeOH 1:1, 21°C). **^{1}H NMR** (400 MHz, $CDCl_3$) δ 3.64 (tt, *J*=11.1, 4.5 Hz, 1H, 3β-**H**), 2.44 (ddd, *J*=15.8, 10.1, 5.3 Hz, 1H, 23-**H'**), 2.31 (ddd, *J*=16.3, 9.8, 6.6 Hz, 1H, 23-**H''**), 1.04-2.00 (m), 1.01 (dd, *J*=6.5, 1.7 Hz, 3H, 21-**CH_3**), 0.93 (s, 3H, 19-**CH_3**), 0.82 (s, 3H, 18-**CH_3**) ppm. **^{13}C NMR** (100 MHz, DMSO-d_6) δ 174.7 (**24-COOH**), 126.8

(dd, *J*=250.5, 246.9 Hz, **12-C**), 69.6 (**3-CH**), 52.3 (d, *J*=7.3 Hz, **14-CH**), 48.7 (br t, *J*=19.8 Hz, **13-C**), 47.6 (d, *J*=1.5 Hz, **17-CH**), 41.0 (**5-CH**), 36.8 (d, *J*=8.8 Hz, **9-CH**), 36.1 (CH_2), 34.8 (**1-CH_2**), 34.0 (**8-CH**), 33.7 (**10-C**), 32.5 (**20-CH**), 31.2 (**23-CH_2**), 30.9 (br t, *J*=24.9 Hz, **11-CH_2**), 30.2 (**22-CH_2**), 30.1 (CH_2), 26.5 (CH_2), 25.8 (CH_2), 25.2 (CH_2), 22.7 (**19-CH_3**), 22.5 (CH_2), 18.9 (d, *J*=10.3 Hz, **21-CH_3**), 10.2 (d, *J*=5.1 Hz, **18-CH_3**) ppm. **^{19}F NMR** (376MHz, DMSO-d_6) δ -89.30 (br d, *J*=228.9 Hz, 1F, 12β-**F**), -111.05--109.92 (m, 1F, 12α-**F**) ppm. **^{19}F [^{1}H] NMR** (376MHz, DMSO-d_6) δ -89.30 (br d, *J*=228.9 Hz, 1F, 12β-**F**), -110.47 (d, *J*=228.9 Hz, 1F, 12α-**F**) ppm. **LRMS (ESI+)** m/z: 430.2 $[M+NH_4]^+$, 842.6 $[2M+NH_4]^+$. **HRMS (ESI+)** $C_{24}H_{38}F_2NaO_3$ $[M+Na]^+$. Calculated: 435.2681; Found: 435.2680 (0.2 ppm error). **IR** (neat, cm^{-1}) 3298 (m), 2925 – 2861 (m), 2571 (m), 1702 (s), 1018 (s).

Methyl 12α,12β-difluoro-3α-hydroxy-5β-cholan-24-oate (2.82)

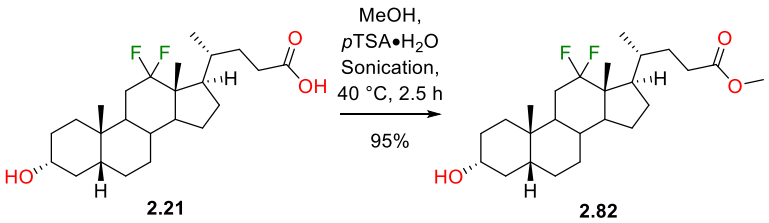

Following general procedure A, **2.21** (1.90 g, 4.61 mmol, 1.0 equiv) was protected to yield **2.82** as a light brown gummy solid (1.87 g, 4.38 mmol, 95%) with no further purification.

R_f 0.56 (Acetone/PE 30/70). **$[\alpha]_D$** + 43.8 (c = 1.0, $CHCl_3$, 21 °C). **^{1}H NMR** (400 MHz, $CDCl_3$) δ 3.66 (s, 3H, 24-COO**CH_3**), 3.62 (tt, *J*=11.1, 4.4 Hz, 1H, 3β-**H**), 2.37 (ddd, *J*=15.4, 10.0, 5.3 Hz, 1H, 23-**H'**), 2.25 (ddd, *J*=16.1, 9.7, 6.7 Hz, 1H, 23-**H''**), 1.00-1.99 (m), 0.98 (dd, *J*=6.5, 1.7 Hz, 3H, 21-**CH_3**), 0.92 (s, 3H, 19-**CH_3**), 0.80 (s, 3H, 18-**CH_3**) ppm. **^{13}C NMR** (100 MHz, $CDCl_3$) δ 174.7 (**24-COO**CH_3), 126.4 (dd, *J*=250.2, 247.2 Hz, **12-C**), 71.5 (**3-CH**), 52.5 (d, *J*=7.3 Hz, **14-CH**), 51.4 (**24-**COO**CH_3**), 49.1 (dd, *J*=21.3, 19.8 Hz, **13-C**), 47.7 (d, *J*=2.2 Hz, **17-CH**), 41.6 (**5-CH**), 37.1 (d, *J*=9.5 Hz, **9-CH**), 36.2 (CH_2), 35.1 (**1-CH_2**), 34.6 (**8-CH**), 34.1 (**10-C**), 33.1 (**20-CH**), 31.5 (**23-CH_2**), 31.2 (br t, *J*=25.7 Hz, **11-CH_2**), 30.4 (**22-CH_2**), 30.3 (**2-CH_2**), 26.9 (CH_2), 26.2 (CH_2), 25.5 (d, *J*=1.5 Hz, CH_2), 23.0 (CH_2), 22.9 (**19-CH_3**), 18.9 (d, *J*=11.0 Hz, **21-CH_3**), 10.5 (dd, *J*=4.4, 1.5 Hz, **18-CH_3**) ppm. **^{19}F NMR** (376MHz, $CDCl_3$) δ -91.18 (br d, *J*=228.9 Hz, 1F, 12β-**F**), -112.17 (ddd, *J*=230.6, 34.7, 12.1 Hz, 1F, 12α-**F**) ppm. **^{19}F [^{1}H] NMR** (376MHz, $CDCl_3$) δ -91.19 (d, *J*=228.9 Hz, 1F, 12β-**F**), -112.17 (d, *J*=228.9 Hz, 1F, 12α-**F**) ppm. **LRMS (ESI+)** m/z: 444.3 $[M+NH_4]^+$. **HRMS (ESI+)** $C_{25}H_{40}F_2NaO_3$ $[M+Na]^+$. Calculated: 449.2838; Found: 449.2844 (1.5 ppm error). **IR** (neat, cm^{-1}) 3351 (m), 2920 – 2861 (m), 1732 (s), 1038 (s).

Methyl 12α,12β-difluoro-3α-(phenoxycarbonothioyl)oxy-5β-cholan-24-oate (2.83)

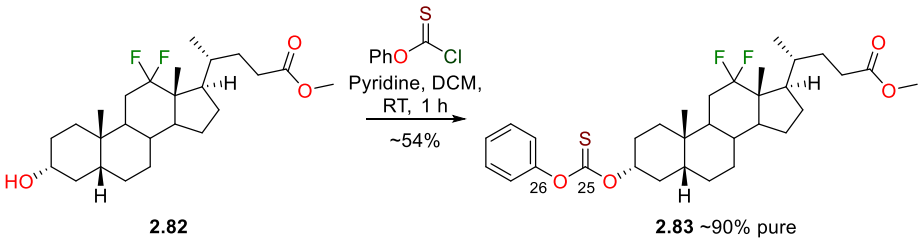

2.82 **2.83** ~90% pure

Following general procedure G, the thiocarbonate of **2.82** (1.65 g, 3.87 mmol, 1.0 equiv) was formed. The crude material was purified by flash chromatography (acetone/PE 0%/100% → 4%/96%) to yield **2.83** as an off-white solid, around 90% pure with aromatic impurities (1.38 g (~1.2 g), ~2.1 mmol, ~54%).

R_f 0.30 (EtOAc/PE 10/90). **^{1}H NMR** (400 MHz, $CDCl_3$) δ 7.40-7.45 (m, 2H, *meta* **CH**), 7.28-7.32 (m, 1H, *para*-**CH**), 7.09-7.14 (m, 2H, *ortho*-**CH**), 5.22 (tt, *J*=11.4, 5.0 Hz, 0.9H, 3β-**H**), 3.68 (s, 3H, 24-COO**CH_3**), 2.40 (ddd, *J*=15.4, 10.0, 5.1 Hz, 1H, 23-**H'**), 2.28 (ddd, *J*=16.0, 9.5, 6.6 Hz, 1H, 23-**H''**), 1.05-2.08 (m), 1.01 (dd, *J*=6.5, 1.4 Hz, 3H, 21-**CH_3**), 0.97 (s, 3H, 19-**CH_3**), 0.84 (s, 3H, 18-**CH_3**) ppm. **^{13}C NMR** (100 MHz, $CDCl_3$) δ 194.3 (**25-C=S**), 174.6 (**24-COO**CH_3), 153.3 (**26-C**), 129.4 (2C, ***meta*-C**), 126.4 (***para*-C**), 126.3 (dd, *J*=250.9, 247.2 Hz, **12-C**), 122.0 (2C, ***ortho*-C**), 84.4 (**3-CH**), 52.5 (d, *J*=7.3 Hz, **14-CH**), 51.4 (**24-**COO**CH_3**), 49.2 (br t, *J*=19.8 Hz, **13-C**), 47.8 (**17-CH**), 41.4 (**5-CH**), 37.1 (d, *J*=9.5 Hz, **9-CH**), 34.6 (**1-CH_2**), 34.6 (**8-CH**), 34.1 (**10-C**), 33.2 (**20-CH**), 31.5 (**23-CH_2**), 31.3 (br t, *J*=25.7 Hz, **11-CH_2**), 31.2 (**4-CH_2**), 30.4 (**22-CH_2**), 26.7 (CH_2), 26.2 (CH_2), 25.6 (**2-CH_2**), 25.4 (CH_2), 23.0 (CH_2), 22.8 (**19-CH_3**), 18.9 (d, *J*=11.0 Hz, **21-CH_3**), 10.5 (d, *J*=4.4 Hz, **18-CH_3**) ppm. **^{19}F NMR** (376MHz, $CDCl_3$) δ -91.26 (br d, *J*=228.9 Hz, 1F, 12β-**H**), -112.19 (ddd, *J*=230.6, 34.7, 12.1 Hz, 1F, 12α-**H**) ppm. **^{19}F [^{1}H] NMR** (376MHz, $CDCl_3$) δ -91.26 (d, *J*=228.9 Hz, 1F, 12β-**H**), -112.19 (d, *J*=230.6 Hz, 1F, 12α-**H**) ppm. **LRMS (ESI+)** m/z: 580.2 $[M+NH_4]^+$.

Methyl 12α,12β-difluoro-5β-cholan-24-oate (2.84)

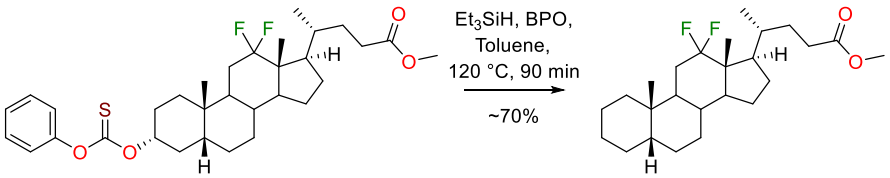

2.83 ~90% pure **2.84** ~90% pure

Following general procedure H, **2.83** (1.30g (~1.17 g), ~2.1 mmol, 1.0 equiv) was deoxygenated. The crude material was purified twice by flash chromatography (both Biotage SNAP KP-Sil 50 g cartridge, Et_2O/PE: 0%/100% → 5%/95%), yielding **2.84** around 90% pure, with aromatic impurities, as a white solid (665 mg (~600 mg), ~1.45 mmol, ~70%).

R_f 0.36 (Et_2O/PE 4/96). **^{1}H NMR** (400 MHz, $CDCl_3$) δ 3.67 (s, 3H, 24-COO**CH_3**), 2.38 (ddd, *J*=15.4, 10.0, 5.3 Hz, 1H, 23-**H'**), 2.26 (ddd, *J*=16.1, 9.7, 6.6 Hz, 1H, 23-**H''**), 1.05-1.99 (m), 0.99 (dd, *J*=6.6, 1.8 Hz, 3H, 21-**CH_3**), 0.92 (s, 3H, 19-**CH_3**), 0.82 (s, 3H, 18-**CH_3**) ppm. **^{13}C NMR** (100 MHz, $CDCl_3$) δ 174.7 (**24-COO**CH_3), 126.7 (dd, *J*=250.5, 246.9 Hz, **12-C**), 52.6 (d, *J*=6.6 Hz, **14-CH**), 51.4 (**24**-COO**CH_3**), 49.2 (t, *J*=19.8 Hz, **13-C**), 47.8 (d, *J*=2.2 Hz, **17-CH**), 43.2 (**5-CH**), 37.3 (CH_2), 37.2 (d, *J*=9.5 Hz, **9-CH**), 34.9 (**10-C**), 34.7 (**8-CH**), 33.2 (**20-CH**), 31.5 (**23-CH_2**), 31.3 (dd, *J*=26.4, 24.2 Hz, **11-CH_2**), 30.4 (**22-CH_2**), 27.2 (CH_2), 27.0 (CH_2), 26.8 (CH_2), 26.3 (**16-CH_2**), 25.6 (d, *J*=1.5 Hz, CH_2), 23.8 (**19-CH_3**), 23.1 (**15-CH_2**), 21.0 (CH_2), 18.9 (d, *J*=11.0 Hz, **21-CH_3**), 10.5 (dd, *J*=5.1, 1.5 Hz, **18-CH_3**) ppm. **^{19}F NMR** (376MHz, $CDCl_3$) δ -91.04 (br d, *J*=228.9 Hz, 1F, 12β-**F**), -112.27 (ddd, *J*=228.9, 34.7, 12.1 Hz, 1F, 12α-**F**) ppm. **^{19}F [^{1}H] NMR** (376MHz, $CDCl_3$) δ -91.04 (d, *J*=228.9 Hz, 1F, 12β-**F**), -112.27 (d, *J*=228.9 Hz, 1F, 12α-**F**) ppm. **LRMS (ESI+)** m/z: 428.2 $[M+NH_4]^+$. **HRMS (ESI+)** $C_{25}H_{40}F_2NaO_2$ $[M+Na]^+$. Calculated: 433.2889; Found: 433.2896 (1.6 ppm error).

12α,12β-Difluoro-5β-cholanic acid (2.19)

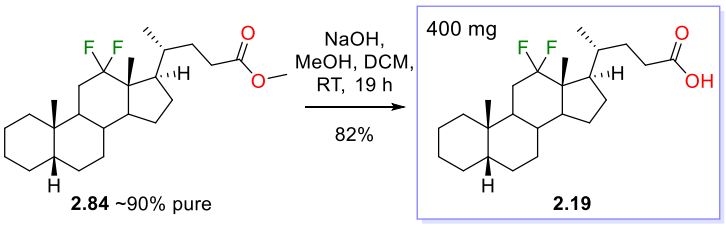

Following general procedure D, **2.84** (~90% pure, 620 mg (~560 mg), ~1.35 mmol, 1.0 equiv) was deprotected. The crude material was purified by flash chromatography (Biotage SNAP KP-Sil 25 g cartridge, acetone/DCM: 0%/100% → 10%/90%), cleanly yielding **2.19** as a white solid (440 mg, 1.11 mmol, ~82%).

mp 147 – 148 °C. **R_f** 0.30 (Acetone/PE 20/80). **[α]$_D$** + 43.1 (c = 1.03, $CHCl_3$, 21 °C). **^{1}H NMR** (400 MHz, $CDCl_3$) δ 2.43 (ddd, *J*=15.7, 10.3, 5.3 Hz, 1H, 23-**H'**), 2.31 (ddd, *J*=16.1, 9.8, 6.5 Hz, 1H, 23-**H''**), 1.03-2.00 (m), 1.01 (dd, *J*=6.5, 1.8 Hz, 3H, 21-**CH_3**), 0.93 (s, 3H, 19-**CH_3**), 0.82 (s, 3H, 18-**CH_3**) ppm. **^{13}C NMR** (100 MHz, $CDCl_3$) δ 180.5 (**24-COOH**), 126.7 (dd, *J*=250.5, 246.9 Hz, **12-C**), 52.6 (d, *J*=7.3 Hz, **14-CH**), 49.2 (dd, *J*=21.3, 19.1 Hz, **13-C**), 47.8 (d, *J*=2.2 Hz, **17-CH**), 43.2 (**5-CH**), 37.3 (CH_2), 37.2 (d, *J*=8.8 Hz, **9-CH**), 34.9 (**10-C**), 34.7 (**8-CH**), 33.2 (**20-CH**), 31.5 (**23-CH_2**), 31.3 (t, *J*=24.9 Hz, **11-CH_2**), 30.2 (**22-CH_2**), 27.2 (CH_2), 27.0 (CH_2), 26.8 (**1-CH_2**), 26.3 (**16-CH_2**), 25.6 (d, *J*=1.5 Hz, **7-CH_2**), 23.8 (**19-CH_3**), 23.1 (d, *J*=1.5 Hz, **15-CH_2**), 21.1 (**2-CH_2**), 18.9 (d, *J*=11.0 Hz, **21-CH_3**), 10.5 (dd, *J*=5.1, 1.5 Hz, **18-CH_3**) ppm. **^{19}F NMR** (376MHz, $CDCl_3$) δ -90.89 (br d, *J*=228.9 Hz, 1F, 12β-**F**), -112.25 (ddd, *J*=229.3, 34.2, 12.1 Hz, 1F, 12α-**F**) ppm. **^{19}F [^{1}H] NMR** (376MHz, $CDCl_3$) δ -90.90 (d, *J*=228.9 Hz, 1F, 12β-**F**), -112.25 (d, *J*=228.9 Hz, 1F, 12α-**F**) ppm. **LRMS (ESI+)** m/z: 414.2 $[M+NH_4]^+$. **HRMS (ESI+)** $C_{24}H_{38}F_2NaO_2$ $[M+Na]^+$.

Calculated: 419.2732; Found: 419.2724 (1.9 ppm error). **IR** ($CHCl_3$, cm^{-1}) 2925 – 2862 (m), 1708 (s), 1449 (m), 1027 (m).

Methyl 12α,12β-difluoro-3-oxo-5β-cholan-24-oate (2.85)

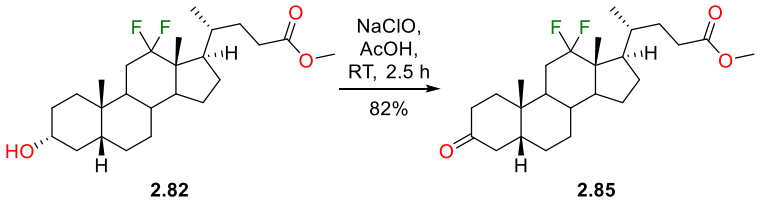

2.82 **2.85**

The alcohol **2.82** (152 mg, 0.36 mmol, 1.0 equiv) was dissolved in acetic acid (6 mL) and NaClO (~10% in H_2O, 0.67 ml, 1.08 mmol, 3.0 equiv) was added dropwise over the course of 3 min. After stirring at RT for 2.5 h, the reaction mixture was diluted with water (25 mL) and filtered. The resulting solid crude material was dissolved in EtOAc (50 mL) and washed with sat. $NaHCO_3$ (50 mL), water (50 mL) and brine (50 mL) before drying over Na_2SO_4 and reducing *in vacuo* to cleanly yield **2.85** as a white solid (125 mg, 0.29 mmol, 82%).

mp 87 – 88 °C. $\mathbf{R_f}$ 0.29 (Acetone/PE 15/85). $\mathbf{[\alpha]_D}$ + 47.3 (c = 0.56, $CHCl_3$, 21 °C). **^{1}H NMR** (400 MHz, $CDCl_3$) δ 3.66 (s, 3H, 24-COO**CH_3**), 2.64 (br t, *J*=13.4 Hz, 1H, 4α-**H**), 2.16-2.43 (m, 4H, 23-**H'**, 23-**H''**, 2α-**H** and 2β-**H**), 2.00-2.08 (m, 1H, 4β-**H**), 1.62-2.00 (m), 1.05-1.60 (m), 1.02 (s, 3H, 19-**CH_3**), 0.99 (dd, *J*=6.7, 1.8 Hz, 3H, 21-**CH_3**), 0.85 (s, 3H, 18-**CH_3**) ppm. **^{13}C NMR** (100 MHz, $CDCl_3$) δ 212.2 (**3-C**), 174.6 (**24-COO**CH_3), 126.2 (dd, *J*=251.3, 246.9 Hz, **12-C**), 52.4 (d, *J*=7.3 Hz, **14-CH**), 51.4 (**24-**COO**CH_3**), 49.2 (br t, *J*=20.5 Hz, **13-C**), 47.8 (d, *J*=2.2 Hz, **17-CH**), 43.7 (**5-CH**), 42.1 (**4-CH_2**), 37.4 (d, *J*=9.5 Hz, **9-CH**), 36.9 (**2-CH_2**), 36.7 (**1-CH_2**), 34.4 (**8-CH**), 34.3 (**10-C**), 33.1 (**20-CH**), 31.6 (br t, *J*=26.0 Hz, **11-CH_2**), 31.5 (**23-CH_2**), 30.4 (**22-CH_2**), 26.3 (**6-CH_2**), 26.2 (**16-CH_2**), 24.8 (d, *J*=1.5 Hz, ***15-CH_2* or *7-CH_2***), 23.0 (d, *J*=1.5 Hz, ***15-CH_2* or *7-CH_2***), 22.2 (**19-CH_3**), 18.9 (d, *J*=10.3 Hz, **21-CH_3**), 10.5 (br dd, *J*=5.1, 1.5 Hz, **18-CH_3**) ppm. **^{19}F NMR** (376MHz, $CDCl_3$) δ -91.47 (br d, *J*=232.3 Hz, 1F, 12β-**F**), -112.97--111.46 (m, 1F, 12α-**F**) ppm. **^{19}F [^{1}H] NMR** (376MHz, $CDCl_3$) δ -91.48 (d, *J*=230.6 Hz, 1F, 12β-**F**), -112.21 (d, *J*=230.6 Hz, 1F, 12α-**F**) ppm. **LRMS (ESI+)** m/z: 447.1 $[M+Na]^+$, 442.2 $[M+NH_4]^+$. **HRMS (ESI+)** $C_{25}H_{38}F_2NaO_3$ $[M+Na]^+$. Calculated: 447.2681; Found: 447.2676 (1.2 ppm error). **IR** (neat, cm^{-1}) 2953 – 2869 (m), 1728 (s), 1207 (m), 1027 (m).

12α,12β-Difluoro-3-oxo-5β-cholanic acid (2.86)

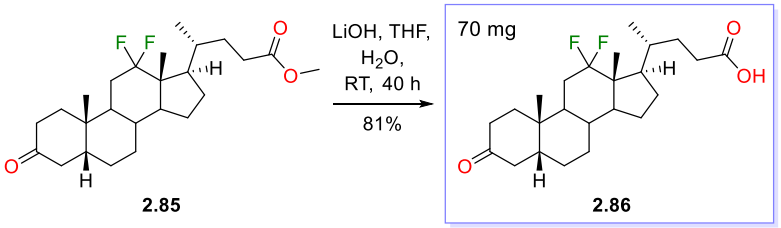

2.85 **2.86**

Following general procedure C, **2.85** (89 mg, 0.21 mmol, 1.0 equiv) was deprotected to yield **2.86** as a white gummy solid (70 mg, 0.17 mmol, 81%) with no further purification.

R_f 0.15 (Acetone/PE 20/80). **$[\alpha]_D$** + 46.1 (c = 0.52, $CHCl_3$, 21 °C). **^{1}H NMR** (400 MHz, $CDCl_3$) δ 2.64 (br t, *J*=14.1 Hz, 1H, 4α-**H**), 2.25-2.48 (m, 3H, 23-**H'**, 23-**H''** and 2α-**H**), 2.16-2.25 (m, 1H, 2β-**H**), 2.02-2.09 (m, 1H, 4β-**H**), 1.05-2.01 (m), 1.03 (s, 3H, 19-**CH_3**), 1.01 (dd, *J*=6.7, 1.4 Hz, 3H, 21-**CH_3**), 0.86 (s, 3H, 18-**CH_3**) ppm. **^{13}C NMR** (100 MHz, $CDCl_3$) δ 212.5 (**3-C**), 180.1 (**24-COOH**), 126.2 (dd, *J*=251.3, 246.9 Hz, **12-C**), 52.4 (d, *J*=6.6 Hz, **14-CH**), 49.2 (t, *J*=20.5 Hz, **13-C**), 47.8 (d, *J*=2.2 Hz, **17-CH**), 43.7 (**5-CH**), 42.0 (**4-CH_2**), 37.4 (d, *J*=9.5 Hz, **9-CH**), 36.9 (**2-CH_2**), 36.6 (**1-CH_2**), 34.4 (**8-CH**), 34.3 (**10-C**), 33.1 (**20-CH**), 31.6 (br t, *J*=26.0 Hz, **11-CH_2**), 31.4 (**23-CH_2**), 30.2 (**22-CH_2**), 26.3 (**6-CH_2**), 26.3 (**16-CH_2**), 24.8 (**7-CH_2**), 23.0 (**15-CH_2**), 22.2 (**19-CH_3**), 18.8 (d, *J*=11.0 Hz, **21-CH_3**), 10.5 (d, *J*=4.4 Hz, **18-CH_3**) ppm. **^{19}F NMR** (376MHz, $CDCl_3$) δ -91.32 (br d, *J*=232.4 Hz, 1F, 12β-**F**), -112.63--111.75 (m, 1F, 12α-**F**) ppm. **^{19}F [^{1}H] NMR** (376MHz, $CDCl_3$) δ -91.33 (d, *J*=230.6 Hz, 1F, 12β-**F**), -112.18 (d, *J*=230.6 Hz, 1F, 12α-**F**) ppm. **LRMS (ESI+)** m/z: 428.2 $[M+NH_4]^+$. **HRMS (ESI+)** $C_{24}H_{36}F_2NaO_3$ $[M+Na]^+$. Calculated: 433.2525; Found: 433.2534 (2.1 ppm error). **IR** ($CHCl_3$, cm^{-1}) 2926 – 2873 (m), 1708 (s), 1024 (m), 754 (m).

Methyl 3,12-dioxo-5β-cholan-24-oate (2.22)

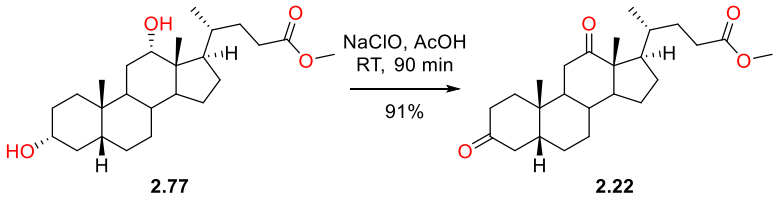

2.77 **2.22**

The alcohol **2.77** (5.0 g, 12.3 mmol, 1.0 equiv) was dissolved in acetic acid (50 mL) and NaClO (11% in H_2O, 28.0 mL, ~49 mmol, ~4 equiv) was added dropwise over the course of an h. After full addition of NaClO, water (450 mL) was added to the reaction mixture and stirred for 15 min. The aqueous phase was filtered and the obtained solid was dissolved in EtOAc (200 mL), which was washed with saturated $NaHCO_3$ (150 mL), water (150 mL) and brine (150 mL) before drying over Na_2SO_4 and reducing *in vacuo* to yield **2.22** as a white solid (4.50 g, 11.2 mmol, 91%).

mp 123 – 124 °C (Lit. 126.8 – 129.2 °C[96,232]). **R_f** 0.69 (EtOAc/PE 40/60). **^{1}H NMR** (400 MHz, $CDCl_3$) δ 3.67 (s, 3H, 24-COO**CH_3**), 2.54-2.66 (m, 2H, 11β-**H** and 4α-**H**), 2.23-2.45 (m, 3H, 23-**H'**, 23-**H''**), 2.15-2.22 (m, 1H), 1.73-2.15 (m), 1.62 (br dq, *J*=13.0, 3.4 Hz, 1H), 1.14-1.51 (m), 1.12 (s, 3H, 19-**CH_3**), 1.06 (s, 3H, 18-**CH_3**), 0.87 (d, *J*=6.5 Hz, 3H, 21-**CH_3**) ppm. **^{13}C NMR** (100 MHz, $CDCl_3$) δ 214.0 (***3-C*** *or* ***12-C***), 212.0 (***3-C*** *or* ***12-C***), 174.5 (**24-COO**CH_3), 58.4 (**14-CH**), 57.5 (**13-C**), 51.4 (**24-**COO**CH_3**), 46.4 (**17-CH**), 44.2 (***5-CH*** *or* ***9-CH***), 43.6 (CH), 42.0 (***4-CH_2*** *or* ***11-CH_2***), 38.3 (***4-CH_2*** *or* ***11-CH_2***), 36.8 (CH_2), 36.7 (**1-CH_2**), 35.5 (**10-C** and **20-CH**), 35.4 (CH), 31.2 (**23-CH_2**), 30.4 (**22-CH_2**), 27.4 (CH_2), 26.5 (**6-CH_2**), 25.4

(CH_2), 24.2 (CH_2), 22.1 (**19-CH_3**), 18.5 (**21-CH_3**), 11.6 (**18-CH_3**) ppm. **LRMS (ESI+)** m/z: 403.5 $[M+H]^+$, 425.5 $[M+Na]^+$. ^1H and ^{13}C NMR data agree with literature.[96,232]

Methyl 3α,3β-difluoro-12-oxo-5β-cholan-24-oate (2.87)

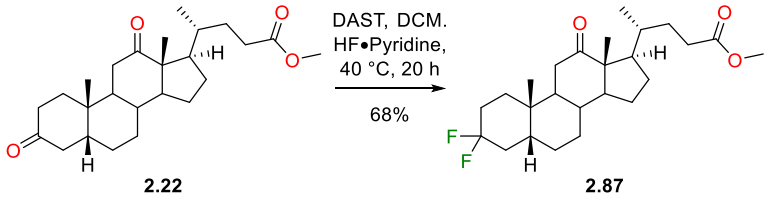

The ketone **2.22** (4.73 g, 11.7 mmol, 1.0 equiv) was dissolved in dry DCM (75 mL) and DAST (~4.8 mL, ~35 mmol, ~3 equiv) and HF.Pyridine (70% HF, ~0.02 mL, ~0.59 mmol, ~0.05 equiv) were added. After heating under reflux at 40 °C for 20 h, the reaction mixture was allowed to cool to RT, was diluted with DCM (50 mL) and was quenched with slow addition of saturated $NaHCO_3$ solution (100 mL) and stirring for 30 min. The aqueous and organic phases were then separated and the aqueous phase was extracted with DCM (3 x 50 mL). The combined organic phases were then washed with water (200 mL) and brine (200 mL) before drying over Na_2SO_4 and reducing *in vacuo* to yield 5.5 g of crude material. The crude was purified by flash chromatography twice (1st: Biotage SNAP KP-Sil 100 g cartridge, EtOAc/PE: 10%/90% → 25%/75%; 2nd: Biotage SNAP KP-Sil 100 g cartridge, Acetone/PE: 3%/97% → 15%/85%), yielding **2.87** as an off-white solid (3.40 g, 8.01 mmol, 68%).

mp 114 – 115 °C. **R_f** 0.29 (Acetone/PE 10/90). **$[\alpha]_D$** + 87.9 (c = 1.02, $CHCl_3$, 22 °C). **^{1}H NMR** (400 MHz, $CDCl_3$) δ 3.66 (s, 3H, 24-COO**CH_3**), 2.52 (t, *J*=12.7 Hz, 1H, 11β-**H**), 2.38 (ddd, *J*=15.4, 9.8, 5.1 Hz, 1H, 23-**H'**), 2.25 (ddd, *J*=15.8, 9.1, 6.8 Hz, 1H, 23-**H''**), 1.08-2.12 (m), 1.06 (s, 3H, 19-**CH_3**), 1.02 (s, 3H, 18-**CH_3**), 0.85 (d, *J*=6.6 Hz, 3H, 21-**CH_3**) ppm. **^{13}C NMR** (100 MHz, $CDCl_3$) δ 214.1 (**12-C**), 174.6 (**24-COO**CH_3), 123.9 (dd, *J*=242.5, 238.8 Hz, **3-C**), 58.5 (**14-CH**), 57.5 (**13-C**), 51.4 (**24-**COO**CH_3**), 46.4 (**17-CH**), 43.4 (**9-CH**), 39.5 (d, *J*=8.8 Hz, **5-CH**), 38.2 (**11-CH_2**), 35.6 (**20-CH**), 35.4 (**8-CH**), 35.2 (**10-C**), 34.4 (dd, *J*=25.7, 21.3 Hz, ***2-CH_2 or 4-CH_2***), 32.9 (d, *J*=9.5 Hz, **1-CH_2**), 31.2 (**23-CH_2**), 30.4 (**22-CH_2**), 29.1 (dd, *J*=25.7, 22.0 Hz, ***2-CH_2 or 4-CH_2***), 27.4 (CH_2), 26.0 (CH_2), 25.7 (CH_2), 24.2 (CH_2), 22.2 (d, *J*=2.2 Hz, **19-CH_3**), 18.5 (**21-CH_3**), 11.6 (**18-CH_3**) ppm. **^{19}F NMR** (376MHz, $CDCl_3$) δ -89.15 (br d, *J*=234.1 Hz, 1F, 3α-**F**), -100.00 (dtt, *J*=233.9, 34.1, 11.9 Hz, 1F, 3β-**F**) ppm. **^{19}F [^{1}H] NMR** (376MHz, $CDCl_3$) δ -89.15 (d, *J*=234.1 Hz, 1F, 3α-**F**), -100.00 (d, *J*=234.1 Hz, 1F, 3β-**F**) ppm. **LRMS (ESI+)** m/z: 447.4 $[M+Na]^+$, 425.4 $[M+H]^+$. **HRMS (ESI+)** $C_{25}H_{39}F_2O_3$ $[M+H]^+$. Calculated: 425.2862; Found: 425.2873 (2.6 ppm error). **IR** (neat, cm^{-1}) 2966 – 2866 (m), 1737 (s), 1703 (s), 1372 (m), 1176 (m).

Methyl 3α,3β,12α,12β-tetrafluoro-5β-cholan-24-oate (2.88)

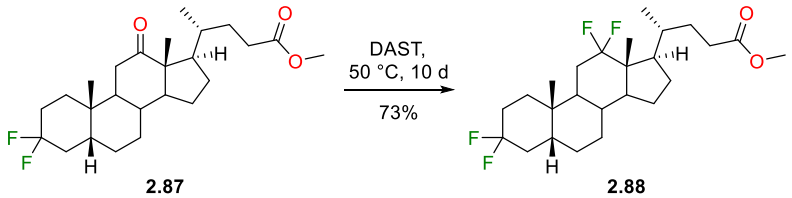

2.87 **2.88**

To a flame-dried flask with condenser attached, under argon, **2.87** (2.82 g, 6.64 mmol, 1.0 equiv) and DAST (~7 mL, ~53 mmol, ~8 equiv) were added. The reaction mixture was heated to 50 °C. Over the course of 3 d, 8 mL of DAST was added to the reaction mixture at RT in two 2 mL portions and a 4 mL portion (~60 mmol, ~9 equiv in total). After 7 d of further heating, the reaction mixture was allowed to cool to RT, diluted with DCM (50 mL) and the mixture was slowly decanted (~5 mL per min) into icy, saturated $NaHCO_3$ solution (~700 mL). After the mixture was fully neutralised, the aqueous and organic phases were separated and the aqueous phase was extracted with DCM (3 x 100 mL). The combined organic phases were then washed with saturated $NaHCO_3$ (200 mL), water (200 mL) and brine (200 mL) before drying over Na_2SO_4 and reducing *in vacuo* to yield 4.2 g of crude material. The crude was purified by flash chromatography (Biotage SNAP KP-Sil 100 g cartridge, EtOAc/PE: 0%/100% → 10%/90%), yielding **2.88** as a yellow solid (2.00 g, 4.87 mmol, 73%).

mp 93 – 94 °C. **R_f** 0.26 (EtOAc/PE 5/95). **$[\alpha]_D$** + 39.6 (c = 0.97, $CHCl_3$, 23 °C). **^{1}H NMR** (400 MHz, $CDCl_3$) δ 3.66 (s, 3H, 24-COO**CH_3**), 2.37 (ddd, *J*=15.4, 9.9, 5.3 Hz, 1H, 23-**H'**), 2.26 (ddd, *J*=16.0, 9.5, 6.7 Hz, 1H, 23-**H''**), 1.01-2.17 (m), 0.95-1.01 (m, 6H, 19-**CH_3** and 21-**CH_3**), 0.82 (s, 3H, 18-**CH_3**) ppm. **^{13}C NMR** (100 MHz, $CDCl_3$) δ 174.6 (**24-COO**CH_3), 125.7 (dd, *J*=250.9, 247.2 Hz, **12-C**), 121.7 (dd, *J*=242.1, 239.2 Hz, **3-C**), 52.4 (d, *J*=7.3 Hz, **14-CH**), 51.4 (**24-**COO**CH_3**), 49.2 (dd, *J*=21.3, 19.8 Hz, **13-C**), 47.8 (d, *J*=2.2 Hz, **17-CH**), 39.5 (d, *J*=8.8 Hz, **5-CH**), 36.6 (d, *J*=9.5 Hz, **9-CH**), 34.3 (d, *J*=1.5 Hz, **8-CH**), 34.1-34.6 (m, **4-CH_2**), 34.0 (**10-C**), 33.1 (**20-CH**), 32.8 (d, *J*=8.8 Hz, **1-CH_2**), 31.5 (**23-CH_2**), 31.5 (t, *J*=26.4 Hz, **11-CH_2**), 30.4 (**22-CH_2**), 29.1 (dd, *J*=25.7, 22.0 Hz, **2-CH_2**), 26.2 (***6-CH_2* or *7-CH_2***), 25.8 (***6-CH_2* or *7-CH_2***), 25.1 (d, *J*=1.5 Hz, ***15-CH_2* or *16-CH_2***), 23.0 (***15-CH_2* or *16-CH_2***), 22.4 (d, *J*=2.2 Hz, **19-CH_3**), 18.9 (d, *J*=11.0 Hz, **21-CH_3**), 10.5 (dd, *J*=5.9, 1.5 Hz, **18-CH_3**) ppm. **^{19}F NMR** (376MHz, $CDCl_3$) δ -89.02 (br d, *J*=232.4 Hz, 1F, 3α-**F**), -91.35 (br d, *J*=230.6 Hz, 1F, 12β-**F**), -99.92 (dtt, *J*=233.8, 34.6, 11.5 Hz, 1F, 3β-**F**), -112.19 (ddd, *J*=230.6, 32.9, 12.1 Hz, 1F, 12α-**F**) ppm. **^{19}F [^{1}H] NMR** (376MHz, $CDCl_3$) δ -89.03 (d, *J*=234.1 Hz, 1F, 3α-**F**), -91.35 (d, *J*=230.6 Hz, 1F, 12β-**F**), -99.92 (d, *J*=234.1 Hz, 1F, 3β-**F**), -112.19 (d, *J*=232.4 Hz, 1F, 12α-**F**) ppm. **LRMS (ESI+)** m/z: 464.3 $[M+NH_4]^+$. **HRMS (ESI+)** $C_{25}H_{38}F_4NaO_2$ $[M+Na]^+$. Calculated: 469.2700; Found: 469.2707 (1.6 ppm error). **IR** (neat, cm^{-1}) 2954 – 2880 (m), 1731 (s), 1370 (m), 1096 (s), 1023 (s).

3α,3β,12α,12β-Tetrafluoro-5β-cholanic acid (2.20)

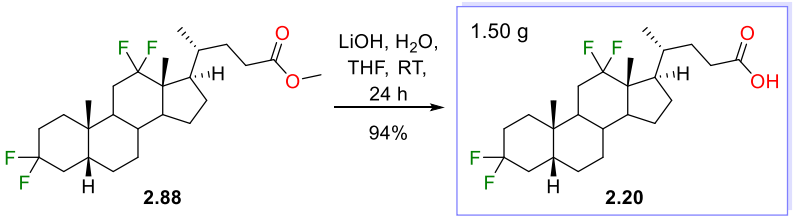

Following general procedure C, **2.88** (1.70 g, 3.81 mmol, 1.0 equiv) was deprotected to yield **2.20** as an off-white solid (1.55 g, 3.58 mmol, 94%) with no further purification.

mp 175 – 177 °C. $\mathbf{R_f}$ 0.11 (EtOAc/PE 15/85). $\mathbf{[\alpha]_D}$ + 40.4 (c = 1.04, $CHCl_3$, 23 °C). **^{1}H NMR** (400 MHz, $CDCl_3$) δ 2.43 (ddd, *J*=15.7, 10.1, 5.3 Hz, 1H, 23-**H'**), 2.31 (ddd, *J*=16.0, 9.7, 6.6 Hz, 1H, 23-**H''**), 1.03-2.23 (m), 1.01 (dd, *J*=6.6, 1.6 Hz, 3H, 21-$\mathbf{CH_3}$), 0.98 (s, 3H, 19-$\mathbf{CH_3}$), 0.83 (s, 3H, 18-$\mathbf{CH_3}$) ppm. **^{13}C NMR** (100 MHz, $CDCl_3$) δ 180.5 (**24-COOH**), 125.7 (dd, *J*=250.9, 247.2 Hz, **12-C**), 121.7 (dd, *J*=242.1, 239.2 Hz, **3-C**), 52.4 (d, *J*=7.3 Hz, **14-CH**), 49.2 (dd, *J*=21.3, 19.1 Hz, **13-C**), 47.8 (d, *J*=2.2 Hz, **17-CH**), 39.6 (d, *J*=8.8 Hz, **5-CH**), 36.6 (d, *J*=9.5 Hz, **9-CH**), 34.3 (d, *J*=1.5 Hz, **8-CH**), 34.1-34.6 (m, **4-CH_2**), 34.1 (**10-C**), 33.1 (**20-CH**), 32.8 (d, *J*=9.5 Hz, **1-CH_2**), 31.5 (**23-CH_2**), 31.5 (t, *J*=25.7 Hz, **11-CH_2**), 30.2 (**22-CH_2**), 29.1 (dd, *J*=25.7, 22.0 Hz, **2-CH_2**), 26.3 (***6-CH_2 or 7-CH_2***), 25.8 (***6-CH_2 or 7-CH_2***), 25.1 (d, *J*=1.5 Hz, ***15-CH_2 or 16-CH_2***), 23.0 (d, *J*=1.5 Hz, ***15-CH_2 or 16-CH_2***), 22.4 (d, *J*=2.9 Hz, **19-CH_3**), 18.8 (d, *J*=11.0 Hz, **21-CH_3**), 10.5 (dd, *J*=5.1, 1.5 Hz, **18-CH_3**) ppm. **^{19}F NMR** (376MHz, $CDCl_3$) δ -89.02 (br d, *J*=234.1 Hz, 1F, 3α-**F**), -91.20 (br d, *J*=230.6 Hz, 1F, 12β-**F**), -99.91 (dtt, *J*=233.9, 34.8, 12.1 Hz, 1F, 3β-**F**), -112.16 (ddd, *J*=231.1, 33.4, 13.0 Hz, 1F, 12α-**F**) ppm. **^{19}F [^{1}H] NMR** (376MHz, $CDCl_3$) δ -89.02 (d, *J*=234.1 Hz, 1F, 3α-**F**), -91.21 (d, *J*=232.3 Hz, 1F, 12β-**F**), -99.91 (d, *J*=234.1 Hz, 1F, 3β-**F**), -112.16 (d, *J*=232.3 Hz, 1F, 12α-**F**) ppm. **LRMS (ESI+)** m/z: 450.3 $[M+NH_4]^+$. **HRMS (ESI+)** $C_{24}H_{36}F_4NaO_2$ $[M+Na]^+$. Calculated: 455.2544; Found: 455.2552 (1.7 ppm error). **IR** (neat, cm^{-1}) 2944 – 2898 (b, m), 1712 (s), 1261 (m), 1091 (s), 1022 (m).

3α,3β-Difluoro-12-oxo-5β-cholanic acid (2.89)

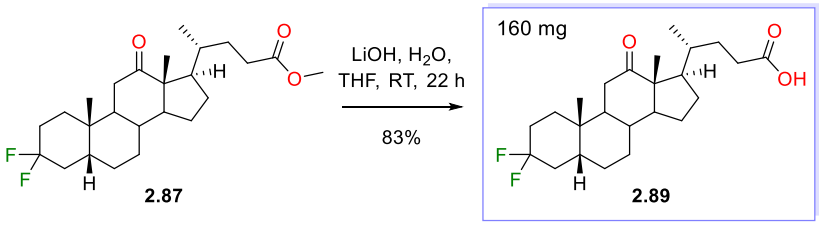

Following general procedure C, **2.87** (200 mg, 0.47 mmol, 1.0 equiv) was deprotected to yield **2.89** as a white solid (162 mg, 0.39 mmol, 83%) with no further purification.

mp 176 – 177 °C. $\mathbf{R_f}$ 0.32 (EtOAc/PE 40/60). $\mathbf{[\alpha]_D}$ + 92.8 (c = 0.97, $CHCl_3$, 22 °C). **^{1}H NMR** (400 MHz, $CDCl_3$) δ 2.53 (t, *J*=12.7 Hz, 1H, 11β-**H**), 2.44 (ddd, *J*=15.5, 9.7, 5.0 Hz, 1H, 23-**H'**), 2.30 (ddd, *J*=16.0, 9.3, 6.7 Hz, 1H, 23-**H''**), 1.08-2.08 (m), 1.07 (s, 3H, 19-**CH_3**), 1.03 (s, 3H, 18-**CH_3**), 0.86 (d, *J*=6.5 Hz, 3H, 21-**CH_3**) ppm. **^{13}C NMR** (100 MHz, $CDCl_3$) δ 214.4 (**12-C**), 180.1 (**24-COOH**), 124.0 (dd, *J*=242.5, 238.8 Hz, **3-C**), 58.5 (**14-CH**), 57.5 (**13-C**), 46.4 (**17-CH**), 43.4 (**9-CH**), 39.5 (d, *J*=9.5 Hz, **5-CH**), 38.2 (**11-CH_2**), 35.5 (**20-CH**), 35.4 (**8-CH**), 35.3 (d, *J*=1.5 Hz, **10-C**), 34.4 (dd, *J*=25.7, 21.3 Hz, ***2-CH_2 or 4-CH_2***), 32.9 (d, *J*=9.5 Hz, **1-CH_2**), 31.2 (**23-CH_2**), 30.2 (**22-CH_2**), 29.1 (dd, *J*=25.3, 22.4 Hz, ***2-CH_2 or 4-CH_2***), 27.4 (CH_2), 26.0 (CH_2), 25.7 (CH_2), 24.3 (CH_2), 22.2 (d, *J*=2.2 Hz, **18-CH_3**), 18.5 (**21-CH_3**), 11.7 (**18-CH_3**) ppm. **^{19}F NMR** (376MHz, $CDCl_3$) δ -89.15 (br d, *J*=234.1 Hz, 1F, 3α-**F**), -100.00 (dtt, *J*=234.0, 34.5, 11.5 Hz, 1F, 3β-**F**) ppm. **^{19}F [^{1}H] NMR** (376MHz, $CDCl_3$) δ -89.15 (d, *J*=234.1 Hz, 1F, 3α-**F**), -100.00 (br d, *J*=234.1 Hz, 1F, 3β-**F**) ppm. **LRMS (ESI+)** m/z: 411.4 $[M+H]^+$, 433.4 $[M+Na]^+$. **HRMS (ESI+)** $C_{24}H_{37}F_2O_3$ $[M+H]^+$. Calculated: 411.2705; Found: 411.2701 (1.1 ppm error). **IR** (neat, cm^{-1}) 3476 (m), 2989 – 2868 (m), 1702 (s), 1257 (m), 1086 (m).

7.4 Synthesis of Mono- and (Non-Geminal) Difluorinated Analogues

7.4.1 Synthesis of 4β,6α-Difluorinated Bile Acid Analogues

6α-Fluoro-7-oxo-lithocholic acid (3.12)

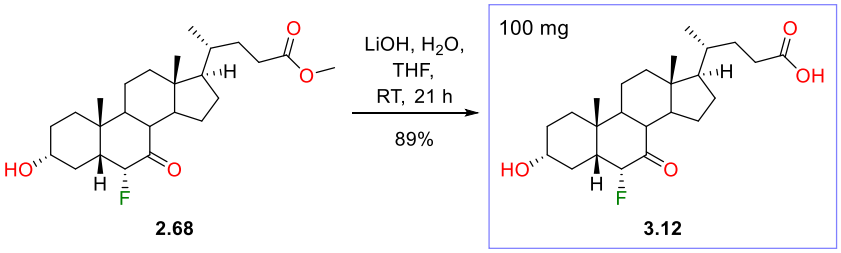

Following general procedure C, **2.68** (124 mg, 0.29 mmol, 1.0 equiv) was deprotected to yield **3.12** as a white solid (105 mg, 0.26 mmol, 89%) with no further purification.

mp 224 – 226 °C. $\mathbf{R_f}$ 0.30 (Acetone/PE 40/60). $\mathbf{[\alpha]_D}$ - 30.0 (c = 0.2, MeOH/$CHCl_3$ 9:1, 22 °C). **^{1}H NMR** (400 MHz, MeOH-d_4) δ 5.39 (dd, *J*=49.5, 6.7 Hz, 1H, 6β-**F**), 3.44-3.57 (m, 1H, 3β-**H**), 2.55 (t, *J*=11.3 Hz, 1H, 8β-**H**), 2.14-2.41 (m, 4H), 2.02-2.10 (m, 1H, 12β-**H**), 1.27-2.01 (m), 1.25 (s, 3H, 19-**CH_3**), 1.12-1.24 (m, 3H), 0.99-1.10 (m, 1H), 0.97 (d, *J*=6.6 Hz, 3H, 21-**CH_3**), 0.86-0.95 (m, 1H, 4α-**H**), 0.71 (s, 3H, 18-**CH_3**) ppm. **^{13}C NMR** (101 MHz, DMSO-d_6) δ 206.1 (d, *J*=13.2 Hz, **7-C**), 174.8 (**24-COOH**), 92.0 (d, *J*=190.0 Hz, **6-CH**), 68.4 (**3-CH**), 54.2 (**17-CH**), 49.9 (d, *J*=15.4 Hz, **5-CH**), 48.3 (**14-CH**), 46.7 (**8-CH**), 42.2 (**13-C**), 42.0 (**9-CH**), 38.3 (**12-CH_2**), 35.6 (d, *J*=7.3 Hz, **10-C**), 34.7 (**20-CH**), 33.9 (**1-CH_2**), 30.7 (**23-CH_2**), 30.7 (**22-CH_2**), 30.1 (**4-CH_2**), 29.6 (CH_2), 27.8 (CH_2), 24.0 (CH_2), 22.8 (**19-CH_3**), 21.1 (CH_2), 18.2 (**21-CH_3**), 11.8 (**18-CH_3**) ppm. **^{19}F NMR** (376MHz, DMSO-d_6) δ -201.08 (br d, *J*=48.5 Hz, 1F, 6α-**F**) ppm. **^{19}F [^{1}H] NMR** (376MHz, DMSO-d_6) δ -201.08 (s, 1F, 6α-**F**) ppm**. LRMS (ESI+)** m/z: 426.2 $[M+NH_4]^+$. **HRMS (ESI+)** $C_{24}H_{37}FNaO_4$ $[M+Na]^+$. Calculated: 431.2568; Found: 431.2570 (0.5 ppm error). **IR** (neat, cm^{-1}) 3262 (m), 2933 – 2874 (m), 2514 (b), 1727 (s), 1698 (s), 1017 (s).

Methyl 6α-fluoro-3α-hydroxy-7-oxo-5β-cholan-24-oate (2.68)

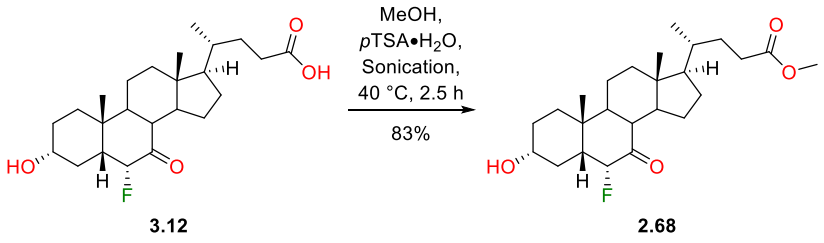

Following general procedure A, **3.12** (3.9 g, 9.58 mmol, 1 equiv) was protected to yield **2.68** as a white gummy solid (3.37 g, 7.97 mmol, 83%) with no further purification.

Data as before.

Methyl 6α-fluoro-3α,7α-dihydroxy-5β-cholan-24-oate (3.14) and Methyl 6α-fluoro-3α-(30α-fluoro-27α,33α-dihydroxy-29β-cholan-48-oxy)-7α-hydroxy-5β-cholan-24-oate (3.15)

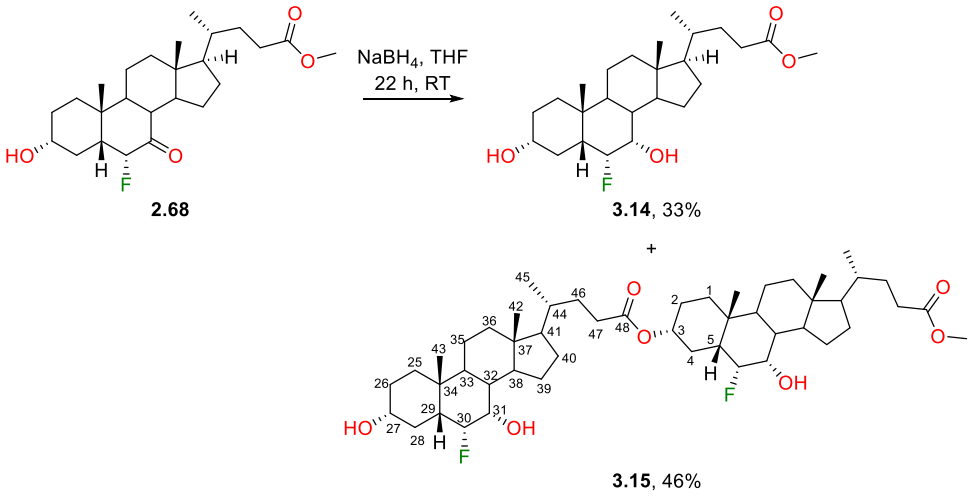

The ketone **2.68** (6.55 g, 15.5 mmol, 1.0 equiv) was dissolved in dry THF (120 mL) and $NaBH_4$ (1.47 g, 38.8 mmol, 2.5 equiv) was added. After stirring for 22 h at RT, the reaction mixture was cooled to 0 °C and quenched with addition of 2M HCl (50 mL), added dropwise over the course of 5 min. Further 2M HCl (200 mL) was added and the mixture was extracted with EtOAc (3 x 150 mL). The combined organic phases were washed with water (400 mL) and brine (400 mL) before drying over Na_2SO_4 and reducing *in vacuo* to give 6.5 g of crude material. The crude was combined with the crude material from a repeat of the reaction (total 24.4 mmol of **2.68**) and purified by flash chromatography (acetone/PE 20%/80%), first giving **3.14** as a white gummy solid (3.40 g, 8.02 mmol, 33%), followed by **3.15** around 90-95% pure as a colourless gum (4.5 g, 5.5 mmol, 46%).

3.14: R_f 0.24 (Acetone/PE 30/70). **$[\alpha]_D$** + 6.90 (c = 0.99, $CHCl_3$, 22 °C). **^{1}H NMR** (400 MHz, $CDCl_3$) δ 4.67 (ddd, *J*=45.1, 5.6, 3.4 Hz, 1H, 6β-**H**), 3.98-4.06 (m, 1H, 7β-**H**), 3.66 (s, 3H, 24-COO**CH_3**), 3.43 (tt, *J*=10.8, 4.8 Hz, 1H, 3β-**H**), 2.35 (ddd, *J*=15.5, 10.3, 5.4 Hz, 1H, 23-**H'**), 2.22 (ddd, *J*=16.0, 9.7, 6.6 Hz, 1H, 23-**H''**), 1.01-2.14 (m), 0.92 (d, *J*=6.4 Hz, 3H, 21-**CH_3**), 0.90 (s, 3H, 19-**CH_3**), 0.64 (s, 3H, 18-**CH_3**) ppm. **^{13}C NMR** (100 MHz, $CDCl_3$) δ 174.7 (**24-COO**CH_3), 91.9 (d, *J*=176.8 Hz, **6-CH**), 71.4 (**3-CH**), 69.9 (d, *J*=16.1 Hz, **7-CH**), 55.6 (**17-CH**), 51.5 (**24-**COO**CH_3**), 49.7 (**14-CH**), 46.2 (d, *J*=16.1 Hz, **5-CH**), 42.6 (**13-C**), 39.3 (**12-CH_2**), 38.0 (d, *J*=5.1 Hz, **8-CH**), 36.2 (d, *J*=7.3 Hz, **10-C**), 35.5 (**1-CH_2**), 35.3 (**20-CH**), 32.6 (**9-CH**), 32.5 (d, *J*=4.4 Hz, **4-CH_2**), 31.0 (**23-CH_2**), 30.9 (**22-CH_2**), 30.4 (**2-CH_2**), 28.0 (**16-CH_2**), 23.4 (**15-CH_2**), 23.0 (**19-CH_3**), 20.5 (**11-CH_2**), 18.2 (**21-CH_2**), 11.6 (**18-CH_3**) ppm. **^{19}F NMR** (376MHz, $CDCl_3$) δ -197.03 (br d, *J*=45.1 Hz, 1F, 6α-**F**) ppm. **^{19}F [^{1}H] NMR** (376MHz, $CDCl_3$) δ -197.04 (s, 1F, 6α-**F**) ppm. **LRMS (ESI+)** m/z: 442.4 $[M+NH_4]^+$. **HRMS (ESI+)** $C_{25}H_{41}FNaO_4$ $[M+Na]^+$. Calculated: 447.2881; Found: 447.2893 (2.6 ppm error). **IR** (neat, cm^{-1}) 3423 (m), 3278 (m), 2940 – 2866 (m), 1742 (s), 1168 (m), 1031 (s).

3.15: R_f 0.18 (Acetone/PE 30/70). **^{1}H NMR** (400 MHz, $CDCl_3$) δ 4.58-4.74 (m, 2H, 6β-**H** and 30β-**H**), 4.50-4.58 (m, 1H, 3β-**H**), 4.01 (br s, 2H, 7β-**H** and 31β-**H**), 3.65 (s, 3H, 24-COO**CH$_3$**), 3.35-3.48 (m, 1H, 27β-**H**), 2.17-2.40 (m, 5H), 0.96-2.15 (m), 0.88-0.92 (m, 12H, 19-**CH$_3$**, 21-**CH$_3$**, 43-**CH$_3$** and 45-**CH$_3$**), 0.63 (m, 6H, 18-**CH$_3$** and 42-**CH$_3$**) ppm. **^{13}C NMR** (100 MHz, $CDCl_3$) δ 174.7 (**24-COO**CH_3), 173.8 (**48-COO**R), 91.8 (d, *J*=176.8 Hz, **6-CH** or **30-CH**), 91.6 (br d, *J*=177.5 Hz, **6-CH** or **30-CH**), 73.3 (**3-CH** or **27-CH**), 71.3 (**3-CH** or **27-CH**), 69.9 (br d, *J*=16.9 Hz, **7-CH** or **31-CH**), 69.8 (br d, *J*=16.9 Hz, **7-CH** or **31-CH**), 55.6 (**17-CH** or **41-CH**), 55.5 (**17-CH** or **41-CH**), 51.4 (**24-**COO**CH$_3$**), 49.7 (**14-CH** and **36-CH**), 46.2 (br d, *J*=16.1 Hz, **5-CH** or **29-CH**), 45.9 (br d, *J*=16.1 Hz, **5-CH** or **29-CH**), 42.6 (**10-C** and **34-C**), 39.2 (**12-CH$_2$** and **36-CH$_2$**), 37.6-38.1 (**8-CH** and **32-CH**), 36.2 (d, *J*=7.3 Hz, **10-C** and **34-C**), 35.5 (CH_2), 35.3 (**20-CH** or **44-CH**), 35.2 (**20-CH** or **44-CH**), 35.1 (CH_2), 32.6 (**9-CH** and **33-CH**), 30.9 (2 CH_2), 30.9 (CH_2), 30.8 (CH_2), 30.4 (CH_2), 28.4 (CH_2), 28.0 (2 CH_2), 26.6 (CH_2), 23.4 (2 CH_2), 23.0 (**19-CH$_3$** or **43-CH$_3$**), 22.9 (**19-CH$_3$** or **43-CH$_3$**), 20.5 (2 CH_2), 18.2 (**21-CH$_3$** or **45-CH$_3$**), 18.2 (**21-CH$_3$** or **45-CH$_3$**), 11.6 (**18-CH$_3$** and **42-CH$_3$**) ppm. **^{19}F NMR** (376MHz, $CDCl_3$) δ -197.70--196.69 (m, 2F, 6α-**F** and 30α-**F**) ppm. **^{19}F [^{1}H] NMR** (376MHz, $CDCl_3$) δ -197.02 (s, 1F, 6α-**F** or 30α-**F**), -197.23 (s, 1F, 6α-**F** or 30α-**F**) ppm. **LRMS (ESI+)** m/z: 839.9 $[M+Na]^+$. **HRMS (ESI+)** $C_{49}H_{79}F_2O_7$ $[M+H]^+$. Calculated: 817.5788; Found: 817.5765 (2.9 ppm error).

6α-Fluorochenodeoxycholic acid (1.20)

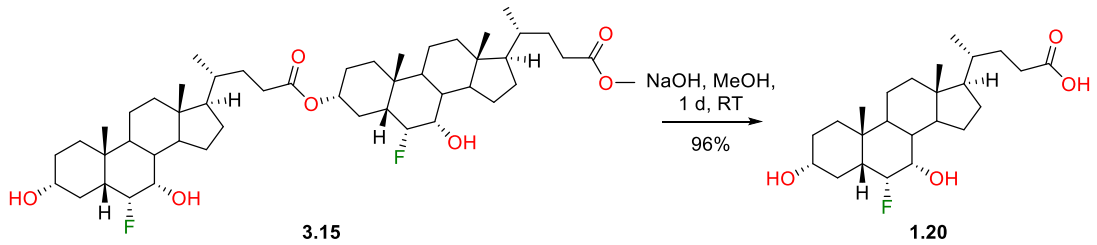

Following general procedure D, **3.15** (4.17 g, 5.10 mmol, 1.0 equiv, 90-95% pure) was hydrolysed to yield **1.20** as a white gummy solid (4.00 g, 9.74 mmol, 96%) with no further purification.

R_f 0.30 (Acetone/PE 40/60). **^{1}H NMR** (400 MHz, MeOH-d_4) δ 4.62 (ddd, *J*=45.2, 5.7, 3.5 Hz, 1H, 6β-**H**), 3.93-4.00 (m, 1H, 7β-**H**), 3.32-3.40 (m, 1H, 3β-**H**), 2.34 (ddd, *J*=15.8, 9.8, 5.3 Hz, 1H, 23-**H'**), 2.20 (ddd, *J*=16.1, 9.4, 7.0 Hz, 1H, 23-**H''**), 2.12 (q, *J*=12.1 Hz, 1H, 4α-**H**), 1.02-2.05 (m), 0.97 (d, *J*=6.5 Hz, 3H, 21-**CH$_3$**), 0.93 (s, 3H, 19-**CH$_3$**), 0.70 (s, 3H, 18-**CH$_3$**) ppm. **^{13}C NMR** (100 MHz, MeOH-d_4) δ 178.2 (**24-COOH**), 92.9 (d, *J*=179.0 Hz, **6-CH**), 72.5 (**3-CH**), 70.9 (d, *J*=16.9 Hz, **7-CH**), 57.4 (**17-CH**), 51.3 (d, *J*=1.5 Hz, **14-CH**), 48.2 (d, *J*=16.9 Hz, **5-CH**), 43.8 (**13-C**), 41.0 (**12-CH$_2$**), 39.6 (d, *J*=6.6 Hz, **8-CH**), 37.5 (d, *J*=8.1 Hz, **10-C**), 36.9 (**20-CH**), 36.8 (**1-CH$_2$**), 34.2 (**9-CH**), 33.5 (d, *J*=4.4 Hz, **4-CH$_2$**), 32.4 (**22-CH$_2$**), 32.1 (**23-CH$_2$**), 31.5 (CH_2), 29.3 (CH_2), 24.6 (CH_2), 23.8 (**19-CH$_3$**), 21.9 (CH_2), 18.9 (**21-CH$_3$**), 12.3 (**18-CH$_3$**) ppm. **^{19}F NMR** (376MHz, MeOH-d_4) δ -196.52 (br d, *J*=45.1 Hz, 1F, 6α-**F**) ppm. **^{19}F [^{1}H] NMR** (376MHz, MeOH-d_4) δ -196.52 (s, 1F, 6α-**F**) ppm. **LRMS (ESI+)** m/z: 428.3 $[M+NH_4]^+$. **HRMS (ESI+)**

$C_{24}H_{39}FNaO_4$ $[M+Na]^+$. Calculated: 433.2725; Found: 433.2726 (0.3 ppm error). ^1H and ^{13}C NMR data agree with data from within the group and literature.[228] ^{19}F NMR data agrees with data from within the group.

Methyl 6α-fluoro-3α,7α-dihydroxy-5β-cholan-24-oate (3.14)

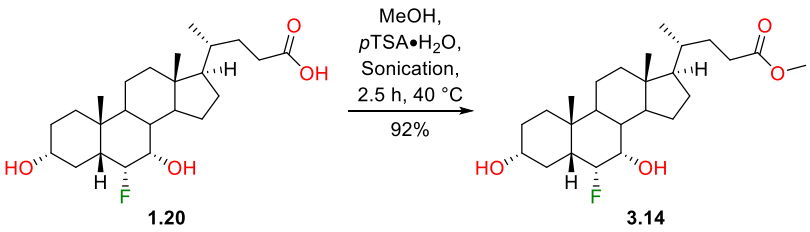

Following general procedure A, **1.20** (4.10 g, 9.99 mmol, 1.0 equiv) was protected to yield **3.14** as a white gummy solid (3.90 g, 9.19 mmol 92%) with no further purification.

Data as before.

Methyl 6α-fluoro-3-oxo-7α-hydroxy-5β-cholan-24-oate (3.11)

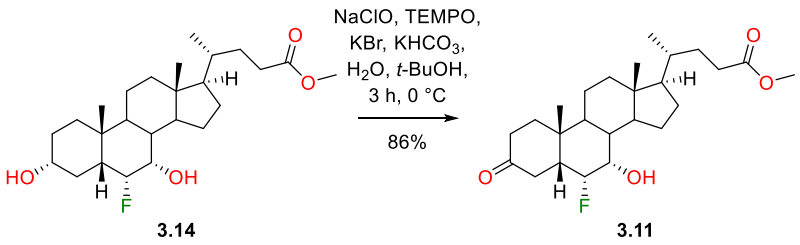

Following general procedure B, **3.14** (10.1 g, 23.8 mmol, 1.0 equiv) was oxidised. The crude material was purified by flash chromatography (acetone/PE: 14%/86% → 20%/80%) yielding **3.11** as a white gummy solid (8.63 g, 20.4 mmol, 86%).

R_f 0.30 (Acetone/PE 20/80). **$[\alpha]_D$** + 8.72 (c = 0.98, $CHCl_3$, 22 °C). **^{1}H NMR** (400 MHz, $CDCl_3$) δ 4.64 (ddd, *J*=44.9, 6.2, 3.4 Hz, 1H, 6β-**H**), 4.07 (br q, *J*=3.2 Hz, 1H, 7β-**H**), 3.65 (s, 3H, 24-COO**CH_3**), 3.22 (dd, *J*=15.6, 13.4 Hz, 1H, 4α-**H**), 2.29-2.50 (m, 3H), 2.12-2.28 (m, 4H), 1.86-2.07 (m, 4H), 1.03-1.85 (m), 1.00 (s, 3H, 19-**CH_3**), 0.92 (d, *J*=6.5 Hz, 3H, 21-**CH_3**), 0.67 (s, 3H, 18-**CH_3**) ppm. **^{13}C NMR** (100 MHz, $CDCl_3$) δ 211.7 (**3-C**), 174.6 (**24-COO**CH_3), 91.0 (d, *J*=177.5 Hz, **6-CH**), 69.9 (d, *J*=16.9 Hz, **7-CH**), 55.6 (**17-CH**), 51.4 (**24-**COO**CH_3**), 49.6 (d, *J*=1.5 Hz, **14-CH**), 47.0 (d, *J*=16.1 Hz, **5-CH**), 42.5 (**13-C**), 39.1 (**12-CH_2**), 38.9 (d, *J*=5.1 Hz, **4-CH_2**), 37.9 (d, *J*=5.9 Hz, **8-CH**), 36.7 (**1-CH_2**), 36.6 (**2-CH_2**), 36.4 (d, *J*=8.1 Hz, **10-C**), 35.3 (**20-CH**), 33.4 (**9-CH**), 30.9 (**23-CH_2**), 30.8 (**22-CH_2**), 27.9 (**16-CH_2**), 23.4 (**15-CH_2**), 22.1 (**19-CH_3**), 20.8 (**11-CH_2**), 18.2 (**21-CH_3**), 11.6 (**18-CH_3**) ppm. **^{19}F NMR** (376MHz, $CDCl_3$) δ -197.27 (br d, *J*=43.4 Hz, 1F, 6α-**F**) ppm. **^{19}F [^{1}H] NMR** (376MHz, $CDCl_3$) δ -197.27 (s, 1F, 6α-**F**) ppm. **LRMS (ESI+)** m/z: 440.2 $[M+NH_4]^+$. **HRMS (ESI+)** $C_{25}H_{39}FNaO_4$ $[M+Na]^+$. Calculated: 445.2725; Found:

445.2726 (0.3 ppm error). **IR** ($CHCl_3$, cm^{-1}) 3464 (b, m), 2939 – 2869 (m), 1711 (b, s), 1031 (m), 753 (m).

6α-Fluoro-3-oxo-7α-hydroxy-5β-cholanic acid (3.16)

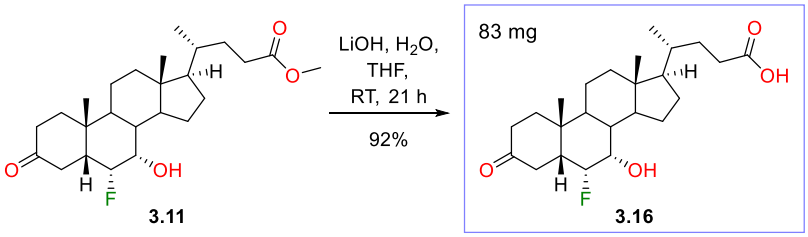

Following general procedure C, **3.11** (91 mg, 0.22 mmol, 1.0 equiv) was deprotected to yield **3.16** as a white gummy solid (83.0 mg, 0.20 mmol, 92%) with no further purification.

R_f 0.21 (Acetone/PE 30/70). **$[\alpha]_D$** + 8.04 (c = 0.55, $CHCl_3$, 22 °C). **^{1}H NMR** (400 MHz, $CDCl_3$) δ 4.65 (ddd, *J*=44.5, 5.7, 2.9 Hz, 1H, 6β-**H**), 4.05-4.11 (m, 1H, 7β-**H**), 3.22 (dd, *J*=15.5, 13.4 Hz, 1H, 4α-**H**), 2.35-2.52 (m, 3H, 4β-**H**, 23-**H'** and 2α/β-**H**), 2.14-2.32 (m, 3H, 5β-**H**, **23-H''** and 2α/β-**H**), 1.08-2.07 (m), 1.01 (s, 3H, 19-**CH_3**), 0.95 (d, *J*=6 .5 Hz, 3H, 21-**CH_3**), 0.69 (s, 3H, 18-**CH_3**) ppm. **^{13}C NMR** (100 MHz, $CDCl_3$) δ 212.0 (**3-C**), 180.0 (**24-COOH**), 91.1 (d, *J*=178.3 Hz, **6-CH**), 70.0 (d, *J*=16.9 Hz, **7-CH**), 55.7 (**17-CH**), 49.6 (**14-CH**), 47.0 (d, *J*=16.1 Hz, **5-CH**), 42.6 (**13-C**), 39.2 (**12-CH_2**), 38.9 (d, *J*=4.4 Hz, **4-CH_2**), 37.9 (d, *J*=5.9 Hz, **8-CH**), 36.7 (**2-CH_2**), 36.6 (**1-CH_2**), 36.4 (d, *J*=8.1 Hz, **10-C**), 35.3 (**20-CH**), 33.5 (**9-CH**), 30.9 (**23-CH_2**), 30.7 (**22-CH_2**), 28.0 (**16-CH_2**), 23.4 (**15-CH_2**), 22.2 (**19-CH_3**), 20.9 (**11-CH_2**), 18.2 (**21-CH_3**), 11.7 (**18-CH_3**) ppm. **^{19}F NMR** (376MHz, $CDCl_3$) δ -197.27 (br d, *J*=45.1 Hz, 1F, 6α-**F**) ppm. **^{19}F [^{1}H] NMR** (376MHz, $CDCl_3$) δ -197.28 (s, 1F, 6α-**F**) ppm. **LRMS (ESI+)** m/z: 426.2 $[M+NH_4]^+$. **HRMS (ESI+)** $C_{24}H_{37}FNaO_4$ $[M+Na]^+$. Calculated: 431.2568; Found: 431.2566 (0.5 ppm error). **IR** (neat, cm^{-1}) 3465 (m), 2932 – 2866 (m), 1730 (s), 1688 (s), 1170 (m), 1035 (m).

Methyl 4β,6α-difluoro-3-oxo-7α-hydroxy-5β-cholan-24-oate (3.17), Methyl 2β,6α-difluoro-3-oxo-7α-hydroxy-5β-cholan-24-oate (3.18) and Methyl 4β,6α-difluoro-3-oxo-7α-(N-methylformamido)methoxy-5β-cholan-24-oate (3.19)

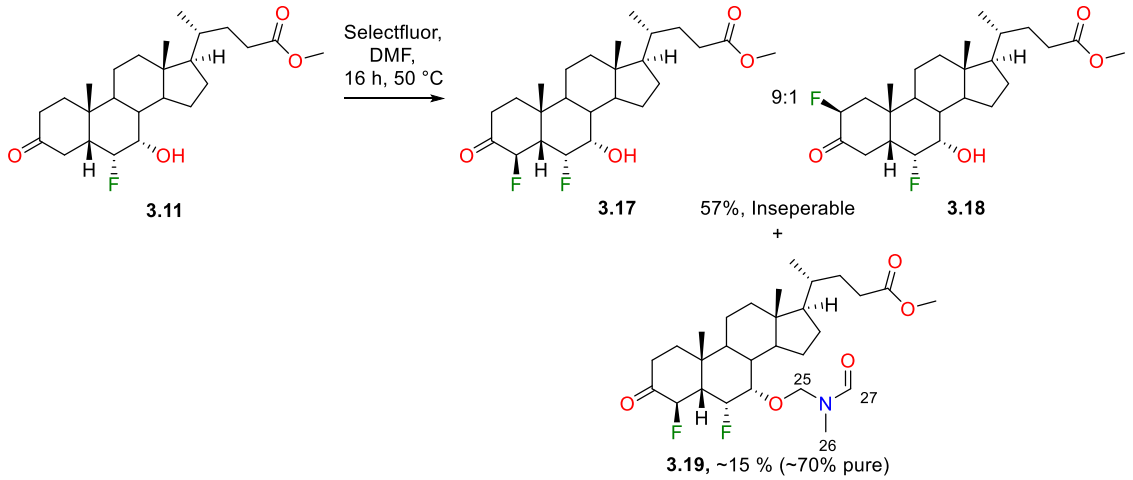

The ketone **3.11** (5.06 g, 12.0 mmol, 1.0 equiv) was dissolved in dry DMF (50 mL) and a suspension of Selectfluor® (6.38 g, 18.0 mmol, 1.5 equiv) in dry DMF (80 mL) was added. After heating at 50 °C for 16 h, the reaction mixture was cooled to RT and added water (250 mL). The resulting mixture was extracted with EtOAc (3 x 100 mL), and the combined organic phases were washed with brine (2 x 200 mL) before drying over Na_2SO_4 and reducing *in vacuo* to give 5.9 g of crude material. The crude was purified by flash chromatography (Biotage ZIP KP-Sil 120g cartridge, acetone/PE: 15%/85% → 30%/70%) to firstly give an impure fraction containing **3.17** and **3.18** (3.9 g) and then secondly give **3.19** ~70% pure as a colourless gum (1.3 g, ~1.8 mmol, ~15%). The impure fraction containing **3.17** and **3.18** was repurified by flash chromatography (acetone/PE 15%/85% → 16%/84%) to yield an inseparable 9:1 mixture of **3.17** and **3.18** as a white gummy solid (3.0 g, 6.81 mmol, 57%).

3.17 and **3.18: R_f** 0.45 (Acetone/PE 30/70). **^{1}H NMR** (400 MHz, $CDCl_3$) δ 6.03 (dd, *J*=47.1, 10.5 Hz, 0.9H, ***3.17*** 4α-**H**), 5.05 (ddd, *J*=49.0, 12.8, 6.1 Hz, 0.1H, ***3.18*** 2α-**H**), 4.53-4.79 (m, 1H, 6β-**H**), 4.17 (br d, *J*=7.3 Hz, 0.9H, ***3.17*** 7β-**H**), 4.06 (br s, 0.1H, ***3.18*** 7β-**H**), 3.64 (s, 3H, 24-COO**CH_3**), 3.39 (t, *J*=14.1 Hz, 0.1H, ***3.18*** 4α-**H**), 2.62 (s, 1H, 7α-**OH**), 2.50 (td, *J*=14.2, 5.3 Hz, 1H, ***3.17*** 2α-**H**), 2.27-2.39 (m, 3H, 5β-**H**, 2β-**H**, 23-**H'**), 2.20 (ddd, *J*=16.4, 10.3, 6.6 Hz, 1H, 23-**H''**), 2.06-2.15 (m, 1H, 1α-**H**), 1.98 (br dt, *J*=12.5, 3.1 Hz, 1H, 12β-**H**), 1.07-1.95 (m), 1.04 (s, 3H, 19-**CH_3**), 0.87-0.94 (m, 3H, 21-**CH_3**), 0.66 (s, 3H, 18-**CH_3**) ppm. **^{13}C NMR** (100 MHz, $CDCl_3$) δ 205.0 (d, *J*=15.4 Hz, **3-C**), 174.6 (**24-COO**CH_3), 92.5 (d, *J*=195.1 Hz, ***3.17*** **4-CH**), 90.7 (d, *J*=189.3 Hz, ***3.17*** **6-CH**), 90.3 (d, *J*=176.8 Hz, ***3.18*** **6-CH**), 88.9 (d, *J*=190.0 Hz, ***3.18*** **2-CH**), 70.3 (d, *J*=17.6 Hz, ***3.17*** **7-CH**), 69.7 (d, *J*=16.9 Hz, ***3.18*** **7-CH**), 55.6 (**17-CH**), 53.3 (t, *J*=14.7 Hz, **5-CH**), 51.5 (**24-**COO**CH_3**), 49.6 (**14-CH**), 42.4 (**13-C**), 39.2 (t, *J*=7.0 Hz, **10-C**), 38.9 (**12-CH_2**), 37.9 (d, *J*=5.9 Hz, **8-CH**), 36.4 (**1-CH_2**), 35.2 (**20-CH**), 34.9 (***3.17*** **2-CH_2**), 34.6 (**9-CH**), 30.9

(**23-CH_2**), 30.8 (**22-CH_2**), 27.9 (**16-CH_2**), 23.2 (**15-CH_2**), 22.2 (**19-CH_3**), 21.0 (**11-CH_2**), 18.1 (**21-CH_3**), 11.6 (**18-CH_3**) ppm. **^{19}F NMR** (376MHz, $CDCl_3$) δ -193.64--193.17 (m, 0.9F, ***3.17*** 4β-**F**), -195.30--194.98 (m, 0.1F, ***3.18*** 2β-**F**), -195.71--195.31 (m, 0.9F, ***3.17*** 6α-**F**), -196.21 (dq, *J*=43.3, 5.2 Hz, 1F, ***3.18*** 6α-**F**) ppm. **^{19}F [^{1}H] NMR** (376MHz, $CDCl_3$) δ -193.44 (d, *J*=38.1 Hz, 0.9F, ***3.17*** 4β-**F**), -195.15 (s, 0.1F, ***3.18*** 2β-**F**), -195.49 (br d, *J*=38.1 Hz, 0.9F, ***3.17*** 6α-**F**), -196.22 (s, 0.1F, ***3.18*** 6α-**F**) ppm. **LRMS (ESI+)** m/z: 458.2 $[M+NH_4]^+$. **HRMS (ESI+)** $C_{25}H_{42}F_2NO_4$ $[M+NH_4]^+$. Calculated: 458.3076; Found: 458.3087 (2.4 ppm error).

3.19: R_f 0.29 (Acetone/PE 30/70). **Selected ^{1}H NMR** (400 MHz, $CDCl_3$) δ 8.17 (s, 1H, 27-**H**), 5.89 (br dd, *J*=47.6, 10.3 Hz, 1H, 4α-**H**), 5.06 (d, *J*=10.0 Hz, 1H, 25-**H'**), 4.74-4.87 (m, 1H, 6β-**H**), 4.72 (d, *J*=10.1 Hz, 1H, 25-**H''**), 3.85-3.95 (m, 1H, 7β-**H**), 3.65 (s, 3H, 24-COO**CH_3**), 2.93 (s, 3H, 26-**CH_3**), 2.48 (td, *J*=14.4, 5.3 Hz, 1H, 2α-**H**), 1.03-1.08 (m, 3H, 19-**CH_3**), 0.88-0.94 (m, 3H, 21-**CH_3**), 0.63-0.69 ppm (s, 3H, 18-**CH_3**) ppm. **Selected ^{13}C NMR** (100 MHz, $CDCl_3$) δ 204.3 (d, *J*=15.4 Hz, **3-C**), 174.4 (**24-COO**CH_3), 163.3 (**27-CH**), 92.4 (d, *J*=190.0 Hz, **4-CH**), 91.9 (d, *J*=187.8 Hz, **6-CH**), 81.7 (d, *J*=7.3 Hz, **25-CH_2**), 75.7 (d, *J*=15.4 Hz, **7-CH**), 55.6 (**17-CH**), 53.7 (t, *J*=14.3 Hz, **5-CH**), 51.4 (**24**-COO**CH_3**), 49.4 (**14-CH**), 42.5 (**13-C**), 39.3 (t, *J*=7.0 Hz**, 10-C**), 38.7 (**12-CH_2**), 38.3 (d, *J*=6.6 Hz, **8-CH**), 36.2 (CH_2), 35.3 (**9-CH**), 35.2 (**20-CH**), 34.9 (**2-CH_2**), 30.9 (CH_2), 30.8 (CH_2), 29.6 (**26-CH_3**), 27.8 (CH_2), 23.8 (CH_2), 22.3 (**19-CH_3**), 21.0 (CH_2), 18.2 (**21-CH_3**), 11.7 (**18-CH_3**) ppm. **Selected ^{19}F NMR** (376MHz, $CDCl_3$) δ -187.65 (br dd, *J*=42.5, 35.5 Hz, 1F, 4β-**F**), -195.98 (dddd, *J*=48.1, 34.2, 14.7, 5.2 Hz, 1F, 6α-**F**) ppm. **Selected ^{19}F [^{1}H] NMR** (376MHz, $CDCl_3$) δ -187.65 (d, *J*=34.7 Hz, 1F, 4β-**F**), -195.98 (d, *J*=34.7 Hz, 1F, 6α-**F**) ppm. **LRMS (ESI+)** m/z: 512.2 $[M+H]^+$.

Methyl 4β,6α-difluoro-chenodeoxycholan-24-oate (3.23), Methyl 2β,6α-difluoro-chenodeoxycholan-24-oate (3.24), Methyl 4β,6α-difluoro-3β,7α-dihydroxy-5β-cholan-24-oate (3.25), Methyl 2β,6α-difluoro-3β,7α-dihydroxy-5β-cholan-24-oate (3.26)

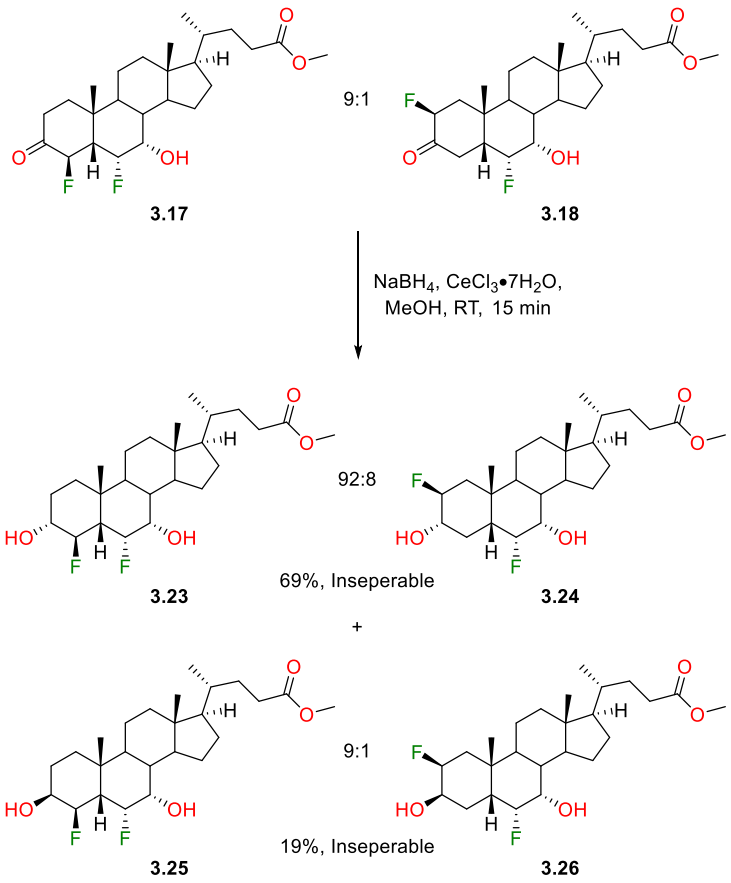

The ketones **3.17** and **3.18** (9:1 mix, 2.68 g, 6.08 mmol, 1.0 equiv) were dissolved in methanol (130 mL) and $CeCl_3 \bullet 7H_2O$ (2.72 g, 7.30 mmol, 1.2 equiv) was added. The reaction mixture was stirred and $NaBH_4$ (276 mg, 7.30 mmol, 1.2 equiv) was added in portions, over 5 min. After 15 min, the reaction mixture was quenched with 2M HCl (150 mL), added water (200 mL) and extracted with EtOAc (4 x 100 mL). The combined organic phases were then washed with water (300 mL) and brine (300 mL) before drying over Na_2SO_4 and reducing *in vacuo* to give 2.8 g of crude material. The crude was purified by flash chromatography (acetone/PE 20%/80%) to firstly yield an inseparable 9:1 mix of **3.25** and **3.26** as a white gummy solid (520 mg, 1.17 mmol, 19%); secondly, **3.23** and **3.24** were yielded in an inseparable 92:8 mixture as a white gummy solid (1.85 g, 4.20 mmol, 69%).

3.23 and 3.24: $\mathbf{R_f}$ 0.34 (Acetone/PE 30/70). **Selected ^{1}H NMR** (400 MHz, $CDCl_3$) δ 5.44 (ddd, *J*=50.5, 10.4, 8.9 Hz, 1H, 4β-**H**), 4.75 (ddd, *J*=44.4, 5.1, 3.3 Hz, 1H, 6α-**H**), 4.15 (apparent br d, *J*=8.1 Hz, 1H, 7β-**H**), 3.67 (s, 3H, 24-COO**CH$_3$**), 3.52-3.65 (m, 1H, 3β-**H**), 1.05-2.48 (m), 0.99 (s, 3H, 19-**CH$_3$**), 0.92 (d, *J*=6.5 Hz, 3H, 21-**CH$_3$**), 0.66 (s, 3H, 18-**CH$_3$**) ppm. **^{19}F NMR** (376MHz, $CDCl_3$) δ -187.79--187.48 (m, 0.1F), -192.04--191.54 (m, 1F), -193.47 (br t, *J*=43.4 Hz, 1F), -195.94 (br d, *J*=45.1 Hz, 0.1F) ppm. **^{19}F**

[^{1}H] NMR (376MHz, $CDCl_3$) δ -187.66 (s, 0.1F), -191.78 (d, *J*=39.9 Hz, 1F), -193.46 (d, *J*=39.9 Hz, 1F), -195.94 (s, 0.1F) ppm.

3.25 and 3.26: R_f 0.44 (Acetone/PE 30/70). **Selected ^{1}H NMR** (400 MHz, $CDCl_3$) δ 5.62 (ddd, *J*=45.6, 10.9, 3.2 Hz, 1H, 4α-**H**), 4.82 (ddd, *J*=44.3, 4.9, 3.2 Hz, 1H, 6β-**H**), 4.11-4.19 (m, *J*=8.2 Hz, 2H, 3α-**H** and 7β-**H**), 3.67 (s, 3H, 24-COO**CH$_3$**), 1.05-2.51 (m), 1.01 (s, 3H, 19-**CH$_3$**), 0.92 (d, *J*=6.5 Hz, 3H, 21-**CH$_3$**), 0.66 (s, 3H, 18-**CH$_3$**) ppm. **^{19}F NMR** (376MHz, $CDCl_3$) δ -187.73--187.43 (m, 0.1F), -191.09--190.70 (m, 1F), -193.08--192.68 (m, 1F), -196.87 (br d, *J*=43.3 Hz, 0.1F) ppm. **^{19}F [^{1}H] NMR** (376MHz, $CDCl_3$) δ -187.56 (s, 0.1F), -190.89 (d, *J*=39.9 Hz, 1F), -192.88 (d, *J*=39.9 Hz, 1F), -196.86 (s, 0.1F) ppm.

Methyl 4β,6α-difluoro-3α,7α-diacteoxy-5β-cholan-24-oate (3.27)

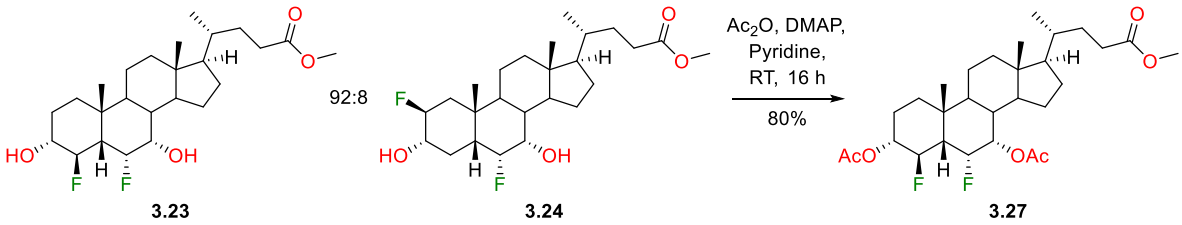

3.23 **3.24** **3.27**

Following general procedure E, the mix of **3.23** and **3.24** (92:8, 3.69 g, 8.34 mmol, 1.0 equiv) was protected. The crude material was purified by flash chromatography (EtOAc/PE 18%/82% → 20%/80% → 50%/50%) to yield **3.27** 95% pure as a white solid (3.50 g, 6.65 mmol, 80%). Note: No 2β-fluorinated acetylated material cleanly isolated.

mp 209 – 210 °C. **R_f** 0.34 (EtOAc/PE 20/80). **[α]$_D$** + 11.1 (c = 0.49, $CHCl_3$, 22 °C). **^{1}H NMR** (400 MHz, $CDCl_3$) δ 5.45-5.56 (m, 1H, 7β-**H**), 5.31 (dt, *J*=50.3, 9.7 Hz, 1H, 4α-**H**), 4.73-4.93 (m, 2H, 6β-**H** and 7β-**H**), 3.65 (s, 3H, 24-COO**CH$_3$**), 2.34 (ddd, *J*=15.4, 10.1, 5.3 Hz, 1H, 23-**H'**), 2.21 (ddd, *J*=16.0, 9.3, 6.8 Hz, 1H, 23-**H''**), 2.15 (s, 3H, 7α-OCO**CH$_3$**), 2.09-2.14 (m, 1H, 5β-**H**), 2.08 (s, 3H, 3α-OCO**CH$_3$**), 1.97 (br d, *J*=12.3 Hz, 1H, 12β-**H**), 1.04-1.92 (m), 1.02 (s, 3H, 19-**CH$_3$**), 0.90 (d, *J*=6.4 Hz, 3H, 21-**CH$_3$**), 0.64 (s, 3H, 18-**CH$_3$**) ppm. **^{13}C NMR** (100 MHz, $CDCl_3$) δ 174.5 (**24-COO**CH_3), 170.4 (**3α-OCO**CH_3), 169.9 (**7α-OCO**CH_3), 91.8 (d, *J*=180.5 Hz, **4-CH**), 89.2 (d, *J*=190.7 Hz, **6-CH**), 75.2 (d, *J*=19.1 Hz, **3-CH**), 70.9 (d, *J*=16.9 Hz, **7-CH**), 55.6 (**17-CH**), 51.4 (**24-**COO**CH$_3$**), 50.3 (t, *J*=13.6 Hz, **5-CH**), 49.9 (**14-CH**), 42.8 (**13-C**), 39.2 (t, *J*=7.3 Hz, **10-C**), 38.9 (**12-CH$_2$**), 37.2 (d, *J*=5.9 Hz, **8-CH**), 36.0 (**9-CH**), 35.1 (**20-CH**), 34.0 (**1-CH$_2$**), 30.9 (**23-CH$_2$**), 30.8 (**22-CH$_2$**), 27.8 (**16-CH$_2$**), 24.1 (d, *J*=7.3 Hz, **2-CH$_2$**), 23.5 (**15-CH$_2$**), 22.8 (**19-CH$_3$**), 21.1 (***3α- or 7α-OCO**CH$_3$*), 21.1 (***3α- or 7α-OCO**CH$_3$*), 20.5 (**11-CH$_2$**), 18.2 (**21-CH$_3$**), 11.7 (**18-CH$_3$**) ppm. **^{19}F NMR** (376MHz, $CDCl_3$) δ -191.22--190.81 (m, 1F, 4β-**F**), -193.54 (br t, *J*=42.5 Hz, 1F, 6α-**F**) ppm. **^{19}F [^{1}H] NMR** (376MHz, $CDCl_3$) δ -191.02 (d, *J*=41.6 Hz, 1F, 4β-**F**), -193.54 (d, *J*=41.6 Hz, 1F, 6α-**F**) ppm. **LRMS (ESI+)** m/z: 544.3 $[M+NH_4]^+$. **HRMS (ESI+)** $C_{29}H_{44}F_2NaO_6$ $[M+Na]^+$. Calculated: 549.2998; Found: 549.2992 (1.1 ppm error). **IR** (neat, cm^{-1}) 2955 – 2885 (m), 1728 (s), 1231 (s), 1037 (m).

4β,6α-Difluorochenodeoxycholic acid (3.2)

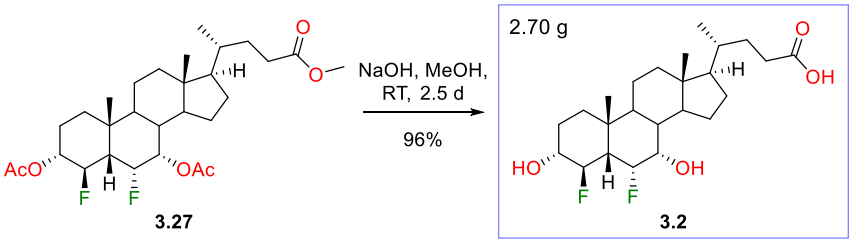

Following general procedure D, **3.27** (1.34 g, 2.54 mmol, 1.0 equiv) was deprotected to yield **3.2** as a white gummy solid (1.04 g, 2.43 mmol, 96%) with no further purification.

R_f 0.05 (EtOAc/PE 30/70). **$[\alpha]_D$** + 11.4 (c = 0.50, MeOH, 22 °C). **^{1}H NMR** (400 MHz, MeOH-d_4) δ 5.45 (ddd, *J*=49.9, 10.0, 8.9 Hz, 1H, 4α-**H**), 4.69 (ddd, *J*=44.6, 5.0, 3.1 Hz, 1H, 6β-**H**), 4.05 (apparent br d, *J*=8.8 Hz, 1H, 7β-**H**), 3.39-3.52 (m, 1H, 3β-**H**), 2.34 (ddd, *J*=15.3, 9.8, 5.4 Hz, 1H, 23-**H'**), 2.21 (ddd, *J*=15.6, 9.1, 6.9 Hz, 1H, 23-**H''**), 1.09-2.04 (m), 1.01 (s, 3H, 19-**CH_3**), 0.96 (d, *J*=6.5 Hz, 3H, 21-**CH_3**), 0.70 (s, 3H, 18-**CH_3**) ppm. **^{13}C NMR** (100 MHz, MeOH-d_4) δ 178.2 (**24-COO**CH_3), 97.5 (d, *J*=173.9 Hz, **4-CH**), 93.0 (d, *J*=183.4 Hz, **6-CH**), 75.2 (d, *J*=19.1 Hz, **3-CH**), 71.2 (d, *J*=16.9 Hz, **7-CH**), 57.4 (**17-CH**), 52.1 (t, *J*=13.9 Hz, **5-CH**), 51.3 (**14-CH**), 43.8 (**13-C**), 40.8 (**12-CH_2**), 40.9 (br t, *J*=7.7 Hz, **10-C**), 39.8 (d, *J*=6.6 Hz, **8-CH**), 36.8 (**20-CH**), 36.2 (**9-CH**), 35.7 (**1-CH_2**), 32.4 (**22-CH_2**), 32.1 (**23-CH_2**), 29.3 (***15-CH_2* *or* *16-CH_2***), 27.9 (d, *J*=8.8 Hz, **2-CH_2**), 24.5 (***15-CH_2* *or* *16-CH_2***), 23.6 (**19-CH_3**), 21.9 (**11-CH_2**), 18.9 (**21-CH_3**), 12.3 (**18-CH_3**) ppm. **^{19}F NMR** (376MHz, MeOH-d_4) δ -188.39--187.94 (m, 1F, 4β-**F**), -192.72--192.32 (m, 1F, 6α-**F**) ppm. **^{19}F [^{1}H] NMR** (376MHz, MeOH-d_4) δ -188.16 (d, *J*=38.1 Hz, 1F, 4β-**F**), -192.53 (d, *J*=38.1 Hz, 1F, 6α-**F**) ppm. **LRMS (ESI+)** m/z: 446.4 $[M+NH_4]^+$. **HRMS (ESI+)** $C_{24}H_{38}F_2NaO_4$ $[M+Na]^+$. Calculated: 451.2630; Found: 451.2635 (0.9 ppm error). **IR** (neat, cm^{-1}) 3428 (b), 2936 – 2870 (m), 1705 (s), 1055 (s), 1019 (s).

Methyl 4β,6α-difluoro-3α,7α-dihydroxy-5β-cholan-24-oate (3.23)

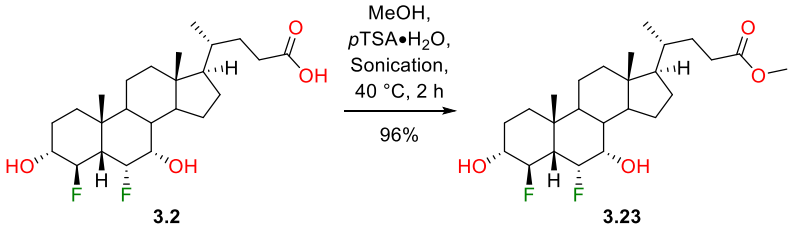

Following general procedure A, **3.2** (2.72 g, 6.35 mmol, 1.0 equiv) was protected to yield **3.23** as a white gummy solid (2.71 g, 6.12 mmol, 96%) with no further purification.

R_f 0.55 (EtOAc/PE 50/50). **$[\alpha]_D$** + 23.8 (c = 0.45, $CHCl_3$, 22 °C). **^{1}H NMR** (400 MHz, $CDCl_3$) δ 5.44 (ddd, *J*=50.5, 10.4, 8.9 Hz, 1H, 4α-**H**), 4.73 (ddd, *J*=44.4, 5.0, 3.1 Hz, 1H, 6β-**H**), 4.13 (apparent br d, *J*=8.3 Hz, 1H, 7β-**H**), 3.66 (s, 3H, 24-COO**CH_3**), 3.50-3.62 (m, 1H, 3β-**H**), 2.63 (br s, 1H, 3α-**OH**), 2.44 (br s,

1H, 7α-**OH**), 2.35 (ddd, *J*=15.4, 10.1, 5.3 Hz, 1H, 23-**H'**), 2.22 (ddd, *J*=16.0, 9.7, 6.7 Hz, 1H, 23-**H''**), 1.04-2.06 (m), 0.98 (s, 3H, 19-**CH_3**), 0.91 (d, *J*=6.4 Hz, 3H, 21-**CH_3**), 0.65 (s, 3H, 18-**CH_3**) ppm. **^{13}C NMR** (100 MHz, $CDCl_3$) δ 174.7 (**24-COO**CH_3), 97.0 (d, *J*=171.7 Hz, **4-CH**), 91.8 (d, *J*=181.9 Hz, **6-CH**), 74.1 (d, *J*=19.1 Hz, **3-CH**), 70.2 (d, *J*=17.6 Hz, **7-CH**), 55.6 (**17-CH**), 51.5 (**24-**COO**CH_3**), 49.8 (t, *J*=13.9 Hz, **5-CH**), 49.7 (d, *J*=1.5 Hz, **14-CH**), 42.5 (**13-C**), 39.9 (t, *J*=7.7 Hz, **10-C**), 39.1 (**12-CH_2**), 38.2 (d, *J*=5.9 Hz, **8-CH**), 35.3 (**20-CH**), 34.7 (**9-CH**), 34.3 (**1-CH_2**), 30.9 (**23-CH_2**), 30.9 (**22-CH_2**), 28.0 (**15-CH_2** or **16-CH_2**), 25.9 (d, *J*=8.1 Hz, **2-CH_2**), 23.3 (**15-CH_2** or **16-CH_2**), 22.9 (**19-CH_3**), 20.6 (**11-CH_2**), 18.2 (**21-CH_3**), 11.7 (**18-CH_3**) ppm. **^{19}F NMR** (376MHz, $CDCl_3$) δ -191.56--191.02 (m, 1F, 4β-**F**), -193.10 (br td, *J*=43.3, 3.5 Hz, 1F, 6α-**F**) ppm. **^{19}F [^{1}H] NMR** (376MHz, $CDCl_3$) δ -191.26 (br d, *J*=39.9 Hz, 1F, 4β-**F**), -193.10 (br d, *J*=39.9 Hz, 1F, 6α-**F**) ppm. **LRMS (ESI+)** m/z: 460.5 $[M+NH_4]^+$. **HRMS (ESI+)** $C_{25}H_{40}F_2NaO_4$ $[M+Na]^+$. Calculated: 465.2787; Found: 465.2795 (1.8 ppm error). **IR** (neat, cm^{-1}) 3451 (b), 2937 – 2870 (m), 1734 (s), 1054 (s), 1019 (s).

Methyl 3α,7α-di(phenoxycarbonothioyl)oxy-5β-cholan-24-oate (3.28)

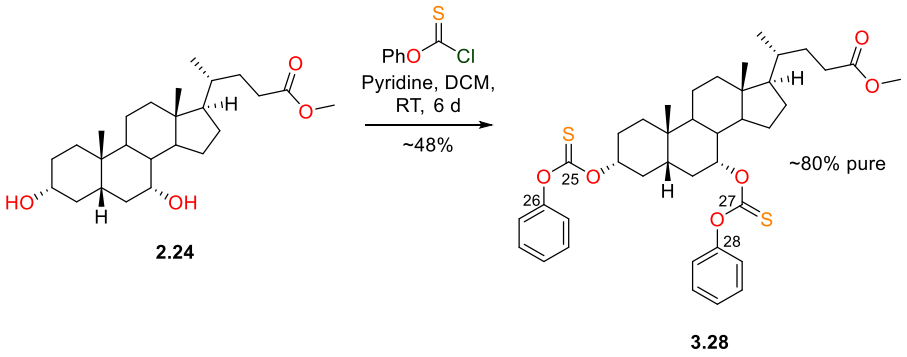

CDCA methyl ester (**2.24**, 300 mg, 0.74 mmol, 1.0 equiv) was dissolved in dry DCM (5 mL) and dry pyridine (0.36 mL, 4.44 mmol, 6.0 equiv) and *O*-phenyl chlorothionoformate (0.23 mL, 1.63 mmol, 2.2 equiv) were added. After stirring for 23 h at RT, further *O*-phenyl chlorothionoformate (~0.06 mL, ~0.4 mmol, ~0.5 equiv) and dry DCM (3 mL) were added to the reaction mixture. After 3 d, further *O*-phenyl chlorothionoformate (~0.06 mL, ~0.4 mmol, ~0.5 equiv), dry pyridine (0.36 mL, 4.44 mmol, 6.0 equiv) and dry DCM (3 mL) were added to the reaction mixture. 6 d after starting the reaction, the reaction mixture was added EtOAc (50 mL). The combined organic phases were then washed with water (50 mL) and brine (50 mL) before drying over Na_2SO_4 and reducing *in vacuo* to give ~650 mg of crude material. The crude was purified twice by flash chromatography (1st: Biotage SNAP KP-Sil 25 g cartridge, acetone/PE 2%/98% → 10%/90% over 15 CV; 2nd: Biotage SNAP KP-Sil 25 g cartridge, acetone/PE 3%/97% → 7%/93% over 16 CV), yielding **3.28** around 80% pure as a white gummy solid (300 mg, ~0.35 mmol, ~48%).

R_f 0.32 (Acetone/PE 10/90). **^{1}H NMR** (400 MHz, $CDCl_3$) δ 7.37-7.50 (m, 4H, *meta* **CH**), 7.27-7.35 (m, 2H, *para*-**CH**), 7.05-7.14 (m, 3.5H, *ortho*-**CH**), 5.29 (br s, 0.8H,7β-**H**), 5.02-5.15 (m, 0.9H, 3β-**H**), 3.61-

3.75 (m, 3H, 24-COO**CH₃**), 2.34-2.46 (m, 1H, 23-**H'**), 1.02-2.33 (m), 0.97 (s, 3H, 19-**CH₃**), 0.95 (d, *J*=6.4 Hz, 3H, 21-**CH₃**), 0.68 (s, 3H, 18-**CH₃**) ppm. **^{13}C NMR** (100 MHz, $CDCl_3$) δ 194.3 (**25-C**), 193.1 (**27-C**), 174.6 (**24-COO**CH_3), 153.3 (***26-C or 28-C***), 153.0 (***26-C or 28-C***), 129.5 (2 C, ***meta*-CH**), 129.5 (2 C, ***meta*-CH**), 126.5 (***para*-CH**), 126.4 (***para*-CH**), 122.0 (2 C, ***ortho*-CH**), 122.0 (2 C, ***ortho*-CH**), 84.4 (**3-CH**), 83.0 (**7-CH**), 55.8 (**17-CH**), 51.5 (**24-**COO**CH₃**), 50.2 (**14-CH**), 42.7 (**13-C**), 40.6 (***5-CH or 9-CH***), 39.4 (**12-CH₂**), 38.4 (**8-CH**), 35.3 (**20-CH**), 34.6 (**1-CH₂**), 34.5 (**10-C**), 34.4 (***5-CH or 9-CH***), 33.4 (CH_2), 31.1 (**23-CH₂**), 31.0 (**22-CH₂**), 29.8 (CH_2), 28.0 (CH_2), 25.9 (**2-CH₂**), 23.7 (CH_2), 22.6 (**19-CH₃**), 20.6 (CH_2), 18.2 (**21-CH₃**), 11.6 (**18-CH₃**) ppm. **LRMS (ESI+)** m/z: 696.3 $[M+NH_4]^+$.

Methyl 5β-cholan-24-oate (3.29)

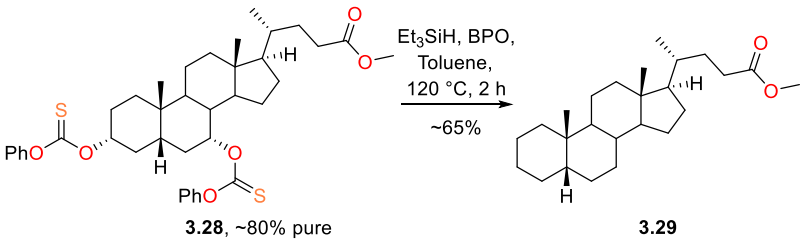

Following general procedure H, **3.28** (~80% pure, 164 mg, ~0.24 mmol, 1.0 equiv) was deoxygenated. The crude material was combined with the crude from a repeat of the reaction (total ~0.31 mmol of **3.28**) and purified by flash chromatography (Et_2O/PE 0%/100% → 2%/98%), yielding **3.29** as a white solid with trace aromatic impurities (76 mg, 0.20 mmol, ~65%).

mp 68 – 70 °C (lit. 87 °C).[233] **R_f** 0.65 (EtOAc/PE 10/90). **^{1}H NMR** (400 MHz, $CDCl_3$) δ 3.67 (s, 3H, 24-COO**CH₃**), 2.35 (ddd, *J*=15.5, 10.4, 5.3 Hz, 1H, 23-**H'**), 2.22 (ddd, *J*=16.0, 9.9, 6.6 Hz, 1H, 23-**H''**), 1.92-1.99 (m, 1H, 12β-**H**), 1.61-1.91 (m, 6H), 1.52-1.61 (m, 1H), 1.00-1.48 (m), 0.92 (s, 3H, 19-**CH₃**), 0.92 (d, *J*=6.5 Hz, 3H, 21-**CH₃**), 0.83-0.90 (m, 1H, 1β-**H**), 0.65 (s, 3H, 18-**CH₃**) ppm. **^{13}C NMR** (100 MHz, $CDCl_3$) δ 174.8 (**24-COO**CH_3), 56.6 (**14-CH**), 56.0 (**17-CH**), 51.4 (**24-**COO**CH₃**), 43.7 (***5-CH or 9-CH***), 42.8 (**13-C**), 40.5 (***5-CH or 9-CH***), 40.3 (**12-CH₂**), 37.6 (**1-CH₂**), 35.9 (**8-CH**), 35.4 (**20-CH**), 35.4 (**10-C**), 31.1 (**23-CH₂**), 31.0 (**22-CH₂**), 28.2 (CH_2), 27.5 (CH_2), 27.2 (**3-CH₂**), 27.0 (CH_2), 26.6 (CH_2), 24.3 (**19-CH₃**), 24.2 (CH_2), 21.3 (**2-CH₂**), 20.8 (**11-CH₂**), 18.3 (**21-CH₃**), 12.0 (**18-CH₃**) ppm. **LRMS (ESI+)** m/z: 392.7 $[M+NH_4]^+$. **HRMS (ESI+)** $C_{25}H_{43}O_2$ $[M+H]^+$. Calculated: 375.3258; Found: 375.3253 (1.3 ppm error). ^{1}H and ^{13}C NMR data agree with literature.[153,234]

5β-Cholanic Acid (1.25)

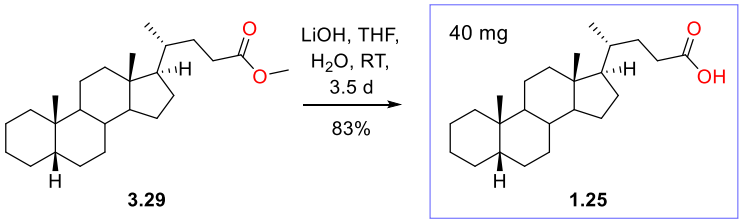

Following general procedure C, **3.29** (56 mg, 0.15 mmol, 1.0 equiv) was deprotected to yield **1.25** as a white solid (45 mg, 0.12 mmol, 83%) with no further purification.

mp 140 – 142 °C. **R_f** 0.38 (Acetone/PE 20/80). **$[\alpha]_D$** + 21.1 (c = 0.32, $CHCl_3$, 22 °C). **^{1}H NMR** (400 MHz, $CDCl_3$) δ 2.41 (ddd, *J*=15.5, 10.4, 5.3 Hz, 1H, 23-**H'**), 2.27 (ddd, *J*=16.0, 9.8, 6.5 Hz, 1H, 23-**H''**), 1.93-1.99 (m, 1H, 12β-**H**), 1.69-1.92 (m, 6H), 1.54-1.62 (m, 1H), 0.99-1.51 (m), 0.94 (d, *J*=6.4 Hz, 3H, 21-**CH_3**), 0.92 (s, 3H, 19-**CH_3**), 0.84-0.91 (m, 1H, 1β-**H**), 0.66 (s, 3H, 18-**CH_3**) ppm. **^{13}C NMR** (100 MHz, $CDCl_3$) δ 180.3 (**24-COOH**), 56.6 (**14-CH**), 56.0 (**17-CH**), 43.7 (**5-CH**), 42.8 (**13-C**), 40.5 (**9-CH**), 40.3 (**12-CH_2**), 37.6 (**1-CH_2**), 35.9 (**8-CH**), 35.4 (**10-C**), 35.3 (**20-CH**), 31.0 (**23-CH_2**), 30.8 (**22-CH_2**), 28.2 (CH_2), 27.5 (CH_2), 27.3 (CH_2), 27.0 (CH_2), 26.6 (CH_2), 24.3 (**19-CH_3**), 24.2 (CH_2), 21.3 (**2-CH_2**), 20.8 (**11-CH_2**), 18.2 (**21-CH_3**), 12.1 (**18-CH_3**) ppm. **LRMS (ESI-)** m/z: 359.3 $[M-H]^-$, 719.7 $[2M-H]^-$. **HRMS (ESI+)** $C_{24}H_{39}O_2$ $[M-H]^-$. Calculated: 359.2956; Found: 359.2950 (1.5 ppm error). ^{1}H and ^{13}C NMR data agree with literature.[234,235]

Methyl 4β,6α-difluoro-3α,7α-di(phenoxycarbonothioyl)oxy-5β-cholan-24-oate (3.30), Methyl 4β,6α-difluoro-3α-(phenoxycarbonothioyl)oxy-7α-hydroxy-5β-cholan-24-oate (3.31), Methyl 4β,6α-difluoro-3α-(phenoxycarbonothioyl)oxy-7α-(phenoxycarbonyl)oxy-5β-cholan-24-oate (3.32)

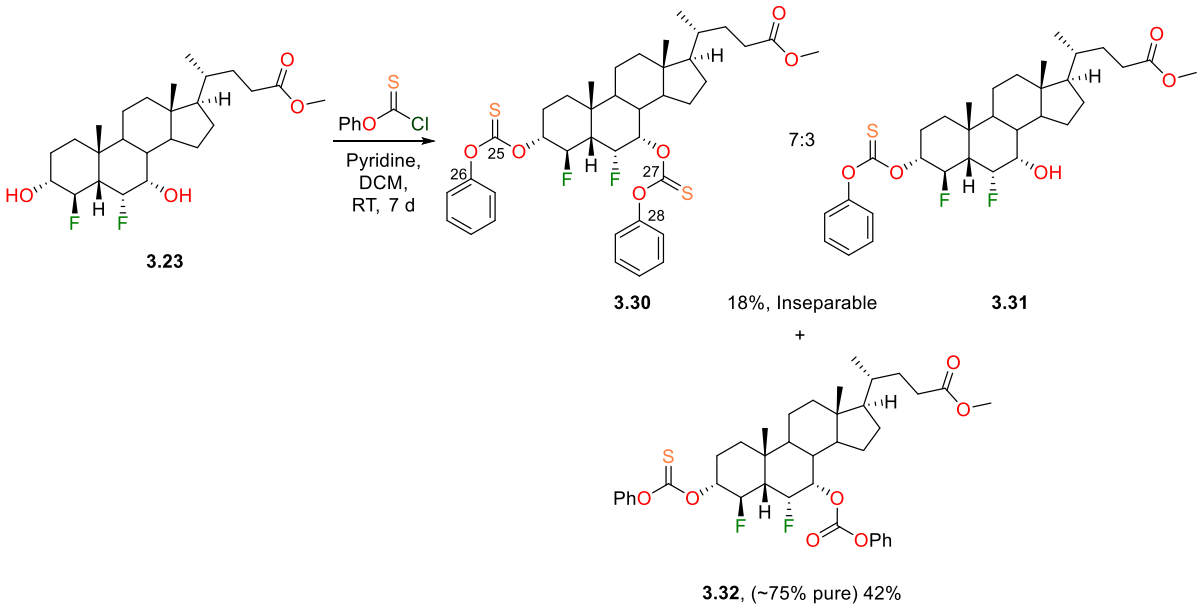

The alcohol **3.23** (680 mg, 1.54 mmol, 1.0 equiv) was dissolved in dry DCM (15 mL) and pyridine (5.0 mL, 62 mmol, 40 equiv) and *O*-phenyl chlorothionoformate (4.3 mL, 31 mmol, 20 equiv) were added. After stirring at RT for 7 d, the reaction mixture was added EtOAc (150 mL). The combined organic phases were washed with 1M HCl (150 mL), water (150 mL) and brine (150 mL) before drying over Na_2SO_4 and reducing *in vacuo* to give 1.2 g of crude material. The crude was purified twice by flash chromatography (1st: Biotage SNAP KP-Sil 25 g cartridge, EtOAc/PE: 10%/90% →

60%/40%; 2nd: Biotage SNAP KP-Sil 25 g cartridge, EtOAc/PE: 15%/85% → 60%/40%) to firstly yield a 7:3 mix of **3.30** and **3.31** (207 mg, ~0.31 mmol, ~20%) and secondly to yield **3.32** around 75% pure (567 mg, ~0.61 mmol, ~40%). Both were isolated as colourless gums.

3.30 and **3.31:** $\mathbf{R_f}$ 0.33 (EtOAc/PE 20/80). **Selected ^{1}H NMR** (400 MHz, $CDCl_3$) δ 7.28-7.53 (m, 5H, *ortho*/*meta*/*para*-CH), 7.08-7.26 (m, 5H, *ortho*/*meta*/*para*-CH), 6.00-6.10 (m, 0.7H, 6β-**H**), 5.48 (dt, *J*=50.1, 9.4 Hz, 0.7H, 4α-**H**), 5.25-5.38 (m, 1H, 3β-**H**), 5.03 (ddd, *J*=42.8, 4.8, 3.5 Hz, 1H, 6β-**H**), 3.62-3.76 (m, 3H, 24-COO**CH_3**), 2.34-2.45 (m, 1H, 23-**H'**), 1.11-2.31 (m), 1.08 (s, 2H, 19-**CH_3**), 0.95 (br d, *J*=6.1 Hz, 3H, 21-**CH_3**), 0.64-0.71 (m, 3H, 18-**CH_3**) ppm. **Selected ^{13}C NMR** (100 MHz, $CDCl_3$) δ 194.4 (**27-C**), 194.1 (**25-C**), 174.5 (**24-COO**CH_3), 153.4 (***26-C** or **28-C***), 153.2 (***26-C** or **28-C***), 129.6 (2 C, ***ortho- or meta-CH***), 129.4 (2 C, ***ortho- or meta-CH***), 126.5 (***para*-CH**), 126.4 (***para*-CH**), 121.9 (2 C, ***ortho- or meta-CH***), 121.8 (2 C, ***ortho- or meta-CH***), 91.0 (d, *J*=182.7 Hz, **4-CH**), 89.5 (d, *J*=192.9 Hz, **6-CH**), 85.3 (d, *J*=19.1 Hz, **3-CH**), 81.5 (d, *J*=15.4 Hz, **7-CH**), 55.5 (**17-CH**), 51.5 (**24-**COO**CH_3**), 50.4 (t, *J*=13.9 Hz, **5-CH**), 49.9 (**14-CH**), 42.9 (**13-C**), 39.2 (t, *J*=7.0 Hz, **10-C**), 38.7 (**12-CH_2**), 37.7 (d, *J*=4.4 Hz, **8-CH**), 36.1 (**9-CH**), 35.2 (**20-CH**), 33.7 (**1-CH_2**), 31.0 (**23-CH_2**), 30.8 (**22-CH_2**), 27.9 (CH_2), 24.2 (CH_2), 22.9 (**2-CH_2**) 22.7 (**19-CH_3**), 20.5 (CH_2), 18.2 (**21-CH_3**), 11.6 (s, **18-CH_3**) ppm. **Selected ^{19}F NMR** (376MHz, $CDCl_3$) δ -189.89--189.44 (m, 1F, 4β-**F**), -192.49 (br t, *J*=43.3 Hz, 1F, 6α-**F**) ppm. **Selected ^{19}F [^{1}H] NMR** (376MHz, $CDCl_3$) δ -189.67 (br d, *J*=41.6 Hz, 1F, 4β-**F**), -192.49 (br d, *J*=41.6 Hz, 1F, 6α-**F**) ppm. **LRMS (ESI+)** m/z: 732.4 $[M+NH_4]^+$.

3.32: $\mathbf{R_f}$ 0.26 (EtOAc/PE 20/80). **Selected ^{1}H NMR** (400 MHz, $CDCl_3$) 7.30-7.53 (m, 5H, *ortho*/*meta*/*para*-CH), 7.10-7.26 (m, 5H, *ortho*/*meta*/*para*-CH), 5.54 (br dt, *J*=50.3, 9.4 Hz, 1H, 4α-**H**), 5.40-5.45 (m, 1H, 7β-**H**), 5.26-5.39 (m, 1H, 3β-**H**), 4.95 (ddd, *J*=42.9, 5.0, 3.5 Hz, 1H, 6β-**H**), 3.67-3.70 (m, 3H, 24-COO**CH_3**), 2.38 (ddd, *J*=15.3, 9.9, 5.1 Hz, 1H, 23-**H'**), 2.20-2.31 (m, 3H), 1.15-2.05 (m), 1.06-1.10 (m, 3H, 19-**CH_3**), 0.95 (d, *J*=6.5 Hz, 3H, 21-**CH_3**), 0.69 (s, 3H, 18-**CH_3**) ppm. **Selected ^{19}F [^{1}H] NMR** (376MHz, $CDCl_3$) δ -189.16 (d, *J*=43.4 Hz, 1F, 4β-**F**), -194.21 (d, *J*=43.4 Hz, 1F, 6α-**F**) ppm. **LRMS (ESI+)** m/z: 716.4 $[M+NH_4]^+$.

Methyl 4β,6α-difluoro-5β-cholan-24-oate (3.33), Methyl 4β,6α-difluoro-7α-hydroxy-5β-cholan-24-oate (3.34)

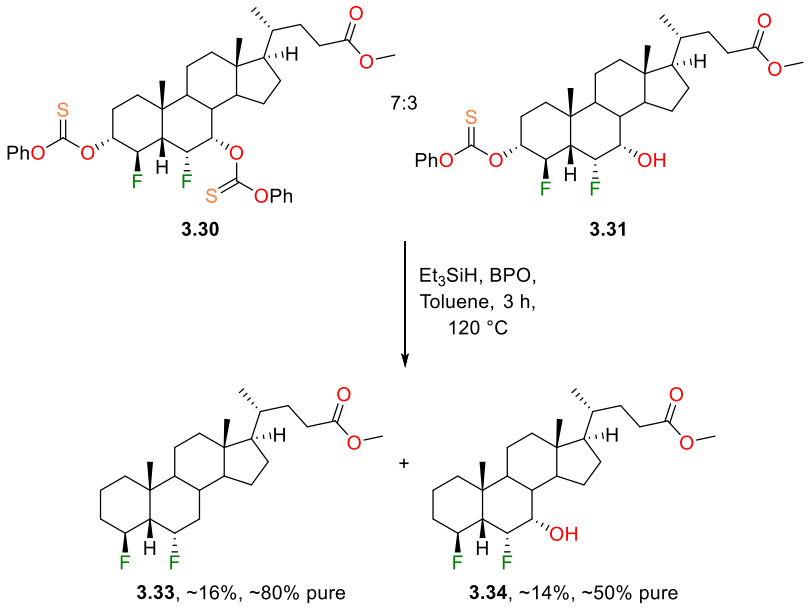

Following general procedure H, the 7:3 mixture of thiocarbonates **3.30** and **3.31** (200 mg, ~0.28 mmol, 1.0 equiv) was deoxygenated. The crude material was purified by flash chromatography (Biotage SNAP KP-Sil 25 g cartridge, EtOAc/PE: 0%/100% → 20%/80% over 20 CV) to firstly yield **3.33**, around 80% pure, as a colourless gum (23 mg, ~0.045 mmol, ~16%), and to secondly yield **3.34**, around 50% pure, as a colourless gum (34 mg, ~0.040 mmol, ~14%).

3.33: $\mathbf{R_f}$ 0.42 (EtOAc/PE 10/90). **Selected ^{1}H NMR** (400 MHz, $CDCl_3$) δ 4.90-5.16 (m, 2H, 4α-**H** and 6β-**H**), 3.67 (s, 3H, 24-COO**CH₃**), 2.36 (ddd, *J*=15.4, 10.1, 5.0 Hz, 1H, 23-**H'**), 1.02-2.28 (m), 1.00 (s, 3H, 19-**CH₃**), 0.91 (d, *J*=6.5 Hz, 3H, 21-**CH₃**), 0.65 (s, 3H, 18-**CH₃**) ppm. **Selected ^{19}F NMR** (376MHz, $CDCl_3$) δ -174.74 (br t, *J*=43.3 Hz, 1F), -180.16 (br t, *J*=43.4 Hz, 1F) ppm. **Selected ^{19}F [^{1}H] NMR** (376MHz, $CDCl_3$) δ -174.74 (d, *J*=39.9 Hz, 1F), -180.16 (d, *J*=39.9 Hz, 1F) ppm. **LRMS (ESI+)** m/z: 428.3 $[M+NH_4]^+$.

3.34: $\mathbf{R_f}$ 0.28 (EtOAc/PE 10/90). **Selected ^{1}H NMR** (400 MHz, $CDCl_3$) δ 5.58 (dtd, *J*=47.6, 10.3, 5.0 Hz, 1H, 4α-**H**), 4.81 (ddd, *J*=44.6, 5.0, 3.3 Hz, 1H, 6β-**H**), 4.15 (br d, *J*=8.3 Hz, 1H, 7β-**H**), 3.68 (s, 3H, 24-COO**CH₃**), 2.36 (ddd, *J*=15.2, 10.1, 5.1 Hz, 1H, 23-**H'**), 1.02-2.30 (m), 1.00 (s, 3H, 19-**CH₃**), 0.93 (d, *J*=6.5 Hz, 3H, 21-**CH₃**), 0.66 (s, 3H, 18-**CH₃**) ppm. **Selected ^{19}F NMR** (376MHz, $CDCl_3$) δ -176.12 (br t, *J*=44.2 Hz, 1F), -193.26--192.89 (m, 1F) ppm. **Selected ^{19}F [^{1}H] NMR** (376MHz, $CDCl_3$) δ -176.13 (d, *J*=39.9 Hz, 1F), -193.06 (d, *J*=39.9 Hz, 1F) ppm. **LRMS (ESI+)** m/z: 444.2 $[M+NH_4]^+$.

Methyl 4β,6α-difluoro-7α-(phenoxycarbonyl)oxy-5β-cholan-24-oate (3.35)

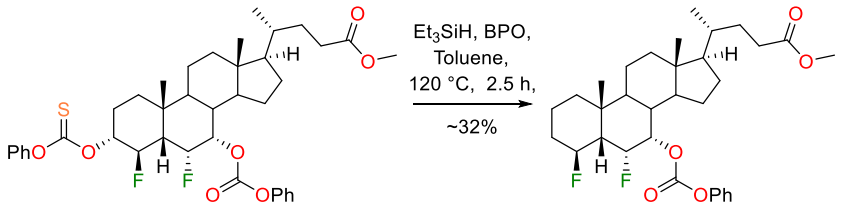

3.32 **3.35**, ~80% pure

Following general procedure H, **3.32** (75% pure, 515 mg, ~0.72 mmol, 0.1 equiv) was deoxygenated. The crude material was purified twice by flash chromatography (1st: Biotage SNAP KP-Sil 25 g cartridge, EtOAc/PE: 0%/100% → 30%/70%; 2nd: Biotage SNAP KP-Sil 25 g cartridge, EtOAc/PE: 10%/90% → 20%/80%) to yield **3.35**, around 80% pure, as a colourless gum (125 mg, ~0.23 mmol, ~32%).

R_f 0.30 (EtOAc/PE 10/90). **^{1}H NMR** (400 MHz, $CDCl_3$) δ 7.35-7.41 (m, 2H, *ortho*-**H**), 7.17-7.26 (m, 3H, *para*-**H**, *meta*-**H**), 5.34-5.41 (m, 1H, 7β-**H**), 5.23 (dtd, *J*=47.9, 10.1, 4.9 Hz, 1H, 4α-**H**), 4.94 (ddd, *J*=43.4, 4.8, 3.7 Hz, 1H, 6β-**H**), 3.66 (s, 3H, 24-COO**CH_3**), 2.37 (ddd, *J*=15.4, 10.0, 5.3 Hz, 1H, 23-**H'**), 2.23 (ddd, *J*=15.9, 9.5, 6.7 Hz, 1H, 23-**H''**), 2.09-2.17 (m, 1H, 3α/β-**H**), 1.03-2.01 (m), 1.01 (s, 3H, 19-**CH_3**), 0.93 (d, *J*=6.5 Hz, 3H, 21-**CH_3**), 0.65 (s, 3H, 18-**CH_3**) ppm. **^{13}C NMR** (100 MHz, $CDCl_3$) δ 174.5 (**24-COO**CH_3), 152.9 (**25-C**), 151.2 (**26-C**), 129.3 (2 C, ***ortho*-CH**), 125.9 (***para*-CH**), 121.1 (2 C, ***meta*-CH**), 90.8 (d, *J*=173.1 Hz, **4-CH**), 89.7 (d, *J*=189.3 Hz, **6-CH**), 76.7 (d, *J*=16.9 Hz, **7-CH**), 55.5 (**17-CH**), 52.2 (t, *J*=13.9 Hz, **5-CH**), 51.4 (**24-**COO**CH_3**), 49.8 (**14-CH**), 42.8 (**13-C**), 39.5 (t, *J*=7.3 Hz, **10-C**), 38.9 (**12-CH_2**), 37.4 (d, *J*=5.1 Hz, **8-CH**), 36.6 (**1-CH_2**), 35.8 (**9-CH**), 35.2 (**20-CH**), 33.4 (d, *J*=19.8 Hz, **3-CH_2**), 30.9 (**23-CH_2**), 30.8 (**22-CH_2**), 27.9 (***15-CH_2* or *16-CH_2***), 23.5 (***15-CH_2* or *16-CH_2***), 23.3 (**19-CH_3**), 20.5 (**11-CH_2**), 18.2 (d, *J*=13.2 Hz, **2-CH_2**), 18.1 (**21-CH_3**), 11.6 (**18-CH_3**) ppm. **^{19}F NMR** (376MHz, $CDCl_3$) δ -176.48 (br t, *J*=43.4 Hz, 1F, 4β-**F**), -193.23 (br t, *J*=43.4 Hz, 1F, 6α-**F**) ppm. **^{19}F [^{1}H] NMR** (376MHz, $CDCl_3$) δ -176.47 (br d, *J*=41.6 Hz, 1F, 4β-**F**), -193.23 (d, *J*=39.9 Hz, 1F, 6α-**F**) ppm. **LRMS (ESI+)** m/z: 564.3 $[M+NH_4]^+$. **IR** (neat, cm^{-1}) 2942 – 2870 (m), 1766 (s), 1735 (s), 1238 (s), 1208 (s), 729 (m).

Methyl 4β,6α-difluoro-3α,7α-di(methylthio)thiocarbonyloxy-5β-cholan-24-oate (3.40)

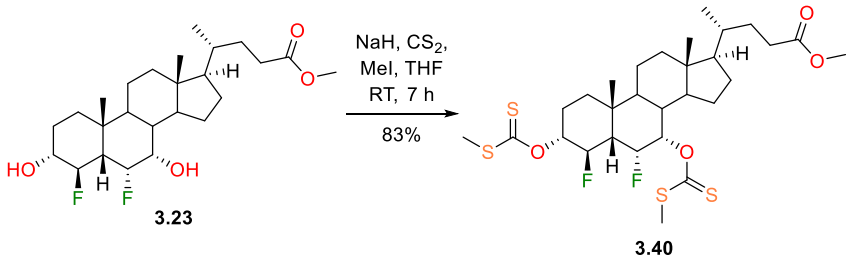

3.23 **3.40**

The alcohol **3.23** (750 mg, 1.69 mmol, 1.0 equiv) was dissolved in dry THF (15 mL) and NaH (~60% in mineral oil, 676 mg, 16.9 mmol, 10 equiv) was added. After stirring for 3 h at RT, CS_2 (1.02 mL, 16.9 mmol, 10 equiv) was added to the reaction mixture. After stirring for a further 3 h at RT, MeI (2.10 mL, 33.8 mmol, 20 equiv) was added. Following 1 h of stirring, NH_4Cl solution (sat., 35 mL) was added to the reaction mixture and the resulting mixture was extracted with EtOAc (3 x 50 mL). The combined organic phases were washed with brine (100 mL) before drying over Na_2SO_4 and reducing *in vacuo* to give a yellow crude. The crude material was purified by flash chromatography (Biotage SNAP KP-Sil 25 g cartridge, EtOAc/PE: 0%/100% → 20%/80% → 50%/50% over 22 CV in total) to yield **3.40** as a pale yellow gummy solid (880 mg, 1.41 mmol, 83%).

R_f 0.30 (EtOAc/PE 15/85). **^{1}H NMR** (400 MHz, $CDCl_3$) δ 6.36-6.51 (m, 1H, 7β-**H**), 5.58-5.68 (m, 1H, 3β-**H**), 5.50 (ddd, *J*=50.1, 10.3, 9.3 Hz, 1H, 4α-**H**), 4.98 (ddd, *J*=43.2, 5.1, 3.4 Hz, 1H, 6β-**H**), 3.66 (s, 3H, 24-COO**CH_3**), 2.64 (s, 3H, S-**CH_3**), 2.56 (s, 3H, S-**CH_3**), 2.34 (ddd, *J*=15.5, 10.3, 5.3 Hz, 1H, 23-**H'**), 2.15-2.27 (m, 3H), 1.98 (br d, *J*=12.2 Hz, 1H, 12β-**H**), 1.09-1.94 (m), 1.07 (s, 3H, 19-**CH_3**), 0.91 (d, *J*=6.5 Hz, 3H, 21-**CH_3**), 0.66 (s, 3H, 18-**CH_3**) ppm. **^{13}C NMR** (100 MHz, $CDCl_3$) δ 216.1 (**C=S**), 215.2 (**C=S**), 174.5 (**24-COO**CH_3), 91.4 (d, *J*=181.9 Hz, **4-CH**), 89.8 (d, *J*=192.9 Hz, **6-CH**), 84.2 (d, *J*=19.8 Hz, **3-CH**), 79.9 (d, *J*=16.1 Hz, **7-CH**), 55.4 (**17-CH**), 51.5 (**24-**COO**CH_3**), 50.5 (t, *J*=13.6 Hz, **5-CH**), 50.0 (**14-CH**), 42.9 (**13-C**), 39.2 (t, *J*=7.3 Hz, **10-C**), 38.7 (**12-CH_2**), 37.9 (d, *J*=4.4 Hz, **8-CH**), 36.2 (**9-CH**), 35.1 (**20-CH**), 33.7 (**1-CH_2**), 30.8 (**23-CH_2**), 30.8 (**22-CH_2**), 27.8 (CH_2), 24.3 (CH_2), 23.0 (d, *J*=7.3 Hz, **2-CH_2**), 22.8 **19-CH_3**), 20.5 (**11-CH_2**), 19.6 (**S-CH_3**), 18.7 (**S-CH_3**), 18.2 (**21-CH_3**), 11.6 (**18-CH_3**) ppm. **^{19}F NMR** (376MHz, $CDCl_3$) δ -188.34 (apparent ddtd, *J*=50.3, 41.6, 13.9, 3.5 Hz, 1F, 4β-**F**), -192.34 (br t, *J*=42.5 Hz, 1F, 6α-**F**) ppm. **^{19}F [^{1}H] NMR** (376MHz, $CDCl_3$) δ -188.34 (d, *J*=41.6 Hz, 1F, 4β-**F**), -192.34 (d, *J*=41.6 Hz, 1F, 6α-**F**) ppm. **LRMS (ESI+)** m/z: 640.4 $[M+NH_4]^+$. **HRMS (ESI+)** $C_{29}H_{44}F_2NaO_4S_4$ $[M+Na]^+$. Calculated: 645.1983; Found: 645.1987 (0.7 ppm error). **IR** (neat, cm^{-1}) 2946 (m), 1732 (m), 1196 (s), 1057 (s).

Methyl 4β,6α-difluoro-5β-cholan-24-oate (3.33)

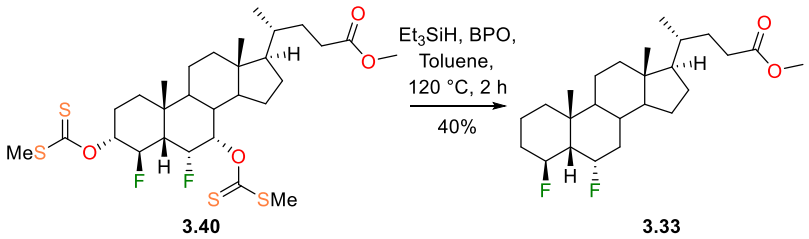

Following general procedure H, **3.40** (840 mg, 1.35 mmol, 1.0 equiv) was deoxygenated. The crude material was purified by flash chromatography (Biotage SNAP KP-Sil 25 g cartridge, EtOAc/PE: 3%/97% → 10%/90% over 18 CV) to yield **3.33** as a white gummy solid (225 mg, 0.55 mmol, 40%).

R_f 0.34 (EtOAc/PE 10/90). **$[\alpha]_D$** + 28.9 (c = 0.6, $CHCl_3$, 22 °C). **^{1}H NMR** (400 MHz, $CDCl_3$) δ 4.89-5.14 (m, 2H, 4α-**H** and 6β-**H**), 3.67 (s, 3H, 24-COO**CH_3**), 2.35 (ddd, *J*=15.4, 10.1, 5.3 Hz, 1H, 23-**H'**), 2.16-2.28 (m, 2H, 23-**H''** and *3-**H** or 6-**H***), 1.03-2.04 (m), 0.99 (s, 3H, 19-**CH_3**), 0.91 (d, *J*=6.5 Hz, 3H, 21-**CH_3**), 0.65 (s, 3H, 18-**CH_3**) ppm. **^{13}C NMR** (100 MHz, $CDCl_3$) δ 174.6 (**24-COO**CH_3), 90.8 (d, *J*=178.3 Hz, **4-CH**), 88.5 (d, *J*=173.1 Hz, **6-CH**), 56.0 (**14-CH**), 55.9 (**17-CH**), 52.5 (t, *J*=13.2 Hz, **5-CH**), 51.5 (**24-COOCH_3**), 42.8 (**13-C**), 42.0 (d, *J*=1.5 Hz, **9-CH**), 40.0 (t, *J*=7.7 Hz, **10-C**), 39.7 (**12-CH_2**), 36.6 (**1-CH_2**), 35.3 (**20-CH**), 34.8 (d, *J*=10.3 Hz, **8-CH**), 33.0 (d, *J*=19.8 Hz, ***3-CH_2 or 7-CH_2***), 32.8 (d, *J*=18.3 Hz, ***3-CH_2 or 7-CH_2***), 31.0 (**23-CH_2**), 30.9 **(22-CH_2)**, 28.0 (***15-CH_2 or 16-CH_2***), 24.1 (***15-CH_2 or 16-CH_2***), 23.7 (**19-CH_3**), 20.7 (**11-CH_2**), 18.3 (d, *J*=12.5 Hz, **2-CH_2**), 18.2 (**21-CH_3**), 12.0 **18-CH_3**) ppm. **^{19}F NMR** (376MHz, $CDCl_3$) δ -174.73 (br t, *J*=46.8 Hz, 1F, 4β-**F**), -180.16 (br t, *J*=43.4 Hz, 1F, 6α-**F**) ppm. **^{19}F [^{1}H] NMR** (376MHz, $CDCl_3$) δ -174.73 (d, *J*=39.9 Hz, 1F, 4β-**F**), -180.16 (d, *J*=39.9 Hz, 1F, 6α-**F**) ppm. **LRMS (ESI+)** m/z: 428.3 $[M+NH_4]^+$. **HRMS (ESI+)** $C_{25}H_{40}F_2NaO_2$ $[M+Na]^+$. Calculated: 433.2889; Found: 433.2879 (2.0 ppm error). **IR** (neat, cm^{-1}) 2933 – 2868 (m), 1739 (s), 1046 (s).

4β,6α-Difluoro-5β-cholanic acid (3.1)

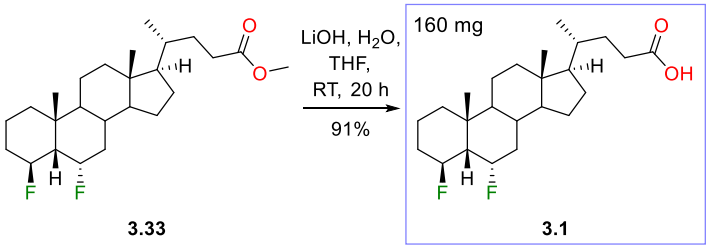

Following general procedure C, **3.33** (183 mg, 0.45 mmol, 1.0 equiv) was deprotected to yield **3.1** as a white solid (162 mg, 0.41 mmol, 91%) with no further purification.

mp 168 – 170 °C. **R_f** 0.23 (EtOAc/PE 30/70). **$[\alpha]_D$** + 28.0 (c = 0.65, $CHCl_3$, 22 °C). **^{1}H NMR** (400 MHz, $CDCl_3$) δ 4.89-5.15 (m, 2H, 4α-**H** and 6β-**H**), 2.40 (ddd, *J*=15.5, 10.1, 5.3 Hz, 1H, 23-**H'**), 2.17-2.33 (m, 2H, 23-**H''** and and *3-**H** or 6-**H***), 1.03-2.04 (m), 1.00 (s, 3H, 19-**CH_3**), 0.92 (d, *J*=6.5 Hz, 3H, 21-**CH_3**), 0.66 (s, 3H, 18-**CH_3**) ppm. **^{13}C NMR** (100 MHz, $CDCl_3$) δ 180.5 (**24-COOH**), 90.8 (d, *J*=179.0 Hz, **4-CH**), 88.5 (d, *J*=172.4 Hz, **6-CH**), 56.0 (**14-CH**), 55.8 (**17-CH**), 52.5 (t, *J*=12.8 Hz, **5-CH**), 42.8 (**13-C**), 42.0 (**9-CH**), 40.0 (t, *J*=7.7 Hz, **10-C**), 39.7 (**12-CH_2**), 36.6 (**1-CH_2**), 35.2 (**20-CH**), 34.8 (d, *J*=11.0 Hz, **8-CH**), 33.0 (d, *J*=20.5 Hz, ***3-CH_2 or 7-CH_2***), 32.8 (d, *J*=18.3 Hz, ***3-CH_2 or 7-CH_2***), 31.0 (**23-CH_2**), 30.6 (**22-CH_2**), 28.0 (***15-CH_2 or 16-CH_2***), 24.1 (***15-CH_2 or 16-CH_2***), 23.7 (**19-CH_3**), 20.7 (**11-CH_2**), 18.4 (d, *J*=12.5 Hz, **2-CH_2**), 18.2 (**21-CH_3**), 12.0 (**18-CH_3**) ppm. **^{19}F NMR** (376MHz, $CDCl_3$) δ -174.70 (br t, *J*=44.2 Hz, 1F, 4β-**F**), -180.13 (br t, *J*=43.3 Hz, 1F, 6α-**F**) ppm. **^{19}F [^{1}H] NMR** (376MHz, $CDCl_3$) δ -174.69 (br d, *J*=39.9 Hz, 1F, 4β-**F**), -180.13 (br d, *J*=39.9 Hz, 1F, 6α-**F**) ppm. **LRMS (ESI-)** m/z: 395.5 $[M-H]^-$. **HRMS (ESI+)** $C_{24}H_{38}F_2NaO_2$ $[M+Na]^+$. Calculated: 419.2732; Found: 419.2727 (1.2 ppm error). **IR** (neat, cm^{-1}) 2941 – 2876 (m), 1705 (s), 1239 (m), 1025 (s).

7.4.2 Synthesis of 7-Fluorinated Bile Acid Analogues

Methyl 3α,6α-dihydroxy-5β-cholan-24-oate (3.44)

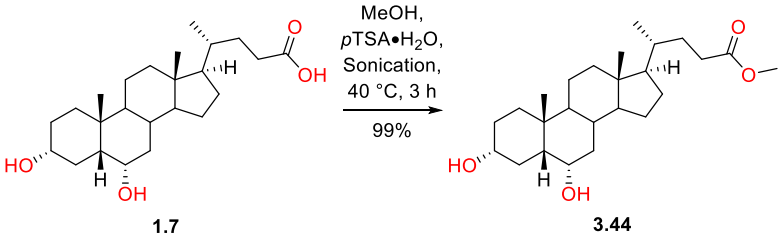

Following general procedure A, HDCA (**1.7**, 50.0 g, 127 mmol, 1.0 equiv) was protected to yield **3.44** as a white gummy solid (51.4 g, 126 mmol, 99%) with no further purification.

R_f 0.18 (EtOAc/PE 60/40). **^{1}H NMR** (400 MHz, $CDCl_3$) δ 4.03 (dt, *J*=11.9, 4.5 Hz, 1H, 6β-**H**), 3.65 (s, 3H, 24-COO**CH_3**), 3.53-3.63 (m, 1H, 3β-**H**), 2.55 (br s, 1H, **OH**), 2.34 (m, 2H, 23-**H'** and **OH**), 2.21 (ddd, *J*=15.7, 9.4, 6.5 Hz, 1H, 23-**H''**), 0.98-2.02 (m), 0.91 (d, *J*=6.2 Hz, 3H, 21-**CH_3**), 0.89 (s, 3H, 19-**CH_3**), 0.63 (s, 3H, 18-**CH_3**) ppm. **^{13}C NMR** (100 MHz, $CDCl_3$) δ 174.7 (**24-COO**CH_3), 71.5 (**3-CH**), 68.0 (**6-CH**), 56.2 (**14-CH**), 55.9 (**17-CH**), 51.4 (**24**-COO**CH_3**), 48.4 (***5-CH or 9-CH***), 42.8 (**13-C**), 39.9 (**12-CH_2**), 39.8 (***5-CH or 9-CH***), 35.9 (**10-C**), 35.6 (**1-CH_2**), 35.3 (**20-CH**), 34.8 (CH_2), 34.8 (**8-CH**), 31.0 (**23-CH_3**), 30.9 (**22-CH_2**), 30.1 (CH_2), 29.2 (CH_2), 28.1 (CH_2), 24.2 (CH_2), 23.5 (**19-CH_3**), 20.7 (CH_2), 18.2 (**21-CH_3**), 12.0 (**18-CH_3**) ppm. **LRMS (ESI+)** m/z: 813.8 $[2M+H]^+$, 389.3 $[M+H-H_2O]^+$, 371.3 $[M+H-2H_2O]^+$. ^{1}H NMR data agrees with data from within the group and literature.[177,236] ^{13}C NMR data agrees with data from within the group.

Methyl 3α-hydroxy-6-oxo-5β-cholan-24-oate (3.57), Methyl 6α-hydroxy-3-oxo-5β-cholan-24-oate (3.58), Methyl 3,6-dioxo-5β-cholan-24-oate (3.59)

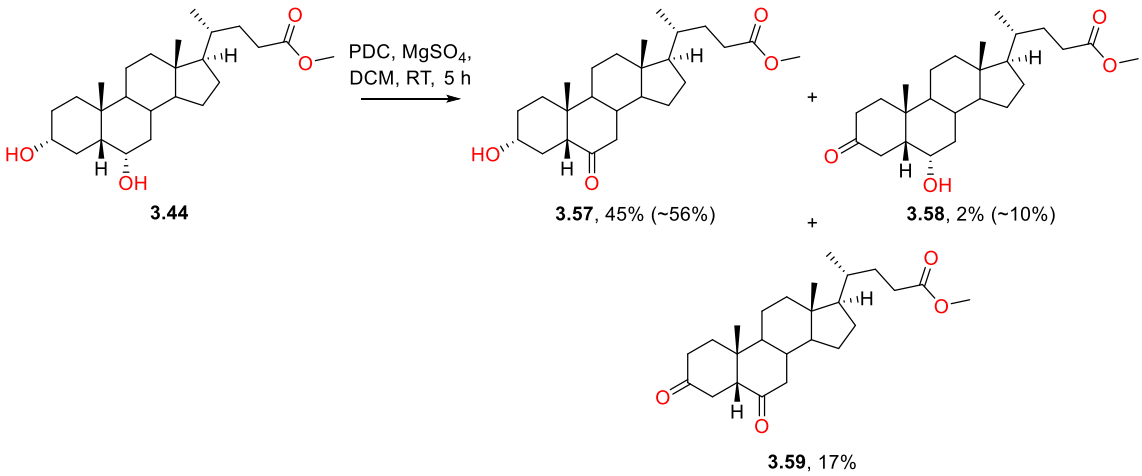

The alcohol **3.44** (24.7 g, 60.7 mmol, 1.0 equiv) was dissolved in DCM (500 mL) and $MgSO_4$ (125 g) and PDC (27.4 g, 72.8 mmol, 1.2 equiv) were added. After stirring at RT for 5 h, the reaction mixture

was filtered over a short layer of silica gel, further rinsed with EtOAc (1.5 L) and reduced in vacuo to give 23.5 g of crude material. The crude was purified by flash chromatography (EtOAc/PE: 30%/70% → 35%/65% → 40%/60%) to firstly yield **3.59** as a white solid (4.41 g, 11.0 mmol, 18%), then a 2:1 mixture of **3.57** and **3.58** (6.62 g) and finally **3.57** as a white gummy solid (10.0 g, 24.7 mmol, 41%). The 2:1 mixture of **3.57** and **3.58** was combined with mixed fractions of repeats of the reaction (total **3.44 =** 122.2 mmol) and purified by flash chromatography (EtOAc/PE 33%/67% → 35%/65% → 50%/50%), to firstly yield **3.58** as a colourless gum (250 mg, 0.62 mmol, 0.51%), then a 3:2 mixture of **3.57** and **3.58** (9.95 g) and finally **3.57** as a white gummy solid (3.29 g, 8.13 mmol, 6.7%).

Combined yields of products over three batches (yield in brackets denotes yield including mixed fractions) **3.57** – 22.0 g, 54.4 mmol, 45% (56%); **3.58** – 900 mg, 2.22 mmol, 2% (10%); **3.59** – 8.37 g, 20.8 mmol, 17%.

3.57: $\mathbf{R_f}$ 0.18 (EtOAc/PE 40/60). ^{1}**H NMR** (400 MHz, $CDCl_3$) δ 3.64 (s, 3H, 24-COO**CH_3**), 3.56-3.63 (m, 1H, 3β-**H**), 2.34 (ddd, *J*=15.7, 10.1, 5.5 Hz, 1H, 23-**H'**), 2.07-2.26 (m, 4H, overlapping 23-**H''**, 5β-**H**, 7α-**H**, 7β-**H**), 1.98-2.05 (m, 1H, 12β-**H**), 0.96-1.93 (m), 0.91 (d, *J*=6.4 Hz, 3H, 19-**CH_3**), 0.82 (s, 3H, 21-**CH_3**), 0.63 (s, 3H, 18-**CH_3**) ppm. ^{13}**C NMR** (100 MHz, $CDCl_3$) δ 213.9 (**6-C**), 174.6 (**24-COO**CH_3), 70.0 (**3-CH**), 59.3 (**5-CH**), 56.7 (**14-CH**), 55.7 (**17-CH**), 51.4 (**24**-COO**CH_3**), 43.0 (**13-C**), 42.8 (**7-CH_2**), 39.9 (**9-CH**), 39.5 (**12-CH_2**), 37.9 (**10-C**), 37.0 (**8-CH**), 35.2 (**20-CH**), 34.8 (**4-CH_2**), 34.3 (**1-CH_2**), 31.0 (**23-CH_2**), 30.8 (**22-CH_2**), 29.7 (**2-CH_2**), 27.9 (**16-CH_2**), 23.9 (**15-CH_2**), 23.1 (**19-CH_3**), 20.8 (**11-CH_2**), 18.2 (**21-CH_3**), 11.9 (**18-CH_3**) ppm. **LRMS (ESI+)** m/z: 422.3 $[M+NH_4]^+$, 405.3 $[M+H]^+$. ^{1}H and ^{13}C NMR data agree with data from within the group and literature.[180]

3.58: $\mathbf{R_f}$ 0.24 (EtOAc/PE 40/60). ^{1}**H NMR** (400 MHz, $CDCl_3$) δ 4.07 (dt, *J*=11.9, 4.7 Hz, 1H, 6β-**H**), 3.63 (s, 3H, 24-COO**CH_3**), 2.26-2.41 (m, 4H), 2.11-2.24 (m, 2H), 1.03-2.07 (m), 0.98 (s, 3H, 19-**CH_3**), 0.90 (d, *J*=6.5 Hz, 3H, 21-**CH_3**), 0.65 (s, 3H, 18-**CH_3**) ppm. ^{13}**C NMR** (100 MHz, $CDCl_3$) δ 212.9 (**3-C**), 174.6 (**24-COO**CH_3), 67.4 (**6-CH**), 56.0 (**14-CH**), 55.8 (**17-CH**), 51.4 (**24**-COO**CH_3**), 50.1 (**5-CH**), 42.7 (**13-C**), 40.1 (**9-CH**), 39.7 (**12-CH_2**), 37.0 (***1-CH_2* or *2-CH_2***), 37.0 (***1-CH_2* or *2-CH_2***), 36.1 (**10-C**), 36.0 (**4-CH_2**), 35.2 (**20-CH**), 34.4 (**8-CH**), 34.2 (**7-CH_2**), 30.9 (**23-CH_2**), 30.8 (**22-CH_2**), 28.0 (***15-CH_2* or *16-CH_2***), 24.1 (***15-CH_2* or *16-CH_2***), 22.7 (**19-CH_3**), 21.0 (**11-CH_2**), 18.2 (**21-CH_3**), 11.9 (**18-CH_3**) ppm. **LRMS (ESI+)** m/z: 422.2 $[M+NH_4]^+$. ^{1}H and ^{13}C NMR data agree with literature.[237]

3.59: mp 129 – 130 °C. $\mathbf{R_f}$ 0.66 (EtOAc/PE 40/60). ^{1}**H NMR** (400 MHz, $CDCl_3$) δ 3.64 (s, 3H, 24-COO**CH_3**), 2.63 (dd, *J*=14.8, 13.3 Hz, 1H, 4α-**H**), 2.15-2.50 (m), 2.03-2.12 (m, 2H, 12α or β-**H** and 1α or β-**H**), 1.72-1.96 (m), 1.19-1.62 (m), 1.03-1.19 (m, 2H, 17α-**H** and 15α or β-**H**), 0.93 (s, 3H, 19-**CH_3**), 0.91 (d, *J*=6.5 Hz, 3H, 21-**CH_3**), 0.67 (s, 3H, 18-**CH_3**) ppm. ^{13}**C NMR** (100 MHz, $CDCl_3$) δ 210.7 (**6-C**), 208.5 (**3-C**), 174.4 (**24-COO**CH_3), 59.6 (**5-CH**), 56.7 (**14-CH**), 55.7 (**17-CH**), 51.4 (**24**-COO**CH_3**), 43.0

(**13-C**), 42.1 (**7-CH$_2$**), 40.8 (**9-CH**), 39.8 (**4-CH$_2$**), 39.4 (**12-CH$_2$**), 38.2 (**10-C**), 36.6 (**8-CH**), 36.4 (**2-CH$_2$**), 35.7 (**1-CH$_2$**), 35.2 (**20-CH**), 30.9 (**23-CH$_2$**), 30.8 (**22-CH$_2$**), 27.8 (**16-CH$_2$**), 23.8 (**15-CH$_2$**), 22.4 (**19-CH$_3$**), 21.2 (**11-CH$_2$**), 18.2 (**21-CH$_3$**), 11.9 (**18-CH$_3$**) ppm. **LRMS (ESI+)** m/z: 420.4 $[M+NH_4]^+$. ^{1}H and ^{13}C NMR data agree with literature.[180]

Methyl 3α,6-bis(trimethylsilyloxy)-5β-cholan-6-en-24-oate (3.60)

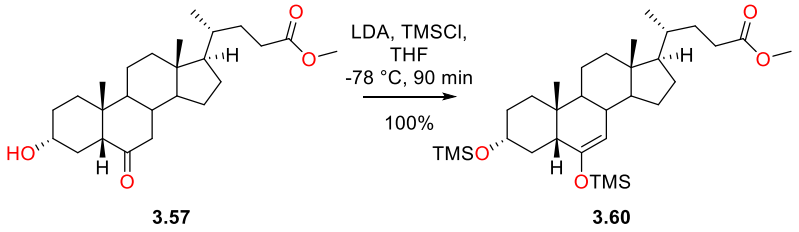

3.57 **3.60**

To a flame-dried flask under argon diisopropylamine (15.5 mL, 111 mmol, 5.0 equiv) and dry THF (130 mL) were added. The solution was cooled to -78 °C and *n*-BuLi (2.5 M in hexanes, 44 mL, 111 mmol, 5.0 equiv) was added dropwise. After stirring for 30 min, chlorotrimethylsilane (14.0 mL, 111 mmol, 5.0 equiv) was added to the reaction mixture. After stirring for a further 30 min, a solution of **3.57** (8.95 g, 22.1 mmol, 1.0 equiv) in dry THF (100 mL) was added to the reaction mixture at -78 °C dropwise over 30 min. After stirring for 90 min, NEt_3 (31 mL, 221 mmol, 10 equiv) was added to the reaction mixture. After stirring for a further 1 h, the reaction mixture was warmed to -10 °C and added sat. $NaHCO_3$ (50 mL). Following a further 20 min of stirring, the mixture was extracted with EtOAc (2 x 250 mL). The combined organic phases were then washed with sat. $NaHCO_3$ (300 mL), water (300 mL) and brine (300 mL) before drying over Na_2SO_4 and reducing *in vacuo* to yield **3.60** (12.9 g, ~100% yield). The crude material was used in the next reaction without purification.

R$_f$ 0.39 (Acetone/PE 10/90). **Selected ^{1}H NMR** (400 MHz, $CDCl_3$) 4.58 (d, *J*=1.7 Hz, 1H, 7-**H**), 3.65 (s, 3H, 24-COO**CH$_3$**), 3.49-3.57 (m, 1H, 3β-**H**), 2.35 (ddd, *J*=15.4, 10.1, 5.3 Hz, 1H, 23-**H'**), 2.21 (ddd, *J*=15.6, 9.4, 6.6 Hz, 1H, 23-**H''**), 0.96-2.12 (m), 0.90 (d, *J*=6.4 Hz, 3H, 21-**CH$_3$**), 0.84 (s, 3H, 19-**CH$_3$**), 0.67 (s, 3H, 18-**CH$_3$**), 0.17 (s, 9H, Si**Me$_3$**), 0.11 (s, 9H, Si**Me$_3$**) ppm. **Selected ^{13}C NMR** (100 MHz, $CDCl_3$) δ 174.7 (**24-COO**CH_3), 153.0 (**6-C**), 104.3 (**7-CH**), 71.5 (**3-CH**), 55.8 (**17-CH**), 55.4 (**14-CH**), 51.4 (**24-**COO**CH$_3$**), 48.3 (***5-CH* or *9-CH***), 43.2 (**13-C**), 40.0 (**12-CH$_2$**), 39.7 (***5-CH* or *9-CH***), 38.2 (CH_2), 35.8 (**8-CH**), 35.2 (**20-CH**), 34.4 (**1-CH$_2$**), 34.1 (**10-C**), 31.0 (**23-CH$_2$**), 30.9 (**22-CH$_2$**), 30.6 (**2-CH$_2$**), 28.1 (CH_2), 23.9 (CH_2), 22.6 (**19-CH$_3$**), 20.4 (**11-CH$_2$**), 18.2 **21-CH$_3$**), 12.1 (**18-CH$_3$**), 0.4 (Si**Me$_3$**), 0.2 (Si**Me$_3$**) ppm. ^{1}H NMR data agrees with literature[238] and data from within the group. ^{13}C NMR data agrees with data from within the group.

Methyl 7α-fluoro-3α-hydroxy-6-oxo-5β-cholan-24-oate (2.74) and Methyl 7β-fluoro-3α-hydroxy-6-oxo-5β-cholan-24-oate (3.42)

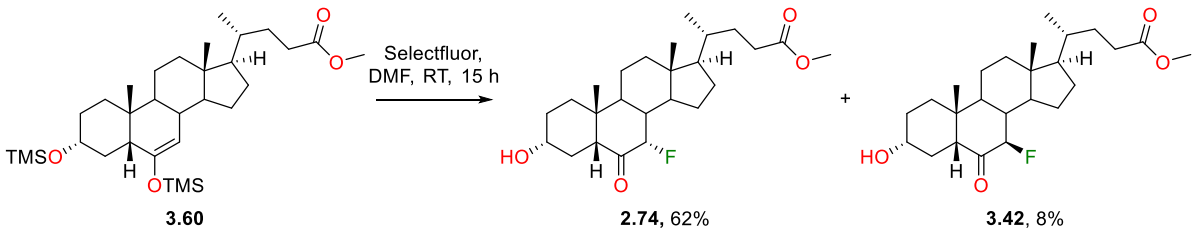

3.60 **2.74**, 62% **3.42**, 8%

The silyl enol ether **3.60** (12.9 g, 22.1 mmol, 1.0 equiv) was dissolved in dry DMF (50 mL), cooled to 0 °C and a suspension of Selectfluor® (11.7 g, 33.2 mmol, 1.5 equiv) in dry DMF (50 mL) was added. After stirring for 15 h, the reaction mixture was quenched with water (300 mL) and the resulting mixture was extracted with EtOAc (3 x 150 mL). The combined organic phases were washed with brine (400 mL) and dried over Na_2SO_4, before reducing *in vacuo* to give 11 g of crude material. The crude was combined with two other batches for purification (total **3.60** = 51.5 mmol). The combined crude materials were purified by flash chromatography (acetone/PE: 15%/85% → 17%/83% → 20%/80% → 25%/75%), first giving **2.74** as a white solid (9.71 g, 23.0 mmol, 44%), followed by a mixed fraction containing ~55% **2.74** and ~40% **3.42** (10.1 g). The mixed fractions were repurified by flash chromatography (acetone/PE 16%/84% → 18%/82% → 40%/60%), first giving **2.74** (3.88 g, 9.18 mmol, 18%), then further mixed fractions of **2.74** and **3.42** (2.84 g) and finally **3.42** around 90% pure (2.30 g). The 90% pure fraction of **3.42** was purified by flash chromatography (acetone/PE 18%/82% → 20%/80%), giving **3.42** as a white solid (1.65 g, 3.90 mmol, 8%).

Combined yields of products over three batches: **2.74** – 13.6 g, 32.2 mmol, 62%; **3.42**– 1.65 g, 3.90 mmol, 8%.

2.74: mp 163 – 165 °C. **R_f** 0.30 (Acetone/PE 25/75). **^{1}H NMR** (400 MHz, $CDCl_3$) δ 4.42 (dd, *J*=51.1, 1.7 Hz, 1H, 7β-**H**), 3.65 (s, 3H, 24-COO**CH_3**), 3.48-3.59 (m, 1H, 3β-**H**), 2.35 (ddd, *J*=15.5, 10.0, 5.4 Hz, 1H, 23-**H'**), 0.98-2.29 (m), 0.92 (d, *J*=6.4 Hz, 3H, 21-**CH_3**), 0.81 (s, 3H, 19-**CH_3**), 0.65 (s, 3H, 18-**CH_3**) ppm. **^{13}C NMR** (100 MHz, $CDCl_3$) δ 207.1 (d, *J*=16.9 Hz, **6-C**), 174.6 (**24-COO**CH_3), 94.6 (d, *J*=180.5 Hz, **7-CH**), 69.9 (**3-CH**), 58.8 (**5-CH**), 55.4 (**17-CH**), 51.5 (**24**-COO**CH_3**), 49.1 (d, *J*=4.4 Hz, **14-CH**), 42.9 (**13-C**), 40.8 (d, *J*=21.3 Hz, **8-CH**), 39.0 (**12-CH_2**), 38.5 (**10-C**), 35.2 (**20-CH**), 34.3 (**1-CH_2**), 33.9 (**9-CH**), 32.9 (d, *J*=7.3 Hz, **4-CH_2**), 30.9 (**23-CH_2**), 30.8 (**22-CH_2**), 29.8 (**2-CH_2**), 27.9 (***15-CH_2* or *16-CH_2***), 23.1 (***15-CH_2* or *16-CH_2***), 22.8 (**19-CH_3**), 20.7 (**11-CH_2**), 18.2 (**21-CH_3**), 11.5 (**18-CH_3**) ppm. **^{19}F NMR** (376MHz, $CDCl_3$) δ -195.82--194.10 (m, 1F, 7α-**F**) ppm. **^{19}F [^{1}H] NMR** (376MHz, $CDCl_3$) δ -194.92 (br s, 1F, 7α-**F**) ppm. **LRMS (ESI+)** m/z: 423.2 $[M+H]^+$. ^{1}H, ^{13}C and ^{19}F NMR data agree with data from within the group.

3.42: mp 162 – 164 °C. **R_f** 0.19 (Acetone/PE 25/75). **^{1}H NMR** (400 MHz, $CDCl_3$) δ 4.84 (dd, *J*=48.5, 10.0 Hz, 1H, 7α-**H**), 3.65 (s, 3H, 24-COO**CH_3**), 3.54-3.63 (m, 1H, 3β-**H**), 2.17-2.40 (m, 3H, 5β-**H**, 23-**H'**,

23-**H''**), 1.00-2.12 (m), 0.92 (d, *J*=6.4 Hz, 3H, **21-CH₃**), 0.86 (s, 3H, 19-**CH₃**), 0.66 (s, 3H, 18-**CH₃**) ppm. **^{13}C NMR** (100 MHz, $CDCl_3$) δ 206.7 (d, *J*=13.9 Hz, **6-C**), 174.6 (**24-COO**CH_3), 94.0 (d, *J*=192.9 Hz, **7-CH**), 69.7 (**3-CH**), 58.8 (**5-CH**), 55.8 (**14-CH**), 55.0 (**17-CH**), 51.5 (**24**-COO**CH₃**), 43.6 (br d, *J*=16.1 Hz, **8-CH**), 43.5 (**13-C**), 39.3 (**12-CH₂**), 38.5 (d, *J*=8.1 Hz, **9-CH**), 37.9 (**10-C**), 35.1 (**20-CH**), 34.2 (**1-CH₂**), 34.0 (**4-CH₂**), 31.0 (**23-CH₂**), 30.9 (**22-CH₂**), 29.6 (**2-CH₂**), 28.1 (d, *J*=2.2 Hz, **16-CH₂**), 25.6 (d, *J*=4.4 Hz, **15-CH₂**), 22.9 (**19-CH₃**), 20.9 (**11-CH₂**), 18.3 (**21-CH₃**), 11.8 (**18-CH₃**) ppm. **^{19}F NMR** (376MHz, $CDCl_3$) δ -194.39--194.00 (m, 7β-**F**) ppm. **^{19}F [^{1}H] NMR** (376MHz, $CDCl_3$) δ -194.18 (s, 1F, 7β-**F**) ppm. **LRMS (ESI+)** m/z: 440.1 $[M+NH_4]^+$, 423.2 $[M+H]^+$. ^{1}H, ^{13}C and ^{19}F NMR data agree with data from within the group.

Methyl 7α-fluoro-3α-acetoxy-6-oxo-5β-cholan-24-oate (3.61)

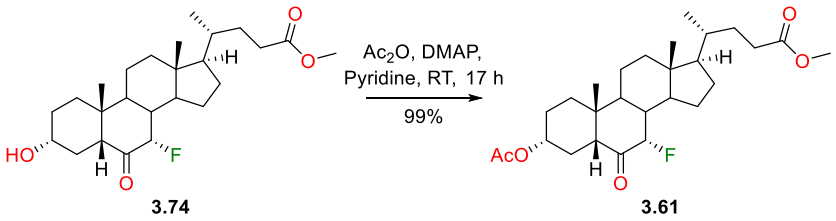

3.74 **3.61**

Following general procedure E, **3.74** (9.63 g, 22.8 mmol, 1.0 equiv) was protected to yield **3.61** as an off-white solid (10.6 g, 22.7 mmol, 99%) with no further purification.

mp 126 – 128 °C. **R_f** 0.48 (EtOAc/PE 20/80). **[α]$_D$** - 62.6 (c = 1.0, $CHCl_3$, 23 °C). **^{1}H NMR** (400 MHz, $CDCl_3$) δ 4.55-4.66 (m, 1H, 3β-**H**), 4.43 (dd, *J*=51.6, 1.5 Hz, 1H, 7β-**H**), 3.66 (s, 3H, 24-COO**CH₃**), 2.10-2.40 (m, 5H, overlapping 23-**H'**, 23-**H''**, 9α-**H**, 5β-**H**, 4-**H**), 2.02 (s, 3H, 3α-OCO**CH₃**), 1.03-2.05 (m), 0.93 (d, *J*=6.4 Hz, 3H, 21-**CH₃**), 0.82 (s, 3H, 19-**CH₃**), 0.66 (s, 3H, 18-**CH₃**) ppm. **^{1}H NMR** ($CDCl_3$, 500MHz) [according to 1D Selective Gradient NOESY at 19-CH_3]: δ 2.33 (dd, *J*=13.3, 2.7 Hz, 1H, 5β-**H**), 1.77 (dtd, *J*=38.5, 11.0, 2.3 Hz, 1H, 8β-**H**), 1.38 (apparent qd, *J*=12.8, 3.7 Hz, 1H, 11β-**H**), 1.14 (td, *J*=14.3, 3.4 Hz, 1H, 1β-**H**) ppm. **^{13}C NMR** (100 MHz, $CDCl_3$) δ 205.9 (d, *J*=16.9 Hz, **6-C**), 174.5 (**24-COO**CH_3), 170.3 (**3α-OCO**CH_3), 94.8 (d, *J*=179.0 Hz, **7-CH**), 72.2 (d, *J*=1.5 Hz, **3-CH**), 58.7 (d, *J*=2.2 Hz, **5-CH**), 55.6 (**17-CH**), 51.4 (**24**-COO**CH₃**), 49.2 (d, *J*=4.4 Hz, **14-CH**), 43.0 (**13-C**), 40.8 (d, *J*=21.3 Hz, **8-CH**), 39.0 (**12-CH₂**), 38.4 (**10-C**), 35.3 (**20-CH**), 34.2 (**1-CH₂**), 33.6 (**9-CH**), 30.9 (**23-CH₂**), 30.8 (**22-CH₂**), 29.1 (d, *J*=8.1 Hz, **4-CH₂**), 27.9 (***15-CH₂ or 16-CH₂***), 26.2 (**2-CH₂**), 23.0 (***15-CH₂ or 16-CH₂***), 22.8 (**19-CH₃**), 21.2 (**3α-**OCO**CH₃**), 20.7 (**11-CH₂**), 18.2 (**21-CH₃**), 11.5 (**18-CH₃**) ppm. **^{19}F NMR** (376MHz, $CDCl_3$) δ -194.89 (br dd, *J*=50.3, 38.1 Hz, 1F, 7α-**F**) ppm. **^{19}F [^{1}H] NMR** (376MHz, $CDCl_3$) δ -194.89 (s, 1F, 7α-**F**) ppm. **LRMS (ESI+)** m/z: 482.2 $[M+NH_4]^+$. **HRMS (ESI+)** $C_{27}H_{41}FNaO_5$ $[M+Na]^+$. Calculated: 487.2830; Found: 487.2825 (1.0 ppm error). **IR** (neat, cm^{-1}) 2943 – 2871 (m), 1734 (s), 1715 (s), 1250 (m), 1234 (m).

Methyl 7β-fluoro-3α-acetoxy-6-oxo-5β-cholan-24-oate (3.62)

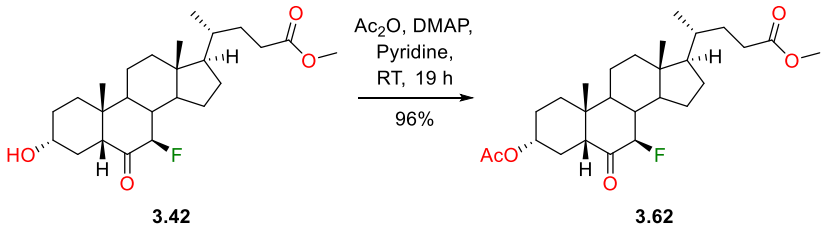

3.42 **3.62**

Following general procedure E, **3.42** (1.58 g, 3.74 mmol, 1.0 equiv) was protected to yield **3.62** as a pale yellow solid (1.67 g, 3.59 mmol, 96%) with no further purification.

mp 130 – 131 °C. **R_f** 0.45 (EtOAc/PE 30/70). **$[\alpha]_D$** + 4.90 (c = 0.5, $CHCl_3$, 21 °C). **^{1}H NMR** (400 MHz, $CDCl_3$) δ 4.83 (dd, *J*=48.5, 10.0 Hz, 1H, 7α-**H**), 4.64 (tt, *J*=11.2, 4.6 Hz, 1H, 3β-**H**), 3.65 (s, 3H, 24-COO**CH_3**), 2.28-2.42 (m, 2H, 23-**H'** and 5β-**H**), 2.22 (ddd, *J*=16.1, 9.7, 6.7 Hz, 1H, 23-**H''**), 2.06 (br dt, *J*=12.7, 3.1 Hz, 1H, 12β-**H**), 2.01 (s, 3H, 3α-OCO**CH_3**), 1.08-2.00 (m), 0.92 (d, *J*=6.4 Hz, 3H, 21-**CH_3**), 0.88 (s, 3H, 19-**CH_3**), 0.66 (s, 3H, 18-**CH_3**) ppm. **^{1}H NMR** ($CDCl_3$, 500MHz) [according to 1D Selective Gradient NOESY at 19-CH_3]: δ 2.40 (dt, *J*=13.7, 4.3 Hz, 1H, 5β-**H**), 1.97 (quin, *J*=10.1 Hz, 1H, 8β-**H**), 1.43 (qd, *J*=11.9, 3.7 Hz, 1H, 11β-**H**), 1.18 (td, *J*=14.3, 3.4 Hz, 1H, 1β-**H**) ppm. **^{13}C NMR** (100 MHz, $CDCl_3$) δ 205.7 (d, *J*=13.9 Hz, **6-C**), 174.5 (**24-COO**CH_3), 170.1 (**3α-OCO**CH_3), 93.9 (d, *J*=192.9 Hz, **7-CH**), 71.7 (**3-CH**), 58.5 (**5-CH**), 55.8 (**14-CH**), 55.1 (**17-CH**), 51.4 (**24**-COO**CH_3**), 43.6 (**13-C**), 43.6 (br d, *J*=16.1 Hz, **8-CH**), 39.3 (**12-CH_2**), 38.5 (d, *J*=8.8 Hz, **9-CH**), 37.8 (**10-C**), 35.1 (**20-CH**), 33.7 (**1-CH_2**), 31.0 (**23-CH_2**), 30.9 (**22-CH_2**), 30.3 (**4-CH_2**), 28.1 (d, *J*=2.9 Hz, **16-CH_2**), 26.0 (**2-CH_2**), 25.5 (d, *J*=4.4 Hz, **15-CH_2**), 22.8 (**19-CH_3**), 21.2 (**3α**-OCO**CH_3**), 21.0 (**11-CH_2**), 18.3 (**21-CH_3**), 11.8 (**18-CH_3**) ppm. **^{19}F NMR** (376MHz, $CDCl_3$) δ -194.56--194.10 (m, 1F, 7β-**F**) ppm. **^{19}F [^{1}H] NMR** (376MHz, $CDCl_3$) δ -194.32 (s, 1F, 7β-**F**) ppm. **LRMS (ESI+)** m/z: 482.5 $[M+NH_4]^+$. **HRMS (ESI+)** $C_{27}H_{42}FO_5$ $[M+H]^+$. Calculated: 465.3011; Found: 465.3015 (0.9 ppm error). **IR** (neat, cm^{-1}) 2953 – 2974 (m), 1727 (s), 1251 (m), 1038 (m).

Methyl 7α-fluoro-3α-acetoxy-6α-hydroxy-5β-cholan-24-oate (3.67) and Methyl 7α-fluoro-3α-acetoxy-6β-hydroxy-5β-cholan-24-oate (3.68)

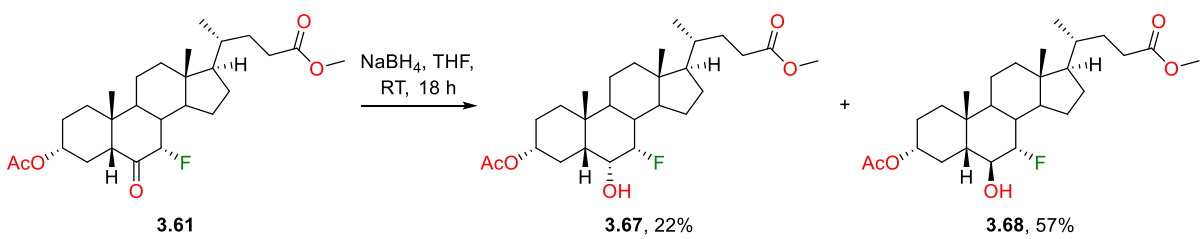

3.61 **3.67**, 22% **3.68**, 57%

The ketone **3.61** (13.1 g, 28.2 mmol, 1.0 equiv) was dissolved in dry THF (250 mL) and $NaBH_4$ (1.60 g, 42.3 mmol, 1.5 equiv) was added. After stirring for ar RT for 18 h, the reaction mixture was cooled

to 0 °C and quenched with portionwise addition of 2M HCl (200 mL). Water (100 mL) was then added to the mixture and was then extracted with EtOAc (3 x 200 mL). The combined organic phases were washed with water (400 mL) and brine (400 mL) before drying over Na_2SO_4 and reducing *in vacuo* to give 14 g of crude material. The crude material was combined with that of a previous batch (total mmol **3.61** = 31.4 mmol) and purified by flash chromatography (acetone/PE 15%/85% → 20%/80%) to firstly give **3.68** as a white solid (7.49 g, 16.1 mmol, 51%), followed by a 3:1 mixture of **3.67** and **3.68** (6.32 g). The mixed fractions were repurified by flash chromatography (acetone/PE 15%/85% → 18%/82%), firstly giving **3.68** (906 mg, 1.94 mmol, 6%), then mixed fractions of **3.67** and **3.68** (1.66 g) and finally **3.67** as a white gummy solid (3.20 g, 6.86 mmol, 22%).

3.67: $\mathbf{R_f}$ 0.25 (Acetone/PE 20/80). $\mathbf{[\alpha]_D}$ + 19.3 (c = 1.0, $CHCl_3$, 22 °C). **^{1}H NMR** (400 MHz, $CDCl_3$) δ 4.56-4.64 (m, 1H, 3β-**H**), 4.60 (br d, *J*=51.8 Hz, 1H, 7β-**H**), 3.75-3.92 (m, contains d *J*=33.9 Hz, 1H, 6β-**H**), 3.65 (s, 3H, 24-COO**CH_3**), 2.35 (ddd, *J*=15.3, 10.1, 5.3 Hz, 1H, 23-**H'**), 2.16-2.27 (m, 2H, 23-**H'** and 6α-**OH**), 2.01 (s, 3H, 3α-OCO**CH_3**), 1.04-2.00 (m), 0.91 (d, *J*=6.4 Hz, 3H, 21-**CH_3**), 0.90 (s, 3H, 19-**CH_3**), 0.64 (s, 3H, 18-**CH_3**) ppm. **^{13}C NMR** (100 MHz, $CDCl_3$) δ 174.6 (**24-COO**CH_3), 170.5 (**3α-OCO**CH_3), 94.2 (d, *J*=176.1 Hz, **7-CH**), 73.8 (**3-CH**), 68.8 (d, *J*=17.6 Hz, **6-CH**), 55.7 (**17-CH**), 51.4 (**24-**COO**CH_3**), 49.8 (d, *J*=3.7 Hz, **14-CH**), 47.3 (***5-CH or 9-CH***), 42.7 (**13-C**), 39.3 (**12-CH_2**), 38.3 (d, *J*=19.1 Hz, **8-CH**), 35.7 (**10-C**), 35.3 (**20-CH**), 34.9 (**1-CH_2**), 33.4 (***5-CH or 9-CH***), 30.9 (**23-CH_2**), 30.9 (**22-CH_2**), 28.0 (***15-CH_2 or 16-CH_2***), 27.7 (d, *J*=8.1 Hz, **4-CH_2**), 26.5 (**2-CH_2**), 23.3 (***15-CH_2 or 16-CH_2***), 22.7 (**19-CH_3**), 21.3 (**3α-**OCO**CH_3**), 20.5 (**11-CH_2**), 18.2 (**21-CH_3**), 11.6 (**18-CH_3**) ppm. **^{19}F NMR** (376MHz, $CDCl_3$) δ -208.52 (dt, *J*=52.0, 37.3 Hz, 1F, 7α-**F**) ppm. **^{19}F [^{1}H] NMR** (376MHz, $CDCl_3$) δ -208.52 (s, 1F, 7α-**F**) ppm. **LRMS (ESI+)** m/z: 484.2 $[M+NH_4]^+$. **HRMS (ESI+)** $C_{27}H_{43}FNaO_5$ $[M+Na]^+$. Calculated: 489.2987; Found: 489.2986 (0.2 ppm error). **IR** (neat, cm^{-1}) 3470 (b), 2939 – 2869 (m), 1731 (s), 1236 (s), 1027 (m).

3.68: mp 124 – 126 °C. $\mathbf{R_f}$ 0.35 (Acetone/PE 20/80). $\mathbf{[\alpha]_D}$ + 30.2 (c = 1.0, $CHCl_3$, 22 °C). **^{1}H NMR** (400 MHz, $CDCl_3$) δ 4.55-4.65 (m, 1H, 3β-**H**), 4.45 (d, *J*=46.2 Hz, 1H, 7α-**F**), 3.81 (br d, *J*=9.8 Hz, 1H, 6α-**H**), 3.66 (s, 3H, 24-COO**CH_3**), 2.35 (ddd, *J*=15.5, 10.3, 5.3 Hz, **23-H'**), 2.22 (ddd, *J*=15.9, 9.8, 6.6 Hz, 1H, 23-**H''**), 2.01 (s, 3H, 3α-OCO**CH_3**), 1.09-2.00 (m), 1.07 (s, 3H, 19-**CH_3**), 0.92 (d, *J*=6.5 Hz, 3H, 21-**CH_3**), 0.68 (s, 3H 18-**CH_3**) ppm. **^{13}C NMR** (100 MHz, $CDCl_3$) δ 174.7 (**24-COO**CH_3), 170.8 (**3α-OCO**CH_3), 92.9 (d, *J*=173.9 Hz, **7-CH**), 73.7 (**3-CH**), 73.1 (d, *J*=27.1 Hz, **6-CH**), 55.7 (**17-CH**), 51.5 (**24-**COO**CH_3**), 49.5 (d, *J*=3.7 Hz, **14-CH**), 47.3 (***5-CH or 9-CH***), 42.6 (**13-C**), 39.4 (**12-CH_2**), 35.3 (**20-CH**), 35.3 (**1-CH_2**), 34.9 (d, *J*=19.1 Hz, **8-CH**), 34.4 (**10-C**), 33.5 (***5-CH or 9-CH***), 31.3 (d, *J*=7.3 Hz, **4-CH_2**), 31.0 (**23-CH_2**), 30.9 (**22-CH_2**), 28.1 (***15-CH_2 or 16-CH_2***), 26.1 (**2-CH_2**), 25.0 (**19-CH_3**), 23.4 (***15-CH_2 or 16-CH_2***), 21.4 (**3α-**OCO**CH_3**), 20.3 (**11-CH_2**), 18.2 (**21-CH_3**), 11.6 (**18-CH_3**) ppm. **^{19}F NMR** (376MHz, $CDCl_3$) δ -194.60 (ddd, *J*=46.8, 37.3, 9.5 Hz, 1F, 7α-**F**) ppm. **^{19}F [^{1}H] NMR** (376MHz, $CDCl_3$) δ -194.60 (s, 1F, 7α-**F**) ppm. **LRMS (ESI+)** m/z: 484.2 $[M+NH_4]^+$. **HRMS (ESI+)** $C_{27}H_{43}FNaO_5$ $[M+Na]^+$. Calculated: 489.2987; Found:

489.2997 (2.1 ppm error). **IR** (neat, cm^{-1}) 3479 (b), 2939 – 2880 (m), 1730 (s), 1711 (s), 1236 (s), 1037 (m).

Methyl 7α-fluoro-3α-acetoxy-6β-(phenoxycarbonothioyl)oxy-5β-cholan-24-oate (3.69)

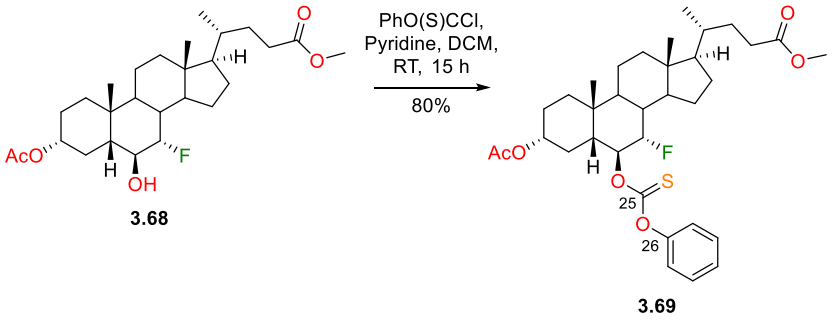

3.68 **3.69**

Following general procedure G, the thiocarbonate of **3.68** (7.31 g, 15.7 mmol, 1.0 equiv) was formed. Note: reaction stirred for 15 h. The crude material was purified by flash chromatography (EtOAc/PE 5%/95% → 10%/90% → 15%/85%) to give **3.69** as a white gummy solid (7.61 g, 12.6 mmol, 80%).

R_f 0.23 (EtOAc/PE 10/90). **^{1}H NMR** (400 MHz, $CDCl_3$) δ 7.42 (br t, *J*=7.6 Hz, 2H, *meta*-**CH**), 7.30 (br t, *J*=7.3 Hz, 1H, *para*-**CH**), 7.09 (br d, *J*=7.5 Hz, 2H, *ortho*-**CH**), 5.28 (br dt, *J*=9.2, 1.8 Hz, 1H, 6α-**H**), 4.60-4.67 (m, 1H, 3β-**H**), 4.62 (d, *J*=44.5 Hz, 1H, 7β-**H**), 3.68 (s, 3H, 24-COO**CH_3**), 2.37 (ddd, *J*=15.5, 10.0, 5.3 Hz, 1H, 23-**H'**), 2.24 (ddd, *J*=16.0, 9.7, 6.7 Hz, 1H, 23-**H''**), 2.03 (s, 3H, 3α-OCO**CH_3**), 1.05-2.09 (m), 0.98 (s, 3H, 19-**CH_3**), 0.94 (d, *J*=6.5 Hz, 3H, 21-**CH_3**), 0.70 (s, 3H, 18-**CH_3**) ppm. **^{13}C NMR** (100 MHz, $CDCl_3$) δ 193.4 (**25-C**), 174.6 (**24-COO**CH_3), 170.5 (**3α-OCO**CH_3), 153.3 (**26-C**), 129.5 (2 C, ***meta*-C**), 126.6 (***para*-C**), 121.8 (2 C, ***ortho*-C**), 89.6 (d, *J*=173.9 Hz, **7-CH**), 82.5 (d, *J*=32.3 Hz, **6-CH**), 73.0 (**3-CH**), 55.7 (**17-CH**), 51.4 (**24-**COO**CH_3**), 49.3 (d, *J*=3.7 Hz, **14-CH**), 43.3 (***5-CH or 9-CH***), 42.7 (**13-C**), 39.3 (**12-CH_2**), 35.8 (d, *J*=19.8 Hz, **8-CH**), 35.3 (**20-CH**), 34.9 (**1-CH_2**), 34.1 (**10-C**), 33.2 (***5-CH or 9-CH***), 31.0 (**23-CH_2**), 30.9 (**22-CH_2**), 30.6 (d, *J*=8.1 Hz, **4-CH_2**), 28.0 (***15-CH_2 or 16-CH_2***), 26.1 (**2-CH_2**), 24.3 (**19-CH_3**), 23.4 (***15-CH_2 or 16-CH_2***), 21.3 (**3α-**OCO**CH_3**), 20.3 (**11-CH_2**), 18.2 (**21-CH_3**), 11.6 (**18-CH_3**) ppm. **^{19}F NMR** (376MHz, $CDCl_3$) δ -195.95 (ddd, *J*=46.8, 41.6, 10.4 Hz, 1F, 7α-**F**) ppm. **^{19}F [^{1}H] NMR** (376MHz, $CDCl_3$) δ -195.95 (s, 1F, 7α-**F**) ppm. **LRMS (ESI+)** m/z: 620.2 $[M+NH_4]^+$. **HRMS (ESI+)** $C_{34}H_{47}FNaO_6S$ $[M+Na]^+$. Calculated: 625.2970; Found: 625.2965 (0.7 ppm error). **IR** (neat, cm^{-1}) 2940 – 2871 (m), 1733 (s), 1196 (s), 1016 (m).

Methyl 7α-fluoro-3α-acetoxy-5β-cholan-24-oate (3.70)

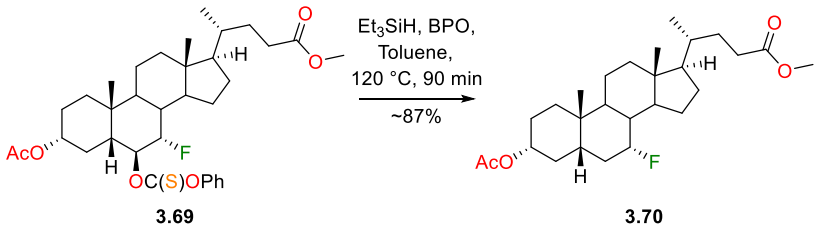

Following general procedure H, **3.69** (3.99 g, 6.62 mmol, 1.0 equiv) was deoxygenated. The crude material was combined with the crude material from a repeat of the reaction (total mmol **3.69** = 12.9 mmol) and purified by flash chromatography (EtOAc/PE 0%/100% → 5%/95% → 7%/93%), giving **3.70** around 80% pure as a white gummy solid (~5.1 g, ~11.3 mmol, ~87%).

R_f 0.28 (EtOAc/PE 10/90). **^{1}H NMR** (400 MHz, $CDCl_3$) δ 4.56-4.65 (m, 1H, 3β-**H**), 4.60 (dq, *J*=48.7, 2.1 Hz, 1H, 7β-**H**), 3.66 (s, 3H, 24-COO**CH_3**), 2.36 (ddd, *J*=15.4, 10.1, 5.3 Hz, 1H, 23-**H'**), 2.22 (ddd, *J*=15.9, 9.8, 6.5 Hz, 1H, 23-**H''**), 2.02 (s, 3H, 3α-OCO**CH_3**), 0.95-2.08 (m), 0.92 (d, *J*=6.5 Hz, 3H, 21-**CH_3**), 0.90 (s, 3H, 19-**CH_3**), 0.65 (s, 3H, 18-**CH_3**) ppm. **^{13}C NMR** (100 MHz, $CDCl_3$) δ 174.8 (**24-COO**CH_3), 170.9 (**3α-OCO**CH_3), 91.1 (d, *J*=171.7 Hz, **7-CH**), 74.1 (**3-CH**), 55.7 (**17-CH**), 51.5 (**24-**COO**CH_3**), 50.0 (d, *J*=3.7 Hz, **14-CH**), 42.6 (**13-C**), 40.6 (d, *J*=1.5 Hz, ***5-CH or 9-CH***), 39.5 (**12-CH_2**), 39.0 (d, *J*=19.8 Hz, **8-CH**), 35.3 (**20-CH**), 34.8 (**1-CH_2**), 34.6 (**10-C**), 34.5 (d, *J*=5.9 Hz, **4-CH_2**), 33.6 (***5-CH or 9-CH***), 32.3 (d, *J*=19.1 Hz, **6-CH_2**), 31.0 (**23-CH_2**), 30.9 (**22-CH_2**), 28.0 (***15-CH_2 or 16-CH_2***), 26.5 (**2-CH_2**), 23.4 (***15-CH_2 or 16-CH_2***), 22.5 (**19-CH_3**), 21.4 (**3α-**OCO**CH_3**), 20.5 (**11-CH_2**), 18.2 (**21-CH_3**), 11.6 (**18-CH_3**) ppm. **^{19}F NMR** (376MHz, $CDCl_3$) δ -186.89 (apparent tdd, *J*=50.3, 38.1, 13.9 Hz, 1F, 7α-**F**) ppm. **^{19}F [^{1}H] NMR** (376MHz, $CDCl_3$) δ -186.88 (s, 1F, 7α-**F**) ppm. **LRMS (ESI+)** m/z: 468.2 $[M+NH_4]^+$. **HRMS (ESI+)** $C_{27}H_{43}FNaO_4$ $[M+Na]^+$. Calculated: 473.3038; Found: 473.3044 (1.4 ppm error).

7α-Fluorolithocholic acid (3.3)

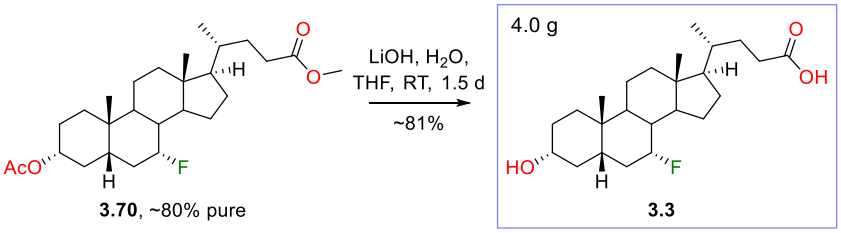

Following general procedure C, **3.70** (~80% pure, 5.65 g, ~11 mmol, 1.0 equiv) was deprotected. The crude material was loaded onto silica gel and was purified by a plug column (EtOAc/PE 20%/80% → EtOAc/PE 100%/0% → MeOH/EtOAc 20%/80%) to give **3.3** as a white solid (4.00 g, 10.1 mmol, ~81%).

mp 194 – 196 °C. **R_f** 0.13 (EtOAc/PE 40/60). **$[\alpha]_D$** + 20.3 (c = 0.4, EtOAc, 22 °C). **^{1}H NMR** (400 MHz, $CDCl_3$) δ 4.62 (br dq, *J*=48.7, 2.0 Hz, 1H, 7β-**F**), 3.51 (ttd, *J*=11.1, 4.5, 2.1 Hz, 1H, 3β-**H**), 2.41 (ddd, *J*=15.5, 10.0, 5.3 Hz, 1H, 23-**H'**), 2.27 (ddd, *J*=16.1, 9.8, 6.7 Hz, 1H, 23-**H''**), 1.66-2.04 (m), 0.97-1.57 (m), 0.95 (d, *J*=6.5 Hz, 3H, 21-**CH_3**), 0.91 (s, 3H, 19-**CH_3**), 0.66 (s, 3H, 18-**CH_3**) ppm. **^{13}C NMR** (100 MHz, MeOH-d_4) δ 178.3 (**24-COOH**), 92.4 (d, *J*=172.4 Hz, **7-CH**), 72.5 (**3-CH**), 57.5 (**17-CH**), 51.7 (d, *J*=3.7 Hz, **14-CH**), 44.0 (**13-C**), 42.5 (d, *J*=1.5 Hz, ***5-CH or 9-CH***), 41.2 (**12-CH_2**), 40.5 (d, *J*=19.8 Hz, **8-CH**), 40.0 (d, *J*=5.1 Hz, **4-CH_2**), 36.9 (**20-CH**), 36.4 (**1-CH_2**), 35.9 (**10-C**), 35.3 (***5-CH or 9-CH***), 33.8 (d, *J*=19.1 Hz, **6-CH_2**), 32.4 (**22-CH_2**), 32.2 (**23-CH_2**), 31.3 (**2-CH_2**), 29.3 (***15-CH_2 or 16-CH_2***), 24.6 (***15-CH_2 or 16-CH_2***), 23.2 (**19-CH_3**), 21.9 (**11-CH_2**), 18.9 (**21-CH_3**), 12.3 (**18-CH_3**) ppm. **^{19}F NMR** (376MHz, MeOH-d_4) δ -187.05 (apparent tdd, *J*=49.4, 36.4, 13.9 Hz, 1F, 7α-**F**) ppm. **^{19}F [^{1}H] NMR** (376MHz, MeOH-d_4) δ -187.05 (s, 1F, 7α-**F**) ppm. **LRMS (ESI+)** m/z: 412.2 $[M+NH_4]^+$. **HRMS (ESI+)** $C_{24}H_{39}FNaO_3$ $[M+Na]^+$. Calculated: 417.2775; Found: 417.2772 (0.9 ppm error). **IR** (neat, cm^{-1}) 3370 (m), 2926 – 2862 (m), 1700 (s), 1108 (m), 971 (m).

7α-Fluorohyodeoxycholic acid (3.43)

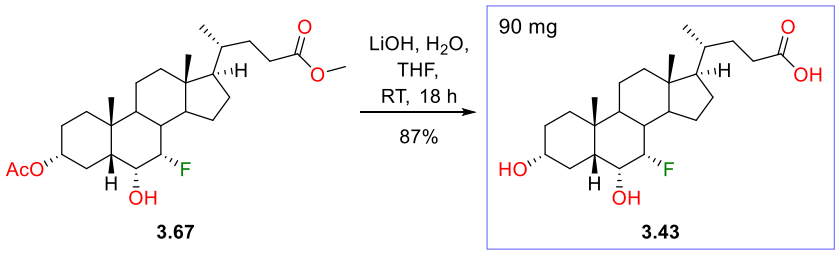

Following general procedure C, **3.67** (120 mg, 0.26 mmol, 1.0 equiv) was deprotected to yield **3.43** as a white gummy solid (93 mg, 0.23 mmol, 87%) with no further purification.

R_f 0.24 (Acetone/PE 50/50). **$[\alpha]_D$** + 10.4 (c = 0.6, MeOH, 22 °C). **^{1}H NMR** (400 MHz, MeOH-d_4) δ 4.58 (br d, *J*=52.6 Hz, 1H, 7β-**H**), 3.85 (apparent dtd, *J*=35.2, 2.6, 1.5 Hz, 1H, 6β-**H**), 3.33-3.46 (m, 1H, 3β-**H**), 2.34 (ddd, *J*=15.3, 9.5, 5.3 Hz, 1H, 23-**H'**), 2.21 (ddd, *J*=16.1, 9.5, 7.0 Hz, 1H, 23-**H''**), 1.03-2.09 (m), 0.97 (d, *J*=6.5 Hz, 3H, 21-**CH_3**), 0.94 (s, 3H, 19-**CH_3**), 0.71 (s, 3H, 18-**CH_3**) ppm. **^{13}C NMR** (100 MHz, MeOH-d_4) δ 178.2 (**24-COOH**), 95.1 (d, *J*=179.7 Hz, **7-CH**), 72.5 (**3-CH**), 69.8 (d, *J*=16.9 Hz, **6-CH**), 57.4 (**17-CH**), 51.5 (d, *J*=2.9 Hz, **14-CH**), 49.4 (**5-CH**), 44.1 (**13-C**), 41.0 (**12-CH_2**), 39.9 (d, *J*=19.1 Hz, **8-CH**), 37.0 (**10-C**), 36.8 **(20-CH**), 36.7 (**1-CH_2**), 35.2 (**9-CH**), 33.0 (d, *J*=7.3 Hz, **4-CH_2**), 32.4 (**22-CH_2**), 32.1 (**23-CH_2**), 31.4 (**2-CH_2**), 29.2 (***15-CH_2 or 16-CH_2***), 24.5 (***15-CH_2 or 16-CH_2***), 23.7 (**19-CH_3**), 21.9 (**11-CH_2**), 18.9 (**21-CH_3**), 12.3 (**18-CH_3**) ppm. **^{19}F NMR** (376MHz, MeOH-d_4) δ -207.15 (dt, *J*=52.0, 34.7 Hz, 1F, 7α-**F**) ppm. **^{19}F [^{1}H] NMR** (376MHz, MeOH-d_4) δ -207.15 (s, 1F, 7α-**F**) ppm. **LRMS (ESI+)** m/z: 428.2 $[M+NH_4]^+$. **HRMS (ESI+)** $C_{24}H_{39}FNaO_4$ $[M+Na]^+$. Calculated: 433.2725; Found: 433.2730 (1.3 ppm error). **IR** (neat, cm^{-1}) 3347 (b), 2932 – 2867 (m), 1706 (s), 1242 (m), 1051 (s).

Methyl 7α-fluoro-3α-acetoxy-6α-methoxy-5β-cholan-24-oate (3.71)

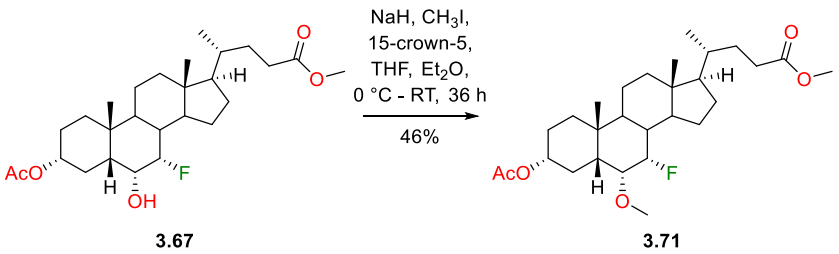

The alcohol **3.67** (300 mg, 0.64 mmol, 1.0 equiv) and 15-crown-5 (0.14 mL, 0.70 mmol, 1.1 equiv) were dissolved in anhydrous THF (6 mL) and were added to a suspension of NaH (~60% dispersion in mineral oil, 36 mg, 0.90 mmol, 1.4 equiv) in anhydrous diethyl ether (20 mL) at 0 °C. A solution of iodomethane (0.05 mL, ~0.70 mmol, ~1.1 equiv) in anhydrous THF (6 mL) was then added to the reaction mixture dropwise. After stirring for 1.5 d from 0 °C to RT, the reaction mixture was cooled back to 0 °C and added water (30 mL). The mixture was extracted with EtOAc (2 x 25 mL) and the combined organic phases were washed with brine (80 mL) before drying over Na_2SO_4 and reducing *in vacuo*. The crude material was purified by flash chromatography (Biotage ZIP KP-Sil 10 g cartridge, EtOAc/PE: 15%/85% → 40%/60% over 18 CV) to give **3.71** as a white gummy solid (142 mg, 0.30 mmol, 46%).

R_f 0.48 (EtOAc/PE 30/70). **^{1}H NMR** (400 MHz, $CDCl_3$) δ 4.72 (br d, *J*=52.2 Hz, 1H, 7β-**H**), 4.56-4.64 (m, 1H, 3β-**H**), 3.66 (s, 3H, 24-COO**CH_3**), 3.37 (s, 3H, 6α-O**CH_3**), 3.34 (ddd, *J*=34.1, 5.0, 2.6 Hz, 1H, 6β-**H**), 2.35 (ddd, *J*=15.4, 10.0, 5.3 Hz, 1H, 23-**H'**), 2.22 (ddd, *J*=16.1, 9.7, 6.8 Hz, 1H, 23-**H''**), 2.00 (s, 3H, 3α-OCO**CH_3**), 1.05-1.99 (m), 0.92 (d, *J*=6.4 Hz, 3H, 21-**CH_3**), 0.91 (s, 3H, 19-**CH_3**), 0.65 (s, 3H, 18-**CH_3**) ppm. **^{1}H NMR** (^{19}F decoupled) (500 MHz, $CDCl_3$) δ 4.73 (br s, 1H, 7β-**H**), 4.61 (tt, *J*=11.3, 4.5 Hz, 1H, 3β-**H**), 3.67 (s, 3H, 24-COO**CH_3**), 3.38 (s, 3H, 6α-O**CH_3**), 3.35 (dd, *J*=5.1, 2.6 Hz, 1H, 6β-**H**), 2.36 (ddd, *J*=15.2, 10.0, 5.1 Hz, 1H, 23-**H'**), 2.23 (ddd, *J*=15.7, 9.3, 6.6 Hz, 1H, 23-**H''**), 2.01 (s, 3H, 3α-OCO**CH_3**), 1.68-2.05 (m), 1.08-1.57 (m), 0.94 (d, *J*=6.4 Hz, 3H, 21-**CH_3**), 0.92 (s, 3H, 19-**CH_3**), 0.66 (s, 3H, 18-**CH_3**) ppm. **^{13}C NMR** (100 MHz, $CDCl_3$) δ 174.6 (**24-COO**CH_3), 170.6 (**3α-OCO**CH_3), 90.7 (d, *J*=181.2 Hz, **7-CH**), 77.5 (d, *J*=16.1 Hz, **6-CH**), 73.7 (**3-CH**), 56.2 (**6α-OCH_3**), 55.7 (**17-CH**), 51.4 (**24-**COO**CH_3**), 49.7 (d, *J*=2.9 Hz, **14-CH**), 44.4 (***5-CH or 9-CH***), 42.7 (**13-C**), 39.3 (**12-CH_2**), 38.4 (d, *J*=19.1 Hz, **8-CH**), 35.5 (**10-C**), 35.3 (**20-CH**), 35.1 (**1-CH_2**), 33.6 (***5-CH or 9-CH***), 31.0 (**23-CH_2**), 30.9 (**22-CH_2**), 28.1 (d, *J*=8.1 Hz, **4-CH_2**), 28.0 (***15-CH_2 or 16-CH_2***), 26.6 (**2-CH_2**), 23.4 (***15-CH_2 or 16-CH_2***), 23.1 (**19-CH_3**), 21.3 (**3α-**OCO**CH_3**), 20.6 (**11-CH_2**), 18.2 (**21-CH_3**), 11.6 (**18-CH_3**) ppm. **^{19}F NMR** (376MHz, $CDCl_3$) δ -206.06 (dt, *J*=52.0, 34.7 Hz, 1F, 7α-**F**) ppm. **^{19}F [^{1}H] NMR** (376MHz, $CDCl_3$) δ -206.06 (s, 1F, 7α-**F**) ppm. **LRMS (ESI+)** m/z: 498.2 $[M+NH_4]^+$. **HRMS (ESI+)** $C_{28}H_{45}FNaO_5$ $[M+Na]^+$. Calculated: 503.3143; Found: 503.3145 (0.3 ppm error). **IR** (neat, cm^{-1}) 2938 – 2869 (m), 1731 (s), 1236 (m), 1100 (m).

7α-Fluoro-6α-methoxylithocholic acid (3.72)

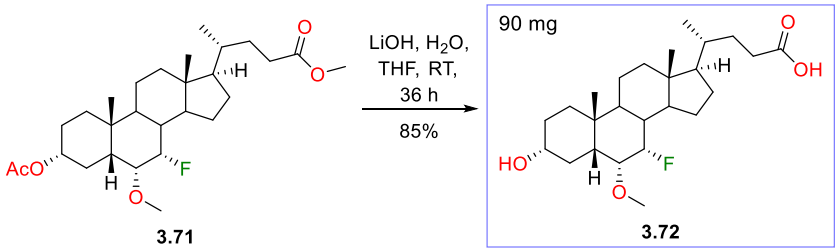

Following general procedure C, **3.71** (122 mg, 0.25 mmol, 1.0 equiv) was deprotected to yield **3.72** as a white gummy solid (90 mg, 0.21 mmol, 85%) with no further purification.

R_f 0.04 (EtOAc/PE 30/70). **$[\alpha]_D$** + 5.70 (c = 0.5, $CHCl_3$, 21 °C). **^{1}H NMR** (400 MHz, $CDCl_3$) δ 4.74 (br d, *J*=52.2 Hz, 1H, 7β-**H**), 3.43-3.54 (m, 1H, 3β-**H**), 3.40 (s, 3H, 6α-O**CH_3**), 3.36 (ddd, *J*=34.0, 5.1, 2.7 Hz, 1H, 6β-**H**), 2.41 (ddd, *J*=15.5, 9.9, 5.1 Hz, 1H, 23-**H'**), 2.28 (ddd, *J*=16.1, 9.7, 6.8 Hz, 1H, 23-**H''**), 1.04-2.04 (m), 0.95 (d, *J*=6.5 Hz, 3H, 21-**CH_3**), 0.92 (s, 3H, 19-**CH_3**), 0.67 (s, 3H, 18-**CH_3**) ppm. **^{13}C NMR** (100 MHz, $CDCl_3$) δ 179.6 (**24-COOH**), 90.6 (d, *J*=181.2 Hz, **7-CH**), 77.7 (d, *J*=16.9 Hz, **6-CH**), 71.6 (**3-CH**), 56.1 (**6α-OCH_3**), 55.7 (**17-CH**), 49.7 (d, *J*=2.9 Hz, **14-CH**), 44.6 (***5-CH or 9-CH***), 42.7 (**13-C**), 39.3 (**12-CH_2**), 38.4 (d, *J*=19.1 Hz, **8-CH**), 35.5 (**10-C**), 35.4 (**1-CH_2**), 35.3 (**20-CH**), 33.7 (***5-CH or 9-CH***), 32.2 (d, *J*=8.1 Hz, **4-CH_2**), 31.0 (**23-CH_2**), 30.7 (**22-CH_2**), 30.2 (**2-CH_2**), 28.0 (***15-CH_2 or 16-CH_2***), 23.4 (***15-CH_2 or 16-CH_2***), 23.1 (**19-CH_3**), 20.6 (**11-CH_2**), 18.2 (**21-CH_3**), 11.6 (**18-CH_3**) ppm. **^{19}F NMR** (376MHz, $CDCl_3$) δ -205.82 (apparent dt, *J*=52.0, 34.7 Hz, 1F, 7α-**F**) ppm. **^{19}F [^{1}H] NMR** (376MHz, $CDCl_3$) δ -205.82 (s, 1F, 7α-**F**) ppm. **LRMS (ESI-)** m/z: 423.5 $[M-H]^-$. **HRMS (ESI+)** $C_{25}H_{41}FNaO_4$ $[M+Na]^+$. Calculated: 447.2881; Found: 447.2877 (0.8 ppm error). **IR** (neat, cm^{-1}) 3428 (b), 2933 – 2868 (m), 1707 (s), 749 (m).

Methyl 7α-fluoro-lithochol-24-oate (3.73)

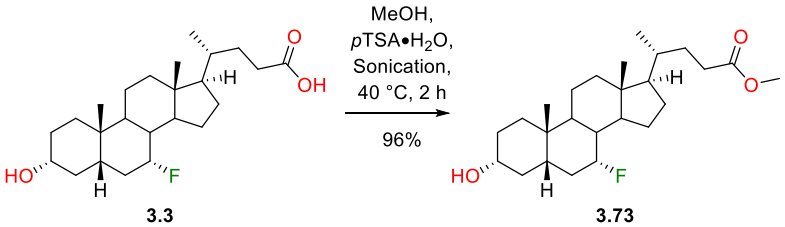

Following general procedure A, **3.3** (3.0 g, 7.60 mmol, 1.0 equiv) was protected to yield **3.73** as a white solid (2.97 g, 7.27 mmol, 96%) with no further purification.

mp 135 – 137 °C. **R_f** 0.21 (EtOAc/PE 20/80). **$[\alpha]_D$** + 16.3 (c = 1.0, $CHCl_3$, 22 °C). **^{1}H NMR** (400 MHz, $CDCl_3$) δ 4.60 (apparent dq, *J*=48.7, 2.0 Hz, 1H, 7β-**F**), 3.66 (s, 3H, 24-COO**CH_3**), 3.48 (ttd, *J*=11.0, 4.4, 2.1 Hz, 1H, 3β-**H**), 2.35 (ddd, *J*=15.5, 10.1, 5.3 Hz, 1H, 23-**H'**), 2.21 (ddd, *J*=16.0, 9.7, 6.7 Hz, 1H, 23-**H''**), 1.64-2.02 (m), 1.58 (br s, 1H, 3α-**OH**), 1.04-1.54 (m), 1.00 (td, *J*=14.2, 3.2 Hz, 1H, 1β-**H**), 0.92 (d,

J=6.5 Hz, 3H, 21-**CH₃**), 0.89 (s, 3H, 19-**CH₃**), 0.64 (s, 3H, 18-**CH₃**) ppm. **^{13}C NMR** (100 MHz, $CDCl_3$) δ 174.7 (**24-COO**CH_3), 91.1 (d, *J*=172.4 Hz, **7-CH**), 71.7 (**3-CH**), 55.7 (**17-CH**), 51.4 (**24**-COO**CH₃**), 50.0 (d, *J*=3.7 Hz, **14-CH**), 42.6 (**13-C**), 40.9 (d, *J*=1.5 Hz, ***5-CH or 9-CH***), 39.5 (**12-CH₂**), 39.1 (d, *J*=5.1 Hz, **4-CH₂**), 39.1 (br d, *J*=19.8 Hz, **8-CH**), 35.3 (**20-CH**), 35.1 (**1-CH₂**), 34.6 (**10-C**), 33.6 (***5-CH or 9-CH***), 32.5 (d, *J*=19.1 Hz, **6-CH₂**), 31.0 (**23-CH₂**), 30.9 (**22-CH₂**), 30.4 (**2-CH₂**), 28.1 (***15-CH₂ or 16-CH₂***), 23.4 (***15-CH₂ or 16-CH₂***), 22.5 (**19-CH₃**), 20.5 (**11-CH₂**), 18.2 (**21-CH₃**), 11.6 (**18-CH₃**) ppm. **^{19}F NMR** (376MHz, $CDCl_3$) δ -186.76 (apparent tdd, *J*=50.3, 38.1, 13.9 Hz, 1F, 7α-**F**) ppm. **^{19}F [^{1}H] NMR** (376MHz, $CDCl_3$) δ -186.76 (s, 1F, 7α-**F**) ppm. **LRMS (ESI+)** m/z: 426.1 $[M+NH_4]^+$. **HRMS (ESI+)** $C_{25}H_{41}FNaO_3$ $[M+Na]^+$. Calculated: 431.2932; Found: 431.2933 (0.4 ppm error). **IR** (neat, cm^{-1}) 3520 (m), 2957 – 2868 (m), 1711 (s), 1076 (m), 1005 (m).

Methyl 3β,7α-difluoro-5β-cholan-24-oate (3.74)

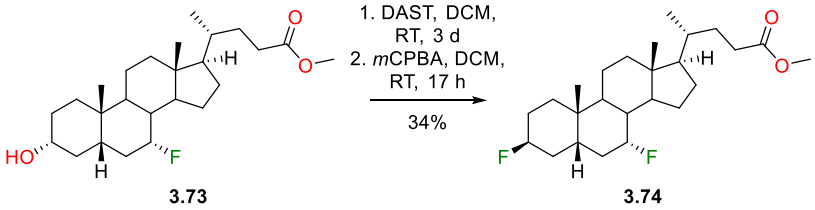

3.73 **3.74**

The alcohol **3.73** (541 mg, 1.32 mmol, 1.0 equiv) was dissolved in dry DCM (5 mL) and DAST (0.52 mL, 3.96 mmol, 3.0 equiv) was added. After stirring at RT for 1.5 d, further DAST (0.17 mL, 1.32 mmol, 1.0 equiv) was added to the reaction mixture. After stirring for a total of 3 d, the reaction mixture was diluted with DCM (10 mL) and was slowly added $NaHCO_3$ solution (sat., 20 mL) with stirring. The resulting mixture was extracted with EtOAc (3 x 50 mL) and the combined organic phases were washed with $NaHCO_3$ solution (sat., 100 mL), water (100 mL) and brine (100 mL) before drying over Na_2SO_4 and reducing *in vacuo*. The crude material was purified by flash chromatography (Biotage SNAP KP-Sil 25 g cartridge, EtOAc/PE 0%/100% → 10%/90% → 20%/80% over 24 CV in total) to yield **3.74** around 80% pure with alkene by-products (204 mg). The 80% pure fraction of **3.74** (204 mg, ~0.50 mmol, 1.0 equiv) was dissolved in DCM (4 mL) and *m*-CPBA (~70% with water, ~57 mg, ~0.23 mmol, ~1.5 equiv based on alkene content) was added. After stirring at RT for 17 h, the reaction mixture was added $NaHCO_3$ solution (sat., 20 mL) and the resulting mixture was extracted with EtOAc (3 x 15 mL). The combined organic phases were washed with $NaHCO_3$ solution (sat., 40 mL), water (40 mL) and brine (40 mL) before drying over Na_2SO_4 and reducing *in vacuo*. The crude material was purified by flash chromatography (Biotage SNAP KP-Sil 25 g cartridge, EtOAc/PE: 0%/100% → 10%/90% → 20%/80% over 22 CV in total) to yield **3.74** as a white solid (184 mg, 0.45 mmol, 34%).

mp 95 – 96 °C. **R_f** 0.53 (EtOAc/PE 10/90) **$[\alpha]_D$** + 7.75 (c = 0.6, $CHCl_3$, 22 °C). **^{1}H NMR** (400 MHz, $CDCl_3$) δ 4.83 (br d, *J*=48.9 Hz, 1H, 3α-**H**), 4.63 (dq, *J*=49.2, 2.4 Hz, 1H, 7β-**H**), 3.66 (s, 3H, 24-COO**CH₃**), 2.36

(ddd, *J*=15.4, 10.1, 5.3 Hz, 1H, 23-**H'**), 1.05-2.28 (m), 0.95 (s, 3H, 19-**CH_3**), 0.93 (d, *J*=6.5 Hz, 3H, 21-**CH_3**), 0.66 (s, 3H, 18-**CH_3**) ppm. **^{1}H [^{19}F] NMR** ($CDCl_3$, 500MHz) δ = 4.84 (br s, 1H, 3α-**H**), 4.64 (q, *J*=2.4 Hz, 1H, 7β-**H**), 3.67 (s, 3H, 24-COO**CH_3**), 2.36 (ddd, *J*=15.4, 10.3, 5.3 Hz, 1H, 23-**H'**), 2.23 (ddd, *J*=16.2, 9.6, 6.8 Hz, 1H, 23-**H''**), 2.12 (ddd, *J*=16.2, 14.1, 2.1 Hz, 1H, 4α-**H**), 1.87-2.02 (m), 1.67-1.85 (m), 1.25-1.62 (m), 1.09-1.23 (m), 0.95 (s, 3H, 19-**CH_3**), 0.93 (s, 3H, 21-**CH_3**), 0.67 (s, 3H, 18-**CH_3**) ppm. **^{13}C NMR** (100 MHz, $CDCl_3$) δ 174.6 (**24-COO**CH_3), 91.6 (d, *J*=171.7 Hz, **7-CH**), 89.7 (dd, *J*=166.5, 1.5 Hz, **3-CH**), 55.7 (**17-CH**), 51.4 (**24**-COO**CH_3**), 50.1 (d, *J*=3.7 Hz, **14-CH**), 42.7 (**13-C**), 39.5 (**12-CH_2**), 39.1 (d, *J*=19.8 Hz, **8-CH**), 35.8 (d, *J*=1.5 Hz, ***5-CH or 9-CH***), 35.4 (**20-CH**), 34.8 (**10-C**), 34.0 (dd, *J*=20.5, 5.9 Hz, **4-CH_2**), 33.0 (***5-CH or 9-CH***), 31.8 (d, *J*=19.1 Hz, **6-CH_2**), 31.0 (**23-CH_2**), 30.9 (**22-CH_2**), 29.9 (**1-CH_2**), 28.1 (***15-CH_2 or 16-CH_2***), 25.8 (d, *J*=21.3 Hz, **2-CH_2**), 23.4 (***15-CH_2 or 16-CH_2***), 22.8 (**19-CH_3**), 20.9 (**11-CH_2**), 18.2 (**21-CH_3**), 11.6 (**18-CH_3**) ppm. **^{19}F NMR** (471MHz, $CDCl_3$) δ -184.98 (apparent tdtd, *J*=48.9, 44.0, 10.4, 5.4 Hz, 1F, 3β-**F**), -186.95--186.55 (m, 1F, 7α-**F**) ppm. **^{19}F [^{1}H] NMR** (471MHz, $CDCl_3$) δ -184.98 (d, *J*=5.4 Hz, 1F, 3β-**F**), -186.76 (d, *J*=5.4 Hz, 1F, 7α-**F**) ppm. **LRMS (ESI+)** m/z: 428.5 $[M+NH_4]^+$. **HRMS (ESI+)** $C_{25}H_{40}F_2NaO_2$ $[M+Na]^+$. Calculated: 433.2889; Found: 433.2893 (1.0 ppm error). **IR** (neat, cm^{-1}) 2937 – 2874 (m), 1737 (s), 1185 (m), 1169 (m), 1001 (m).

3β,7α-Difluoro-5β-cholan-24-oate (3.7)

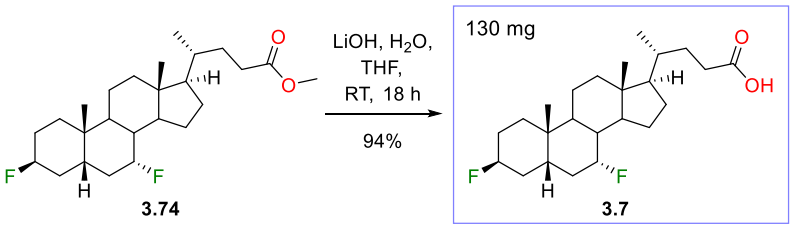

Following general procedure C, **3.74** (150 mg, 0.37 mmol, 1.0 equiv) was deprotected to yield **3.7** as a white solid (138 mg, 0.35 mmol, 94%) with no further purification.

mp 157 – 158 °C. **R_f** 0.13 (EtOAc/PE 20/80). **[α]$_D$** + 7.86 (c = 0.70, $CHCl_3$, 22 °C). **^{1}H NMR** (400 MHz, $CDCl_3$) δ 11.30 (br s, 1H, 24-**COOH**), 4.84 (d, *J*=48.8 Hz, 1H, 3α-**H**), 4.64 (dq, *J*=49.3, 2.3 Hz, 1H, 7β-**H**), 2.41 (ddd, *J*=15.5, 10.1, 5.3 Hz, 1H, 23-**H'**), 2.27 (ddd, *J*=15.9, 9.6, 6.5 Hz, 1H, 23-**H''**), 1.04-2.22 (m), 0.95 (s, 3H, 19-**CH_3**), 0.93 (d, *J*=6.5 Hz, 3H, 21-**CH_3**), 0.67 (s, 3H, 18-**CH_3**) ppm. **^{13}C NMR** (100 MHz, $CDCl_3$) δ 180.7 (**24-COOH**), 91.6 (d, *J*=170.9 Hz, **7-CH**), 89.7 (d, *J*=165.1 Hz, **3-CH**), 55.7 (**17-CH**), 50.1 (d, *J*=3.7 Hz, **14-CH**), 42.7 (**13-C**), 39.5 (**12-CH_2**), 39.0 (d, *J*=19.8 Hz, **8-CH**), 35.8 (d, *J*=1.5 Hz, ***5-CH or 9-CH***), 35.3 (**20-CH**), 34.8 (**10-C**), 34.0 (dd, *J*=20.5, 5.1 Hz, **4-CH_2**), 33.0 (***5-CH or 9-CH***), 31.8 (d, *J*=19.8 Hz, **6-CH_2**), 31.0 (**23-CH_2**), 30.7 (**22-CH_2**), 29.9 (**1-CH_2**), 28.1 (***15-CH or 16-CH_2***), 25.8 (d, *J*=21.3 Hz, **2-CH_2**), 23.4 (***15-CH_2 or 16-CH_2***), 22.8 (**19-CH_3**), 20.9 (**11-CH_2**), 18.2 (**21-CH_3**), 11.7 (**18-CH_3**) ppm. **^{19}F NMR** (376MHz, $CDCl_3$) δ -185.19 (apparent tdtd, *J*=48.5, 43.4, 10.4, 5.2 Hz, 1F, 3β-**F**), -187.23--186.66 (m, 1F, 7α-**F**) ppm. **^{19}F [^{1}H] NMR** (376MHz, $CDCl_3$) δ -185.19 (d, *J*=5.2 Hz, 1F, 3β-**F**), -186.96

(d, *J*=5.2 Hz, 1F, 7α-**F**) ppm. **LRMS (ESI-)** m/z: 395.2 $[M-H]^-$. **HRMS (ESI+)** $C_{24}H_{38}F_2NaO_2$ $[M+Na]^+$. Calculated: 419.2732; Found: 419.2742 (2.0 ppm error). **IR** (neat, cm^{-1}) 2942 – 2859 (m), 1702 (s), 1412 (m), 1352 (m), 882 (m).

Methyl 7α-fluoro-3β-benzoloxy-5β-cholan-24-oate (3.77)

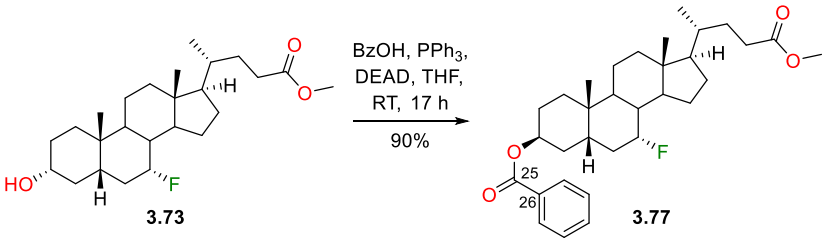

The alcohol **3.73** (2.0 g, 4.89 mmol, 1.0 equiv) was dissolved in dry THF (40 mL) and benzoic acid (896 mg, 7.34 mmol, 1.5 equiv) and triphenylphosphine (1.93 g, 7.34 mmol, 1.5 equiv) were added. DEAD (1.16 mL, 7.34 mmol, 1.5 equiv) was then added dropwise over the course of 5 min. After stirring at RT for 17 h, the reaction mixture was reduced *in vacuo*. The crude material was purified by flash chromatography (Biotage SNAP KP-Sil 100 g cartridge, EtOAc/PE: 0%/100% → 20%/80% over 14 CV) to give **3.77** as an off-white gummy solid, around 95% pure with benzoic acid and DEAD-related impurities (2.25 g, 4.39 mmol 90%).

R_f 0.50 (EtOAc/PE 10/90). **^{1}H NMR** (400 MHz, $CDCl_3$) δ 8.05 (br dd, *J*=8.4, 1.1 Hz, 2H, *ortho*-C**H**), 7.55 (tt, *J*=7.5, 1.3 Hz, 1H, *para*-C**H**), 7.45 (br t, *J*=7.8 Hz, 2H, *meta*-C**H**), 5.30 (br s, 1H, 3α-**H**), 4.64 (apparent dq, *J*=49.0, 2.2 Hz, 1H, 7β-**H**), 3.67 (s, 3H, 24-COO**CH₃**), 2.37 (ddd, *J*=15.4, 10.1, 5.3 Hz, 1H, 23-**H'**), 2.18-2.32 (m, 2H, 23-**H''** and 4α or 4β-**H**), 1.07-2.11 (m), 1.00 (s, 3H, 19-**CH₃**), 0.94 (d, *J*=6.5 Hz, 3H, 21-**CH₃**), 0.68 (s, 3H, 18-**CH₃**) ppm. **^{13}C NMR** (100 MHz, $CDCl_3$) δ 174.7 (**24-COO**CH_3), 165.8 (**25-C**), 132.6 (*para*-**CH**), 131.1 (**26-C**), 129.4 (2 C, *ortho*-**CH**), 128.3 (2 C, *meta*-**CH**), 91.5 (d, *J*=171.7 Hz, **7-CH**), 71.0 (**3-CH**), 55.7 (**17-CH**), 51.4 (**24-**COO**CH₃**), 50.1 (d, *J*=3.7 Hz, **14-CH**), 42.7 (**13-C**), 39.5 (**12-CH₂**), 39.1 (d, *J*=19.8 Hz, **8-CH**), 36.7 (d, *J*=1.5 Hz, **5-CH**), 35.3 (**20-CH**), 35.0 (**10-C**), 33.2 (d, *J*=5.1 Hz, **4-CH₂**), 33.1 (**9-CH**), 32.0 (d, *J*=19.8 Hz, **6-CH₂**), 31.0 (**23-CH₂**), 30.9 (**22-CH₂**), 30.8 (**1-CH₂**), 28.1 (***15-CH₂ or 16-CH₂***), 25.0 (**2-CH₂**), 23.4 (***15-CH₂ or 16-CH₂***), 23.2 (**19-CH₃**), 20.9 (**11-CH₂**), 18.2 (**21-CH₃**), 11.6 (**18-CH₃**) ppm. **^{19}F NMR** (376MHz, $CDCl_3$) δ -186.82 (apparent tdd, *J*=50.5, 37.7, 13.9 Hz, 1F, 7α-**F**) ppm. **^{19}F [^{1}H] NMR** (376MHz, $CDCl_3$) δ -186.82 (s, 1F, 7α-**F**) ppm. **LRMS (ESI+)** m/z: 530.5 $[M+NH_4]^+$. **HRMS (ESI+)** $C_{32}H_{45}FNaO_4$ $[M+Na]^+$. Calculated: 535.3194; Found: 535.3181 (2.4 ppm error). **IR** (neat, cm^{-1}) 2943 – 2867 (m), 1735 (s), 1710 (s), 1273 (s), 708 (s).

Methyl 7α-fluoro-3β-hydroxy-5β-cholan-24-oate (3.78)

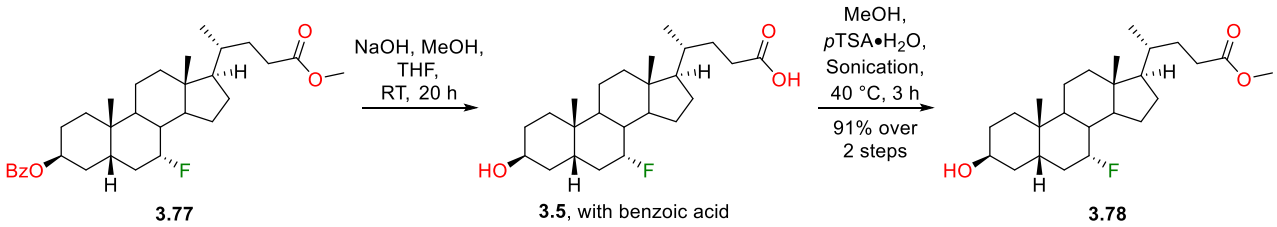

3.77 **3.5**, with benzoic acid **3.78**

Following general procedure D, **3.77** (1.44 g, 2.81 mmol, 1.0 equiv) was deprotected. The benzoic acid formed in the reaction was inseparable from **3.5**, so the mixture was esterified to enable purification. Assumed quantitative yield (2.81 mmol). Following general procedure A, **3.5** (impure with benzoic acid, ~1.7 g, 2.81 mmol, 1.0 equiv) was protected. The crude material was purified by flash chromatography (Biotage ZIP KP-Sil 45 g cartridge, EtOAc/PE: 10%/90% → 20%/70% → 50%/50% over 20 CV in total) to yield **3.78** as a white gummy solid (1.05 g, 2.57 mmol, 91% from **3.77**).

R_f 0.33 (EtOAc/PE 30/70). **$[\alpha]_D$** + 8.33 (c = 0.45, $CHCl_3$, 21 °C). **^{1}H NMR** (400 MHz, $CDCl_3$) δ 4.61 (apparent dq, *J*=49.4, 2.0 Hz, 1H, 7β-**H**), 4.06 (br s, 1H, 3β-**H**), 3.66 (s, 3H, 24-COO**CH_3**), 2.35 (ddd, *J*=15.4, 10.1, 5.3 Hz, 1H, 23-**H'**), 2.09-2.27 (m, 2H, 23-**H''** and 4α or 4β-**H**), 1.03-2.07 (m), 0.93 (s, 3H, 19-**CH_3**), 0.92 (d, *J*=6.5 Hz, 3H, 21-**CH_3**), 0.65 (s, 3H, 18-**CH_3**) ppm. **^{13}C NMR** (100 MHz, $CDCl_3$) δ 174.7 (**24-COO**CH_3), 91.6 (d, *J*=171.7 Hz, **7-CH**), 66.7 (**3-CH**), 55.7 (**17-CH**), 51.4 (**24-**OO**CH_3**), 50.1 (d, *J*=3.7 Hz, **14-CH**), 42.7 (**13-C**), 39.6 (**12-CH_2**), 39.1 (d, *J*=19.8 Hz, **8-CH**), 36.0 (d, *J*=5.1 Hz, **4-CH_2**), 35.4 (d, *J*=1.5 Hz, **5-CH**), 35.3 (**20-CH**), 35.1 (**10-C**), 32.9 (**9-CH**), 32.1 (d, *J*=19.1 Hz, **6-CH_2**), 31.0 (**23-CH_2**), 30.9 (**22-CH_2**), 29.6 (**1-CH_2**), 28.1 (***15-CH_2* or *16-CH_2***), 27.7 (**2-CH_2**), 23.4 (***15-CH_2* or *16-CH_2***), 23.0 (**19-CH_3**), 20.8 (**11-CH_2**), 18.2 (**21-CH_3**), 11.6 (**18-CH_3**) ppm. **^{19}F NMR** (376MHz, $CDCl_3$) δ -186.73 (apparent tdd, *J*=50.9, 38.6, 13.9 Hz, 1F, 7α-**F**) ppm. **^{19}F [^{1}H] NMR** (376MHz, $CDCl_3$) δ -186.73 (s, 1F, 7α-**F**) ppm. **LRMS (ESI+)** m/z: 426.5 $[M+NH_4]^+$. **HRMS (ESI+)** $C_{25}H_{41}FNaO_3$ $[M+Na]^+$. Calculated: 431.2932; Found: 431.2929 (0.6 ppm error). **IR** (neat, cm^{-1}) 3479 (b), 2930 – 2873 (m), 1718 (s), 1165 (m).

7α-Fluoro-3β-hydroxy-5α-cholanic acid (3.5)

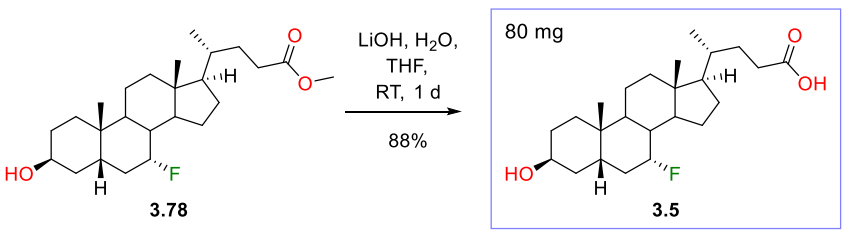

3.78 **3.5**

Following general procedure C, **3.78** (100 mg, 0.24 mmol, 1.0 equiv) was deprotected to yield **3.5** as a white solid (83 mg, 0.21 mmol, 88%) with no further purification.

mp 170 – 171 °C. **R_f** 0.10 (EtOAc/PE 30/70). **$[\alpha]_D$** + 7.00 (c = 0.3, $CHCl_3$, 21 °C). **^{1}H NMR** (400 MHz, MeOH-d_4) δ 4.60 (dq, *J*=49.9, 2.2 Hz, 1H, 7β-**H**), 3.98 (br s, 1H, 3α-**H**), 2.34 (ddd, *J*=15.3, 9.8, 5.3 Hz, 1H, 23-**H'**), 1.08-2.26 (m), 0.97 (d, *J*=6.5 Hz, 3H, 21-**CH_3**), 0.96 (s, 3H, 19-**CH_3**), 0.71 (s, 3H, 18-**CH_3**) ppm. **^{13}C NMR** (100 MHz, MeOH-d_4) δ 178.2 (**24-COOH**), 92.7 (d, *J*=171.7 Hz, **7-CH**), 67.6 (**3-CH**), 57.4 (**17-CH**), 51.8 (d, *J*=3.7 Hz, **14-CH**), 44.0 (**13-C**), 41.2 (**12-CH_2**), 40.6 (d, *J*=19.8 Hz, **8-CH**), 37.2 (d, *J*=5.1 Hz, **4-CH_2**), 36.9 (d, *J*=1.5 Hz, **5-CH**), 36.9 (**20-CH**), 36.4 (**10-C**), 34.6 (**9-CH**), 33.4 (d, *J*=19.1 Hz, **6-CH_2**), 32.4 (**22-CH_2**), 32.1 (**23-CH_2**), 30.9 (**1-CH_2**), 29.3 (***15-CH_2 or 16-CH_2***), 28.6 (**2-CH_2**), 24.6 (***15-CH_2 or 16-CH_2***), 23.8 (**19-CH_3**), 22.2 (**11-CH_2**), 19.0 (**21-CH_3**), 12.3 (**18-CH_3**) ppm. **^{19}F NMR** (376MHz, $CDCl_3$) -186.77 (apparent tdd, *J*=50.7, 39.0, 13.9 Hz, 1F, 7α-**F**) ppm. **^{19}F [^{1}H] NMR** (376MHz, $CDCl_3$) δ -186.77 (s, 1F, 7α-**F**) ppm. **LRMS (ESI-)** m/z: 393.4 $[M-H]^-$. **HRMS (ESI-)** $C_{24}H_{38}FO_3$ $[M-H]^-$. Calculated: 393.2810; Found: 393.2815 (1.1 ppm error). **IR** (neat, cm^{-1}) 3469 (m), 2927 – 2867 (m), 1702 (s), 1158 (m).

Methyl 3α,7α-difluoro-5β-cholan-24-oate (3.79)

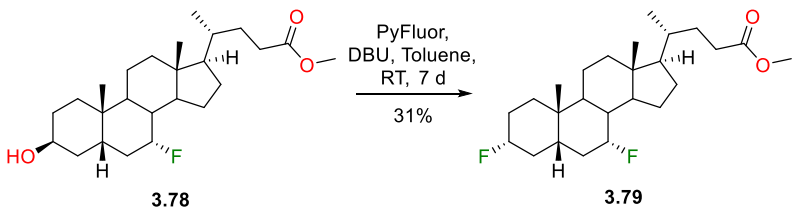

The alcohol **3.78** (834 mg, 2.04 mmol, 1.0 equiv) was dissolved in dry toluene (5 mL) and DBU (0.61 mL, 4.08 mmol, 2.0 equiv) and PyFluor (493 mg, 3.06 mmol, 1.5 equiv) as a solution in toluene (1 mL) were added. After stirring at RT for 7 d, the reaction mixture was added $NaHCO_3$ solution (sat., 40 mL) and the resulting mixture was extracted with EtOAc (3 x 50 mL). The combined organic phases were washed with $NaHCO_3$ solution (sat., 100 mL), water (100 mL) and brine (100 mL) before drying over Na_2SO_4 and reducing *in vacuo*. The crude material was purified twice by flash chromatography (1st: Biotage SNAP KP-Sil 25 g cartridge, EtOAc/PE: 0%/100% → 15%/85% → 50%/50% over 22 CV in total; 2nd: Biotage SNAP KP-Sil 25 g cartridge, EtOAc/PE: 0%/100% → 10%/90% over 20 CV) to yield **3.79** as a white solid (258 mg, 0.63 mmol, 31%).

mp 125 – 127 °C. **R_f** 0.43 (EtOAc/PE 10/90). **$[\alpha]_D$** + 11.1 (c = 0.5, $CHCl_3$, 22 °C). **^{1}H NMR** (400 MHz, $CDCl_3$) δ 4.62 (dq, *J*=48.4, 2.6 Hz, 1H, 7β-**H**), 4.38 (apparent dttd, *J*=49.8, 11.3, 4.7, 2.0 Hz, 1H, 3β-**H**), 3.66 (s, 3H, 24-COO**CH_3**), 2.36 (ddd, *J*=15.4, 10.1, 5.3 Hz, 1H, 23-**H'**), 2.22 (ddd, *J*=15.7, 9.4, 6.6 Hz, 1H, 23-**H''**), 2.07-2.18 (m, 1H, 4α or 4β-**H**), 1.04-2.04 (m), 0.98 (br t, *J*=14.6 Hz, 1H, 1β-**H**), 0.93 (d, *J*=6.5 Hz, 3H, 21-**CH_3**), 0.90 (s, 3H, 19-**CH_3**), 0.65 (s, 3H, 18-**CH_3**) ppm. **^{13}C NMR** (100 MHz, $CDCl_3$) δ 174.7 (**24-COO**CH_3), 93.1 (d, *J*=171.7 Hz, **3-CH**), 91.0 (d, *J*=171.7 Hz, **7-CH**), 55.7 (**17-CH**), 51.4 (**24-**COO**CH_3**), 50.0 (d, *J*=3.7 Hz, **14-CH**), 42.6 (**13-C**), 40.3 (dd, *J*=11.0, 1.5 Hz, **5-CH**), 39.4 (**12-CH_2**), 39.1 (d, *J*=19.8 Hz, **8-CH**), 35.7 (dd, *J*=17.6, 5.1 Hz, **4-CH_2**), 35.3 (**20-CH**), 34.6 (d, *J*=1.5 Hz, **10-C**), 34.2 (d,

J=11.0 Hz, **1-CH₂**), 33.6 (**9-CH**), 32.3 (d, *J*=19.8 Hz, **6-CH₂**), 31.0 (**23-CH₂**), 30.9 (**22-CH₂**), 28.1 (***15-CH₂ or 16-CH₂***), 27.7 (d, *J*=17.6 Hz, **2-CH₂**), 23.4 (***15-CH₂ or 16-CH₂***), 22.3 (d, *J*=2.9 Hz, **19-CH₃**), 20.6 (**11-CH₂**), 18.2 (**21-CH₃**), 11.6 (**18-CH₃**) ppm. **^{19}F NMR** (376MHz, $CDCl_3$) δ -168.02 (br d, *J*=48.5 Hz, 1F, 3α-**F**), -187.25 (apparent tdd, *J*=49.9, 37.3, 13.9 Hz, 1F, 7α-**F**) ppm. **^{19}F [^{1}H] NMR** (376MHz, $CDCl_3$) δ -168.02 (s, 1F, 3α-**F**), -187.25 (s, 1F, 7α-**F**) ppm. **LRMS (ESI+)** m/z: 428.5 $[M+NH_4]^+$. **HRMS (ESI+)** $C_{25}H_{40}F_2NaO_2$ $[M+Na]^+$. Calculated: 433.2889; Found: 433.2886 (0.7 ppm error). **IR** (neat, cm^{-1}) 2939 – 2875 (m), 1732 (s), 1002 (m), 966 (m).

3α,7α-Difluoro-5β-cholanic acid (3.6)

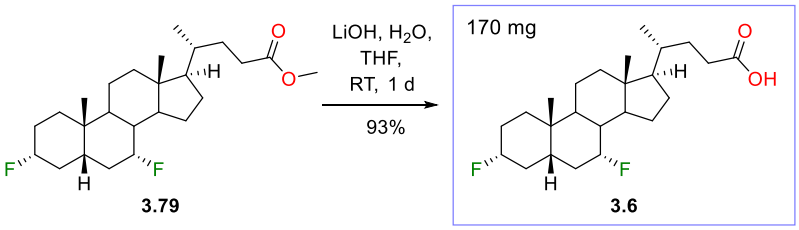

Following general procedure C, **3.79** (195 mg, 0.47 mmol, 1.0 equiv) was deprotected to yield **3.6** as a white solid (173 mg, 0.44 mmol, 93%) with no further purification.

mp 175 – 176 °C. **R_f** 0.20 (EtOAc/PE 20/80). **$[\alpha]_D$** + 11.5 (c = 0.8, $CHCl_3$, 24 °C). **^{1}H NMR** (400 MHz, $CDCl_3$) δ 4.62 (dq, *J*=49.0, 2.5 Hz, 1H, 7β-**H**), 4.39 (apparent dttd, *J*=49.8, 11.1, 4.8, 1.6 Hz, 1H, 3β-**H**), 2.41 (ddd, *J*=15.7, 10.0, 5.3 Hz, 1H, 23-**H'**), 2.27 (ddd, *J*=15.9, 9.5, 6.5 Hz, 1H, 23-**H''**), 2.08-2.22 (m, 1H, 4α-**H**), 1.67-2.05 (m), 1.05-1.62 (m), 0.99 (br t, *J*=14.3 Hz, 1H, 1β-**H**), 0.95 (d, *J*=6.4 Hz, 3H, 21-**CH₃**), 0.91 (s, 3H, 19-**CH₃**), 0.66 (s, 3H, 18-**CH₃**) ppm. **^{13}C NMR** (100 MHz, $CDCl_3$) δ 180.2 (**24-COOH**), 93.1 (d, *J*=171.7 Hz, **3-CH**), 91.0 (d, *J*=172.4 Hz, **7-CH**), 55.7 (**17-CH**), 50.0 (d, *J*=3.7 Hz, **14-CH**), 42.7 (**13-C**), 40.4 (br d, *J*=11.0 Hz, **5-CH**), 39.5 (**12-CH₂**), 39.1 (d, *J*=19.8 Hz, **8-CH**), 35.8 (dd, *J*=17.6, 5.9 Hz, **4-CH₂**), 35.3 (**20-CH**), 34.6 (d, *J*=1.5 Hz, **10-C**), 34.3 (d, *J*=11.0 Hz, **1-CH₂**), 33.6 (**9-CH**), 32.4 (d, *J*=19.1 Hz, **6-CH₂**), 31.0 (**23-CH₂**), 30.7 (**22-CH₂**), 28.1 (***15-CH₂ or 16-CH₂***), 27.7 (d, *J*=18.3 Hz, **2-CH₂**), 23.4 (***15-CH₂ or 16-CH₂***), 22.4 (d, *J*=2.9 Hz, **19-CH₃**), 20.6 (**11-CH₂**), 18.2 (**21-CH₃**), 11.7 (**18-CH₃**) ppm. **^{19}F NMR** (376MHz, $CDCl_3$) δ -168.00 (br d, *J*=48.6 Hz, 1F, 3α-**F**), -187.24 (apparent tdd, *J*=49.4, 36.4, 13.9 Hz, 1F, 7α-**F**) ppm. **^{19}F [^{1}H] NMR** (376MHz, $CDCl_3$) δ -168.00 (s, 1F, 3α-**F**), -187.24 (s, 1F, 7α-**F**) ppm. **LRMS (ESI-)** m/z: 395.5 $[M-H]^-$. **HRMS (ESI-)** $C_{24}H_{37}F_2O_2$ $[M-H]^-$. Calculated: 395.2767; Found: 395.2762 (1.3 ppm error). **IR** (neat, cm^{-1}) 2932 – 2874 (m), 1720 (s), 1003 (m), 967 (m).

Methyl 7β-fluoro-3α-acetoxy-6α-hydroxy-5β-cholan-24-oate (3.80) and Methyl 7β-fluoro-3α-acetoxy-6β-hydroxy-5β-cholan-24-oate (3.81)

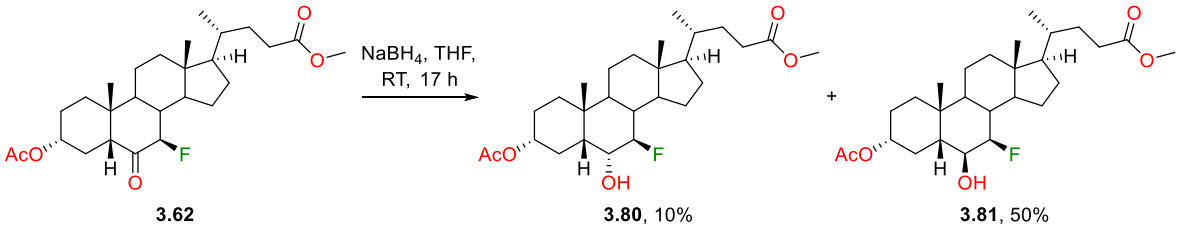

3.62 **3.80**, 10% **3.81**, 50%

The ketone **3.62** (1.60 g, 3.44 mmol, 1.0 equiv) was dissolved in dry THF (30 mL) and $NaBH_4$ (195 mg, 5.16 mmol, 1.5 equiv) was added. After stirring at RT for 17 h, the reaction mixture was cooled to 0 °C and added 2M HCl (30 mL) and water (30 mL). The mixture was extracted with EtOAc (3 x 50 mL) and the combined organic phases were washed with water (100 mL) and brine (100 mL) before drying over Na_2SO_4 and reducing *in vacuo*. The crude material was purified by flash chromatography (Biotage ZIP KP-Sil 45 g cartridge, EtOAc/PE: 15%/85% → 35%/65% over 18 CV) to firstly yield **3.81** as a colourless gum (809 mg, 1.73 mmol, 50%) and secondly yield **3.80** also as a colourless gum (158 mg, 0.34 mmol, 10%).

3.80: **R_f** 0.33 (EtOAc/PE 30/70). **$[\alpha]_D$** + 25.8 (c = 0.3, $CHCl_3$, 23 °C). **^{1}H NMR** (400 MHz, $CDCl_3$) δ 4.65 (tt, *J*=11.4, 4.6 Hz, 1H, 3β-**H**), 4.24 (dt, *J*=51.8, 9.4 Hz, 1H, 7α-**H**), 4.01 (ddd, *J*=14.8, 8.7, 6.1 Hz, 1H, 6β-**H**), 3.66 (s, 3H, 24-COO**CH_3**), 2.28-2.41 (m, 2H, 23-**H'** and 6α-**OH**), 2.12-2.27 (m, 2H, 23-**H''** and *4α or 4β-**H***), 2.01 (s, 3H, 3α-OCO**CH_3**), 1.97-2.04 (m, 1H, *12α or 12β-**H***), 1.01-1.93 (m), 0.97 (s, 3H, 19-**CH_3**), 0.92 (d, *J*=6.4 Hz, 3H, 21-**CH_3**), 0.66 (s, 3H, 18-**CH_3**) ppm. **^{13}C NMR** (100 MHz, $CDCl_3$) δ 174.6 (**24-COO**CH_3), 170.3 (**3α-OCO**CH_3), 97.9 (d, *J*=171.7 Hz, **7-CH**), 73.4 (**3-CH**), 70.5 (d, *J*=19.1 Hz, **6-CH**), 55.0 (**17-CH**), 55.0 (br s, **14-CH**), 51.5 (**24-**COO**CH_3**), 47.3 (d, *J*=8.1 Hz, **5-CH**), 43.3 (**13-C**), 39.8 (d, *J*=15.4 Hz, **8-CH**), 39.6 (**12-CH_2**), 38.9 (d, *J*=8.8 Hz, **9-CH**), 35.2 (**20-CH**), 35.1 (**10-C**), 34.5 (**1-CH_2**), 31.0 (**23-CH_2**), 30.9 (**22-CH_2**), 28.3 (d, *J*=2.2 Hz, **16-CH_2**), 26.7 (**4-CH_2**), 26.3 (**2-CH_2**), 25.7 (d, *J*=4.4 Hz, **15-CH_2**), 23.4 (**19-CH_3**), 21.3 (**3α-**OCO**CH_3**), 21.0 (**11-CH_2**), 18.3 (**21-CH_3**), 11.9 (**18-CH_3**) ppm. **^{19}F NMR** (376MHz, $CDCl_3$) δ -187.19 (apparent dt, *J*=52.0, 12.1 Hz, 1F, 7β-**F**) ppm. **^{19}F [^{1}H] NMR** (376MHz, $CDCl_3$) δ -187.19 (s, 1F, 7β-**F**) ppm. **LRMS (ESI+)** m/z: 484.6 $[M+NH_4]^+$. **HRMS (ESI+)** $C_{27}H_{43}FNaO_5$ $[M+Na]^+$. Calculated: 489.2987; Found: 489.2986 (0.1 ppm error). **IR** ($CHCl_3$, cm^{-1}) 3502 (b), 2949 – 2873 (m), 1736 (s), 1244 (m), 1030 (m).

3.81: **R_f** 0.43 (EtOAc/PE 30/70). **$[\alpha]_D$** + 47.7 (c = 1.0, $CHCl_3$, 23 °C). **^{1}H NMR** (400 MHz, $CDCl_3$) δ 4.65 (tt, *J*=11.1, 4.7 Hz, 1H, 3β-**H**), 4.39 (ddd, *J*=46.6, 10.4, 3.7 Hz, 1H, 7α-**H**), 3.84-3.90 (m, 1H, 6α-**H**), 3.66 (s, 3H, 24-COO**CH_3**), 2.35 (ddd, *J*=15.5, 10.1, 5.3 Hz, 1H, 23-**H'**), 2.17-2.27 (m, 2H, 23-**H''** and 6α-**OH**), 2.01 (s, 3H, 3α-OCO**CH_3**), 1.97-2.10 (m, 2H, *12α or 12β-**H*** and 8β-**H**), 1.64-1.95 (m), 1.02-

1.49 (m), 1.13 (s, 3H, 19-**CH₃**), 0.92 (d, *J*=6.4 Hz, 3H, 21-**CH₃**), 0.69 (s, 3H, 18-**CH₃**) ppm. **^{13}C NMR** (100 MHz, $CDCl_3$) δ 174.6 (**24-COO**CH_3), 170.4 (**3α-OCO**CH_3), 95.9 (d, *J*=175.3 Hz, **7-CH**), 73.4 (d, *J*=18.3 Hz, **6-CH**), 73.1 (**3-CH**), 55.1 (**17-CH**), 54.8 (**14-CH**), 51.5 (**24-**COO**CH₃**), 46.9 (d, *J*=5.9 Hz, **5-CH**), 43.2 (**13-C**), 39.7 (**12-CH₂**), 39.2 (d, *J*=8.8 Hz, **9-CH**), 36.2 (d, *J*=16.1 Hz, **8-CH**), 35.2 (**20-CH**), 34.8 (**1-CH₂**), 33.9 (**10-C**), 31.5 (**4-CH₂**), 31.0 (**23-CH₂**), 31.0 (**22-CH₂**), 28.3 (d, *J*=2.9 Hz, **16-CH₂**), 26.1 (d, *J*=5.1 Hz, **15-CH₂**), 26.1 (**2-CH₂**), 25.4 (**19-CH₃**), 21.3 (**3α-**OCO**CH₃**), 20.6 (**11-CH₂**), 18.3 (**21-CH₃**), 11.9 (**18-CH₃**) ppm. **^{19}F NMR** (376MHz, $CDCl_3$) δ -189.14 (br d, *J*=46.8 Hz, 1F, 7β-**F**) ppm. **^{19}F [^{1}H] NMR** (376MHz, $CDCl_3$) δ -189.13 (s, 1F, 7β-**F**) ppm. **LRMS (ESI+)** m/z: 484.5 $[M+NH_4]^+$. **HRMS (ESI+)** $C_{27}H_{43}FNaO_5$ $[M+Na]^+$. Calculated: 489.2987; Found: 489.2982 (0.9 ppm error). **IR** ($CHCl_3$, cm^{-1}) 3521 (b), 2948 – 2873 (m), 1736 (s), 1238 (m).

Methyl 7β-fluoro-3α-acetoxy-6α-(phenoxycarbonothioyl)oxy-5β-cholan-24-oate (3.82)

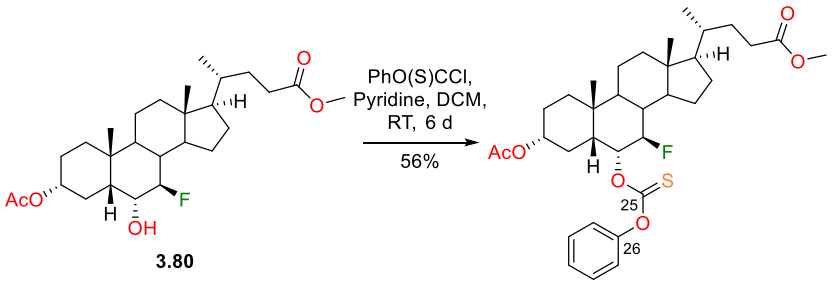

3.80 **3.82**

Following general procedure G, the thiocarbonate of **3.80** (149 mg, 0.32 mmol, 1.0 equiv) was formed. Note: reaction stirred for 16 h. The crude material was purified by flash chromatography (Biotage SNAP KP-Sil 10 g cartridge, EtOAc/PE: 5%/95% → 25%/75% over 18 CV) to yield **3.82** as a pale yellow gum (106 mg, 0.18 mmol, 56%).

R_f 0.38 (EtOAc/PE 20/80). **^{1}H NMR** (400 MHz, $CDCl_3$) δ 7.42 (br t, *J*=7.5 Hz, 2H, *meta*-**CH**), 7.30 (br t, *J*=7.5 Hz, 1H, *para*-**CH**), 7.14 (dd, *J*=8.7, 1.1 Hz, 2H, *ortho*-**CH**), 5.77 (ddd, *J*=13.7, 9.5, 5.6 Hz, 1H, 6β-**H**), 4.70 (tt, *J*=11.3, 4.8 Hz, 1H, 3β-**H**), 4.58 (dt, *J*=51.8, 9.8 Hz, 1H, 7α-**H**), 3.68 (s, 3H, 24-COO**CH₃**), 2.37 (ddd, *J*=15.5, 10.3, 5.6 Hz, 1H, 23-**H'**), 2.19-2.31 (m, 2H, 23-**H''** and 5β-**H**), 2.05 (s, 3H, 3α-OCO**CH₃**), 1.12-2.09 (m), 1.10 (s, 3H, 19-**CH₃**), 0.94 (d, *J*=6.4 Hz, 3H, 21-**CH₃**), 0.70 (s, 3H, 18-**CH₃**) ppm. **^{13}C NMR** (100 MHz, $CDCl_3$) δ 194.3 (**25-C**), 174.6 (**24-COO**CH_3), 170.3 (**3α-OCO**CH_3), 153.3 (**26-C**), 129.4 (2 C, ***meta*-CH**), 126.5 (***para*-CH**), 122.0 (2 C, ***ortho*-CH**), 93.3 (d, *J*=179.7 Hz, **7-CH**), 83.3 (d, *J*=19.1 Hz, **6-CH**), 72.7 (**3-CH**), 55.1 (**17-CH** and **14-CH**), 51.5 (**24-**COO**CH₃**), 44.2 (d, *J*=7.3 Hz, **5-CH**), 43.4 (**13-C**), 40.5 (d, *J*=15.4 Hz, **8-CH**), 39.6 (**12-CH₂**), 38.6 (d, *J*=8.8 Hz, **9-CH**), 35.6 (d, *J*=1.5 Hz, **10-C**), 35.2 (**20-CH**), 34.4 (**1-CH₂**), 31.0 (**23-CH₂**), 31.0 (**22-CH₂**), 28.3 (br s, **16-CH₂**), 27.4 (**4-CH₂**), 26.1 (**2-CH₂**), 25.5 (d, *J*=5.1 Hz, **15-CH₂**), 22.8 (**19-CH₃**), 21.3 (**3α-**OCO**CH₃**), 20.9 (**11-CH₂**), 18.3 (**21-CH₃**), 12.0 (**18-CH₃**) ppm. **^{19}F NMR** (376MHz, $CDCl_3$) δ -185.51 (apparent dt, *J*=52.0, 13.0 Hz, 1F, 7β-**F**) ppm. **^{19}F**

[^{1}H] NMR (376MHz, $CDCl_3$) δ -185.51 (s, 1F, 7β-**F**) ppm. **LRMS (ESI+)** m/z: 603.2 $[M+H]^+$. **HRMS (ESI+)** $C_{34}H_{47}FNaO_6S$ $[M+Na]^+$. Calculated: 625.2970; Found: 625.2967 (0.4 ppm error). **IR** (neat, cm^{-1}) 2950 – 2874 (m), 1734 (s), 1287 – 1199 (b, s), 1031 (m), 753 (m).

Methyl 7β-fluoro-3α-acetoxy-6β-(phenoxycarbonothioyl)oxy-5β-cholan-24-oate (3.83)

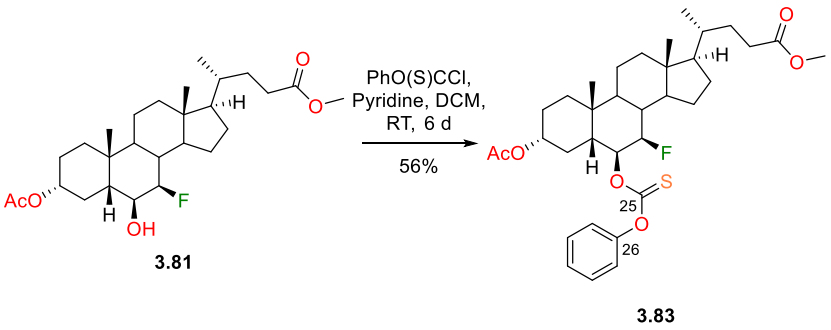

The alcohol **3.81** (760 mg, 1.63 mmol, 1.0 equiv) was dissolved in dry DCM (10 mL) and dry pyridine (0.40 mL, 4.89 mmol, 3.0 equiv) and *O*-phenyl chlorothionoformate (0.25 mL, 1.79 mmol, 1.1 equiv) were added. After stirring at RT for 2 d, further *O*-phenyl chlorothionoformate (0.10 mL, 0.72 mmol, 0.4 equiv) was added to the reaction mixture. After a further 1 d of stirring, further *O*-phenyl chlorothionoformate (0.25 mL, 1.79 mmol, 1.1 equiv), dry pyridine (0.40 mL, 4.89 mmol, 3.0 equiv) and dry DCM (3 mL) were added to the reaction mixture. Following a total of 6 d of stirring, the reaction mixture was added EtOAc (100 mL) and the combined organic phases were washed with water (100 mL) and brine (100 mL) before drying over Na_2SO_4 and reducing *in vacuo*. The crude material was purified by flash chromatography (Biotage SNAP KP-Sil 25 g cartridge, EtOAc/PE: 5%/95% → 25%/75% over 20 CV) to yield **3.83** as a pale yellow gummy solid (550 mg, 0.91 mmol, 56%).

R_f 0.37 (EtOAc/PE 20/80). **^{1}H NMR** (400 MHz, $CDCl_3$) δ 7.41 (br t, *J*=7.6 Hz, 2H, *meta*-**CH**), 7.28 (br t, *J*=7.3 Hz, 1H, *para*-**CH**), 7.11 (br d, *J*=7.6 Hz, 2H, *ortho*-**CH**), 5.47 (dt, *J*=6.0, 3.2 Hz, 1H, 6α-**H**), 4.69 (tt, *J*=11.1, 4.5 Hz, 1H, 3β-**H**), 4.55 (ddd, *J*=45.0, 10.8, 3.7 Hz, 1H, 7β-**H**), 3.68 (s, 3H, 24-COO**CH_3**), 2.37 (ddd, *J*=15.5, 10.3, 5.3 Hz, 1H, 23-**H'**), 2.17-2.29 (m, 2H, 23-**H''** *ortho*-**CH** and 5β-**H**), 2.03 (s, 3H, 3α-OCO**CH_3**), 1.68-2.08 (m), 1.03-1.56 (m), 0.97 (s, 3H, 19-**CH_3**), 0.94 (d, *J*=6.4 Hz, 3H, 21-**CH_3**), 0.68 (s, 3H, 18-**CH_3**) ppm. **^{13}C NMR** (100 MHz, $CDCl_3$) δ 193.6 (**25-C**), 174.6 (**24-COO**CH_3), 170.3 (**3α-OCO**CH_3), 153.2 (**26-C**), 129.4 (2 C, ***meta*-CH**), 126.5 (***para*-CH**), 121.9 (2 C, ***ortho*-CH**), 91.9 (d, *J*=185.6 Hz, **7-CH**), 84.1 (d, *J*=16.1 Hz, **6-CH**), 72.5 (**3-CH**), 55.1 (**17-CH**), 54.7 (**14-CH**), 51.5 (**24-**COO**CH_3**), 44.6 (d, *J*=5.1 Hz, **5-CH**), 43.3 (**13-C**), 39.6 (**12-CH_2**), 39.2 (d, *J*=8.8 Hz**, 9-CH**), 37.5 (d, *J*=16.1 Hz, **8-CH**), 35.2 (**20-CH**), 34.5 (**1-CH_2**), 33.8 (**10-C**), 31.1 (**23-CH_2**), 31.0 (**22-CH_2**), 30.9 (**4-CH_2**), 28.3 (d, *J*=2.2 Hz, **16-CH_2**), 26.1 (**2-CH_2**), 26.1 (d, *J*=5.1 Hz, **15-CH_2**), 25.0 (**19-CH_3**), 21.3 (**3α**-OCO**CH_3**), 20.6 (**11-CH_2**), 18.3 (**21-CH_3**), 12.0 (**18-CH_3**) ppm. **^{19}F NMR** (376MHz, $CDCl_3$) δ -189.01 (br d, *J*=45.1 Hz, 1F,

7β-**F**) ppm. **^{19}F [^{1}H] NMR** (376MHz, $CDCl_3$) δ -189.01 (s, 1F, 7β-**F**) ppm. **LRMS (ESI+)** m/z: 603.5 $[M+H]^+$. **HRMS (ESI+)** $C_{34}H_{47}FNaO_6S$ $[M+Na]^+$. Calculated: 625.2970; Found: 625.2966 (0.6 ppm error). **IR** (neat, cm^{-1}) 2947 – 2872 (m), 1733 (s), 1198 (b), 1017 (m).

Methyl 7β-fluoro-3α-acetoxy-5β-cholan-24-oate (3.84)

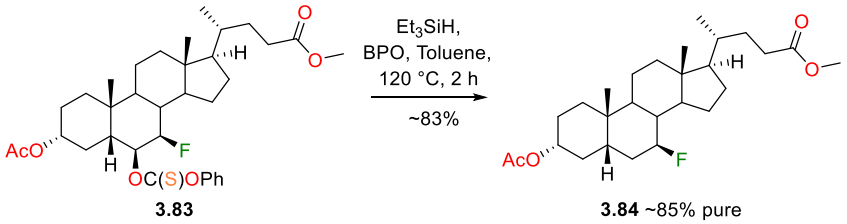

Following general procedure H, **3.83** (510 mg, 0.85 mmol, 1.0 equiv) was deoxygenated. The crude material was purified by flash chromatography (Biotage SNAP KP-Sil 25 g cartridge, EtOAc/PE: 0%/100% → 12%/88% over 20 CV) to give **3.84** around 85% pure as a white gummy solid (~320 mg, ~0.71 mmol, ~83%).

R_f 0.22 (EtOAc/PE 10/90). **^{1}H NMR** (400 MHz, $CDCl_3$) δ 4.66 (tt, *J*=10.9, 4.9 Hz, 1H, 3β-**H**), 4.41 (dddd, *J*=49.2, 11.2, 10.0, 5.3 Hz, 1H, 7α-**H**), 3.67 (s, 3H, 24-COO**CH_3**), 2.36 (ddd, *J*=15.5, 10.4, 5.3 Hz, 1H, 23-**H'**), 2.23 (ddd, *J*=16.0, 9.8, 6.6 Hz, 1H, 23-**H''**), 2.03 (s, 3H, 3α-OCO**CH_3**), 1.01-2.02 (m), 0.98 (s, 3H, 19-**CH_3**), 0.93 (d, *J*=6.4 Hz, 3H, 21-**CH_3**), 0.68 (s, 3H, 18-**CH_3**) ppm. **^{13}C NMR** (100 MHz, $CDCl_3$) δ 174.8 (**24-COO**CH_3), 170.6 (**3α-OCO**CH_3), 93.7 (d, *J*=171.7 Hz, **7-CH**), 73.6 (**3-CH**), 55.2 (**17-CH**), 55.1 (**14-CH**), 51.5 (**24**-COO**CH_3**), 43.2 (**13-C**), 42.2 (d, *J*=12.5 Hz**, 5-CH**), 41.6 (d, *J*=16.1 Hz, **8-CH**), 39.9 (**12-CH_2**), 38.6 (d, *J*=8.8 Hz, **9-CH**), 35.3 (**20-CH**), 34.3 (d, *J*=1.5 Hz, **1-CH_2**), 34.1 (d, *J*=1.5 Hz, **10-C**), 33.5 (d, *J*=19.8 Hz, **6-CH_2**), 33.1 (**4-CH_2**), 31.1 (**23-CH_2**), 31.0 (**22-CH_2**), 28.3 (d, *J*=2.2 Hz, **16-CH_2**), 26.4 (**2-CH_2**), 25.9 (d, *J*=5.1 Hz, **15-CH_2**), 23.2 (**19-CH_3**), 21.4 (**3α**-OCO**CH_3**), 21.0 (**11-CH_2**), 18.3 (**21-CH_3**), 12.0 (**18-CH_3**) ppm. **^{19}F NMR** (376MHz, $CDCl_3$) δ -172.97 (br dt, *J*=48.6, 12.1 Hz, 1F, 7β-**F**) ppm. **^{19}F [^{1}H] NMR** (376MHz, $CDCl_3$) δ -172.97 (s, 1F, 7β-**F**) ppm. **LRMS (ESI+)** m/z: 468.6 $[M+NH_4]^+$. **HRMS (ESI+)** $C_{27}H_{43}FNaO_4$ $[M+Na]^+$. Calculated: 473.3038; Found: 473.3039 (0.2 ppm error). **IR** (neat, cm^{-1}) 2949 – 2876 (m), 1728 (s), 1248 (m), 1039 (m).

7β-Fluorolithocholic acid (3.4)

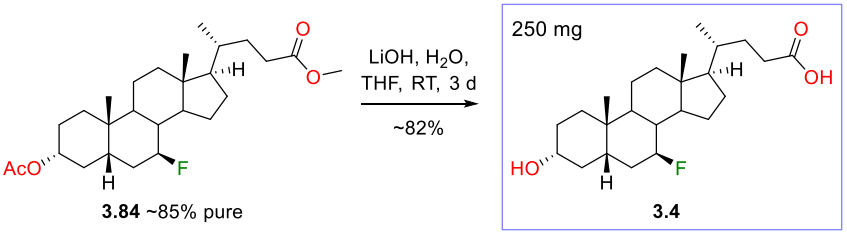

Following general procedure C, **3.84** (~85% pure, ~350 mg, ~0.78 mmol, 1.0 equiv) was deprotected. The crude material was purified by flash chromatography (Biotage SNAP KP-Sil 10 g cartridge, EtOAc/PE: 20%/80% → 100%/0% over 13 CV then MeOH/EtOAc: 0%/100% → 30%/70% over 7 CV) to yield **3.4** as a white solid (253 mg, 0.64 mmol, ~82%).

mp 196 – 197 °C. **R_f** 0.08 (EtOAc/PE 50/50). **$[\alpha]_D$** + 46.2 (c = 0.3, EtOAc, 22 °C). **^{1}H NMR** (400 MHz, MeOH-d_4) δ 4.41 (dddd, *J*=49.5, 11.4, 9.9, 5.3 Hz, 1H, 7α-**H**), 3.49 (tt, *J*=10.5, 4.8 Hz, 1H, 3β-**H**), 2.34 (ddd, *J*=15.3, 9.8, 5.4 Hz, 1H, 23-**H'**), 2.20 (ddd, *J*=15.7, 9.2, 7.0 Hz, 1H, 23-**H''**), 2.05 (dt, *J*=12.8, 3.2 Hz, 1H, 12β-**H**), 1.01-2.00 (m), 0.99 (s, 3H, 19-**CH_3**), 0.96 (d, *J*=6.5 Hz, 3H, 21-**CH_3**), 0.71 (s, 3H, 18-**CH_3**) ppm. **^{13}C NMR** (100 MHz, DMSO-d_6) δ 174.8 (**24-COOH**), 93.5 (d, *J*=170.2 Hz, **7-CH**), 69.5 (**3-CH**), 54.6 (**17-CH**), 54.4 (**14-CH**), 42.7 (**13-C**), 41.8 (d, *J*=11.7 Hz, **5-CH**), 41.3 (d, *J*=15.4 Hz, **8-CH**), 39.4 (**12-CH_2**), 38.0 (d, *J*=9.5 Hz, **9-CH**), 37.0 (**4-CH_2**), 34.7 (**20-CH**), 34.4 (**1-CH_2**), 33.7 (**10-C**), 33.6 (d, *J*=19.1 Hz, **6-CH_2**), 30.7 (2 C, **23-CH_2** and **22-CH_2**), 30.1 (**2-CH_2**), 27.9 (**16-CH_2**), 25.8 (d, *J*=5.1 Hz, **15-CH_2**), 23.1 (**19-CH_3**), 20.6 (**11-CH_2**), 18.2 (**21-CH_3**), 11.7 (**18-CH_3**) ppm. **^{19}F NMR** (376MHz, DMSO-d_6) δ -170.52 (br dt, *J*=48.6, 10.4 Hz, 1F, 7β-**F**) ppm. **^{19}F [^{1}H] NMR** (376MHz, DMSO-d_6) δ -170.52 (s, 1F, 7β-**F**) ppm. **LRMS (ESI-)** m/z: 393.5 $[M-H]^-$. **HRMS (ESI-)** $C_{24}H_{38}FO_3$ $[M-H]^-$. Calculated: 393.2810; Found: 393.2804 (1.7 ppm error). **IR** (neat, cm^{-1}) 3267 (b), 2928 – 2859 (m), 2565 (b), 1701 (s), 1208 (m), 1054 (m).

7.5 Synthesis of Chlorinated Analogues

7.5.1 Synthesis of Analogues from CDCA and its Derivatives

7α-Methoxymethoxyl-3-oxo-5β-cholanic acid (4.7)

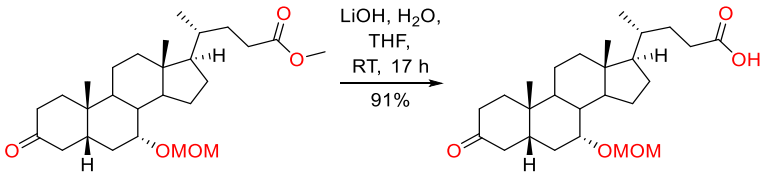

2.26 **4.7**

Following general procedure C, **2.26** (300 mg, 0.67 mmol, 1.0 equiv) was deprotected to yield **4.7** as a white solid (266 mg, 0.61 mmol, 91%) with no further purification.

mp 147 – 148 °C. **R_f** 0.29 (EtOAc/PE 50/50). **$[\alpha]_D$** - 14.7 (c = 0.90, $CHCl_3$, 22 °C). **^{1}H NMR** (400 MHz, $CDCl_3$) δ 4.67 (d, *J*=6.8 Hz, 1H, 7α-O**CH_2**OCH_3), 4.54 (d, *J*=6.8 Hz, 1H, 7α-O**CH_2**OCH_3), 3.67 (br s, 1H, 7β-**H**), 3.27-3.41 (m, 4H, 4α-**H** and 7α-OCH_2O**CH_3**), 1.04-2.46 (m), 1.02 (s, 3H, 19-**CH_3**), 0.94 (d, *J*=6.5 Hz, 3H, 21-**CH_3**), 0.68 (s, 3H, 18-**CH_3**) ppm. **^{13}C NMR** (100 MHz, $CDCl_3$) δ 213.4 (**3-C**), 180.0 (**24-COO**CH_3), 95.9 (**7α**-O**CH_2**OCH_3), 75.0 (**7-CH**), 56.3 (**7α**-OCO**CH_3**), 55.6 (**17-CH**), 49.7 (CH), 45.1 (**4-CH_2**), 43.1 (**5-CH**), 42.5 (**13-C**), 39.3 (CH), 39.2 (**12-CH_2**), 36.8 (CH_2), 36.7 (**1-CH_2**), 35.3 (**20-CH**), 35.2 (**10-C**), 33.7 (**9-CH**), 31.0 (CH_2), 30.7 (**22-CH_2**), 30.4 (**2-CH_2**), 28.0 (CH_2), 23.7 (CH_2), 21.9 (**19-CH_3**), 20.9 (CH_2), 18.3 (**21-CH_3**), 11.7 (**18-CH_3**) ppm. **LRMS (ESI+)** m/z: 457.5 $[M+Na]^+$, 373.5 $[M+H\text{-}MOMOH]^+$, 355.5 $[M+H\text{-}MOMOH\text{-}H_2O]^+$. **HRMS (ESI+)** $C_{26}H_{42}NaO_5$ $[M+Na]^+$. Calculated: 457.2924; Found: 457.2935 (2.3 ppm error). **IR** (neat, cm^{-1}) 3090 (bw), 2936 – 2871 (m), 1732 (s), 1683 (s), 1033 (s).

Methyl 7α-Acetoxy-3-oxo-5β-cholan-24-oate (4.8)

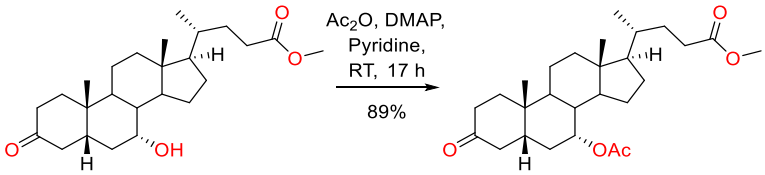

2.25 **4.8**

Following general procedure E, **2.25** (3.00 g, 7.41 mmol, 1.0 equiv) was protected. The crude material was purified by flash chromatography (EtOAc/PE: 20%/80% → 25%/75%) to yield **4.8** as a white solid (2.95 g, 6.61 mmol, 89%).

mp 110 – 112 °C (lit. 117 – 118 °C[138]). **R_f** 0.42 (EtOAc/PE 30/70). **^{1}H NMR** (400 MHz, $CDCl_3$) δ 4.95 (apparent br d, *J*=2.8 Hz, 1H, 7β-**H**), 3.65 (s, 3H, 24-COO**CH_3**), 2.98 (t, *J*=14.4 Hz, 1H, 4α-**H**), 2.02 (s, 3H, **7α**-OCO**CH_3**), 2.44 – 1.04 (m), 1.02 (s, 3H, 19-**CH_3**), 0.92 (d, *J*=6.5 Hz, 3H, 21-**CH_3**), 0.68 (s, 3H, 18-**CH_3**) ppm. **^{13}C NMR** (100 MHz, $CDCl_3$) δ 212.4 (**3-C**), 174.6 (**24-COO**CH_3), 170.2 (**7α-OCO**CH_3), 71.1

(**7-CH**), 55.7 (CH), 51.4 (**24-COOCH$_3$**), 50.3 (CH), 44.7 (CH_2), 42.7 (C), 42.5 (CH), 39.3 (CH_2), 37.9 (CH), 36.8 (CH_2), 36.5 (CH_2), 35.2 (CH), 34.9 (CH), 34.9 (C), 31.0 (CH_2), 30.9 (CH_2), 30.9 (CH_2), 27.9 (CH_2), 23.5 (CH_2), 21.8 (**19-CH$_3$**), 21.4 (**7α-OCOCH$_3$**), 21.0 (CH_2), 18.2 (**21-CH$_3$**), 11.7 (**18-CH$_3$**) ppm. ^{1}H NMR data agrees with literature.[138] ^{13}C NMR data not available. ^{1}H and ^{13}C NMR data consistent with data from within the group.

3β-Hydroxy-7α-methoxymethoxyl-5β-cholanic acid (4.9)

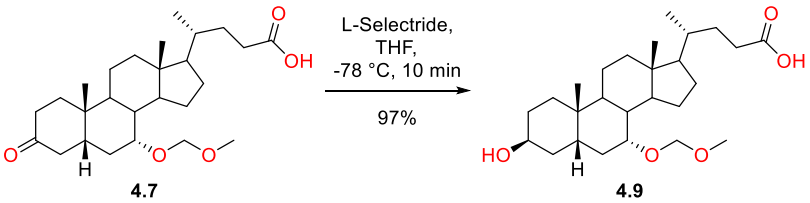

4.7 4.9

The ketone **4.7** (100 mg, 0.23 mmol, 1.0 equiv) was dissolved in dry THF (4 mL), was cooled to -78 °C and L-Selectride (1M in THF, 0.60 mL, 0.60 mmol, 2.5 equiv) was added over the course of 5 min. After 10 min of stirring, a mixture of H_2O_2 (1 mL), 2M NaOH (1 mL) and water (5 mL) was added to the reaction mixture and stirred at RT. After 10 min, 2M HCl (5 mL) was added to the mixture and stirred. After 5 min, the mixture was extracted with EtOAc (2 x 25 mL) and the combined organic phases were washed with water (2 x 50 mL) and brine (50 mL) before drying over Na_2SO_4 and reducing *in vacuo* to cleanly yield **4.9** as a white solid (97.0 mg, 0.22 mmol, 97%).

mp 65 – 66°C. **R$_f$** 0.41 (EtOAc/PE 80/20). **[α]$_D$** - 14.0 (c = 0.40, $CHCl_3$, 21 °C). **^{1}H NMR** (400 MHz, $CDCl_3$) δ 4.70 (d, *J*=6.7 Hz, 1H, 7α-O**CH$_2$**OCH$_3$), 4.57 (d, *J*=6.7 Hz, 1H, 7α-O**CH$_2$**OCH$_3$), 4.07 (br s, 1H, 3α-**H**), 3.62 (apparent br d, *J*=2.2 Hz, 1H, 7β-**H**), 3.40 (s, 3H, 7α-OCH$_2$O**CH$_3$**), 2.21-2.53 (m, 4H), 1.00-2.00 (m), 0.97 (s, 3H, 19-**CH$_3$**), 0.95 (d, *J*=6.4 Hz, 3H, 21-**CH$_3$**), 0.79-0.91 (m, 1H), 0.67 (s, 3H, 18-**CH$_3$**) ppm. **^{13}C NMR** (100 MHz, $CDCl_3$) δ 179.7 (**24-COOH**), 95.8 (**7α-OCH$_2$**OCH$_3$), 75.1 (**7-CH**), 67.1 (**3-CH**), 56.2 (**7α**-OCH$_2$O**CH$_3$**), 55.6 (**17-CH**), 49.9 (CH), 42.6 (**13-C**), 39.4 (**12-CH$_2$**), 39.4 (CH), 36.1 (**5-CH**), 35.9 (CH_2), 35.5 (**10-C**), 35.3 (CH), 32.4 (**5-CH**), 30.9 (CH_2), 30.8 (CH_2), 30.3 (CH_2), 29.8 (CH_2), 28.1 (CH_2), 27.7 (CH_2), 23.7 (CH_2), 23.2 (**19-CH$_3$**), 20.9 (CH_2), 18.3 (**21-CH$_3$**), 11.8 (**18-CH$_3$**) ppm. **LRMS (ESI+)** m/z: 454.7 $[M+NH_4]^+$. **HRMS (ESI+)** $C_{26}H_{44}NaO_5$ $[M+Na]^+$. Calculated: 459.3081; Found: 459.3082 (0.1 ppm error). **IR** (neat, cm^{-1}) 3439 (b,m), 2926.2 (m), 1706 (s), 1032 (s), 917 (m), 730 (s).

Methyl 3β-hydroxy-7α-acetoxy-5β-cholan-24-oate (4.10)

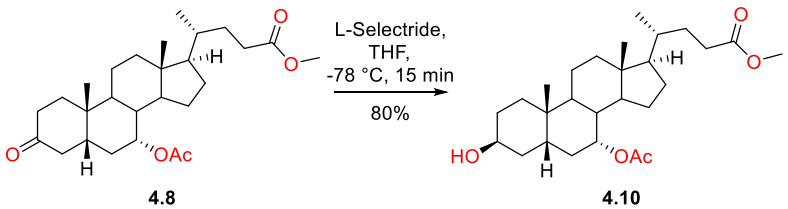

4.8 4.10

The ketone **4.8** (4.0 g, 8.96 mmol, 1.0 equiv) was dissolved in dry THF (25 mL) and L-Selectride (1M in THF, 12 mL, ~11.7 mmol, ~1.3 equiv) was added over the course of 10 min at -78 °C. After 5 min, the reaction mixture was quenched with a mixture of H_2O_2 (~30% in H_2O, 30 mL), 2M NaOH (30 mL) and water (30 mL) at RT. After stirring for 15 min, the mixture was acidified with 2M HCl (200 mL) and extracted with EtOAc (3 x 100 mL). The combined organic phases were washed with water (200 mL) and brine (200 mL) before dying over Na_2SO_4 and reducing *in vacuo* to give 4.5 g of crude material. The crude was purified by flash chromatography (Biotage ZIP KP-Sil 120 g cartridge, EtOAc/PE: 25%/75% → 45%/55%), yielding **4.10** as a white gummy solid (3.20 g, 7.13 mmol, 80%).

R_f 0.27 (EtOAc/PE 40/60). **$[\alpha]_D$** + 0.40 (c = 0.51, $CHCl_3$, 22 °C). **^{1}H NMR** (400 MHz, $CDCl_3$) δ 44.89 (apparent br d, *J*=2.3 Hz, 1H, 7β-**H**), 4.08 (br s, 1H, 3α-**H**), 3.67 (s, 3H, 24-COO**CH_3**), 2.36 (ddd, *J*=15.4, 10.1, 5.0 Hz, 1H, 23-**H'**), 2.15-2.30 (m, 2H), 2.04 (s, 3H, 7α-OCO**CH_3**), 1.02-2.01 (m), 0.97 (s, 3H, 19-**CH_3**), 0.93 (d, *J*=6.5 Hz, 3H, 21-**CH_3**), 0.66 (s, 3H, 18-**CH_3**) ppm. **^{13}C NMR** (100 MHz, $CDCl_3$) δ 174.6 (**24-COO**CH_3), 170.4 (**7α-OCO**CH_3), 71.6 (**7-CH**), 66.6 (**3-CH**), 55.6 (**17-CH**), 51.4 (**24-**OCO**CH_3**), 50.4 (**14-CH**), 42.7 (**13-C**), 39.5 (**12-CH_2**), 37.8 (**8-CH**), 35.8 (CH_2), 35.5 (**5-CH**), 35.2 (**20-CH**), 35.2 (**10-C**), 33.3 (**9-CH**), 31.0 (**23-CH_2**), 30.9 (**22-CH_2**), 30.9 (CH_2), 29.7 (**1-CH_2**), 27.9 (**2-CH_2**), 27.7 (CH_2), 23.5 (CH_2), 23.1 (**19-CH_3**), 21.5 (**7α-**OCO**CH_3**), 20.8 (**11-CH_2**), 18.2 (**21-CH_3**), 11.6 (**18-CH_3**) ppm. **LRMS (ESI+)** m/z: 466.5 $[M+NH_4]^+$. **HRMS (ESI+)** $C_{27}H_{44}NaO_5$ $[M+Na]^+$. Calculated: 471.3081; Found: 471.3077 (0.8 ppm error). **IR** (neat, cm^{-1}) 3398 (b, w), 2933-2870 (m), 1731 (s), 1246 (m), 730 (s).

Methyl 3α-chloro-7α-hydroxy-5β-cholan-24-oate (4.12)

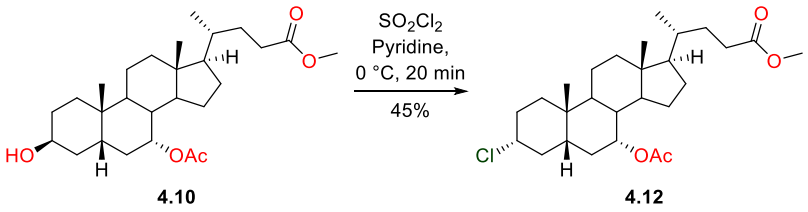

The alcohol **4.10** (2.47 g, 5.53 mmol, 1.0 equiv) was dissolved in dry pyridine (25 mL), cooled to 0 °C and sulfuryl chloride (~1.4 mL, ~17 mmol, ~ 3 equiv) was added over the course of 5 min. After 15 min, the reaction mixture was poured into ice-chilled 2M HCl (200 mL) and the mixture was extracted with EtOAc (3 x 100 mL). The combined organic phases were washed with 2M HCl (100 mL), water (100 mL) and brine (100 mL) before drying over Na_2SO_4 and reducing *in vacuo* to give 2.64 g of crude material. The crude was purified by flash chromatography (Biotage SNAP KP-Sil 50 g cartridge, EtOAc/PE: 5%/95% → 10%/90%), yielding **4.12** as a white solid (1.16 g, 2.48 mmol, 45%).

mp 89 – 90 °C. **R_f** 0.32 (EtOAc/PE 15/85). **$[\alpha]_D$** - 2.80 (c = 0.57, $CHCl_3$, 23 °C). **^{1}H NMR** (400 MHz, $CDCl_3$) δ 4.87 (br q, *J*=2.7 Hz, 1H, 7β-**H**), 3.75 (tt, *J*=11.8, 4.1 Hz, 1H, 3β-**H**), 3.66 (s, 3H, 24-COO**CH_3**), 2.28-2.42 (m, 2H, 23-**H'** and 4α- or 4β-**H**), 2.22 (ddd, *J*=16.1, 9.9, 6.6 Hz, 1H, 23-**H''**), 2.07 (s, 3H, 7α-

OCO**CH₃**), 0.98-2.01 (m), 0.88-0.97 (m, 6H, 21-**CH₃** and 19-**CH₃**), 0.65 (s, 3H, 18-**CH₃**) ppm. **^{13}C NMR** (100 MHz, $CDCl_3$) δ 174.6 (**24-COO**CH_3), 170.5 (**7α-OCO**CH_3), 71.1 (**7-CH**), 60.4 (**3-CH**), 55.7 (**17-CH**), 51.5 (**24-**COO**CH₃**), 50.3 (**14-CH**), 42.8 (***5-CH or 9-CH***), 42.6 (**13-C**), 40.2 (**4-CH₂**), 39.4 (**12-CH₂**), 37.8 (**8-CH**), 36.8 (**1-CH₂**), 35.2 (**20-CH**), 34.5 (**10-C**), 34.0 (***5-CH or 9-CH***), 32.3 (**2-CH₂**), 31.2 (**6-CH₂**), 30.9 (**23-CH₂**), 30.9 (**22-CH₂**), 28.0 (***15-CH₂ or 16-CH₂***), 23.5 (***15-CH₂ or 16-CH₂***), 22.7 (**19-CH₃**), 21.5 (**7α-**OCO**CH₃**), 20.6 (**11-CH₂**), 18.2 (**21-CH₃**), 11.7 (**18-CH₃**) ppm. **LRMS (ESI+)** m/z: 486.5 [^{37}ClM+NH_4]$^+$, 484.5 [^{35}ClM+NH_4]$^+$. **HRMS (ESI+)** $C_{27}H_{43}{}^{35}ClNaO_4$ [^{35}ClM+Na]$^+$. Calculated: 489.2742; Found: 489.2735 (1.4 ppm error). **IR** (neat, cm^{-1}) 2936-2873 (m), 1728 (s), 1243 (s), 1170 (m), 1020 (m), 744 (m).

3α-Chloro-7α-hydroxy-5β-cholanic acid (4.2)

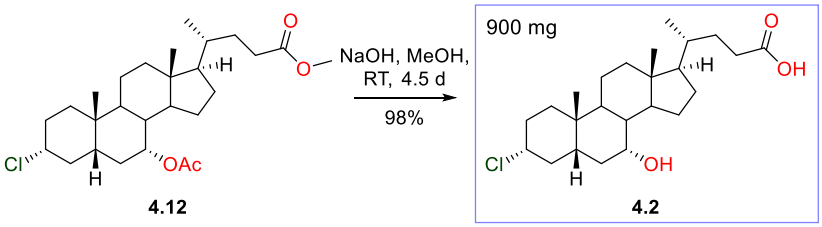

Following general procedure D, **4.12** (1.07 g, 2.29 mmol, 1.0 equiv) was deprotected to yield **4.2** as a white solid (925 mg, 2.25 mmol, 98%) with no further purification.

mp 84 – 85 °C. **R_f** 0.49 (EtOAc/PE 70/30). **$[\alpha]_D$** + 18.0 (c = 0.2, $CHCl_3$, 23 °C). **^{1}H NMR** (400 MHz, $CDCl_3$) δ 3.86 (br q, *J*=2.4 Hz, 1H, 7β-**H**), 3.75 (tt, *J*=11.9, 4.0 Hz, 1H, 3β-**H**), 2.60 (q, *J*=13.0 Hz, 1H, 4α-**H**), 2.33-2.44 (ddd, *J*=15.7, 10.4, 5.1 Hz, 1H, 23-**H'**), 2.22 (ddd, *J*=15.7, 9.7, 6.2 Hz, 1H, 23-**H''**), 0.97-2.01 (m), 0.93 (d, *J*=6.5 Hz, 3H, 21-**CH₃**), 0.90 (s, 3H, 19-**CH₃**), 0.66 (s, 3H, **18-CH₃**) ppm. **^{13}C NMR** (100 MHz, $CDCl_3$) δ 180.2 (**24-COO**CH_3), 68.3 (**7-CH**), 60.9 (**3-CH**), 55.8 (**17-CH**), 50.3 (**14-CH**), 43.2 (**5-CH**), 42.6 (**13-C**), 40.7 (**4-CH₂**), 39.5 (**12-CH₂**), 39.3 (**8-CH**), 36.9 (**1-CH₂**), 35.4 (**20-CH**), 34.8 (**10-C**), 34.4 (**6-CH₂**), 32.8 (**9-CH**), 32.3 (**2-CH₂**), 31.4 (**23-CH₂**), 30.9 (**22-CH₂**), 28.1 (***15-CH₂ or 16-CH₂***), 23.6 (***15-CH₂ or 16-CH₂***), 22.7 (**19-CH₃**), 20.5 (**11-CH₂**), 18.2 (**21-CH₃**), 11.7 (**18-CH₃**) ppm. **LRMS (ESI+)** m/z: 428.4 [^{35}ClM+NH_4]$^+$. **HRMS (ESI+)** $C_{24}H_{43}{}^{35}ClNO_3$ [^{35}ClM+NH_4]$^+$. Calculated: 428.2926; Found: 428.2924 (0.4 ppm error). **IR** (neat, cm^{-1}) 3441 (b), 2933-2866 (m), 1705 (s), 1240 (m b), 1070 (m).

7.5.2 Synthesis of Analogues from UDCA

Methyl 3α,7β-dihydroxy-5β-cholan-24-oate (4.15)

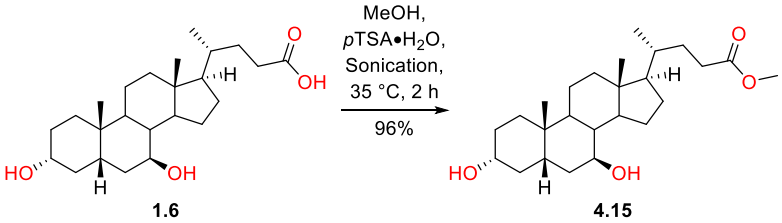

Following general procedure A, UDCA (**1.6**, 10.0 g, 25.5 mmol, 1.0 equiv) was protected to yield **4.15** as a white solid (10.0 g, 24.6 mmol, 96%) with no further purification.

mp 163-164 °C (Lit. 210-212 °C[95]). **R_f** 0.37 (EtOAc/PE 50/50). **^{1}H NMR** (400 MHz, $CDCl_3$) δ 3.65 (s, 3H, 24-COO**CH_3**), 3.52-3.61 (m, 2H, 3β-**H** and 7α-**H**), 2.34 (ddd, *J*=15.4, 10.1, 5.3 Hz, 1H, 23-**H'**), 2.21 (ddd, *J*=16.0, 9.9, 6.5 Hz, 1H, 23-**H''**), 0.95-2.01 (m), 0.93 (s, 3H, 19-**CH_3**), 0.91 (d, *J*=6.4 Hz, 3H, 21-**CH_3**), 0.66 (s, 3H, 18-**CH_3**) ppm. **^{13}C NMR** (100 MHz, $CDCl_3$) δ 174.7 (**24-COO**CH_3), 71.3 (***3-CH*** *or* ***7-CH***), 71.2 (***3-CH*** *or* ***7-CH***), 55.7 (**14-CH**), 54.9 (**17-CH**), 51.4 (**24-**COO**CH_3**), 43.7 (**13-C** and CH), 42.4 (***5-CH*** *or* ***9-CH***), 40.1 (**12-CH_2**), 39.2 (***5-CH*** *or* ***9-CH***), 37.3 (CH_2), 36.9 (CH_2), 35.2 (**20-CH**), 34.9 (CH_2), 34.0 (**10-C**), 31.0 (**23-CH_2**), 31.0 (**22-CH_2**), 30.3 (s, CH_2), 28.5 (CH_2), 26.8 (CH_2), 23.3 (**19-CH_3**), 21.1 (CH_2), 18.3 (**21-CH_3**), 12.1 (**18-CH_3**) ppm. **LRMS (ESI+)** m/z: 389.5 $[M+H-H_2O]^+$, 371.5 $[M+H-2H_2O]^+$. ^{1}H and ^{13}C NMR data agree with literature.[95]

Methyl 3-oxo-7β-hydroxy-5β-cholan-24-oate (4.5)

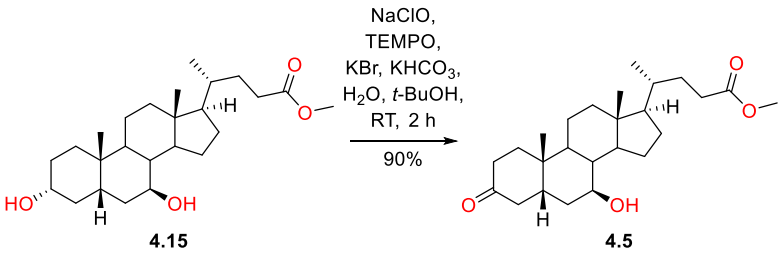

Following general procedure B, **4.15** (6.0 g, 14.8 mmol, 1.0 equiv) was oxidised. The crude material was purified by flash chromatography (Biotage ZIP KP-Sil 120 g cartridge, EtOAc/PE: 35%/65% → 50%/50%), yielding **4.5** as a white gummy solid (5.37 g, 13.3 mmol, 90%).

R_f 0.24 (EtOAc/PE 40/60). **$[\alpha]_D$** + 54.7 (c = 2.86, $CHCl_3$, 23 °C). **^{1}H NMR** (400 MHz, $CDCl_3$) δ 3.66 (s, 3H, 24-COO**CH_3**), 3.57-3.64 (m, 1H, 7α-**H**), 2.52 (t, *J*=14.4 Hz, 1H, 4α-**H**), 2.35 (ddd, *J*=15.4, 10.1, 5.3 Hz, 1H, 23-**H'**), 2.13-2.31 (m, 4H), 1.06-2.11 (m), 1.05 (s, 3H, 19-**CH_3**), 0.93 (d, *J*=6.5 Hz, 3H, 21-**CH_3**), 0.71 (s, 3H, 18-**CH_3**) ppm. **^{13}C NMR** (100 MHz, $CDCl_3$) δ 211.9 (**3-C**), 174.6 (**24-COO**CH_3), 70.8 (**7-CH**), 55.6 (**14-CH**), 54.9 (**17-CH**), 51.5 (**24-**COO**CH_3**), 44.3 (**5-CH**), 43.7 (**13-C**), 43.4 (**8-CH**), 43.1 (**4-CH_2**),

40.0 (**12-CH_2**), 39.4 (**9-CH**), 37.0 (CH_2), 36.3 (CH_2), 36.2 (CH_2), 35.2 (**20-CH**), 34.4 (**10-C**), 31.0 (**23-CH_2**), 30.9 (**22-CH_2**), 28.5 (**16-CH_2**), 26.8 (**15-CH_2**), 22.6 (**19-CH_3**), 21.6 (CH_2), 18.3 (**21-CH_3**), 12.1 (**18-CH_3**) ppm**. LRMS (ESI+)** m/z: 387.4 $[M+H-H_2O]^+$, 405.4 $[M+H]^+$. **HRMS (ESI+)** $C_{25}H_{40}NaO_4$ $[M+Na]^+$. Calculated: 427.2819; Found: 427.2815 (0.9 ppm error). **IR** (neat, cm^{-1}) 3479 (m), 2987 – 2809 (m), 1710 (s), 1291 (m).

Methyl 3-oxo-7β-acetoxy-5β-cholan-24-oate (4.16)

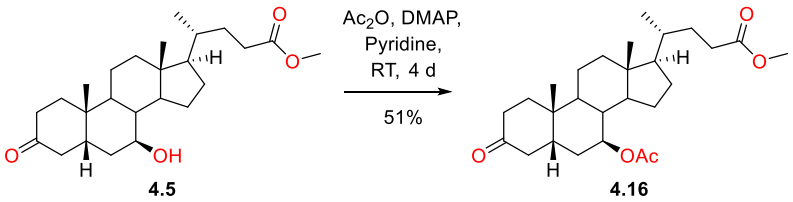

Following general procedure E, **4.5** (5.00 g, 12.4 mmol, 1.0 equiv) was protected. The crude material was purified by flash chromatography (Biotage ZIP KP-Sil 120 g cartridge, EtOAc/PE: 15%/85% → 35%/65%), yielding **4.16** as a colourless gum (2.85 g, 6.38 mmol, 51%).

R_f 0.18 (EtOAc/PE 20/80). **$[\alpha]_D$** + 51.0 (c = 1.05, $CHCl_3$, 23 °C). **^{1}H NMR** (400 MHz, $CDCl_3$) δ 4.77 (td, *J*=10.7, 5.4 Hz, 1H, 7α-**H**), 3.65 (s, 3H, 24-COO**CH_3**), 2.58 (t, *J*=14.5 Hz, 1H, 4α-**H**), 2.12-2.38 (m, 5H), 2.00-2.08 (m, 2H), 1.98 (s, 3H, 7β-OCO**CH_3**), 1.71-1.93 (m, 5H), 1.14-1.69 (m), 1.00-1.10 (m, 4H, 19-**CH_3** and 17α-**H**), 0.91 (d, *J*=6.4 Hz, 3H, 21-**CH_3**), 0.70 (s, 3H, 18-**CH_3**) ppm. **^{13}C NMR** (100 MHz, $CDCl_3$) δ 211.3 (**3-C**), 174.5 (**24-COO**CH_3), 170.4 (**7β-OCO**CH_3), 72.9 (**7-CH**), 55.1 (**14-CH**), 54.9 (**17-CH**), 51.4 (**24-**COO**CH_3**), 44.1 (**5-CH**), 43.5 (**13-C**), 42.8 (**4-CH_2**), 39.7 (**12-CH_2**), 39.6 (**8-CH**), 39.5 (**9-CH**), 36.9 (CH_2), 36.2 (CH_2), 35.1 (**20-CH**), 34.2 (**10-C**), 32.4 (**6-CH_2**), 30.9 (**23-CH_2**), 30.9 (**22-CH_2**), 28.3 (**16-CH_2**), 25.5 (**15-CH_2**), 22.5 (**19-CH_3**), 21.7 (**7β-**OCO**CH_3**), 21.6 (CH_2), 18.3 (**21-CH_3**), 12.0 (**18-CH_3**) ppm. **LRMS (ESI+)** m/z: 464.3 $[M+NH_4]^+$. **HRMS (ESI+)** $C_{27}H_{42}NaO_5$ $[M+Na]^+$. Calculated: 469.2924; Found: 469.2930 (1.3 ppm error). **IR** (neat, cm^{-1}) 2944 – 2861 (m), 1733 – 1718 (s), 1251 – 1231 (s), 1094 (m).

Methyl 3β-hydroxy-7β-acetoxy-5β-cholan-24-oate (4.17) and Methyl 3α-hydroxy-7β-acetoxy-5β-cholan-24-oate (4.18)

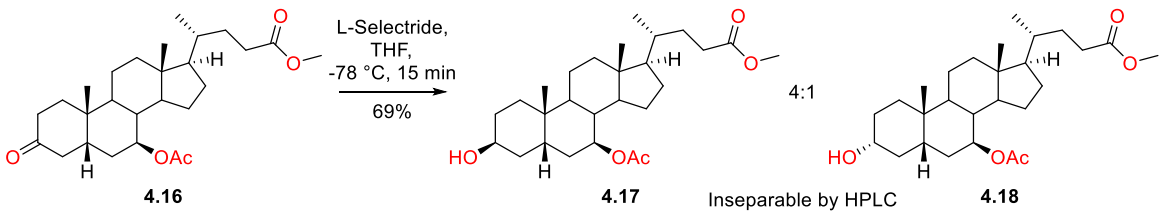

The ketone **4.16** (1.71 g, 3.83 mmol, 1.0 equiv) was dissolved in dry THF (20 mL), cooled to -78 °C and L-Selectride (1M in THF, ~6 mL, ~6 mmol, ~1.6 equiv) was added over the course of 5 min. 8

min after addition, a mixture of H_2O_2 (aq., 20 mL), 2M NaOH (20 mL) and water (20 mL) was added to the reaction mixture and stirred at RT. After 10 min, 2M HCl (40 mL) was added to neutralise and the mixture was extracted with EtOAc (3 x 100 mL). The combined organic phases were then washed with water (200 mL) and brine (200 mL) before drying over Na_2SO_4 and reducing *in vacuo* to yield 1.8 g of crude material. The crude was purified by flash chromatography (Biotage ZIP KP-Sil 30 g cartridge, EtOAc/PE: 30%/70% → 45%/55%), yielding a 4:1 mix of **4.17** and **4.18** (1.18 g total, ~0.94 g **4.17**, ~2.1 mmol **4.17**, ~55% **4.17**).

R_f 0.27 (EtOAc/PE 40/60). **^{1}H NMR** (400 MHz, $CDCl_3$) δ 4.68-4.82 (m, 1H, 7α-**H**), 4.09 (br s, 0.8H, 3α-**H**), 3.66 (s, 3H, 24-COO**CH_3**), 3.53-3.62 (m, 0.2H, 3β-**H**), 2.33 (ddd, *J*=15.3, 10.0, 5.3 Hz, 1H, 23-**H'**), 2.21 (ddd, *J*=16.0, 9.5, 6.6 Hz, 1H, 23-**H''**), 2.01 (br s, 1H), 1.98 (s, 3H, 7β-OCO**CH_3**), 1.01-1.90 (m), 0.94-1.01 (m, 3H, 19-**CH_3**), 0.91 (d, *J*=6.4 Hz, 3H, 21-**CH_3**), 0.68 (s, 3H, 18-**CH_3**) ppm. **^{13}C NMR** (100 MHz, $CDCl_3$) δ 174.7 (**24-COO**CH_3), 170.7 + 170.6 (**7β-OCO**CH_3), 73.9 + 73.8 (**7-C**), 71.3 (**3-C** *of 3α-OH*), 66.4 (**3-C** *of 3β-OH*), 55.3 + 55.2 (**14-CH**), 55.0 + 54.9 (**17-CH**), 51.5 (**24-**COO**CH_3**), 43.6 + 43.5 (**13-C**), 42.2 (***5-CH or 9-CH*** *of 3α-OH*), 40.0 + 39.9 (**12-CH_2**), 39.8 (**8-CH**), 39.3 (***5-CH or 9-CH*** *of 3α-OH*), 38.7 (**9-CH** *of 3β-OH*), 37.1 (CH_2), 36.9 (**5-CH** *of 3β-OH*), 35.2 (**20-CH**), 34.8 (CH_2), 34.5 (**10-C** *of 3β-OH*), 34.2 (CH_2), 33.9 (**10-C** *of 3α-OH*), 33.0 (CH_2), 32.6 (**6-CH_2** of 3β-OH), 31.0 (**23-CH_2**), 30.9 (**22-CH_2**), 30.1 (CH_2), 29.5 (CH_2), 28.4 (CH_2), 27.6 (CH_2), 25.6 (CH_2), 25.5 (CH_2), 23.7 (**19-CH_3** *of 3β-OH*), 23.2 (**19-*CH_3*** *of 3α-OH*), 21.8 (**7β-**OCO**CH_3**), 21.4 (CH_2), 21.1 (CH_2), 18.3 (**21-CH_3**), 12.0 (**18-CH_3**) ppm. **LRMS (ESI+)** m/z: 466.5 $[M+NH_4]^+$. **HRMS (ESI+)** $C_{27}H_{44}NaO_5$ $[M+Na]^+$. Calculated: 471.3081; Found: 471.3089 (1.7 ppm error).

Methyl 3α-chloro-7β-acetoxy-5β-cholan-24-oate (4.19)

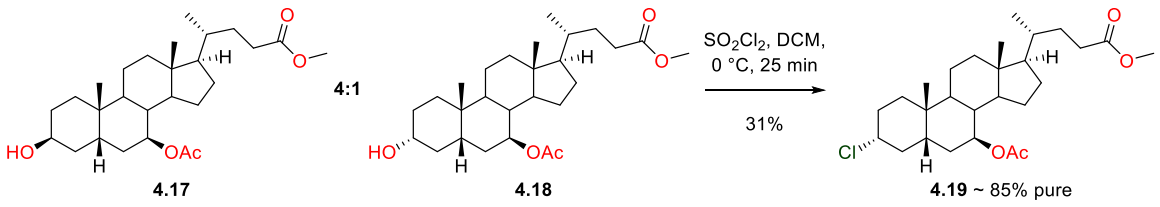

A 4:1 mix of **4.17** and **4.18** (1.01 g, 2.25 mmol, 1.0 equiv of mix) was dissolved in dry pyridine (30 mL), cooled to 0 °C and SO_2Cl_2 (0.55 mL, 6.75 mmol, 3.0 equiv) was added over the course of 5 min. 20 min following addition, the reaction mixture was poured into ice-chilled 2M HCl (50 mL), which was added further 2M HCl (50 mL) and extracted with EtOAc (3 x 100 mL). The combined organic phases were washed with 2M HCl (150 mL), water (100 mL) and brine (100 mL) before drying over Na_2SO_4 and reducing *in vacuo* to yield 900 mg of crude material. The crude was purified by flash chromatography (Biotage SNAP KP-Sil 25 g cartridge, Acetone/PE: 3%/97% → 8%/92%), yielding a fraction containing **4.19** ~80% pure. The fraction was purified further by HPLC (Acetone/Hexane

4%/96%), yielding **4.19** as a gummy solid, 85% pure (307 mg total, ~260 mg **4.19**, 0.56 mmol **4.19**, ~31% **4.19**).

R_f 0.35 (Acetone/PE 10/90). **^{1}H NMR** (400 MHz, $CDCl_3$) δ 4.76 (td, *J*=11.2, 5.5 Hz, 0.8H, 7α-**H**), 3.81 (tt, *J*=11.7, 4.9 Hz, 0.8H, 3β-**H**), 3.66 (s, 3H, 24-COO**CH_3**), 2.29-2.40 (m, 1H, 23-**H'**), 2.17-2.27 (m, 1H, 23-**H''**), 1.98 (s, 3H, 7β-OCO**CH_3**), 1.03-1.97 (m), 0.94-1.03 (m, 3H, 19-**CH_3**), 0.90-0.94 (m, 3H, 21-**CH_3**), 0.68 (s, 3H, 18-**CH_3**) ppm. **^{13}C NMR** (100 MHz, $CDCl_3$) δ 174.6 (**24-COO**CH_3), 170.5 (**7β-OCO**CH_3), 73.4 (**7-CH**), 59.7 (**3-CH**), 55.1 (**14-CH**), 54.9 (**17-CH**), 51.4 (**24-**COO**CH_3**), 43.9 (***5-CH or 9-CH***), 43.5 (**13-C**), 39.9 (**8-CH**), 39.8 (**12-CH_2**), 39.3 (***5-CH or 9-CH***), 38.3 (CH_2), 36.4 (**1-CH_2**), 35.2 (**20-CH**), 33.8 (**10-C**), 32.8 (CH_2), 32.0 (CH_2), 31.0 (**23-CH_2**), 30.9 (**22-CH_2**), 28.4 (CH_2), 25.6 (CH_2), 23.2 (**19-CH_3**), 21.7 (**7β-**OCO**CH_3**), 21.2 (CH_2), 18.3 (**21-CH_3**), 12.0 (**18-CH_3**) ppm. **LRMS (ESI+)** m/z: 484.6 [^{35}ClM+NH_4]$^+$. HRMS **(ESI+)** $C_{27}H_{43}{}^{35}ClNaO_4$ [M+Na]$^+$. Calculated: 489.2742; Found: 429.2747 (1.1 ppm error).

3α-chloro-7β-hydroxy-5β-cholan-24-oate (4.4)

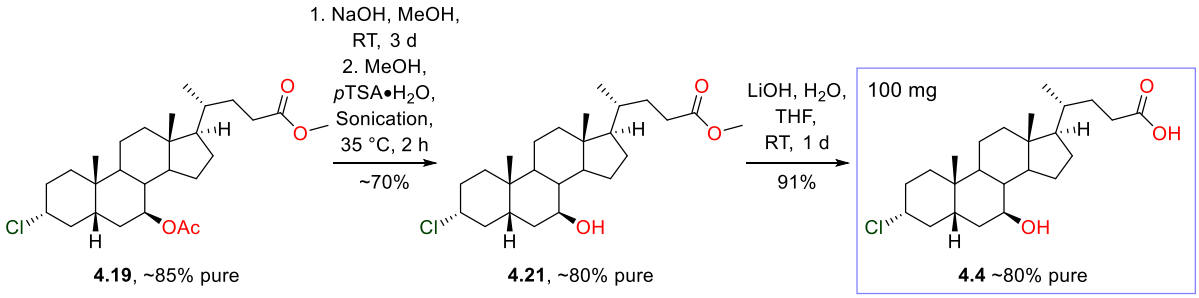

Following general procedure D, **4.19** (~85% pure, 260 mg, ~0.47 mmol, 1.0 equiv) was deprotected. The 80% pure crude material was used in further reactions with no purification. Following general procedure A, the crude carboxylic acid (230 mg, ~0.47 mmol, 1.0 equiv) was protected. The crude material was purified by flash chromatography (Biotage ZIP KP-Sil 10 g cartridge, Acetone/PE: 20%/80%→35%/65%) to yield **4.21** ~80% pure (176 mg, 0.41 mmol, ~88%). Following general procedure C, **4.21** (~80% pure, 135 mg, 0.32 mmol, 1.0 equiv) was deprotected to yield **4.4** ~80% pure as a white solid (120 mg, 0.29 mmol, 91%) with no further purification.

R_f 0.11 (EtOAc/PE 40/60). **Selected ^{1}H NMR** (400 MHz, $CDCl_3$) δ 3.76-3.92 (m, 1H, 3β-**H**), 3.48-3.66 (m, 1H, 7α-**H**), 2.37-2.46 (m, 1H, 23-**H'**), 2.23-2.33 (m, 1H, 23-**H''**), 1.00-2.04 (m), 0.91-0.98 (m, 6H, 19-**CH_3** and 21-**CH_3**), 0.69 (s, 3H, 18-**CH_3**) ppm. **Selected ^{13}C NMR** (100 MHz, DMSO-*d6*) δ 174.8 (**24-COOH**), 69.1 (**7-CH**), 60.6 (**3-CH**), 55.6 (**14-CH**), 54.6 (**17-CH**), 43.6 (***5-CH or 9-CH***), 43.0 (**13-C**), 42.9 (**8-CH**), 39.6 (**12-CH_2**), 38.6 (***5-CH or 9-CH***), 38.4 (CH_2), 37.2 (CH_2), 36.0 (**1-CH_2**), 34.8 (**20-CH**), 33.4 (**10-C**), 31.8 (CH_2), 30.8 (**23-CH_2**), 30.7 (**22-CH_2**), 28.1 (CH_2), 26.6 (CH_2), 23.0 (**19-CH_3**), 20.9 (CH_2), 18.3 (**21-CH_3**), 12.0 (**18-CH_3**) ppm. **LRMS (ESI+)** m/z: 436.5 [^{35}ClM+Na]$^+$, 395.4 [^{37}ClM+H-H_2O]$^+$.

Methyl 3α-chloro-7α-hydroxy-5β-cholan-24-oate (4.23)

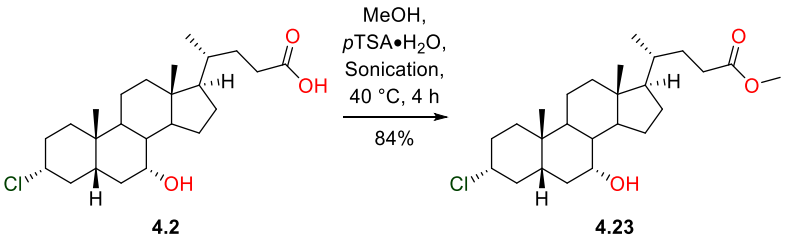

Following general procedure A, **4.2** (900 mg, 2.19 mmol, 1.0 equiv) was protected to yield **4.23** as an off-white solid (780 mg, 1.84 mmol, 84%) with no further purification.

mp 114 – 115 °C. **R_f** 0.70 (EtOAc/PE 30/70). **$[\alpha]_D$** + 16.2 (c = 0.95, $CHCl_3$, 22 °C). **^{1}H NMR** (400 MHz, $CDCl_3$) δ 3.85 (br q, *J*=2.7 Hz, 1H, 7β-**H**), 3.75 (tt, *J*=11.9, 4.1 Hz, 1H, 3β-**H**), 3.67 (s, 3H, 24-COO**CH_3**), 2.62 (q, *J*=13.1 Hz, 1H, 4α-**H**), 2.35 (ddd, *J*=15.5, 10.1, 5.3 Hz, 1H, 23-**H'**), 2.23 (ddd, *J*=16.0, 9.7, 6.7 Hz, 1H, 23-**H''**), 0.96-2.09 (m), 0.93 (d, *J*=6.5 Hz, 3H, 21-**CH_3**), 0.91 (s, 3H, 19-**CH_3**), 0.66 (s, 3H, 18-**CH_3**) ppm. **^{13}C NMR** (100 MHz, $CDCl_3$) δ 174.7 (**24-COO**CH_3), 68.3 (**7-CH**), 60.8 (**3-CH**), 55.7 (**17-CH**), 51.5 (**24-**COO**CH_3**), 50.3 (**14-CH**), 43.2 (**5-CH**), 42.7 (**13-C**), 40.7 (**4-CH_2**), 39.5 (**12-CH_2**), 39.3 (**8-CH**), 37.0 (**1-CH_2**), 35.3 (**20-CH**), 34.8 (**10-C**), 34.4 (**6-CH_2**), 32.8 (**9-CH**), 32.3 (**2-CH_2**), 31.0 (**23-CH_2**), 30.9 (**22-CH_2**), 28.1 (***15-CH_2 or 16-CH_2***), 23.7 (***15-CH_2 or 16-CH_2***), 22.7 (**19-CH_3**), 20.5 (**11-CH_2**), 18.2 (**21-CH_3**), 11.7 (**18-CH_3**) ppm. **LRMS (ESI+)** m/z: 442.3 $[^{35}ClM+NH_4]^+$, 444.3 $[^{37}ClM+NH_4]^+$. **HRMS (ESI+)** $C_{25}H_{41}{}^{35}ClNaO_3$ $[^{35}ClM+Na]^+$. Calculated: 447.2636; Found: 447.2637 (0.2 ppm error). **IR** (neat, cm^{-1}) 3502 (m, s), 2934 – 2864 (m), 1717 (s), 1217 (m), 1165 (m).

Methyl 3α-chloro-7-oxo-5β-cholan-24-oate (4.30)

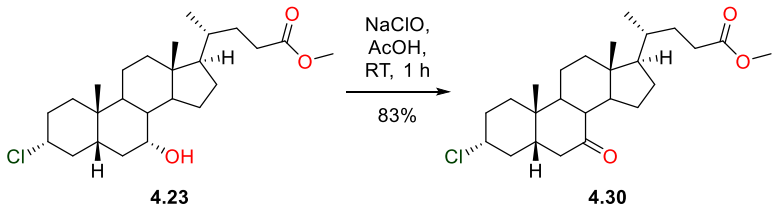

The alcohol **4.23** (500 mg, 1.18 mmol, 1.0 equiv) was dissolved in acetic acid (15 mL) and NaClO (~11% in H_2O, 1.4 mL, ~2.4 mmol, ~2.0 equiv) was added dropwise over the course of 45 min. After 1 h (from beginning the addition of NaClO) of stirring at RT, the reaction mixture was diluted with water (200 mL) and filtered. The resulting crude solid product was dissolved in EtOAc (100 mL) and washed with sat. $NaHCO_3$ (100 mL), water (100 mL) and brine (100 mL) before drying over Na_2SO_4 and reducing *in vacuo* to yield **4.30** as a white solid (415 mg, 0.98 mmol, 83%).

mp 154 – 155 °C. **R_f** 0.20 (EtOAc/PE 10/90). **$[\alpha]_D$** - 28.9 (c = 0.75, $CHCl_3$, 22 °C). **^{1}H NMR** (400 MHz, $CDCl_3$) δ 3.81 (tt, *J*=11.9, 4.0 Hz, 1H, 3β-**H**), 3.65 (s, 3H, 24-COO**CH_3**), 2.84 (dd, *J*=12.7, 5.7 Hz, 1H, 6β-

H), 2.29-2.42 (m, 2H, 8β-**H** and 23-**H'**), 2.14-2.27 (m, 2H, 23-**H''** and 15β-**H**), 1.20-2.03 (m), 1.19 (s, 3H, 19-**CH_3**), 1.07-1.18 (m, 2H), 0.93-1.00 (m, 1H, 15α-**H**), 0.91 (d, *J*=6.4 Hz, 3H, 21-**CH_3**), 0.64 (s, 3H, 18-**CH_3**) ppm. **^{13}C NMR** (100 MHz, $CDCl_3$) δ 211.2 (**7-C**), 174.6 (**24-COO**CH_3), 58.8 (**3-CH**), 54.7 (**17-CH**), 51.4 (**24**-COO**CH_3**), 49.4 (**8-CH**), 48.8 (**14-CH**), 47.4 (**5-CH**), 45.1 (**6-CH_2**), 42.6 (**9-CH** and **13-C**), 38.8 (**12-CH_2**), 38.4 (**4-CH_2**), 35.7 (**2-CH_2**), 35.1 (**20-CH**), 34.9 (**10-C**), 31.6 (**1-CH_2**), 31.0 (**23-CH_2**), 30.9 (**22-CH_2**), 28.2 (**16-CH_2**), 24.7 (**15-CH_2**), 23.0 (**19-CH_3**), 21.6 (**11-CH_2**), 18.3 (**21-CH_3**), 12.0 (**18-CH_3**) ppm. **LRMS (ESI+)** m/z: 440.3 [^{35}ClM+NH_4]$^+$, 442.3 [^{37}ClM+NH_4]$^+$. **HRMS (ESI+)** $C_{25}H_{40}ClO_3$ [^{35}ClM+H]$^+$. Calculated: 423.2660; Found: 423.2668 (1.7 ppm error). **IR** (neat, cm^{-1}) 2950 – 2871 (m), 1739 (s), 1708 (s), 1165 (m).

3α-Chloro-7-oxo-5β-cholanic acid (4.31)

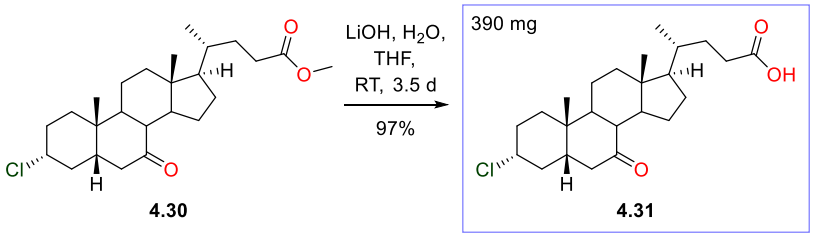

Following general procedure C, **4.30** (420 mg, 0.99 mmol, 1.0 equiv) was to yield **4.31** as an off-white solid (392 mg, 0.96 mmol, 97%) with no further purification.

mp 142 – 143 °C. **R_f** 0.15 (EtOAc/PE 30/70). **[α]$_D$** - 21.7 (c = 0.54, $CHCl_3$, 22 °C). **^{1}H NMR** (400 MHz, $CDCl_3$) δ 3.82 (tt, *J*=11.8, 4.3 Hz, 3β-**H**), 2.85 (dd, *J*=12.5, 5.6 Hz, 1H, 6β-**H**), 2.35-2.46 (m, 2H, 23-**H'** and 8β-**H**), 2.16-2.32 (m, 2H, 23-**H''** and 15β-**H**), 1.76-2.04 (m, 10H), 1.21-1.70 (m, 10H), 1.20 (s, 3H, 19-**CH_3**), 1.08-1.19 (m, 3H), 0.95-1.02 (m, 1H, 15α-**H**), 0.94 (d, *J*=6.5 Hz, 3H, 21-**CH_3**), 0.66 (s, 3H, 18-**CH_3**) ppm. **^{13}C NMR** (100 MHz, $CDCl_3$) δ 211.4 (**7-C**), 179.9-180.2 (**24-COO**CH_3), 58.9 (**3-CH**), 54.7 (**17-CH**), 49.5 (**8-CH**), 48.8 (**14-CH**), 47.5 (**5-CH**), 45.1 (**6-CH_2**), 42.6 (**13-C**), 42.6 (**9-CH**), 38.8 (**12-CH_2**), 38.5 (**4-CH_2**), 35.7 (**2-CH_2**), 35.1 (**20-CH**), 34.9 (**10-C**), 31.6 (**1-CH_2**), 31.0 (**23-CH_2**), 30.7 (**22-CH_2**), 28.2 (**16-CH_2**), 24.8 (**15-CH_2**), 23.0 (**19-CH_3**), 21.7 (**11-CH_2**), 18.3 (**21-CH_3**), 12.0 (**18-CH_3**) ppm. **LRMS (ESI+)** m/z: 426.1 [^{35}ClM+NH_4]$^+$, 428.1 [^{37}ClM+NH_4]$^+$. **HRMS (ESI+)** $C_{24}H_{38}{}^{35}ClO_3$ [^{35}ClM+H]$^+$. Calculated: 409.2504; Found: 409.2510 (1.4 ppm error). **IR** (neat, cm^{-1}) 2940 – 2870 (m), 1704 (s), 759 (m).

Bibliography

(1) Masters, C. L.; Bateman, R.; Blennow, K.; Rowe, C. C.; Sperling, R. A.; Cummings, J. L. *Nat. Rev. Dis. Primers* **2015**, *1*, 15056.

(2) Ramalho, R. M.; Viana, R. J. S.; Low, W. C.; Steer, C. J.; Rodrigues, C. M. P. *Trends Mol. Med.* **2008**, *14*, 54.

(3) Vang, S.; Longley, K.; Steer, C. J.; Low, W. C. *Glob. Adv. Health Med.* **2014**, *3*, 58.

(4) Poewe, W.; Seppi, K.; Tanner, C. M.; Halliday, G. M.; Brundin, P.; Volkmann, J.; Schrag, A.-E.; Lang, A. E. *Nat. Rev. Dis. Primers* **2017**, *3*, 17013.

(5) Webb, W. G. In *Neurology for the Speech-Language Pathologist (Sixth Edition)*; Webb, W. G., Ed.; Mosby: 2017, p 13.

(6) Aldred, E. M.; Buck, C.; Vall, K. In *Pharmacology*; Aldred, E. M., Buck, C., Vall, K., Eds.; Churchill Livingstone: Edinburgh, 2009, p 255.

(7) Klein, C.; Westenberger, A. *Cold Spring Harb. Perspect. Med.* **2012**, *2*, (1):a008888.

(8) Cancer Research UK https://www.cancerresearchuk.org/health-professional/cancer-statistics/risk, Access Date: 31/07/2018.

(9) Cancer Research UK https://www.cancerresearchuk.org/health-professional/cancer-statistics/mortality, Access Date: 31/07/2018.

(10) Siegel, R. L.; Miller, K. D.; Jemal, A. *CA Cancer J. Clin.* **2018**, *68*, 7.

(11) Cancer Research UK https://www.cancerresearchuk.org/health-professional/cancer-statistics/incidence, Access Date: 31/07/2018.

(12) Cancer Research UK https://www.cancerresearchuk.org/health-professional/cancer-statistics/statistics-by-cancer-type/breast-cancer, Access Date: 31/07/2018.

(13) Uhr, K.; Prager-van der Smissen, W. J. C.; Heine, A. A. J.; Ozturk, B.; Smid, M.; Göhlmann, H. W. H.; Jager, A.; Foekens, J. A.; Martens, J. W. M. *SpringerPlus* **2015**, *4*, 611.

(14) Bertram, J. S. *Mol. Aspects Med.* **2000**, *21*, 167.

(15) Lowe, S. W.; Lin, A. W. *Carcinogenesis* **2000**, *21*, 485.

(16) Hanahan, D.; Weinberg, Robert A. *Cell* **2011**, *144*, 646.

(17) Moss, G. P. *Pure Appl. Chem.* **1989**, *61*, 1783.

(18) Russell, D. W.; Setchell, K. D. R. *Biochemistry* **1992**, *31*, 4737.

(19) Hofmann, A. F.; Hagey, L. R.; Krasowski, M. D. *J. Lipid Res.* **2010**, *51*, 226.

(20) Li, T.; Chiang, J. Y. *Pharmacol. Rev.* **2014**, *66*, 948.

(21) Russell, D. W. *Annu. Rev. Biochem.* **2003**, *72*, 137.

(22) De Marino, S.; Carino, A.; Masullo, D.; Finamore, C.; Marchianò, S.; Cipriani, S.; Di Leva, F. S.; Catalanotti, B.; Novellino, E.; Limongelli, V.; Fiorucci, S.; Zampella, A. *Sci. Rep.* **2017**, *7*, 43290.

(23) Trauner, M.; Graziadei, I. W. *Aliment. Pharmacol. Ther.* **1999**, *13*, 979.

(24) Makishima, M.; Lu, T. T.; Xie, W.; Whitfield, G. K.; Domoto, H.; Evans, R. M.; Haussler, M. R.; Mangelsdorf, D. J. *Science* **2002**, *296*, 1313.

(25) Xie, W.; Radominska-Pandya, A.; Shi, Y.; Simon, C. M.; Nelson, M. C.; Ong, E. S.; Waxman, D. J.; Evans, R. M. *Proc. Natl. Acad. Sci. U. S. A.* **2001**, *98*, 3375.

(26) Garcia Linares, G.; Antonela Zigolo, M.; Simonetti, L.; Longhi, S. A.; Baldessari, A. *Bioorg. Med. Chem.* **2015**, *23*, 4804.

(27) Tonin, F.; Arends, I. W. C. E. *Beilstein J. Org. Chem.* **2018**, *14*, 470.

(28) Makishima, M.; Okamoto, A. Y.; Repa, J. J.; Tu, H.; Learned, R. M.; Luk, A.; Hull, M. V.; Lustig, K. D.; Mangelsdorf, D. J.; Shan, B. *Science* **1999**, *284*, 1362.

(29) Parks, D. J.; Blanchard, S. G.; Bledsoe, R. K.; Chandra, G.; Consier, T. G.; Kliewer, S. A.; Stimmel, J. B.; Wilson, T. M.; Zavacki, A. M.; Moore, D. D.; Lehmann, J. M. *Science* **1999**, *284*, 1365.

(30) Maloney, P. R.; Parks, D. J.; Haffner, C. D.; Fivush, A. M.; Chandra, G.; Plunket, K. D.; Creech, K. L.; Moore, L. B.; Wilson, J. G.; Lewis, M. C.; Jones, S. A.; Willson, T. M. *J. Med. Chem.* **2000**, *43*, 2971.

(31) Pellicciari, R.; Fiorucci, S.; Camaioni, E.; Clerici, C.; Costantino, G.; Maloney, P. R.; Morelli, A.; Parks, D. J.; Willson, T. M. *J. Med. Chem.* **2002**, *45*, 3569.

(32) Lowe, E. S.; Balis, F. M. In *Principles of Clinical Pharmacology (Second Edition)*; Atkinson, A. J., Abernethy, D. R., Daniels, C. E., Dedrick, R. L., Markey, S. P., Eds.; Academic Press: Burlington, 2007, p 289.

(33) Maruyama, T.; Miyamoto, Y.; Nakamura, T.; Tamai, Y.; Okada, H.; Sugiyama, E.; Itadani, H.; Tanaka, K. *Biochem. Biophys. Res. Commun.* **2002**, *298*, 714.

(34) Kawamata, Y.; Fujii, R.; Hosoya, M.; Harada, M.; Yoshida, H.; Miwa, M.; Fukusumi, S.; Habata, Y.; Itoh, T.; Shintani, Y.; Hinuma, S.; Fujisawa, Y.; Fujino, M. *J. Biol. Chem.* **2003**, *278*, 9435.

(35) Pellicciari, R.; Gioiello, A.; Macchiarulo, A.; Thomas, C.; Rosatelli, E.; Natalini, B.; Sardella, R.; Pruzanski, M.; Roda, A.; Pastorini, E.; Schoonjans, K.; Auwerx, J. *J. Med. Chem.* **2009**, *52*, 7958.

(36) Fiorucci, S.; Mencarelli, A.; Palladino, G.; Cipriani, S. *Trends Pharmacol. Sci.* **2009**, *30*, 570.

(37) Mathiesen, J. M.; Vedel, L.; Bräuner-Osborne, H. In *Methods Enzymol.*; Conn, P. M., Ed.; Academic Press: 2013; Vol. 522, p 191.

(38) Zhang, W.; Liu, H. T. *Cell Res.* **2002**, *12*, 9.

(39) Nguyen, A.; Bouscarel, B. *Cell. Signal.* **2008**, *20*, 2180.

(40) Watanabe, M.; Houten, S. M.; Mataki, C.; Christoffolete, M. A.; Kim, B. W.; Sato, H.; Messaddeq, N.; Harney, J. W.; Ezaki, O.; Kodama, T.; Schoonjans, K.; Bianco, A. C.; Auwerx, J. *Nature* **2006**, *439*, 484.

(41) Katsuma, S.; Hirasawa, A.; Tsujimoto, G. *Biochem. Biophys. Res. Commun.* **2005**, *329*, 386.

(42) Keitel, V.; Reinehr, R.; Gatsios, P.; Rupprecht, C.; Gorg, B.; Selbach, O.; Haussinger, D.; Kubitz, R. *Hepatology* **2007**, *45*, 695.

(43) Danzinger, R. G.; Hofmann, A. F. S., L.J.; Thistle, J. L. *New Engl. J. Med.* **1972**, *286*, 1.

(44) Poupon, R. E.; Balkau, B.; Eschwege, E.; Poupon, R. *New Engl. J. Med.* **1991**, *324*, 1548.

(45) Yang, L.; Zhang, H.; Fawcett, J. P.; Mikov, M.; Tucker, I. G. *J. Pharm. Sci.* **2011**, *100*, 1516.

(46) Hassan, N.; Ahad, A.; Ali, M.; Ali, J. *Expert Opin. Drug Deliv.* **2010**, *7*, 97.

(47) Shi, Z.; Zhao, Z.; Liu, M.; Wang, X. *Comptes Rendus Chimie* **2013**, *16*, 977.

(48) Bansal, S.; Singh, M.; Kidwai, S.; Bhargava, P.; Singh, A.; Sreekanth, V.; Singh, R.; Bajaj, A. *Med. Chem. Commun.* **2014**, *5*, 1761.

(49) Omura, K.; Ohsaki, A.; Zhou, B.; Kushida, M.; Mitsuma, T.; Kobayashi, A.; Hagey, L. R.; Hofmann, A. F.; Iida, T. *Lipids* **2014**, *49*, 1169.

(50) Omura, K.; Adachi, Y.; Kobayashi, Y.; Sekiguchi, S.; Zhou, B.; Iida, T. *Lipids* **2015**, *50*, 919.

(51) Clerici, C.; Castellani, D.; Asciutti, S.; Pellicciari, R.; Setchell, K. D.; O'Connell, N. C.; Sadeghpour, B.; Camaioni, E.; Fiorucci, S.; Renga, B.; Nardi, E.; Sabatino, G.; Clementi, M.; Giuliano, V.; Baldoni, M.; Orlandi, S.; Mazzocchi, A.; Morelli, A.; Morelli, O. *Toxicol. Appl. Pharmacol.* **2006**, *214*, 199.

(52) Roda, A.; Pellicciari, R.; Polimeni, C.; Cerre, C.; Cantelli Forti, G.; Sadeghpour, B.; Sapigni, E.; Gioacchini, A. M.; Natalini, B. *Gastroenterology* **1995**, *108*, 1204.

(53) Markham, A.; Keam, S. J. *Drugs* **2016**, *76*, 1221.

(54) Xiao, H.; Li, P.; Li, X.; He, H.; Wang, J.; Guo, F.; Zhang, J.; Wei, L.; Zhang, H.; Shi, Y.; Hou, L.; Shen, L.; Chen, Z.; Du, C.; Fu, S.; Zhang, P.; Hao, F.; Wang, P.; Xu, D.; Liang, W.; Tian, X.; Zhang, A.; Cheng, X.; Yang, L.; Wang, X.; Zhang, X.; Li, J.; Chen, S. *ACS Med. Chem. Lett.* **2017**, *8*, 1246.

(55) Pellicciari, R.; Passeri, D.; De Franco, F.; Mostarda, S.; Filipponi, P.; Colliva, C.; Gadaleta, R. M.; Franco, P.; Carotti, A.; Macchiarulo, A.; Roda, A.; Moschetta, A.; Gioiello, A. *J. Med. Chem.* **2016**, *59*, 9201.

(56) Pellicciari, R.; Sato, H.; Gioiello, A.; Constantino, G.; Macchiarulo, A.; Sadeghpour, B. M.; Giorgi, G.; Schoonjans, K.; Auwerx, J. *J. Med. Chem.* **2007**, *50*, 4265.

(57) Pellicciari, R.; Constantino, G.; Camaioni, E.; Sadeghpour, B. M.; Entrena, A.; Willson, T. M.; Fiorucci, S.; Clerici, C.; Gioiello, A. *J. Med. Chem.* **2004**, *47*, 4559.

(58) Downes, M.; Verdecia, M. A.; Roecker, A. J.; Hughes, R.; Hogenesch, J. B.; Kast-Woelbern, H. R.; Bowman, M. E.; Ferrer, J.-L.; Anisfeld, A. M.; Edwards, P. A.; Rosenfeld, J. M.; Alvarez, J. G. A.; Noel, J. P.; Nicolaou, K. C.; Evans, R. M. *Mol. Cell* **2003**, *11*, 1079.

(59) Sato, H.; Genet, C.; Strehle, A.; Thomas, C.; Lobstein, A.; Wagner, A.; Mioskowski, C.; Auwerx, J.; Saladin, R. *Biochem. Biophys. Res. Commun.* **2007**, *362*, 793.

(60) Lamers, C.; Merk, D.; Gabler, M.; Flesch, D.; Kaiser, A.; Schubert-Zsilavecz, M. *Future Med. Chem.* **2016**, *8*, 133.

(61) Genin, M. J.; Bueno, A. B.; Francisco, J. A.; Manninen, P. R.; Bocchinfuso, W. P.; Montrose-Rafizadeh, C.; Cannady, E. A.; Jones, T. M.; Stille, J. R.; Raddad, E.; Reidy, C.; Cox, A.; Michael, M. D.; Michael, L. F. *J. Med. Chem.* **2015**, *58*, 9768.

(62) Elmore, S. *Toxicol. Pathol.* **2007**, *35*, 495.

(63) Duane, W. C. *J. Lipid Res.* **2009**, *50*, 1507.

(64) Perez, M. J.; Briz, O. *World J. Gastroenterol.* **2009**, *15*, 1677.

(65) Martinez, J. D.; Stratagoules, E. D.; LaRue, J. M.; Powell, A. A.; Gause, P. R.; Craven, M. T.; Payne, C. M.; Powell, M. B.; Gerner, E. W.; Earnest, D. L. *Nutr. Cancer* **1998**, *31*, 111.

(66) Amaral, J. D.; Castro, R. E.; Solá, S.; Steer, C. J.; Rodrigues, C. M. P. *J. Biol. Chem.* **2007**, *282*, 34250.

(67) Amaral, J. D.; Viana, R. J.; Ramalho, R. M.; Steer, C. J.; Rodrigues, C. M. *J. Lipid Res.* **2009**, *50*, 1721.

(68) Heuman, D. M.; Mills, A. S.; McCall, J.; Hylemon, P. B.; Pandak, W. M.; Vlahcevic, Z. R. *Gastroenterology* **1991**, *100*, 203.

(69) Keene, C. D.; Rodrigues, C. M. P.; Eich, T.; Linehan-Stieers, C.; Abt, A.; Kren, B. T.; Steer, C. J.; Low, W. C. *Exp. Neurol.* **2001**, *171*, 351.

(70) Solá, S.; Castro, R. E.; Laires, P. A.; Steer, C. J.; Rodrigues, C. M. P. *Mol. Med.* **2003**, *9*, 226.

(71) Abdelkader, N. F.; Safar, M. M.; Salem, H. A. *Mol. Neurobiol.* **2016**, *53*, 810.

(72) Ackerman, H. D.; Gerhard, G. S. *Front. Aging Neurosci.* **2016**, *8*.

(73) Mortiboys, H.; Furmston, R.; Bronstad, G.; Aasly, J.; Elliott, C.; Bandmann, O. *Neurology* **2015**, *85*, 846.

(74) Castro-Caldas, M.; Carvalho, A. N.; Rodrigues, E.; Henderson, C. J.; Wolf, C. R.; Rodrigues, C. M. P.; Gama, M. J. *Mol. Neurobiol.* **2012**, *46*, 475.

(75) Fonseca, I.; Gordino, G.; Moreira, S.; Nunes, M. J.; Azevedo, C.; Gama, M. J.; Rodrigues, E.; Rodrigues, C. M. P.; Castro-Caldas, M. *Mol. Neurobiol.* **2017**, *54*, 6107.

(76) Keene, C. D.; Rodrigues, C. M. P.; Eich, T.; Chhabra, M. S.; Steer, C. J.; Low, W. C. *Proc. Natl. Acad. Sci. U.S.A* **2002**, *99*, 10671.

(77) Park, I. H.; Kim, M. K.; Kim, S. U. *Biochem. Biophys. Res. Commun.* **2008**, *377*, 1025.

(78) Low, W. C.; Steer, C.; Chun, H. S. M., R.; WO 2014/036379 A2 ed. 2014.

(79) Lo, A. C.; Callaerts-Vegh, Z.; Nunes, A. F.; Rodrigues, C. M. P.; D'Hooge, R. *Neurobiol. Dis.* **2013**, *50*, 21.

(80) Mortiboys, H.; Aasly, J.; Bandmann, O. *Brain* **2013**, *136*, 3038.

(81) Parry, G. J.; Rodrigues, C. M. P.; Aranha, M. M.; Hilbert, S. J.; Davey, C.; Kelkar, P.; Low, W. C.; Steer, C. J. *Clin. Neuropharmacol.* **2010**, *33*, 17.

(82) Earnest, D. L.; Holubec, H.; Wali, R. K.; Jolley, C. S.; Bissonette, M.; Bhattacharyya, A. K.; Roy, H.; Khare, S.; Brasitus, T. A. *Cancer Res.* **1994**, *54*, 5071.

(83) Hori, T.; Matsumoto, K.; Sakaitani, Y.; Sato, M.; Morotomi, M. *Cancer Lett.* **1998**, *124*, 79.

(84) Bayerdörffer, E.; Mannes, G. A.; Richter, W. O.; Ochsenkühn, T.; Wiebecke, B.; Köpcke, W.; Paumgartner, G. *Gastroenterology* **1993**, *104*, 145.

(85) Mahmoud, N. N.; Dannenberg, A. J.; Bilinski, R. T.; Mestre, J. R.; Chadburn, A.; Churchill, M.; Martucci, C.; Bertagnolli, M. M. *Carcinogenesis* **1999**, *20*, 299.

(86) Luu, T. H.; Bard, J.-M.; Carbonnelle, D.; Chaillou, C.; Huvelin, J.-M.; Bobin-Dubigeon, C.; Nazih, H. *Cell. Oncol.* **2018**, *41*, 13.

(87) Phelan, J. P.; Reen, F. J.; Dunphy, N.; O'Connor, R.; O'Gara, F. *BMC Cancer* **2016**, *16*, 1.

(88) Lo, Y. L.; Ho, C. T.; Tsai, F. L. *Eur. J. Pharm. Sci.* **2008**, *35*, 52.

(89) Roberto Mazzanti M.D.; Ornella Fantappié; Yukkio Kamimoto; Zenaida Gatmaitan; Paolo Gentilini; Arias, I. M. *Hepatology* **1994**, *20*, 170.

(90) Bansal, R.; Acharya, P. C. *Chem. Rev.* **2014**, *114*, 6986.

(91) Dahlmann, H. A. *Chem. Res. Toxicol.* **2013**, *26*, 1776.

(92) Solit, D. B.; Garraway, L. A.; Pratilas, C. A.; Sawai, A.; Getz, G.; Basso, A.; Ye, Q.; Lobo, J. M.; She, Y.; Osman, I.; Golub, T. R.; Sebolt-Leopold, J.; Sellers, W. R.; Rosen, N. *Nature* **2005**, *439*, 358.

(93) Agarwal, D. S.; Anantaraju, H. S.; Sriram, D.; Yogeeswari, P.; Nanjegowda, S. H.; Mallu, P.; Sakhuja, R. *Steroids* **2016**, *107*, 87.

(94) He, X.-L.; Xing, Y.; Gu, X.-Z.; Xiao, J.-X.; Wang, Y.-Y.; Yi, Z.; Qiu, W.-W. *Steroids* **2017**, *125*, 54.

(95) Ren, J.; Wang, Y.; Wang, J.; Lin, J.; Wei, K.; Huang, R. *Steroids* **2013**, *78*, 53.

(96) Popadyuk, II; Markov, A. V.; Salomatina, O. V.; Logashenko, E. B.; Shernyukov, A. V.; Zenkova, M. A.; Salakhutdinov, N. F. *Biorg. Med. Chem.* **2015**, *23*, 5022.

(97) O'Hagan, D. *Chem. Soc. Rev.* **2008**, *37*, 308.

(98) Harsanyi, A.; Sandford, G. *Green Chem.* **2015**, *17*, 2081.

(99) Wang, J.; Sánchez-Roselló, M.; Aceña, J. L.; del Pozo, C.; Sorochinsky, A. E.; Fustero, S.; Soloshonok, V. A.; Liu, H. *Chem. Rev.* **2014**, *114*, 2432.

(100) Hunter, L. *Beilstein J. Org. Chem.* **2010**, *6*, 38.

(101) Gillis, E. P.; Eastman, K. J.; Hill, M. D.; Donnelly, D. J.; Meanwell, N. A. *J. Med. Chem.* **2015**, *58*, 8315.

(102) Smart, B. E. *J. Fluorine Chem.* **2001**, *109*, 3.

(103) Hagmann, W. K. *J. Med. Chem.* **2008**, *51*, 4359.

(104) van Niel, M. B.; Collins, I.; Beer, M. S.; Broughton, H. B.; Cheng, S. K. F.; Goodacre, S. C.; Heald, A.; Locker, K. L.; MacLeod, A. M.; Morrison, D.; Moyes, C. R.; O'Connor, D.; Pike, A.; Rowley, M.; Russell, M. G. N.; Sohal, B.; Stanton, J. A.; Thomas, S.; Verrier, H.; Watt, A. P.; Castro, J. L. *J. Med. Chem.* **1999**, *42*, 2087.

(105) Bohm, H. J.; Banner, D.; Bendels, S.; Kansy, M.; Kuhn, B.; Muller, K.; Obst-Sander, U.; Stahl, M. *ChemBioChem* **2004**, *5*, 637.

(106) Champagne, P. A.; Desroches, J.; Paquin, J.-F. *Synthesis* **2015**, *47*, 306.

(107) Dalvit, C.; Invernizzi, C.; Vulpetti, A. *Chem. Eur. J* **2014**, *20*, 11058.

(108) Linclau, B.; Peron, F.; Bogdan, E.; Wells, N.; Wang, Z.; Compain, G.; Fontenelle, C. Q.; Galland, N.; Le Questel, J. Y.; Graton, J. *Chem. Eur. J* **2015**, *21*, 17808.

(109) Takemura, H.; Kotoku, M.; Yasutake, M.; Shinmyozu, T. *Eur. J. Org. Chem.* **2004**, *2004*, 2019.

(110) Struble, M. D.; Kelly, C.; Siegler, M. A.; Lectka, T. *Angew. Chem. Int. Ed.* **2014**, *53*, 8924.

(111) Graton, J.; Wang, Z.; Brossard, A. M.; Goncalves Monteiro, D.; Le Questel, J. Y.; Linclau, B. *Angew. Chem. Int. Ed. Engl.* **2012**, *51*, 6176.

(112) Arnott, J. A.; Planey, S. L. *Expert Opin. Drug Discov.* **2012**, *7*, 863.

(113) Purser, S.; Moore, P. R.; Swallow, S.; Gouverneur, V. *Chem. Soc. Rev.* **2008**, *37*, 320.

(114) Lipinski, C. A.; Lombardo, F.; Dominy, B. W.; Feeney, P. J. *Adv. Drug Del. Rev.* **1997**, *23*, 3.

(115) Linclau, B.; Wang, Z.; Compain, G.; Paumelle, V.; Fontenelle, C. Q.; Wells, N.; Weymouth-Wilson, A. *Angew. Chem. Int. Ed. Engl.* **2016**, *55*, 674.

(116) Swallow, S. In *Prog. Med. Chem.*; Elsevier, Ed. 2015; Vol. 54, p 65.

(117) Huchet, Q. A.; Kuhn, B.; Wagner, B.; Fischer, H.; Kansy, M.; Zimmerli, D.; Carreira, E. M.; Müller, K. *J. Fluorine Chem.* **2013**, *152*, 119.

(118) Huchet, Q. A.; Kuhn, B.; Wagner, B.; Kratochwil, N. A.; Fischer, H.; Kansy, M.; Zimmerli, D.; Carreira, E. M.; Muller, K. *J. Med. Chem.* **2015**, *58*, 9041.

(119) Muller, N. *J. Pharm. Sci.* **1986**, *75*, 987.

(120) Müller, K.; Faeh, C.; Diederich, F. *Science* **2007**, *317*, 1881.

(121) Wang, J.; Sanchez-Rosello, M.; Acena, J. L.; del Pozo, C.; Sorochinsky, A. E.; Fustero, S.; Soloshonok, V. A.; Liu, H. *Chem. Rev.* **2014**, *114*, 2432.

(122) O'Hagan, D. H., D.B. *J. Fluorine Chem.* **1999**, *100*, 127.

(123) Hamada, Y.; Kiso, Y. *Expert Opin. Drug Discov.* **2012**, *7*, 903.

(124) Meanwell, N. A. *J. Med. Chem.* **2018**, *61*, 5822.

(125) Muehlbacher, M.; Poulter, C. D. *J. Am. Chem. Soc.* **1985**, *107*, 8307.

(126) Olsen, J. A.; Banner, D. W.; Seiler, P.; Wagner, B.; Tschopp, T.; Obst-Sander, U.; Kansy, M.; Müller, K.; Diederich, F. *ChemBioChem* **2004**, *5*, 666.

(127) Hiedelberger, C.; Chaudhuri, N. K.; Danneberg, P.; Mooren, D.; Griesbach, L. *Nature* **1957**, *179*, 663.

(128) Fried, J.; Sabo, E. F. *J. Am. Chem. Soc.* **1954**, *76*, 1455.

(129) Yamazaki, T.; Taguchi, T.; Ojima, I. In *Fluorine in Medicinal Chemistry and Chemical Biology*; John Wiley & Sons, Ltd: 2009.

(130) Jasem, Y. A.; Thiemann, T.; Gano, L.; Oliveira, M. C. *J. Fluorine Chem.* **2016**, *185*, 48.

(131) Zhou, Y.; Wang, J.; Gu, Z.; Wang, S.; Zhu, W.; Aceña, J. L.; Soloshonok, V. A.; Izawa, K.; Liu, H. *Chem. Rev.* **2016**, *116*, 422.

(132) Dong, Z.; Mai, L.; Norio, Y.; H., A.-Q. M.; S., D. C.; Sally, S.; A., K. J. *J. Labelled Compd. Radiopharm.* **2014**, *57*, 371.

(133) Testa, A.; Dall'Angelo, S.; Mingarelli, M.; Augello, A.; Schweiger, L.; Welch, A.; Elmore, C. S.; Sharma, P.; Zanda, M. *Biorg. Med. Chem.* **2017**, *25*, 963.

(134) Poopadyuk, II; Salomatina, O. V.; Salakhutdinov, N. F. *Russ. Chem. Rev.* **2017**, *86*, 388.

(135) Pellicciari, R.; Gioiello, A.; Sabbatini, P.; Venturoni, F.; Nuti, R.; Colliva, C.; Rizzo, G.; Adorini, L.; Pruzanski, M.; Roda, A.; Macchiarulo, A. *ACS Med. Chem. Lett.* **2012**, *3*, 273.

(136) Dangate, P. S.; Salunke, C. L.; Akamanchi, K. G. *Steroids* **2011**, *76*, 1397.

(137) Wolfrum, C.; Carreira, E.; Meissburger, B.; Organization, W. I. P., Ed. 2013; Vol. WO2013/041519 A1.

(138) Masahiko Tohma, R. M., Hiromi Takeshita, Takao Kurosawa, Shigeo Ikeagawa *Chem. Pharm. Bull.* **1986**, *34*, 2890.

(139) Riva, S.; Bovara, R.; Zetta, L.; Pasta, P.; Ottolina, G.; Carrea, G. *J. Org. Chem.* **1988**, *53*, 88.

(140) Burns, A. C.; Sorensen, P. W.; Hoye, T. R. *Steroids* **2011**, *76*, 291.

(141) Marcus, A.; Magnus, H.; Hai, D.; Olof, R. *Eur. J. Org. Chem.* **2006**, *2006*, 4323.

(142) Hasek, W. R.; Smith, W. C.; Engelhardt, V. A. *J. Am. Chem. Soc.* **1960**, *82*, 543.

(143) Middleton, W. J. *J. Org. Chem.* **1975**, *40*, 574.

(144) Lal, G. S.; Pez, G. P.; Pesaresi, R. J.; Prozonic, F. M.; Cheng, H. *J. Org. Chem.* **1999**, *64*, 7048.

(145) Messina, P. A.; Mange, K. C.; Middleton, W. J. *J. Fluorine Chem.* **1989**, *42*, 137.

(146) Coe, P. L.; Mott, A. W.; Tatlow, J. C. *J. Fluorine Chem.* **1982**, *20*, 243.

(147) Dayal, B.; Salen, G.; Toome, B.; Tint, G. S.; Shefer, S.; Padia, J. *Steroids* **1990**, *55*, 233.

(148) Giordano, C.; Perdoncin, G.; Castaldi, G. *Angew. Chem.* **1985**, *97*, 510.

(149) Sepe, V.; Ummarino, R.; D'Auria, M. V.; Chini, M. G.; Bifulco, G.; Renga, B.; D'Amore, C.; Debitus, C.; Fiorucci, S.; Zampella, A. *J. Med. Chem.* **2012**, *55*, 84.

(150) Ikonen, S.; Nonappa; Valkonen, A.; Juvonen, R.; Salo, H.; Kolehmainen, E. *Org. Biomol. Chem.* **2010**, *8*, 2784.

(151) Fantin, G.; Fogagnolo, M.; Medici, A.; Pedrini, P.; Cova, U. *Tetrahedron Lett.* **1992**, *33*, 3235.

(152) Bortolini, O.; Fantin, G.; Fogagnolo, M.; Forlani, R.; Maietti, S.; Pedrini, P. *J. Org. Chem.* **2002**, *67*, 5802.

(153) Festa, C.; Renga, B.; D'Amore, C.; Sepe, V.; Finamore, C.; De Marino, S.; Carino, A.; Cipriani, S.; Monti, M. C.; Zampella, A.; Fiorucci, S. *J. Med. Chem.* **2014**, *57*, 8477.

(154) Inoue, H.; Iijima, I.; Takeda, M. *Chem. Pharm. Bull. (Tokyo)* **1980**, *28*, 1022.

(155) Ji, L.; Zhang, D.-f.; Zhao, Q.; Hu, S.-m.; Qian, C.; Chen, X.-Z. *Tetrahedron* **2013**, *69*, 7031.

(156) Ogawa, S.; Tezuka, Y. *Bioorg. Med. Chem. Lett.* **2006**, *16*, 5238.

(157) Fukase, H.; Horii, S. *J. Org. Chem.* **1992**, *57*, 3642.

(158) Miura, K.; Tomita, M.; Yamada, Y.; Hosomi, A. *J. Org. Chem.* **2007**, *72*, 787.

(159) Barton, D. H. R.; Blundell, P.; Dorchak, J.; Jang, D. O.; Jaszberenyi, J. C. *Tetrahedron* **1991**, *47*, 8969.

(160) Barton, D. H. R.; Jang, D. O.; Jaszberenyi, J. C. *Tetrahedron Lett.* **1991**, *32*, 7187.

(161) Barton, D. H. R.; McCombie, S. W. *J. Chem. Soc., Perkin Trans. 1* **1975**, 1574.

(162) Kobayashi, S.; Kuroda, H.; Ohtsuka, Y.; Kashihara, T.; Masuyama, A.; Watanabe, K. *Tetrahedron* **2013**, *69*, 2251.

(163) Yuan, H.; Bi, K.; Chang, W.; Yue, R.; Li, B.; Ye, J.; Sun, Q.; Jin, H.; Shan, L.; Zhang, W. *Tetrahedron* **2014**, *70*, 9084.

(164) Barton, D. H. R.; Doo Ok, J.; Jaszberenyi, J. C. *Tetrahedron Lett.* **1990**, *31*, 3991.

(165) Umemoto, T.; Singh, R. P.; Xu, Y.; Saito, N. *J. Am. Chem. Soc.* **2010**, *132*, 18199.

(166) Jiang, X.; Liu, X.; Greiner, J.; Szucs, S.; Visnick, M.; WO 2009/129548 A1 ed. 2009, p 1.

(167) Li W-S; Hung W-C; Shen C-N; WO2017035501 (A1) ed. 2017.

(168) Dai, C.; Meschini, F.; Narayanam, J. M. R.; Stephenson, C. R. J. *J. Org. Chem.* **2012**, *77*, 4425.

(169) Albert-Soriano, M.; Pastor, I. M. *Eur. J. Org. Chem.* **2016**, *2016*, 5180.

(170) Zhang, S.; Guo, L.-N.; Wang, H.; Duan, X.-H. *Org. Biomol. Chem.* **2013**, *11*, 4308.

(171) T., N. P.; Gonzalez, D. S.; D., B. M.; P., V. S.; Chi-Huey, W. *Angew. Chem. Int. Ed.* **2005**, *44*, 192.

(172) Luche, J. L. *J. Am. Chem. Soc.* **1978**, *100*, 2226.

(173) Černý, I.; Buděšínský, M.; Pouzar, V.; Vyklický, V.; Krausová, B.; Vyklický Jr, L. *Steroids* **2012**, *77*, 1233.

(174) Litvinovskaya, R. P.; Minin, P. S.; Raiman, M. E.; Zhilitskaya, G. A.; Kurtikova, A. L.; Kozharnovich, K. G.; Derevyanchuk, M. V.; Kravets, V. S.; Khripach, V. A. *Chem. Nat. Compd.* **2013**, *49*, 478.

(175) Togo, H.; Matsubayashi, S.; Yamazaki, O.; Yokoyama, M. *J. Org. Chem.* **2000**, *65*, 2816.

(176) Mukai, K.; Urabe, D.; Kasuya, S.; Aoki, N.; Inoue, M. *Angew. Chem. Int. Ed.* **2013**, *52*, 5300.

(177) Zhang, J.-l.; Wang, H.; Pi, H.-f.; Ruan, H.-l.; Zhang, P.; Wu, J.-z. *Steroids* **2009**, *74*, 424.

(178) Yang, Y.-X.; Zheng, L.-T.; Shi, J.-J.; Gao, B.; Chen, Y.-K.; Yang, H.-C.; Chen, H.-L.; Li, Y.-C.; Zhen, X.-C. *Bioorg. Med. Chem. Lett.* **2014**, *24*, 1222.

(179) W., S. A.; Thomas, D.; Sigrid, G.; Margit, G.; Fanny, M.; V., K. T.; Hans-Joachim, K. *Eur. J. Org. Chem.* **2006**, *2006*, 3687.

(180) Herrera, H.; Carvajal, R.; Olea, A.; Espinoza, L. *Molecules* **2016**, *21*, 1139.

(181) Iida, T.; Tamaru, T.; Chang, F. C.; Niwa, T.; Goto, J.; Nambara, T. *Steroids* **1993**, *58*, 362.

(182) Nielsen, M. K.; Ugaz, C. R.; Li, W.; Doyle, A. G. *J. Am. Chem. Soc.* **2015**, *137*, 9571.

(183) Bennua-Skalmowski, B.; Vorbrüggen, H. *Tetrahedron Lett.* **1995**, *36*, 2611.

(184) Geoffroy, P.; Ressault, B.; Marchioni, E.; Miesch, M. *Steroids* **2011**, *76*, 1166.

(185) Yu-Rui, Z.; Bing, G.; Roger, B.; Annemieke, V.; Pierre, D. C.; Maurits, V. *Eur. J. Org. Chem.* **2005**, *2005*, 4414.

(186) Göndös, G.; Orr, J. C. *J. Chem. Soc., Chem. Commun.* **1982**, 1239.

(187) Gunning, P. J.; Tiffin, P. D.; WO 2004/037845 A1 ed. United Kingdom, 2004.

(188) Brown, H. C.; Krishnamurthy, S. *J. Am. Chem. Soc.* **1972**, *94*, 7159.

(189) Kovács, D.; Wölfling, J.; Szabó, N.; Szécsi, M.; Minorics, R.; Zupkó, I.; Frank, É. *Eur. J. Med. Chem.* **2015**, *98*, 13.

(190) Babcock, J. C.; Campbell, J. A.; Lobl, T. J.; US4297350 ed. Unted States, 1981.

(191) Schneider, H. J.; Buchheit, U.; Becker, N.; Schmidt, G.; Siehl, U. *J. Am. Chem. Soc.* **1985**, *107*, 7027.

(192) Mariangela, D.; Giancarlo, F.; Marco, F.; Alessandro, M.; Paola, P.; Silvia, P. *Chem. Lett.* **1999**, *28*, 693.

(193) Pedrini, P.; Andreotti, E.; Guerrini, A.; Dean, M.; Fantin, G.; Giovannini, P. P. *Steroids* **2006**, *71*, 189.

(194) Iida, T.; Chang, F. C. *J. Org. Chem.* **1982**, *47*, 2972.

(195) Yu, D. D.; Andrali, S. S.; Li, H.; Lin, M.; Huang, W.; Forman, B. M. *Biorg. Med. Chem.* **2016**, *24*, 3986.

(196) Li, M.; Zhou, P.; Wu, A. *Tetrahedron Lett.* **2006**, *47*, 3409.

(197) Ali, A.; Asif, M.; Khanam, H.; Mashrai, A.; Sherwani, M. A.; Owais, M.; Shamsuzzaman *RSC Advances* **2015**, *5*, 75964.

(198) Saïah, M.; Bessodes, M.; Antonakis, K. *Tetrahedron Lett.* **1992**, *33*, 4317.

(199) Nunnari, J.; Suomalainen, A. *Cell* **2012**, *148*, 1145.

(200) Birsoy, K.; Wang, T.; Chen, Walter W.; Freinkman, E.; Abu-Remaileh, M.; Sabatini, David M. *Cell* **2015**, *162*, 540.

(201) Friedman, J. R.; Nunnari, J. *Nature* **2014**, *505*, 335.

(202) Zorova, L. D.; Popkov, V. A.; Plotnikov, E. Y.; Silachev, D. N.; Pevzner, I. B.; Jankauskas, S. S.; Babenko, V. A.; Zorov, S. D.; Balakireva, A. V.; Juhaszova, M.; Sollott, S. J.; Zorov, D. B. *Anal. Biochem.* **2018**, *552*, 50.

(203) Sakamuru, S.; Attene-Ramos, M. S.; Xia, M. *Methods Mol. Biol.* **2016**, *1473*, 17.

(204) Perry, S. W.; Norman, J. P.; Barbieri, J.; Brown, E. B.; Gelbard, H. A. *BioTechniques* **2011**, *50*, 98.

(205) Szewczyk, A.; Wojtczak, L. *Pharmacol. Rev.* **2002**, *54*, 101.

(206) Chen, F.; Cushion, M. T. *J. Clin. Microbiol.* **1994**, *32*, 2791.

(207) Kaja, S.; Payne, A. J.; Singh, T.; Ghuman, J. K.; Sieck, E. G.; Koulen, P. *J. Pharmacol. Toxicol. Methods* **2015**, *73*, 1.

(208) Chan, F. K.-M.; Moriwaki, K.; De Rosa, M. J. *Methods Mol. Biol.* **2013**, *979*, 65.

(209) Xu, Z.; Chu, X.; Jiang, H.; Schilling, H.; Chen, S.; Feng, J. *Redox Biology* **2017**, *11*, 606.

(210) Deschamps, J. R. *Life Sci.* **2010**, *86*, 585.

(211) Stubbs, M. T. In *Comprehensive Medicinal Chemistry II*; Taylor, J. B., Triggle, D. J., Eds.; Elsevier: Oxford, 2007, p 449.

(212) Williams, S. P.; Kuyper, L. F.; Pearce, K. H. *Curr. Opin. Chem. Biol.* **2005**, *9*, 371.

(213) Thompson, H. P. G.; Day, G. M. *Chem. Sci.* **2014**, *5*, 3173.

(214) Desiraju, G. R. *J. Am. Chem. Soc.* **2013**, *135*, 9952.

(215) R., D. G. *Angew. Chem. Int. Ed.* **2007**, *46*, 8342.

(216) Bishop, R. *CrystEngComm* **2015**, *17*, 7448.

(217) Chopra, D.; Row, T. N. G. *CrystEngComm* **2011**, *13*, 2175.

(218) Reichenbacher, K.; Suss, H. I.; Hulliger, J. *Chem. Soc. Rev.* **2005**, *34*, 22.

(219) Dolle, F.; Hetru, C.; Rousseau, B.; Sobrio, F.; Blais, C.; Lafont, R.; Descamp, M.; Luu, B. *Tetrahedron* **1993**, *49*, 2485.

(220) Li, Q.; Tochtrop, G. P. *Tetrahedron Lett.* **2011**, *52*, 4137.

(221) Huang, L.; Sun, Y.; Zhu, H.; Zhang, Y.; Xu, J.; Shen, Y. M. *Steroids* **2009**, *74*, 701.

(222) Sasaki, T.; Nakamori, R.; Yamaguchi, T.; Kasuga, Y.; Iida, T.; Nambara, T. *Chem. Phys. Lipids* **2001**, *109*, 135.

(223) Maslov, M. A.; Morozova, N. G.; Solomatina, T. V.; Shaforostova, N. G.; Serebrennikova, G. A. *uss. J. Bioorg. Chem.* **2011**, *37*, 507.

(224) Travaglini, L.; Bridgland, L. N.; Davis, A. P. *Chem. Commun.* **2014**, *50*, 4803.

(225) Gil, R. P.; Martínez, C. S. P.; Manchado, F. C. *Synth. Commun.* **1998**, *28*, 3387.

(226) Stoltz, K. L.; Erickson, R.; Staley, C.; Weingarden, A. R.; Romens, E.; Steer, C. J.; Khoruts, A.; Sadowsky, M. J.; Dosa, P. I. *J. Med. Chem.* **2017**, *60*, 3451.

(227) Gioiello, A.; Macchiarulo, A.; Carotti, A.; Filipponi, P.; Costantino, G.; Rizzo, G.; Adorini, L.; Pellicciari, R. *Biorg. Med. Chem.* **2011**, *19*, 2650.

(228) Medici, A.; Pedrini, P.; Bianchini, E.; Fantin, G.; Guerrini, A.; Natalini, B.; Pellicciari, R. *Steroids* **2002**, *67*, 51.

(229) Li, W.; Xu, Q.; Li, Y.; Zhu, W.; Cui, J.; Ju, Y.; Li, G. *Tetrahedron Lett.* **2013**, *54*, 3868.

(230) Zürcher, R. F. *Helv. Chim. Acta* **1963**, *46*, 2054.

(231) Ray Dias, J.; Gao, H.; Kolehmainen, E. *Spectrochim. Acta A* **2000**, *56*, 53.

(232) Moriarty, R.; David, N.; Mahmood, N.; Parasad, A.; Swaringen, R.; Reid, J.; Sahoo, A.; EP 2 407 475 A2 ed. 2008.

(233) Cushman, M.; Golebiewski, W. M.; Pommier, Y.; Mazunder, A.; Reymen, D.; De Clercq, E.; Grahm, L.; Rice, W. G. *J. Med. Chem.* **1995**, *38*, 443.

(234) Sepe, V.; Renga, B.; Festa, C.; Finamore, C.; Masullo, D.; Carino, A.; Cipriani, S.; Distrutti, E.; Fiorucci, S.; Zampella, A. *Steroids* **2016**, *105*, 59.

(235) Bettarello, L.; Bortolini, O.; Fantin, G.; Guerrini, A. *Il Farmaco* **2000**, *55*, 51.

(236) Byrd, K. M.; Arieno, M. D.; Kennelly, M. E.; Estiu, G.; Wiest, O.; Helquist, P. *Biorg. Med. Chem.* **2015**, *23*, 3843.

(237) Grenot, C.; Cuilleron, C.; WO 2011/073419 ed. 2011.

(238) Zhou, W.-S.; Jiang, B.; Pan, X.-F. *J. Chem. Soc., Chem. Commun.* **1988**, 791.

Appendix A Bile Acid X-Ray Crystallography Data

A.1 Molecular structure of 2.37

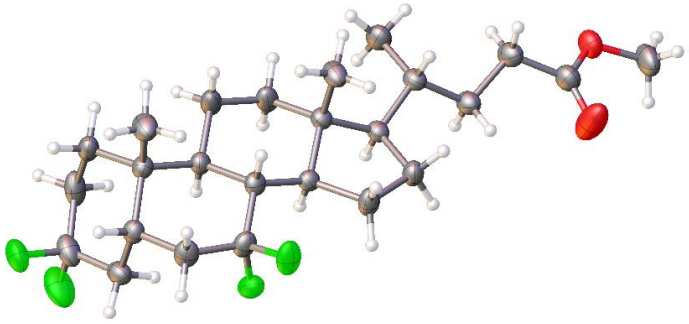

Thermal ellipsoids drawn at the 50% probability level.

Experimental. Single clear colourless prism-shaped crystals of (**RW-7704-37**) were recrystallised from a mixture of methanol and $CHCl_3$ by slow evaporation. A suitable crystal (0.46×0.44×0.16) mm^3 was selected and mounted on a MITIGEN holder silicon oil on a Rigaku R-AXIS Spider diffractometer. The crystal was kept at T = 150(2) K during data collection. Using **Olex2** (Dolomanov et al., 2009), the structure was solved with the **ShelXT** (Sheldrick, 2015) structure solution program, using the Intrinsic Phasing solution method. The model was refined with version 2016/6 of **ShelXL** (Sheldrick, 2015) using Least Squares minimisation.

Crystal Data. $C_{25}H_{38}F_4O_2$, M_r = 446.55, orthorhombic, $P2_12_12_1$ (No. 19), a = 10.4072(3) Å, b = 11.1018(3) Å, c = 20.0202(5) Å, α = β = γ = 90°, V = 2313.11(11) $Å^3$, T = 150(2) K, Z = 4, Z' = 1, $\mu(CuK_\alpha)$ = 0.843, 27222 reflections measured, 4466 unique (R_{int} = 0.0284) which were used in all calculations. The final wR_2 was 0.0935 (all data) and R_1 was 0.0362 (I > 2(I)).

Compound	2017sot0008
Formula	$C_{25}H_{38}F_4O_2$
$D_{calc.}$/ g cm^{-3}	1.282
μ/mm^{-1}	0.843
Formula Weight	446.55
Colour	clear colourless
Shape	prism
Size/mm^3	0.46×0.44×0.16
T/K	150(2)
Crystal System	orthorhombic
Flack Parameter	0.10(3)
Hooft Parameter	0.09(3)
Space Group	$P2_12_12_1$
a/Å	10.4072(3)
b/Å	11.1018(3)
c/Å	20.0202(5)
α/°	90
β/°	90
γ/°	90
V/$Å^3$	2313.11(11)
Z	4
Z'	1
Wavelength/Å	1.54187
Radiation type	CuK_α
Θ_{min}/°	4.417
Θ_{max}/°	71.701
Measured Refl.	27222
Independent Refl.	4466
Reflections Used	4228
R_{int}	0.0284
Parameters	284
Restraints	0
Largest Peak	0.234
Deepest Hole	-0.210
GooF	1.039
wR_2 (all data)	0.0935
wR_2	0.0922
R_1 (all data)	0.0381
R_1	0.0362

A.2 Molecular Structure of 2.38

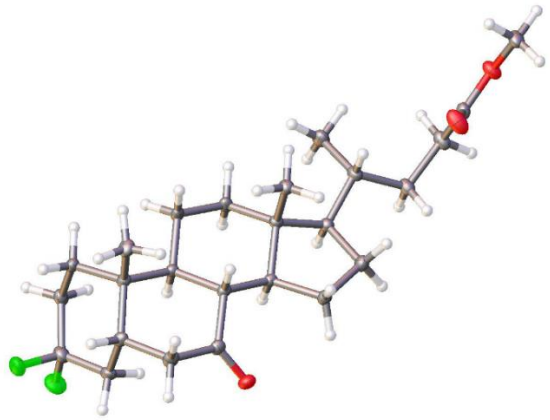

Thermal ellipsoids drawn at the 50% probability level.

Experimental. Single clear colourless prism-shaped crystals of (**RW-7704-38**) were recrystallised from a mixture of methanol and $CHCl_3$ by slow evaporation. A suitable crystal (0.41×0.22×0.06) mm^3 was selected and mounted on a MITIGEN holder silicon oil on a Rigaku AFC12 FRE-HF diffractometer. The crystal was kept at T = 100(2) K during data collection. Using **Olex2** (Dolomanov et al., 2009), the structure was solved with the **ShelXT** (Sheldrick, 2015) structure solution program, using the Intrinsic Phasing solution method. The model was refined with version 2014/7 of **ShelXL** (Sheldrick, 2015) using Least Squares minimisation.

Crystal Data. $C_{25}H_{38}O_3F_2$, M_r = 424.55, monoclinic, $P2_1$ (No. 4), a = 10.0313(2) Å, b = 7.5000(2) Å, c = 14.8179(3) Å, β = 94.180(2)°, α = γ = 90°, V = 1111.86(4) $Å^3$, T = 100(2) K, Z = 2, Z' = 1, $\mu(MoK_\alpha)$ = 0.092, 17264 reflections measured, 5718 unique (R_{int} = 0.0373) which were used in all calculations. The final wR_2 was 0.0947 (all data) and R_1 was 0.0396 (I > 2(I)).

Compound	**2017sot0007**
Formula	$C_{25}H_{38}O_3F_2$
$D_{calc.}$/ g cm^{-3}	1.268
μ/mm^{-1}	0.092
Formula Weight	424.55
Colour	clear colourless
Shape	prism
Size/mm^3	0.41×0.22×0.06
T/K	100(2)
Crystal System	monoclinic
Flack Parameter	-0.2(3)
Hooft Parameter	-0.1(3)
Space Group	$P2_1$
a/Å	10.0313(2)
b/Å	7.5000(2)
c/Å	14.8179(3)
α/°	90
β/°	94.180(2)
γ/°	90
V/$Å^3$	1111.86(4)
Z	2
Z'	1
Wavelength/Å	0.71073
Radiation type	MoK_α
Θ_{min}/°	3.720
Θ_{max}/°	28.699
Measured Refl.	17264
Independent Refl.	5718
Reflections Used	5533
R_{int}	0.0373
Parameters	275
Restraints	1
Largest Peak	0.305
Deepest Hole	-0.192
GooF	1.058
wR_2 (all data)	0.0947
wR_2	0.0937
R_1 (all data)	0.0412
R_1	0.0396

A.3 Molecular Structure of 2.41

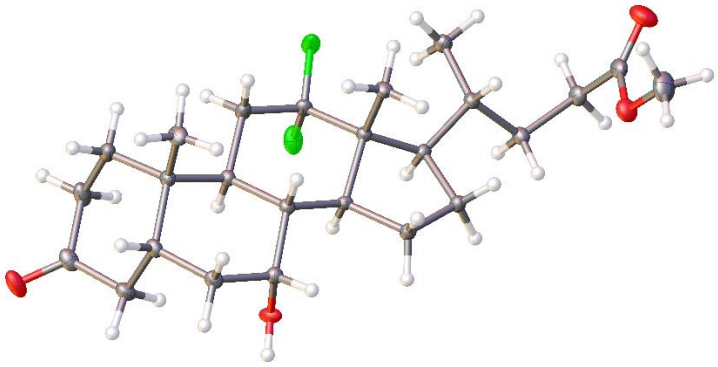

Thermal ellipsoids drawn at the 50% probability level.

Experimental: Single clear colourless prism-shaped crystals of (**RW-7704-28**) were recrystallised from DCM by slow evaporation. A suitable crystal (0.44×0.39×0.24) mm^3 was selected and mounted on a MITIGEN holder with silicon oil on a Rigaku R-AXIS Spider diffractometer. The crystal was kept at T = 100(2) K during data collection. Using **Olex2** (Dolomanov et al., 2009), the structure was solved with the **ShelXT** (Sheldrick, 2015) structure solution program, using the Intrinsic Phasing solution method. The model was refined with version 2014/7 of **ShelXL** (Sheldrick, 2015) using Least Squares minimisation.

Crystal Data. $C_{25}H_{38}F_2O_4$, M_r = 440.55, orthorhombic, $P2_12_12_1$ (No. 19), a = 24.4860(4) Å, b = 7.63480(10) Å, c = 12.1594(2) Å, $\alpha = \beta = \gamma = 90^\circ$, V = 2273.15(6) $Å^3$, T = 100(2) K, Z = 4, Z' = 1, $\mu(CuK_\alpha)$ = 0.789, 27017 reflections measured, 4396 unique (R_{int} = 0.0337) which were used in all calculations. The final wR_2 was 0.0776 (all data) and R_1 was 0.0309 (I > 2(I)).

Compound	**2016sot0064**
Formula	$C_{25}H_{38}F_2O_4$
$D_{calc.}$/ g cm^{-3}	1.287
μ/mm^{-1}	0.789
Formula Weight	440.55
Colour	clear colourless
Shape	prism
Size/mm^3	0.44×0.39×0.24
T/K	100(2)
Crystal System	orthorhombic
Flack Parameter	0.05(2)
Hooft Parameter	0.07(2)
Space Group	$P2_12_12_1$
a/Å	24.4860(4)
b/Å	7.63480(10)
c/Å	12.1594(2)
$\alpha/^\circ$	90
$\beta/^\circ$	90
$\gamma/^\circ$	90
V/$Å^3$	2273.15(6)
Z	4
Z'	1
Wavelength/Å	1.54187
Radiation type	CuK_α
$\Theta_{min}/^\circ$	3.610
$\Theta_{max}/^\circ$	71.795
Measured Refl.	27017
Independent Refl.	4396
Reflections Used	4367
R_{int}	0.0337
Parameters	288
Restraints	0
Largest Peak	0.205
Deepest Hole	-0.227
GooF	1.080
wR_2 (all data)	0.0776
wR_2	0.0773
R_1 (all data)	0.0312
R_1	0.0309

A.4 Molecular Structure of 2.42

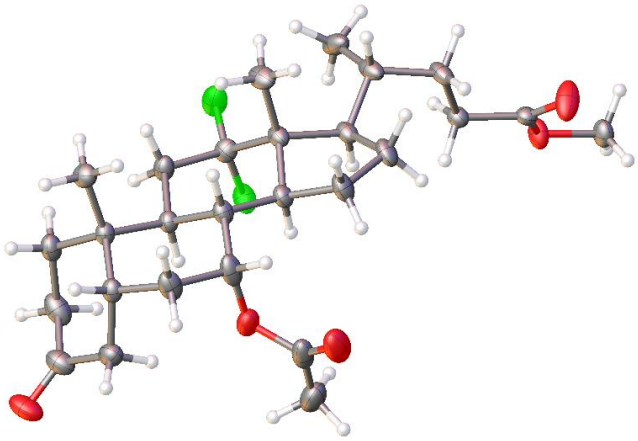

Thermal ellipsoids drawn at the 50% probability level.

Experimental. Single clear colourless block-shaped crystals of (**RW-7704-31**) were recrystallised from DCM by slow evaporation. A suitable crystal (0.14×0.05×0.04) mm^3 was selected and mounted on a MITIGEN holder with silicon oil on a Rigaku AFC12 FRE-VHF diffractometer. The crystal was kept at T = 100(2) K during data collection. Using **Olex2** (Dolomanov et al., 2009), the structure was solved with the **ShelXT** (Sheldrick, 2015) structure solution program, using the Intrinsic Phasing solution method. The model was refined with version 2014/7 of **ShelXL** (Sheldrick, 2015) using Least Squares minimisation.

Crystal Data. $C_{27}H_{40}F_2O_5$, M_r = 482.59, orthorhombic, $P2_12_12$ (No. 18), a = 16.9434(4) Å, b = 23.1004(7) Å, c = 6.3622(2) Å, α = β = γ = 90°, V = 2490.16(12) $Å^3$, T = 100(2) K, Z = 4, Z' = 1, μ (MoK_α) = 0.097, 23811 reflections measured, 6439 unique (R_{int} = 0.0318) which were used in all calculations. The final wR_2 was 0.1400 (all data) and R_1 was 0.0529 (I > 2(I)).

Compound	**2016sot0065**
Formula	$C_{27}H_{40}F_2O_5$
$D_{calc.}$/ g cm^{-3}	1.287
μ/mm^{-1}	0.097
Formula Weight	482.59
Colour	clear colourless
Shape	block
Size/mm^3	0.14×0.05×0.04
T/K	100(2)
Crystal System	orthorhombic
Flack Parameter	0.1(3)
Hooft Parameter	-0.0(3)
Space Group	$P2_12_12$
a/Å	16.9434(4)
b/Å	23.1004(7)
c/Å	6.3622(2)
α/°	90
β/°	90
γ/°	90
V/$Å^3$	2490.16(12)
Z	4
Z'	1
Wavelength/Å	0.71073
Radiation type	MoK_α
Θ_{min}/°	2.982
Θ_{max}/°	28.699
Measured Refl.	23811
Independent Refl.	6439
Reflections Used	5624
R_{int}	0.0318
Parameters	312
Restraints	0
Largest Peak	0.690
Deepest Hole	-0.238
GooF	1.020
wR_2 (all data)	0.1400
wR_2	0.1333
R_1 (all data)	0.0624
R_1	0.0529

A.5 Molecular Structure of 2.44

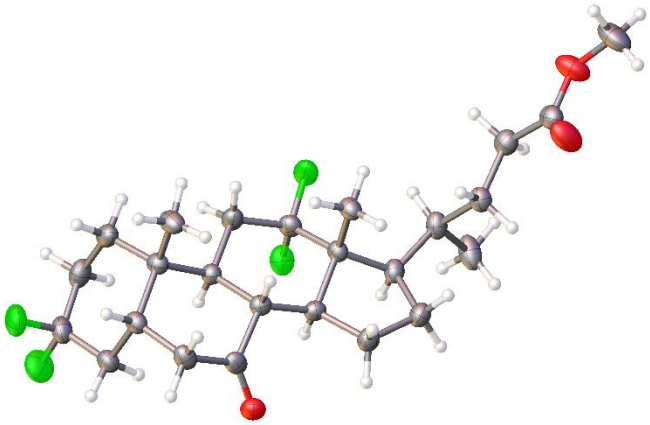

Thermal ellipsoids drawn at the 50% probability level.

Experimental. Single clear colourless prism-shaped crystals of (**RW-7704-93**) were recrystallised from a mixture of water and acetone by slow evaporation. A suitable crystal (0.42×0.36×0.18) mm^3 was selected and mounted on a MITIGEN holder silicon oil on a Rigaku R-AXIS Spider diffractometer. The crystal was kept at T = 150(2) K during data collection. Using **Olex2** (Dolomanov et al., 2009), the structure was solved with the **ShelXT** (Sheldrick, 2015) structure solution program, using the Intrinsic Phasing solution method. The model was refined with version 2016/6 of **ShelXL** (Sheldrick, 2015) using Least Squares minimisation.

Crystal Data. $C_{25}H_{36}F_4O_3$, M_r = 460.54, monoclinic, $P2_1$ (No. 4), a = 8.3764(3) Å, b = 12.3323(5) Å, c = 10.9601(4) Å, β = 92.818(7)°, α = γ = 90°, V = 1130.81(7) $Å^3$, T = 150(2) K, Z = 2, Z' = 1, μ (CuK_α) = 0.915, 12715 reflections measured, 3891 unique (R_{int} = 0.0460) which were used in all calculations. The final wR_2 was 0.0856 (all data) and R_1 was 0.0349 (I > 2(I)).

Compound	**2017sot0038**
Formula	$C_{25}H_{36}F_4O_3$
$D_{calc.}$/ g cm^{-3}	1.353
μ /mm^{-1}	0.915
Formula Weight	460.54
Colour	clear . colourless
Shape	prism
Size/mm^3	0.42×0.36×0.18
T/K	150(2)
Crystal System	monoclinic
Flack Parameter	0.05(5)
Hooft Parameter	0.07(5)
Space Group	$P2_1$
a/Å	8.3764(3)
b/Å	12.3323(5)
c/Å	10.9601(4)
α/°	90
β/°	92.818(7)
γ/°	90
V/$Å^3$	1130.81(7)
Z	2
Z'	1
Wavelength/Å	1.54187
Radiation type	CuK_α
Θ_{min}/°	4.038
Θ_{max}/°	66.479
Measured Refl.	12715
Independent Refl.	3891
Reflections Used	3713
R_{int}	0.0460
Parameters	293
Restraints	1
Largest Peak	0.158
Deepest Hole	-0.141
GooF	1.041
wR_2 (all data)	0.0856
wR_2	0.0842
R_1 (all data)	0.0371
R_1	0.0349

A.6 Molecular Structure of 2.5

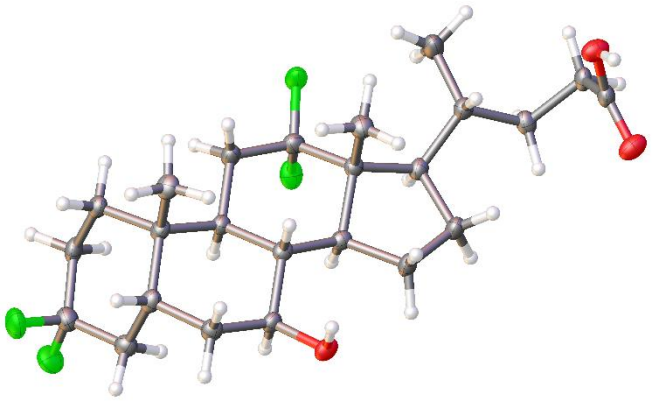

Thermal ellipsoids drawn at the 50% probability level.

Experimental. Single clear colourless plate-shaped crystals of (**RW-7704-97**) were recrystallised from a mixture of $CDCl_3$ and methanol by slow evaporation. A suitable crystal (0.59×0.16×0.02) mm^3 was selected and mounted on a MITIGEN holder silicon oil on a Rigaku R-AXIS Spider diffractometer. The crystal was kept at T = 100(2) K during data collection. Using **Olex2** (Dolomanov et al., 2009), the structure was solved with the **ShelXT** (Sheldrick, 2015) structure solution program, using the Intrinsic Phasing solution method. The model was refined with version 2016/6 of **ShelXL** (Sheldrick, 2015) using Least Squares minimisation.

Crystal Data. $C_{24}H_{36}F_4O_3$, M_r = 448.53, monoclinic, $I2$ (No. 5), a = 14.3757(4) Å, b = 6.1311(2) Å, c = 26.542(2) Å, β = 104.761(7)°, α = γ = 90°, V = 2262.2(2) $Å^3$, T = 100(2) K, Z = 4, Z' = 1, $\mu(CuK_\alpha)$ = 0.899, 12828 reflections measured, 3987 unique (R_{int} = 0.0355) which were used in all calculations. The final wR_2 was 0.0888 (all data) and R_1 was 0.0384 (I > 2(I)).

Compound	**2017sot0042**
Formula	$C_{24}H_{36}F_4O_3$
$D_{calc.}$/ g cm^{-3}	1.317
μ/mm^{-1}	0.899
Formula Weight	448.53
Colour	clear colourless
Shape	plate
Size/mm^3	0.59×0.16×0.02
T/K	100(2)
Crystal System	monoclinic
Flack Parameter	0.06(6)
Hooft Parameter	0.06(5)
Space Group	$I2$
a/Å	14.3757(4)
b/Å	6.1311(2)
c/Å	26.542(2)
α/°	90
β/°	104.761(7)
γ/°	90
V/$Å^3$	2262.2(2)
Z	4
Z'	1
Wavelength/Å	1.54187
Radiation type	CuK_α
Θ_{min}/°	3.207
Θ_{max}/°	68.444
Measured Refl.	12828
Independent Refl.	3987
Reflections Used	3623
R_{int}	0.0355
Parameters	291
Restraints	1
Largest Peak	0.172
Deepest Hole	-0.198
GooF	1.061
wR_2 (all data)	0.0888
wR_2	0.0857
R_1 (all data)	0.0443
R_1	0.0384

A.7 Molecular Structure of 2.7

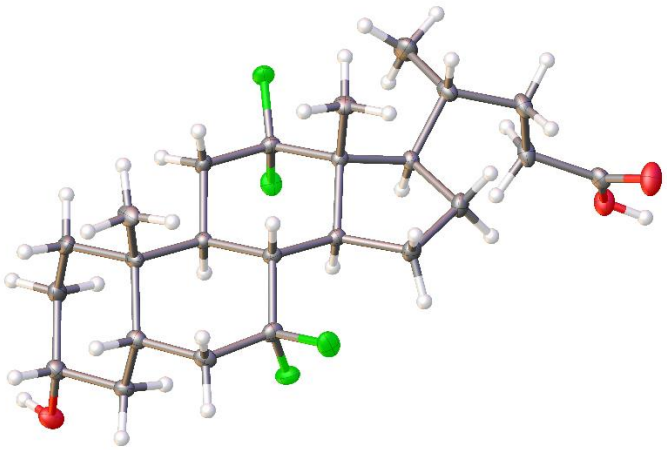

Thermal ellipsoids drawn at the 50% probability level.

Experimental. Single clear colourless prism-shaped crystals of (**RW-7704-70**) were recrystallised from ethyl acetate by slow evaporation. A suitable crystal (0.11×0.06×0.04) mm^3 was selected and mounted on a MITIGEN holder with silicon oil on a Rigaku AFC12 FRE-VHF diffractometer. The crystal was kept at T = 100(2) K during data collection. Using **Olex2** (Dolomanov et al., 2009), the structure was solved with the **ShelXT** (Sheldrick, 2015) structure solution program, using the Intrinsic Phasing solution method. The model was refined with version 2014/7 of **ShelXL** (Sheldrick, 2015) using Least Squares minimisation.

Crystal Data. $C_{24}H_{36}F_4O_3$, M_r = 448.53, orthorhombic, $P2_12_12_1$ (No. 19), a = 6.9602(2) Å, b = 12.2831(3) Å, c = 26.5929(5) Å, α = β = γ = 90°, V = 2273.50(10) $Å^3$, T = 100(2) K, Z = 4, Z' = 1, μ(MoK_α) = 0.106, 21727 reflections measured, 5846 unique (R_{int} = 0.0229) which were used in all calculations. The final wR_2 was 0.0827 (all data) and R_1 was 0.0320 (I > 2(I)).

Compound	**2016sot0068**
Formula	$C_{24}H_{36}F_4O_3$
$D_{calc.}$/ g cm^{-3}	1.310
μ /mm^{-1}	0.106
Formula Weight	448.53
Colour	clear colourless
Shape	prism
Size/mm^3	0.11×0.06×0.04
T/K	100(2)
Crystal System	orthorhombic
Flack Parameter	0.06(17)
Hooft Parameter	-0.00(13)
Space Group	$P2_12_12_1$
a/Å	6.9602(2)
b/Å	12.2831(3)
c/Å	26.5929(5)
α/°	90
β/°	90
γ/°	90
V/$Å^3$	2273.50(10)
Z	4
Z'	1
Wavelength/Å	0.71073
Radiation type	MoK_α
Θ_{min}/°	3.025
Θ_{max}/°	28.698
Measured Refl.	21727
Independent Refl.	5846
Reflections Used	5438
R_{int}	0.0229
Parameters	291
Restraints	0
Largest Peak	0.368
Deepest Hole	-0.162
GooF	1.023
wR_2 (all data)	0.0827
wR_2	0.0808
R_1 (all data)	0.0357
R_1	0.0320

A.8 Molecular Structure of 2.46

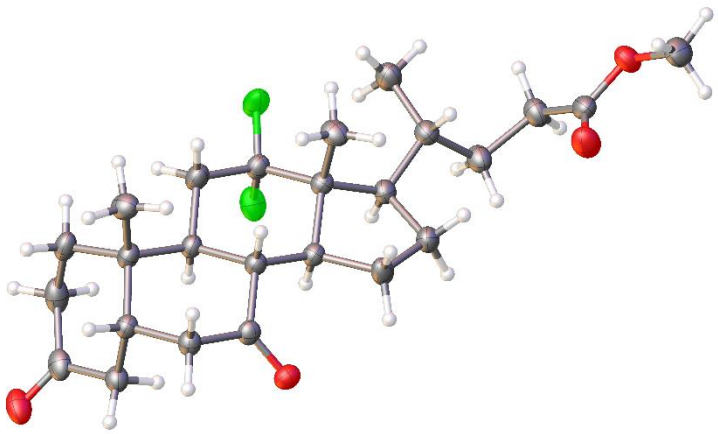

Thermal ellipsoids drawn at the 50% probability level.

Experimental. Single clear colourless rod-shaped crystals of (**RW-7704-94**) were recrystallised from a mixture of $CHCl_3$ and DCM by slow evaporation. A suitable crystal (0.30×0.06×0.04) mm^3 was selected and mounted on a MITIGEN holder silicon oil on a Rigaku AFC12 FRE-HF diffractometer. The crystal was kept at T = 99.94(19) K during data collection. Using **Olex2** (Dolomanov et al., 2009), the structure was solved with the **ShelXT** (Sheldrick, 2015) structure solution program, using the Intrinsic Phasing solution method. The model was refined with version 2016/6 of **ShelXL** (Sheldrick, 2015) using Least Squares minimisation.

Crystal Data. $C_{25}H_{36}F_2O_4$, M_r = 438.54, monoclinic, $P2_1$ (No. 4), a = 10.8660(5) Å, b = 6.7557(3) Å, c = 16.1814(8) Å, β = 108.987(6)°, α = γ = 90°, V = 1123.21(10) $Å^3$, T = 99.94(19) K, Z = 2, Z' = 1, $\mu(MoK_\alpha)$ = 0.097, 13548 reflections measured, 5764 unique (R_{int} = 0.0377) which were used in all calculations. The final wR_2 was 0.1873 (all data) and R_1 was 0.0626 (I > 2(I)).

Compound	**2017sot0019**
Formula	$C_{25}H_{36}F_2O_4$
$D_{calc.}$/ g cm^{-3}	1.297
μ/mm^{-1}	0.097
Formula Weight	438.54
Colour	clear colourless
Shape	rod
Size/mm^3	0.30×0.06×0.04
T/K	99.94(19)
Crystal System	monoclinic
Flack Parameter	-0.6(5)
Hooft Parameter	-0.4(4)
Space Group	$P2_1$
a/Å	10.8660(5)
b/Å	6.7557(3)
c/Å	16.1814(8)
α/°	90
β/°	108.987(6)
γ/°	90
V/$Å^3$	1123.21(10)
Z	2
Z'	1
Wavelength/Å	0.71073
Radiation type	MoK_α
Θ_{min}/°	3.751
Θ_{max}/°	28.698
Measured Refl.	13548
Independent Refl.	5764
Reflections Used	4306
R_{int}	0.0377
Parameters	284
Restraints	1
Largest Peak	0.332
Deepest Hole	-0.370
GooF	1.167
wR_2 (all data)	0.1873
wR_2	0.1521
R_1 (all data)	0.0824
R_1	0.0626

A.9 Molecular Structure of 2.54

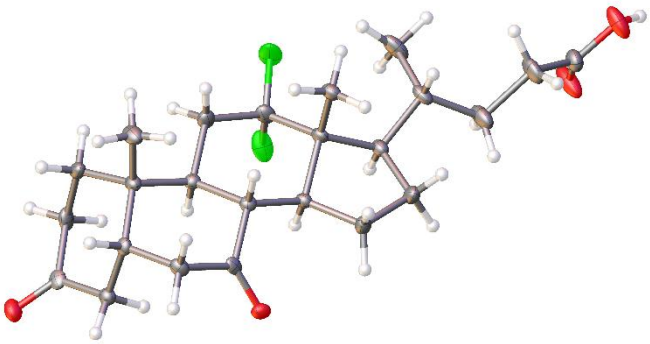

Thermal ellipsoids drawn at the 50% probability level.

Experimental. Single clear colourless needle-shaped crystals of (**RW-7704-96**) were recrystallised from a mixture of $CHCl_3$ and methanol by slow evaporation. A suitable crystal (0.22×0.02×0.01) mm^3 was selected and mounted on a MITIGEN holder silicon oil on a Rigaku AFC12 FRE-HF diffractometer. The crystal was kept at *T* = 100(2) K during data collection. Using **Olex2** (Dolomanov et al., 2009), the structure was solved with the **ShelXT** (Sheldrick, 2015) structure solution program, using the Intrinsic Phasing solution method. The model was refined with version 2016/6 of **ShelXL** (Sheldrick, 2015) using Least Squares minimisation.

Crystal Data. $C_{24}H_{34}O_4F_2$, M_r = 424.51, triclinic, P1 (No. 1), a = 6.8453(7) Å, b = 10.4878(10) Å, c = 15.5575(15) Å, α = 76.857(8)°, β = 85.884(8)°, γ = 89.316(8)°, V = 1084.83(19) Å^3, T = 100(2) K, Z = 2, Z' = 2, μ(MoK_α) = 0.098, 22327 reflections measured, 10951 unique (R_{int} = 0.0420) which were used in all calculations. The final wR_2 was 0.1213 (all data) and R_1 was 0.0715 (I > 2(I)).

Compound	**2017sot0041**
Formula	$C_{24}H_{34}O_4F_2$
$D_{calc.}$/ g cm^{-3}	1.300
μ/mm^{-1}	0.098
Formula Weight	424.51
Colour	clear colourless
Shape	needle
Size/mm^3	0.22×0.02×0.01
T/K	100(2)
Crystal System	triclinic
Flack Parameter	0.8(4)
Hooft Parameter	0.8(4)
Space Group	P1
a/Å	6.8453(7)
b/Å	10.4878(10)
c/Å	15.5575(15)
α/°	76.857(8)
β/°	85.884(8)
γ/°	89.316(8)
V/Å^3	1084.83(19)
Z	2
Z'	2
Wavelength/Å	0.71073
Radiation type	MoK_α
Θ_{min}/°	2.984
Θ_{max}/°	28.498
Measured Refl.	22327
Independent Refl.	10951
Reflections Used	8999
R_{int}	0.0420
Parameters	549
Restraints	525
Largest Peak	0.272
Deepest Hole	-0.249
GooF	1.087
wR_2 (all data)	0.1213
wR_2	0.1135
R_1 (all data)	0.0897
R_1	0.0715

A.10 Molecular Structure of 2.60

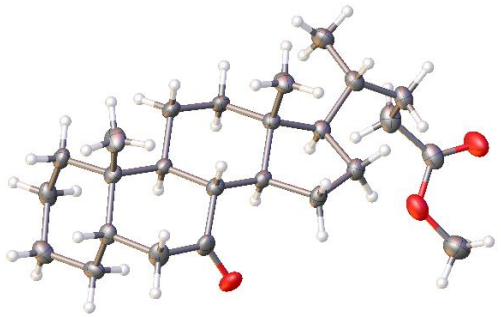

Thermal ellipsoids drawn at the 50% probability level.

Experimental. Single clear colourless slab-shaped crystals of (**RW-7991-17**) were recrystallised from a mixture of chloroform and methanol by slow evaporation. A suitable crystal (0.19×0.08×0.03) mm^3 was selected and mounted on a MITIGEN holder silicon oil on a Rigaku R-AXIS Spider diffractometer. The crystal was kept at T = 150(2) K during data collection. Using **Olex2** (Dolomanov et al., 2009), the structure was solved with the **ShelXT** (Sheldrick, 2015) structure solution program, using the Intrinsic Phasing solution method. The model was refined with version 2016/6 of **ShelXL** (Sheldrick, 2015) using Least Squares minimisation.

Crystal Data. $C_{25}H_{40}O_3$, M_r = 388.57, orthorhombic, $P2_12_12_1$ (No. 19), a = 7.73960(10) Å, b = 9.9370(2) Å, c = 28.4732(5) Å, $\alpha = \beta = \gamma = 90^\circ$, V = 2189.83(6) $Å^3$, T = 150(2) K, Z = 4, Z' = 1, $\mu(CuK_\alpha)$ = 0.582, 25634 reflections measured, 4205 unique (R_{int} = 0.0248) which were used in all calculations. The final wR_2 was 0.0836 (all data) and R_1 was 0.0337 (I > 2(I)).

Compound	**2017sot0027**
Formula	$C_{25}H_{40}O_3$
$D_{calc.}$/ g cm^{-3}	1.179
μ/mm^{-1}	0.582
Formula Weight	388.57
Colour	clear colourless
Shape	slab
Size/mm^3	0.19×0.08×0.03
T/K	150(2)
Crystal System	orthorhombic
Flack Parameter	0.05(4)
Hooft Parameter	0.07(4)
Space Group	$P2_12_12_1$
a/Å	7.73960(10)
b/Å	9.9370(2)
c/Å	28.4732(5)
α/°	90
β/°	90
γ/°	90
V/$Å^3$	2189.83(6)
Z	4
Z'	1
Wavelength/Å	1.54187
Radiation type	CuK_α
Θ_{min}/°	3.104
Θ_{max}/°	71.677
Measured Refl.	25634
Independent Refl.	4205
Reflections Used	4034
R_{int}	0.0248
Parameters	257
Restraints	0
Largest Peak	0.175
Deepest Hole	-0.180
GooF	1.057
wR_2 (all data)	0.0836
wR_2	0.0826
R_1 (all data)	0.0355
R_1	0.0337

A.11 Molecular Structure of 2.66

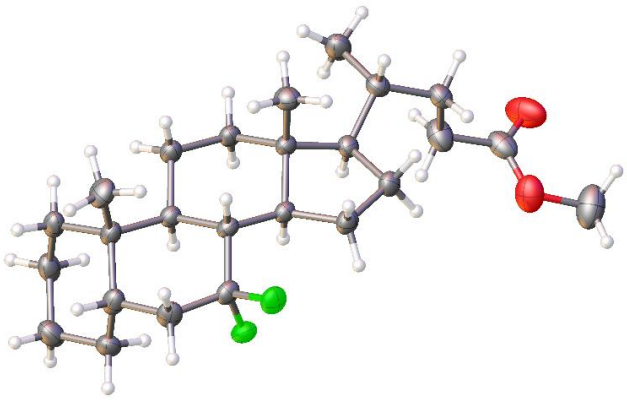

Thermal ellipsoids drawn at the 50% probability level.

Experimental. Single colourless prism-shaped crystals of (**RW-7991-44**) were recrystallised from a mixture of methanol and ethyl acetate by slow evaporation. A suitable crystal (0.54×0.14×0.04) mm^3 was selected and mounted on a MITIGEN holder silicon oil on a Rigaku R-AXIS Spider diffractometer. The crystal was kept at T = 150(2) K during data collection. Using **Olex2** (Dolomanov et al., 2009), the structure was solved with the **ShelXT** (Sheldrick, 2015) structure solution program, using the Intrinsic Phasing solution method. The model was refined with version 2016/6 of **ShelXL** (Sheldrick, 2015) using Least Squares minimisation.

Crystal Data. $C_{25}H_{40}F_2O_2$, M_r = 410.57, orthorhombic, $P2_12_12_1$ (No. 19), a = 7.4350(3) Å, b = 10.3193(4) Å, c = 29.3598(10) Å, $\alpha = \beta = \gamma = 90^\circ$, V = 2252.60(15) $Å^3$, T = 150(2) K, Z = 4, Z' = 1, $\mu(CuK_\alpha)$ = 0.689, 25017 reflections measured, 3960 unique (R_{int} = 0.0497) which were used in all calculations. The final wR_2 was 0.0857 (all data) and R_1 was 0.0368 (I > 2(I)).

Compound	**2017sot0043**
Formula	$C_{25}H_{40}F_2O_2$
$D_{calc.}$/ g cm^{-3}	1.211
μ/mm^{-1}	0.689
Formula Weight	410.57
Colour	colourless
Shape	prism
Size/mm^3	0.54×0.14×0.04
T/K	150(2)
Crystal System	orthorhombic
Flack Parameter	0.03(5)
Hooft Parameter	0.06(5)
Space Group	$P2_12_12_1$
a/Å	7.4350(3)
b/Å	10.3193(4)
c/Å	29.3598(10)
α/°	90
β/°	90
γ/°	90
V/$Å^3$	2252.60(15)
Z	4
Z'	1
Wavelength/Å	1.54187
Radiation type	CuK_α
Θ_{min}/°	3.010
Θ_{max}/°	66.447
Measured Refl.	25017
Independent Refl.	3960
Reflections Used	3545
R_{int}	0.0497
Parameters	266
Restraints	0
Largest Peak	0.170
Deepest Hole	-0.175
GooF	1.048
wR_2 (all data)	0.0857
wR_2	0.0824
R_1 (all data)	0.0431
R_1	0.0368

A.12 Molecular Structure of 2.13

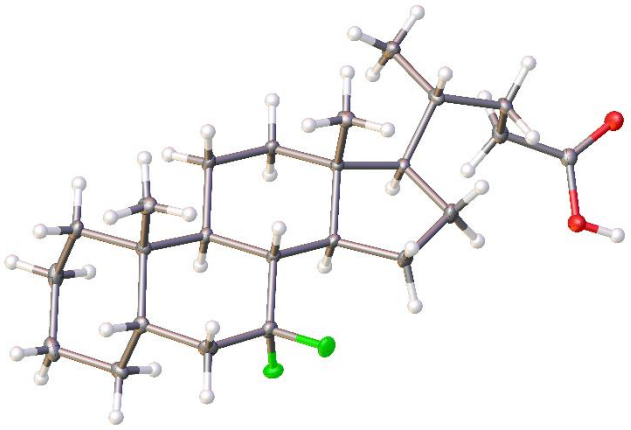

Thermal ellipsoids drawn at the 50% probability level.

Experimental. Single clear colourless block-shaped crystals of (**RW-7991-49**) were recrystallised from a mixture of DCM and methanol by slow evaporation. A suitable crystal (0.22×0.18×0.04) mm^3 was selected and mounted on a MITIGEN holder silicon oil on a Rigaku AFC12 FRE-VHF diffractometer. The crystal was kept at T = 100(2) K during data collection. Using **Olex2** (Dolomanov et al., 2009), the structure was solved with the **ShelXT** (Sheldrick, 2015) structure solution program, using the Intrinsic Phasing solution method. The model was refined with version 2016/6 of **ShelXL** (Sheldrick, 2015) using Least Squares minimisation.

Crystal Data. $C_{24}H_{38}F_2O_2$, M_r = 396.54, orthorhombic, $P2_12_12_1$ (No. 19), a = 7.34200(10) Å, b = 10.6343(2) Å, c = 27.1499(5) Å, $\alpha = \beta = \gamma = 90^\circ$, V = 2119.78(6) $Å^3$, T = 100(2) K, Z = 4, Z' = 1, $\mu(MoK_\alpha)$ = 0.088, 16660 reflections measured, 5482 unique (R_{int} = 0.0258) which were used in all calculations. The final wR_2 was 0.0928 (all data) and R_1 was 0.0413 (I > 2(I)).

Compound	**2017sot0028**
Formula	$C_{24}H_{38}F_2O_2$
$D_{calc.}$/ g cm^{-3}	1.243
μ/mm^{-1}	0.088
Formula Weight	396.54
Colour	clear colourless
Shape	block
Size/mm^3	0.22×0.18×0.04
T/K	100(2)
Crystal System	orthorhombic
Flack Parameter	-0.1(2)
Hooft Parameter	-0.1(2)
Space Group	$P2_12_12_1$
a/Å	7.34200(10)
b/Å	10.6343(2)
c/Å	27.1499(5)
$\alpha/^\circ$	90
$\beta/^\circ$	90
$\gamma/^\circ$	90
V/$Å^3$	2119.78(6)
Z	4
Z'	1
Wavelength/Å	0.71073
Radiation type	MoK_α
$\Theta_{min}/^\circ$	2.956
$\Theta_{max}/^\circ$	28.699
Measured Refl.	16660
Independent Refl.	5482
Reflections Used	5216
R_{int}	0.0258
Parameters	260
Restraints	0
Largest Peak	0.344
Deepest Hole	-0.185
GooF	1.119
wR_2 (all data)	0.0928
wR_2	0.0914
R_1 (all data)	0.0442
R_1	0.0413

A.13 Molecular Structure of 2.21

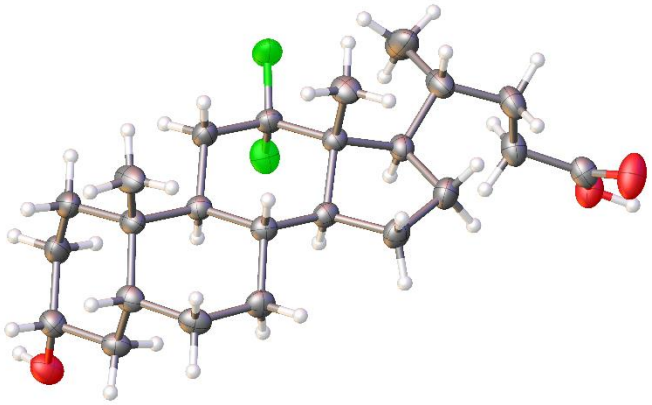

Thermal ellipsoids drawn at the 50% probability level.

Experimental. Single clear, colourless slab-shaped crystals of (**RW-7991-67**) were recrystallised from a mixture of acetone and $CHCl_3$ by slow evaporation. A suitable crystal (0.72×0.41×0.13) mm^3 was selected and mounted on a MITIGEN holder silicon oil on a Rigaku R-AXIS Spider diffractometer. The crystal was kept at T = 150(2) K during data collection. Using **Olex2** (Dolomanov et al., 2009), the structure was solved with the **ShelXT** (Sheldrick, 2015) structure solution program, using the Intrinsic Phasing solution method. The model was refined with version 2016/6 of **ShelXL** (Sheldrick, 2015) using Least Squares minimisation.

Crystal Data. $C_{24}H_{38}F_2O_3$, M_r = 412.54, orthorhombic, $P2_12_12_1$ (No. 19), a = 12.3323(2) Å, b = 26.4741(5) Å, c = 6.85570(10) Å, $\alpha = \beta = \gamma = 90^\circ$, V = 2238.29(6) $Å^3$, T = 150(2) K, Z = 4, Z' = 1, $\mu(CuK_\alpha)$ = 0.731, 24650 reflections measured, 3914 unique (R_{int} = 0.0368) which were used in all calculations. The final wR_2 was 0.0802 (all data) and R_1 was 0.0322 (I > 2(I)).

Compound	**2017sot0040**
Formula	$C_{24}H_{38}F_2O_3$
$D_{calc.}$/ g cm^{-3}	1.224
μ/mm^{-1}	0.731
Formula Weight	412.54
Colour	clear, colourless
Shape	slab
Size/mm^3	0.72×0.41×0.13
T/K	150(2)
Crystal System	orthorhombic
Flack Parameter	0.02(4)
Hooft Parameter	0.03(4)
Space Group	$P2_12_12_1$
a/Å	12.3323(2)
b/Å	26.4741(5)
c/Å	6.85570(10)
α/°	90
β/°	90
γ/°	90
V/$Å^3$	2238.29(6)
Z	4
Z'	1
Wavelength/Å	1.54187
Radiation type	CuK_α
Θ_{min}/°	3.339
Θ_{max}/°	66.500
Measured Refl.	24650
Independent Refl.	3914
Reflections Used	3799
R_{int}	0.0368
Parameters	273
Restraints	0
Largest Peak	0.134
Deepest Hole	-0.261
GooF	1.085
wR_2 (all data)	0.0802
wR_2	0.0794
R_1 (all data)	0.0334
R_1	0.0322

A.14 Molecular Structure of 2.19

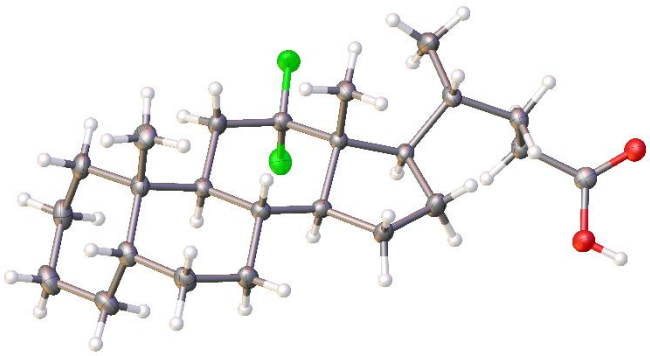

Thermal ellipsoids drawn at the 50% probability level.

Experimental. Single clear colourless prism-shaped crystals of (**RW-7991-75)** were recrystallised from a mixture of methanol and DCM by slow evaporation. A suitable crystal (0.45×0.18×0.12) mm^3 was selected and mounted on a MITIGEN holder silicon oil on a Rigaku R-AXIS Spider diffractometer. The crystal was kept at T = 150(2) K during data collection. Using **Olex2** (Dolomanov et al., 2009), the structure was solved with the **ShelXT** (Sheldrick, 2015) structure solution program, using the Intrinsic Phasing solution method. The model was refined with version 2016/6 of **ShelXL** (Sheldrick, 2015) using Least Squares minimisation.

Crystal Data. $C_{24}H_{38}F_2O_2$, M_r = 396.54, orthorhombic, $P2_12_12_1$ (No. 19), a = 7.1924(2) Å, b = 8.9361(2) Å, c = 32.7835(7) Å, $\alpha = \beta = \gamma = 90^\circ$, V = 2107.06(9) $Å^3$, T = 150(2) K, Z = 4, Z' = 1, $\mu(CuK_\alpha)$ = 0.719, 24188 reflections measured, 3774 unique (R_{int} = 0.0206) which were used in all calculations. The final wR_2 was 0.0748 (all data) and R_1 was 0.0296 (I > 2(I)).

Compound	**2017sot0044**
Formula	$C_{24}H_{38}F_2O_2$
$D_{calc.}$/ g cm^{-3}	1.250
μ/mm^{-1}	0.719
Formula Weight	396.54
Colour	clear colourless
Shape	prism
Size/mm^3	0.45×0.18×0.12
T/K	150(2)
Crystal System	orthorhombic
Flack Parameter	0.02(2)
Hooft Parameter	0.016(18)
Space Group	$P2_12_12_1$
a/Å	7.1924(2)
b/Å	8.9361(2)
c/Å	32.7835(7)
α/°	90
β/°	90
γ/°	90
V/$Å^3$	2107.06(9)
Z	4
Z'	1
Wavelength/Å	1.54187
Radiation type	CuK_α
Θ_{min}/°	5.130
Θ_{max}/°	67.496
Measured Refl.	24188
Independent Refl.	3774
Reflections Used	3697
R_{int}	0.0206
Parameters	260
Restraints	0
Largest Peak	0.158
Deepest Hole	-0.215
GooF	1.063
wR_2 (all data)	0.0748
wR_2	0.0743
R_1 (all data)	0.0303
R_1	0.0296

A.15 Molecular Structure of 2.20

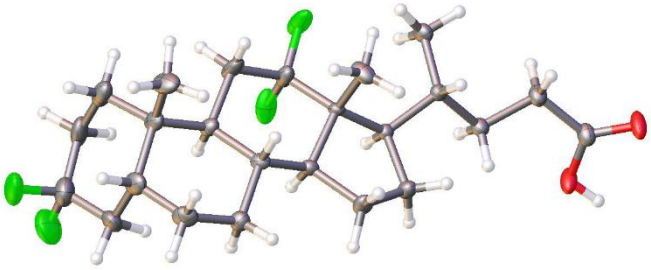

Thermal ellipsoids drawn at the 50% probability level, 3 other molecules in the asymmetric unit omitted for clarity.

Experimental. Single clear colourless prism-shaped crystals of (**RW-7991-7**) were recrystallised from a mixture of $CHCl_3$ and methanol by slow evaporation. A suitable crystal (0.33×0.20×0.15) mm^3 was selected and mounted on a MITIGEN holder silicon oil on a Rigaku AFC12 FRE-HF diffractometer. The crystal was kept at T = 100(2) K during data collection. Using **Olex2** (Dolomanov et al., 2009), the structure was solved with the **ShelXT** (Sheldrick, 2015) structure solution program, using the Intrinsic Phasing solution method. The model was refined with version 2014/7 of **ShelXL** (Sheldrick, 2015) using Least Squares minimisation.

Crystal Data. $C_{24}H_{36}F_4O_2$, M_r = 432.53, monoclinic, $P2_1$ (No. 4), a = 12.7705(2) Å, b = 12.7430(2) Å, c = 27.7098(4) Å, β = 103.121(2)°, α = γ = 90°, V = 4391.61(12) $Å^3$, T = 100(2) K, Z = 8, Z' = 4, $\mu(MoK_\alpha)$ = 0.104, 67480 reflections measured, 22561 unique (R_{int} = 0.0416) which were used in all calculations. The final wR_2 was 0.1200 (all data) and R_1 was 0.0500 (I > 2(I)).

Compound	**2017sot0018**
Formula	$C_{24}H_{36}F_4O_2$
$D_{calc.}$/ g cm^{-3}	1.308
μ/mm^{-1}	0.104
Formula Weight	432.53
Colour	clear colourless
Shape	prism
Size/mm^3	0.33×0.20×0.15
T/K	100(2)
Crystal System	monoclinic
Flack Parameter	0.21(16)
Hooft Parameter	0.26(19)
Space Group	$P2_1$
a/Å	12.7705(2)
b/Å	12.7430(2)
c/Å	27.7098(4)
α/°	90
β/°	103.121(2)
γ/°	90
V/$Å^3$	4391.61(12)
Z	8
Z'	4
Wavelength/Å	0.71073
Radiation type	MoK_α
Θ_{min}/°	3.650
Θ_{max}/°	28.700
Measured Refl.	67480
Independent Refl.	22561
Reflections Used	21583
R_{int}	0.0416
Parameters	1098
Restraints	1
Largest Peak	0.485
Deepest Hole	-0.301
GooF	1.047
wR_2 (all data)	0.1200
wR_2	0.1178
R_1 (all data)	0.0525
R_1	0.0500

A.16 Molecular Structure of 2.87

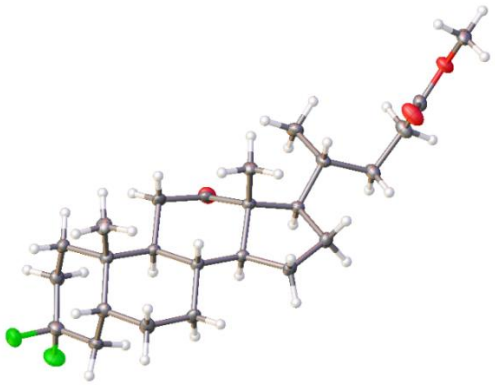

Thermal ellipsoids drawn at the 50% probability level.

Experimental. Single clear colourless fragment-shaped crystals of (**RW-7991-1**) were recrystallised from a mixture of methanol and chloroform by slow evaporation. A suitable crystal (0.32×0.14×0.05) mm^3 was selected and mounted on a MITIGEN holder silicon oil on a Rigaku AFC12 FRE-HF diffractometer. The crystal was kept at T = 100(2) K during data collection. Using **Olex2** (Dolomanov et al., 2009), the structure was solved with the **ShelXT** (Sheldrick, 2015) structure solution program, using the Intrinsic Phasing solution method. The model was refined with version 2016/6 of **ShelXL** (Sheldrick, 2015) using Least Squares minimisation.

Crystal Data. $C_{25}H_{38}F_2O_3$, M_r = 424.55, monoclinic, $P2_1$ (No. 4), a = 9.88690(10) Å, b = 7.63260(10) Å, c = 14.8219(2) Å, β = 92.2880(10)°, α = γ = 90°, V = 1117.61(2) $Å^3$, T = 100(2) K, Z = 2, Z' = 1, μ(MoK_α) = 0.092, 13402 reflections measured, 5761 unique (R_{int} = 0.0240) which were used in all calculations. The final wR_2 was 0.0890 (all data) and R_1 was 0.0346 (I > 2(I)).

Compound	**2017sot0026**
Formula	$C_{25}H_{38}F_2O_3$
$D_{calc.}$/ g cm^{-3}	1.262
μ/mm^{-1}	0.092
Formula Weight	424.55
Colour	clear colourless
Shape	fragment
Size/mm^3	0.32×0.14×0.05
T/K	100(2)
Crystal System	monoclinic
Flack Parameter	0.0(2)
Hooft Parameter	-0.1(2)
Space Group	$P2_1$
a/Å	9.88690(10)
b/Å	7.63260(10)
c/Å	14.8219(2)
α/°	90
β/°	92.2880(10)
γ/°	90
V/$Å^3$	1117.61(2)
Z	2
Z'	1
Wavelength/Å	0.71073
Radiation type	MoK_α
Θ_{min}/°	3.002
Θ_{max}/°	28.700
Measured Refl.	13402
Independent Refl.	5761
Reflections Used	5649
R_{int}	0.0240
Parameters	275
Restraints	1
Largest Peak	0.281
Deepest Hole	-0.185
GooF	1.072
wR_2 (all data)	0.0890
wR_2	0.0885
R_1 (all data)	0.0352
R_1	0.0346

A.17 Molecular Structure of 2.89

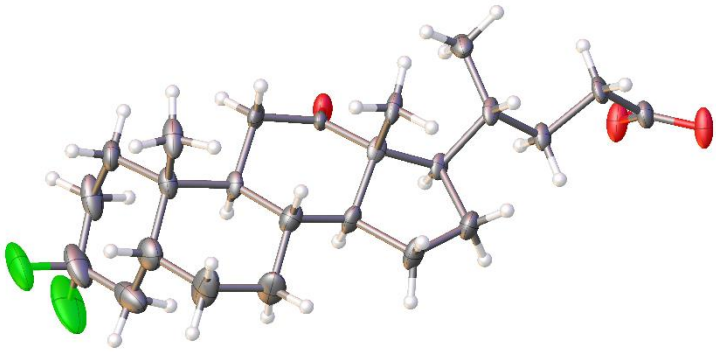

Thermal ellipsoids drawn at the 50% probability level. 2nd molecule omitted for clarity.

Experimental. Single clear colourless rod-shaped crystals of (**RW-7991-3**) were recrystallised from a mixture of methanol and DCM by slow evaporation. A suitable crystal (0.20×0.08×0.05) mm^3 was selected and mounted on a MITIGEN holder silicon oil on a Rigaku AFC12 FRE-HF diffractometer. The crystal was kept at T = 100(2) K during data collection. Using **Olex2** (Dolomanov et al., 2009), the structure was solved with the **ShelXT** (Sheldrick, 2015) structure solution program, using the Intrinsic Phasing solution method. The model was refined with version 2016/6 of **ShelXL** (Sheldrick, 2015) using Least Squares minimisation.

Crystal Data. $C_{24}H_{36}F_2O_3$, M_r = 410.53, monoclinic, $P2_1$ (No. 4), a = 6.4416(2) Å, b = 26.6970(9) Å, c = 12.8013(6) Å, β = 93.831(4)°, α = γ = 90°, V = 2196.54(15) $Å^3$, T = 100(2) K, Z = 4, Z' = 2, $\mu(MoK_\alpha)$ = 0.091, 30102 reflections measured, 11309 unique (R_{int} = 0.0505) which were used in all calculations. The final wR_2 was 0.3302 (all data) and R_1 was 0.1281 (I > 2(I)).

Compound	2017sot0025
Formula	$C_{24}H_{36}F_2O_3$
$D_{calc.}$/ g cm^{-3}	1.241
μ/mm^{-1}	0.091
Formula Weight	410.53
Colour	clear colourless
Shape	rod
Size/mm^3	0.20×0.08×0.05
T/K	100(2)
Crystal System	monoclinic
Flack Parameter	0.3(4)
Hooft Parameter	0.1(4)
Space Group	$P2_1$
a/Å	6.4416(2)
b/Å	26.6970(9)
c/Å	12.8013(6)
α/°	90
β/°	93.831(4)
γ/°	90
V/$Å^3$	2196.54(15)
Z	4
Z'	2
Wavelength/Å	0.71073
Radiation type	MoK_α
Θ_{min}/°	3.052
Θ_{max}/°	28.698
Measured Refl.	30102
Independent Refl.	11309
Reflections Used	9067
R_{int}	0.0505
Parameters	531
Restraints	532
Largest Peak	0.822
Deepest Hole	-0.363
GooF	1.161
wR_2 (all data)	0.3302
wR_2	0.3149
R_1 (all data)	0.1478
R_1	0.1281

A.18 Molecular Structure of 3.16

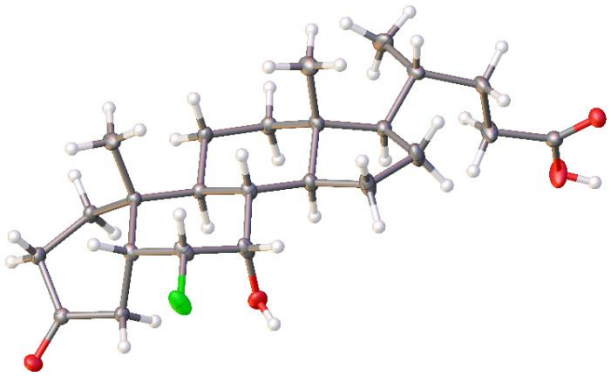

Thermal ellipsoids drawn at the 50% probability level.

Experimental. Single clear colourless prism-shaped crystals of (**RW-7991-92**) were recrystallised from a mixture of DCM and chloroform by slow evaporation. A suitable crystal (0.56×0.15×0.04) mm^3 was selected and mounted on a MITIGEN holder with silicon oil on a Rigaku AFC12 FRE-HF diffractometer. The crystal was kept at T = 100(2) K during data collection. Using **Olex2** (Dolomanov et al., 2009), the structure was solved with the **ShelXT** (Sheldrick, 2015) structure solution program, using the Intrinsic Phasing solution method. The model was refined with version 2016/6 of **ShelXL** (Sheldrick, 2015) using Least Squares minimisation.

Crystal Data. $C_{24}H_{37}O_4F$, M_r = 408.53, orthorhombic, $P2_12_12_1$ (No. 19), a = 6.3407(2) Å, b = 12.8451(4) Å, c = 27.6314(9) Å, $\alpha = \beta = \gamma = 90^\circ$, V = 2250.49(12) $Å^3$, T = 100(2) K, Z = 4, Z' = 1, $\mu(MoK_\alpha)$ = 0.085, 29061 reflections measured, 5700 unique (R_{int} = 0.0311) which were used in all calculations. The final wR_2 was 0.0954 (all data) and R_1 was 0.0398 (I > 2(I)).

Compound	**2017sot0073**
Formula	$C_{24}H_{37}O_4F$
$D_{calc.}$/ g cm^{-3}	1.206
μ/mm^{-1}	0.085
Formula Weight	408.53
Colour	clear colourless
Shape	prism
Size/mm^3	0.56×0.15×0.04
T/K	100(2)
Crystal System	orthorhombic
Flack Parameter	0.1(2)
Hooft Parameter	0.1(2)
Space Group	$P2_12_12_1$
a/Å	6.3407(2)
b/Å	12.8451(4)
c/Å	27.6314(9)
α/°	90
β/°	90
γ/°	90
V/$Å^3$	2250.49(12)
Z	4
Z'	1
Wavelength/Å	0.71073
Radiation type	MoK_α
Θ_{min}/°	2.949
Θ_{max}/°	28.496
Measured Refl.	29061
Independent Refl.	5700
Reflections Used	5599
R_{int}	0.0311
Parameters	273
Restraints	0
Largest Peak	0.335
Deepest Hole	-0.153
GooF	1.131
wR_2 (all data)	0.0954
wR_2	0.0949
R_1 (all data)	0.0406
R_1	0.0398

A.19 Molecular Structure of 3.19

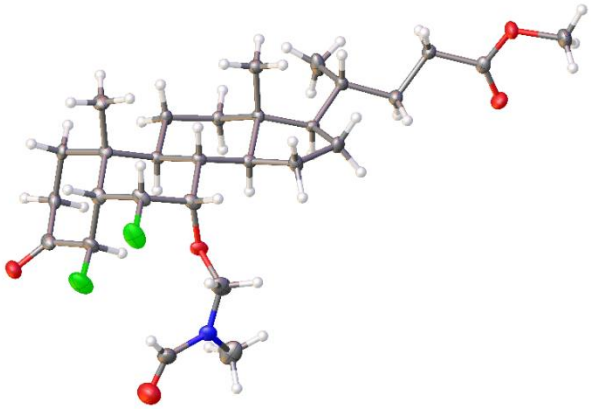

Thermal ellipsoids drawn at the 50% probability level, 2nd molecule and disorder omitted for clarity.

Experimental. Single clear colourless prism-shaped crystals of (**RW-7991-93-MIX2)** were recrystallised from a mixture of acetone and petrol by slow evaporation. A suitable crystal (0.42×0.22×0.07) mm^3 was selected and mounted on a MITIGEN holder with silicon oil on a Rigaku AFC12 FRE-HF diffractometer. The crystal was kept at T = 100(2) K during data collection. Using **Olex2** (Dolomanov et al., 2009), the structure was solved with the **ShelXT** (Sheldrick, 2015) structure solution program, using the Intrinsic Phasing solution method. The model was refined with version 2016/6 of **ShelXL** (Sheldrick, 2015) using Least Squares minimisation.

Crystal Data. $C_{28}H_{43}F_2NO_5$, M_r = 511.63, orthorhombic, $P2_12_12$ (No. 18), a = 35.3956(7) Å, b = 19.0314(3) Å, c = 7.83840(10) Å, $\alpha = \beta = \gamma = 90^{\circ}$, V = 5280.16(15) $Å^3$, T = 100(2) K, Z = 8, Z' = 2, $\mu(MoK_\alpha)$ = 0.096, 69385 reflections measured, 13383 unique (R_{int} = 0.0496) which were used in all calculations. The final wR_2 was 0.1490 (all data) and R_1 was 0.0687 (I > 2(I)).

Compound	**2017sot0071**
Formula	$C_{28}H_{43}F_2NO_5$
$D_{calc.}$/ g cm^{-3}	1.287
μ/mm^{-1}	0.096
Formula Weight	511.63
Colour	clear colourless
Shape	prism
Size/mm^3	0.42×0.22×0.07
T/K	100(2)
Crystal System	orthorhombic
Flack Parameter	-0.2(2)
Hooft Parameter	-0.2(2)
Space Group	$P2_12_12$
a/Å	35.3956(7)
b/Å	19.0314(3)
c/Å	7.83840(10)
α/°	90
β/°	90
γ/°	90
V/$Å^3$	5280.16(15)
Z	8
Z'	2
Wavelength/Å	0.71073
Radiation type	MoK_α
Θ_{min}/°	2.842
Θ_{max}/°	28.500
Measured Refl.	69385
Independent Refl.	13383
Reflections Used	12481
R_{int}	0.0496
Parameters	657
Restraints	20
Largest Peak	0.995
Deepest Hole	-0.422
GooF	1.177
wR_2 (all data)	0.1490
wR_2	0.1460
R_1 (all data)	0.0743
R_1	0.0687

A.20 Molecular Structure of 3.27

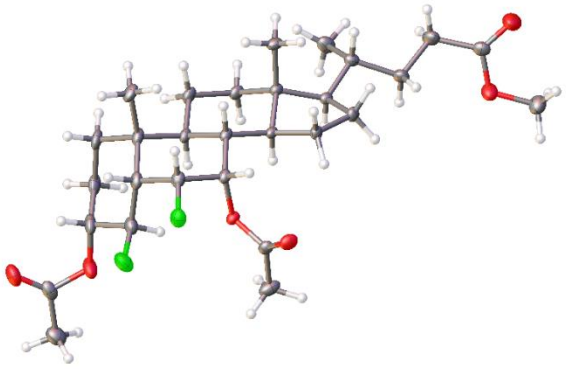

Thermal ellipsoids drawn at the 50% probability level.

Experimental. Single clear colourless prism-shaped crystals of (**RW-8313-1**) were recrystallised from a mixture of petrol and acetone by slow evaporation. A suitable crystal (0.17×0.13×0.04) mm^3 was selected and mounted on a MITIGEN holder with silicon oil on a Rigaku AFC12 FRE-HF diffractometer. The crystal was kept at T = 100(2) K during data collection. Using **Olex2** (Dolomanov et al., 2009), the structure was solved with the **ShelXT** (Sheldrick, 2015) structure solution program, using the Intrinsic Phasing solution method. The model was refined with version 2016/6 of **ShelXL** (Sheldrick, 2015) using Least Squares minimisation.

Crystal Data. $C_{29}H_{44}O_6F_2$, M_r = 526.64, monoclinic, $P2_1$ (No. 4), a = 11.1169(2) Å, b = 9.87310(10) Å, c = 13.4551(2) Å, β = 107.609(2)°, α = γ = 90°, V = 1407.61(4) $Å^3$, T = 100(2) K, Z = 2, Z' = 1, $\mu(MoK_\alpha)$ = 0.094, 36254 reflections measured, 7122 unique (R_{int} = 0.0271) which were used in all calculations. The final wR_2 was 0.0887 (all data) and R_1 was 0.0368 (I > 2(I)).

Compound	**2017sot0072**
Formula	$C_{29}H_{44}O_6F_2$
$D_{calc.}$/ g cm^{-3}	1.243
μ/mm^{-1}	0.094
Formula Weight	526.64
Colour	clear colourless
Shape	prism
Size/mm^3	0.17×0.13×0.04
T/K	100(2)
Crystal System	monoclinic
Flack Parameter	0.12(15)
Hooft Parameter	0.05(14)
Space Group	$P2_1$
a/Å	11.1169(2)
b/Å	9.87310(10)
c/Å	13.4551(2)
α/°	90
β/°	107.609(2)
γ/°	90
V/$Å^3$	1407.61(4)
Z	2
Z'	1
Wavelength/Å	0.71073
Radiation type	MoK_α
Θ_{min}/°	2.937
Θ_{max}/°	28.497
Measured Refl.	36254
Independent Refl.	7122
Reflections Used	6914
R_{int}	0.0271
Parameters	340
Restraints	1
Largest Peak	0.293
Deepest Hole	-0.187
GooF	1.074
wR_2 (all data)	0.0887
wR_2	0.0880
R_1 (all data)	0.0381
R_1	0.0368

A.21 Molecular Structure of 3.1

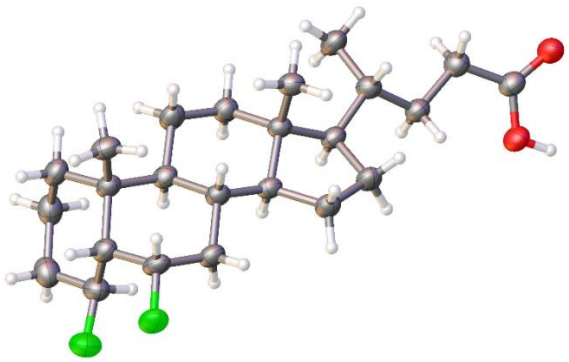

Thermal ellipsoids drawn at the 50% probability level.

Experimental. Single clear colourless rod-shaped crystals of **RW-8525-17** were recrystallised from a mixture of ethyl acetate and acetone by slow evaporation. A suitable crystal 0.52×0.10×0.04 mm^3 was selected and mounted on a MITIGEN holder with silicon oil on an Rigaku R-AXIS Spider diffractometer. The crystal was kept at a steady T = 120(2) K during data collection. The structure was solved with the **ShelXT** (Sheldrick, 2015) structure solution program using the Intrinsic Phasing solution method and by using **Olex2** (Dolomanov et al., 2009) as the graphical interface. The model was refined with version 2018/3 of **ShelXL** (Sheldrick, 2015) using Least Squares minimisation.

Crystal Data. $C_{24}H_{38}F_2O_2$, M_r = 396.54, orthorhombic, $P2_12_12_1$ (No. 19), a = 7.1033(2) Å, b = 10.3943(2) Å, c = 28.9901(7) Å, $\alpha = \beta = \gamma = 90^\circ$, V = 2140.45(9) $Å^3$, T = 120(2) K, Z = 4, Z' = 1, $\mu(CuK_\alpha)$ = 0.708, 23647 reflections measured, 3860 unique (R_{int} = 0.0970) which were used in all calculations. The final wR_2 was 0.1495 (all data) and R_1 was 0.0581 (I > 2(I)).

Compound	**2018sot0016**
Formula	$C_{24}H_{38}F_2O_2$
$D_{calc.}$/ g cm^{-3}	1.231
μ/mm^{-1}	0.708
Formula Weight	396.54
Colour	clear colourless
Shape	rod
Size/mm^3	0.52×0.10×0.04
T/K	120(2)
Crystal System	orthorhombic
Flack Parameter	0.07(12)
Hooft Parameter	0.12(10)
Space Group	$P2_12_12_1$
a/Å	7.1033(2)
b/Å	10.3943(2)
c/Å	28.9901(7)
α/°	90
β/°	90
γ/°	90
V/$Å^3$	2140.45(9)
Z	4
Z'	1
Wavelength/Å	1.54187
Radiation type	CuK_α
Θ_{min}/°	3.049
Θ_{max}/°	68.490
Measured Refl.	23647
Independent Refl.	3860
Reflections with I > 2(I)	3197
R_{int}	0.0970
Parameters	260
Restraints	0
Largest Peak	0.201
Deepest Hole	-0.174
GooF	1.069
wR_2 (all data)	0.1495
wR_2	0.1394
R_1 (all data)	0.0700
R_1	0.0581

A.22 Molecular Structure of 2.72

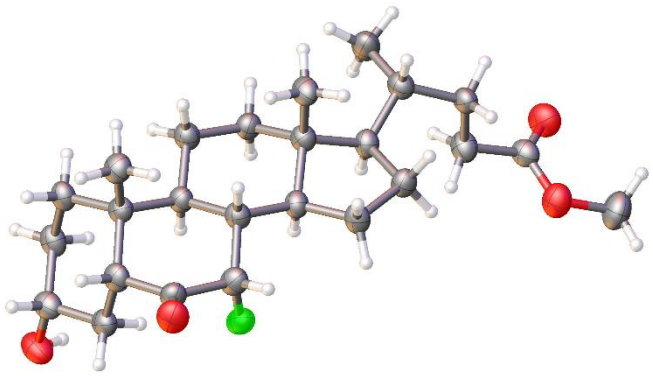

Thermal ellipsoids drawn at the 50% probability level.

Experimental. Single clear colourless plate-shaped crystals of (**RW-8313-63A**) were recrystallised from a mixture of pet-ether and acetone by slow evaporation. A suitable crystal (0.40×0.12×0.03) mm^3 was selected and mounted on a MITIGEN holder with silicon oil on a Rigaku R-AXIS Spider diffractometer. The crystal was kept at T = 120(2) K during data collection. Using **Olex2** (Dolomanov et al., 2009), the structure was solved with the ShelXD (Sheldrick, 2008) structure solution program, using the Dual Space solution method. The model was refined with version 2018/3 of **ShelXL** (Sheldrick, 2015) using Least Squares minimisation.

Crystal Data. $C_{25}H_{39}FO_4$, M_r = 422.56, orthorhombic, $P2_12_12_1$ (No. 19), a = 7.2126(2) Å, b = 10.4835(3) Å, c = 29.9762(8) Å, $\alpha = \beta = \gamma = 90^\circ$, V = 2266.60(11) $Å^3$, T = 120(2) K, Z = 4, Z' = 1, $\mu(CuK_\alpha)$ = 0.704, 25122 reflections measured, 4103 unique (R_{int} = 0.0793) which were used in all calculations. The final wR_2 was 0.1615 (all data) and R_1 was 0.0626 (I > 2(I)).

Compound	**2018sot0007**
Formula	$C_{25}H_{39}FO_4$
$D_{calc.}$/ g cm^{-3}	1.238
μ/mm^{-1}	0.704
Formula Weight	422.56
Colour	clear colourless
Shape	plate
Size/mm^3	0.40×0.12×0.03
T/K	120(2)
Crystal System	orthorhombic
Flack Parameter	-0.11(12)
Hooft Parameter	-0.01(12)
Space Group	$P2_12_12_1$
a/Å	7.2126(2)
b/Å	10.4835(3)
c/Å	29.9762(8)
α/°	90
β/°	90
γ/°	90
V/$Å^3$	2266.60(11)
Z	4
Z'	1
Wavelength/Å	1.54187
Radiation type	CuK_α
Θ_{min}/°	2.948
Θ_{max}/°	68.486
Measured Refl.	25122
Independent Refl.	4103
Reflections Used	2903
R_{int}	0.0793
Parameters	278
Restraints	0
Largest Peak	0.196
Deepest Hole	-0.267
GooF	1.040
wR_2 (all data)	0.1615
wR_2	0.1405
R_1 (all data)	0.0937
R_1	0.0626

A.23 Molecular Structure of 3.42

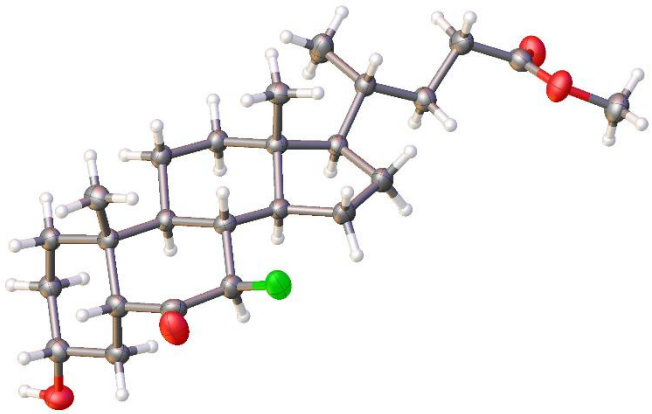

Thermal ellipsoids drawn at the 50% probability level.

Experimental. Single clear colourless rod-shaped crystals of (**RW-8313-63B**) were recrystallised from a mixture of pet-ether and acetone by slow evaporation. A suitable crystal (0.50×0.10×0.06) mm^3 was selected and mounted on a MITIGEN holder with silicon oil on a Rigaku R-AXIS Spider diffractometer. The crystal was kept at T = 120(2) K during data collection. Using **Olex2** (Dolomanov et al., 2009), the structure was solved with the **ShelXT** (Sheldrick, 2015) structure solution program, using the Intrinsic Phasing solution method. The model was refined with version 2018/3 of **ShelXL** (Sheldrick, 2015) using Least Squares minimisation.

Crystal Data. $C_{25}H_{39}FO_4$, M_r = 422.56, orthorhombic, $P2_12_12_1$ (No. 19), a = 7.06770(10) Å, b = 12.2239(2) Å, c = 26.0618(5) Å, $\alpha = \beta = \gamma = 90^\circ$, V = 2251.61(7) $Å^3$, T = 120(2) K, Z = 4, Z' = 1, $\mu(CuK_\alpha)$ = 0.708, 25865 reflections measured, 4136 unique (R_{int} = 0.0390) which were used in all calculations. The final wR_2 was 0.0849 (all data) and R_1 was 0.0376 (I > 2(I)).

Compound	**2018sot0008**
Formula	$C_{25}H_{39}FO_4$
$D_{calc.}$/ g cm^{-3}	1.247
μ/mm^{-1}	0.708
Formula Weight	422.56
Colour	clear colourless
Shape	rod
Size/mm^3	0.50×0.10×0.06
T/K	120(2)
Crystal System	orthorhombic
Flack Parameter	0.11(6)
Hooft Parameter	0.10(5)
Space Group	$P2_12_12_1$
a/Å	7.06770(10)
b/Å	12.2239(2)
c/Å	26.0618(5)
α/°	90
β/°	90
γ/°	90
V/$Å^3$	2251.61(7)
Z	4
Z'	1
Wavelength/Å	1.54187
Radiation type	CuK_α
Θ_{min}/°	3.392
Θ_{max}/°	68.499
Measured Refl.	25865
Independent Refl.	4136
Reflections Used	3750
R_{int}	0.0390
Parameters	279
Restraints	0
Largest Peak	0.163
Deepest Hole	-0.154
GooF	1.062
wR_2 (all data)	0.0849
wR_2	0.0816
R_1 (all data)	0.0436
R_1	0.0376

A.24 Molecular Structure of 3.61

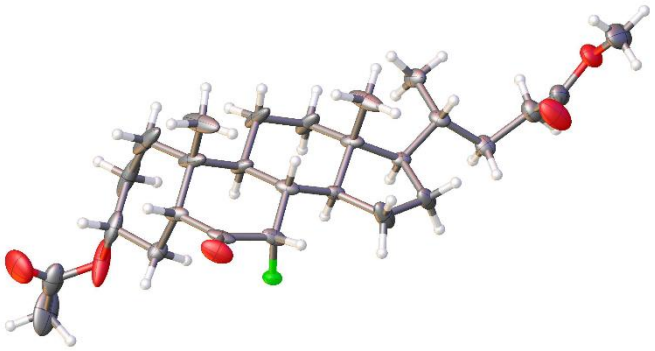

Thermal ellipsoids drawn at the 50% probability level.

Experimental. Single clear colourless needle-shaped crystals of **RW-8313-67** were recrystallised from CHCl3 by slow evaporation. A suitable crystal 0.25×0.02×0.02 mm^3 was selected and mounted on a MITIGEN holder silicon oil on an on a Rigaku AFC12 FRE-VHF diffractometer. The crystal was kept at a steady T = 100(2) K during data collection. The structure was solved with the ShelXT structure solution program using the intrinsic phasing methods solution method and by using **Olex2** (Dolomanov et al., 2009) as the graphical interface. The model was refined with version 2016/6 of **ShelXL** (Sheldrick, 2015) using Least Squares minimisation.

Crystal Data. $C_{27}H_{41}FO_5$, M_r = 464.60, orthorhombic, $P2_12_12_1$ (No. 19), a = 7.5750(3) Å, b = 12.0398(7) Å, c = 55.017(4) Å, $\alpha = \beta = \gamma = 90^\circ$, V = 5017.7(5) $Å^3$, T = 100(2) K, Z = 8, Z' = 2, μ (MoK$_\alpha$) = 0.088, 34885 reflections measured, 12307 unique (R_{int} = 0.0737) which were used in all calculations. The final wR_2 was 0.1920 (all data) and R_1 was 0.0858 (I > 2(I)).

Compound	**2018sot0005**
Formula	$C_{27}H_{41}FO_5$
$D_{calc.}$/ g cm^{-3}	1.230
μ/mm^{-1}	0.088
Formula Weight	464.60
Colour	clear colourless
Shape	needle
Size/mm^3	0.25×0.02×0.02
T/K	100(2)
Crystal System	orthorhombic
Flack Parameter	0.2(5)
Hooft Parameter	0.2(5)
Space Group	$P2_12_12_1$
a/Å	7.5750(3)
b/Å	12.0398(7)
c/Å	55.017(4)
α/°	90
β/°	90
γ/°	90
V/$Å^3$	5017.7(5)
Z	8
Z'	2
Wavelength/Å	0.71073
Radiation type	MoK α
Θ_{min}/°	1.731
Θ_{max}/°	28.499
Measured Refl.	34885
Independent Refl.	12307
Reflections with I > 2(I)	8220
R_{int}	0.0737
Parameters	612
Restraints	588
Largest Peak	0.503
Deepest Hole	-0.351
GooF	1.050
wR_2 (all data)	0.1920
wR_2	0.1722
R_1 (all data)	0.1312
R_1	0.0858

A.25 Molecular Structure of 3.62

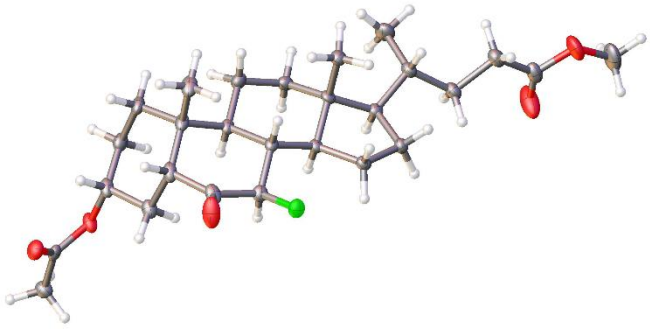

Thermal ellipsoids drawn at the 50% probability level.

Experimental. Single clear colourless block-shaped crystals of **RW-8525-21** were recrystallised from AcOH by slow evaporation. A suitable crystal 0.20×0.15×0.10 mm^3 was selected and mounted on a Mitigen mount on a Rigaku AFC12 FRE-VHF diffractometer. The crystal was kept at a steady T = 100(2) K during data collection. The structure was solved with the **ShelXT** (Sheldrick, 2015) structure solution program using the Intrinsic Phasing solution method and by using **Olex2** (Dolomanov et al., 2009) as the graphical interface. The model was refined with version 2016/6 of **ShelXL** (Sheldrick, 2015) using Least Squares minimisation.

Crystal Data. $C_{27}H_{41}FO_5$, M_r = 464.60, orthorhombic, $P2_12_12_1$ (No. 19), a = 7.5499(3) Å, b = 11.3968(3) Å, c = 57.870(3) Å, $\alpha = \beta = \gamma = 90^\circ$, V = 4979.4(3) $Å^3$, T = 100(2) K, Z = 8, Z' = 2, $\mu(MoK_\alpha)$ = 0.088, 31300 reflections measured, 12262 unique (R_{int} = 0.0435) which were used in all calculations. The final wR_2 was 0.0992 (all data) and R_1 was 0.0485 (I > 2(I)).

Compound	**2018sot0018**
Formula	$C_{27}H_{41}FO_5$
$D_{calc.}$/ g cm^{-3}	1.239
μ/mm^{-1}	0.088
Formula Weight	464.60
Colour	clear colourless
Shape	block
Size/mm^3	0.20×0.15×0.10
T/K	100(2)
Crystal System	orthorhombic
Flack Parameter	-0.1(3)
Hooft Parameter	-0.1(3)
Space Group	$P2_12_12_1$
a/Å	7.5499(3)
b/Å	11.3968(3)
c/Å	57.870(3)
α/°	90
β/°	90
γ/°	90
V/$Å^3$	4979.4(3)
Z	8
Z'	2
Wavelength/Å	0.71073
Radiation type	MoK_α
Θ_{min}/°	1.920
Θ_{max}/°	28.499
Measured Refl.	31300
Independent Refl.	12262
Reflections with I > 2(I)	9759
R_{int}	0.0435
Parameters	605
Restraints	0
Largest Peak	0.206
Deepest Hole	-0.202
GooF	1.025
wR_2 (all data)	0.0992
wR_2	0.0936
R_1 (all data)	0.0673
R_1	0.0485

A.26 Molecular Structure of 3.70

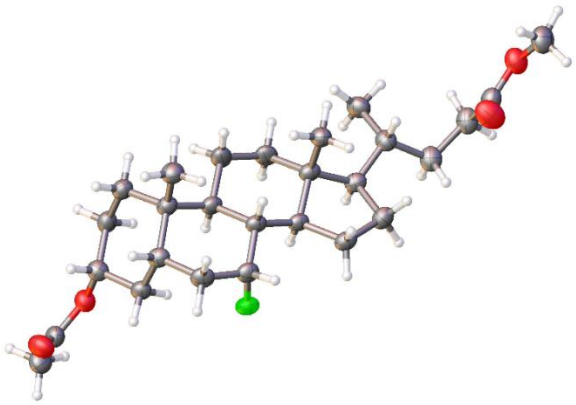

Thermal ellipsoids drawn at the 50% probability level.

Experimental. Single clear colourless irregular-shaped crystals of (**RW-8313-80**) were recrystallised from a mixture of DCM and water by slow evaporation. A suitable crystal (0.42×0.10×0.08) mm^3 was selected and mounted on a MITIGEN holder with silicon oil on a Rigaku R-AXIS Spider diffractometer. The crystal was kept at T = 120(2) K during data collection. Using **Olex2** (Dolomanov et al., 2009), the structure was solved with the **ShelXT** (Sheldrick, 2015) structure solution program, using the Intrinsic Phasing solution method. The model was refined with version 2018/3 of **ShelXL** (Sheldrick, 2015) using Least Squares minimisation.

Crystal Data. $C_{27}H_{43}FO_4$, M_r = 450.61, monoclinic, $P2_1$ (No. 4), a = 10.2736(3) Å, b = 7.5745(2) Å, c = 15.9202(5) Å, β= 96.112(7)°, α = γ = 90°, V = 1231.83(6) $Å^3$, T = 120(2) K, Z = 2, Z' = 1, μ(CuK_α) = 0.677, 13803 reflections measured, 4393 unique (R_{int} = 0.0478) which were used in all calculations. The final wR_2 was 0.1048 (all data) and R_1 was 0.0486 (I > 2(I)).

Compound	2018sot0006
Formula	$C_{27}H_{43}FO_4$
$D_{calc.}$/ g cm^{-3}	1.215
μ/mm^{-1}	0.677
Formula Weight	450.61
Colour	clear colourless
Shape	irregular
Size/mm^3	0.42×0.10×0.08
T/K	120(2)
Crystal System	monoclinic
Flack Parameter	0.13(10)
Hooft Parameter	0.18(9)
Space Group	$P2_1$
a/Å	10.2736(3)
b/Å	7.5745(2)
c/Å	15.9202(5)
α/°	90
β/°	96.112(7)
γ/°	90
V/$Å^3$	1231.83(6)
Z	2
Z'	1
Wavelength/Å	1.54187
Radiation type	CuK_α
Θ_{min}/°	4.328
Θ_{max}/°	68.498
Measured Refl.	13803
Independent Refl.	4393
Reflections Used	3515
R_{int}	0.0478
Parameters	294
Restraints	1
Largest Peak	0.152
Deepest Hole	-0.151
GooF	1.032
wR_2 (all data)	0.1048
wR_2	0.0979
R_1 (all data)	0.0649
R_1	0.0486

A.27 Molecular Structure of 3.3

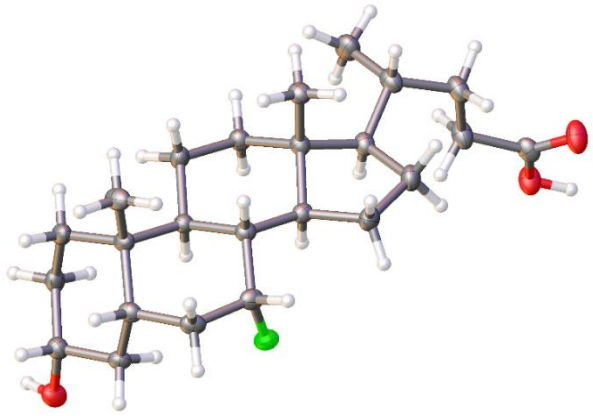

Thermal ellipsoids drawn at the 50% probability level.

Experimental. Single clear colourless plate-shaped crystals of (**RW-8313-89**) were recrystallised from a mixture of CHCl3 and water by slow evaporation. A suitable crystal (0.40×0.40×0.08) mm^3 was selected and mounted on a MITIGEN holder with silicon oil on a Rigaku R-AXIS Spider diffractometer. The crystal was kept at T = 150(2) K during data collection. Using **Olex2** (Dolomanov et al., 2009), the structure was solved with the **ShelXS** (Sheldrick, 2008) structure solution program, using the Direct Methods solution method. The model was refined with version 2018/3 of **ShelXL** (Sheldrick, 2015) using Least Squares minimisation.

Crystal Data. $C_{24}H_{39}FO_3$, M_r = 394.55, orthorhombic, $P2_12_12_1$ (No. 19), a = 6.89110(10) Å, b = 12.0438(2) Å, c = 26.7358(5) Å, $\alpha = \beta = \gamma = 90^\circ$, V = 2218.94(6) $Å^3$, T = 150(2) K, Z = 4, Z' = 1, $\mu(CuK_\alpha)$ = 0.648, 24374 reflections measured, 3905 unique (R_{int} = 0.0292) which were used in all calculations. The final wR_2 was 0.0720 (all data) and R_1 was 0.0297 (I > 2(I)).

Compound	**2018sot0004**
Formula	$C_{24}H_{39}FO_3$
$D_{calc.}$/ g cm^{-3}	1.181
μ/mm^{-1}	0.648
Formula Weight	394.55
Colour	clear colourless
Shape	plate
Size/mm^3	0.40×0.40×0.08
T/K	150(2)
Crystal System	orthorhombic
Flack Parameter	0.04(3)
Hooft Parameter	0.03(3)
Space Group	$P2_12_12_1$
a/Å	6.89110(10)
b/Å	12.0438(2)
c/Å	26.7358(5)
α/°	90
β/°	90
γ/°	90
V/$Å^3$	2218.94(6)
Z	4
Z'	1
Wavelength/Å	1.54187
Radiation type	CuK_α
Θ_{min}/°	3.306
Θ_{max}/°	66.492
Measured Refl.	24374
Independent Refl.	3905
Reflections Used	3797
R_{int}	0.0292
Parameters	264
Restraints	0
Largest Peak	0.124
Deepest Hole	-0.166
GooF	1.082
wR_2 (all data)	0.0720
wR_2	0.0713
R_1 (all data)	0.0309
R_1	0.0297

A.28 Molecular Structure of 3.74

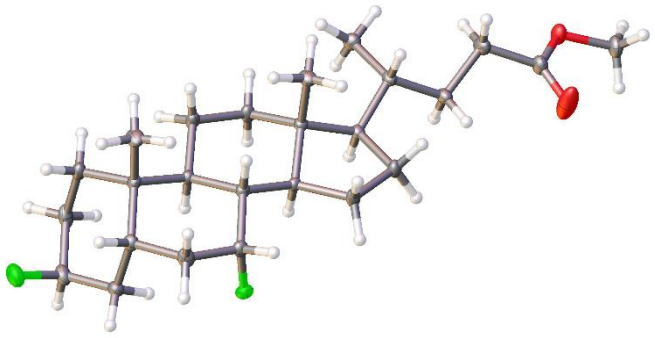

Thermal ellipsoids drawn at the 50% probability level.

Experimental. Single clear colourless prism-shaped crystals of **RW-8525-5** were recrystallised from a mixture of petrol and acetone by slow evaporation. A suitable crystal 0.22×0.10×0.04 mm^3 was selected and mounted on a MITIGEN holder silicon oil on a Rigaku AFC12 FRE-VHF diffractometer. The crystal was kept at a steady T = 100(2) K during data collection. The structure was solved with the **ShelXT** (Sheldrick, 2015) structure solution program using the Intrinsic Phasing solution method and by using **Olex2** (Dolomanov et al., 2009) as the graphical interface. The model was refined with version 2016/6 of **ShelXL** (Sheldrick, 2015) using Least Squares minimisation.

Crystal Data. $C_{25}H_{40}F_2O_2$, M_r = 410.57, orthorhombic, $P2_12_12_1$ (No. 19), a = 10.7927(2) Å, b = 10.8550(2) Å, c = 19.1728(4) Å, $\alpha = \beta = \gamma = 90^\circ$, V = 2246.18(8) $Å^3$, T = 100(2) K, Z = 4, Z' = 1, $\mu(MoK_\alpha)$ = 0.086, 24772 reflections measured, 6523 unique (R_{int} = 0.0211) which were used in all calculations. The final wR_2 was 0.0938 (all data) and R_1 was 0.0337 (I > 2(I)).

Compound	**2018sot0014**
Formula	$C_{25}H_{40}F_2O_2$
$D_{calc.}$/ g cm^{-3}	1.214
μ/mm^{-1}	0.086
Formula Weight	410.57
Colour	clear colourless
Shape	prism
Size/mm^3	0.22×0.10×0.04
T/K	100(2)
Crystal System	orthorhombic
Flack Parameter	-0.15(14)
Hooft Parameter	-0.14(13)
Space Group	$P2_12_12_1$
a/Å	10.7927(2)
b/Å	10.8550(2)
c/Å	19.1728(4)
α/°	90
β/°	90
γ/°	90
V/$Å^3$	2246.18(8)
Z	4
Z'	1
Wavelength/Å	0.71073
Radiation type	MoK_α
Θ_{min}/°	2.124
Θ_{max}/°	32.315
Measured Refl.	24772
Independent Refl.	6523
Reflections with I > 2(I)	6116
R_{int}	0.0211
Parameters	266
Restraints	0
Largest Peak	0.386
Deepest Hole	-0.248
GooF	1.029
wR_2 (all data)	0.0938
wR_2	0.0921
R_1 (all data)	0.0366
R_1	0.0337

A.29 Molecular Structure of 3.7

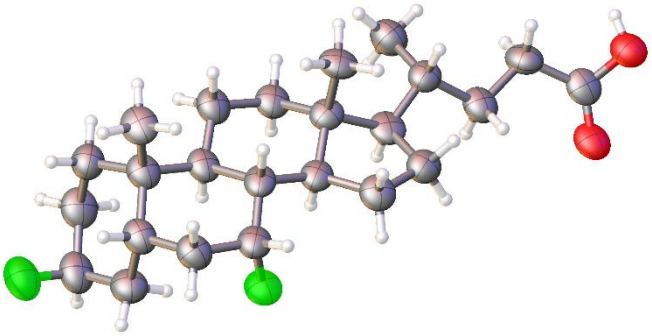

Thermal ellipsoids drawn at the 50% probability level.

Experimental. Single clear colourless slab-shaped crystals of **RW-8525-10** were recrystallised from a mixture of water and acetone by slow evaporation. A suitable crystal 0.62×0.22×0.08 mm^3 was selected and mounted on a MITIGEN holder with silicon oil on an Rigaku R-AXIS Spider diffractometer. The crystal was kept at a steady T = 120(2) K during data collection. The structure was solved with the **ShelXT** (Sheldrick, 2015) structure solution program using the Intrinsic Phasing solution method and by using **Olex2** (Dolomanov et al., 2009) as the graphical interface. The model was refined with version 2018/3 of **ShelXL** (Sheldrick, 2015) using Least Squares minimisation.

Crystal Data. $C_{24}H_{38}F_2O_2$, M_r = 396.54, orthorhombic, $P2_12_12_1$ (No. 19), a = 7.4619(5) Å, b = 9.9017(6) Å, c = 28.649(2) Å, $\alpha = \beta = \gamma = 90^\circ$, V = 2116.7(2) $Å^3$, T = 120(2) K, Z = 4, Z' = 1, $\mu(CuK_\alpha)$ = 0.716, 22406 reflections measured, 3862 unique (R_{int} = 0.1201) which were used in all calculations. The final wR_2 was 0.3063 (all data) and R_1 was 0.1040 (I > 2(I)).

Compound	2018sot0015
Formula	$C_{24}H_{38}F_2O_2$
$D_{calc.}$/ g cm^{-3}	1.244
μ/mm^{-1}	0.716
Formula Weight	396.54
Colour	clear colourless
Shape	slab
Size/mm^3	0.62×0.22×0.08
T/K	120(2)
Crystal System	orthorhombic
Flack Parameter	0.0(3)
Hooft Parameter	0.00(19)
Space Group	$P2_12_12_1$
a/Å	7.4619(5)
b/Å	9.9017(6)
c/Å	28.649(2)
$\alpha/^\circ$	90
$\beta/^\circ$	90
$\gamma/^\circ$	90
V/$Å^3$	2116.7(2)
Z	4
Z'	1
Wavelength/Å	1.54187
Radiation type	CuK_α
$\Theta_{min}/^\circ$	3.085
$\Theta_{max}/^\circ$	68.460
Measured Refl.	22406
Independent Refl.	3862
Reflections Used	2103
R_{int}	0.1201
Parameters	257
Restraints	240
Largest Peak	0.286
Deepest Hole	-0.381
GooF	1.026
wR_2 (all data)	0.3063
wR_2	0.2623
R_1 (all data)	0.1564
R_1	0.1040

A.30 Molecular Structure of 3.5

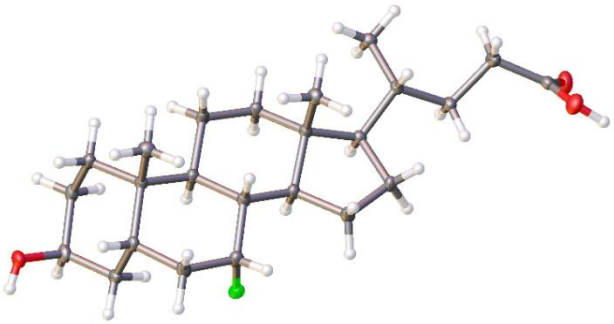

Thermal ellipsoids drawn at the 50% probability level.

Experimental. Single clear colourless prism-shaped crystals of **RW-8525-20** were recrystallised from acetone by slow evaporation. A suitable crystal 0.13×0.10×0.08 mm^3 was selected and mounted on a MITIGEN holder silicon oil on a Rigaku AFC12 FRE-VHF diffractometer. The crystal was kept at a steady T = 100(2) K during data collection. The structure was solved with the **ShelXT** (Sheldrick, 2015) structure solution program using the Intrinsic Phasing solution method and by using **Olex2** (Dolomanov et al., 2009) as the graphical interface. The model was refined with version 2016/6 of **ShelXL** (Sheldrick, 2015) using Least Squares minimisation.

Crystal Data. $C_{24}H_{39}FO_3$, M_r = 394.55, orthorhombic, $P2_12_12_1$ (No. 19), a = 11.7613(3) Å, b = 15.9730(4) Å, c = 23.0746(5) Å, $\alpha = \beta = \gamma = 90^\circ$, V = 4334.87(18) $Å^3$, T = 100(2) K, Z = 8, Z' = 2, $\mu(MoK_\alpha)$ = 0.083, 42404 reflections measured, 10989 unique (R_{int} = 0.0390) which were used in all calculations. The final wR_2 was 0.0885 (all data) and R_1 was 0.0401 (I > 2(I)).

Compound	**2018sot0017**
Formula	$C_{24}H_{39}FO_3$
$D_{calc.}$/ g cm^{-3}	1.209
μ/mm^{-1}	0.083
Formula Weight	394.55
Colour	clear colourless
Shape	prism
Size/mm^3	0.13×0.10×0.08
T/K	100(2)
Crystal System	orthorhombic
Flack Parameter	0.2(2)
Hooft Parameter	0.3(2)
Space Group	$P2_12_12_1$
a/Å	11.7613(3)
b/Å	15.9730(4)
c/Å	23.0746(5)
α/°	90
β/°	90
γ/°	90
V/$Å^3$	4334.87(18)
Z	8
Z'	2
Wavelength/Å	0.71073
Radiation type	MoK_α
Θ_{min}/°	1.765
Θ_{max}/°	28.495
Measured Refl.	42404
Independent Refl.	10989
Reflections with I > 2(I)	9586
R_{int}	0.0390
Parameters	527
Restraints	0
Largest Peak	0.252
Deepest Hole	-0.172
GooF	1.026
wR_2 (all data)	0.0885
wR_2	0.0855
R_1 (all data)	0.0501
R_1	0.0401

A.31 Molecular Structure of 3.6

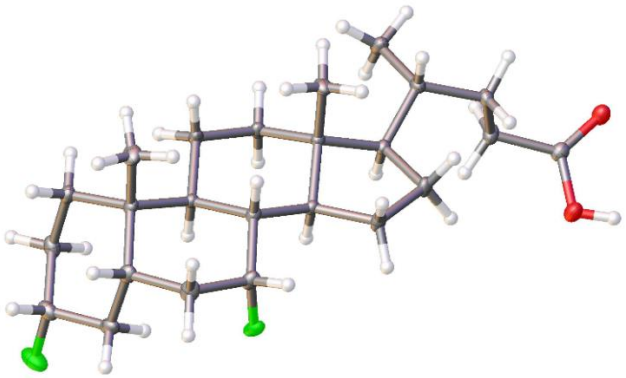

Thermal ellipsoids drawn at the 50% probability level.

Experimental. Single clear colourless prism-shaped crystals of **RW-8523-31** were recrystallised from pet-ether by slow evaporation. A suitable crystal 0.14×0.10×0.08 mm^3 was selected and mounted on a MITIGEN holder with silicon oil on a Rigaku AFC12 FRE-VHF diffractometer. The crystal was kept at a steady T = 100(2) K during data collection. The structure was solved with the ShelXT structure solution program using the intrinsic phasing methods solution method and by using **Olex2** (Dolomanov et al., 2009) as the graphical interface. The model was refined with version 2016/6 of **ShelXL** (Sheldrick, 2015) using Least Squares minimisation.

Crystal Data. $C_{24}H_{38}F_2O_2$, M_r = 396.54, orthorhombic, $P2_12_12_1$ (No. 19), a = 7.32730(10) Å, b = 9.3457(2) Å, c = 30.8186(7) Å, $\alpha = \beta = \gamma = 90^\circ$, V = 2110.42(7) $Å^3$, T = 100(2) K, Z = 4, Z' = 1, $\mu(MoK_\alpha)$ = 0.089, 26874 reflections measured, 5344 unique (R_{int} = 0.0287) which were used in all calculations. The final wR_2 was 0.0803 (all data) and R_1 was 0.0304 (I > 2(I)).

Compound	2018sot0019
Formula	$C_{24}H_{38}F_2O_2$
$D_{calc.}$/ g cm^{-3}	1.248
μ/mm^{-1}	0.089
Formula Weight	396.54
Colour	clear colourless
Shape	prism
Size/mm^3	0.14×0.10×0.08
T/K	100(2)
Crystal System	orthorhombic
Flack Parameter	0.16(16)
Hooft Parameter	0.17(15)
Space Group	$P2_12_12_1$
a/Å	7.32730(10)
b/Å	9.3457(2)
c/Å	30.8186(7)
α/°	90
β/°	90
γ/°	90
V/$Å^3$	2110.42(7)
Z	4
Z'	1
Wavelength/Å	0.71073
Radiation type	MoK_α
Θ_{min}/°	2.277
Θ_{max}/°	28.493
Measured Refl.	26874
Independent Refl.	5344
Reflections with I > 2(I)	5028
R_{int}	0.0287
Parameters	260
Restraints	0
Largest Peak	0.276
Deepest Hole	-0.163
GooF	1.031
wR_2 (all data)	0.0803
wR_2	0.0788
R_1 (all data)	0.0331
R_1	0.0304

A.32 Molecular Structure of 3.4

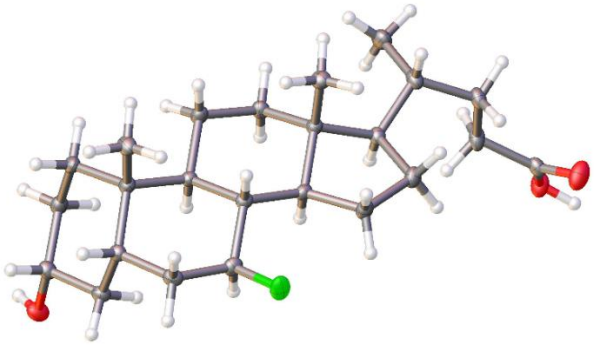

Thermal ellipsoids drawn at the 50% probability level.

Experimental. Single clear colourless prism-shaped crystals of **RW-8525-33** were recrystallised from acetone by slow evaporation. A suitable crystal 0.50×0.40×0.15 mm^3 was selected and mounted on a MITIGEN holder with silicon oil on an Rigaku R-AXIS SPIDER IP diffractometer. The crystal was kept at a steady T = 100(2) K during data collection. The structure was solved with the **ShelXS** (Sheldrick, 2008) structure solution program using the Direct Methods solution method and by using **Olex2** (Dolomanov et al., 2009) as the graphical interface. The model was refined with version 2016/6 of **ShelXL** (Sheldrick, 2015) using Least Squares minimisation.

Crystal Data. $C_{24}H_{39}FO_3$, M_r = 394.55, orthorhombic, $P2_12_12_1$ (No. 19), a = 6.6777(5) Å, b = 12.1376(10) Å, c = 26.8586(18) Å, $\alpha = \beta = \gamma = 90^\circ$, V = 2176.9(3) $Å^3$, T = 100(2) K, Z = 4, Z' = 1, μ(MoK_α) = 0.083, 17505 reflections measured, 4921 unique (R_{int} = 0.0376) which were used in all calculations. The final wR_2 was 0.0821 (all data) and R_1 was 0.0358 (I > 2(I)).

Compound	**2018sot0020**
Formula	$C_{24}H_{39}FO_3$
$D_{calc.}$/ g cm^{-3}	1.204
μ/mm^{-1}	0.083
Formula Weight	394.55
Colour	clear colourless
Shape	prism
Size/mm^3	0.50×0.40×0.15
T/K	100(2)
Crystal System	orthorhombic
Flack Parameter	0.0(3)
Hooft Parameter	0.0(3)
Space Group	$P2_12_12_1$
a/Å	6.6777(5)
b/Å	12.1376(10)
c/Å	26.8586(18)
α/°	90
β/°	90
γ/°	90
V/$Å^3$	2176.9(3)
Z	4
Z'	1
Wavelength/Å	0.71075
Radiation type	MoK_α
Θ_{min}/°	3.034
Θ_{max}/°	27.436
Measured Refl.	17505
Independent Refl.	4921
Reflections with I > 2(I)	4467
R_{int}	0.0376
Parameters	264
Restraints	0
Largest Peak	0.218
Deepest Hole	-0.202
GooF	1.027
wR_2 (all data)	0.0821
wR_2	0.0795
R_1 (all data)	0.0424
R_1	0.0358

A.33 Molecular Structure of 4.12

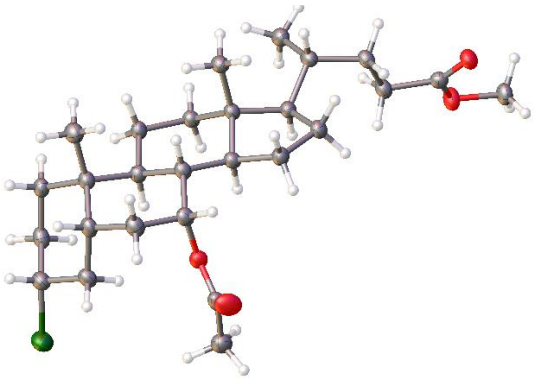

Thermal ellipsoids drawn at the 50% probability level.

Experimental. Single clear colourless prism-shaped crystals of (**RW-7704-57**) were recrystallised from DCM by slow evaporation. A suitable crystal (0.77×0.10×0.03) mm^3 was selected and mounted on a MITIGEN holder with silicon oil on a Rigaku R-AXIS Spider diffractometer. The crystal was kept at T = 100(2) K during data collection. Using **Olex2** (Dolomanov et al., 2009), the structure was solved with the **ShelXT** (Sheldrick, 2015) structure solution program, using the Intrinsic Phasing solution method. The model was refined with version 2014/7 of **ShelXL** (Sheldrick, 2015) using Least Squares minimisation.

Crystal Data. $C_{27}H_{43}ClO_4$, M_r = 467.06, orthorhombic, $P2_12_12$ (No. 18), a = 15.3820(3) Å, b = 26.1105(5) Å, c = 6.25240(10) Å, $\alpha = \beta = \gamma = 90^\circ$, V = 2511.16(8) $Å^3$, T = 100(2) K, Z = 4, Z' = 1, $\mu(CuK_\alpha)$ = 1.579, 28699 reflections measured, 4563 unique (R_{int} = 0.0668) which were used in all calculations. The final wR_2 was 0.0896 (all data) and R_1 was 0.0362 (I > 2(I)).

Compound	**2016sot0066**
Formula	$C_{27}H_{43}ClO_4$
$D_{calc.}$/ g cm^{-3}	1.235
μ/mm^{-1}	1.579
Formula Weight	467.06
Colour	clear colourless
Shape	prism
Size/mm^3	0.77×0.10×0.03
T/K	100(2)
Crystal System	orthorhombic
Flack Parameter	0.069(8)
Hooft Parameter	0.080(8)
Space Group	$P2_12_12$
a/Å	15.3820(3)
b/Å	26.1105(5)
c/Å	6.25240(10)
$\alpha/^\circ$	90
$\beta/^\circ$	90
$\gamma/^\circ$	90
V/$Å^3$	2511.16(8)
Z	4
Z'	1
Wavelength/Å	1.54187
Radiation type	CuK_α
$\Theta_{min}/^\circ$	3.335
$\Theta_{max}/^\circ$	68.252
Measured Refl.	28699
Independent Refl.	4563
Reflections Used	4169
R_{int}	0.0668
Parameters	294
Restraints	0
Largest Peak	0.186
Deepest Hole	-0.279
GooF	1.054
wR_2 (all data)	0.0896
wR_2	0.0831
R_1 (all data)	0.0426
R_1	0.0362

A.34 Molecular Structure of 4.2

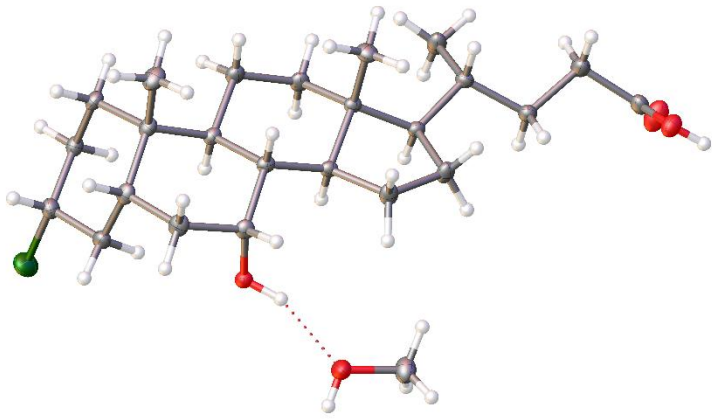

Thermal ellipsoids drawn at the 50% probability level.

Experimental. Single clear colourless prism-shaped crystals of (**RW-7704-64**) were recrystallised from methanol by slow evaporation. A suitable crystal (0.21×0.07×0.02) mm^3 was selected and mounted on a MITIGEN holder with silicon oil on a Rigaku AFC12 FRE-HF diffractometer. The crystal was kept at T = 100(2) K during data collection. Using **Olex2** (Dolomanov et al., 2009), the structure was solved with the **ShelXT** (Sheldrick, 2015) structure solution program, using the Intrinsic Phasing solution method. The model was refined with version 2014/7 of **ShelXL** (Sheldrick, 2015) using Least Squares minimisation.

Crystal Data. $C_{25}H_{43}ClO_4$, M_r = 443.04, orthorhombic, $P2_12_12_1$ (No. 19), a = 6.5095(2) Å, b = 16.9001(3) Å, c = 21.5962(5) Å, α = β = γ = 90°, V = 2375.82(10) $Å^3$, T = 100(2) K, Z = 4, Z' = 1, μ(MoK_α) = 0.189, 13032 reflections measured, 5870 unique (R_{int} = 0.0214) which were used in all calculations. The final wR_2 was 0.1004 (all data) and R_1 was 0.0389 (I > 2(I)).

Compound	**2016sot0067**
Formula	$C_{25}H_{43}ClO_4$
	$C_{24}H_{39}ClO_3$, CH_4O
$D_{calc.}$/ g cm^{-3}	1.239
μ /mm^{-1}	0.189
Formula Weight	443.04
Colour	clear colourless
Shape	prism
Size/mm^3	0.21×0.07×0.02
T/K	100(2)
Crystal System	orthorhombic
Flack Parameter	-0.01(3)
Hooft Parameter	0.01(2)
Space Group	$P2_12_12_1$
a/Å	6.5095(2)
b/Å	16.9001(3)
c/Å	21.5962(5)
α/°	90
β/°	90
γ/°	90
V/$Å^3$	2375.82(10)
Z	4
Z'	1
Wavelength/Å	0.71073
Radiation type	MoK_α
Θ_{min}/°	3.061
Θ_{max}/°	28.692
Measured Refl.	13032
Independent Refl.	5870
Reflections Used	5477
R_{int}	0.0214
Parameters	287
Restraints	1
Largest Peak	0.339
Deepest Hole	-0.190
GooF	1.060
wR_2 (all data)	0.1004
wR_2	0.0976
R_1 (all data)	0.0431
R_1	0.0389

A.35 Molecular Structure of 4.30

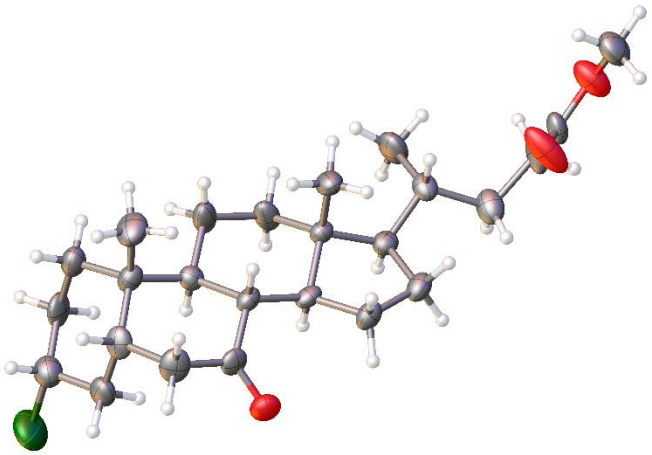

Thermal ellipsoids drawn at the 50% probability level.

Experimental. Single clear colourless irregular-shaped crystals of (**RW-7991-41**) were recrystallised from a mixture of acetone and methanol by slow evaporation. A suitable crystal (0.24×0.12×0.03) mm^3 was selected and mounted on a MITIGEN holder silicon oil on a Rigaku AFC12 FRE-HF diffractometer. The crystal was kept at T = 200(2) K during data collection. Using **Olex2** (Dolomanov et al., 2009), the structure was solved with the **ShelXT** (Sheldrick, 2015) structure solution program, using the Intrinsic Phasing solution method. The model was refined with version 2016/6 of **ShelXL** (Sheldrick, 2015) using Least Squares minimisation.

Crystal Data. $C_{25}H_{39}ClO_3$, M_r = 423.01, triclinic, P1 (No. 1), a = 7.6770(7) Å, b = 9.8365(10) Å, c = 15.2334(8) Å, α = 95.367(6)°, β = 90.834(6)°, γ = 90.447(8)°, V = 1145.13(17) $Å^3$, T = 200(2) K, Z = 2, Z' = 2, μ (MoK_α) = 0.190, 16030 reflections measured, 8848 unique (R_{int} = 0.0402) which were used in all calculations. The final wR_2 was 0.1545 (all data) and R_1 was 0.1000 (I > 2(I)).

Compound	**2017sot0039**
Formula	$C_{25}H_{39}ClO_3$
$D_{calc.}$/ g cm^{-3}	1.227
μ/mm^{-1}	0.190
Formula Weight	423.01
Colour	clear colourless
Shape	irregular
Size/mm^3	0.24×0.12×0.03
T/K	200(2)
Crystal System	triclinic
Flack Parameter	0.00(5)
Hooft Parameter	0.02(5)
Space Group	P1
a/Å	7.6770(7)
b/Å	9.8365(10)
c/Å	15.2334(8)
α/°	95.367(6)
β/°	90.834(6)
γ/°	90.447(8)
V/$Å^3$	1145.13(17)
Z	2
Z'	2
Wavelength/Å	0.71073
Radiation type	MoK_α
Θ_{min}/°	2.956
Θ_{max}/°	27.913
Measured Refl.	16030
Independent Refl.	8848
Reflections Used	6438
R_{int}	0.0402
Parameters	531
Restraints	501
Largest Peak	0.267
Deepest Hole	-0.261
GooF	1.163
wR_2 (all data)	0.1545
wR_2	0.1379
R_1 (all data)	0.1431
R_1	0.1000